BEILSTEIN JOURNAL OF ORGANIC CHEMISTRY

New advances in asymmetric organocatalysis II

Edited by Radovan Šebesta

Imprint

Beilstein Journal of Organic Chemistry
www.bjoc.org
ISSN 1860-5397
Email: journals-support@beilstein-institut.de

The *Beilstein Journal of Organic Chemistry* is published by the Beilstein-Institut zur Förderung der Chemischen Wissenschaften.

Beilstein-Institut zur Förderung der Chemischen Wissenschaften
Trakehner Straße 7–9
60487 Frankfurt am Main
Germany
www.beilstein-institut.de

BEILSTEIN JOURNAL OF ORGANIC CHEMISTRY

New advances in asymmetric organocatalysis II

Radovan Šebesta

Editorial

Open Access

Address:
Department of Organic Chemistry, Faculty of Natural Sciences, Comenius University in Bratislava, Mlynská dolina, Ilkovičova 6, 842 15 Bratislava, Slovakia

Email:
Radovan Šebesta - radovan.sebesta@uniba.sk

Keywords:
asymmetric organocatalysis; covalent activation; noncovalent activation

Beilstein J. Org. Chem. **2025,** *21,* 766–769.
https://doi.org/10.3762/bjoc.21.60

Received: 10 March 2025
Accepted: 28 March 2025
Published: 15 April 2025

This article is part of the thematic issue "New advances in asymmetric organocatalysis II".

Guest Editor: R. Šebesta

Organocatalysis is commonly defined as a form of catalysis where a small organic molecule, an organocatalyst, accelerates a chemical reaction. Unlike previously regarded traditional catalysts involving metals or enzymes, organocatalysts are composed of nonmetal elements, such as carbon, hydrogen, nitrogen, oxygen, phosphorus, or sulfur. The year 2000 is typically regarded as the birth of organocatalysis, which was at that time regarded as a new mode of action for chemical catalysts. In that year, List and MacMillan et al. published their landmark studies on proline- and imidazolidine-catalyzed aldol, Mannich, and cycloaddition reactions [1-4]. The history of scientific discoveries, however, is rarely defined by single specific dates that can unambiguously be connected to the discoveries. Instead, the chronology often seems to be quite convoluted but also ultimately more interesting, as can also be seen for organocatalysis. Even toward the end of the 20th century, there have been a few pioneering studies that should be counted as examples of asymmetric organocatalysis. The works of Jacobsen, Miller, Shi, and Denmark et al. marked the early sparks of interest in this type of chemistry based on catalysis by peptides, carbohydrates, or thiourea [5-8]. Going even more back in time, we shall recognize the work of Eder, Sauer, Wiechert, Hajos, and Parrish on the proline-catalyzed Robinson annulation in the 1970s [9,10]. In light of this, organocatalysis appears to be 50 rather than 25 years old. But is even that correct? Or should we look even more deeply into its history? Well, we can go even further back in time and acknowledge the inspirations from Kuhn and Langebeck in the 1930s, which ultimately leads us to research by Knoevenagel published in 1896 [11,12]. Another interesting historical note is tied to the now prominent Hayashi–Jørgensen catalyst. This prolinol silyl ether was independently discovered by the respective Hayashi and Jørgensen research teams in 2005 [13,14]. Interestingly, the use of prolinol alkyl ethers for asymmetric Michael additions, although at the time added in a stoichiometric manner, has already been described by Seebach et al. in 1982 [15]. From this perspective, organocatalysis is more than 100 years old, building on a long thread of illustrious past discoveries.

Asymmetric organocatalysis is now considered one of the three main pillars of asymmetric catalysis, along with metal-catalyzed reactions and biocatalysis. In the past 25 years, organocatalysis has grown rapidly into a broad area of research, with industrial applications now being developed [16]. The usefulness of any idea or methodology is ultimately often measured by its applications. The robustness, reliability, as well

as the eco- and user-friendliness of asymmetric organocatalysis contribute to its growing applicability in the synthesis of complex target molecules, such as therapeutic agents [17,18]. However, nowadays organocatalysis does go well beyond the boundaries of organic chemistry. This can also be seen from a brief Web of Science analysis of the 6,700 articles, published within the past 25 years, retrieved through a search of the keywords "asymmetric organocatalysis". Organocatalysis is now part of various areas of chemistry, spanning as far as polymer, materials, as well as green and sustainable science and technology (Figure 1).

In 2012, there was a thematic issue in the *Beilstein Journal of Organic Chemistry* devoted to asymmetric organocatalysis edited by one of the pioneers in this field, Benjamin List [19]. After a decade, another thematic issue was devoted to new advances in this field [20]. In 2022, three Review articles and nine research papers showcased the diversity and breadth into which asymmetric organocatalysis had grown. This follow-up thematic issue "New advances in asymmetric organocatalysis II" aims to monitor the progress in this exciting area and highlights excellent contributions in stereoselective organocatalytic transformations. The collection contains nine articles featuring various aspects of asymmetric organocatalysis.

In the first contribution, Waser et al. examined how chiral phase-transfer catalysts promote β-selective additions of azlactones to allenoates. Maruoka´s quaternary ammonium salts provided the corresponding substituted azlactones comprising a quaternary stereogenic center with the highest enantiomeric purity [21]. A contribution by Chowdhury and Dubey further underscored the importance of heterocyclic moieties in chiral compounds. Their article describes the enantioselective Michael addition of pyrazoline-5-ones to α,β-unsaturated ketones. The enantioselectivity and chemical efficiency of this transformation were achieved with a cinchona-alkaloid-derived primary-amine–Brønsted acid composite [22].

A good demonstration of how organocatalysis progressed from the original amine catalysts is the work of Shirakawa and co-workers. In this contribution, the authors employed a binaphthalene-derived sulfide organocatalyst for enantioselective bromolactonizations of α- and β-substituted 5-hexenoic acids to produce the corresponding chiral lactones [23]. Kowalczyk and co-workers showed how asymmetric organocatalysis can benefit from mechanochemical activation. They established that Michael additions of thiomalonates to enones, catalyzed by cinchona-derived primary amines, is efficient and enantioselective under ball-milling conditions [24]. Kondratyev and Malkov reviewed the recent progress in the organocatalytic synthesis of chiral homoallylic amines. This important structural motif is typically made by asymmetric allylation of imines, and the authors describe various catalytic approaches as well as applications of these strategies in total synthesis [25]. The enantioselective addition of propargyltrichlorosilane to aldehydes was studied by Prabhakar, Takenaka, and co-workers. This transformation was catalyzed by a biisoquinoline *N*,*N*'-dioxide catalyst, which acted as a chiral Lewis base [26]. Torres-Oya and Zurro

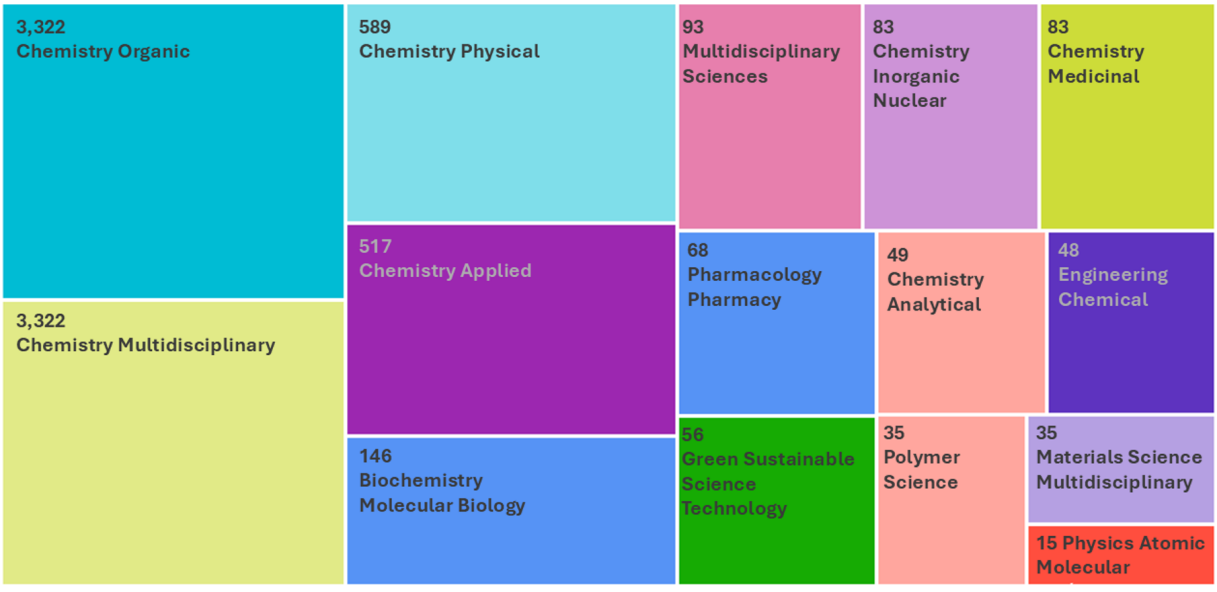

Figure 1: TreeMap chart of the top 15 Web of Science categories for 6,700 articles containing the keywords "asymmetric organocatalysis" published in 2001–2025.

reviewed the recent developments in organocatalytic cycloaddition reactions of unsaturated imines. A broad variety of activation modes, as well as catalyst structures, was covered and found to be useful in affording a diverse array of chiral N-heterocycles [27]. In my group, we recently became interested in atroposelective catalytic syntheses. Therefore, my team reviewed the recent progress in organocatalytic syntheses of axially chiral compounds [28]. The final article within this thematic issue was contributed by Tsogoeva, Harder, and co-workers. They developed and mechanistically studied the hydrocyanation of hydrazones. This interesting transformation was catalyzed by a calcium complex of BINOL phosphate [29].

As can be seen from the summary above, the articles in this thematic issue cover a diverse array of topics in contemporary asymmetric organocatalysis. Moreover, they also reflect the diversity of our scientific community, as researchers at various career stages are involved. Contributions to this issue also highlight its truly global character, with research teams from nine countries (Austria, India, Japan, Poland, UK, USA, Spain, Slovakia, and Germany) across three continents contributing to this remarkable selection.

As guest editor of this thematic issue, I am grateful to all authors for their excellent contributions. I sincerely thank the referees for providing their expertise and time, and the team at the *Beilstein Journal of Organic Chemistry* for their outstanding professionalism and support.

Radovan Šebesta

Bratislava, March 2025

ORCID® iDs

Radovan Šebesta - https://orcid.org/0000-0002-7975-3608

Data Availability Statement

Data sharing is not applicable as no new data was generated or analyzed in this study.

References

1. List, B.; Lerner, R. A.; Barbas, C. F. *J. Am. Chem. Soc.* **2000,** *122,* 2395–2396. doi:10.1021/ja994280y
2. List, B. *J. Am. Chem. Soc.* **2000,** *122,* 9336–9337. doi:10.1021/ja001923x
3. Ahrendt, K. A.; Borths, C. J.; MacMillan, D. W. C. *J. Am. Chem. Soc.* **2000,** *122,* 4243–4244. doi:10.1021/ja000092s
4. Jen, W. S.; Wiener, J. J. M.; MacMillan, D. W. C. *J. Am. Chem. Soc.* **2000,** *122,* 9874–9875. doi:10.1021/ja005517p
5. Miller, S. J.; Copeland, G. T.; Papaioannou, N.; Horstmann, T. E.; Ruel, E. M. *J. Am. Chem. Soc.* **1998,** *120,* 1629–1630. doi:10.1021/ja973892k
6. Sigman, M. S.; Jacobsen, E. N. *J. Am. Chem. Soc.* **1998,** *120,* 4901–4902. doi:10.1021/ja980139y
7. Tu, Y.; Wang, Z.-X.; Shi, Y. *J. Am. Chem. Soc.* **1996,** *118,* 9806–9807. doi:10.1021/ja962345g
8. Denmark, S. E.; Wu, Z.; Crudden, C. M.; Matsuhashi, H. *J. Org. Chem.* **1997,** *62,* 8288–8289. doi:10.1021/jo971781y
9. Eder, U.; Sauer, G.; Wiechert, R. *Angew. Chem., Int. Ed. Engl.* **1971,** *10,* 496–497. doi:10.1002/anie.197104961
10. Hajos, Z. G.; Parrish, D. R. *J. Org. Chem.* **1974,** *39,* 1615–1621. doi:10.1021/jo00925a003
11. Knoevenagel, E. *Ber. Dtsch. Chem. Ges.* **1896,** *29,* 172–174. doi:10.1002/cber.18960290133
12. List, B. *Angew. Chem., Int. Ed.* **2010,** *49,* 1730–1734. doi:10.1002/anie.200906900
13. Hayashi, Y.; Gotoh, H.; Hayashi, T.; Shoji, M. *Angew. Chem., Int. Ed.* **2005,** *44,* 4212–4215. doi:10.1002/anie.200500599
14. Marigo, M.; Wabnitz, T. C.; Fielenbach, D.; Jørgensen, K. A. *Angew. Chem., Int. Ed.* **2005,** *44,* 794–797. doi:10.1002/anie.200462101
15. Blarer, S. J.; Schweizer, W. B.; Seebach, D. *Helv. Chim. Acta* **1982,** *65,* 1637–1654. doi:10.1002/hlca.19820650537
16. List, B.; Maruoka, K., Eds. *Asymmetric Organocatalysis – Workbench Edition;* Georg Thieme Verlag: Stuttgart, Germany, 2012.
17. Han, B.; He, X.-H.; Liu, Y.-Q.; He, G.; Peng, C.; Li, J.-L. *Chem. Soc. Rev.* **2021,** *50,* 1522–1586. doi:10.1039/d0cs00196a
18. Yang, H.; Yu, H.; Stolarzewicz, I. A.; Tang, W. *Chem. Rev.* **2023,** *123,* 9397–9446. doi:10.1021/acs.chemrev.3c00010
19. List, B. *Beilstein J. Org. Chem.* **2012,** *8,* 1358–1359. doi:10.3762/bjoc.8.156
20. Šebesta, R. *Beilstein J. Org. Chem.* **2022,** *18,* 240–242. doi:10.3762/bjoc.18.28
21. Nasiri, B.; Pasdar, G.; Zebrowski, P.; Röser, K.; Naderer, D.; Waser, M. *Beilstein J. Org. Chem.* **2024,** *20,* 1504–1509. doi:10.3762/bjoc.20.134
22. Goyal, P.; Dubey, A. K.; Chowdhury, R.; Wadawale, A. *Beilstein J. Org. Chem.* **2024,** *20,* 1518–1526. doi:10.3762/bjoc.20.136
23. Sumida, S.; Okuno, K.; Mori, T.; Furuya, Y.; Shirakawa, S. *Beilstein J. Org. Chem.* **2024,** *20,* 1794–1799. doi:10.3762/bjoc.20.158
24. Błauciak, M.; Andrzejczyk, D.; Dziuk, B.; Kowalczyk, R. *Beilstein J. Org. Chem.* **2024,** *20,* 2313–2322. doi:10.3762/bjoc.20.198
25. Kondratyev, N. S.; Malkov, A. V. *Beilstein J. Org. Chem.* **2024,** *20,* 2349–2377. doi:10.3762/bjoc.20.201
26. Brako, N.; Narayanan, S. M.; Burns, A.; Auter, L.; Cesiliano, V.; Prabhakar, R.; Takenaka, N. *Beilstein J. Org. Chem.* **2024,** *20,* 3069–3076. doi:10.3762/bjoc.20.255
27. Torres-Oya, S.; Zurro, M. *Beilstein J. Org. Chem.* **2024,** *20,* 3221–3255. doi:10.3762/bjoc.20.268
28. Szabados, H.; Šebesta, R. *Beilstein J. Org. Chem.* **2025,** *21,* 55–121. doi:10.3762/bjoc.21.6
29. Tortora, C.; Fischer, C. A.; Kohlbauer, S.; Zamfir, A.; Ballmann, G. M.; Pahl, J.; Harder, S.; Tsogoeva, S. B. *Beilstein J. Org. Chem.* **2025,** *21,* 755–765. doi:10.3762/bjoc.21.59

License and Terms

BEILSTEIN JOURNAL OF ORGANIC CHEMISTRY

Towards an asymmetric β-selective addition of azlactones to allenoates

Behzad Nasiri‡[1,2], Ghaffar Pasdar‡[1], Paul Zebrowski[1], Katharina Röser[1], David Naderer[1] and Mario Waser*[1]

Full Research Paper

Open Access

Address:
[1]Institute of Organic Chemistry, Johannes Kepler University Linz, Altenbergerstrasse 69, 4040 Linz, Austria and [2]Department of Chemistry, Faculty of Science, University of Kurdistan, 66177-15175 Sanandaj, Kurdistan, Iran

Email:
Mario Waser* - mario.waser@jku.at

* Corresponding author ‡ Equal contributors

Keywords:
allenoates; amino acids; azlactones; organocatalysis; quaternary ammonium salt catalysis

Beilstein J. Org. Chem. **2024,** *20,* 1504–1509.
https://doi.org/10.3762/bjoc.20.134

Received: 03 May 2024
Accepted: 24 June 2024
Published: 04 July 2024

This article is part of the thematic issue "New advances in asymmetric organocatalysis II".

Guest Editor: R. Šebesta

Abstract

We herein report the asymmetric organocatalytic addition of azlactones to allenoates. Upon using chiral quaternary ammonium salt catalysts, i.e., Maruoka's binaphthyl-based spirocyclic ammonium salts, the addition of various azlactones to allenoates proceeds in a β-selective manner with moderate levels of enantioselectivities (up to 83:17 er). Furthermore, the obtained products can be successfully engaged in nucleophilic ring opening reactions, thus giving highly functionalized α-amino acid derivatives.

Introduction

The development of asymmetric synthesis routes to access non-natural amino acids has for decades been one of the most heavily investigated tasks in organic synthesis and catalysis-oriented research [1-13]. As a consequence, a broad variety of conceptually orthogonal strategies to access differently functionalized non-natural α-amino acids (α-AA) [2-7] as well as β-amino acids (β-AA) [8-13] have been introduced and there is still considerable interest in the development of new concepts and synthesis approaches. Our group has a longstanding focus on the development of asymmetric organocatalytic methods to access non-natural chiral α- and β-AA [14-19]. Hereby we are especially interested in utilizing simple (prochiral) starting materials and carry out stereoselective α-functionalizations by reacting them with suited C- or heteroatom electrophiles. α-Amino acid-derived azlactones **1** are amongst the most commonly utilized starting materials to access more diverse chiral α,α-disubstituted amino acids (Scheme 1A) [20-22]. More specifically, these compounds can be engaged in a variety of asymmetric α-carbo- and α-heterofunctionalization reactions by utilizing different catalysis strategies [20-22]. We have recently carried out systematic investigations concerning the syntheses of advanced β-AA by means of asymmetric α-carbofunctional-

ization reactions and during these studies we also realized that the masked β-AA derivatives **2** undergo enantioselective β-addition to allenoates **3** under chiral ammonium salt catalysis (Scheme 1B) [18]. Interestingly, hereby we also found that the use of alternative catalyst systems (i.e., tertiary phosphines) allows for a γ-selective addition of **2** to the allenoate instead, thus resulting in two complementary catalyst-controlled pathways [18]. Based on these previous results, and also the well-documented different reactivity trends of allenoates **3** when using different organocatalysts and activation modes [23-27], we were thus wondering if we could extend this ammonium salt-catalyzed β-selective allenoate functionalization strategy to other amino acid classes. Azlactones **1** have previously been used for γ-selective additions to allenoates under chiral phosphine catalysis [28]. In addition, glycine Schiff base derivatives [29] as well as α-amino acid-based thiazolones [30] have successfully been used for asymmetric β-selective additions to allenoates when using chiral ammonium salt catalysts or chiral organobase catalysts. However, to the best of our knowledge the β-selective asymmetric addition of azlactones **1** to allenoates **3** delivering highly functionalized α,α-disubstituted α-amino acid derivatives **5** has so far not been systematically addressed (for recent other β-selective additions of enolate precursors to allenoates please see references [31-34]). Thus, we now became interested in testing this transformation under asymmetric ammonium salt catalysis [35-38] and the results of these investigations are outlined in this contribution (Scheme 1C).

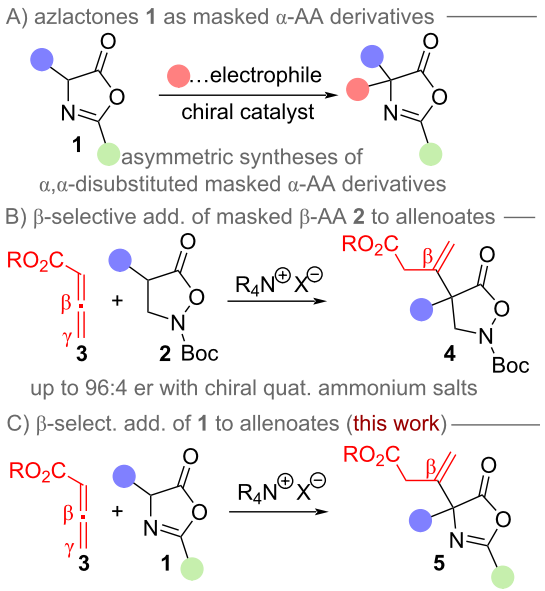

Scheme 1: General use of azlactones **1** to access more advanced α-AA derivatives (A), our recently reported ammonium salt-catalyzed β-selective addition of compounds **2** to allenoates **3** (B), and the herein investigated β-selective addition of azlactones **1** to allenoates **3** (C).

Results and Discussion

We started our investigations by testing the quaternary ammonium salt-catalyzed addition of azlactone **1a** to allenoate **3a** (Table 1 gives an overview of the most significant results obtained hereby). First experiments using cinchona alkaloid-based quaternary ammonium salts **A** showed that the expected β-addition product **5a** can be accessed under typical phase-transfer conditions, but with low selectivities and yields only when using these catalysts (Table 1, entries 1–4, other cinchona alkaloid-based ammonium salt derivatives as well as free base cinchona alkaloids were tested too but did not allow for any improvement). Using the established and commercially available Maruoka catalysts **B1** and **B2** [39] next turned out to be more promising (Table 1, entries 5–8). Testing the bis-CF_3-substituted **B1** first allowed for 75:25 er, but with moderate yield only when carrying out the reaction in toluene in the presence of 3 equiv of K_2CO_3 (Table 1, entry 5). Lower amounts of base (Table 1, entry 6) or other solvents, as exemplified for CH_2Cl_2 (Table 1, entry 7, similar non-selective results were obtained when using THF), were found to be less-suited however. Testing the 3,4,5-trifluorobenzene-decorated catalyst **B2** with K_2CO_3 in toluene next (Table 1, entry 8) allowed for a slightly higher selectivity but still gave only a relatively low yield. Spirobiindane-based salts **C** emerged as promising alternative for quaternary ammonium salt scaffolds recently [40,41] and were also the catalysts of choice in our recently developed β-selective allenoate addition of isoxazolidinones **2** (compare with Scheme 1B [18]). Unfortunately, these catalysts were found to be less-suited for our azlactone protocol, as exemplified for derivative **C1** (Table 1, entry 9). Accordingly, we carried out our final optimization using Maruoka's catalyst **B2** (Table 1, entries 10–14). By testing different bases and lower temperatures as well as lower catalyst loadings we identified the use of 3 equiv Cs_2CO_3 in toluene (0.05 M) at room temperature as the best-suited conditions (Table 1, entry 13), allowing for the synthesis of **5a** in moderate yield (61%) and enantioselectivity (81:19 er).

With optimized conditions for the synthesis of enantioenriched (−)-**5a** at hand, we next investigated the generality of this protocol. As outlined in Scheme 2, differently substituted allenoates were reasonably well tolerated (see products **5a–d**), albeit some erosion in enantioselectivity was observed when using a *tert*-butyl ester containing allenoate (product **5d**). Various α-arylmethyl-substituted azlactones **1** performed similarly as compared to the parent system **1a** (products **5e–i**), and analogous α-alkyl-substituted derivatives were reasonably well accepted too (**5j–o**). When varying the aryl substituent in position **2** of the oxazolone core (compare products **5a**, **5g**, and **5p**) we found that increasing the steric bulk (**5p**) leads to a somewhat lower enantioselectivity, while the methoxy-substituent

Table 1: Optimization of the addition of azlactone **1a** to allenoate **3a**[a].

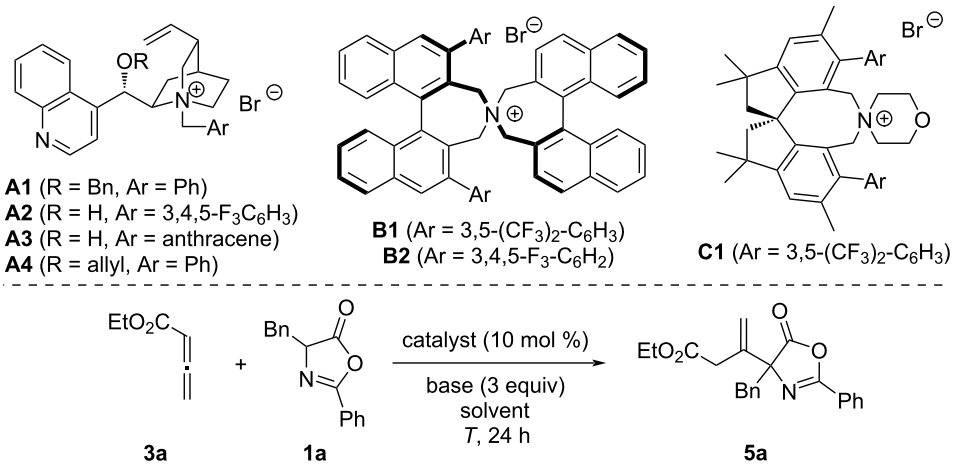

Entry	Cat.	Base	Solvent	*T* [°C]	Yield[b]	er[c]
1	**A1**	K_2CO_3	toluene	25	41	58:42
2	**A2**	K_2CO_3	toluene	25	45	60:40
3	**A3**	K_2CO_3	toluene	25	40	58:42
4	**A4**	K_2CO_3	toluene	25	45	60:40
5	**B1**	K_2CO_3	toluene	25	55	75:25
6	**B1**	K_2CO_3 (1 equiv)	toluene	25	20	72:28
7	**B1**	K_2CO_3	CH_2Cl_2	25	33	51:49
8	**B2**	K_2CO_3	toluene	25	50	80:20
9	**C1**	K_2CO_3	toluene	25	40	68:32
10	**B2**	K_2CO_3	toluene	0	45	80:20
11	**B2** (5%)	K_2CO_3	toluene	0	41	77:23
12	**B2**	K_3PO_4	toluene	25	55	81:19
13	**B2**	Cs_2CO_3	toluene	25	61	81:19
14	**B2**	Cs_2CO_3	toluene (0.1 M)	25	75	73:27

[a]Unless otherwise stated, all reactions were carried out by stirring **1a** (0.1 mmol), the allenoate (2 equiv), the indicated base and the catalyst, in the given solvent (0.05 M based on **1a**) at the given temperature for 24 h. [b]Isolated yield. [c]Determined by HPLC using a chiral stationary phase, (–)-**5a** was obtained as the major enantiomer when using the (*R*,*R*)-configurated catalysts **B**.

does not have a strong impact on the yield. It should, however, be stated that some of the methoxy-containing products, i.e., the α-alkyl-substituted **5j** and **5k** tend to undergo partial nucleophilic ring opening by residual water during column chromatography. Unfortunately, attempts to assign the absolute configuration of products **5** failed, as we have not been able to obtain any crystals suited for single crystal X-ray diffraction analysis.

Finally, we also tested the suitability of products **5** to access acyclic α-AA derivatives by means of nucleophilic azlactone-opening reactions. Gratifyingly primary amines can be easily utilized under reflux conditions to access the amide derivatives **6a** and **6b** straightforwardly (Scheme 3), thus demonstrating the versatility of compounds **5** to access more complex acyclic α-AA derivatives in a straightforward manner.

Conclusion

The development of novel catalytic methods for the asymmetric synthesis of non-natural amino acid derivatives is a contemporary task and we herein introduce an organocatalytic protocol for the β-selective addition of various azlactones **1** to allenoates **3**. Upon using Maruoka's spirocyclic binaphthyl-based quaternary ammonium salts **B** as catalysts this transformation can be achieved with enantioselectivities up to 83:17 er. Furthermore, the herein accessed cyclic products **5** could be successfully engaged in ring-opening reactions with different

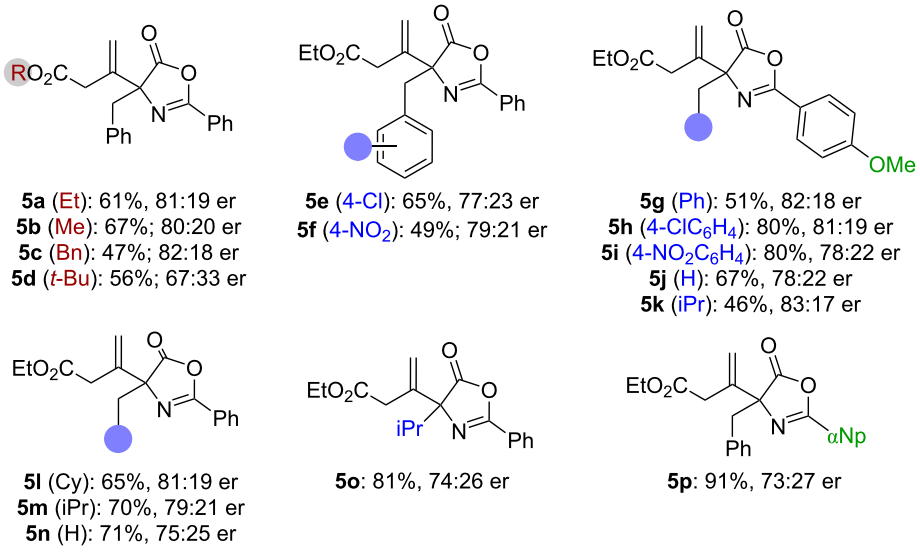

Scheme 2: Application scope (conditions as detailed in Table 1, entry 13).

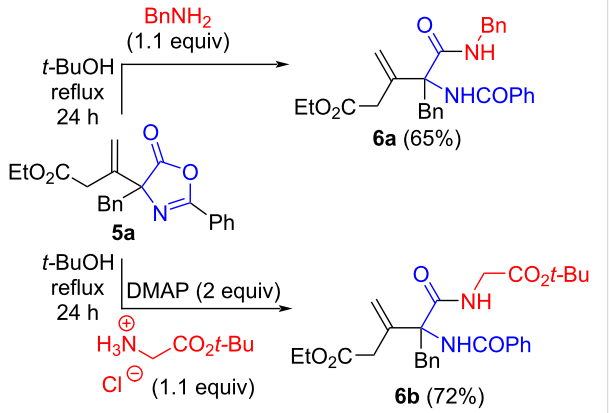

Scheme 3: Azlactone opening reactions.

amines, thus giving access to the acyclic α-amino acid-based amides **6** straightforwardly.

Experimental

General details

^{1}H and ^{13}C NMR spectra were recorded on a Bruker Avance III 300 MHz spectrometer with a broad band observe probe. All NMR spectra were referenced on the solvent residual peak ($CDCl_3$: δ 7.26 ppm for ^{1}H NMR and δ 77.16 ppm for ^{13}C NMR). NMR data are reported as follows: chemical shift (δ ppm), multiplicity (s = singlet, d = doublet, t = triplet, q = quartet, m = multiplet, dd = doublet of doublet), coupling constants (Hz), relative integration value. High-resolution mass spectra were obtained using a Thermo Fisher Scientific LTQ Orbitrap XL spectrometer with an Ion Max API source and analyses were made in the positive ionization mode if not otherwise stated. Infrared (IR) spectra were recorded on a Bruker Alpha II FTIR spectrometer with diamond ATR-module using the OPUS software package and are reported in terms of frequency of absorption (cm^{-1}). HPLC was performed using a Shimadzu Prominence system with a diode array detector with a CHIRALPAK AD-H, CHIRAL ART Amylose-SA, (250 × 4.6 mm, 5 µm) chiral stationary phase. Optical rotations were recorded on a Schmidt + Haensch Polarimeter Model UniPol L1000 at 589 nm ($[\alpha]_D$ values are listed in deg/(dm(g/cm^3)); concentration c is given in g/100 mL).

Unless otherwise stated, all chemicals were purchased from commercial suppliers and used without further purification. Dry solvents were obtained from an MBraun-SPS-800 solvent purification system. All reactions were carried out under argon atmosphere unless stated otherwise. Azlactones **1** and allenoates **3** were synthesized according to previously published procedures [18,42-44].

General procedure

An oven-dried Schlenk tube equipped with a stirring bar was charged with azlactone **1** (0.05–0.1 mmol), catalyst **B2** (10 mol % related to **1**), and Cs_2CO_3 (3 equiv). Then the respective allenoate **3** (2 equiv) and toluene (0.05 M with respect to **1**) were added and the mixture was stirred at room temperature for 24 h (Ar atmosphere). The crude product was passed through a short column of silicagel (rinsed with DCM and EtOAc), concentrated under reduced pressure, and subsequently purified by preparative TLC (silica gel, heptanes/EtOAc 4:1) to obtain the products **2** in the given yields and enantiopurities.

Details for the parent compound 5a (details for the other targets can be found in Supporting Information File 1). Obtained as a colorless oil in 61% yield (81:19 er) on 0.1 mmol scale. $[\alpha]_D^{22} = -11.4$ (*c* 1.1, $CHCl_3$); ^{1}H NMR (300 MHz, $CDCl_3$, 298.0 K) δ/ppm = 7.85 (dd, *J* = 8.6, 1.4 Hz, 2H), 7.54 (t, *J* = 7.4 Hz, 1H), 7.43 (t, *J* = 7.53 Hz, 2H), 7.24–7.11 (m, 5H), 5.79 (s, 1H), 5.37 (s, 1H), 4.14–3.90 (m, 2H), 3.52–3.16 (m, 4H), 1.15 (t, *J* = 7.1 Hz, 3H); ^{13}C NMR (75 MHz, $CDCl_3$, 298.0 K) δ/ppm = 177.4, 171.0, 160.3, 139.1, 133.8, 132.6, 130.5, 128.6, 128.0, 127.8, 127.3, 125.6, 118.1, 75.9, 60.9, 44.9, 39.3, 13.9; IR (neat): 3080, 3070, 2917, 1815, 1732, 1656, 1480, 1175, 1093, 1059, 1030, 974, 893, 694 cm^{-1}; HRESIMS *m*/*z*: $[C_{22}H_{21}NO_4 + H]^+$ calcd for 364.1543; found, 364.1554; HPLC: (Chiralpak SA, eluent: *n*-hexane/iPrOH = 100:2, 0.5 mL·min^{-1}, 20 °C, λ = 254 nm) retention times: t_{major} = 16.15 min, t_{minor} = 17.00 min.

Supporting Information

Supporting Information File 1

Full experimental and analytical details and copies of NMR spectra and HPLC traces.
[https://www.beilstein-journals.org/bjoc/content/supplementary/1860-5397-20-134-S1.pdf]

Acknowledgements

We are grateful to Prof. Dr. Himmelsbach (Institute of Analytical Chemistry, JKU Linz) for support with HRMS analysis.

Funding

The used NMR spectrometers were acquired in collaboration with the University of South Bohemia (CZ) with financial support from the European Union through the EFRE INTERREG IV ETC-AT-CZ program (project M00146, "RERI-uasb").

ORCID® iDs

Paul Zebrowski - https://orcid.org/0000-0002-6154-7160
David Naderer - https://orcid.org/0009-0001-1378-4495
Mario Waser - https://orcid.org/0000-0002-8421-8642

Data Availability Statement

All data that supports the findings of this study is available in the published article and/or the supporting information to this article.

Preprint

A non-peer-reviewed version of this article has been previously published as a preprint: https://doi.org/10.3762/bxiv.2024.28.v1

References

1. Hughes, A., Ed. *Amino Acids, Peptides and Proteins in Organic Chemistry;* Wiley-VCH: Weinheim, Germany, 2009; Vol. 1–5. doi:10.1002/9783527631766
2. Soloshonok, V. A.; Izawa, K., Eds. *Asymmetric Synthesis and Application of α-Amino Acids;* American Chemical Society: Washington, DC, USA, 2009.
3. O'Donnell, M. J., Ed. *α-Amino Acid Synthesis;* Tetrahedron Symposia-in-Print, No. 33; Pergamon: Oxford, UK, 1988.
4. Nájera, C.; Sansano, J. M. *Chem. Rev.* **2007,** *107,* 4584–4671. doi:10.1021/cr050580o
5. Metz, A. E.; Kozlowski, M. C. *J. Org. Chem.* **2015,** *80,* 1–7. doi:10.1021/jo502408z
6. Vogt, H.; Bräse, S. *Org. Biomol. Chem.* **2007,** *5,* 406–430. doi:10.1039/b611091f
7. Cativiela, C.; Ordonez, M. *Tetrahedron: Asymmetry* **2009,** *20,* 1–63. doi:10.1016/j.tetasy.2009.01.002
8. Juaristi, E.; López-Ruiz, H. *Curr. Med. Chem.* **1999,** *6,* 983–1004. doi:10.2174/092986730610220401161510
9. Abele, S.; Seebach, D. *Eur. J. Org. Chem.* **2000,** 1–15. doi:10.1002/(sici)1099-0690(200001)2000:1<1::aid-ejoc1>3.0.co;2-6
10. Juaristi, E.; Soloshonok, V. A., Eds. *Enantioselective Synthesis of b-Amino Acids,* 2nd ed.; John Wiley & Sons: Hoboken, NJ, USA, 2005. doi:10.1002/0471698482
11. Weiner, B.; Szymański, W.; Janssen, D. B.; Minnaard, A. J.; Feringa, B. L. *Chem. Soc. Rev.* **2010,** *39,* 1656. doi:10.1039/b919599h
12. Ashfaq, M.; Tabassum, R.; Ahmad, M. M.; Hassan, N. A.; Oku, H.; Rivera, G. *Med. Chem.* **2015,** *5,* 295.
13. Noda, H.; Shibasaki, M. *Eur. J. Org. Chem.* **2020,** 2350–2361. doi:10.1002/ejoc.201901596
14. Tiffner, M.; Novacek, J.; Busillo, A.; Gratzer, K.; Massa, A.; Waser, M. *RSC Adv.* **2015,** *5,* 78941–78949. doi:10.1039/c5ra14466c
15. Eitzinger, A.; Winter, M.; Schörgenhumer, J.; Waser, M. *Chem. Commun.* **2020,** *56,* 579–582. doi:10.1039/c9cc09239k
16. Zebrowski, P.; Eder, I.; Eitzinger, A.; Mallojjala, S. C.; Waser, M. *ACS Org. Inorg. Au* **2022,** *2,* 34–43. doi:10.1021/acsorginorgau.1c00025
17. Haider, V.; Zebrowski, P.; Michalke, J.; Monkowius, U.; Waser, M. *Org. Biomol. Chem.* **2022,** *20,* 824–830. doi:10.1039/d1ob02235k
18. Zebrowski, P.; Röser, K.; Chrenko, D.; Pospíšil, J.; Waser, M. *Synthesis* **2023,** *55,* 1706–1713. doi:10.1055/a-1948-5493
19. Stockhammer, L.; Craik, R.; Monkowius, U.; Cordes, D. B.; Smith, A. D.; Waser, M. *ChemistryEurope* **2023,** *1,* e202300015. doi:10.1002/ceur.202300015
20. Alba, A.-N. R.; Rios, R. *Chem. – Asian J.* **2011,** *6,* 720–734. doi:10.1002/asia.201000636
21. de Castro, P. P.; Carpanez, A. G.; Amarante, G. W. *Chem. – Eur. J.* **2016,** *22,* 10294–10318. doi:10.1002/chem.201600071
22. Marra, I. F. S.; de Castro, P. P.; Amarante, G. W. *Eur. J. Org. Chem.* **2019,** 5830–5855. doi:10.1002/ejoc.201901076
23. Lu, X.; Zhang, C.; Xu, Z. *Acc. Chem. Res.* **2001,** *34,* 535–544. doi:10.1021/ar000253x
24. Cowen, B. J.; Miller, S. J. *Chem. Soc. Rev.* **2009,** *38,* 3102. doi:10.1039/b816700c
25. Yu, S.; Ma, S. *Angew. Chem., Int. Ed.* **2012,** *51,* 3074–3112. doi:10.1002/anie.201101460
26. Fan, Y. C.; Kwon, O. *Chem. Commun.* **2013,** *49,* 11588. doi:10.1039/c3cc47368f

27. Wang, Z.; Xu, X.; Kwon, O. *Chem. Soc. Rev.* **2014,** *43,* 2927–2940. doi:10.1039/c4cs00054d
28. Wang, T.; Yu, Z.; Hoon, D. L.; Phee, C. Y.; Lan, Y.; Lu, Y. *J. Am. Chem. Soc.* **2016,** *138,* 265–271. doi:10.1021/jacs.5b10524
29. Elsner, P.; Bernardi, L.; Salla, G. D.; Overgaard, J.; Jørgensen, K. A. *J. Am. Chem. Soc.* **2008,** *130,* 4897–4905. doi:10.1021/ja710689c
30. Uraguchi, D.; Kawai, Y.; Sasaki, H.; Yamada, K.; Ooi, T. *Chem. Lett.* **2018,** *47,* 594–597. doi:10.1246/cl.180031
31. Shu, L.; Wang, P.; Gu, C.; Liu, W.; Alabanza, L. M.; Zhang, Y. *Org. Process Res. Dev.* **2013,** *17,* 651–657. doi:10.1021/op300306c
32. Jin, N.; Misaki, T.; Sugimura, T. *Chem. Lett.* **2013,** *42,* 894–896. doi:10.1246/cl.130295
33. Vaishanv, N. K.; Zaheer, M. K.; Kant, R.; Mohanan, K. *Eur. J. Org. Chem.* **2019,** 6138–6142. doi:10.1002/ejoc.201901199
34. Liu, Y.-L.; Wang, X.-P.; Wei, J.; Li, Y. *Tetrahedron* **2022,** *103,* 132577. doi:10.1016/j.tet.2021.132577
35. Shirakawa, S.; Maruoka, K. *Angew. Chem., Int. Ed.* **2013,** *52,* 4312–4348. doi:10.1002/anie.201206835
36. Qian, D.; Sun, J. *Chem. – Eur. J.* **2019,** *25,* 3740–3751. doi:10.1002/chem.201803752
37. Albanese, D. C. M.; Penso, M. *Eur. J. Org. Chem.* **2023,** *26,* 10.1002/ejoc.202300224. doi:10.1002/ejoc.202300224
38. Otevrel, J.; Waser, M. Asymmetric Phase-Transfer Catalysis- From Classical Applications to New Concepts. In *Asymmetric Organocatalysis: New Strategies, Catalysts, and Opportunities;* Albrecht, L.; Albrecht, A.; Dell'Amico, L., Eds.; Wiley-VCH: Weinheim, Germany, 2023; pp 71–120. doi:10.1002/9783527832217.ch3
39. Lee, H.-J.; Maruoka, K. *Chem. Rec.* **2023,** *23,* e202200286. doi:10.1002/tcr.202200286
40. Xu, C.; Qi, Y.; Yang, X.; Li, X.; Li, Z.; Bai, L. *Org. Lett.* **2021,** *23,* 2890–2894. doi:10.1021/acs.orglett.1c00535
41. Xu, C.; Yang, X. *Synlett* **2022,** *33,* 664–668. doi:10.1055/a-1795-7740
42. Macovei, C.; Vicennati, P.; Quinton, J.; Nevers, M.-C.; Volland, H.; Créminon, C.; Taran, F. *Chem. Commun.* **2012,** *48,* 4411. doi:10.1039/c2cc31312j
43. de Mello, A. C.; Momo, P. B.; Burtoloso, A. C. B.; Amarante, G. W. *J. Org. Chem.* **2018,** *83,* 11399–11406. doi:10.1021/acs.joc.8b01683
44. Žabka, M.; Kocian, A.; Bilka, S.; Andrejčák, S.; Šebesta, R. *Eur. J. Org. Chem.* **2019,** 6077–6087. doi:10.1002/ejoc.201901052

License and Terms

BEILSTEIN JOURNAL OF ORGANIC CHEMISTRY

Primary amine-catalyzed enantioselective 1,4-Michael addition reaction of pyrazolin-5-ones to α,β-unsaturated ketones

Pooja Goyal[1,2], Akhil K. Dubey[1], Raghunath Chowdhury[*1,2,§] and Amey Wadawale[3]

Full Research Paper

Open Access

Address:
[1]Bio-Organic Division, Bhabha Atomic Research Centre, Trombay, Mumbai 400085, India, [2]Homi Bhabha National Institute, Anushaktinagar, Mumbai 400094, India and [3]Chemistry Division, Bhabha Atomic Research Centre, Trombay, Mumbai 400085, India

Email:
Raghunath Chowdhury[*] - raghuc@barc.gov.in

* Corresponding author
§ Fax: +91-22-25505151

Keywords:
α,β-unsaturated ketones; iminium catalysis; organocatalysis; pyrazoles

Beilstein J. Org. Chem. **2024,** *20,* 1518–1526.
https://doi.org/10.3762/bjoc.20.136

Received: 09 April 2024
Accepted: 24 June 2024
Published: 09 July 2024

This article is part of the thematic issue "New advances in asymmetric organocatalysis II".

Guest Editor: R. Šebesta

Abstract

The enantioselective 1,4-addition reaction of pyrazolin-5-ones to α,β-unsaturated ketones catalyzed by a cinchona alkaloid-derived primary amine–Brønsted acid composite is reported. Both enantiomers of the anticipated pyrazole derivatives were obtained in good to excellent yields (up to 97%) and high enantioselectivities (up to 98.5% ee) under mild reaction conditions. In addition, this protocol was further expanded to synthesize highly enantioenriched hybrid molecules bearing biologically relevant heterocycles.

Introduction

N-Heterocycles are attractive molecules owing to their extensive applications in small-molecule drugs, natural products, and agrochemical products [1-3]. Among the *N*-heterocycles, pyrazole is an important structural scaffold, found in several marketed drugs and bioactive molecules (Figure 1) [4-7]. In addition, this moiety is an integral part of various agrochemical products and chelating agents [4-9]. Given the importance and widespread applications of pyrazoles, considerable efforts have been devoted to develop new protocols to access structurally diverse pyrazole derivatives [4-7,10-12].

4-Unsubstituted pyrazolin-5-ones are well known precursors for the construction of optically active structurally diverse pyrazoles [10-12]. In this context, the organocatalyzed asymmetric Michael addition of 4-unsubstituted pyrazolin-5-ones to a variety of Michael acceptors has emerged as one of the most powerful strategies to access enantioenriched pyrazole derivatives [10-21]. In the majority of these cases, the reactivities of the pyrazolin-5-one derivatives were harnessed under non-covalent catalysis via bifunctional hydrogen-bonding organocatalysts. The C-4 nucleophilicity of pyrazolin-5-ones was also

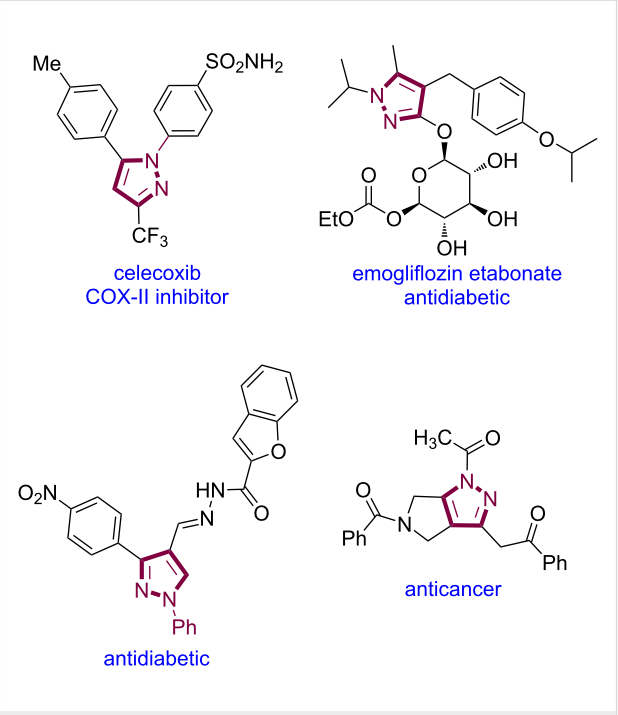

Figure 1: Selected examples of drugs and bioactive molecules bearing a pyrazole core.

explored in enantioselective reactions with α,β-unsaturated carbonyl compounds through covalent catalysis with chiral amine-based catalysts; however, it has achieved limited success [10-21].

Among the developed organocatalyzed enantioselective 1,4-addition reactions of pyrazolin-5-ones, the catalytic asymmetric reactions of pyrazolin-5-ones with α,β-unsaturated ketones are comparatively less studied. In 2009, Zhao's group were the first who reported a chiral amine-catalysed aza-Michael addition reaction of pyrazolin-5-ones with α,β-unsaturated ketones to access β-(3-hydroxypyrazol-1-yl)ketones (Scheme 1a) [22]. The developed reaction was restricted to α,β-unsaturated ketones with aliphatic substituents (Scheme 1a) [22]. Ji and Wang disclosed organocatalyzed [5 + 1] double Michael additions between pyrazolones and dienones (Scheme 1b) [23]. Very recently, the Chimni group reported a cinchona-derived squaramide-catalyzed 1,4-Michael addition reaction of pyrazolin-5-ones with 2-enoylpyridines (Scheme 1c) [24]. Recently, we developed an organocatalyzed asymmetric Michael addition reaction of 4-monosubstituted pyrazol-5-ones to simple enones for the synthesis of pyrazolone derivatives [25]. Despite these progresses, arylidene/heteroarylideneacetones have remained untapped by 4-unsubstituted pyrazolin-5-ones under asymmetric organocatalytic or metal catalytic conditions. In continuation of our work in the field of organocatalysis [26-29], herein, we present the Michael addition reaction of 4-unsubstituted pyrazolin-5-ones with arylidene/heteroarylideneacetones using cinchona alkaloid-derived primary amine catalysts. The developed protocol delivered both enantiomers of the desired products in good to excellent yields and enantioselectivities.

Results and Discussion

At the outset, the reaction between commercially available benzylideneacetone (**1a**) and 3-methyl-1-phenyl-2-pyrazolin-5-one (**2a**) was studied in the presence of a panel of primary amine catalysts (see Table S1 in Supporting Information File 1) in toluene at room temperature (30–32 °C). When the test reaction was conducted in the presence of 15 mol % of 9-amino-9-deoxy-epicinchonidine (**I**) as catalyst [30] for 12 h and treated with Ac_2O followed by DABCO, the reaction gave the conjugate addition product **3aa** in 58–62% yield with 74% ee (Table 1, entry 1). On the other hand, 9-amino-9-deoxyepicinchonine (**II**) [30] furnished the opposite enantiomer *ent*-**3aa** in 62% yield and 66% ee (Table 1, entry 2). Among the screened organocatalysts (see Table S1 in Supporting Information File 1), the catalyst **I** imparted the highest enantioselectivity (74% ee) of the Michael product **3aa** (Table 1, entry 1). Different solvents (see details in Supporting Information File 1) were screened for the test reaction using 15 mol % of catalyst **I**. Among them, $CHCl_3$ turned out to be the optimal solvent, as the product **3aa** was isolated in reproducible yield (77%) and enantioselectivity 74% ee (Table 1, entry 3). Next, we explored a variety of achiral and/or chiral Brønsted acids **A1**–**6** as additives in order to increase the yield and the enantioselectivity of the reaction (Table 1, entries 4–9). A marked increase in both the yield and enantioselectivity of the product **3aa** were observed. Among the screened Brønsted acids **A1**–**6**, the combination of 15 mol % of the catalyst **I** and 30 mol % of (±)-mandelic acid (**A5**) was found to be superior in terms of enantioselectivity (92% ee) of the product **3aa** (Table 1, entry 8). When the catalyst loading was lowered (10 mol % of **I**/20 mol % of **A5**), the desired product **3aa** was obtained in 71% yield and 91% ee (Table 1, entry 10). Lowering the temperature (−20 °C) of the reaction improved the enantioselectivity of the product **3aa** slightly but decreased its yield (Table 1, entry 11). Subsequently, the effect of concentration on the reaction outcome was also studied. In dilute conditions, both the yield and enantioselectivity of the product **3aa** were improved to 80% and 94%, respectively, at room temperature (Table 1, entry 12).

Taking into account the results of the optimization studies mentioned above, the catalytic system **I** (15 mol %)/**A5** (30 mol %) in $CHCl_3$ (1 mL) at room temperature (30–32 °C) was selected as the optimum reaction conditions (Table 1, entry 12). Under identical optimized reaction conditions, the catalytic system **II** (15 mol %)/**A5** (30 mol %) furnished *ent*-**3aa** in 76% yield and 87.5% ee (Table 1, entry 13).

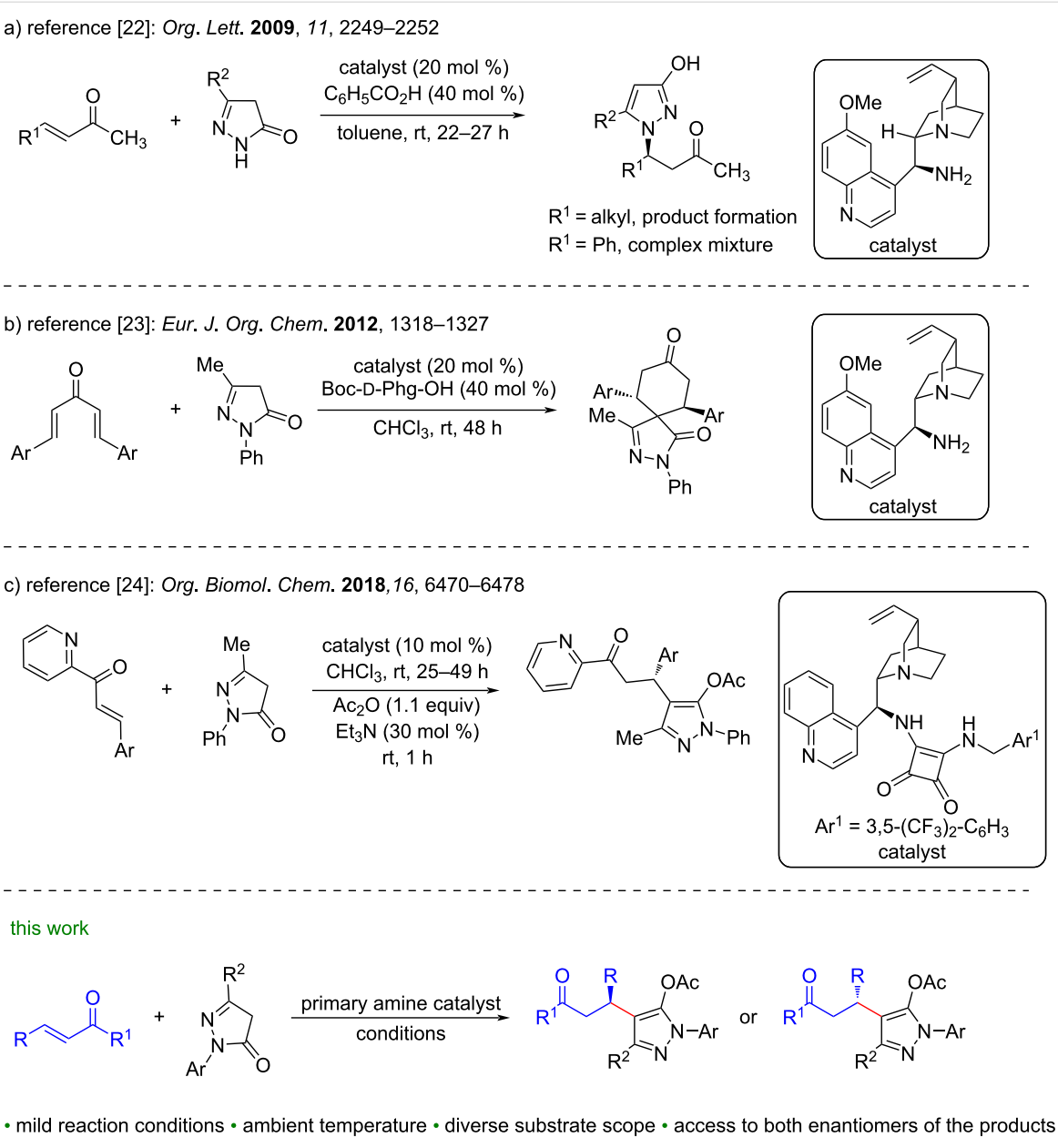

Scheme 1: Representative examples of asymmetric organocatalytic conjugate addition of pyrazolin-5-ones to α,β-unsaturated ketones and present study.

With the optimal reaction conditions at hands, the 1,4-conjugate addition reaction of a series of α,β-unsaturated ketones **1** with pyrazolin-5-one (**2a**) were studied next (Scheme 2). Aryl α,β-unsaturated ketones bearing a halogen, electron-withdrawing, or electron-donating group at the *para*-position of the benzene ring were compatible and led to the corresponding products **3ba**–**fa** in good to excellent yields (72–97%) and enantioselectivities (90–95% ee). The α,β-unsaturated ketone **1f** with a strong electron-withdrawing group (cyano) in the *para*-position of the benzene ring, was found to be more reactive as the reaction was completed within 4 h and the desired Michael adduct **3fa** was isolated in 89% yield and 92% ee. Notably, the α,β-unsaturated ketone with a substituent in the *meta*-position of the benzene ring was also tolerated and the desired product **3ga** was isolated in good yield (82%) and excellent enantioselectivity (95% ee). To our delight, the α,β-unsaturated ketone with a substituent in the *ortho*-position of the benzene ring, led to the product **3ha** in good yield (76.5%) and highest enantioselectivity (98.5% ee). Moreover, 1-naphthyl-substituted and 2-thienyl-substituted α,β-unsaturated ketones also took part in the reaction and the desired products (**3ia** and **3ja**) were isolated in good yields (77.5% and 80%, respectively) and enantioselectiv-

Table 1: Optimization of reaction conditions.[a]

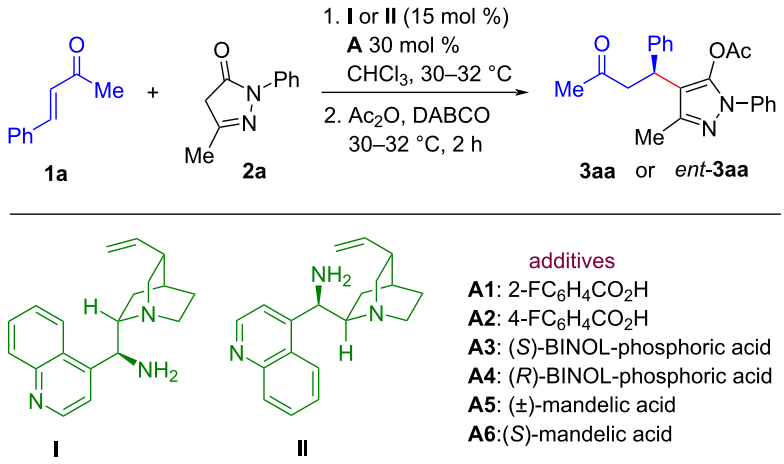

Entry	Cat.	Additive	Yield (%)[b]	ee (%)[c]
1	**I**	–	58[d]	74
2	**II**	–	62	–66
3	**I**	–	77	74
4	**I**	**A1**	80	90
5	**I**	**A2**	76	88.5
6	**I**	**A3**	86	83
7	**I**	**A4**	83	87
8	**I**	**A5**	77	92
9	**I**	**A6**	77	90
10[e]	**I**	**A5**	71	91
11[f]	**I**	**A5**	58	94
12[g]	**I**	**A5**	80	94
13[g]	**II**	**A5**	76	–87.5

[a]Reaction conditions: **1a** (0.3 mmol), **2a** (0.2 mmol), 15 mol % of catalyst **I** or **II** in 0.5 mL toluene (entries 1 and 2) or catalyst **I** (15 mol %) and 30 mol % **A** in 0.5 mL $CHCl_3$ (entries 3–9) for 12–14 h. Next, Ac_2O (0.52 mmol, 50 µL) was added followed by DABCO (0.1 mmol, 11 mg) and the reaction mixture was further stirred for 2 h at 30–32 °C. [b]Isolated yield of **3aa** or *ent*-**3aa** after column chromatography. [c]Enantiomeric excess (ee) was measured by HPLC analysis using a chiralcel OD-H column. [d]The yield of the reaction product varied from 58–62%. [e]The reaction was performed in the presence of 10 mol % **I** and 20 mol % **A5**. [f]The reaction was performed at –20 °C using 15 mol % of catalyst **I** in combination with 30 mol % **A5** in 0.5 mL $CHCl_3$ for 24 h. [g]The reaction was carried out using 15 mol % of catalyst **I** or **II** in combination with 30 mol % **A5** in 1.0 mL $CHCl_3$ for 14 h at 30–32 °C. Next, Ac_2O (0.52 mmol, 50 µL) was added followed by DABCO (0.1 mmol, 11 mg) and the reaction mixture was further stirred for 2 h at 30–32 °C.

ities (92% ee and 90% ee, respectively). Interestingly, the reaction also worked well with (*E*)-1-phenylpent-1-en-3-one (**1k**) as α,β-unsaturated ketone. The corresponding product, **3ka** was obtained in 91% yield and 95% ee. Moreover, ethyl (*E*)-5-oxohex-2-enoate (**1l**) also showed good reactivity and the expected product (−)-**3la** was isolated in 68% yield and 95% ee.

Next, we explored the scope of pyrazolin-5-ones **2** (Scheme 2, lower part) with diverse substituents (Br, Cl, F, Me or CN) in the *para*-position of the *N*-aryl group. These substrates reacted smoothly with α,β-unsaturated ketone **1c** and the corresponding products **3cb**–**cf** were obtained in good yields (61–85.5%) and good to excellent enantioselectivities (84.5–95% ee). In addition, pyrazolone **2g** with a substituent in the *meta*-position of the *N*-aryl group also participated in the reaction and the desired product **3cg** was isolated in 87% yield and 95% ee. Notably, a phenyl substituent at the C3 position of pyrazolone **2h** was found to be compatible, and the desired product **3ch** was obtained in 87% yield and 90% ee.

In general, enantiomers of a bioactive molecule have different biological activities. Therefore, there is a huge demand to develop methods to access both enantiomers of a chiral compound. We turned our attention to the synthesis of enantiomeric products *ent*-**3**. Under identical optimized reaction conditions

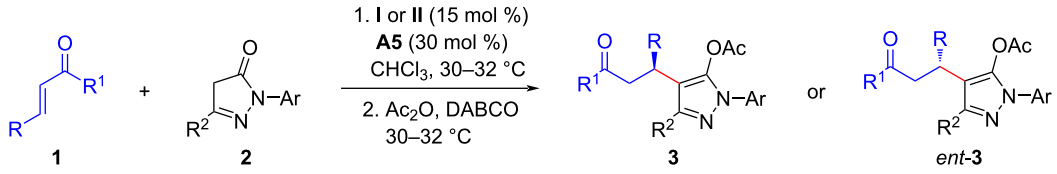

1 2 3 *ent*-3

scope of α,β-unsaturated ketones

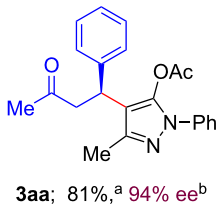

3aa; 81%,[a] 94% ee[b]
ent-**3aa**, 77%,[a] 87.5% ee[b]

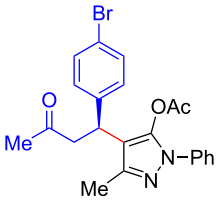

3ba; 85%,[a] 92% ee[b] (99% ee)[c]
ent-**3ba**; 85%,[a] 85% ee[b](98% ee)[c]

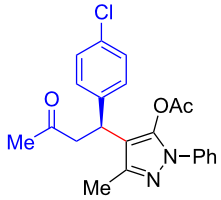

3ca; 97%,[a] 94% ee,[b] (97% ee)[c]
ent-**3ca**; 97%,[a] 90% ee,[b] (97% ee)[c]

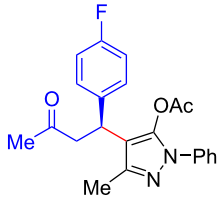

3da; 72%,[a] 95% ee[b]
ent-**3da**; 77.5%,[a] 93% ee[b]

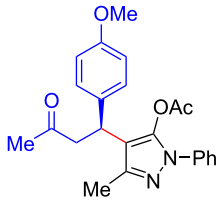

3ea; 86%,[a] 90% ee[b]

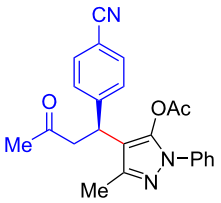

3fa[d]; 89%,[a] 92% ee[b]
ent-**3fa**[d]; 82.5%,[a] 91.5% ee[b]

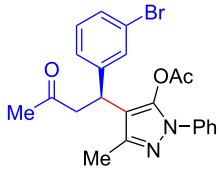

3ga, 82%,[a] ≈95% ee[b]
ent-**3ga**, 79%,[a] 94% ee[b]

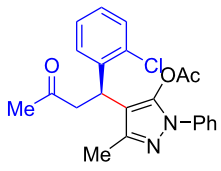

3ha, 76.5%,[a] 98.5% ee[b]
ent-**3ha**, 73%,[a]98% ee[b]

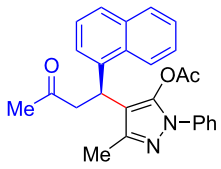

3ia, 77.5%[a], 92% ee[b] (98% ee)[c]
ent-**3ia,** 71.5%,[a] 90% ee,[b] (98% ee)[c]

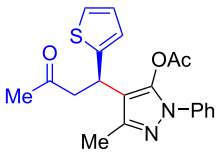

3ja, 80%,[a] 90% ee[b]
ent-**3ja**,73%,[a] 83.5% ee[b]

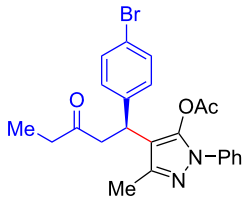

3ka, 91%,[a] 95% ee[b] (>99% ee)[c]
ent-**3ka**, 91%,[a] 90% ee[b] (96% ee)[c]

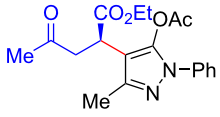

(–)-**3la**, 68%,[a] 95% ee[b]
(+)-*ent*-**3la,** 71,[a] 90% ee[b]

scope of pyrazolin-5-ones

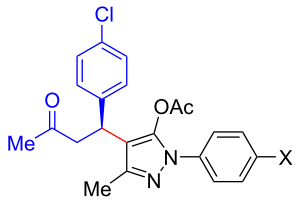

3cb; X = Br, 77.5%,[a] ≈95% ee[b]
ent-**3cb**; 79.5%,[a] 87.5% ee,[b] (95.5% ee)[c]

3cc; X = Cl, 85.5%,[a] 94% ee[b] (98% ee)[c]
ent-**3cc**; 81%,[a] 88% ee[b] (95% ee)[c]

3cd; X = F, 80.5%,[a] 93% ee[b]
ent-**3cd**; 78%,[a] 89% ee[b]

3ce; X = Me, 78%,[a] 89.5% ee[b]
ent-**3ce**; 84%,[a] 84.5% ee[b]

3cf; X = CN, 61.5%,[a] 95% ee[b]

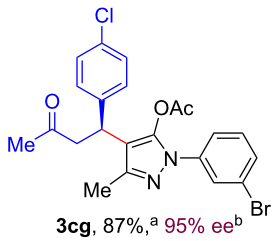

3cg, 87%,[a] 95% ee[b]
ent-**3cg**, 87%,[a] 85% ee[b]

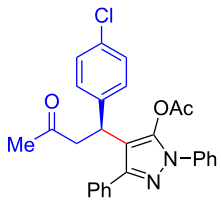

3ch, 87%,[a] 90% ee[b]

Scheme 2: Scope of substrates. Reaction conditions: **1** (0.3 mmol), **2** (0.2 mmol), 15 mol % of catalyst **I**, 30 mol % **A5 (**for **3**) or 15 mol % catalyst **II**, 30 mol % **A5** (for *ent*-**3**) in 1.0 mL $CHCl_3$ for 4–14 h. Next, Ac_2O (0.52 mmol, 50 µL) was added followed by DABCO (0.1 mmol, 11 mg) and the reaction mixture was further stirred for 2 h at 30–32 °C. [a]Isolated yield of **3** or *ent*-**3** after column chromatography. [b]Enantiomeric excess (ee) was measured by HPLC analysis using a stationary phase chiral column. [c]Values in parentheses represent % ee after single recrystallization. [d]Reaction time for the first step was 4 h.

(Table 1, entry 12), a panel of aryl/heteroaryl α,β-unsaturated ketones **1** and pyrazolin-5-ones **2** were studied (Scheme 2) using the catalytic system **II** (15 mol %)/**A5** (30 mol %). To our delight, the enantiomeric products *ent*-**3aa**–*ent*-**3cg** (Scheme 2) were obtained in good to excellent yields (71–97%) and enantioselectivities (83.5–98% ee).

Molecules containing two or more biologically relevant heterocycle motifs are receiving attention in drug discovery research [31-33]. The enantioselective synthesis of such hybrid molecules is fascinating but at the same time challenging. Pyrazoles [4-7], benzofurans [34], and indoles [35,36] are popular scaffolds as they are prevalent in many bioactive molecules. Compounds bearing both pyrazole and indole moieties or pyrazole and benzofuran moieties (Figure 1) are highly attractive since such compounds might be endowed with potent biological activities.

Under the disclosed optimized reaction conditions, the reaction between pyrazolin-5-one (**2a**) and indole-derived α,β-unsaturated ketone **1m** was performed. The resulting hybrid molecule **3ma** was isolated in 96% yield and 90% ee (Scheme 3). On the other hand, the reaction of pyrazolin-5-one (**2a**) with benzofuran-derived α,β-unsaturated ketone **1n** delivered the product **3na** in 85.5% yield and 95.5% ee (Scheme 3). Moreover, by employing the catalytic composite **II** (15 mol %) and **A5** (30 mol %) under otherwise identical optimized reaction conditions, the corresponding enantiomeric products (*ent*-**3ma** and *ent*-**3na**) were obtained (Scheme 3) in good yields (91.5% and 85.5%, respectively) and enantioselectivities (84% ee and 91.5% ee, respectively).

The practical utility of the developed method was demonstrated by carrying out the synthesis of **3aa** on a 1 mmol scale under the optimized reaction conditions (Scheme 4). The product **3aa** was isolated in slightly lower yield and similar enantioselectivity compared to the 0.2 mmol scale reaction.

Subsequently, we turned our attention to determine the absolute configuration of the newly formed chiral center. Under the disclosed optimized conditions, the product *ent*-**3ba** was isolated as white solid with 85% ee and the enantiopurity of the prod-

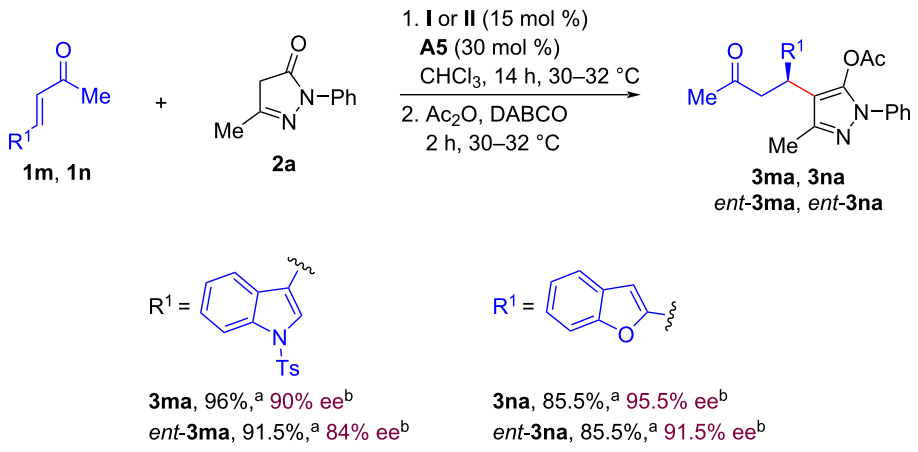

Scheme 3: Synthesis of pyrazole-benzofuran and pyrazole–indole hybrid molecules. Reaction conditions: **1m** or **1n** (0.3 mmol), **2a** (0.2 mmol), 15 mol % of catalyst **I**, 30 mol % **A5** (for **3**) or 15 mol % catalyst **II**, 30 mol % **A5** (for *ent*-**3**) in 1.0 mL $CHCl_3$ for 14 h. Next, Ac_2O (0.52 mmol, 50 µL) was added followed by DABCO (0.1 mmol, 11 mg) and the reaction mixture was further stirred for 2 h at 30–32 °C. [a]Isolated yield of **3** or *ent*-**3** after column chromatography. [b]Enantiomeric excess (ee) was measured by HPLC analysis using a stationary phase chiral column.

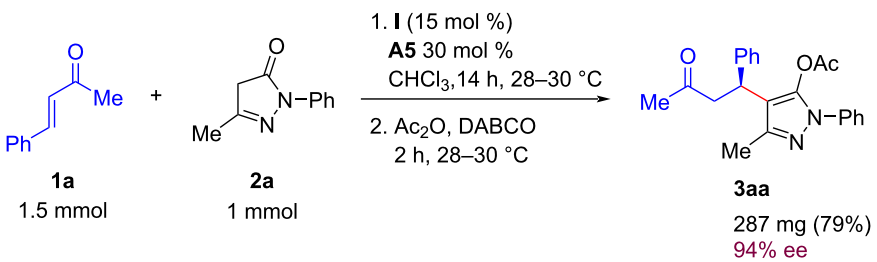

Scheme 4: Synthesis of **3aa** on preparative scale.

uct could be enriched to 98% ee by single recrystallization. The absolute stereochemistry was determined to be "*R*" on the basis of single-crystal X-ray crystallography data of *ent*-**3ba** (Figure 2) [37]. The stereochemistry of the products in this series was assigned by analogy.

Based on the observed absolute configuration of product *ent*-**3ba** and preceding literature reports [38,40], a plausible mechanistic pathway is outlined in Scheme 5. Initially, in the presence of one equivalent Brønsted acid additive **A5**, the catalyst **II** generates the monoprotonated diamine **II**-**A5**. The condensation of the primary amine moiety in **II**-**A5** with the carbonyl group of the α,β-unsaturated ketone **1b** in presence of the Brønsted acid leads to the formation of the iminium ion assembly **4** (Scheme 5). It is known that Brønsted acids facilitate the iminium ion formation step [38,39] and the counteranion of the acid plays an important role in the stereocontrolling event [38,40]. On the other hand, the protonated quinuclidine nitrogen atom of the catalyst **II** (in the iminium ion assembly) activates the pyrazol-5-one **2a** through hydrogen bonding and forms the corresponding enol. Simultaneously, the enol form of the pyrazol-5-one attacks the *Re*-face of the α,β-unsaturated ketone **1b** to provide the intermediate **5** (Scheme 5), which after hydrolysis leads to product *ent*-**3ba'**. In situ acetyla-

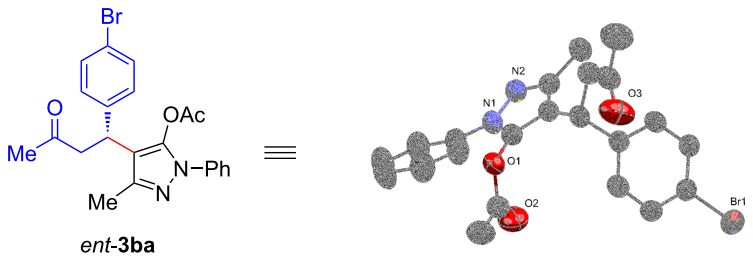

Figure 2: Single crystal X-ray structure of *ent*-**3ba** (CCDC 2234286).

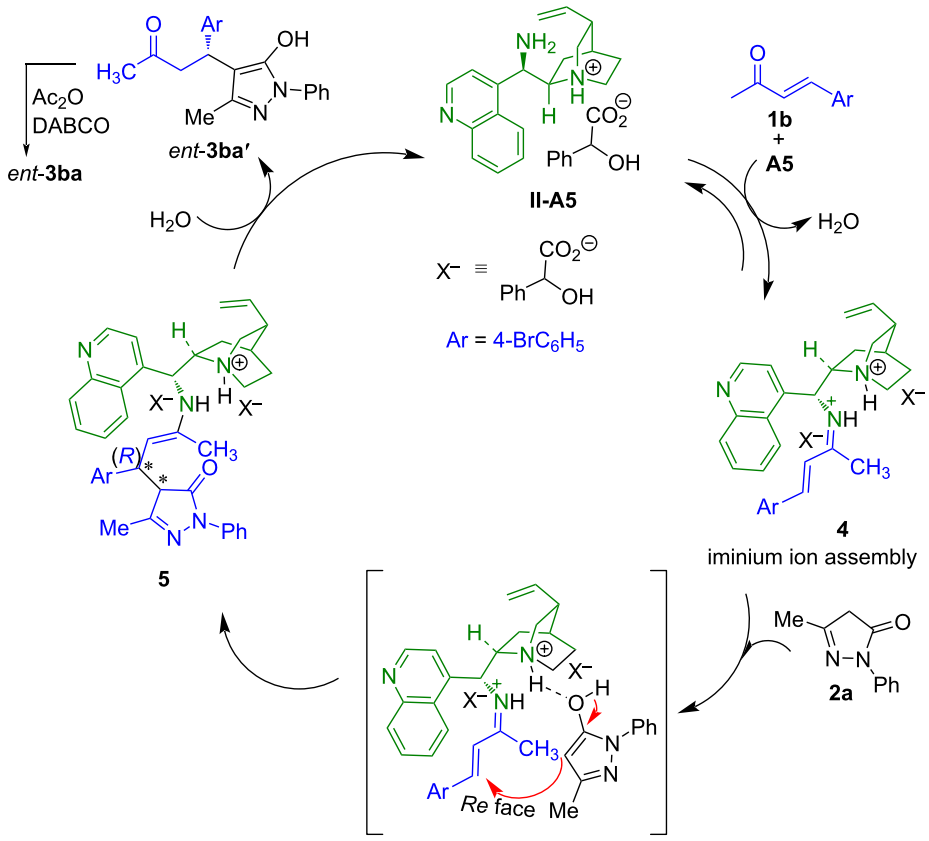

Scheme 5: Proposed reaction mechanism.

tion of the *ent*-**3ba'** using acetic anhydride and DABCO, furnishes the desired product *ent*-**3ba**.

Conclusion

In summary, we have realized the Michael addition reaction of 4-unsubstituted pyrazolin-5-ones to α,β-unsaturated ketones under organocatalytic conditions. The developed protocol was efficiently applied to diverse α,β-unsaturated ketones and a pool of pyrazolin-5-ones. The formed Michael adducts were isolated in good to excellent yields and enantioselectivities. The method also led to enantioenriched hybrid molecules bearing pyrazole–indole moieties and pyrazole–benzofuranone moieties. It is worth mentioning that the current protocol delivers both enantiomers of the Michael adducts.

Experimental

General procedure for the synthesis of **3** and *ent*-**3**.

In an oven-dried 4 mL glass vial fitted with a magnetic stirring bar, the mixture of catalyst **I** (15 mol %, ≈9.0 mg) and (±)-mandelic acid (30 mol %, 9.0 mg) or catalyst **II** (15 mol %, ≈9.0 mg) and (±)-mandelic acid (30 mol %) in $CHCl_3$ (1.0 mL) was stirred at room temperature (30–32 °C) for 5 min. Next, α,β-unsaturated ketone (0.3 mmol, 1.5 equiv) was added in one portion and the reaction mixture was further stirred for 5 min. Then, the pyrazolin-5-one **2** (0.2 mmol, 1.0 equiv) was added to the mixture and stirred for 4–14 h. Once the pyrazolin-5-one **2** was consumed (monitored by TLC), Ac_2O (50 µL, ≈0.52 mmol, 2.6 equiv) and DABCO (11 mg, 50 mol %) were sequentially added. The resulting reaction mixture was further stirred for 2 h at room temperature. The crude reaction mixture was purified by silica gel (230–400 mesh) column chromatography (petroleum ether/EtOAc as the eluent) to give the product **3** or *ent*-**3**.

Supporting Information

Supporting Information File 1

Additional optimization studies, characterization data of compounds **3aa**–**na** and *ent*-**3aa**-*ent*-**3na**, ^1H, ^{13}C NMR spectra of **3aa**–**na**, ^1H NMR of *ent*-**3aa**–*ent*-**3na** and their HPLC traces and single crystal data of *ent*-**3ba**.
[https://www.beilstein-journals.org/bjoc/content/supplementary/1860-5397-20-136-S1.pdf]

Acknowledgements

The authors are thankful to Ms. Ketki Lele for her help in some preliminary experiments.

Funding

The authors thank the Department of Atomic Energy (DAE), Government of India for financial support. P.G thanks the Bhabha Atomic Research Centre (BARC) for her research fellowship.

ORCID® iDs

Pooja Goyal - https://orcid.org/0009-0006-0701-2786
Raghunath Chowdhury - https://orcid.org/0000-0002-0395-7014

Data Availability Statement

All data that supports the findings of this study is available in the published article and/or the supporting information to this article.

References

1. Vitaku, E.; Smith, D. T.; Njardarson, J. T. *J. Med. Chem.* **2014,** *57,* 10257–10274. doi:10.1021/jm501100b
2. Rajput, A. P.; Kankhare, A. R. *Int. J. Pharm. Sci. Invent.* **2017,** *6,* 19.
3. Vinogradov, M. G.; Turova, O. V.; Zlotin, S. G. *Org. Biomol. Chem.* **2019,** *17,* 3670–3708. doi:10.1039/c8ob03034k
4. Schmidt, A.; Dreger, A. *Curr. Org. Chem.* **2011,** *15,* 1423–1463. doi:10.2174/138527211795378263
5. Fustero, S.; Sánchez-Roselló, M.; Barrio, P.; Simón-Fuentes, A. *Chem. Rev.* **2011,** *111,* 6984–7034. doi:10.1021/cr2000459
6. Kumar, V.; Kaur, K.; Gupta, G. K.; Sharma, A. K. *Eur. J. Med. Chem.* **2013,** *69,* 735–753. doi:10.1016/j.ejmech.2013.08.053
7. Neto, J. S. S.; Zeni, G. *Chem. – Eur. J.* **2020,** *26,* 8175–8189. doi:10.1002/chem.201905276
8. Stricker, L.; Fritz, E.-C.; Peterlechner, M.; Doltsinis, N. L.; Ravoo, B. J. *J. Am. Chem. Soc.* **2016,** *138,* 4547–4554. doi:10.1021/jacs.6b00484
9. Orrego-Hernández, J.; Cobo, J.; Portilla, J. *ACS Omega* **2019,** *4,* 16689–16700. doi:10.1021/acsomega.9b02796
10. Chauhan, P.; Mahajan, S.; Enders, D. *Chem. Commun.* **2015,** *51,* 12890–12907. doi:10.1039/c5cc04930j
11. Liu, S.; Bao, X.; Wang, B. *Chem. Commun.* **2018,** *54,* 11515–11529. doi:10.1039/c8cc06196c
12. Bao, X.; Wang, X.; Tian, J.-M.; Ye, X.; Wang, B.; Wang, H. *Org. Biomol. Chem.* **2022,** *20,* 2370–2386. doi:10.1039/d1ob02426d
13. Rao, K. S.; Ramesh, P.; Trivedi, R.; Kantam, M. L. *Tetrahedron Lett.* **2016,** *57,* 1227–1231. doi:10.1016/j.tetlet.2016.02.008
14. Kim, Y. H.; Yoon, J. H.; Lee, M. Y.; Kim, D. Y. *Bull. Korean Chem. Soc.* **2017,** *38,* 1242–1245. doi:10.1002/bkcs.11241
15. Phelan, J. P.; Ellman, J. A. *Adv. Synth. Catal.* **2016,** *358,* 1713–1718. doi:10.1002/adsc.201600110
16. Sharma, A.; Sharma, V.; Chimni, S. S. *Org. Biomol. Chem.* **2019,** *17,* 9514–9523. doi:10.1039/c9ob01700c
17. Yang, M.; Zhang, M.; Wang, Z.; Tang, L.; Chen, W.; Ban, S.; Li, Q. *Chirality* **2018,** *30,* 1096–1104. doi:10.1002/chir.23003
18. Aydin, A. E.; Culha, S. *Chirality* **2021,** *33,* 106–114. doi:10.1002/chir.23295
19. Sharma, V.; Kaur, J.; Chimni, S. S. *Eur. J. Org. Chem.* **2018,** 3489–3495. doi:10.1002/ejoc.201800589
20. Carceller-Ferrer, L.; Vila, C.; Blay, G.; Fernández, I.; Muñoz, M. C.; Pedro, J. R. *Org. Biomol. Chem.* **2019,** *17,* 9859–9863. doi:10.1039/c9ob02252j
21. Chowdhury, R.; Dubey, A. K.; Ghosh, S. K. *Asian J. Org. Chem.* **2021,** *10,* 1173–1183. doi:10.1002/ajoc.202100120

22. Gogoi, S.; Zhao, C.-G.; Ding, D. *Org. Lett.* **2009,** *11,* 2249–2252. doi:10.1021/ol900538q
23. Wu, B.; Chen, J.; Li, M.-Q.; Zhang, J.-X.; Xu, X.-P.; Ji, S.-J.; Wang, X.-W. *Eur. J. Org. Chem.* **2012,** 1318–1327. doi:10.1002/ejoc.201101529
24. Sharma, V.; Kaur, A.; Sahoo, S. C.; Chimni, S. S. *Org. Biomol. Chem.* **2018,** *16,* 6470–6478. doi:10.1039/c8ob01588k
25. Goyal, P.; Dubey, A. K.; Chowdhury, R. *Eur. J. Org. Chem.* **2024,** *27,* e202400002. doi:10.1002/ejoc.202400002
26. Chowdhury, R.; Kumar, M.; Ghosh, S. K. *Org. Biomol. Chem.* **2016,** *14,* 11250–11260. doi:10.1039/c6ob02104b
27. Vamisetti, G. B.; Chowdhury, R.; Ghosh, S. K. *Org. Biomol. Chem.* **2017,** *15,* 3869–3873. doi:10.1039/c7ob00796e
28. Chowdhury, R.; Dubey, A. K.; Ghosh, S. K. *Eur. J. Org. Chem.* **2020,** 2962–2972. doi:10.1002/ejoc.202000306
29. Dubey, A. K.; Chowdhury, R. *Beilstein J. Org. Chem.* **2021,** *17,* 2642–2649. doi:10.3762/bjoc.17.177
30. Vakulya, B.; Varga, S.; Csámpai, A.; Soós, T. *Org. Lett.* **2005,** *7,* 1967–1969. doi:10.1021/ol050431s
31. Shaveta; Mishra, S.; Singh, P. *Eur. J. Med. Chem.* **2016,** *124,* 500–536. doi:10.1016/j.ejmech.2016.08.039
32. Viegas-Junior, C.; Danuello, A.; da Silva Bolzani, V.; Barreiro, E. J.; Fraga, C. A. M. *Curr. Med. Chem.* **2007,** *14,* 1829–1852. doi:10.2174/092986707781058805
33. Fu, R.-g.; Sun, Y.; Sheng, W.-b.; Liao, D.-f. *Eur. J. Med. Chem.* **2017,** *136,* 195–211. doi:10.1016/j.ejmech.2017.05.016
34. Khanam, H.; Shamsuzzaman. *Eur. J. Med. Chem.* **2015,** *97,* 483–504. doi:10.1016/j.ejmech.2014.11.039
35. Wan, Y.; Li, Y.; Yan, C.; Yan, M.; Tang, Z. *Eur. J. Med. Chem.* **2019,** *183,* 111691. doi:10.1016/j.ejmech.2019.111691
36. Thanikachalam, P. V.; Maurya, R. K.; Garg, V.; Monga, V. *Eur. J. Med. Chem.* **2019,** *180,* 562–612. doi:10.1016/j.ejmech.2019.07.019
37. The crystallographic data (CCDC 2234286) for *ent*-**3ba**, can be obtained free of charge from the Cambridge crystallographic Data Centre via https://www.ccdc.cam.ac.uk/data_request/cif.
38. Melchiorre, P. *Angew. Chem., Int. Ed.* **2012,** *51,* 9748–9770. doi:10.1002/anie.201109036
39. Hine, J.; Via, F. A. *J. Org. Chem.* **1977,** *42,* 1972–1978. doi:10.1021/jo00431a031
40. Moran, A.; Hamilton, A.; Bo, C.; Melchiorre, P. *J. Am. Chem. Soc.* **2013,** *135,* 9091–9098. doi:10.1021/ja404784t

License and Terms

BEILSTEIN JOURNAL OF ORGANIC CHEMISTRY

Chiral bifunctional sulfide-catalyzed enantioselective bromolactonizations of α- and β-substituted 5-hexenoic acids

Sao Sumida, Ken Okuno, Taiki Mori, Yasuaki Furuya and Seiji Shirakawa*

Full Research Paper

Open Access

Address:
Institute of Integrated Science and Technology, Nagasaki University, 1-14 Bunkyo-machi, Nagasaki 852-8521, Japan

Email:
Seiji Shirakawa* - seijishirakawa@nagasaki-u.ac.jp

* Corresponding author

Keywords:
asymmetric catalysis; enantioselectivity; halogenation; lactones; organocatalysis

Beilstein J. Org. Chem. **2024,** *20,* 1794–1799.
https://doi.org/10.3762/bjoc.20.158

Received: 26 April 2024
Accepted: 16 July 2024
Published: 30 July 2024

This article is part of the thematic issue "New advances in asymmetric organocatalysis II".

Guest Editor: R. Šebesta

Abstract

Enantioselective halolactonizations of sterically less hindered alkenoic acid substrates without substituents on the carbon–carbon double bond have remained a formidable challenge. To address this limitation, we report herein the asymmetric bromolactonization of 5-hexenoic acid derivatives catalyzed by a BINOL-derived chiral bifunctional sulfide.

Introduction

Catalytic asymmetric halolactonizations of alkenoic acids are powerful methods for the preparation of important chiral lactones in enantioenriched forms [1-11]. A wide variety of chiral catalysts have been applied to asymmetric halolactonizations, especially for the synthesis of chiral γ-butyrolactones and δ-valerolactones via the reaction of 4-pentenoic acid and 5-hexenoic acid derivatives (Scheme 1). Notably, however, substituents on the carbon–carbon double bond of alkenoic acid substrates are generally required to achieve highly enantioselective halolactonizations (Scheme 1a) [1-22]. Enantioselective halolactonizations of sterically less hindered alkenoic acid substrates without substituents on the carbon–carbon double bond have remained a formidable challenge in the field of catalytic asymmetric synthesis (Scheme 1b) [23-25]. To address this limitation, we have investigated the use of BINOL-derived chiral bifunctional sulfide catalysts, which were developed by our group [10], in asymmetric bromolactonizations of α-substituted 4-pentenoic acids without additional substituents on the carbon–carbon double bond (Scheme 1c) [26,27]. Chiral α-substituted γ-butyrolactone products as important building blocks for pharmaceutical development were obtained in a highly enantioselective manner in our catalytic system using bifunctional sulfide (*S*)-**1** [26-31]. To further demonstrate the utility of our chiral bifunctional sulfide catalysts in challenging halolactonizations, we next turned our attention to the asymmetric bromolactonizations of 5-hexenoic acid derivatives **2** for

the synthesis of optically active δ-valerolactones **3** (Scheme 1d). Herein, we report our additional efforts to overcome limitations in catalytic asymmetric halolactonizations.

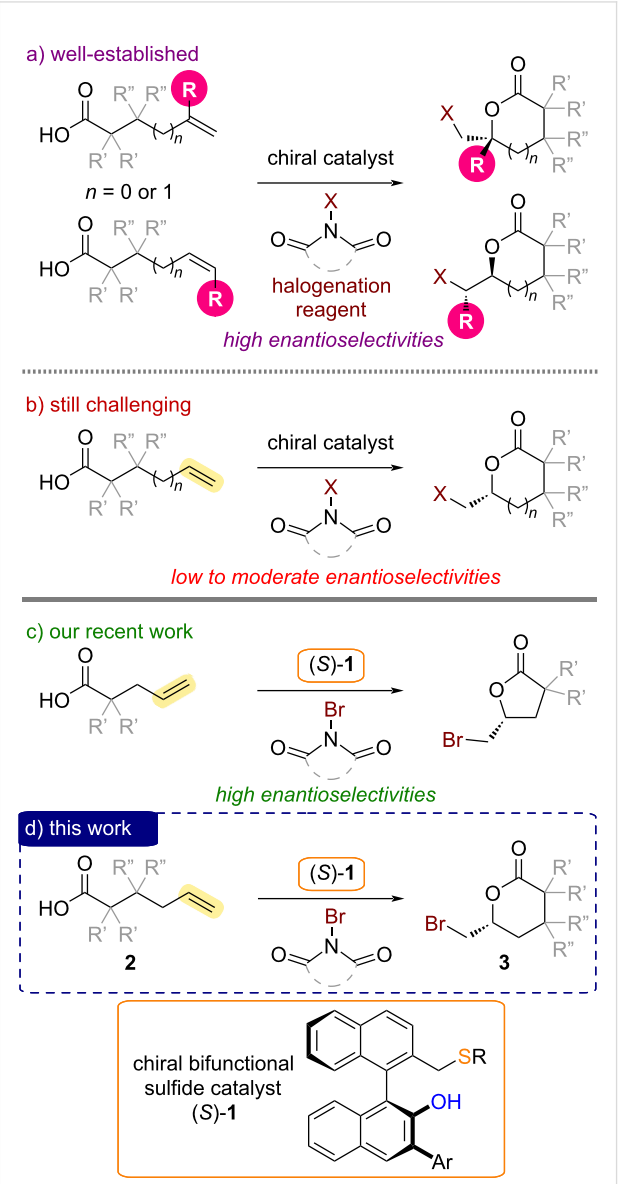

Scheme 1: Catalytic asymmetric halolactonizations of alkenoic acids.

Results and Discussion

α,α-Diphenyl-5-hexenoic acid (**2a**) was selected as a model substrate to evaluate the performance of our BINOL-derived chiral bifunctional sulfide catalysts in the asymmetric bromolactonization of 5-hexenoic acid derivatives without additional substituents on the carbon–carbon double bond (Scheme 2). The catalytic asymmetric bromolactonization of model substrate **2a** with *N*-bromophthalimide (NBP) was conducted at −78 °C for 24 hours using chiral bifunctional sulfide (*S*)-**1a** (10 mol %) bearing a hydroxy group. This reaction yielded the desired δ-valerolactone product **3a** with good yield and enantioselectivity [83% yield, 86:14 enantiomeric ratio (er)]. We further tested the reaction of **2a** with a hydroxy-protected sulfide catalyst (*S*)-**4** under the same conditions to evaluate the importance of the bifunctional design of the hydroxy-type chiral sulfide catalyst (*S*)-**1a**. As expected, the use of the hydroxy-protected catalyst (*S*)-**4** produced **3a** with significantly lower enantioselectivity (51:49 er). This outcome clearly underscores the crucial role of the bifunctional design in chiral sulfide catalysts (*S*)-**1** for enantioselective bromolactonizations of 5-hexenoic acid derivatives without additional substituents on the carbon–carbon double bond [26-31]. We also investigated the effects of other types of BINOL-derived chiral bifunctional sulfide catalysts. Asymmetric bromolactonizations of model substrate **2a** with amide- and urea-type chiral bifunctional sulfides (*S*)-**5** and **6**, known to be effective for other asymmetric halocyclizations [32-35], resulted in δ-valerolactone product **3a** with low enantioselectivities (50:50 and 56:44 er, respectively). These findings led us to further optimize the hydroxy-type chiral sulfide catalysts of type (*S*)-**1**. Substituting an alkyl group on sulfur of catalyst (*S*)-**1** with isobutyl and *tert*-butyl [(*S*)-**1b** and **1c**, respectively] decreased enantioselectivity compared with the *n*-butyl group-substituted catalyst [(*S*)-**1a**]. Next, the effects of aryl substituents at the 3-position of a binaphthyl unit on the hydroxy-type chiral sulfide catalysts [(*S*)-**1d**–**g**] were investigated. Fortunately, the attachments of 3,5-di-*tert*-butylphenyl and 3,5-diphenylphenyl groups [(*S*)-**1f** and **1g**, respectively] slightly improve the enantioselectivity (87:13 er).

We next examined the effects of brominating reagents in the asymmetric bromolactonization of **2a** under the influence of chiral bifunctional sulfide catalyst (*S*)-**1g** in dichloromethane (Scheme 3). Among the examined brominating reagents, NBP provided higher enantioselectivity for the bromolactonization product **3a**. It should be noted that the asymmetric reaction using bromine (Br_2) as a brominating reagent gave product **3a** in a racemic form. Additionally, iodolactonization of **2a** using *N*-iodosuccinimide in the presence of catalyst (*S*)-**1g** was performed. The reaction in dichloromethane, however, provided the corresponding iodolactonization product in racemic form with a good yield (80% yield, 50:50 er) [36].

To improve the enantioselectivity in the asymmetric bromolactonization of **2a** using NBP and catalyst (*S*)-**1g**, the optimization of reaction solvents was also performed. Based on our recent studies of chiral bifunctional sulfide-catalyzed bromolactonizations [26-31], mixed solvent systems were investigated. Among the examined solvent systems, a dichloromethane/toluene mixed solvent (3:1 ration) showed the best enantioselectivity (89:11 er).

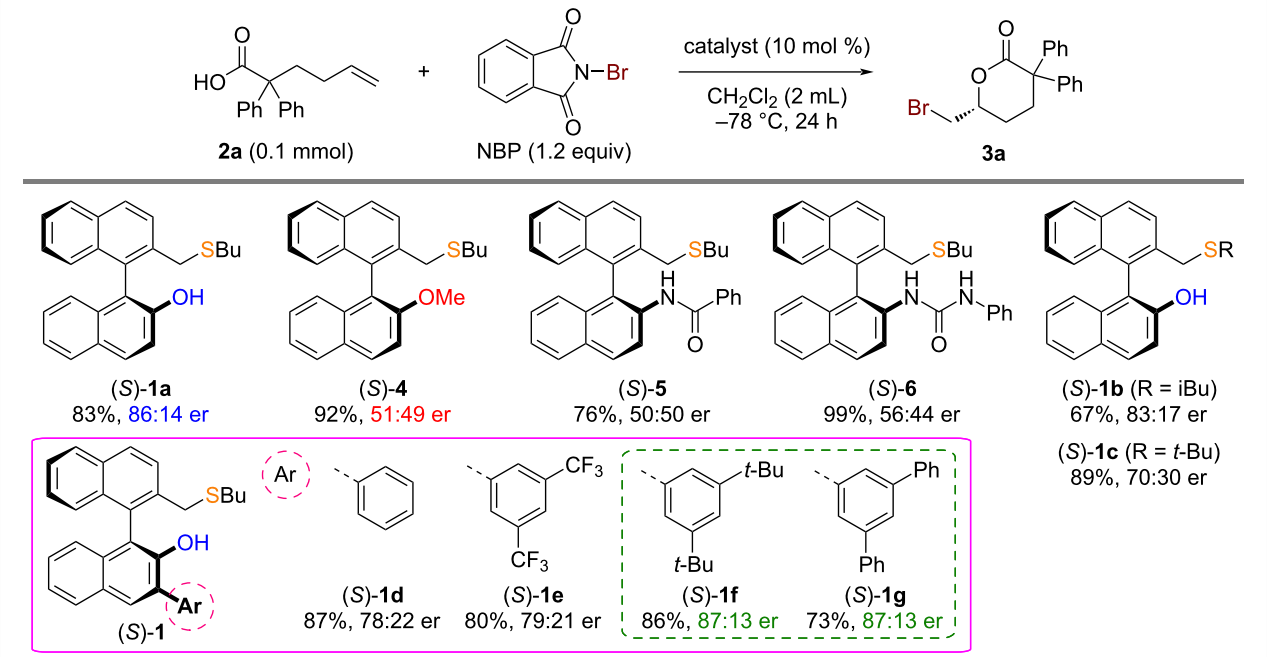

Scheme 2: Effects of chiral sulfide catalysts.

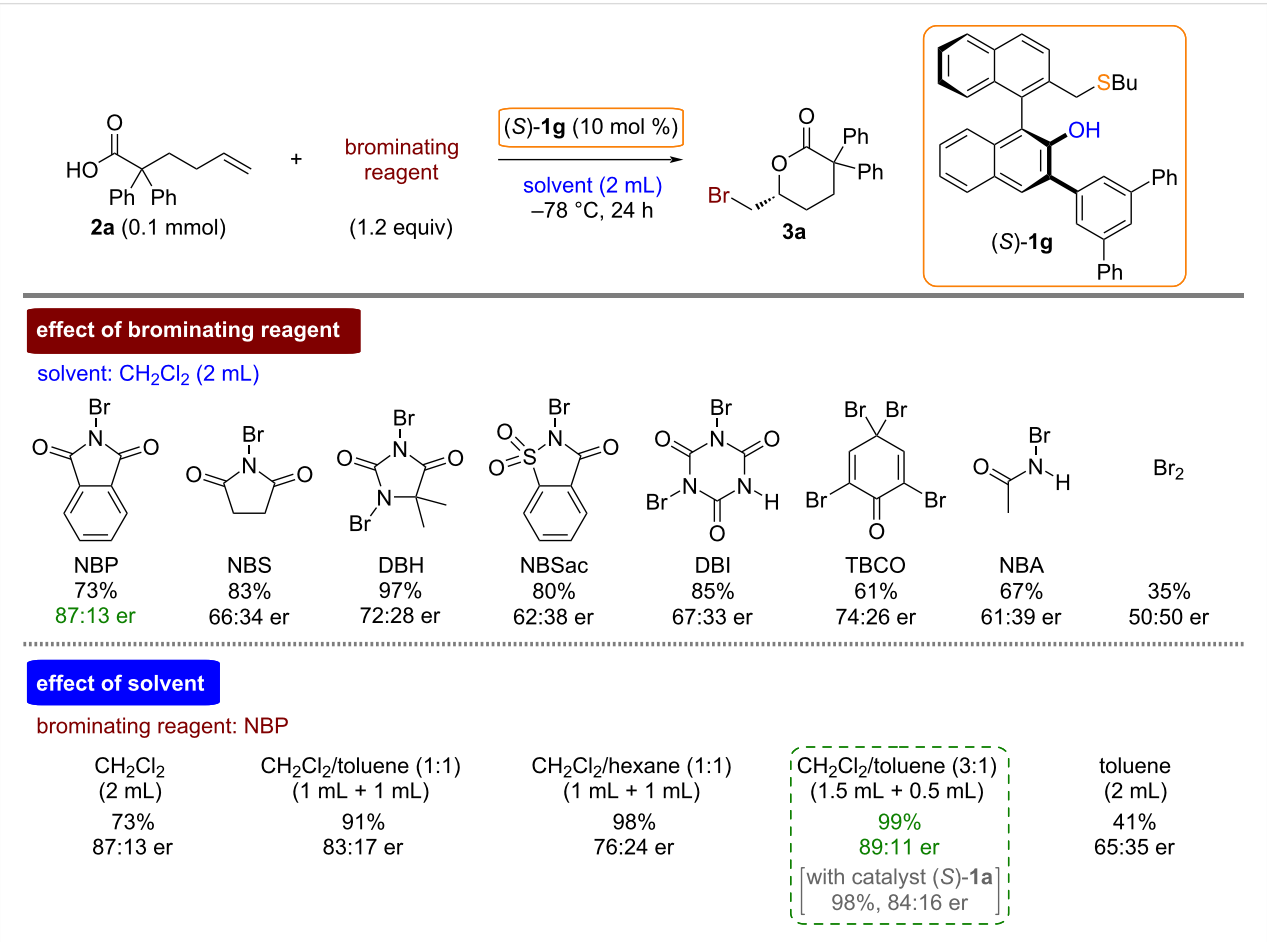

Scheme 3: Effects of brominating reagents and solvents.

With the optimal catalyst (*S*)-**1g** and reaction conditions in hand, we investigated the generality of catalytic asymmetric bromolactonizations of 5-hexenoic acids **2** (Scheme 4). Asymmetric bromolactonizations with α,α-diaryl type 5-hexenoic acids **2a**–**d** provided δ-valerolactone products **3a**–**d** in high yields with good levels of enantioselectivity. The reactions of α,α-dialkyl-5-hexenoic acids **2e** and **2f** gave the corresponding bromolactonization products **3e** and **3f** with moderate enantioselectivities. The present catalytic method could also be applied to the asymmetric synthesis of spirolactones [37-39]. For example, α-spiro-δ-lactone products **3g** and **3h** were obtained with moderate to good levels of enantioselectivity. Unfortunately, the reaction with a simple 5-hexenoic acid **2i** gave a δ-valerolactone **3i** in low enantioselectivity. To expand the substrate scope of chiral bifunctional sulfide-catalyzed asymmetric bromolactonizations of 5-hexenoic acids **2**, β-substituted substrates **2j**–**n** were submitted to the present catalytic system. As a result of these asymmetric reactions, β,β-dialkyl-δ-valerolactones **3j**–**k** and β-spiro-δ-lactones **3l**–**n** were obtained in good levels of enantioselectivity. The reaction of 2-allylbenzoic acid **2o** as a related substrate was also examined to give a dihydroisocoumarin product **3o** in high yield with moderate enantioselectivity. The absolute stereochemistry of the bromolactonization product **3o** was confirmed by comparison with reported data [24].

The transformations of the optically active bromolactonization product **3a** were explored to demonstrate the broader applicability of the current synthetic method (Scheme 5). Asymmetric bromolactonization of α,α-diphenyl-5-hexenoic acid (**2a**), using

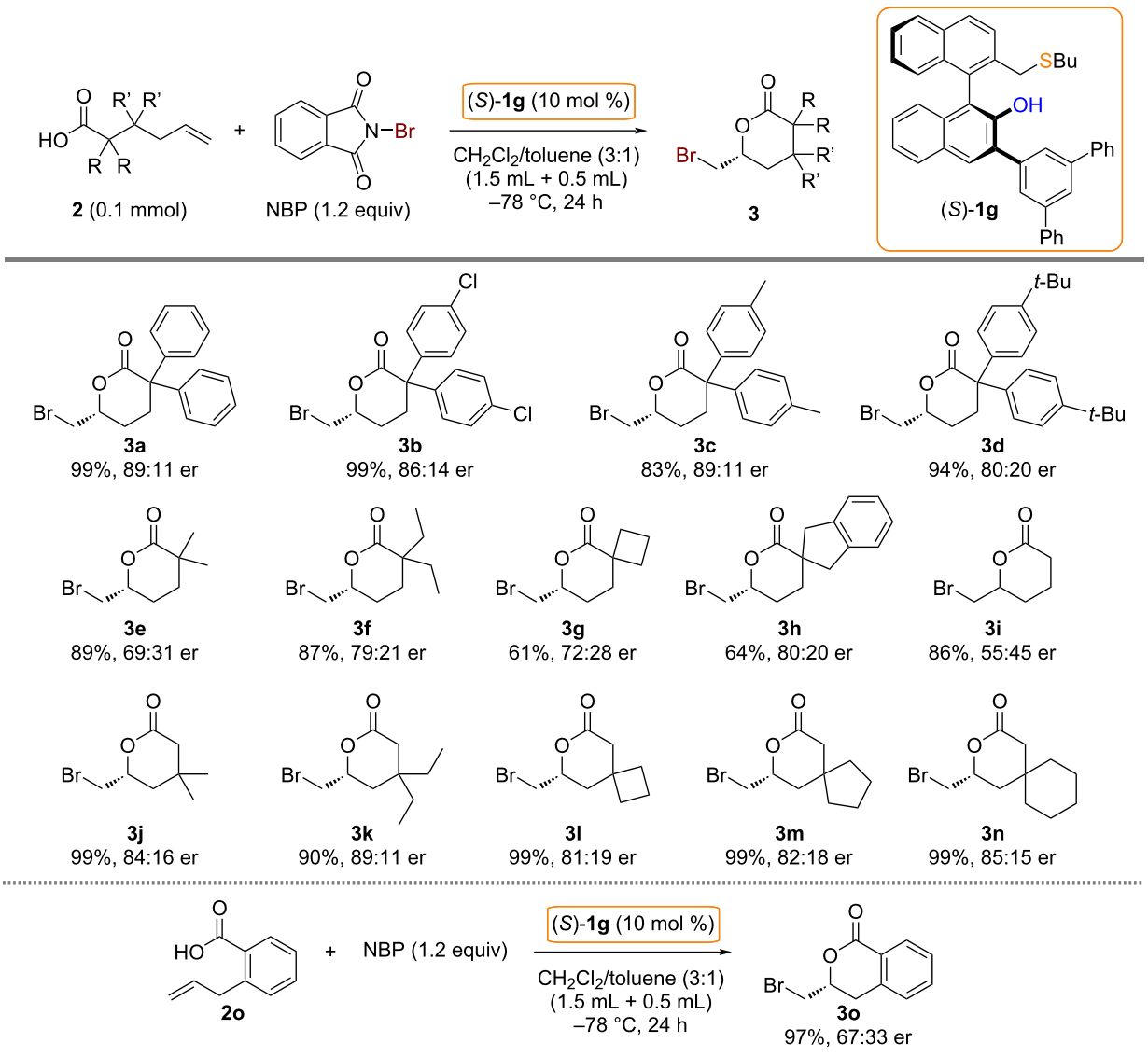

Scheme 4: Substrate scope.

a chiral bifunctional sulfide catalyst (*S*)-**1g**, was scaled up to a 1.0 mmol scale to obtain the optically active bromolactonization product **3a** for further transformations. Comparable yield and enantioselectivity were observed relative to those of the smaller-scale reaction (0.1 mmol scale, Scheme 4). The bromomethyl group in **3a** readily undergoes nucleophilic substitution reactions, leading to the formation of optically active δ-valerolactones **7** and **8**, which are functionalized with sulfur and nitrogen, in high yields. Additionally, optically active δ-valerolactone **3a** was converted to optically active epoxy-ester **9** upon treatment with potassium carbonate in methanol. Notably, the transformed products were obtained without any loss of optical purity.

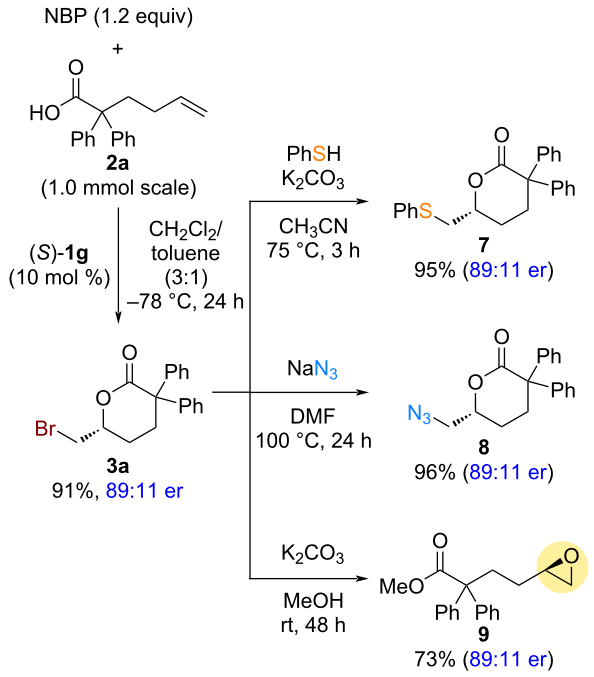

Scheme 5: Larger-scale synthesis and transformations of bromolactonization product **3a**.

Conclusion

In summary, our BINOL-derived chiral bifunctional sulfide-catalyzed enantioselective halocyclization technology was successfully applied to the catalytic asymmetric bromolactonization of α- and β-substituted 5-hexenoic acids. The target optically active δ-valerolactone products were obtained in moderate to good levels of enantioselectivity. The utility of the prepared optically active bromolactonization products was demonstrated in the transformations to functionalized δ-valerolactones and epoxy-esters. These transformations proceeded with no loss of optical purity. This report provides a valuable example of catalytic enantioselective halolactonization of 5-hexenoic acid derivatives without extra substituents on the carbon–carbon double bond.

Supporting Information

Supporting Information File 1

Experimental procedures, characterization data, copies of NMR spectra, and copies of HPLC charts.
[https://www.beilstein-journals.org/bjoc/content/supplementary/1860-5397-20-158-S1.pdf]

Funding

K.O. thanks the JSPS for a research fellowship (DC2). T.M. thanks the Nagasaki University for a planetary health research fellowship. This work was supported by JSPS KAKENHI (Grant Numbers 23K04752 for S. Shirakawa & 24KJ1826 for K.O.), and the Joint Usage/Research Center for Catalysis (24DS0655 for S. Shirakawa).

Author Contributions

Sao Sumida: data curation; formal analysis; investigation; writing – review & editing. Ken Okuno: investigation; writing – review & editing. Taiki Mori: investigation; writing – review & editing. Yasuaki Furuya: investigation; writing – review & editing. Seiji Shirakawa: conceptualization; data curation; formal analysis; funding acquisition; investigation; methodology; project administration; resources; supervision; validation; visualization; writing – original draft.

ORCID® iDs

Seiji Shirakawa - https://orcid.org/0000-0003-1027-8922

Data Availability Statement

All data that supports the findings of this study is available in the published article and/or the supporting information to this article.

References

1. Castellanos, A.; Fletcher, S. P. *Chem. – Eur. J.* **2011,** *17,* 5766–5776. doi:10.1002/chem.201100105
2. Denmark, S. E.; Kuester, W. E.; Burk, M. T. *Angew. Chem., Int. Ed.* **2012,** *51,* 10938–10953. doi:10.1002/anie.201204347
3. Hennecke, U. *Chem. – Asian J.* **2012,** *7,* 456–465. doi:10.1002/asia.201100856
4. Cheng, Y. A.; Yu, W. Z.; Yeung, Y.-Y. *Org. Biomol. Chem.* **2014,** *12,* 2333–2343. doi:10.1039/c3ob42335b
5. Gieuw, M. H.; Ke, Z.; Yeung, Y.-Y. *Chem. Rec.* **2017,** *17,* 287–311. doi:10.1002/tcr.201600088
6. Kristianslund, R.; Tungen, J. E.; Hansen, T. V. *Org. Biomol. Chem.* **2019,** *17,* 3079–3092. doi:10.1039/c8ob03160f
7. Ashtekar, K. D.; Jaganathan, A.; Borhan, B.; Whitehead, D. C. *Org. React.* **2021,** 1–266. doi:10.1002/0471264180.or105.01

8. Liu, S.; Zhang, B.-Q.; Xiao, W.-Y.; Li, Y.-L.; Deng, J. *Adv. Synth. Catal.* **2022,** *364,* 3974–4005. doi:10.1002/adsc.202200611
9. Liao, L.; Zhao, X. *Acc. Chem. Res.* **2022,** *55,* 2439–2453. doi:10.1021/acs.accounts.2c00201
10. Nishiyori, R.; Mori, T.; Okuno, K.; Shirakawa, S. *Org. Biomol. Chem.* **2023,** *21,* 3263–3275. doi:10.1039/d3ob00292f
11. Egami, H.; Hamashima, Y. *Chem. Rec.* **2023,** *23,* e202200285. doi:10.1002/tcr.202200285
12. Murai, K.; Matsushita, T.; Nakamura, A.; Fukushima, S.; Shimura, M.; Fujioka, H. *Angew. Chem., Int. Ed.* **2010,** *49,* 9174–9177. doi:10.1002/anie.201005409
13. Veitch, G. E.; Jacobsen, E. N. *Angew. Chem., Int. Ed.* **2010,** *49,* 7332–7335. doi:10.1002/anie.201003681
14. Jiang, X.; Tan, C. K.; Zhou, L.; Yeung, Y.-Y. *Angew. Chem., Int. Ed.* **2012,** *51,* 7771–7775. doi:10.1002/anie.201202079
15. Murai, K.; Nakamura, A.; Matsushita, T.; Shimura, M.; Fujioka, H. *Chem. – Eur. J.* **2012,** *18,* 8448–8453. doi:10.1002/chem.201200647
16. Lee, H. J.; Kim, D. Y. *Tetrahedron Lett.* **2012,** *53,* 6984–6986. doi:10.1016/j.tetlet.2012.10.051
17. Arai, T.; Sugiyama, N.; Masu, H.; Kado, S.; Yabe, S.; Yamanaka, M. *Chem. Commun.* **2014,** *50,* 8287–8290. doi:10.1039/c4cc02415j
18. Aursnes, M.; Tungen, J. E.; Hansen, T. V. *J. Org. Chem.* **2016,** *81,* 8287–8295. doi:10.1021/acs.joc.6b01375
19. Nishikawa, Y.; Hamamoto, Y.; Satoh, R.; Akada, N.; Kajita, S.; Nomoto, M.; Miyata, M.; Nakamura, M.; Matsubara, C.; Hara, O. *Chem. – Eur. J.* **2018,** *24,* 18880–18885. doi:10.1002/chem.201804630
20. Klosowski, D. W.; Hethcox, J. C.; Paull, D. H.; Fang, C.; Donald, J. R.; Shugrue, C. R.; Pansick, A. D.; Martin, S. F. *J. Org. Chem.* **2018,** *83,* 5954–5968. doi:10.1021/acs.joc.8b00490
21. Jana, S.; Verma, A.; Rathore, V.; Kumar, S. *Synlett* **2019,** *30,* 1667–1672. doi:10.1055/s-0037-1610715
22. Chan, Y.-C.; Wang, X.; Lam, Y.-P.; Wong, J.; Tse, Y.-L. S.; Yeung, Y.-Y. *J. Am. Chem. Soc.* **2021,** *143,* 12745–12754. doi:10.1021/jacs.1c05680
23. Dobish, M. C.; Johnston, J. N. *J. Am. Chem. Soc.* **2012,** *134,* 6068–6071. doi:10.1021/ja301858r
24. Armstrong, A.; Braddock, D. C.; Jones, A. X.; Clark, S. *Tetrahedron Lett.* **2013,** *54,* 7004–7008. doi:10.1016/j.tetlet.2013.10.043
25. Wilking, M.; Daniliuc, C. G.; Hennecke, U. *Synlett* **2014,** *25,* 1701–1704. doi:10.1055/s-0034-1378278
26. Hiraki, M.; Okuno, K.; Nishiyori, R.; Noser, A. A.; Shirakawa, S. *Chem. Commun.* **2021,** *57,* 10907–10910. doi:10.1039/d1cc03874e
27. Mori, T.; Abe, K.; Shirakawa, S. *J. Org. Chem.* **2023,** *88,* 7830–7838. doi:10.1021/acs.joc.2c02283
28. Okada, M.; Kaneko, K.; Yamanaka, M.; Shirakawa, S. *Org. Biomol. Chem.* **2019,** *17,* 3747–3751. doi:10.1039/c9ob00417c
29. Nishiyori, R.; Okada, M.; Maynard, J. R. J.; Shirakawa, S. *Asian J. Org. Chem.* **2021,** *10,* 1444–1448. doi:10.1002/ajoc.202000644
30. Okuno, K.; Chan, B.; Shirakawa, S. *Adv. Synth. Catal.* **2023,** *365,* 1496–1504. doi:10.1002/adsc.202300145
31. Mori, T.; Sumida, S.; Furuya, Y.; Shirakawa, S. *Synlett* **2024,** *35,* 479–483. doi:10.1055/a-2161-9513
32. Nishiyori, R.; Tsuchihashi, A.; Mochizuki, A.; Kaneko, K.; Yamanaka, M.; Shirakawa, S. *Chem. – Eur. J.* **2018,** *24,* 16747–16752. doi:10.1002/chem.201803703
33. Tsuchihashi, A.; Shirakawa, S. *Synlett* **2019,** *30,* 1662–1666. doi:10.1055/s-0037-1610716
34. Nakamura, T.; Okuno, K.; Kaneko, K.; Yamanaka, M.; Shirakawa, S. *Org. Biomol. Chem.* **2020,** *18,* 3367–3373. doi:10.1039/d0ob00459f
35. Okuno, K.; Hiraki, M.; Chan, B.; Shirakawa, S. *Bull. Chem. Soc. Jpn.* **2022,** *95,* 52–58. doi:10.1246/bcsj.20210347
36. Nishiyori, R.; Okuno, K.; Chan, B.; Shirakawa, S. *Chem. Pharm. Bull.* **2022,** *70,* 599–604. doi:10.1248/cpb.c22-00049
37. Bartoli, A.; Rodier, F.; Commeiras, L.; Parrain, J.-L.; Chouraqui, G. *Nat. Prod. Rep.* **2011,** *28,* 763–782. doi:10.1039/c0np00053a
38. Thorat, S. S.; Kontham, R. *Org. Biomol. Chem.* **2019,** *17,* 7270–7292. doi:10.1039/c9ob01212e
39. Hiesinger, K.; Dar'in, D.; Proschak, E.; Krasavin, M. *J. Med. Chem.* **2021,** *64,* 150–183. doi:10.1021/acs.jmedchem.0c01473

License and Terms

BEILSTEIN JOURNAL OF ORGANIC CHEMISTRY

Stereoselective mechanochemical synthesis of thiomalonate Michael adducts via iminium catalysis by chiral primary amines

Michał Błauciak[1], Dominika Andrzejczyk[1,2], Błażej Dziuk[3] and Rafał Kowalczyk[*1]

Full Research Paper

Open Access

Address:
[1]Faculty of Bioorganic Chemistry, Wrocław University of Science and Technology, wyb. Wyspiańskiego 27, 50-370 Wrocław, Poland, [2]Current company: PCC EXOL, Poland and [3]Institute of Advanced Materials, Wrocław University of Science and Technology, wyb. Wyspiańskiego 27, 50-370 Wrocław, Poland

Email:
Rafał Kowalczyk[*] - rafal.kowalczyk@pwr.edu.pl

* Corresponding author

Keywords:
asymmetric catalysis; iminium catalysis; mechanochemistry; organocatalysis; thioesters

Beilstein J. Org. Chem. **2024,** *20,* 2313–2322.
https://doi.org/10.3762/bjoc.20.198

Received: 05 June 2024
Accepted: 30 August 2024
Published: 12 September 2024

This article is part of the thematic issue "New advances in asymmetric organocatalysis II".

Guest Editor: R. Šebesta

Abstract

The study presents a novel approach utilizing iminium salt activation and mild enolization of thioesters, offering an efficient and rapid synthesis of Michael adducts with promising stereoselectivity and marking a significant advancement in mechanocatalysis. The stereoselective addition of bisthiomalonates **1**–**4** to cyclic enones and 4-chlorobenzylideneacetone proceeds stereoselectively under iminium activation conditions secured by chiral primary amines, in contrast to oxo-esters as observed in dibenzyl malonate addition. Mild enolization of thioesters allows for the generation of Michael adducts with good yields and stereoselectivities. Reactions in a ball mill afford product formation with similar efficacy to solution-phase reactions but with slightly reduced enantioselectivity, yet they yield products in just one hour compared to 24 or even 168 hours in solution-based reactions. It is noteworthy that this represents one of the early reports on the application of iminium catalysis using first-generation chiral amines under mechanochemical conditions, along with the utilization of easily enolizable thioesters as nucleophiles in this transformation.

Introduction

Mechanochemistry, particularly solventless processes under ball milling conditions, offers the opportunity to devise unconventional reaction pathways [1-5]. The transient impact of kinetic energy, channeled into the reaction, facilitates overcoming the constraints inherent in equilibrium models. Thus, employing limited substrates could potentially yield diverse products through a simple alteration of conditions, compared to solvent-based methods [6-8]. Furthermore, the integration of mechanochemistry and organocatalysis leads to the development of more sustainable transformations, characterized by reduced reaction times, decreased catalyst loadings, and significantly diminished solvent usage and waste production [9-11].

The pioneering studies by Bolm [12,13], and Juaristi et al. [14]. have significantly advanced chiral secondary amine-catalyzed stereoselective reactions under ball milling conditions, representing a widely explored activation mode in mechanochemical-mediated transformations. However, reports on chiral primary iminium [15,16] or iminium-ion catalysis [17] under ball-mill conditions are scarce, in contrast to the abundance of transformations catalyzed by such covalent catalysis.

Among the numerous organocatalytic reactions facilitated by primary amine-based iminium ions, Michael-type additions deserve special attention. The controlled formation of C–C and C–X bonds in a stereoselective fashion has found extensive application in asymmetric synthesis. Notably, the addition of malonates has attracted significant interest, albeit primarily limited to methyl or ethyl diesters [18-20]. The combination of iminium catalysis with hydrogen bonding units has been essential for achieving high reactivity and enantioselectivities [21,22]. Additionally, the reactivity of the nucleophilic addition is influenced by substitutions near the electron-poor double bond. This approach requires 30 mol % of catalyst and a reaction time of two days under a pressure of 0.8 GPa [23].

Less reactive benzyl malonates, which allow for the cleavage of a free carboxylic group without the need for harsh base- or acid-mediated conditions [24], undergo additions catalyzed by primary amines [19]. However, these transformations are hampered by extended reaction times, sometimes up to 168 hours. An intriguing example involves the use of a bifunctional primary amine-sulfonamide catalyst, which activates benzylideneacetone towards dibenzyl malonate, with the presence of water accelerating the reaction [25].

An alternative approach, where enhancing the reactivity of a relatively inert acceptor does not necessarily lead to increased reaction rates, involves the use of more reactive nucleophiles. In this context, varying the stabilization energy of carboxylic acid derivatives by switching from oxoesters to thioesters is the significant acceleration of the reaction progress [26,27]. The crucial enhancement of anion stabilization by deprotonation of the methylene group in bisthiomalonates was hypothesized to surpass that of analogous dibenzyl malonate [28,29].

Surprisingly, the employment of NaH, NaSEt, or *t*-BuOLi as relatively strong bases proved ineffective in facilitating the Michael addition of bisthiomalonates to conjugated ketones, whereas DABCO enabled the formation of desired products under mild conditions [30]. However, reports of highly stereoselective protocols utilizing hydrogen bonding catalysis have mainly focused on nitroalkenes or guanidine-mediated addition of bisthiomalonates to maleimides, cyclic enones, and acyclic 1,4-dicarbonylbutenes, albeit at low temperatures and with relatively long reaction times, further limited to a narrow scope of thioesters (Scheme 1) [31].

Recently, we described a cinchona-squaramide-based catalytic system for the highly stereoselective addition of various bisthiomalonates to chalcones and dienones [29]. While recog-

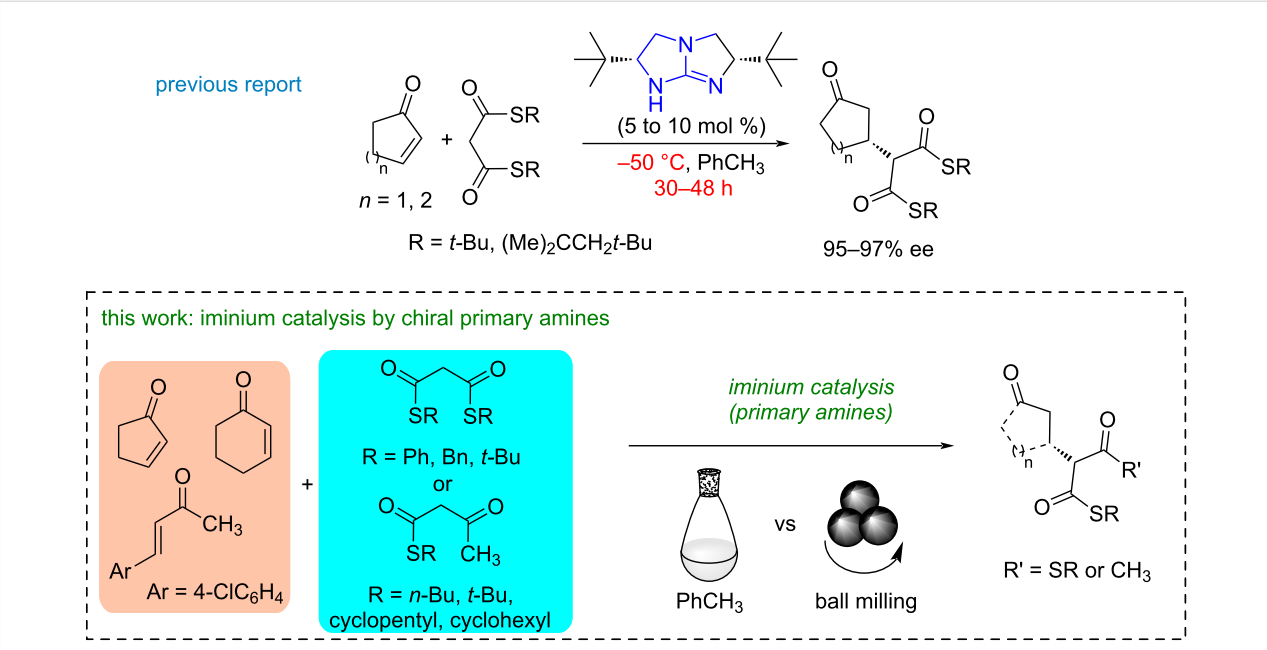

Scheme 1: Two examples of base-catalyzed addition of thiomalonates to enones and the scope of the work.

nizing the potential for greater selectivity enhancement and time savings with ball milling, hydrogen-bonding catalysis was effective only with aromatic enones, yielding low conversions and stereoselectivities when applied to benzylidene acetones or cyclic enones (vide infra).

In our latest research in establishing a mild organocatalytic protocol for incorporating benzyl malonates and bisthiomalonates into cyclic enones and benzylidene acetones, we have developed a novel approach based on iminium catalysis employing chiral primary amines under ball milling conditions. Ball milling induces localized and transient temperature and pressure increases which could influence changes in the free activation volume [32-34], favoring Michael additions [35]. Furthermore, condensation reactions, including the formation of transient C=N bonds, are significantly promoted under ball milling conditions [12-14]. It is noteworthy that the application of primary amines for activating cyclic ketones under mechanochemical conditions remains largely unexplored [36]. We aim to fill this research gap by introducing an effective methodology for generating enantiomerically enriched products, thereby expanding the scope of applications and contributing to a deeper understanding of stereoselective covalent catalysis, particularly in the field of mechanochemistry.

Results and Discussion

Based on our previous experiences with low-reactive Michael acceptors [29], initial attempts were carried out using bifunctional squaramides, derivatives of cinchona. However, up to 45% yield of the desired product was obtained with poor enantioselectivity (14%, Scheme 2). Considering the stability of thioester groups in aqueous environments, we also decided to apply conditions conducive to hydrophobic amplification [37], which unfortunately also did not yield the intended effect. Another approach is to generate and stabilize the active nucleophile form as an anion thus increasing its reactivity by chiral quaternary ammonium salt in the asymmetric variant of the phase-transfer catalysis. Nevertheless, no product was formed despite several conditions being examined. Finally, an attempt to activate the electrophile was performed. We chose iminium salt catalysis particularly employing chiral primary amines for this purpose to enable activation of the enone system. Such a method lowers the energy of the LUMO orbital and subsequently reduces the energy barrier between the nucleophile's HOMO orbital resultingly, expedites the entire transformation [38]. Moreover, the presence of the stereogenic center in proximity to the reactive moiety of the covalent substrate adduct to the catalyst contributes to the efficient transfer of chirality to the resulting product, even in the distant position of the 1,6-conjugated system [39]. For these reasons, iminium catalysis using primary amines appears to be the ideal tool in addition to reactions to cyclic enones and benzylidene acetones. However, our concern was whether the thioester group, whose activity towards nitrogen nucleophiles significantly exceeds that of analogous oxo-esters [26,27,40], would remain unaffected in the presence of a nucleophilic catalyst. Test reactions between cyclohexenone and thiomalonate **1** conducted in toluene at room temperature indicated the formation of the product with high conversions and efficiencies (Scheme 2).

Application of *epi*-aminoquinine (**AQ-1**) in combination with 2-fluorobenzoic acid (system A) led to the product with 93% ee after 24 h, while the bifunctional primary amine-thiourea catalysts (system B) required 4 days to provide an adduct with similar enantioselectivity. Prolonged reaction time is in general the innate nature of organocatalytic reactions employing iminium activation approaches. With the aim to decrease the time along with the generation of a product with an acceptable yield, we decided to perform the reaction under ball milling conditions reasoning that choice by limiting the solvent, increasing the concentration of both reagents and catalyst accompanying with the efficient mixing supported moreover by the local pressure increase. Albeit the transformation performed in the planetary ball mill required 20 h to proceed, the same reaction in the mixer mill offering the greater energy impact by the rise of mixing frequency led to the product after 1 hour with an acceptable yield of isolated product. However, the decrease in the enantioselectivity was noted in comparison to the reaction under standard conditions in toluene (93% vs 85% in ball mill). Surprisingly, the essential loss of enantioselectivity was noted when system B was applied in analogous transformation.

Although an impressive boost of the reaction rate in the ball mill was observed (3 h vs 4 days), the stereochemical outcome suffered giving the desired adduct with 59% ee instead of 94% ee in solution. Owing to the introduction of an additional functional group in the form of a thiourea moiety does not entail a significant enhancement of catalytic system efficiency and results from the dramatic decrease in enantioselectivity observed in mill reactions. Additionally, the catalyst's synthesis requires an extra synthetic step. We decided to conduct further investigations utilizing system A or its modifications.

First, changes in the *epi*-amino alkaloid core of the two-component catalytic system were investigated. Introduction of the 2'-substitution to the quinine core as in **AQ-2** and **AQ-4** (Scheme 2) resulted in the decrease of chirality transfer providing the product with 50% and 72% ee, respectively. A similar trend was observed when **AQ-3** was applied. Besides, the modifications of the quinuclidine ring through replacing the vinyl substituent in the parent quinine core by a triple bond (**AQ-5**) led to no substantial improvement in the mixer mill, but the de-

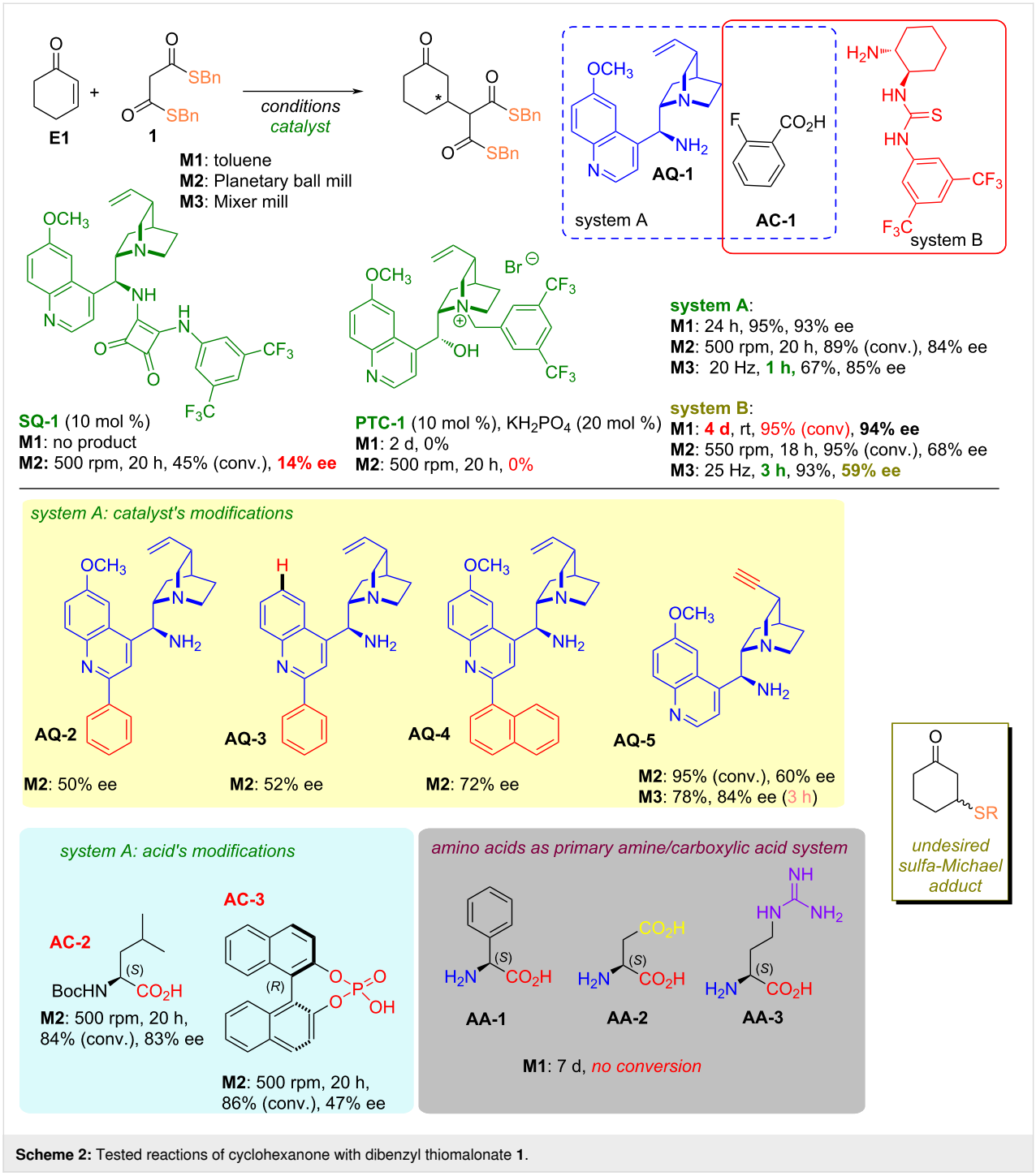

Scheme 2: Tested reactions of cyclohexanone with dibenzyl thiomalonate **1**.

crease of enantioselectivity in the reaction performed in the planetary mill. Further variations of system A concerned the acid's role. However, no impact of the acid was noted while using the amino acid derivative **AC-2**, but the dramatic loss of selectivity was observed in the case of chiral phosphoric acid's application **AC-3**. Thus, it is rather unlikely the iminium-ion catalysis to operate. Moreover, three amino acids (20 mol %) were utilized to generate iminium ions and subsequently to stabilize them by the presence of a carboxyl group. However, no conversion was observed after 7 days despite the additional structural elements as a carboxylic group in **AA-2** or guanidine motif in **AA-3** compared to simple **AA-1**.

Alterations in the thiol structure within thiomalonates significantly impact their stability and reactivity, thereby influencing both reaction efficiency and stereochemical outcome, as demon-

strated in the case of catalysis employing bifunctional hydrogen bond donors [29]. In the context of imine catalysis using acid, the catalyst **AQ-1**'s ability to abstract protons from bisthiomalonate, thereby activating the nucleophile may be at least restricted. Consequently, we chose to investigate the impact of the thioester group on the outcome, including stereochemical, of the reaction between cyclohexenone and bisthiomalonates catalyzed by system A under standard conditions and mechanochemical (mixer mill) conditions (Scheme 3).

Under optimized conditions, the dibenzyl malonate adduct was formed in a ball mill with 67% yield and 85% ee of (*S*)-isomer, which was proved by X-ray studies. Assuming the mechanism of addition is similar in the case of other nucleophiles, the configuration of others was assigned by analogy. More sterically demanding di-*tert*-butyl thiomalonate (**2**) reacted in a similar fashion as the dibenzyl thiomalonate (**1**), leading also to desired products with 61% and 63% yield in the solution and mixer mill, respectively. However, the drop of stereoselectivity was noted in comparison to the reaction in toluene (94% ee vs 86% ee in mixer mill, Δee = 8). It should be noted that the dibenzyl malonate remained inactive for subjecting to reaction under both conditions. This result could be ascribed to the lower affinity of the oxo-ester to form active nucleophiles in comparison to the more favorable enolization of thiomalonates.

The stereochemical outcome of the thiomalonate's addition could be rationalized by the assumption the iminium ion stabilized by an intramolecular hydrogen bond with a protonated amine unit activates the Michael acceptor (Scheme 4). Moreover, a strong but reversible covalent bond locates the electrophile upon the quinoline unit of the catalyst and thus subsequently blocks the bottom approach of the thiomalonate. Hence, such a sterically demanding nucleophile preferentially reaches the face of the reactive site from above the plane leading to the observed (*S*)-product.

The most pronounced effect exhibited by the thioester group concerning nucleophilic reactivity and stereochemical outcome of the reaction was observed for phenyl bis-thiomalonate **3**. The

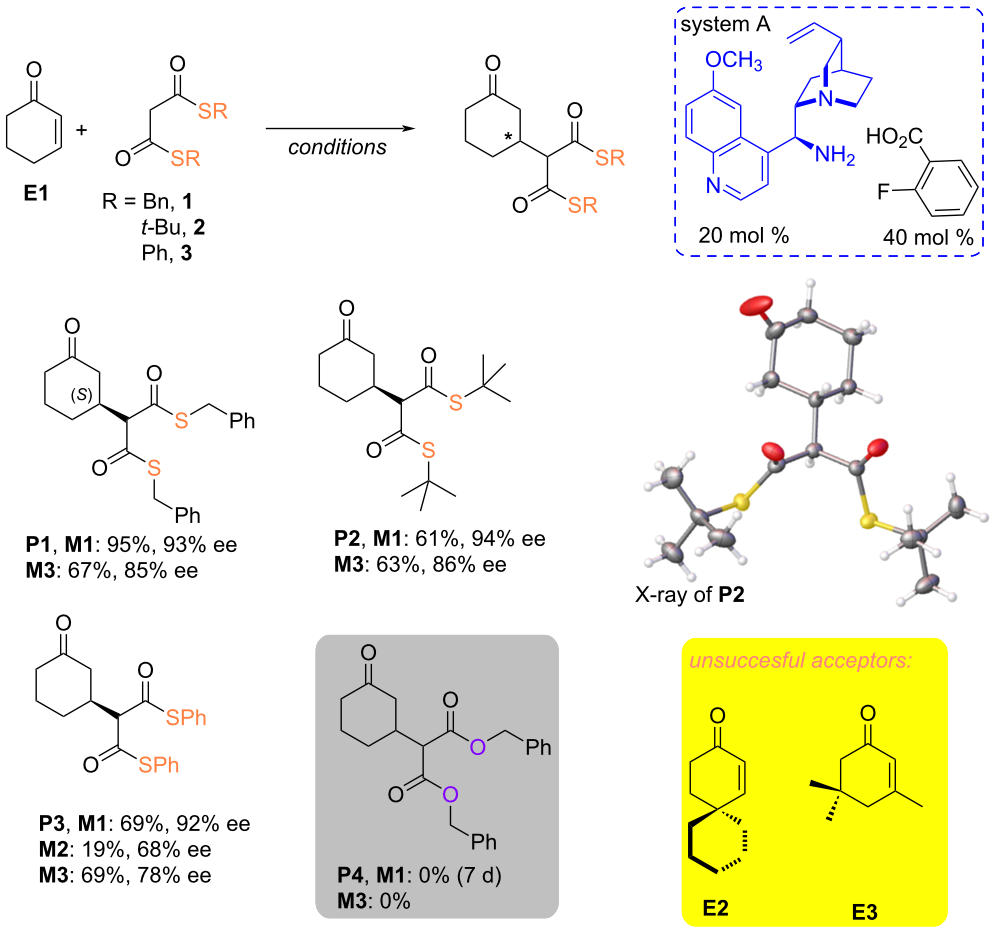

Scheme 3: Impact of the bisthiomalonate on the yield and the stereoselectivity of the products.

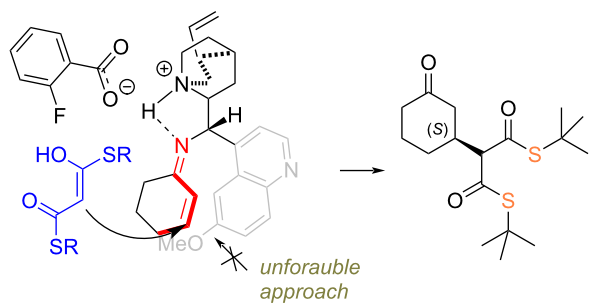

Scheme 4: Plausible stereochemical model of the addition to cyclohexenone.

reaction in toluene required 24 hours to yield an enantiomerically enriched product (92% ee) with a 69% yield. However, achieving such a degree of over-reaction was associated with prolonged reaction times, which may affect the stability of both the substrate and its adduct. Hence, after 24 hours up to 9% of sulfa-adduct was formed (see Supporting Information File 1 for details). Unfavorable in this case is the formation of ketene via thiol elimination [40], leading to the formation of a mixture of products where the thia-Michael adduct predominates over the desired Michael product. We were sincerely interested in shortening the reaction time. This could be achieved by conducting the reaction under conditions of efficient mixing, increasing substrate concentration without solvents, and utilizing transient but repeatable pressure and temperature increases. These conditions are provided by mechanochemistry methods in ball mills. The reaction performed in a mixer mill over 1 hour only led to 13% of sulfa-Michael adduct (see Supporting Information File 1) beside the expected enantioenriched product (69%, 78% ee). We assumed the energy impact generated in the mixer mill could allow the reaction to occur also without the assistance of a catalyst, thereby following the non-stereoselective path. However, changing the milling system to a planetary ball mill affording fewer energy portions than the mixer mill, the Michael adduct was isolated with a rather low yield (19%) and moderate enantioselectivity (68%). Moreover, the steric bias in proximity (**E2**, Scheme 3) or the subunit of the conjugated system (**E3**) of acceptors revealed the nucleophiles (**1** and **3**) were unable to reach the reactive center or to form a stable bond.

Interestingly, when the reaction with bis-thiomalonate **3** was applied to cyclopentenone, which exhibits electrophilicity on the Mayer scale of −20.60 compared to cyclohexenone (E = −22.10, in DMSO) [41], comparable results were obtained both in solution and in a ball mill (Scheme 5). Therefore, a slightly more reactive electrophile does not significantly react less selectively in the ball mill than in solution, leading to the adduct with a low, 24% ee value, but higher than the analogous transformation in toluene. On the other hand, the transformation in the ball mill leads to the formation of 9% of the sulfa-Michael product (see Supporting Information File 1). However, the low stereoselectivity is not surprising. The analysis of the covalent adduct of cyclopentenone with amines may result from the "flattened" of the small system that renders them less sensitive to steric interactions generated by the catalyst compared to cyclohexenone [42-44]. In the case of thiomalonates **1** and **2**, reactions conducted in solution surpass those occurring in the

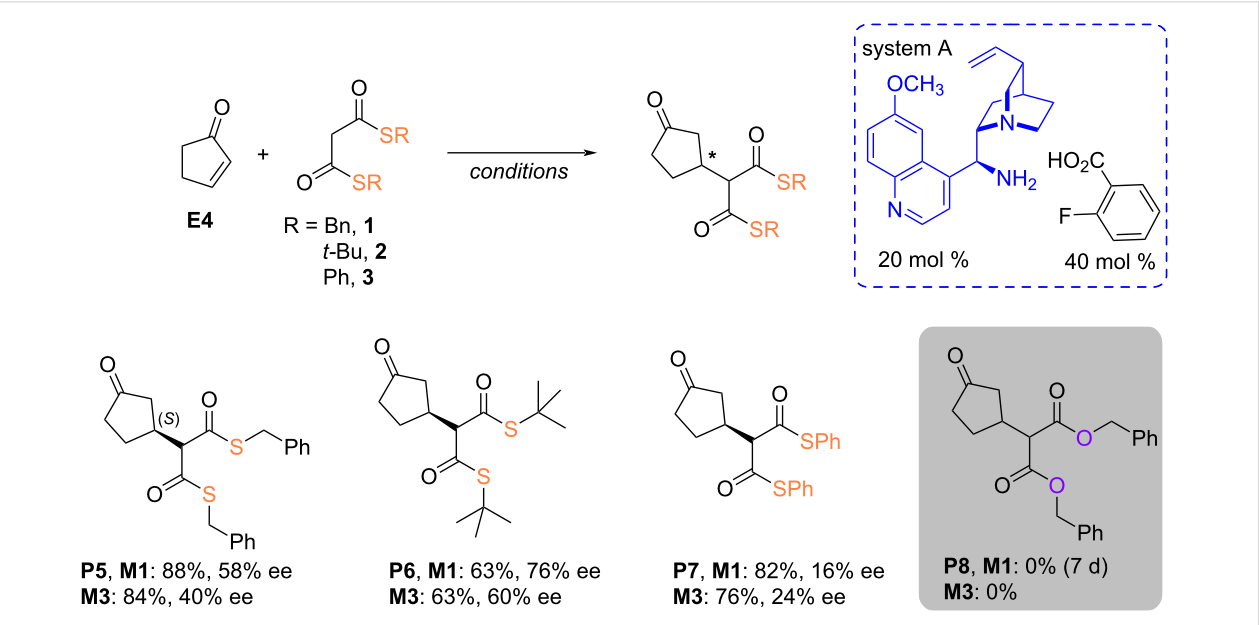

Scheme 5: Addition of bisthiomalonates **1**–**3** to cyclopentenone.

ball mill in terms of stereoselectivity, and yield in case of **P5** and **P7**. Therefore, 1 hour in the ball mill versus 24 hours in solution is sufficient to obtain the desired product with similar efficiency.

Motivated by our curiosity surrounding the reactivity of alicyclic enones with bis-thiomalonates, we embarked on a study to evaluate a chosen catalytic system's efficacy under both standard conditions and mechanochemical milling. We aimed to facilitate the nucleophilic addition of **1**–**4** to 4-chlorobenzylideneacetone (**E5**). In contrast to previous examples, where the use of 1.5 equiv of the electrophile was a necessary step to ensure product formation in a ball mill (see Schemes 2–4), an equimolar mixture of acceptor **E5** and nucleophile **1**–**4** was subjected to Michael addition reaction using system A (Scheme 6). Despite the long reaction time (45 h for thiomalonate **1** up to 70 h for nucleophile **2**), the expected adducts were obtained with yields of 44% and 56%, respectively. Similar transformations conducted in a ball mill afforded products with slightly higher yields (58% for **1** and 64% for **2**) and slightly lower stereoselectivities requiring only 1 hour instead of 45 and 70 hours. Unfortunately, attempts to add thiomalonate **3** and dibenzyl malonate failed. In the first case, instead of forming the expected product, only the thiophenol adduct is formed (see Scheme 2, right chart, for the structure of sulfa-Michael adduct; R = Ph).

Finally, an interesting group of β-ketothioesters **5**–**8**, which are rarely utilized in asymmetric catalysis [45], were employed as nucleophiles in reactions with acceptor **E1** (Scheme 7). While additions of various β-ketothioesters, including **5**–**8**, to nitrostyrenes proceeded efficiently, leading to products with enantiomeric excesses above 95% ee [46], changing the catalytic system and activation method from non-covalent to covalent substrate activation, allowed for the synthesis of products with moderate to good yields (46–72%). However, it was not possible to determine the enantiomeric excesses for nearly equimolar pairs of diastereomeric products due to the lack of appropriate conditions for resolution among the six tested chiral stationary phases. To our surprise, reactions conducted in the ball mill did not lead to the formation of new C–C bonds, and even after extending the reaction time, a mixture of unreacted reagents was recovered.

The observations indicate a significant role of factors related to the physical contact between substances, milling balls, and the walls of the grinding vessel on the final outcome of the reaction when the system is in a liquid state. Interestingly, the transformations conducted under ball mill conditions only failed when the crude product, rather than the initial system, was in a liquid state. Thus, while the reaction of liquid enones with thiomalonate **2** successfully yielded the expected products, the adducts **5**–**8** were only formed in solution when they were in a liquid form. We assume the keto–enol interactions between the substrate molecules or substrate reagents might essentially decreased the reactivity in comparison to solution, as indicated in the recent precedent [47].

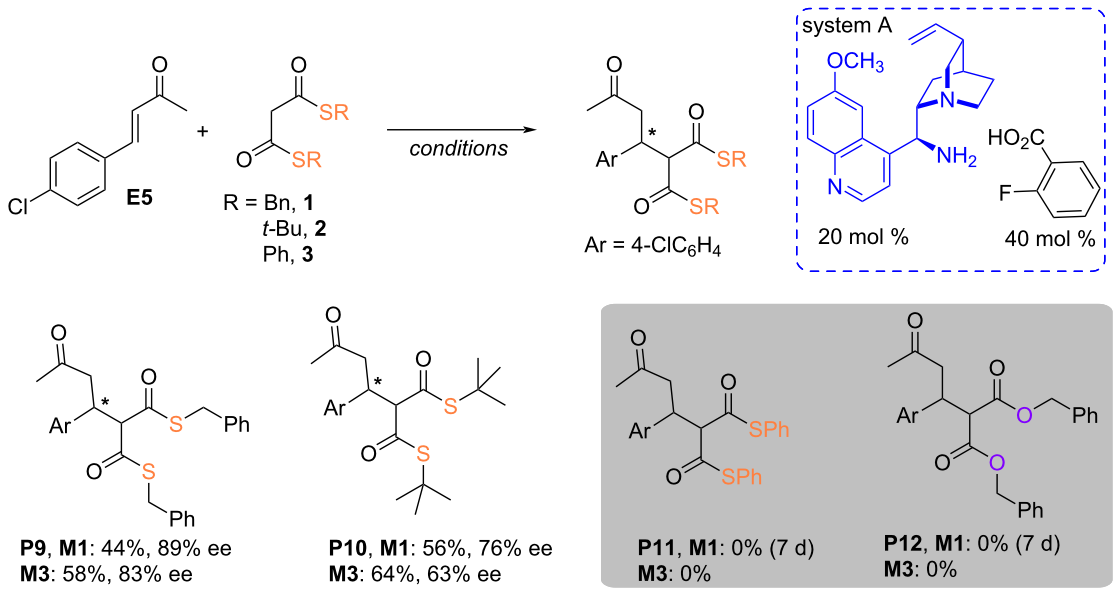

Scheme 6: Acyclic enone in reactions with thiomalonates **1**–**4**.

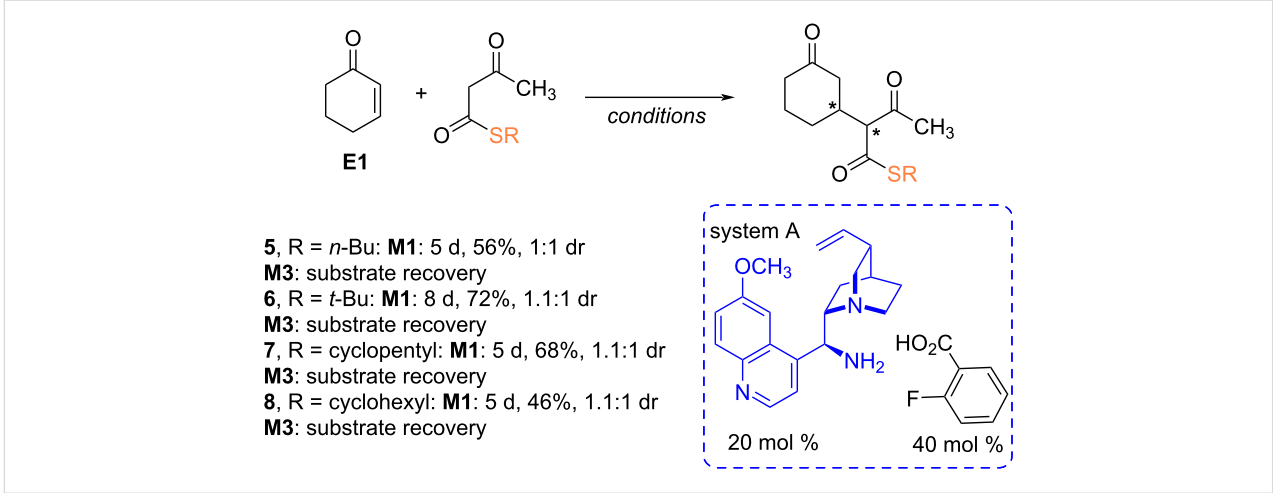

Scheme 7: Reaction of β-ketothioesters with acceptor **E1**.

Conclusion

Mechanochemistry, particularly ball milling, represents a promising avenue for unconventional reaction pathways by exploiting kinetic energy to surpass equilibrium constraints. This methodology presents several advantages over conventional solvent-based approaches, including the potential for diverse product formation with limited substrates and the development of sustainable transformations characterized by reduced reaction times.

An unprecedented combination of mechanochemistry with organocatalysis, notably chiral amine-catalyzed stereoselective reactions, has been extensively investigated. While primary amine-catalyzed reactions under ball milling conditions are less documented, they offer prospects for substrate diversification using a more sustainable approach. Efforts to enhance reactivity through nucleophile modifications, such as transitioning from oxoesters to thioesters, show promise in enhancing reaction progress. However, the efficacy of catalysts varies, with certain systems proving ineffective or leading to diminished stereoselectivity under mechanochemical conditions. Despite a slight decrease in stereoselectivity with the usual Δee of about 8%, reactions conducted in the mill allow for reaction completion within 1 hour compared to the 24 to 168 hours needed when conducting reactions in solution. Therefore, thiomalonates exhibit distinctive reactivity compared to oxoesters, impacting reaction efficiency. Moreover, despite being more reactive acylating agents than oxoesters, thioesters are effectively utilized as nucleophiles in reactions catalyzed by primary amines in transformation requiring the formation of the imines without catalyst deactivation. The study underscores the potential of mechanochemistry in broadening the scope of organocatalytic and stereoselective transformations including the application of rather unexplored thioesters.

Supporting Information

Supporting Information File 1

Experimental and analytical data, crystallographic information and NMR spectra.
[https://www.beilstein-journals.org/bjoc/content/supplementary/1860-5397-20-198-S1.pdf]

Acknowledgments

We are grateful to Miss Aleksandra Motyka for some initial results and Dr. Maciej Dajek for samples of β-ketothioesters **5**–**8**.

Funding

National Science Center, Poland is acknowledged for financial support (Grant No. 2016/22/E/ST5/00046).

Author Contributions

Michał Błauciak: investigation; methodology; writing – review & editing. Dominika Andrzejczyk: investigation. Błażej Dziuk: investigation; writing – review & editing. Rafał Kowalczyk: conceptualization; funding acquisition; methodology; writing – original draft.

ORCID® iDs

Michał Błauciak - https://orcid.org/0000-0002-6363-8146
Rafał Kowalczyk - https://orcid.org/0000-0001-5228-9131

Data Availability Statement

All data that supports the findings of this study is available in the published article and/or the supporting information to this article.

References

1. Margetić, D. *Pure Appl. Chem.* **2023,** *95,* 315–328. doi:10.1515/pac-2022-1202
2. Cuccu, F.; De Luca, L.; Delogu, F.; Colacino, E.; Solin, N.; Mocci, R.; Porcheddu, A. *ChemSusChem* **2022,** *15,* e202200362. doi:10.1002/cssc.202200362
3. Howard, J. L.; Cao, Q.; Browne, D. L. *Chem. Sci.* **2018,** *9,* 3080–3094. doi:10.1039/c7sc05371a
4. Hernández, J. G.; Bolm, C. *J. Org. Chem.* **2017,** *82,* 4007–4019. doi:10.1021/acs.joc.6b02887
5. James, S. L.; Adams, C. J.; Bolm, C.; Braga, D.; Collier, P.; Friščić, T.; Grepioni, F.; Harris, K. D. M.; Hyett, G.; Jones, W.; Krebs, A.; Mack, J.; Maini, L.; Orpen, A. G.; Parkin, I. P.; Shearouse, W. C.; Steed, J. W.; Waddell, D. C. *Chem. Soc. Rev.* **2012,** *41,* 413–447. doi:10.1039/c1cs15171a
6. Pladevall, B. S.; de Aguirre, A.; Maseras, F. *ChemSusChem* **2021,** *14,* 2763–2768. doi:10.1002/cssc.202100497
7. Delogu, F.; Takács, L. *J. Mater. Sci.* **2018,** *53,* 13331–13342. doi:10.1007/s10853-018-2090-1
8. Chen, Z.; Lu, S.; Mao, Q.; Buekens, A.; Wang, Y.; Yan, J. *Environ. Sci. Pollut. Res.* **2017,** *24,* 24562–24571. doi:10.1007/s11356-017-0028-9
9. Némethová, V.; Krištofíková, D.; Mečiarová, M.; Šebesta, R. *Chem. Rec.* **2023,** *23,* e202200283. doi:10.1002/tcr.202200283
10. Juaristi, E.; Avila-Ortiz, C. G. *Synthesis* **2023,** *55,* 2439–2459. doi:10.1055/a-2085-3410
11. Chauhan, P.; Chimni, S. S. *Beilstein J. Org. Chem.* **2012,** *8,* 2132–2141. doi:10.3762/bjoc.8.240
12. Rodríguez, B.; Rantanen, T.; Bolm, C. *Angew. Chem., Int. Ed.* **2006,** *45,* 6924–6926. doi:10.1002/anie.200602820
13. Rodríguez, B.; Bruckmann, A.; Bolm, C. *Chem. – Eur. J.* **2007,** *13,* 4710–4722. doi:10.1002/chem.200700188
14. Hernández, J. G.; Juaristi, E. *J. Org. Chem.* **2011,** *76,* 1464–1467. doi:10.1021/jo1022469
15. Zhang, Y.; Duan, H.-X.; Wang, Y.-Q. *Chin. J. Org. Chem.* **2020,** *40,* 1514–1528. doi:10.6023/cjoc201908030
16. Melchiorre, P. *Angew. Chem., Int. Ed.* **2012,** *51,* 9748–9770. doi:10.1002/anie.201109036
17. Brazier, J. B.; Tomkinson, N. C. O. *Top. Curr. Chem.* **2010,** *291,* 281–347. doi:10.1007/978-3-642-02815-1_28
18. Krištofíková, D.; Modrocká, V.; Mečiarová, M.; Šebesta, R. *ChemSusChem* **2020,** *13,* 2828–2858. doi:10.1002/cssc.202000137
19. Procopio, A.; De Nino, A.; Nardi, M.; Oliverio, M.; Paonessa, R.; Pasceri, R. *Synlett* **2010,** 1849–1853. doi:10.1055/s-0030-1258126
20. Mao, Z.; Jia, Y.; Li, W.; Wang, R. *J. Org. Chem.* **2010,** *75,* 7428–7430. doi:10.1021/jo101188m
21. Li, P.; Wen, S.; Yu, F.; Liu, Q.; Li, W.; Wang, Y.; Liang, X.; Ye, J. *Org. Lett.* **2009,** *11,* 753–756. doi:10.1021/ol802892h
22. Dudziński, K.; Pakulska, A. M.; Kwiatkowski, P. *Org. Lett.* **2012,** *14,* 4222–4225. doi:10.1021/ol3019055
23. Miyamae, N.; Watanabe, N.; Moritaka, M.; Nakano, K.; Ichikawa, Y.; Kotsuki, H. *Org. Biomol. Chem.* **2014,** *12,* 5847–5855. doi:10.1039/c4ob00733f
24. Luo, C.; Jin, Y.; Du, D.-M. *Org. Biomol. Chem.* **2012,** *10,* 4116–4123. doi:10.1039/c2ob07191f
25. Kamito, Y.; Masuda, A.; Yuasa, H.; Tada, N.; Itoh, A.; Nakashima, K.; Hirashima, S.-i.; Koseki, Y.; Miura, T. *Tetrahedron: Asymmetry* **2014,** *25,* 974–979. doi:10.1016/j.tetasy.2014.05.009
26. Castro, E. A. *Chem. Rev.* **1999,** *99,* 3505–3524. doi:10.1021/cr990001d
27. Hupe, D. J.; Jencks, W. P. *J. Am. Chem. Soc.* **1977,** *99,* 451–464. doi:10.1021/ja00444a023
28. Pan, Y.; Kee, C. W.; Jiang, Z.; Ma, T.; Zhao, Y.; Yang, Y.; Xue, H.; Tan, C.-H. *Chem. – Eur. J.* **2011,** *17,* 8363–8370. doi:10.1002/chem.201100687
29. Mała, Ż. A.; Janicki, M. J.; Góra, R. W.; Konieczny, K. A.; Kowalczyk, R. *Adv. Synth. Catal.* **2023,** *365,* 3342–3352. doi:10.1002/adsc.202300636
30. Liu, H.-J.; Oppong, I. V. *Can. J. Chem.* **1982,** *60,* 94–96. doi:10.1139/v82-017
31. Ye, W.; Jiang, Z.; Zhao, Y.; Goh, S. L. M.; Leow, D.; Soh, Y.-T.; Tan, C.-H. *Adv. Synth. Catal.* **2007,** *349,* 2454–2458. doi:10.1002/adsc.200700326
32. Van Eldik, R.; Asano, T.; Le Noble, W. J. *Chem. Rev.* **1989,** *89,* 549–688. doi:10.1021/cr00093a005
33. Drljaca, A.; Hubbard, C. D.; van Eldik, R.; Asano, T.; Basilevsky, M. V.; le Noble, W. J. *Chem. Rev.* **1998,** *98,* 2167–2290. doi:10.1021/cr970461b
34. Schettino, V.; Bini, R. *Chem. Soc. Rev.* **2007,** *36,* 869–880. doi:10.1039/b515964b
35. Kwiatkowski, P.; Dudziński, K.; Łyżwa, D. *Org. Lett.* **2011,** *13,* 3624–3627. doi:10.1021/ol201275h
36. Dalpozzo, R.; Bartoli, G.; Bencivenni, G. *Symmetry* **2011,** *3,* 84–125. doi:10.3390/sym3010084
37. Song, C. E.; Park, S. J.; Hwang, I.-S.; Jung, M. J.; Shim, S. Y.; Bae, H. Y.; Jung, J. Y. *Nat. Commun.* **2019,** *10,* 851. doi:10.1038/s41467-019-08792-z
38. Ahrendt, K. A.; Borths, C. J.; MacMillan, D. W. C. *J. Am. Chem. Soc.* **2000,** *122,* 4243–4244. doi:10.1021/ja000092s
39. Kowalczyk, R.; Boratyński, P. J.; Wierzba, A. J.; Bąkowicz, J. *RSC Adv.* **2015,** *5,* 66681–66686. doi:10.1039/c5ra09631f
40. Yang, W.; Drueckhammer, D. G. *J. Am. Chem. Soc.* **2001,** *123,* 11004–11009. doi:10.1021/ja010726a
41. Mayer, R. J.; Allihn, P. W. A.; Hampel, N.; Mayer, P.; Sieber, S. A.; Ofial, A. R. *Chem. Sci.* **2021,** *12,* 4850–4865. doi:10.1039/d0sc06628a
42. Sanders, J. N.; Jun, H.; Yu, R. A.; Gleason, J. L.; Houk, K. N. *J. Am. Chem. Soc.* **2020,** *142,* 16877–16886. doi:10.1021/jacs.0c08427
43. Wang, X.; Reisinger, C. M.; List, B. *J. Am. Chem. Soc.* **2008,** *130,* 6070–6071. doi:10.1021/ja801181u
44. Lifchits, O.; Mahlau, M.; Reisinger, C. M.; Lee, A.; Farès, C.; Polyak, I.; Gopakumar, G.; Thiel, W.; List, B. *J. Am. Chem. Soc.* **2013,** *135,* 6677–6693. doi:10.1021/ja402058v
45. Wang, X.; Ji, Z.; Liu, J.; Wang, B.; Jin, H.; Zhang, L. *Acta Chim. Sin. (Chin. Ed.)* **2023,** *81,* 64–83. doi:10.6023/a22100422
46. Dajek, M.; Kubiak, P.; Bąkowicz, J.; Dziuk, B.; Kowalczyk, R. *ChemRxiv* **2024**. doi:10.26434/chemrxiv-2023-nl054-v2
47. Kralj, M.; Lukin, S.; Miletić, G.; Halasz, I. *J. Org. Chem.* **2021,** *86,* 14160–14168. doi:10.1021/acs.joc.1c01817

BEILSTEIN JOURNAL OF ORGANIC CHEMISTRY

Asymmetric organocatalytic synthesis of chiral homoallylic amines

Nikolay S. Kondratyev[*1,2] and Andrei V. Malkov[*1]

Review

Open Access

Address:
[1]Department of Chemistry, Loughborough University, Loughborough, LE11 3TU, UK and [2]Faculty of Science and Engineering, University of Wolverhampton, Wolverhampton, WV1 1LY, UK

Email:
Nikolay S. Kondratyev[*] - n.kondratyev@lboro.ac.uk;
Andrei V. Malkov[*] - A.Malkov@lboro.ac.uk

* Corresponding author

Keywords:
asymmetric catalysis; asymmetric synthesis; chiral amines; organicatalysis; rearrangement

Beilstein J. Org. Chem. **2024,** *20,* 2349–2377.
https://doi.org/10.3762/bjoc.20.201

Received: 18 June 2024
Accepted: 30 August 2024
Published: 16 September 2024

This article is part of the thematic issue "New advances in asymmetric organocatalysis II".

Guest Editor: R. Šebesta

Abstract

In recent decades, the chiral allylation of imines emerged as a key methodology in the synthesis of alkaloids and natural products with 4-, 5- and 6-membered cyclic amine motifs. Initially reliant on stoichiometric reagents, synthetic chemists predominantly used *N*-substituted chiral imines, organometallic chiral reagents and achiral reagents with an equimolar chiral controller. However, recent years have witnessed the rise of asymmetric transition-metal catalysts and, importantly, organocatalytic allylation, reshaping the landscape of modern synthetic chemistry. This review explores the latest developments in the asymmetric allylation of imines, encompassing cutting-edge advances in hydrogen-bond catalysis and non-classical approaches. Furthermore, practical examples showcasing the application of these innovative methodologies in total synthesis are presented.

Introduction

Nitrogen-containing organic compounds (sometimes referred to as alkaloids due to their basic properties) are of critical importance in medicinal chemistry because of their unique binding properties to biomolecules [1]. Out of 55 drug candidates, approved by the FDA in 2023, 28 (51%) are nitrogen-containing organic compounds, with many featuring amino groups adjacent to a stereogenic centre. Some reports suggest that 75% of all FDA-approved compounds are alkaloids [2]. The industrial production of amines on a million-ton scale underscores the significance of methods for their synthetic utilisation [3]. Both, nature and humanity utilise ammonia as the central precursor to introduce nitrogen into organic compounds. Nature achieves this through enzymatic processes, sourcing ammonia from geological origins or directly from the air [4], while humanity relies on the Haber–Bosch process and the rich toolkit of advanced organic synthesis [5]. Homoallylic amines occupy a sig-

nificant niche in alkaloid synthesis as they frequently appear as key intermediates in syntheses of the various nitrogen-containing natural products [6-14]. Additionally, they can be directly prepared by combining three readily accessible synthons: an amine, an allyl nucleophile, and a carbonyl compound (Scheme 1) [15,16]. A selection of structural motifs accessible via homoallylic amines is shown in Scheme 1.

Despite several reviews on homoallylic amine syntheses being published [17-23], none have focused specifically on organocatalytic approaches, which are particularly important for medicinal chemistry due to their greener credentials. Given the wide range of organocatalytic methods for synthesising homoallylic amines developed in the past decade, it is essential to provide a comprehensive overview of this significant topic.

Review

Asymmetric allylation with boron-based reagents

The research on the metal-free, asymmetric organocatalytic allylation of acylimines was pioneered in 2007 by Schaus and co-workers [24]. In their elegant approach, high enantioselectivities (90–99% ee) and good yields (75–94%) have been achieved on a wide range of aromatic and aliphatic *N*-acylimines **2** using chiral 3,3'-diaryl-BINOL **3** as catalyst (Scheme 2).

The reaction proved to be highly tolerant to the nature of the R^1 substituent in imine **2**, demonstrating high yields and enantioselectivities for both electron-rich and electron-poor *N*-benzoylarylimines, aliphatic *N*-benzoylimines, and bulkier *N*-carboxyalkylimines. However, less sterically hindered *N*-carboxyalkyl- and *N*-carbamoylimines showed a significant drop in both enantioselectivity and yield.

The observed enantioselectivity was attributed to the chair-like transition state where the organoboron reagent **1** exchanges one isopropoxy group for one of the BINOL **3** oxygen atoms, whereas the free OH group of the BINOL forms a hydrogen bond to the carbonyl of substrate **2**. The flanking phenyl groups on the BINOL facilitate recognition between two enantiotopic faces of acylimine **2**, exposing only one face to the attack by the allyl group. The replacement of one isopropoxy (iPrO) group between allylboronate **1** with BINOL was confirmed by ESI-MS and NMR analysis of the reaction mixture. Interestingly, both (*E*)- and (*Z*)-crotyl boronates **6** and **8** almost exclusively produced *anti*-homoallylamine **7**, with (*E*)-**6** being slightly more efficient. This was explained by the reaction switching from the chair-like TS in (*E*)-crotylation to the boat-like TS in (*Z*)-crotylation. The developed methodology was successfully applied for the total synthesis of Maraviroc, an HIV-1 drug of the CCR5-receptor antagonists class that was approved by the FDA in 2007.

In 2013, a significant work was published by Hoveyda and co-workers [6], who demonstrated that small organic molecules like hindered aminophenol **11** can serve as highly efficient and versatile catalysts in the asymmetric addition of organoboron reagents to imines (Scheme 3). An intermolecular hydrogen bonding between a non-rigid organocatalyst and a non-rigid

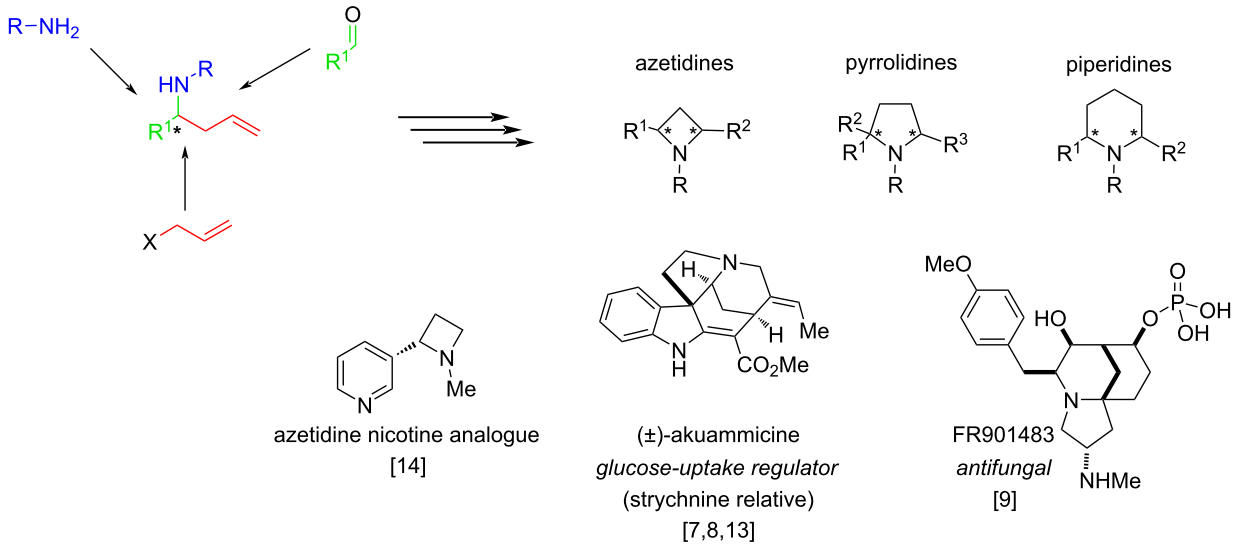

Scheme 1: The position of homoallylic amines in the landscape of alkaloid and nitrogen compounds syntheses.

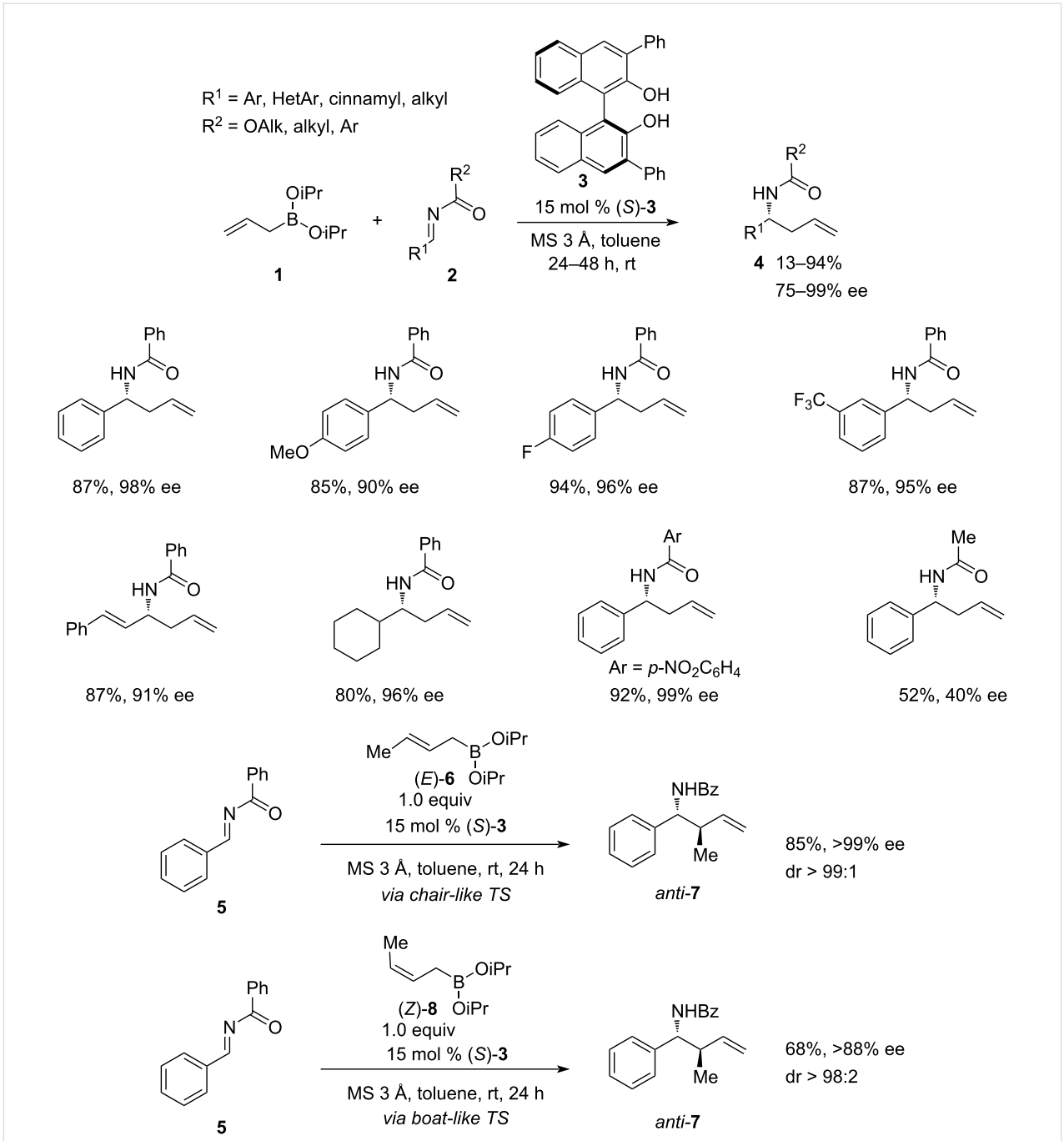

Scheme 2: 3,3'-Diaryl-BINOL-catalysed asymmetric organocatalytic allylation of acylimines [24].

substrate was shown to play a key role in assembling a configurationally stable transition structure. As a result, this approach unveiled the highly enantioselective nucleophilic addition of primary (**10**), secondary, and even tertiary allylboronates, as well as allenylboronates to a broad set of imines, bearing the *N*-phosphinoyl group. The new approach allowed the activation of both the substrate and the reagent using aminophenol organocatalyst **11**. It was proposed, that the internal hydrogen bond between the catalyst **11** and the P=O fragment of the protecting group of imine **9** is responsible for the observed high enantioselectivities (76–98% ee). The scope included a wide range of substrates, such as aromatic, heteroaromatic, aliphatic, and α,β-unsaturated imines **9**.

However, with ethynylimines **12**, the enantioselectivity dropped to a modest level. In addition, the reaction

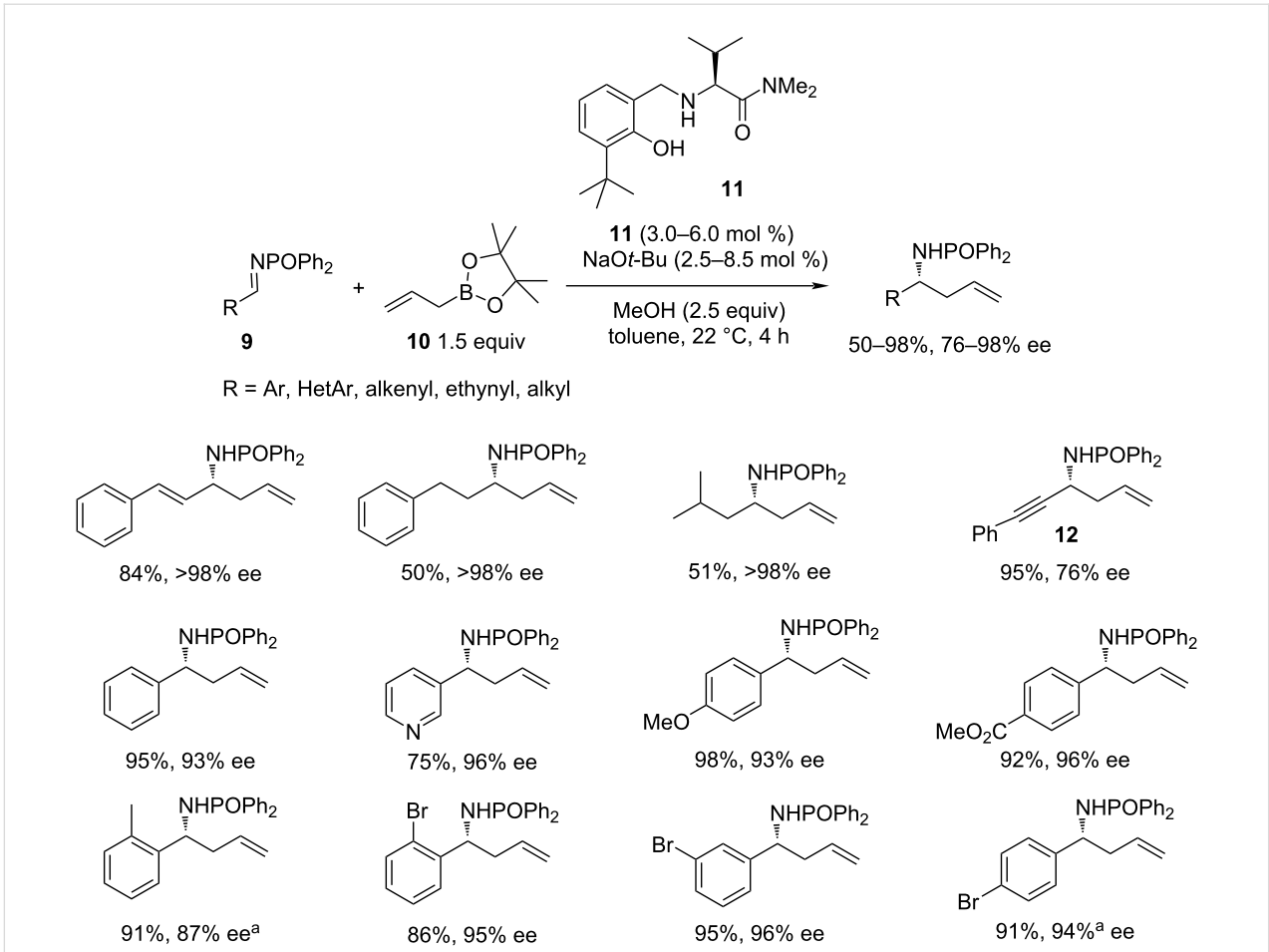

Scheme 3: Aminophenol-catalysed reaction between *N*-phosphinoylimines and pinacol allylboronic ester. Imine scope [6]. [a]Reaction time: 6 h.

with sterically hindered tertiary allylboronates, such as the chiral (*R*)-α-cyclohexyl-α-methyl-allylboronate required the use of catalytic amounts of zinc *tert*-butoxide as an activator.

Interesting examples of a direct asymmetric allylation of indoles **15** (Scheme 4) and 3,4-dihydroisoquinolines **22** (Scheme 5) with geranyl- and prenylboronic acids **14** in the presence of BINOL derivatives were reported by Szabó [25]. In the case of 3-methylindole, the methodology enabled simultaneous construction of homoallylamine scaffolds, exemplified by compounds **16**–**20** with up to 3 contiguous stereocentres, including a quaternary centre in moderate to high yields (60–94%) with 90–99% ee and dr in the range from 97:3 to >99:1 (Scheme 4).

The selectivity of the reaction arises from the reversible coordination of BINOLs **13** or **21** to the prenyl- or geranylboronic acids **14**, favouring one of the four possible chair-like transition states.

The reaction scope for indoles **15** was demonstrated on a limited set of 5-methoxyindole, 5-bromoindole, and 4-indolylpinacol boronates reacting with *E*- and Z-geranyl and prenylboronic acids **14** with yields in the range of 60–94%. *Z*-Geranylboronic acid (**14**, R = prenyl) proved to be less reactive, while stereoselectivities remained high (Scheme 4).

A modified procedure was developed for 3,4-dihydroisoquinolines **22**, which necessitated the use of 40 mol % of 2-(2-pyridyl)phenol (**23**) as an activator, 3 equivalents of HFIP and a slightly different catalyst, 3,3'-bis(3,5-bis(trifluoromethyl)phenyl)-BINOL **21** at 20 mol % loading (Scheme 5).

Interestingly, the reaction showed an opposite trend and worked better with *Z*-geranylboronic acid (**14**). The scope was tested over a few dihydroisoquinolines, including 7-bromo-3,4-dihydroisoquinoline and 6,7-dimethoxy-3,4-dihydroisoquinoline leading to **24** and **25**, respectively. The yields varied between 42–97% and were lower for the electron-rich substrates and higher for the electron-deficient substrates. The enantioselectiv-

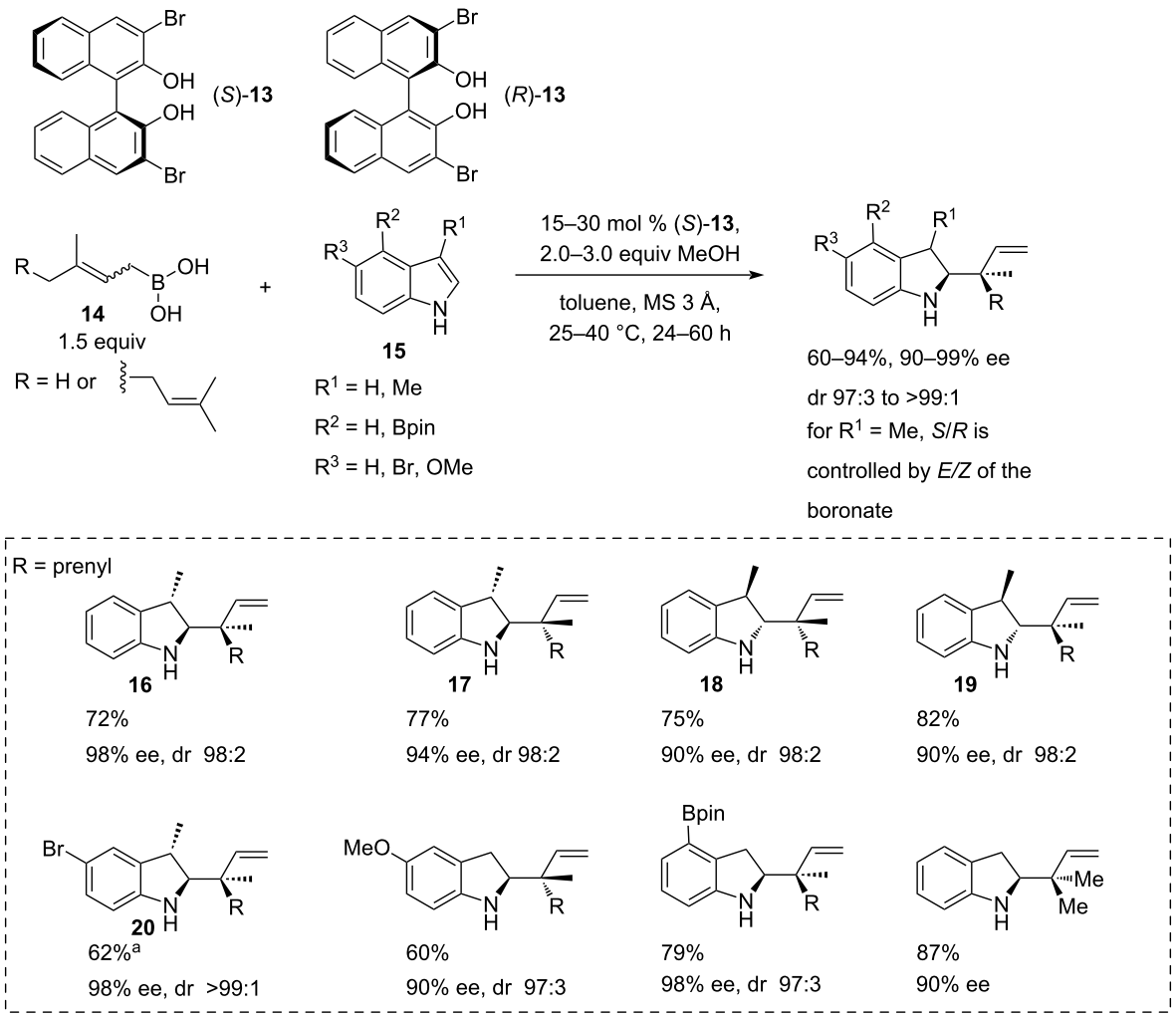

Scheme 4: Asymmetric geranylation and prenylation of indoles catalysed by (*R*)- or (*S*)-3,3'-dibromo-BINOL [25]. [a]Absolute configuration was confirmed by a single crystal XRD of the corresponding hydrochloride salt.

ities were in the range of 82–97% and were lowest for the prenylation, and highest for *Z*-geranylboronic acid. The absolute configurations of the products were established by X-ray crystallography of the hydrochloride salts of the corresponding bromoindole and bromodihydroisoquinoline derivatives **20** and **24**, which supported the hypotheses regarding the selectivity-determining transition states arrangement.

It is important to note, that boronic acids **14** are highly sensitive to oxidation by air and could only be purified in air-free conditions and stored in airtight containers. Additionally, prenylboronic acid (R = H) was synthesised in only 31% yield. Given the 1.5 equiv loading of the boronic acids in the allylation protocol, the overall atom economy is not ideal.

Asymmetric allylation of in situ-formed imines catalysed by chiral BINOLs received further development in the work of Schaus [26]. The new methodology used bench-stable allyl-1,3,2-dioxaborinane (**27**) in the reaction with preformed crude *N*-aryl-, *N*-benzyl- and *N*-allylimines in the presence of 2–8 mol % of the relatively simple 3,3'-Ph_2-BINOL catalyst **3** at 50 °C in a microwave reactor at 10 W irradiation for 1 hour to afford amines **26** (Scheme 6).

The study explored a broad range of *p*-methoxyphenyl (PMP)imines derived from aryl, heteroaryl and alkyl aldehydes (including ethyl glyoxylate), demonstrating yields of 57–98% and high enantioselectivity of 90–98%. Screening of aldehyde and amine components indicated that the method is generally tolerant to diverse *N*-aryl-, *N*-heteroaryl-, and *N*-benzylimines. Additionally, the authors conducted asymmetric crotylations of *N*-(PMP)- and *N*-benzylimines using *E*- and *Z*-crotyldioxaborinanes **29** and **30** to furnish amines **28** (Scheme 7). With (*E*)-crotyldioxaborinane **29**, the *anti*-products **31** and **33** were

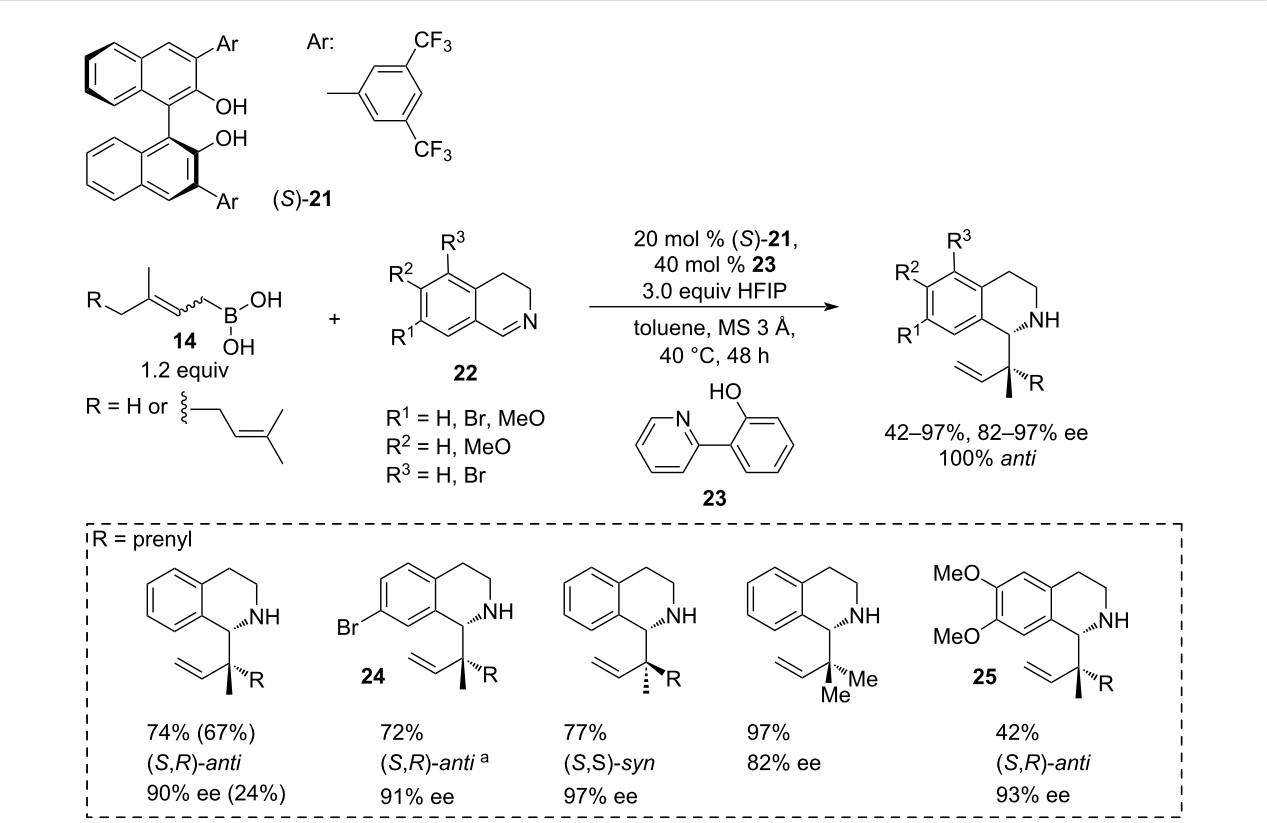

Scheme 5: (*R*)-3,3'-Di(3,5-di(trifluoromethyl)phenyl-BINOL-catalysed asymmetric geranylation and prenylation of dihydroisoquinolines [25]. [a]Absolute configuration was established by single crystal XRD of the corresponding hydrochloride salt.

achieved exclusively (dr > 20:1) in good yields (83% and 89%) and enantioselectivity (96% and 90%). On the other hand, the reactions with (*Z*)-crotyldioxaborinane **30** resulted in lower yields (33% for **32** and 61% for **34**). However, the diastereoselectivity towards the *syn* products remained notably high (9:1 and >20:1), along with impressive enantioselectivity levels (92% and 98% ee). A slight loss of diastereoselectivity in the reaction of the PMP-imine with (*Z*)-crotyldioxaborinane **30** was attributed to the spontaneous isomerisation of the imine to the *cis*-isomer. The crotylboronates were synthesised from the respective *cis* and *trans*-butenes by deprotonation followed by reaction with triisopropylborate [27], therefore the presence of *E* isomer in the *Z*-product **30** cannot be excluded.

Chiral BINOL-derived phosphoric acids have been known since the 1970s as industrially relevant chiral counterions for the resolution of chiral amines [28]. However, it was not until 2004 that they were recognised as efficient chiral Brønsted acid organocatalysts for asymmetric Mannich reactions [29].

Malkov and co-workers revealed [30] that (*R*)-TRIP can act as a very efficient catalyst for the kinetic resolution of racemic, configurationally stable *sec*-allylboronates (±)-**35** (Scheme 8A). Using 2.5 equivalents of racemic boronate **35**, the reaction with aldehydes produced enantioenriched *Z*-homoallylic alcohols **36**. While this protocol was effective for aldehydes, it proved challenging to perform it with *N*-substituted aldimines.

This was later addressed by the same researchers [15], who developed an organocatalytic kinetic resolution of secondary boronates to furnish bench-stable homochiral (*S*)-**35**. The latter were then employed in the asymmetric allylation of in situ-formed primary aldimines **37**, leading directly to the unprotected chiral (*S*,*Z*)-homoallylic amines **38** in high yields and with an excellent retention of the enantiopurity (Scheme 8B). The method remains the only direct *Z*-selective crotylation to attain enantioenriched unprotected homoallylic amines, and the only example of an effective kinetic resolution of chiral secondary allylboronates **35**.

In late 2020, an important method for synthesising enantiopure terminal (*E*)-trifluoromethyl homoallylic amines **44** was described by Szabó and co-workers (Scheme 9) [31]. This methodology is based on the use of enantiopure α-trifluoromethylallylboronic acids **43**, obtained by a 3,3'-diiodo-BINOL **39**-catalysed asymmetric $CH(CF_3)$-homologation of dehydrated vinyl-

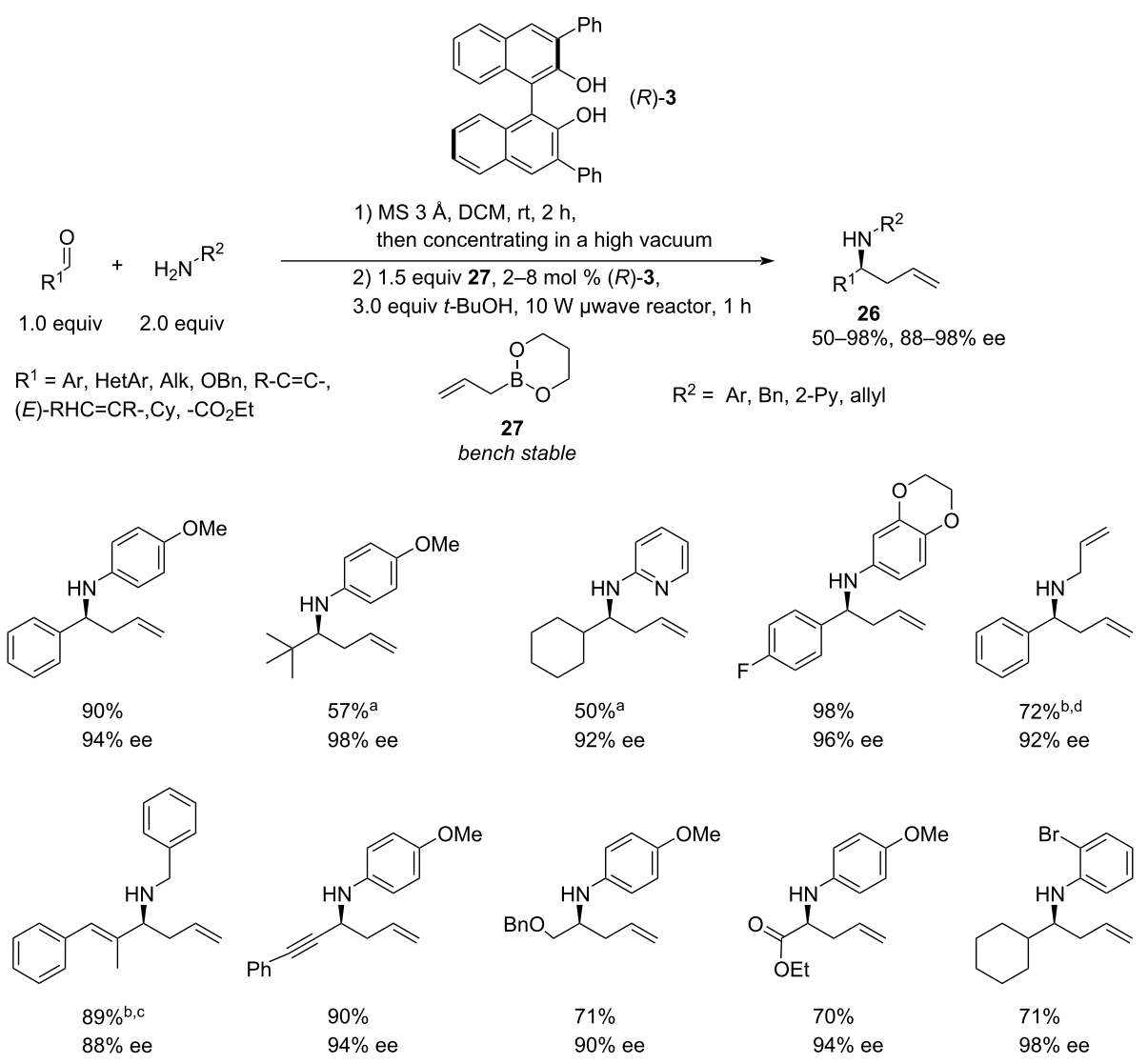

Scheme 6: Microwave-induced one-pot asymmetric allylation of in situ-formed arylimines, catalysed by (*R*)-3,3'-diphenyl-BINOL. Aldehyde and amine scope [26]. [a]The reaction was conventionally heated at 50 °C for 24 hours instead of microwave irradiation. [b]1.0 equiv amine was used. [c]8 mol % BINOL catalyst was used. [d]4 mol % BINOL catalyst was used.

boronic acids **40** with trifluoromethyl diazomethane at 40 °C. The resulting enantioenriched transient (α-trifluoromethyl)allylboronic acid diethyl esters **41** were converted into the chromatographically stable 1,8-diaminonaphthalene derivatives **42**, which after hydrolysis and extraction into toluene, were reacted with indole, 3-methylindole, 3,4-dihydroisoquinoline, and benzoyl hydrazone ethyl glyoxylate ester to afford terminal (*E*)-trifluoromethyl homoallylic amines **44** with up to 3 adjacent stereocentres with high to excellent enantioselectivities (89–98% ee) and low to moderate yields (48–72%).

The homologation step proceeds via the stereoretentive 1,2-migration of the vinyl group from the tetracoordinated boron to the highly electrophilic carbon of the diazomethane, concerted with the elimination of the nitrogen molecule. The BINOL catalyst **39** forming arylboronate species, enables the shift to occur asymmetrically. In the second step, the hydrolysis of unreactive diaminonaphthalene derivative **42** gives the poorly reactive and highly air-sensitive trifluoromethylallylboronic acid **43**, but after the dehydration forms boroxine with dramatically increased reactivity towards C=N electrophiles. Because of the small steric size of the (BO_2) group, the reaction is highly selective towards (*E*)-α-trifluoromethyl homoallylic amine **44**, which otherwise is difficult to obtain in a regiospecific manner. It has to be noted though that manipulations with air-sensitive materials **41** and **43** during the reaction sequence result in reduced total yields of 29–56%. Also, the reaction scope is currently represented by only 4 examples.

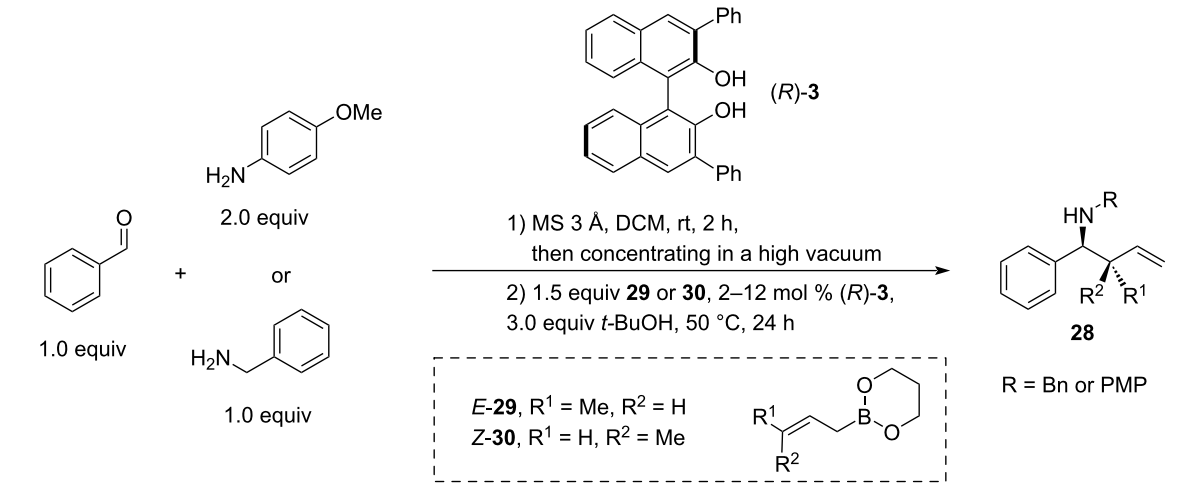

RNH_2	equiv RNH_2 (per 1 equiv PhCHO)	borinane	mol % BINOL	product	yield	dr	ee
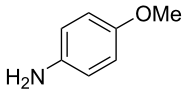	2.0 equiv	**29**	3.0 mol %	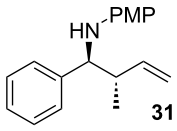 **31**	83%	47:1	96%
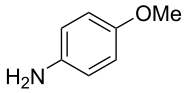	2.0 equiv	**30**	6.0 mol %	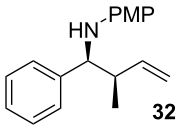 **32**	33%	9:1	92%
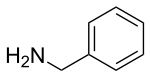	1.0 equiv	**29**	12.0 mol %	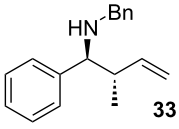 **33**	89%	ND[a]	90%
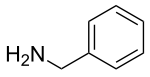	1.0 equiv	**30**	12.0 mol %	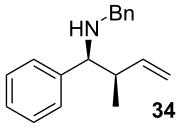 **34**	61%	ND[a]	98%

Scheme 7: Microwave-induced one-pot asymmetric allylation of in situ-formed arylimines, catalysed by (*R*)-3,3'-diphenyl-BINOL. Crotylation studies [26]. [a]Not determined, but estimated to be high; racemate did not produce 4 clear separate peaks on chiral HPLC.

Asymmetric allylation with organosilicon and organotin-based reagents

The first example of a successful organocatalytic enantioselective Hosomi–Sakurai reaction of imines using allyltrimethylsilane was reported by List and co-worker [32]. In this approach, the direct synthesis of Fmoc-protected homoallylic amines **47** was achieved by a three-component coupling of allyltrimethylsilane (**46**) with the in situ-formed *N*-Fmoc-aryl- and -alkylimines, catalysed by a chiral disulfonimide **45** (Scheme 10).

Since allyltrimethylsilane (**46**) belongs to the type 2 allylation reagents [33], the nucleophilic addition proceeds via an open transition state (Figure 1). Two possible mechanistic pathways were proposed, where the Fmoc-imine is activated either with a Brønsted or Lewis acid. In both cases, the allyl group of the silane reagent **46** attacks from the *Re*-face of the imine, leading to the major (*R*)-enantiomer of **47**. Based on the experimental data obtained with the preformed silylated catalyst and preformed imine, the Lewis acid activation mode appears to be the most plausible.

Interestingly, chiral phosphoric acids failed to catalyse this reaction, but the use of chiral sulphonimide **45** afforded 82–97% ee and 65–84% yield on a set of aromatic and aliphatic aldehydes. The low reactivity of the allyltrimethylsilane (**46**) re-

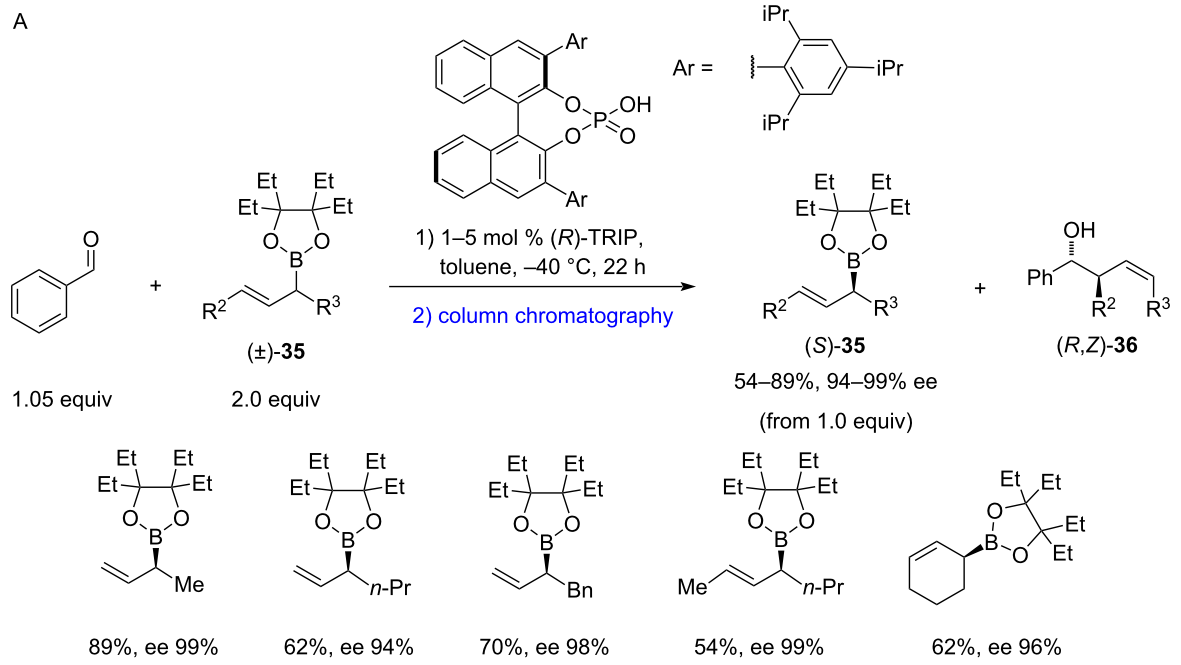

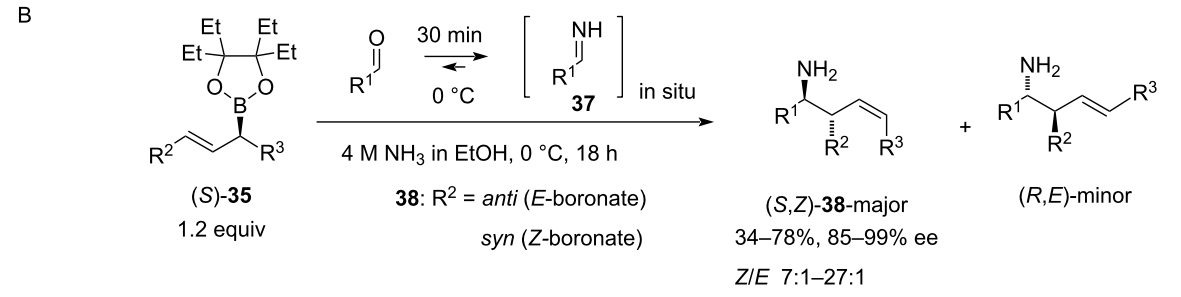

entry	R^1	R^2	R^3	*T*, °C	yield	*Z*/*E*	ee (major)
1	Ph	H	Me	0 °C	76%	8:1	97%
2	Cy	H	Me	25 °C	34%	8:1	91%
3	4-FC_6H_4	H	Me	0 °C	53%	7:1	99%
4	3-$MeOC_6H_4$	H	Me	0 °C	78%	9:1	98%
5	2-$MeOC_6H_4$	H	Me	25 °C	61%	10:1	85%
6	Ph	H	Bn	0 °C	62%	27:1	97%
7	Ph	*anti*-Me	*n*-Pr	0 °C	71%	11:1	99%
8	Ph	*syn*-$(CH_2)_3$-		0 °C	53%	*Z*	95%
9	(*E*)-PhC=CH	H	*n*-Pr	0 °C	55%	10:1	94%

Scheme 8: Kinetic resolution of chiral secondary allylboronates [15,30].

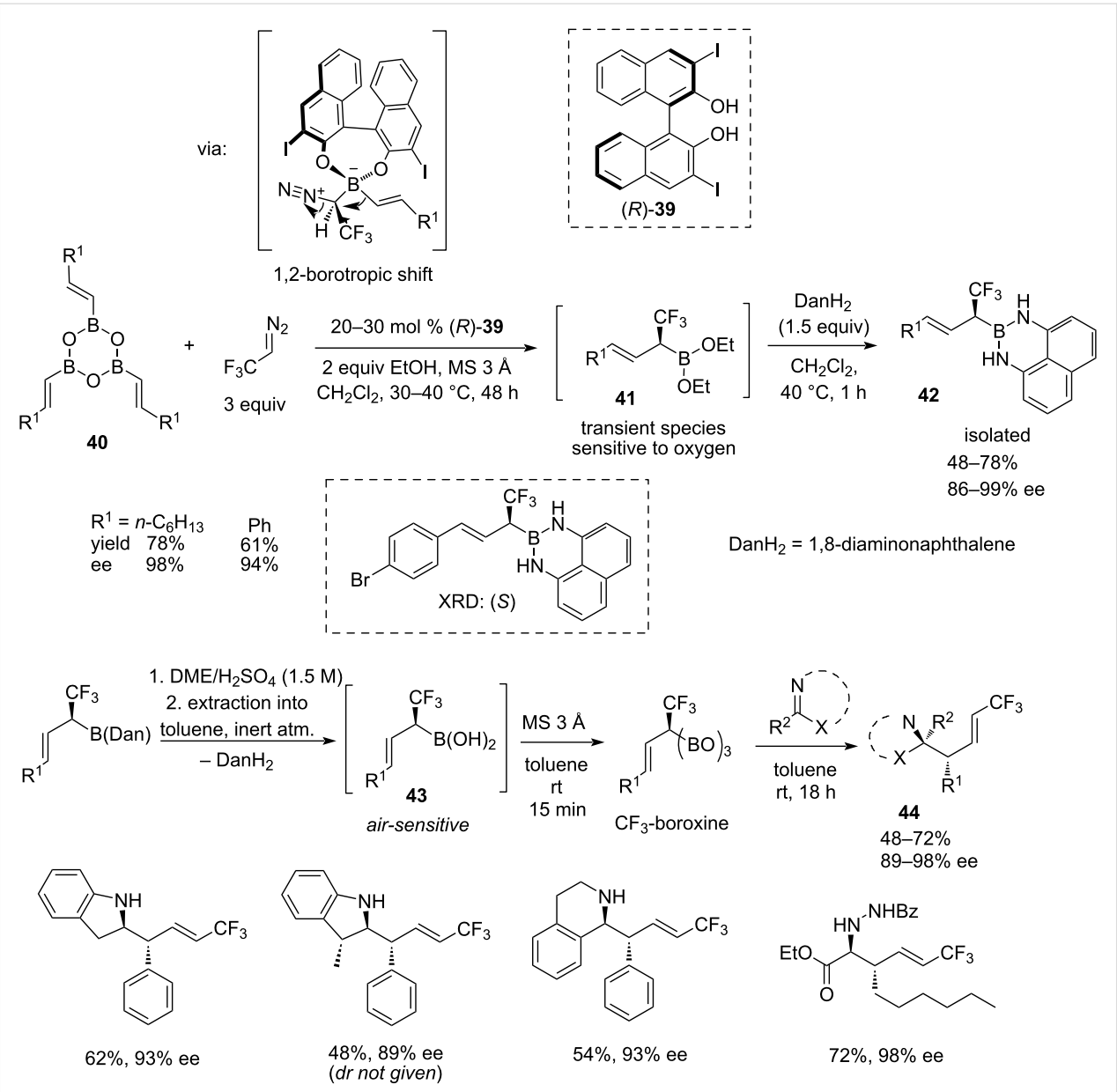

Scheme 9: (*E*)-Stereospecific asymmetric α-trifluoromethylallylation of cyclic imines and hydrazones [31].

quired an extended reaction time (10 days). The relatively low activity of the sulphonamide catalyst **45** also necessitates higher loadings of 10 mol % (Scheme 10).

In 2019, a novel catalytic approach to homoallylic *N*-carbamoylamino esters **50** was described by Jacobsen and co-workers [34]. This allylation method involves squaramide **51**-catalysed chloride abstraction from readily accessible *N*-carbamoyl α-chloroglycinates **48** or **54** (Scheme 11) [35], with a simultaneous nucleophilic attack of allylsilane **49** (Scheme 11A) or allylstannane **55** (Scheme 11B). The reactions are highly sensitive to moisture and oxygen. Therefore, it was conducted under an inert atmosphere in anhydrous dichloromethane with 3 Å molecular sieves.

Benzyl carbamates **48** showed excellent enantioselectivities (90–97%) and moderate to high yields (58–94%) across a wide range of allylation reagents **49** on a submillimolar scale, including 2-methylcrotylsilane (product **52**) and disubstituted cyclic silanes (such as the silane, leading to **53**), locked in *syn*-conformation. For the 2,3-disubstituted allylation products such as **52** and **53**, the diastereomeric ratio spanned across 18:1 to >50:1. Notably, all 2,3-disubstituted silanes required an increased reaction temperature (–5 °C).

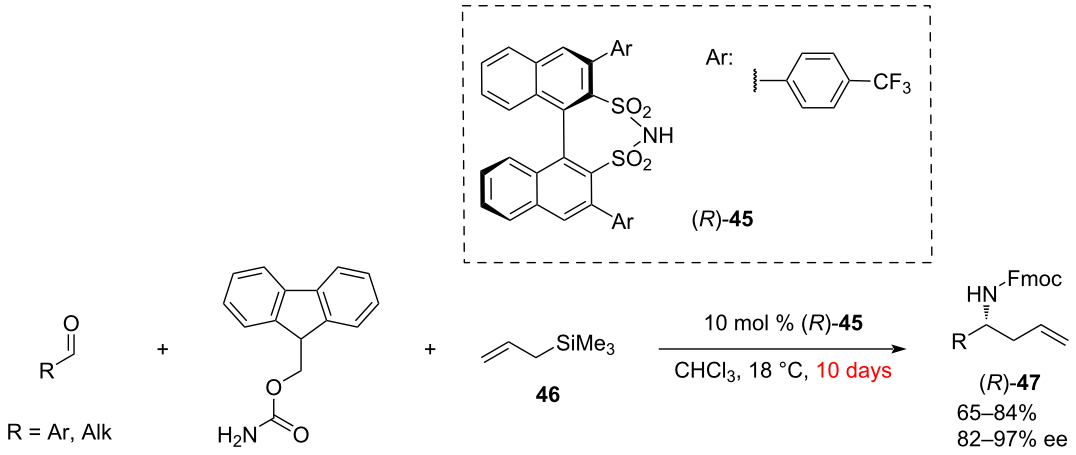

Scheme 10: Hosomi–Sakurai-type allylation of in situ-formed *N*-Fmoc aldimines [32].

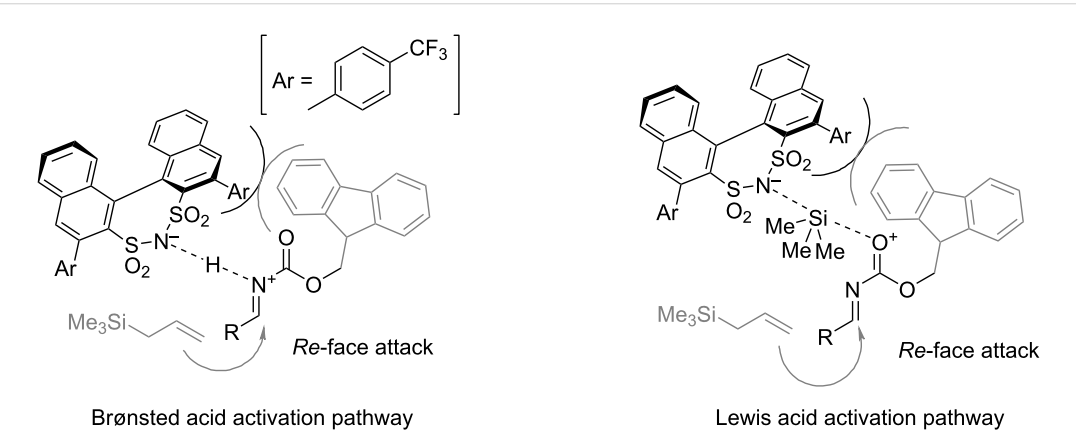

Figure 1: Two different pathways for the Hosomi–Sakurai reaction of allyltrimethylsilane with *N*-Fmoc aldimines.

A slightly different protocol was elaborated for *N*-Fmoc carbamates **54** using the same catalyst **51**. Instead of allylsilanes **49**, stannanes **55** were employed and the method proved effective in simple allylation, prenylation, and crotylation (**57**–**59**). The yields were also generally higher (87–95%) than with silanes. However, the reaction required an increased loading of stannanes **55** (3.0 or 4.0 equiv) and an increased reaction time (72 vs 36 hours). Also, higher loadings of catalyst **51** (5–10 mol %) were required to achieve the same level of enantioselectivity. It is noteworthy that selected recrystallised products showed 98–99% ee. Importantly, both silane and stannane-based protocols were successfully performed on a 5 mmol scale using substrates **52** and **59**. There was a slight loss in yield and a negligible decrease in stereoselectivity in the case of 2,3-dimethylallylation product **52**.

The limitations in the scope of this methodology include a poor stereoselectivity achieved with 5-membered cyclic 2,3-disubstituted silanes in contrast to the 6-membered analogues (**53**). A lower efficiency was recorded with 2-substituted allylsilanes bearing either a halogen or an alkyl group with terminal halogen or acetate. The 2-ethynylallylsilane decomposed in the reaction conditions, while simple allyltrimethylsilane was unreactive. Among allylstannanes, the (3-phenylallyl)tri-*n*-butylstannane was also unreactive. Interestingly, both tetraallylsilane and tetraallylstannane gave racemic products.

Optimisation of the catalysts structure revealed that the 3-phenanthrylpyrrolidine derivative provided superior yields and selectivities. Notably, the isomeric 9-phenanthrylpyrrolidines remained selective but gave noticeably lower yields. The methyl group, geminal to the phenanthryl, plays an important part in securing the enantioselectivity of the reaction by locking the catalyst in the more active and enantioselective *Z*-configuration (Figure 2).

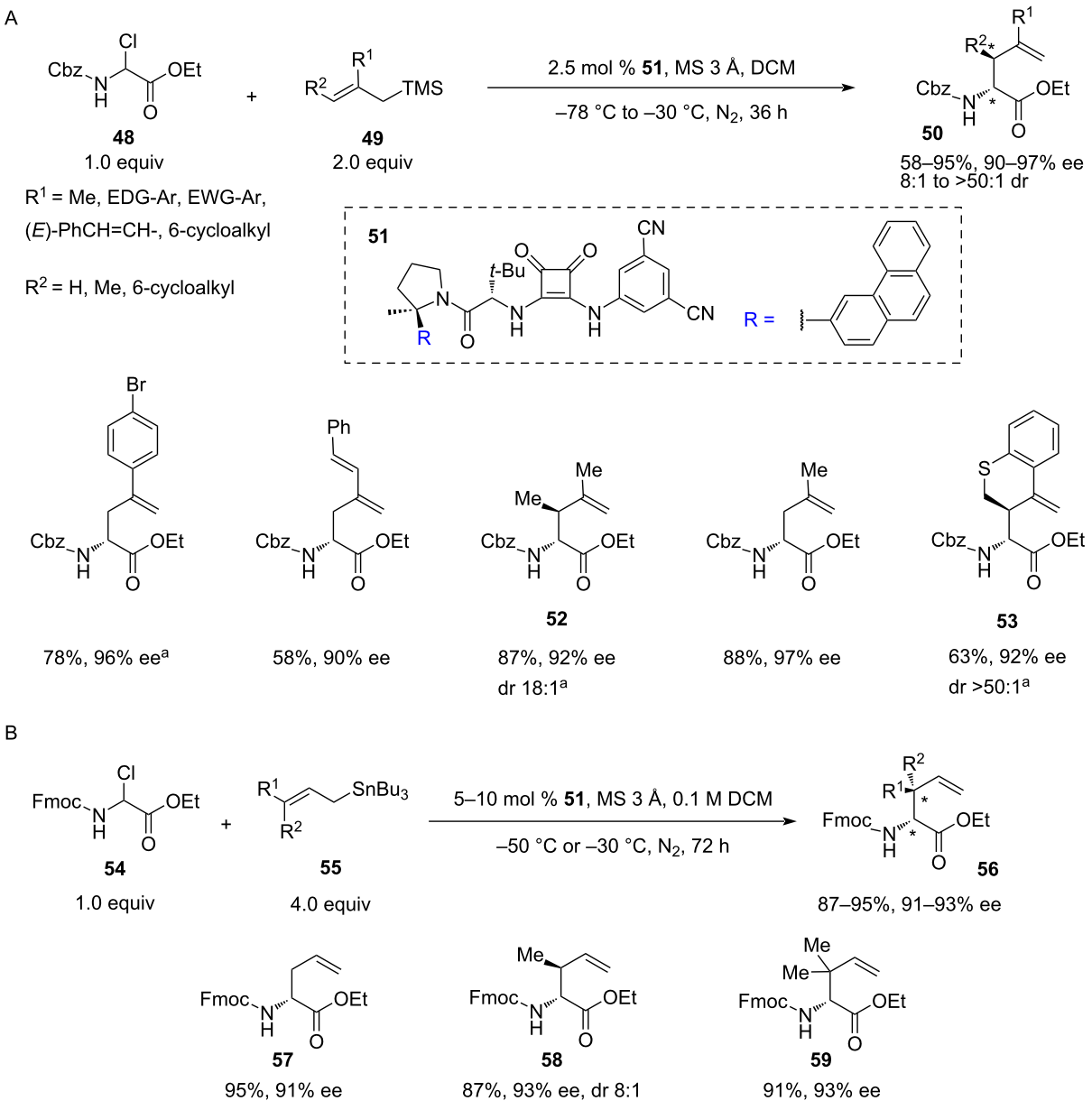

Scheme 11: Chiral squaramide-catalysed hydrogen bond-assisted chloride abstraction–allylation of *N*-carbamoyl α-chloroglycinates with trimethylsilane and tri-(*n*-butyl)stannane reagents [34]. [a]The reaction was conducted at –5 °C.

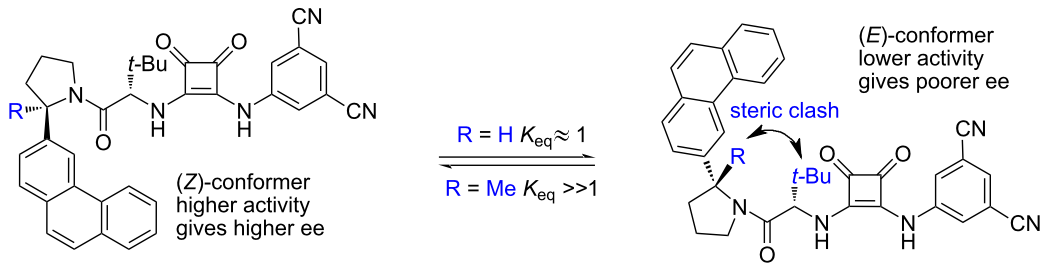

Figure 2: The pyrrolidine unit *gem*-methyl group conformational control in the squaramide-based catalyst [34].

Further, the authors found that H-bond donors featuring urea, thiourea, and guanidine motifs were either inactive or provided racemic mixtures. Among 3,5-dichloro-, 3,5-di(trifluormethyl)- and 3,5-dicyanophenylsquaramides, the latter proved to be the most active but all three provided a similar enantioselectivity.

Kinetic studies revealed that the reaction displayed the 1st order in both the allyl reagent and the glycinate substrate, which may indicate either a concerted S_N2 mechanism or S_N1 mechanism with the allyl nucleophile addition step as rate-determining. Interestingly, the authors observed a 0.55 order in the catalyst, which indicates that a substantial part of the catalyst forms a hydrogen-bonded dimer with $K_{diss} \approx 1000\ M^{-1}$ when not in the catalytic cycle, an observation that is in good agreement with previously obtained data on bisurea catalysts [36]. To further distinguish between the S_N1 and S_N2 mechanisms, the authors performed an in silico simulation of the non-catalysed reaction to determine the possible potential energy surface and found that concerted S_N2-key intermediate **60** must be at least 18.9 kcal/mol more favoured than a separated imine–chloride ion pair **61** attacked by the free allylsilane (Figure 3).

Altogether, the developed methodology can be formally viewed as a useful tool for the enantioselective synthesis of chiral α-carboxyl-2,3-disubstituted homoallylic amines **50** and **56** (Scheme 11). However, the high sensitivity of silanes **49** to air and moisture along with an increased toxicity of organotin compounds **55** may be considered challenging factors in its application on a larger scale.

In 2019, an interesting approach to the organocatalytic enantioselective allylation of imines was described by Ryu's group as a part of a wider asymmetric nucleophilic addition methodology [37]. The method is based on the use of 20 mol % of sterically hindered chiral oxazaborolidinium ion (COBI) **63**, that can be readily prepared from a relatively inexpensive commercially available derivative of L-proline, (*S*)-(−)-α,α-bis(3,5-dimethylphenyl)-2-pyrrolidinemethanol (**62**) (Scheme 12). This catalyst is capable of asymmetric activation of *N*-(2-hydroxyphenyl)imines through the reversible chelation to the *N*-(2-hydroxyphenyl) group, forming a rigid intermediate, while the aryl group of the oxaza-borolidinium ion is restricting the allyltributylstannane attack to only one enantioface of the imine C=N bond (Scheme 13, COBI–aldimine complex). The catalyst was used in the allylation of a wide range of aliphatic and aromatic *N*-(2-hydroxyphenyl)imines **64**, providing good to excellent yields (77–91%) and excellent enantioselectivities (90–96%) on a millimolar scale (Scheme 13).

It is worth noting the use of optimised minimal excess of allyltributyltin (**65**), which to some extent addresses the higher toxicity of trialkylstannanes compared to their silicon counterparts. The absolute configurations of homoallylamines **66** were

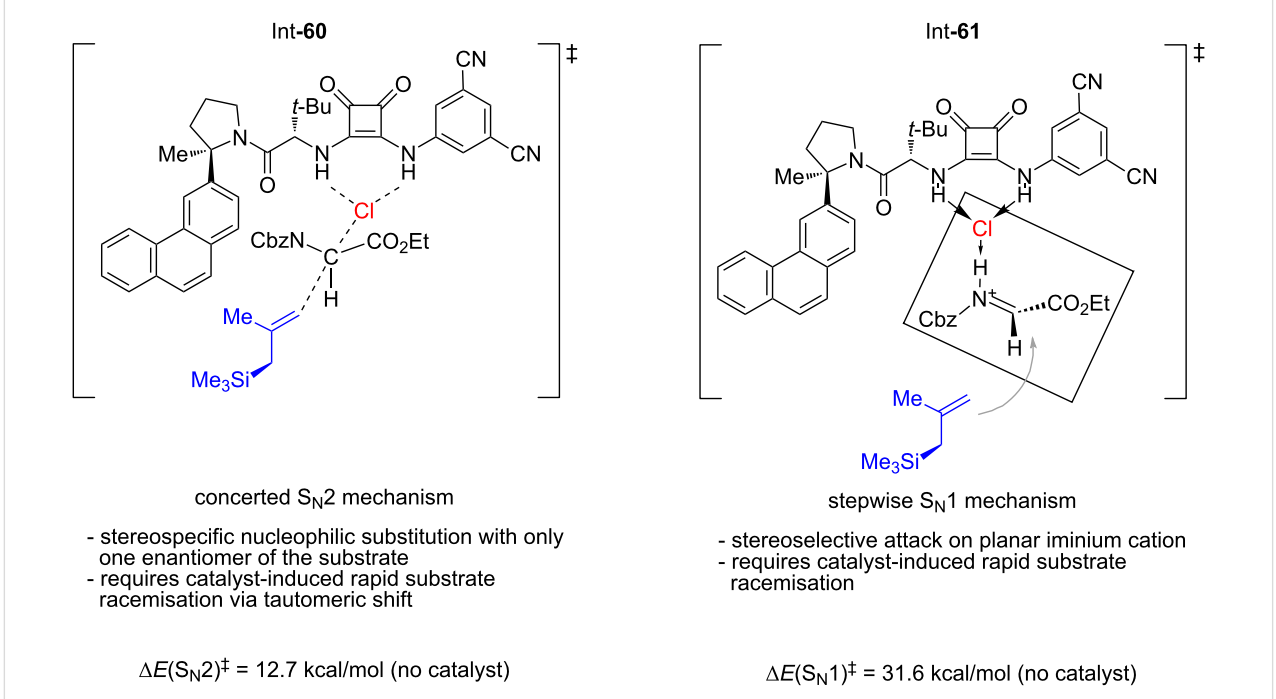

Figure 3: The energetic difference between the transition states of the two proposed modes of the reaction (S_N1 and S_N2 mechanisms). The concerted S_N2 mechanism is energetically more favoured [34].

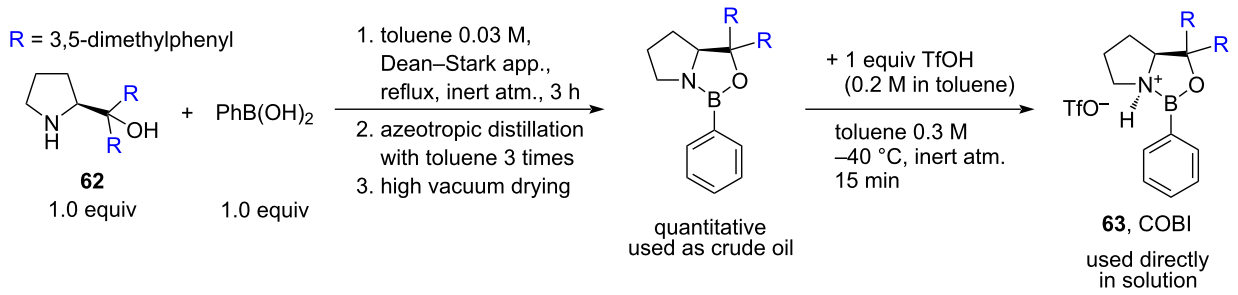

Scheme 12: One-pot preparation procedure for oxazaborolidinium ion (COBI) **63** [37].

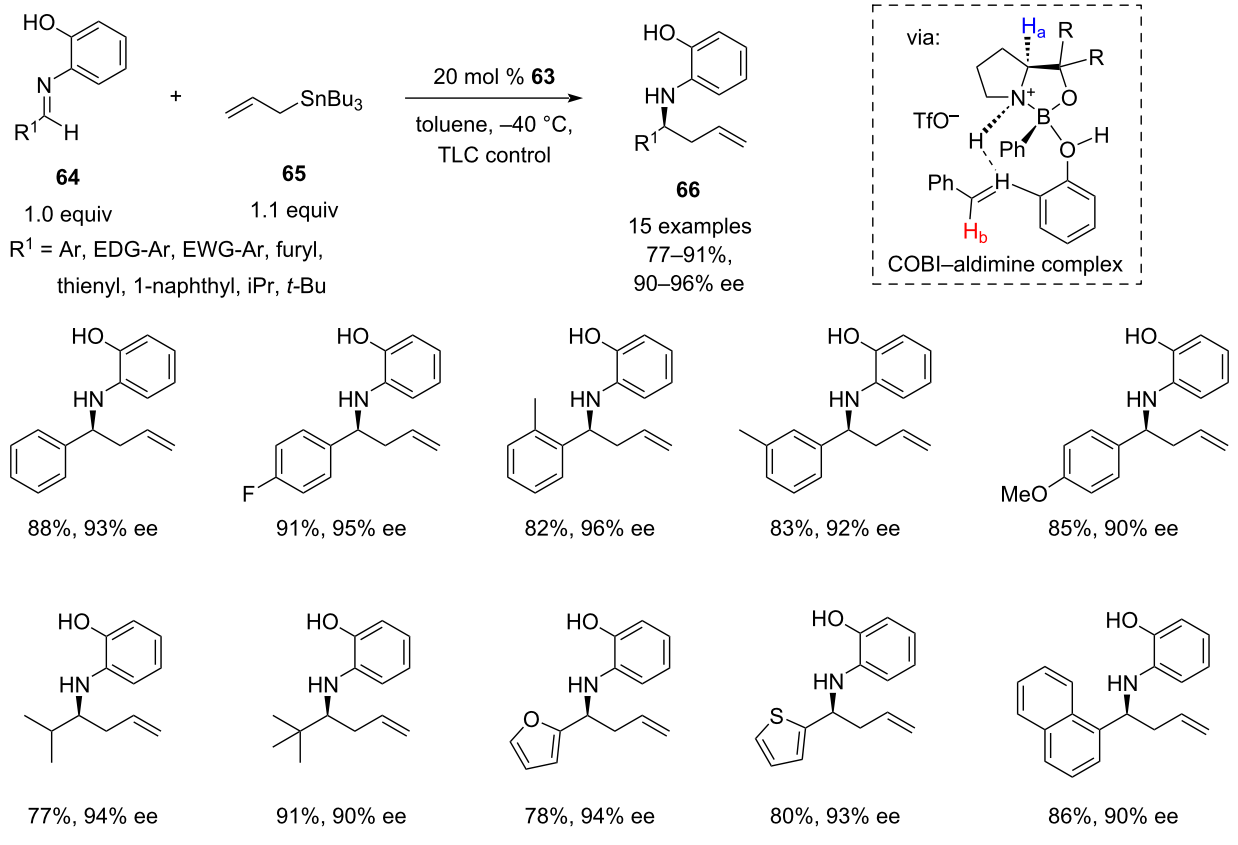

Scheme 13: Chiral oxazaborolidinium ion (COBI)-catalysed allylation of *N*-(2-hydroxy)phenylimines with allyltributyltin. Scope of the reaction [37].

assigned by analogy to **67**, the configuration of which was determined after removal of the *N*-aryl group and comparing the optical rotation with the literature values for the known enantiomer (*S*)-**69** (Scheme 14).

The proposed stereochemical model suggests, that the 2-aminophenol functionality in the substrates is a prerequisite for attaining high enantioselectivity in the allylation. Interestingly, the aldimines synthesised from 2-hydroxy-4-methylaniline produced inferior yields. While the *N*-aryl homoallylic amines **66** can be useful intermediates in total synthesis, the deprotected derivatives such as **69** are desired for the synthesis of natural products. Therefore, an easy-to-perform two-step deprotection procedure was developed that is based on methylation of the phenolic hydroxy group with an excess of MeI in acetone at rt (**68**), followed by oxidative cleavage of the methoxyphenyl group in aqueous methanol using excess of ceric ammonium nitrate (CAN) as a soft oxidant (Scheme 14). The sequence afforded the target (*S*)-homoallylic amine **69** in 64% overall yield with a complete retention of chirality.

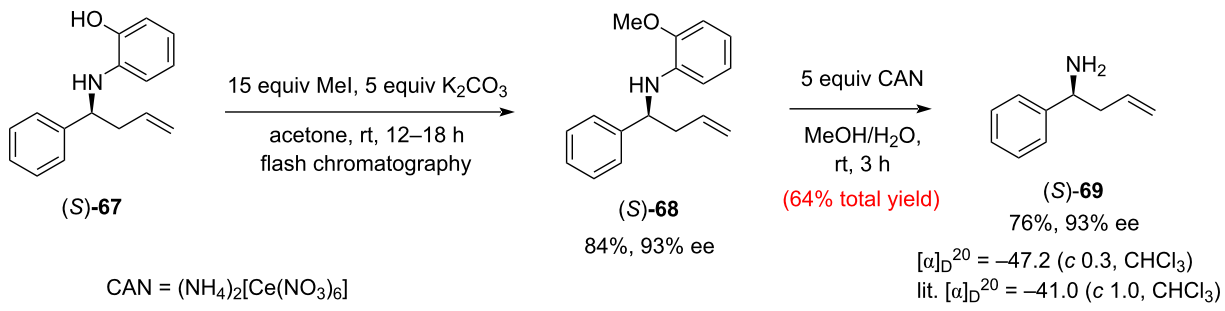

Scheme 14: The two-step *N*-(2-hydroxy)phenyl group deprotection procedure [37].

To gain a mechanistic insight into the formation of the active catalytic species in COBI-catalysed allylations, chemical equilibria in a solution containing catalyst **72**, triflic acid, and aldimine **73** were investigated by low-temperature NMR spectroscopy (Scheme 15).

Protonation of oxazaborolidine **70** with triflic acid resulted in an 8.3:1 mixture of **71** and **72**, the latter acting as a catalytically active species. After the addition of 1 equiv of imine **73** at −40 °C, proton H_a of **72** shifted upfield which was close to what was observed in the TfOH adduct **71**, and which supported the formation of intermediate **74**. The authors estimated the equilibrated ratio between COBI **72** and coordinated COBI–imine complex **74** as 1 to 4.6. Despite the low accuracy of this estimate, it is clear that both species **72** and **74** are present, and that coordination is reversible under the reaction conditions. The formation of the COBI–imine complex was further evidenced by comparing chemical shifts of the H_b proton in **74** with the same signals in the free substrate **73** and protonated **75** at −40 °C. It was revealed that the aldimine proton H_b in the free imine appears as a singlet at 7.95 ppm, while in both **74** and **75** it becomes a doublet with a 15 Hz *trans* $J_{H–H}$ coupling constant. However, in the COBI–imine complex **74** it appears at 8.41 ppm, while in the imine TfOH salt **75** it shows at 9.24 ppm.

This detailed NMR investigation sparked further interest in the structure of the transition state of this reaction. An analysis of the potential energy profiles of the two hypothetical pathways of the analogous nucleophilic addition of cyanide was reported by Chen and Qiao [38] in 2023 (Figure 4).

The calculations revealed that Δ*G* profile for the reaction pathway via **76**, in which the imine molecule is activated by the direct chiral proton transfer from the COBI ion and then later attacked by a nucleophile, is energetically favoured over pathway via **77**, in which the imine is activated directly by coordination to the Lewis acidic boron atom of the free imine complex. This supports the mechanism proposed in the original study based on the NMR experiments.

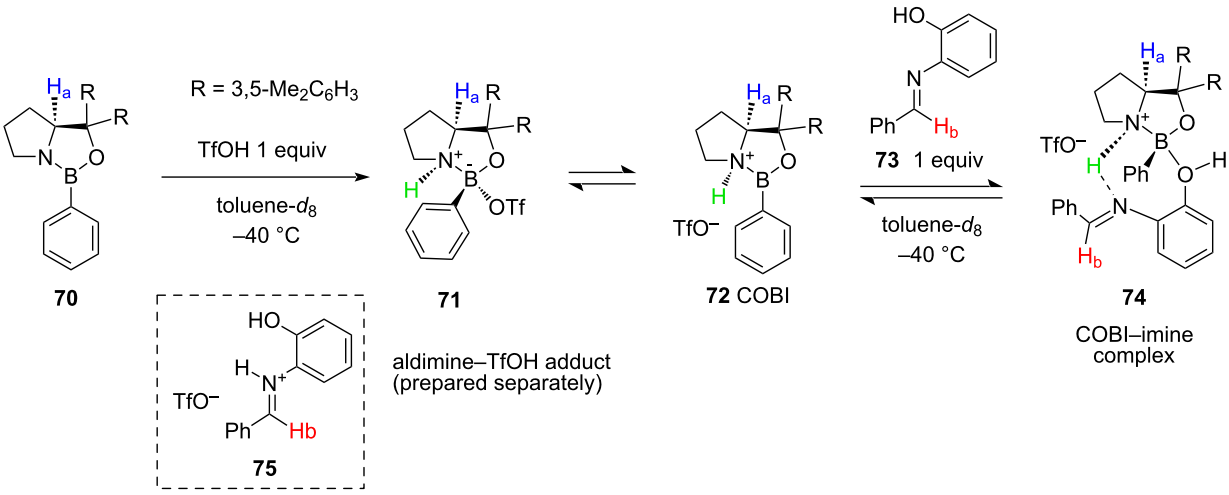

Scheme 15: Low-temperature (−40 °C) NMR experiments evidencing the reversible formation of the active COBI–imine chiral complex [37].

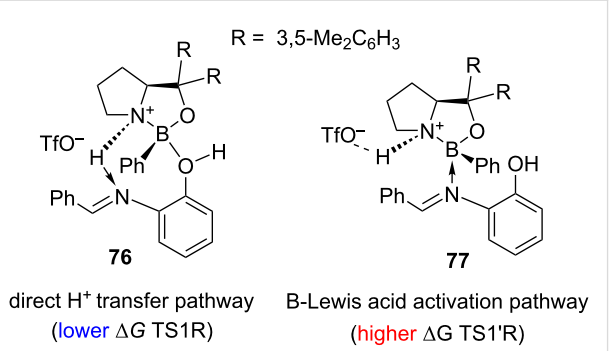

Figure 4: Two computed reaction pathways for the COBI-catalysed Strecker reaction (TS1 identical to allylation – COBI–imine complex) reported by Chen and Qiao in 2023 [38].

In 2021, Jacobsen and co-workers [39] developed a direct, highly enantioselective three-component reaction between aromatic acetals, $BocNH_2$, and various 2-monosubstituted or 2,3-disubstituted allyltrimethylsilanes in the presence of 10 mol % of triethylsilyl triflate (TESOTf) and 10 mol % of the chiral bifunctional thiourea catalyst **78** with a pending 4-pyrenyl group. The catalyst acts as H-bond donor but additionally it controls the chiral environment through π-stacking interaction with the aryl group of the substrate, blocking one of the enantiofaces of the iminium intermediate **79**. The reaction proceeds in Et_2O at −50 °C and requires 18 hours (Scheme 16).

A proposed catalytic cycle is shown in Scheme 17. In this reaction, the aromatic acetal **80** gives rise to a hydrogen-bonded triflate **82** and oxocarbenium ion **81**. The latter quickly reacts with $BocNH_2$ forming the $ArCH{=}HN^+$-Boc iminium–triflate ion pair **83**. Notably, the attack of the C-nucleophile on **81** is very slow, which determines the chemoselectivity of the reaction. Complex **83** of the iminium ion and the catalyst then reacts with allylsilane **84** through an open, type 2 [33] transition state from the exposed enantiotopic face, as in int-**79**, to afford product **85** and to release catalyst **78** completing the catalytic cycle (Scheme 17).

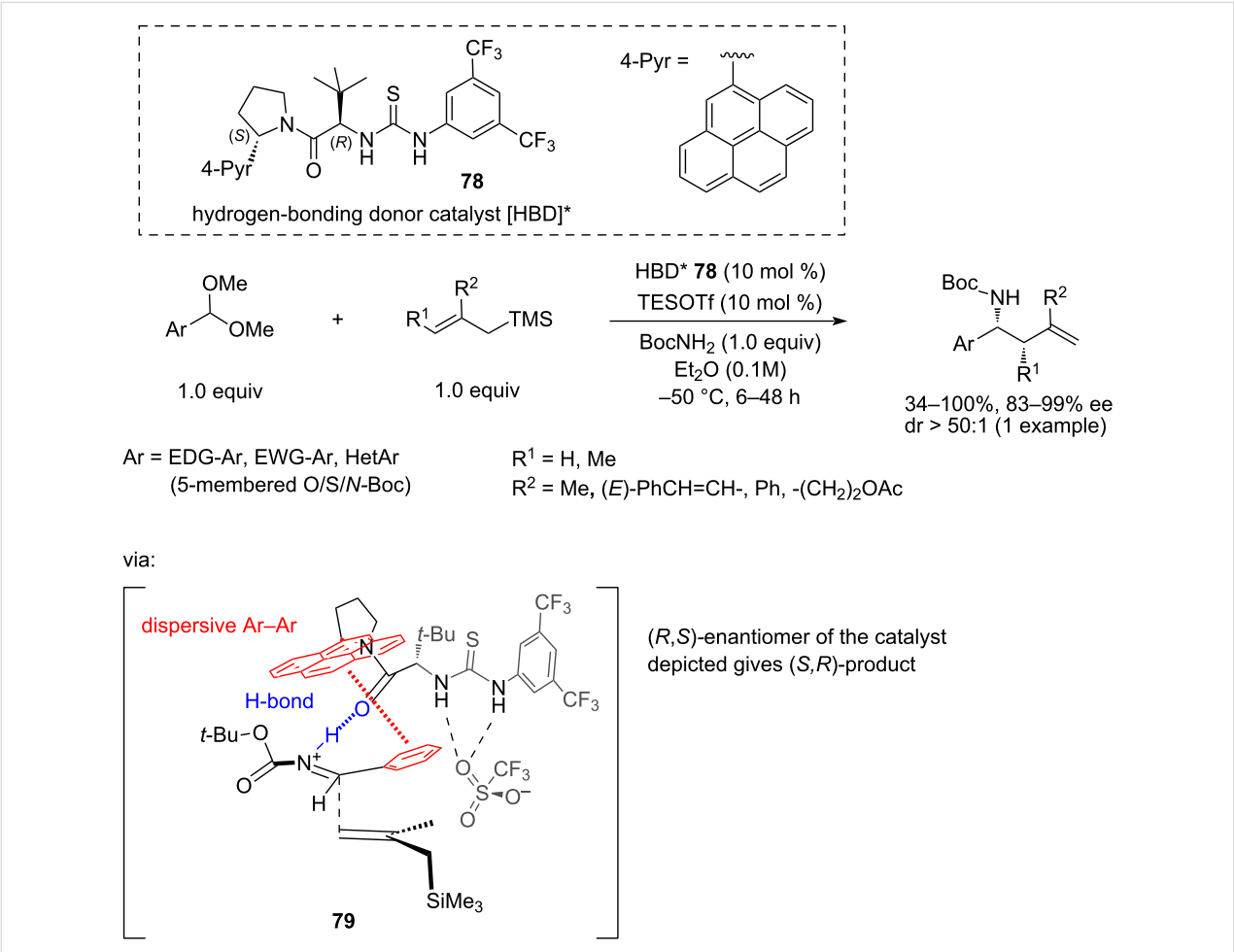

Scheme 16: Highly chemoselective and stereospecific synthesis of γ- and γ,δ-substituted homoallylic amines by a three-component reaction between an aryl acetal, $BocNH_2$ carbamate and a 2,3-disubstituted allylsilane, in presence of the triflate-assisted bifunctional HBD/$\pi_{Ar\text{-}Ar}$ catalyst [39].

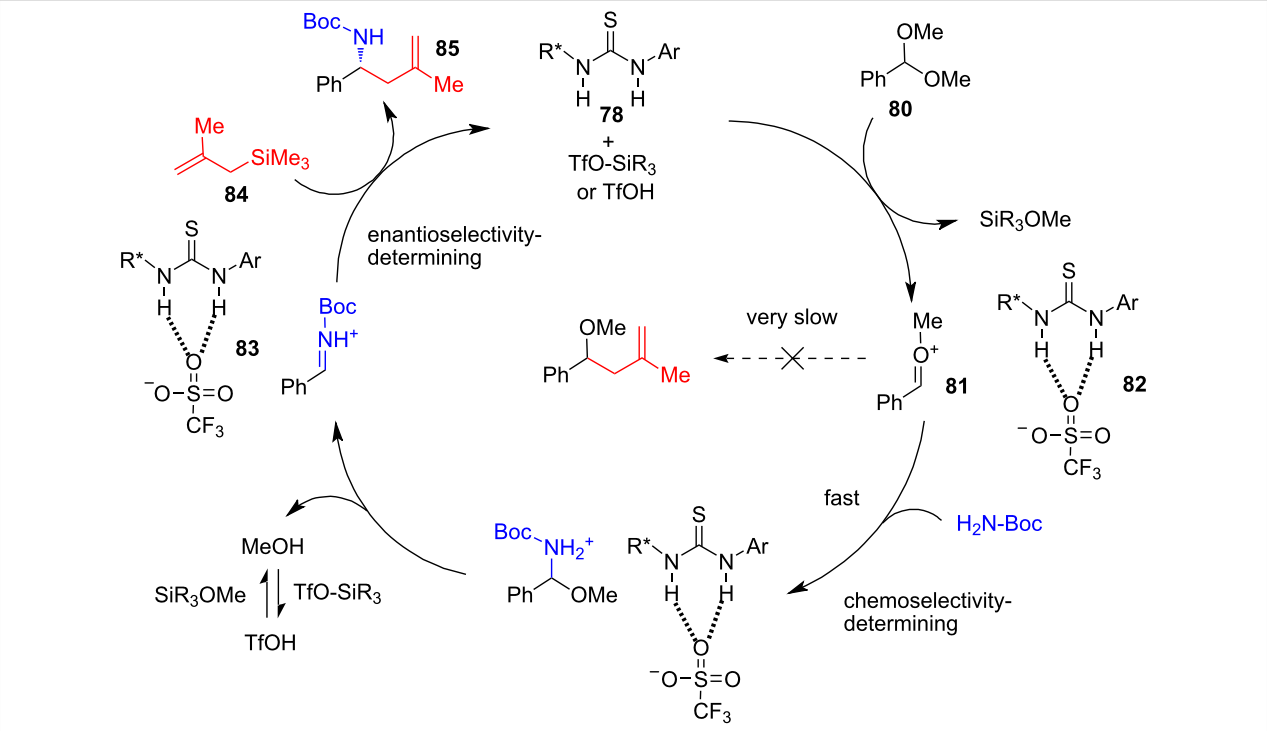

Scheme 17: Catalytic cycle for the three-component allylation with HBD/$\pi_{Ar–Ar}$ catalyst [39].

In a mechanistic probe, the proposed reaction intermediates were used as starting electrophiles under the standard reaction conditions (Scheme 18). In all three cases, identical outcomes were achieved, supporting the proposed catalytic cycle.

In the optimisation of the catalyst **78** structure, several important observations were made (Scheme 19). Replacing thiourea (**91**) as the H-bond donor unit with squaramide (**93**) or urea (**92**) did not affect the enantioselectivity of the allylation of the benzaldehyde-derived acetal. On the other hand, blocking (**94**) or removing (**95**) one of the N–H groups responsible for H-bonding resulted in a dramatic loss of enantioselectivity (7% ee in **94** and 26% ee in **95**), while removing both of the N–H groups gave the racemate (1% ee for **96**). Interestingly,

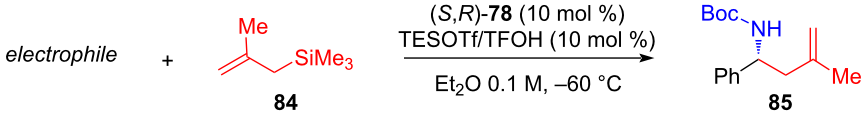

entry	electrophile	co-catalyst	yield %	ee %
1	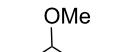	TESOTf	86%	90%
2		TfOH	81%	92%
3	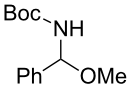	TESOTf (2.5 mol %)	98%	92%
4		TfOH (2.5 mol %)	98%	92%
5	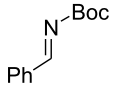	TESOTf (2.5 mol %)	83%	89%
6	(+ 1 equiv MeOH)	TfOH (2.5 mol %)	85%	90%

Scheme 18: Reactivity of model electrophiles [39].

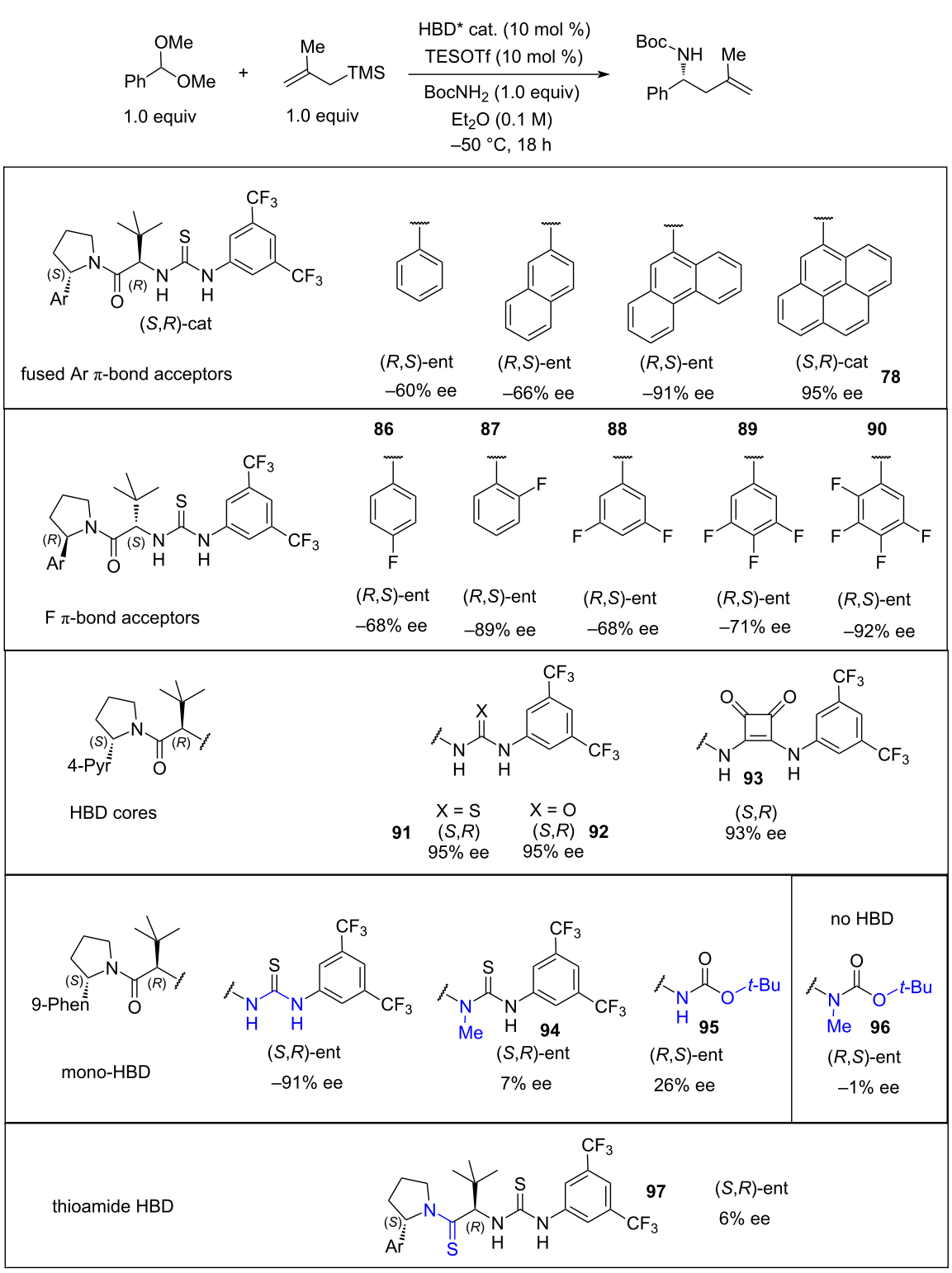

Scheme 19: HBD/$\pi_{Ar–Ar}$ catalyst rational design and optimisation [39].

thioamide **97** also showed a low ee. Replacing the 3,5-bis(trifluoromethylphenyl) group with other fluorinated aromatics (**86**–**90**) showed a gradual decrease in ee (92% ee in **90** to 68% ee in **86** and **88**) depending on the degree of fluorination. Computational modelling for the 3,5-bis(trifluoromethylphenyl) catalyst **78** revealed that π-stacking interactions of the 4-pyrene

group with the aromatic group of the substrate had a significant contribution to the stereoselectivity of the reaction.

The reaction demonstrated a broad scope both in the acetal **98** and in the allylsilane (Scheme 20). A high enantioselectivity was achieved even with the non-aromatic 1-cyclohexene-1-carboxaldehyde-derived acetal **100** (82% yield, 90% ee). 2-Methallylsilane showed universally high enantioselectivity across a range of acetal components (95–99% ee), except for a slight drop in the case of 5-bromo-2-furan (**102**, 86% ee) and 2-benzofuran-substituted (**103**, 86% ee) substrates. Regarding the silane scope, good results were achieved with (*E*)-trimethyl(2-methylbut-2-en-1-yl)silane to give homoallylic amine **105** with 80% yield, 98% ee, and >50:1 dr. The reactions of benzaldehyde dimethyl acetal with (2-[2-(acetoxy)ethyl]allyl)trimethylsilane (producing **104**) and with 2-(cinnamyl)allyltrimethylsilane (producing **106**) also showed high enantioselectivity, although the yields varied from modest to good (Scheme 20).

Limitations of the scope include the inertness of ketals and methyl dimethoxy acetal (glyoxalic acid derivative) in this reaction. Also, allylation with a simple allyltrimethylsilane failed to give the desired product **99** after 72 h returning hemiaminal (Scheme 21). Alkyl acetals, such as cyclohexyl carboxaldehyde acetal reacted sluggishly with low yield and selectivity (<10%

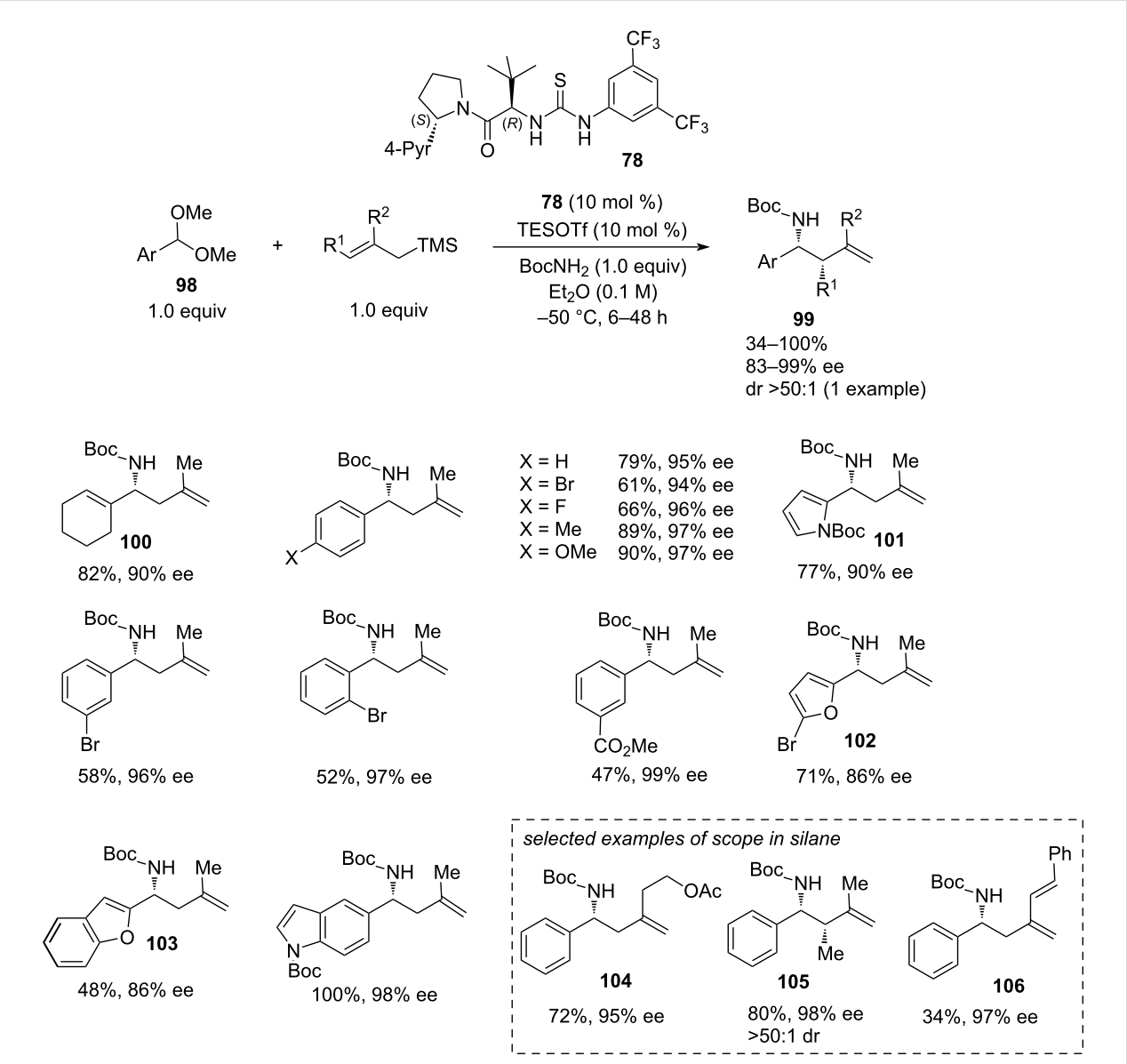

Scheme 20: Scope of the three-component HBD/$\pi_{Ar–Ar}$-catalysed reaction [39].

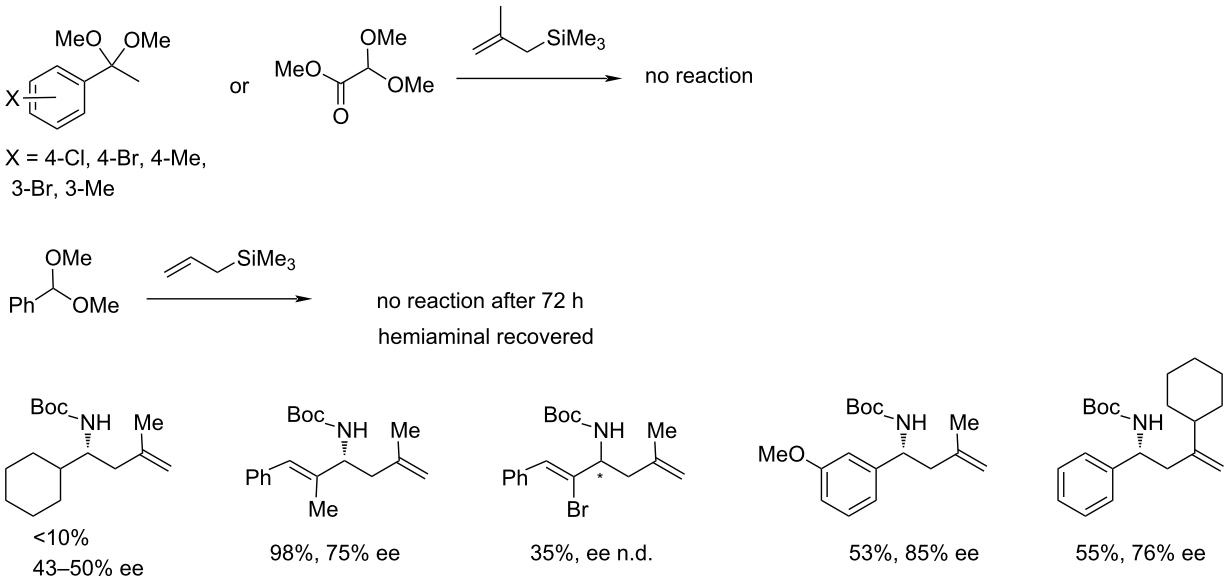

Scheme 21: Limitations of the HBD/$\pi_{Ar–Ar}$-catalysed reaction [39].

yield, 43–50% ee), possibly due to their inability to participate in π–π interactions. In general, the π-stacking interaction between the catalyst and the aryl group of the substrate in the enantio-determining step appears to affect the scope. Other problematic substrates included (*Z*)-α-methylcinnamyl and (*Z*)-α-bromocinnamyl acetals giving the respective products with lower ee. Despite some phenyl substrates with 3-substitution (CO_2Me, OCH_2, Br) showing excellent enantioselectivity, the 3-methoxyphenyl-substituted substrate afforded the homoallylic amine in only 85% ee. The bulky 2-cyclohexylallyltrimethylsilane showed only moderate yield and enantioselectivity (55%, 76% ee).

In 2022, Mancheño and co-workers [40] exploited the application of hydrogen-bond donor catalysis in asymmetric dearomative α-allylations of in situ-generated *N*-acylquinolinium salts **108** generated with 2,2,2-trichloroethyl chloroformate (TrocCl) (Scheme 22). Screening through a range of catalysts including the known squaramide and thiourea analogues, a novel tetrakis-triazole-based H-bond donor catalyst **111** was identified as most promising. Among different nucleophilic allylating reagents, 2-methallyltributyltin (**107**) emerged as optimal in terms of reactivity and enantioselectivity. It was speculated that the enantioinduction is realised via the H-bond-donor association of catalysts **111** to the Cl^- ion of the *N*-acylquinolinium intermediate **108**, though a detailed investigation into the mechanism of the enantiodifferentiation has not been carried out (Scheme 22).

In total 15 different quinolines were tested. The yields varied in the range of 28–96%, whereas enantioselectivities remained modest (20–78% ee). To illustrate the synthetic utility of the products, a double $Cu(acac)_2$-catalysed aziridination of the model substrate **109** was carried out using a large excess of PhI=NNs reagent (15 equiv, Ns = nosyl) to afford diastereoselectively diaziridine **110** with 88% ee albeit with a modest 42% yield. Overall, this is an interesting example of dearomative allylation of *N*-acylquinolinium salts, though enantioselectivity currently is too low to ensure wider practical application of the method.

Enantioselective 2-aza-Cope rearrangement

In 2008, a conceptually different methodology was reported by Rueping and co-workers [41] that was based on the aza-Cope rearrangement of in situ-formed *N*-α,α'-diphenyl-(α''-allyl)methyliminium cations catalysed by the BINOL-derived chiral phosphoric acid **112** (Scheme 23). The amine **113** acting as the allyl donor source was obtained by the addition of allylmagnesium bromide to benzophenone imine on a 3 gram scale in 80% yield. The rearrangement products **114** were readily converted to free homoallylic amines employing hydroxylamine in THF.

The reaction showed moderate to high yields on various aromatic aldehydes, being slightly more efficient with electron-poor substrates. On the other hand, high enantioselectivity was maintained over the aldehyde scope regardless of steric size and position of the substituents.

A few years later, Wulff and co-workers [42] further elaborated the aza-Cope rearrangement methodology by employing a bulkier allyl-transfer reagent **116**. They used a novel pre-formed chiral triborate catalyst **115** in tandem with a non-chiral

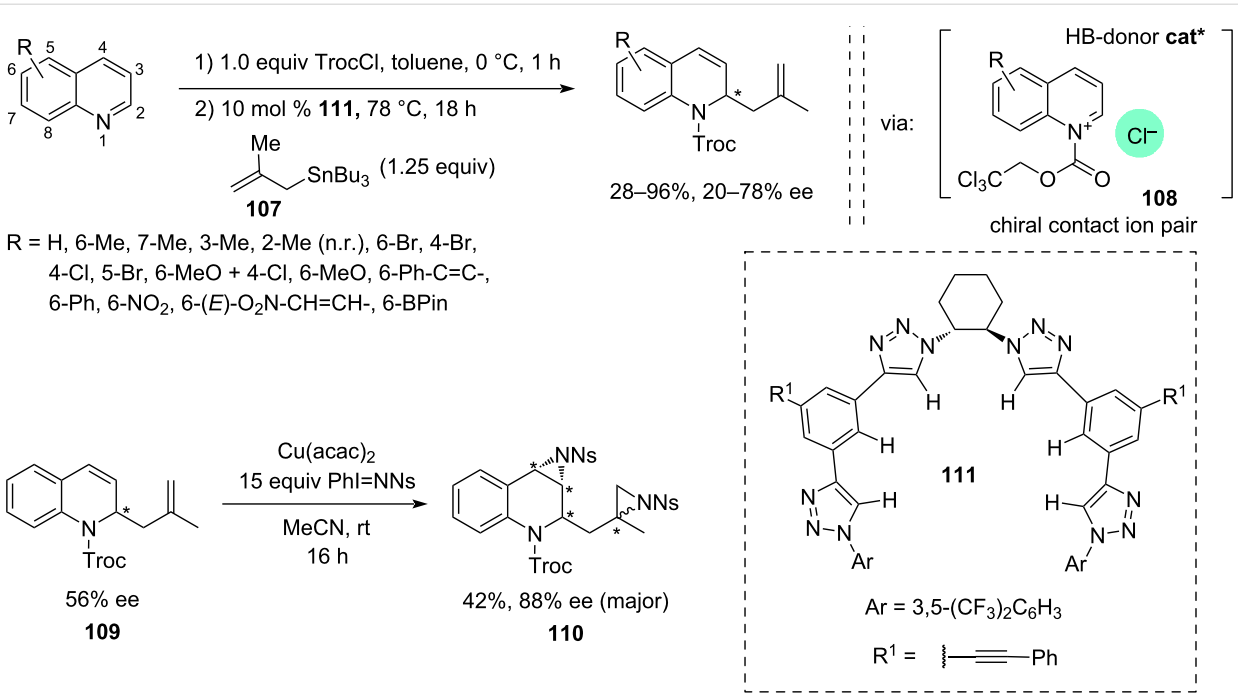

Scheme 22: Asymmetric chloride-directed dearomative allylation of in situ-generated *N*-acylquinolinium ions, catalysed by a tetrakis-triazole HBD catalyst [40].

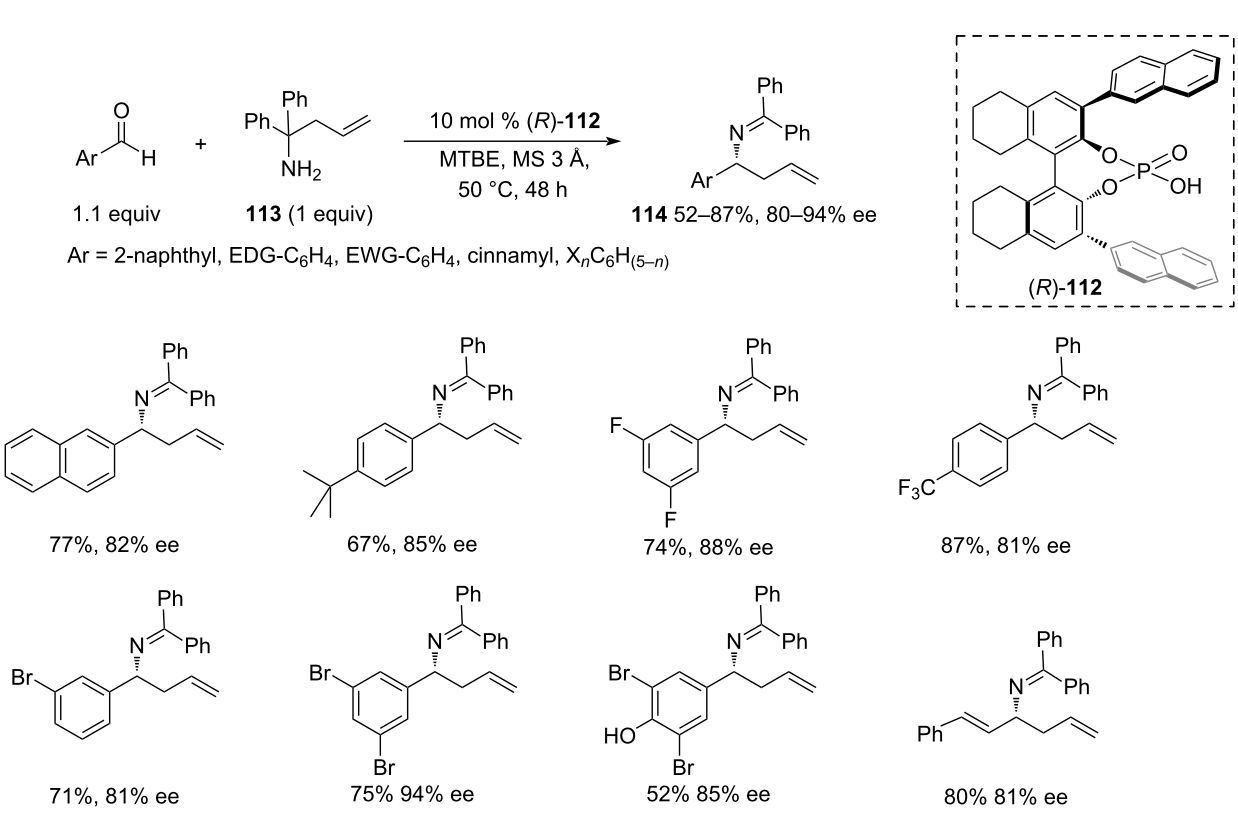

Scheme 23: Chiral phosphoric acid-catalysed aza-Cope rearrangement of in situ-formed *N*-α,α'-diphenyl-(α''-allyl)methyliminium cations reported by Rueping et al. 2008 [41].

Brønsted acid and expanded the scope to aliphatic homoallylic amines (Scheme 24). The new method established a scalable, chromatography-free purification protocol for the synthesis of homoallylic amines **117** and showed increased yields and enantioselectivities for aromatic aldehydes. In addition, a simple, ambient-temperature hydrolysis procedure was reported that yielded the unprotected analytically pure homoallylic amines in high yields without the need for chromatographic purification. The bulky aryl groups in **116** were synthesized in a one-pot procedure, starting from 3,5-dimethylbenzonitrile, by the addition of 3,5-dimethylphenylmagnesium bromide and allylmagnesium chloride (24% combined yield on a 1 g scale). The authors also optimised the protocol for a large-scale synthesis of the allyl donor reagent (up to 25 g). Importantly, benzophenone was easily recovered by recrystallisation after the workup (no chromatography, 80% yield) and then converted back into the allyl donor **116** (86% yield), thus boosting the overall atom-economy of the process. Also, the recovery of the (*R*)-VANOL ligand **115** was attained by column chromatography in 92%.

In 2015, further development of the 2-aza-Cope rearrangement strategy was reported by Johnson [43]. This work expanded the scope of the reaction to β-formyl amides **119** under the conditions of dynamic kinetic resolution (DKR) by employing chiral Brønsted acid catalyst (*S*)-TRIP (**118**) (Scheme 25). In this approach, the racemic β-formyl amide forms the iminium intermediate that undergoes fast equilibration via the enamine tautomer to form preferentially one enantiomer which then undergoes the acid-catalysed aza-Cope rearrangement, creating the desired *syn*-(2*R*,3*S*)-homoallylic amine **120** in high diastereo- and enantioselectivity.

The reaction was tested with various aryl, benzyl, allyl, and alkyl-functionalised β-formyl *N*-morpholinyl amides **119**; the amide function was also varied. Yields were scattered across the 31–90% range, with the diastereoselectivities varying from 1.1:1 to >20:1 (Scheme 25). Interestingly, almost all isolated products, except for the amine resulting from methyl β-formyl *N*-morpholinyl amide (**119**, R = Me), showed dr > 20:1. Enantioselectivity followed the trend and varied between 64–94%,

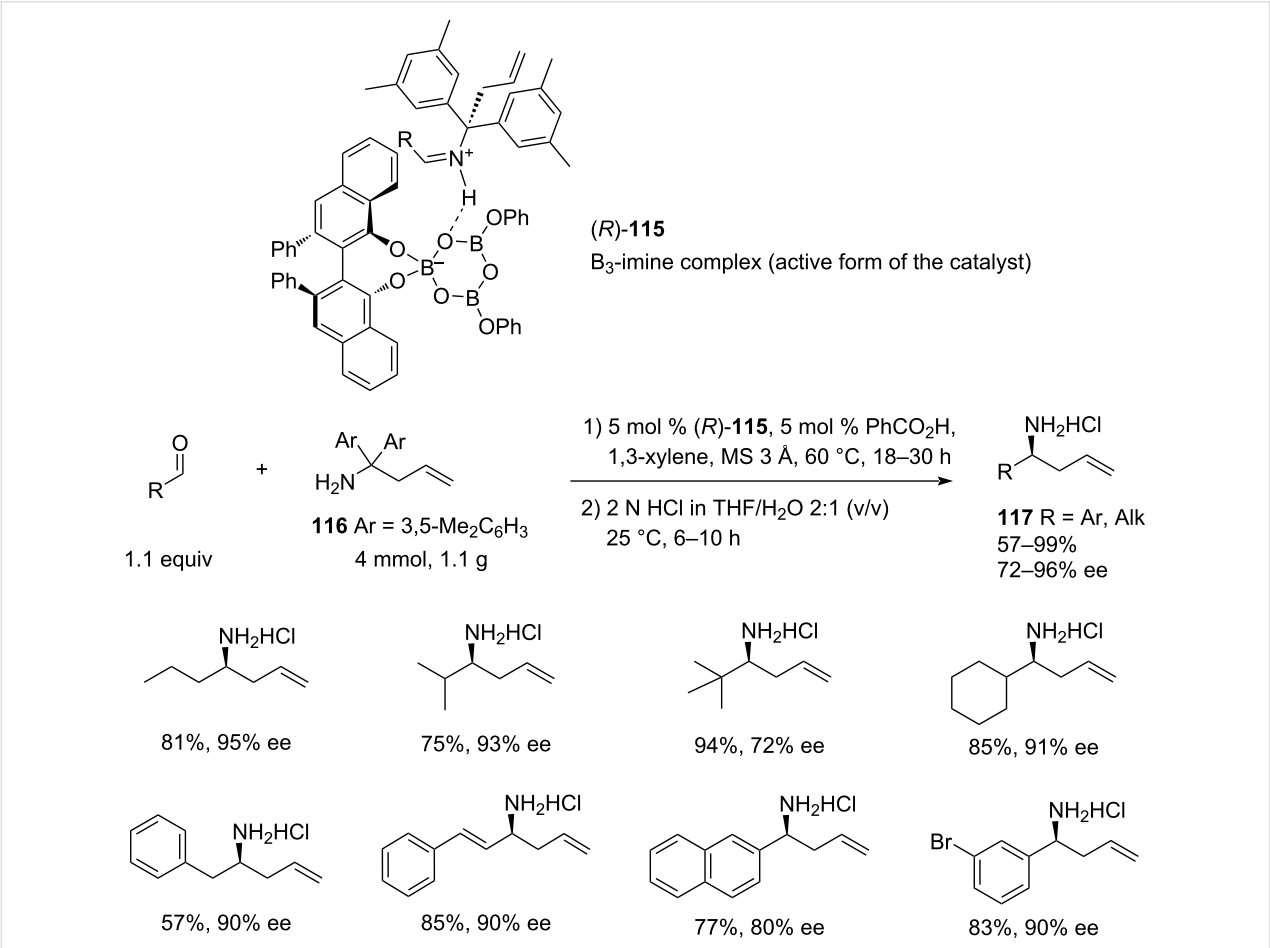

Scheme 24: Tandem (*R*)-VANOL-triborate-catalysed asymmetric aza-Cope rearrangement of in situ-formed aldimines using allyl transfer reagent **116** [42].

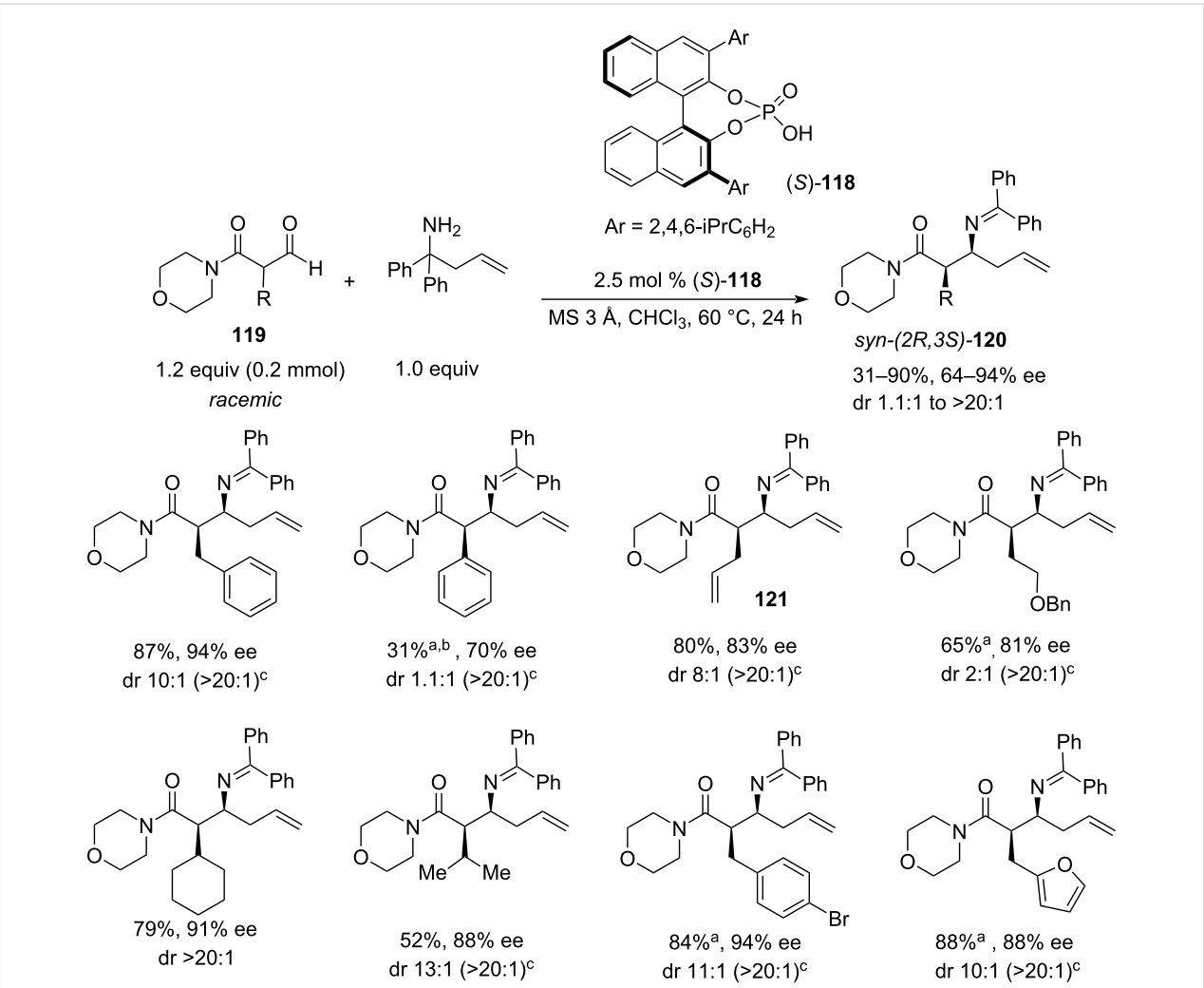

Scheme 25: (*S*)-TRIP-catalysed enantioconvergent aza-Cope rearrangement of β-formyl amides, substrate scope [43]. [a]The yield was measured after hydrolysis of the benzophenone imine. [b]The reaction required 300 W microwave irradiation at 130 °C for 6 hours. [c]Isolated dr.

the lowest being obtained for the methyl-substituted substrate **119** and the highest for bulky benzyl substrates. Several reactions showed 94% ee which appears to be an upper limit for this particular (*S*)-TRIP-catalysed reaction. Screening the amide group revealed, that *N*-morpholinyl (**122**), *N*-piperidinyl (**123**), *N*-pyrrolidinyl (**124**), and *N,N*-dimethyl (**125**) amides produced the corresponding homoallylic amines **126**–**130** with dr ≥ 9:1. In the case of R = Bn, all these amides showed yields greater 85% and ees above 86% for the unsubstituted allyl group transfer (**126**–**129**). The reaction showed low tolerance to changes in the allyl fragment: with a methallyl derivative **130**, the stereoselectivity dropped to a modest level (dr 5:1, ee 60%, yield 60%), whereas higher allyl homologues such as phenyl and benzyl proved to be inactive (Scheme 26).

The synthetic utility of the resulting homoallylic *N*-benzophenone imines **131** was illustrated on a laboratory scale (Scheme 27). Thus, the hydrolysis of the N=CPh_2 group in the *N*-morpholinyl product **129** with hydroxylamine hydrochloride afforded the deprotected homoallylic amine **133** in a 99% yield without need for chromatographical purification. In a separate experiment, the sequential reduction of the *N*-morpholinyl amido and benzophenone imino groups with $LiAlH_4$ and $NaBH_4$ afforded the corresponding *syn*-2-benzyl-1,3-amino alcohol **134** in 83% yield. In the case of the dimethylamide derivative, deprotection of benzophenone imine **128** with $NH_2OH{\cdot}HCl$ followed by the $LiAlH_4$ reduction gave rise to chiral *syn*-2-benzyl-1,3-diamine **132** in 57% yield. The ring-closing metathesis of **121** (R^1 = allyl, from Scheme 25) provided pure *N*-cyclohexenyl imine **135** in 98% yield.

Asymmetric alkylation of imine-carbanion

In 2023, a team of Huang and Yan [44] presented a novel approach towards synthetically important homoallylic α-trifluoro-

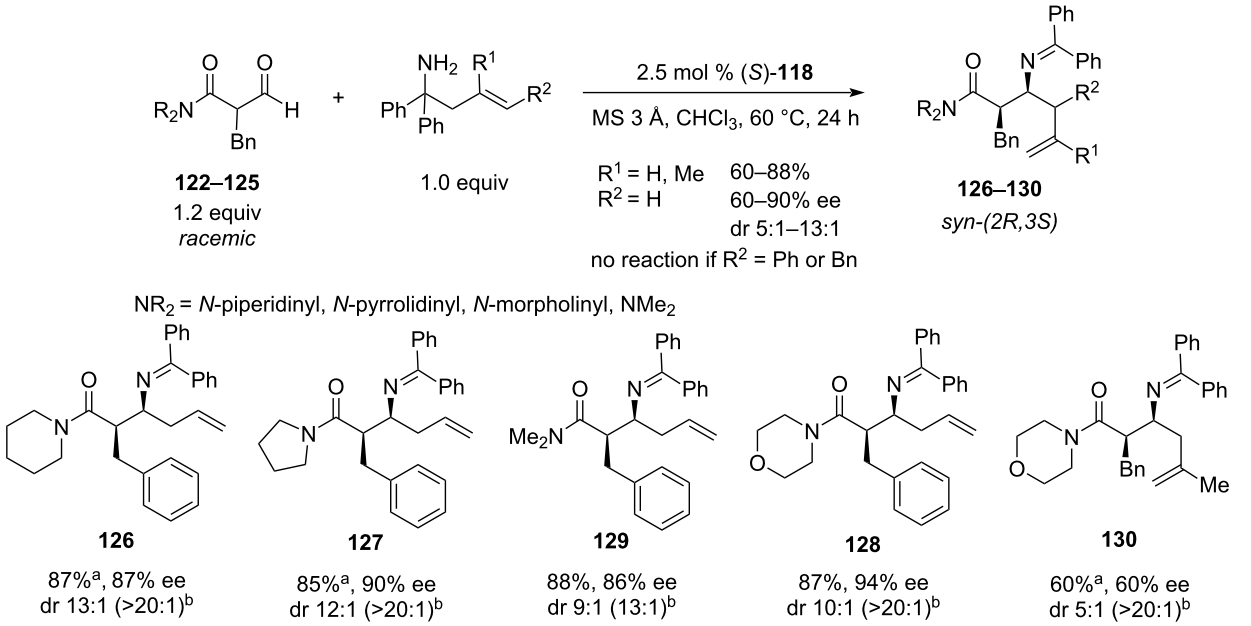

Scheme 26: (*S*)-TRIP-catalysed enantioconvergent aza-Cope rearrangement of β-formyl amides **16**–**19**, amide and allyl group scope [43]. [a]The yield was measured after the benzophenone imine hydrolysis. [b]The isolated dr.

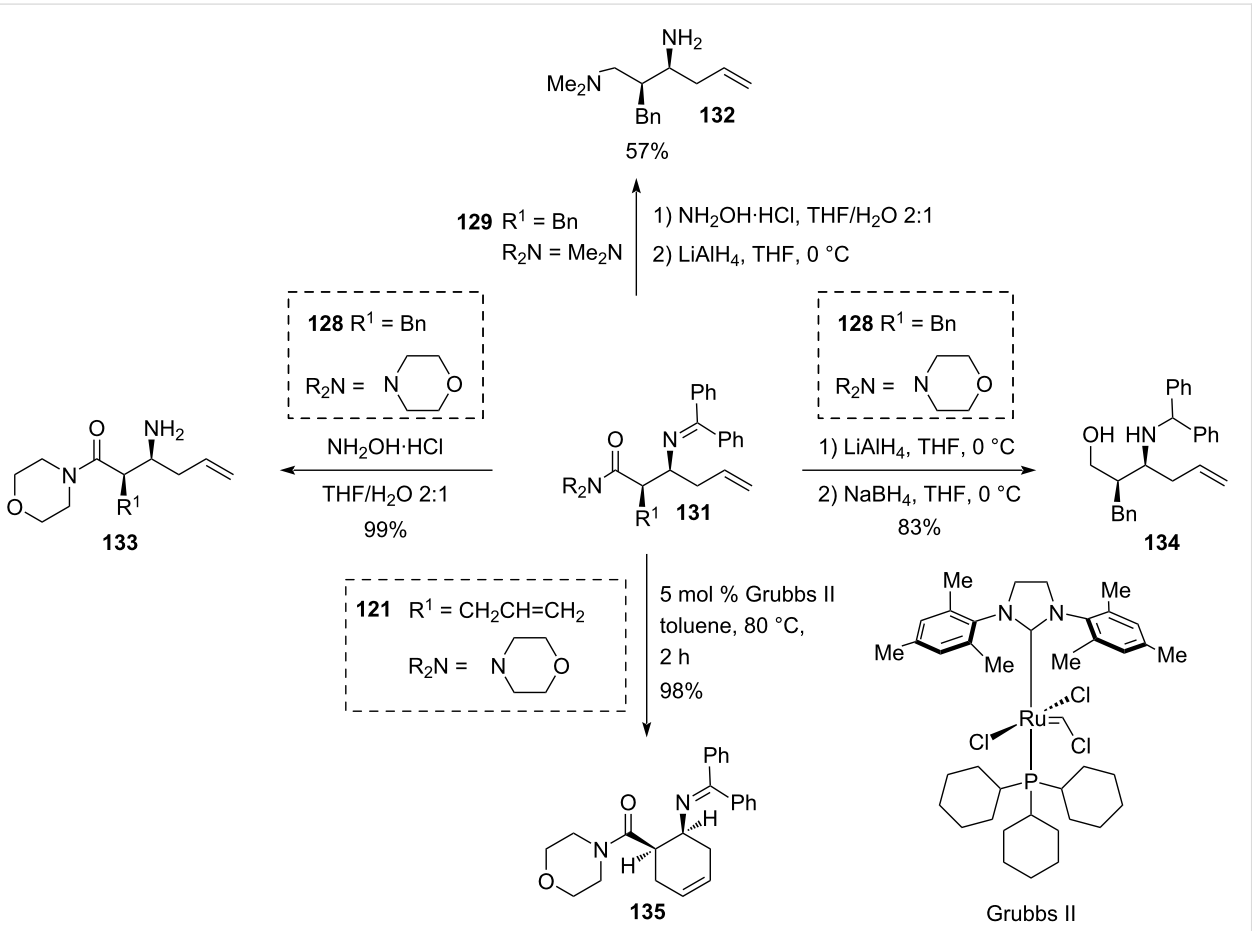

Scheme 27: Synthetic applications of homoallylic *N*-benzophenone imine products **131** [43].

methylamine derivatives of high molecular complexity (Scheme 28). The process involves a highly enantioselective reaction of the isatin-derived Morita–Baylis–Hillman carbonate **137** with a novel α-CF_3-substituted imine **136**, derived from inexpensive benzothiophene-2,3-dione. A C_2-symmetrical cinchona-derived $(DHQ)_2PHAL$ catalyst **138** has been identified as the most efficient that afforded high yield and enantioselectivity with a 10 mol % loading. The diastereoselectivity was 20:1 or better in most cases and was found to be independent of the reaction conditions.

The optimised protocol involved stirring 1 equiv of isatin with a 50% excess of the α-CF_3-substituted imine in toluene at room temperature in the presence of 10 mol % of organocatalyst **138** for times between 1 and 80 h. The reaction exhibited a broad scope in the isatin carbonate derivatives with high to excellent enantioselectivities (89–99%), good to excellent yields (65–98%), and consistently high diasterioselectivities (>20:1). For selected examples, the reaction was successfully performed on a 1 gram scale. Apart from benzothiophene-2-one imine, the reaction also worked well with diethyl oxomalonate-derived trifluoromethylimine.

A practical potential of the methodology was illustrated by constructing the medicinal chemistry-relevant highly fused spiro compound **140** featuring 5 stereocentres (3 quaternary) in 99% ee and 76% overall yield from achiral **136** and racemic **137** in just 2 steps. Selected substrates were converted to the corresponding free amines by hydrolysis with aqueous HCl. The reaction proceeded in good yields and with complete retention of stereointegrity.

In a proposed mechanism, isatin carbonate **137** reacts with a quinuclidine unit of the catalyst **138** by an S_N2' attack to form cationic intermediate **142**. The *t*-BuO^- anion formed in this process abstracts the γ-CH proton of the CF_3-imine (**136** → **141**), facilitating its nucleophilic attack on the isatin cation (**141** + **142** → **143**), followed by elimination of the catalyst **138**, which completes the cycle liberating **139** (Scheme 29).

Overall, this methodology represents a convenient tool for the rapid construction of medicinal chemistry-relevant heterocyclic homoallylic amines in an enantioselective manner without involving nucleophilic allylation. The highly functionalised products offer the possibility of further derivatisation.

Other catalytic approaches

In 2017, the deracemisation of an unsaturated amine **144** was reported by Li Dang and Xin-Yuan Liu (Scheme 30) [45]. They used CF_3-radical-induced remote CH-activation, combined with Brønsted acid-catalysed chiral hydrogen atom transfer (HAT).

In this reaction, triphenylphosphine first mediated the addition of the CF_3-radical generated from Togni's reagent (**145**) to a double bond of the δ-alkenylamine, followed by intramolecular hydrogen atom transfer and a single-electron oxidation of the intermediate alkyl radical to form an imine that is then reduced by hydrogen donor **147** catalysed by CPA (*R*)-VAPOL (**148**).

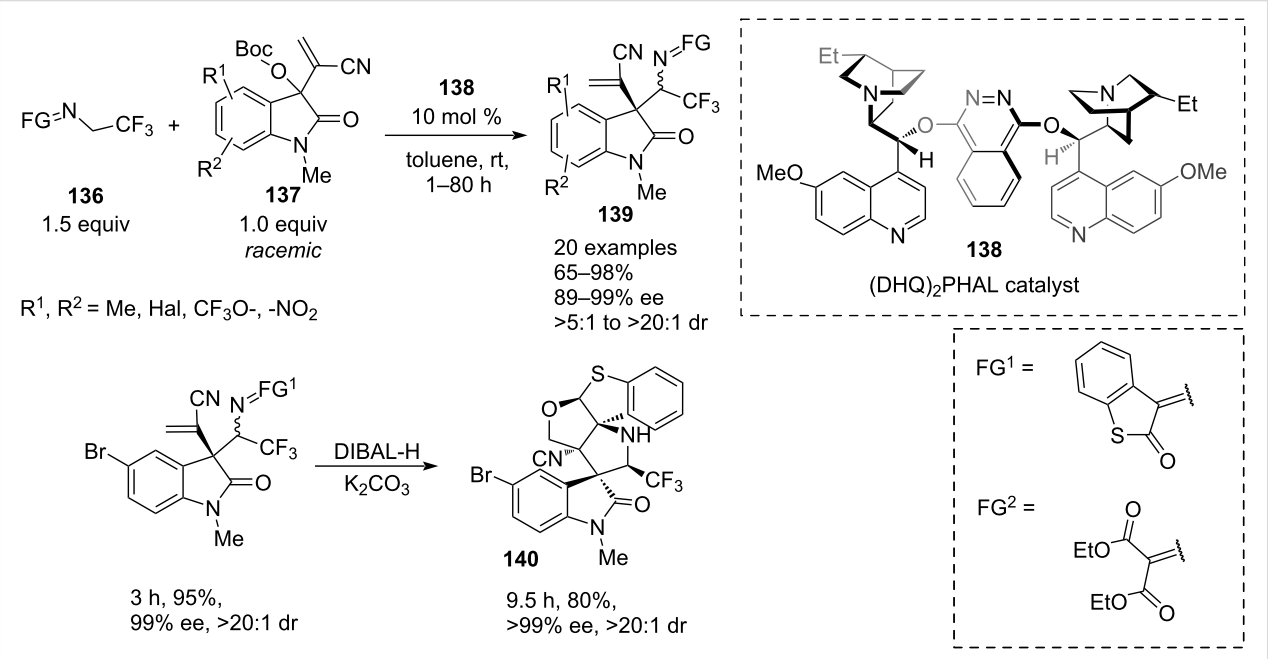

Scheme 28: Chiral organocatalysed addition of 2,2,2-trifluoroethyl ketimines to isatin-derived Morita–Baylis–Hilman carbonates [44].

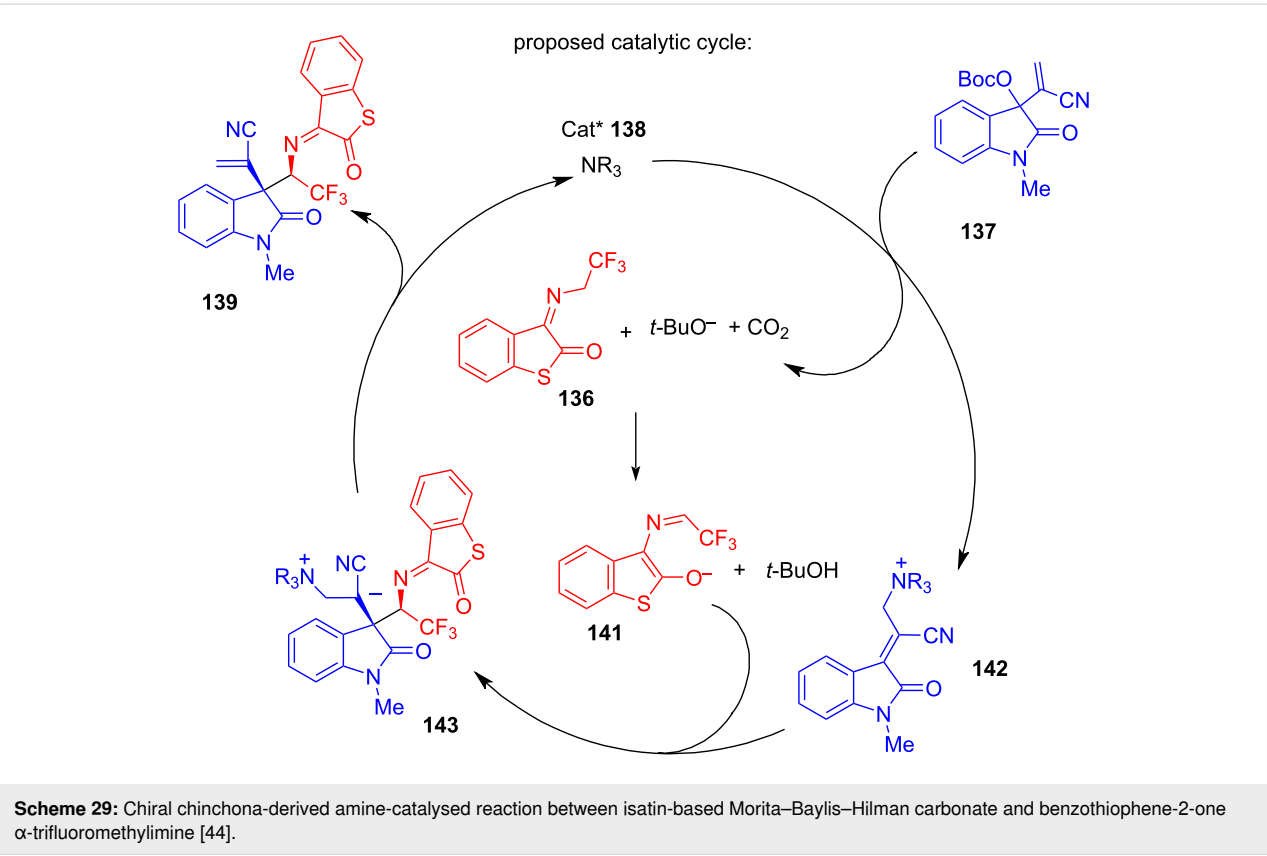

Scheme 29: Chiral chinchona-derived amine-catalysed reaction between isatin-based Morita–Baylis–Hilman carbonate and benzothiophene-2-one α-trifluoromethylimine [44].

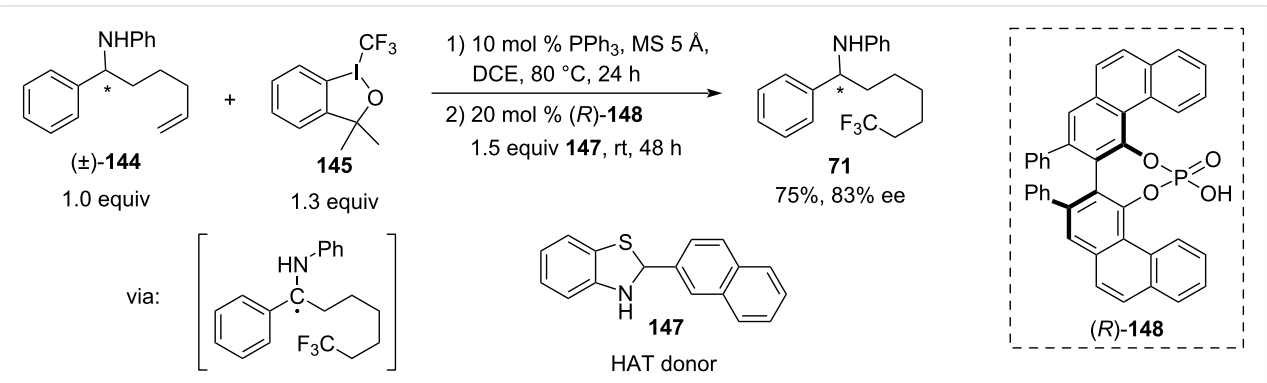

Scheme 30: (*R*)-VAPOL-catalysed hydrogen atom transfer deracemisation [45].

The trifluoromethylated amine **146** was obtained in 75% yield and 83% ee. The scope of this reaction is yet to be explored.

In 2022, Momiyama and co-workers presented a novel synthetic approach towards enantioenriched homoallylic amines **150** that bear a chiral centre on the β-carbon, based on an asymmetric [1,3]-rearrangement of ene-aldimines **149**, catalysed by the BINOL-derived chiral phosphoric acid (CPA) (*R*)-**151** (Scheme 31) [46]. DFT computational analysis suggested that the reaction proceeds via a complex cascade that involves the fragmentation of ene-aldimine **149** to form an imine methylene cation, which in turn catalyses the methylene group transfer, resulting in azonia-[3,3]-sigmatropic rearrangement, followed by regeneration of methylene imine by an elimination step [47]. The reaction proceeded in toluene at 80 °C with 20 mol % of the CPA catalyst **151** over 20 hours resulting in low to moderate enantioselectivities (30–65% ee) and low to moderate yields (49–81%). However, despite the modest enantioselectivity, the proposed approach presents an appealing strategy towards chiral homoallylic amine scaffolds **150** that are difficult to achieve using other methods.

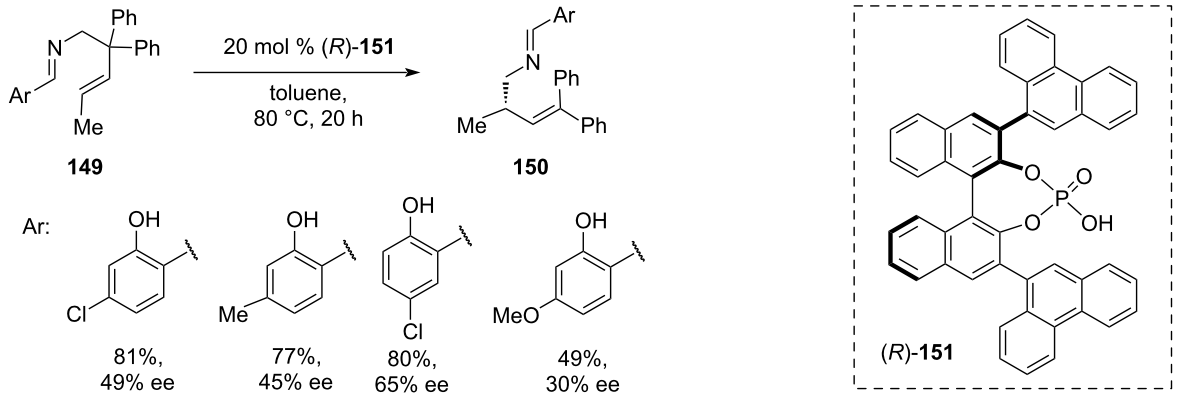

Scheme 31: Chiral PA-catalysed [1,3]-rearrangement of ene-aldimines [46].

Conclusion

Summarising all the analysed approaches, 4 distinct methodological classes can be outlined: (i) Open TS-type [33] Si/Sn reagent-based asymmetric allylations; (ii) closed TS-type [33] allylation of imines with boron-based reagents; (iii) 2-aza-Cope rearrangement methodologies that use achiral *gem*-diaryl homoallylic amines as allyl group transfer reagents; (iv) direct metal-free imine carbanion addition to electrophilic alkene.

Class (i) underwent an evolution from catalysis by covalent interaction to chiral hydrogen-bonded catalysis, which allowed the expansion of the allyl component scope from simple allyl to substituted allyl groups, along with a higher tolerance to imine components. However, one of the unsolved challenges within this class remains the asymmetric allylation of unprotected aldimines. In addition, the use of secondary chiral allylsilanes to access (*E*)- or (*Z*)-homoallylic amines remains unexplored.

Class (ii) was enriched significantly over the last 2 decades and transitioned from the use of unstable unsubstituted non-cyclic dialkylallylboronates and air-sensitive allylboronic acids in combination with chiral BINOL catalysts to the bench-stable purified linear and branched crotylboronates, their activated boroxine forms, and catalysis by more active chiral phosphoric acids. The catalytic asymmetric allylation of unprotected aldimines remains a challenge. In addition, while the enantioselective and regiospecific methodology towards chiral (*E*)-CF_3-homoallylic amines has been established, the regiospecific enantioselective approach towards the formation of chiral (*Z*)-homoallylic amines remains unexplored.

Class (iii) attracted the greatest attention in the previous decade mainly due to the absence of atom-economical protocols for enantioselective allylations of both aromatic and aliphatic imines, and due to the necessity to pre-synthesise imines. As both challenges in the last decade were addressed to a certain extent, the aza-Cope methodology slipped to the second plan. However, a revival of interest towards the recently developed [1,3]-formal rearrangement approach may be expected as such transformation may offer access to the homoallylic amine scaffolds, difficult to access by the direct allylation methodologies from the two previous classes.

Class (iv) on the other hand, so far is represented by the sole methodology which is capable of producing quaternary stereogenic centres. Despite this methodology is not a classic allylation but rather a Mannich-type reaction, further investigation into the scope and the expansion of this methodology to other substrate classes will be beneficial. Its application to the synthesis of alkaloids and natural products can be also expected.

To draw an endline, it is apparent from the presented work, that metal-free organocatalytic nucleophilic asymmetric allylations of ketimines remains a significant challenge for all four general classes of allylation, the solution of which is likely to be revealed in the forthcoming research.

Author Contributions

Nikolay S. Kondratyev: writing – original draft; writing – review & editing. Andrei V. Malkov: writing – review & editing.

ORCID® iDs

Nikolay S. Kondratyev - https://orcid.org/0000-0001-6965-5302
Andrei V. Malkov - https://orcid.org/0000-0001-6072-2353

Data Availability Statement

Data sharing is not applicable as no new data was generated or analyzed in this study.

References

1. Ferreira, M.-J. U. *Molecules* **2022,** *27,* 1347. doi:10.3390/molecules27041347
2. Kerru, N.; Gummidi, L.; Maddila, S.; Gangu, K. K.; Jonnalagadda, S. B. *Molecules* **2020,** *25,* 1909. doi:10.3390/molecules25081909
3. Hayes, K. S. *Appl. Catal., A* **2001,** *221,* 187–195. doi:10.1016/s0926-860x(01)00813-4
4. Schmidt, F. V.; Schulz, L.; Zarzycki, J.; Prinz, S.; Oehlmann, N. N.; Erb, T. J.; Rebelein, J. G. *Nat. Struct. Mol. Biol.* **2024,** *31,* 150–158. doi:10.1038/s41594-023-01124-2
5. *Ammonia: Zero-Carbon Fertiliser, Fuel and Energy Store. Policy Briefing;* The Royal Society: London, UK, 2020; pp 5–11.
6. Silverio, D. L.; Torker, S.; Pilyugina, T.; Vieira, E. M.; Snapper, M. L.; Haeffner, F.; Hoveyda, A. H. *Nature* **2013,** *494,* 216–221. doi:10.1038/nature11844
7. Bird, H. Synthesis of 4- and 5-Membered Nitrogen-Containing Heterocycles from Homoallyl Amines. Ph.D. Thesis, University of Birmingham, Birmingham, U.K., 2023.
8. Kokkonda, P. Total Synthesis of Strychnos and Aspidospermatan Alkaloids. Ph.D. Thesis, Temple University, Philadelphia, PA, USA, 2017.
9. Kropf, J. E.; Meigh, I. C.; Bebbington, M. W. P.; Weinreb, S. M. *J. Org. Chem.* **2006,** *71,* 2046–2055. doi:10.1021/jo052466b
10. Grellepois, F.; Ben Jamaa, A.; Saraiva Rosa, N. *Org. Biomol. Chem.* **2017,** *15,* 9696–9709. doi:10.1039/c7ob02506h
11. Ramachandran, P. V.; Burghardt, T. E. *Chem. – Eur. J.* **2005,** *11,* 4387–4395. doi:10.1002/chem.200401295
12. Schaus, J. V.; Jain, N.; Panek, J. S. *Tetrahedron* **2000,** *56,* 10263–10274. doi:10.1016/s0040-4020(00)00870-x
13. Sirasani, G.; Andrade, R. B. Total Synthesis of *Strychnos* Alkaloids Akuammicine, Strychnine, and Leuconicines A and B. In *Strategies and Tactics in Organic Synthesis;* Harmata, M., Ed.; Academic Press: Oxford, UK, 2013; Vol. 9, pp 1–44. doi:10.1016/b978-0-08-099362-1.00001-1
14. Feula, A.; Dhillon, S. S.; Byravan, R.; Sangha, M.; Ebanks, R.; Hama Salih, M. A.; Spencer, N.; Male, L.; Magyary, I.; Deng, W.-P.; Müller, F.; Fossey, J. S. *Org. Biomol. Chem.* **2013,** *11,* 5083–5093. doi:10.1039/c3ob41007b
15. Villar, L.; Orlov, N. V.; Kondratyev, N. S.; Uria, U.; Vicario, J. L.; Malkov, A. V. *Chem. – Eur. J.* **2018,** *24,* 16262–16265. doi:10.1002/chem.201804395
16. Sugiura, M.; Hirano, K.; Kobayashi, S. *J. Am. Chem. Soc.* **2004,** *126,* 7182–7183. doi:10.1021/ja049689o
17. Zhang, Q.; Wang, C.; Zhao, W. *Mini-Rev. Org. Chem.* **2014,** *11,* 508–516. doi:10.2174/1570193x11999140327113509
18. Puentes, C. O.; Kouznetsov, V. *J. Heterocycl. Chem.* **2002,** *39,* 595–614. doi:10.1002/jhet.5570390401
19. Ramadhar, T. R.; Batey, R. A. *Synthesis* **2011,** 1321–1346. doi:10.1055/s-0030-1258434
20. Ramachandran, P. V.; Burghardt, T. E. *Pure Appl. Chem.* **2006,** *78,* 1397–1406. doi:10.1351/pac200678071397
21. Friestad, G. K.; Mathies, A. K. *Tetrahedron* **2007,** *63,* 2541–2569. doi:10.1016/j.tet.2006.11.076
22. Ding, H.; Friestad, G. K. *Synthesis* **2005,** 2815–2829. doi:10.1055/s-2005-872181
23. Yus, M.; González-Gómez, J. C.; Foubelo, F. *Chem. Rev.* **2013,** *113,* 5595–5698. doi:10.1021/cr400008h
24. Lou, S.; Moquist, P. N.; Schaus, S. E. *J. Am. Chem. Soc.* **2007,** *129,* 15398–15404. doi:10.1021/ja075204v
25. Alam, R.; Diner, C.; Jonker, S.; Eriksson, L.; Szabó, K. J. *Angew. Chem.* **2016,** *128,* 14629–14633. doi:10.1002/ange.201608605
26. Jiang, Y.; Schaus, S. E. *Angew. Chem., Int. Ed.* **2017,** *56,* 1544–1548. doi:10.1002/anie.201611332
27. Barnett, D. S.; Moquist, P. N.; Schaus, S. E. *Angew. Chem., Int. Ed.* **2009,** *48,* 8679–8682. doi:10.1002/anie.200904715
28. Jacques, J.; Fouquey, C.; Viterbo, R. *Tetrahedron Lett.* **1971,** *12,* 4617–4620. doi:10.1016/s0040-4039(01)97544-6
29. Akiyama, T.; Itoh, J.; Yokota, K.; Fuchibe, K. *Angew. Chem., Int. Ed.* **2004,** *43,* 1566–1568. doi:10.1002/anie.200353240
30. Incerti–Pradillos, C. A.; Kabeshov, M. A.; Malkov, A. V. *Angew. Chem., Int. Ed.* **2013,** *52,* 5338–5341. doi:10.1002/anie.201300709
31. Jonker, S. J. T.; Jayarajan, R.; Kireilis, T.; Deliaval, M.; Eriksson, L.; Szabó, K. J. *J. Am. Chem. Soc.* **2020,** *142,* 21254–21259. doi:10.1021/jacs.0c09923
32. Gandhi, S.; List, B. *Angew. Chem., Int. Ed.* **2013,** *52,* 2573–2576. doi:10.1002/anie.201209776
33. Denmark, S. E.; Weber, E. J. *Helv. Chim. Acta* **1983,** *66,* 1655–1660. doi:10.1002/hlca.19830660604
34. Bendelsmith, A. J.; Kim, S. C.; Wasa, M.; Roche, S. P.; Jacobsen, E. N. *J. Am. Chem. Soc.* **2019,** *141,* 11414–11419. doi:10.1021/jacs.9b05556
35. Samanta, S. S.; Roche, S. P. *J. Org. Chem.* **2017,** *82,* 8514–8526. doi:10.1021/acs.joc.7b01274
36. Kennedy, C. R.; Lehnherr, D.; Rajapaksa, N. S.; Ford, D. D.; Park, Y.; Jacobsen, E. N. *J. Am. Chem. Soc.* **2016,** *138,* 13525–13528. doi:10.1021/jacs.6b09205
37. Kang, K.-T.; Park, S. H.; Ryu, D. H. *Org. Lett.* **2019,** *21,* 6679–6683. doi:10.1021/acs.orglett.9b02280
38. Shi, Y.; Shi, Y.; Yang, S.; Chen, X.; Qiao, Y. *J. Org. Chem.* **2023,** *88,* 9803–9810. doi:10.1021/acs.joc.3c00416
39. Ronchi, E.; Paradine, S. M.; Jacobsen, E. N. *J. Am. Chem. Soc.* **2021,** *143,* 7272–7278. doi:10.1021/jacs.1c03024
40. Joseph, S.; Duong, Q.-N.; Schifferer, L.; García Mancheño, O. *Tetrahedron* **2022,** *114,* 132767. doi:10.1016/j.tet.2022.132767
41. Rueping, M.; Antonchick, A. P. *Angew. Chem., Int. Ed.* **2008,** *47,* 10090–10093. doi:10.1002/anie.200803610
42. Ren, H.; Wulff, W. D. *J. Am. Chem. Soc.* **2011,** *133,* 5656–5659. doi:10.1021/ja1110865
43. Goodman, C. G.; Johnson, J. S. *J. Am. Chem. Soc.* **2015,** *137,* 14574–14577. doi:10.1021/jacs.5b09593
44. Chen, D.; Deng, Y.; Sun, S.; Jia, P.; Huang, J.; Yan, W. *Adv. Synth. Catal.* **2023,** *365,* 178–193. doi:10.1002/adsc.202201091
45. Li, L.; Ye, L.; Ni, S.-F.; Li, Z.-L.; Chen, S.; Du, Y.-M.; Li, X.-H.; Dang, L.; Liu, X.-Y. *Org. Chem. Front.* **2017,** *4,* 2139–2146. doi:10.1039/c7qo00500h
46. Momiyama, N.; Jongwohan, C.; Ohtsuka, N.; Chaibuth, P.; Fujinami, T.; Adachi, K.; Suzuki, T. *J. Org. Chem.* **2022,** *87,* 9399–9407. doi:10.1021/acs.joc.2c00742
47. Momiyama, N.; Honda, Y.; Suzuki, T.; Jongwohan, C. *Asian J. Org. Chem.* **2021,** *10,* 2205–2212. doi:10.1002/ajoc.202100302

BEILSTEIN JOURNAL OF ORGANIC CHEMISTRY

Enantioselective regiospecific addition of propargyltrichlorosilane to aldehydes catalyzed by biisoquinoline *N,N'*-dioxide

Noble Brako[1], Sreerag Moorkkannur Narayanan[2], Amber Burns[1], Layla Auter[1], Valentino Cesiliano[2], Rajeev Prabhakar[*2] and Norito Takenaka[*1]

Letter

Open Access

Address:
[1]Department of Chemistry and Chemical Engineering, Florida Institute of Technology, 150 West University Boulevard, Melbourne, Florida 32901-6975, USA and [2]Department of Chemistry, University of Miami, 1301 Memorial Drive, Coral Gables, Florida 33146-0431, USA

Email:
Rajeev Prabhakar[*] - rpr@miami.edu; Norito Takenaka[*] - ntakenaka@fit.edu

* Corresponding author

Keywords:
α-allenic alcohol; computational chemistry; Lewis base catalysis; organocatalysis; propargyltrichlorosilane

Beilstein J. Org. Chem. **2024,** *20,* 3069–3076.
https://doi.org/10.3762/bjoc.20.255

Received: 26 July 2024
Accepted: 12 November 2024
Published: 25 November 2024

This article is part of the thematic issue "New advances in asymmetric organocatalysis II".

Guest Editor: R. Šebesta

Abstract

Distilled propargyltrichlorosilane with >99% isomeric purity was prepared for the first time, and its asymmetric catalytic regiospecific addition reaction to aldehydes was developed through a systematic catalyst structure–reactivity and selectivity relationship study. The observed catalyst structure–enantioselectivity relationship of the present allenylation reaction was found exactly opposite to that of the analogous allylation reaction. The method provided eleven α-allenic alcohols in 22–99% yield with 61:39–92:8 enantiomeric ratios. Furthermore, possible mechanisms of propargyl–allenyl isomerization of propargyltrichlorosilane were computationally investigated.

Introduction

Enantioenriched α-allenic alcohols are an important class of chiral building blocks used for the chemical synthesis of biologically relevant molecules [1-5]. Their strength comes from the rich synthetic versatility [6-9] and biological relevance [10] of the allene functionality. Accordingly, the development of efficient access to optically active chiral α-allenic alcohols continues to be of significant interest in organic chemistry [11-13]. The asymmetric catalytic addition of allenylation reagents to aldehydes provides direct access to chiral α-allenic alcohols in an enantioenriched form [11,12]. However, such metal/metalloid reagents and the corresponding metal catalyst-bound intermediates often equilibrate between possible regioisomeric

forms and can undergo both, S_E2 and S_E2' addition reactions, resulting in a mixture of homopropargylic alcohols and α-allenic alcohols [14-19], the separation of which is by no means trivial [20] (Scheme 1). Nonetheless, substituents at the carbon atom indicated by γ (R^2) of these reagents have been shown to bias the metallotropic rearrangement and/or the kinetic reactivity of the competing regioisomeric intermediates toward electrophiles [14-19]. Consequently, all reported asymmetric catalytic aldehyde allenylation methods are currently limited to metal/metalloid reagents bearing R^2 substituents [21-34], except for the methods with propargyltrichlorosilane [35,36] (Scheme 2). Other notable asymmetric catalytic approaches to prepare α-allenic alcohols (R^2 = H) include the Corey–Bakshi–Shibata reduction of allenyl ketones [37], enzymatic [38-40], non-enzymatic [41] kinetic resolution of racemic α-allenic alcohols, and asymmetric 1,4-difunctionalization of borylenynes by catalytic conjugative cross-coupling [42].

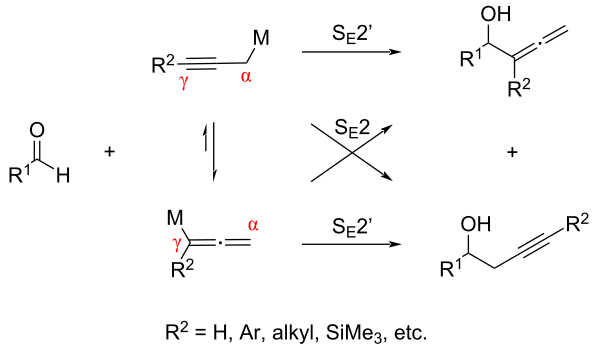

Scheme 1: Metallotropic rearrangement and regioselectivity issues.

Allenylation reagents that require regio-controlling auxiliaries such as a trimethylsilyl group (Scheme 2a) add steps before and/or after the reaction, thus they are less efficient in terms of atom- and step-economy [21-24,33,34]. In sharp contrast, propargyltrichlorosilane is configurationally stable and only reacts through the S_E2' mechanism under Lewis base-catalyzed conditions [43-45], although it was reported that distillation of propargyltrichlorosilane substantially isomerizes it to the thermodynamically more stable allenyltrichlorosilane that affords undesired homopropargylic alcohols [35,36] (Scheme 2b). Furthermore, Iseki [35] and Nakajima [36] evaluated only one chiral catalyst in their independent studies (i.e., no catalyst structure–reactivity and selectivity relationship study). In this context, we became interested in investigating propargyltrichlorosilane for the development of asymmetric catalytic allenylation methods [46]. It is worthy of note that propargyltrichlorosilane is an easy-to-handle liquid and only produces innoxious NaCl and SiO_2 as easy-to-separate inorganic byproducts upon quenching with aqueous NaOH or $NaHCO_3$ solutions.

Results and Discussion

Our group recently reported that *N*,*N*-diisopropylethylamine required for the synthesis of propargyltrichlorosilane isomerized

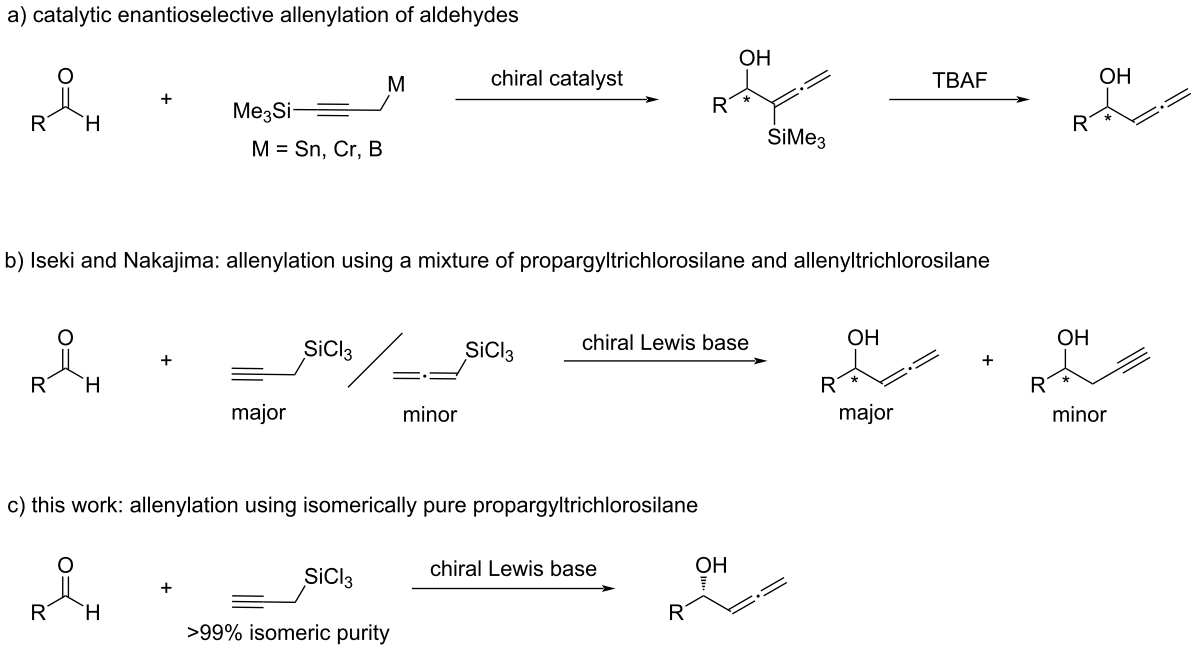

Scheme 2: Asymmetric catalytic allenylation of aldehydes.

it to allenyltrichlorosilane in the absence of solvents, and that removal of the amine before the distillation significantly suppressed the isomerization [46]. In this study, however, we could not prepare isomerically pure propargyltrichlorosilane on a preparative scale from propargyl chloride and CuCl by following Kobayashi's protocol [45] (propargyltrichlorosilane/allenyltrichlorosilane = 10:1) while we fully reproduced the reported result (2 mmol scale, propargyltrichlorosilane/allenyltrichlorosilane = >99:1). In the same report, Kobayashi also described that the combination of propargyl bromide and CuF_2 generated propargyltrichlorosilane faster than using propargyl chloride/CuCl without attenuating the selectivity. Although both protocols reported the same result with respect to the selectivity, we decided to test whether the combination of propargyl bromide and CuF_2 could afford isomerically pure propargyltrichlorosilane on a preparative scale. To our delight, we were able to generate propargyltrichlorosilane free of allenyltrichlorosilane on a 50 mmol scale albeit in 43% chemical yield (determined by ^{1}H NMR analysis of the reaction mixture using freshly distilled anhydrous methylene chloride as an internal standard, Scheme 3). There was no sign of allenyltrichlorosilane observable by ^{1}H NMR in the reaction mixture, but a trace amount of it was detected after the distillation (propargyltrichlorosilane/allenyltrichlorosilane = 200:1 by ^{1}H NMR spectroscopy, see Supporting Information File 1 for details).

With distilled propargyltrichlorosilane (>99% isomeric purity) in hand, we set out on our study on the allenylation reaction of benzaldehyde (**1a**) as model aldehyde with catalyst **3** (Scheme 4). Catalyst **3** was the only catalyst previously studied by Nakajima for propargyltrichlorosilane [36]. Ever since Nakajima reported the beneficial effect of *N*,*N*-diisopropylethylamine on the reaction rate of the aldehyde allylation reaction with allyltrichlorosilane [47], it has been routinely employed in analogous chlorosilane reactions [48-55]. However, a mechanistic basis of its role on the observed rate acceleration remains elusive while it certainly functions as a scavenger of HCl inherently present in chlorosilane reagents. Given our observation regarding propargyl–allenyl isomerization as discussed above, we wanted to avoid its use. Thus, we briefly tested whether 1) it is necessary for achieving a reasonable reaction rate, and 2) if it could be substituted with 4 Å molecular sieves as an acid scavenger. The reactions with catalyst **3** in the presence of either *N*,*N*-diisopropylethylamine or 4 Å molecular sieves gave identical results (99% yield, 78:22 er), and thus we decided to proceed with molecular sieves (Scheme 4).

It is often the case that the narrower the chiral pocket of a catalyst is (i.e., less degree of conformational freedom for a bound substrate), the better is the enantioselectivity for analogous chlorosilane-mediated reactionss [47-49,51,54]. Therefore, we gradually narrowed the chiral pocket of catalysts from **3** to **4**, **5** [53], and **6** [56,57]. To our surprise, the enantioselectivity consistently decreased as the chiral pocket became narrower while the reactivity remained the same. As such, we reduced the size of the substituents that craft the chiral pocket (**7**) and found that unsubstituted catalyst **8** was the most enantioselective. This observed catalyst structure–enantioselectivity relationship is exactly opposite to that for the analogous allylation reaction reported by Nakajima [47], thus it raises a possibility that the asymmetric induction mechanism could be fundamentally different between the present allenylation with propargyltrichlorosilane and the extensively investigated allylation with allyltrichlorosilane [58,59].

In light of the excellent reactivity and promising selectivity displayed by catalyst **8** for the model reaction, we proceeded to evaluate its ability to enantioselectively promote the allenylation of various aldehydes (Scheme 5). The catalyst tolerated all *p*-, *m*-, *o*-Cl-substituted benzaldehydes in terms of both reactivity and selectivity, affording the essentially same results as benzaldehyde (**2b**–**d**). Other electron-deficient substituents CF_3 (**2e**) and Br (**2f**) did not adversely affect the reaction. However, electron-donating substituents (Me and MeO) on the benzene ring substantially lowered the chemical yields while they did not affect the enantioselectivity (**2g**,**h**). Likewise, electron-rich aldehydes **1i**,**j** as well as the aliphatic aldehyde **1k** provided moderate yields. These aldehydes gave substantially lower enantioselectivities than benzaldehydes, which may be attributable to that they have smaller steric demands in the vicinity of the carbonyl carbon atom than benzaldehyde. Importantly, we did not observe the corresponding homopropargylic alcohols

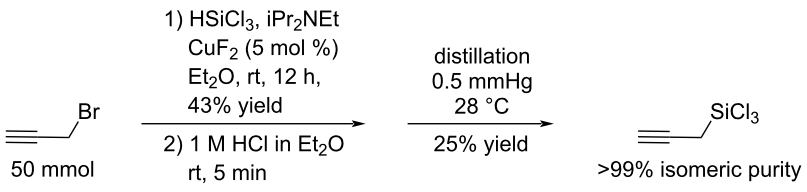

Scheme 3: Selective preparation of propargyltrichlorosilane.

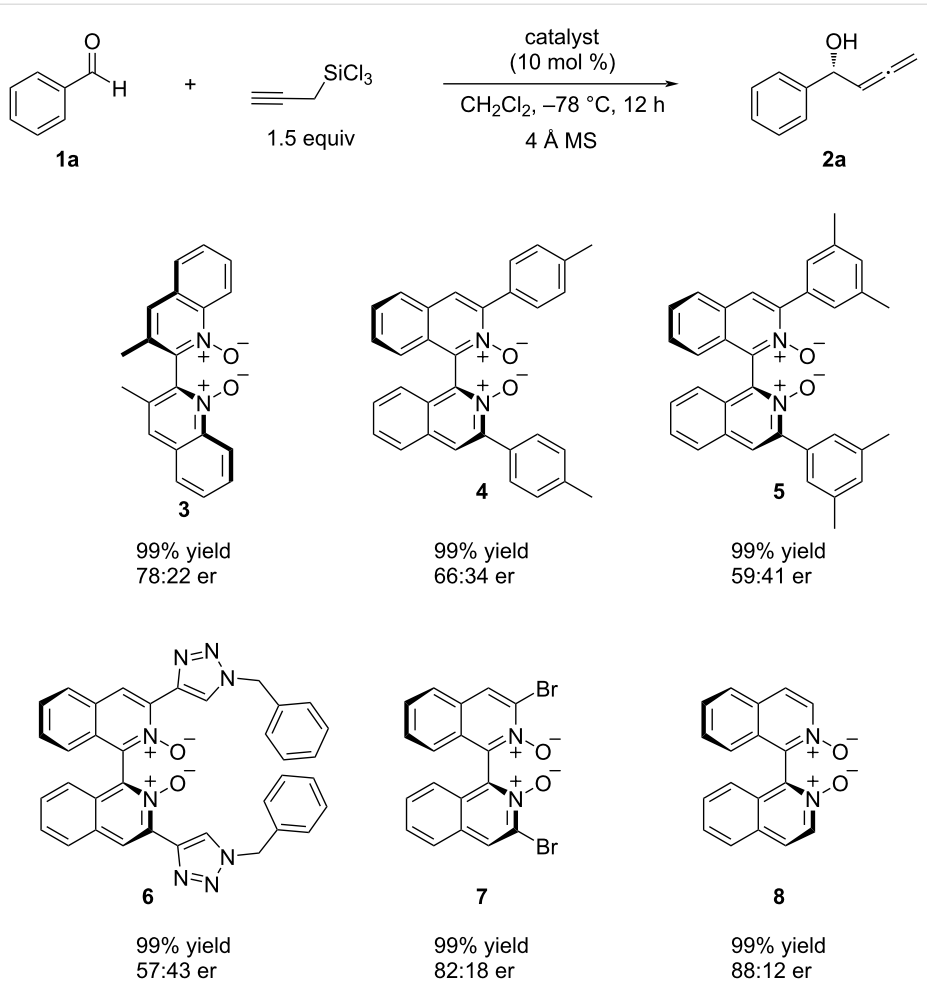

Scheme 4: Evaluation of C_2-symmetric catalysts with benzaldehyde (**1a**) as a model aldehyde. Reaction conditions: **1a** (0.1 mmol), silane (0.15 mmol), catalyst (0.01 mmol), CH_2Cl_2 (0.4 mL); yields were determined by ^{1}H NMR spectroscopy with 1,1,2,2-tetrachloroethane as an internal standard following workup and enantiomeric ratios were determined by HPLC on a chiral stationary phase.

[51] in all cases. Since this work is the first asymmetric catalysis study of isomerically pure propargyltrichlorosilane, it clearly demonstrated that this class of chiral Lewis bases regiospecifically catalyzed the addition of propargyltrichlorosilane to aldehydes, and that these catalysts did not induce the propargyl–allenyl metallotropic rearrangement albeit activating the C–Si bond. Thus, these findings underscore the importance of propargyltrichlorosilane as a regiospecific allenylation reagent and bode well for the development of new reactions.

As we recently reported [46], we noticed during our initial investigation that propargyltrichlorosilane underwent isomerization to allenyltrichlorosilane in the presence of *N*,*N*-diisopropylethylamine upon standing after distillation (i.e., without solvent). Although the base-promoted propargyl–allenyl isomerization is well precedented in literature [60,61], we decided to investigate possible mechanisms of the propargyltrichlorosilane isomerization in the absence and presence of *N*,*N*-diisopropylethylamine using density functional theory (DFT) calculations (Figure 1).

According to the DFT calculations, the free propargyltrichlorosilane ($\mathbf{I_{prop}}$) can isomerize to allenyltrichlorosilane ($\mathbf{I_{all}}$) with a prohibitively high barrier of 43.8 kcal/mol (Figure 1a). This suggests that the isomerization is not energetically feasible on its own. However, in the presence of *N*,*N*-diisopropylethylamine this process can occur readily. In the reactant ($\mathbf{R_{prop}}$ in Figure 1b), the nitrogen atom of *N*,*N*-diisopropylethylamine forms a hydrogen bond with the H_1 proton of propargyltrichlorosilane and significantly activates the C_1–H_1 bond (1.11 Å). It is noteworthy that the nitrogen atom can also interact with the Si atom of propargyltrichlorosilane which is a stronger electrophile compared to the H_1 atom. However, the bulky groups around nitrogen and three chlorine atoms coordinated to Si prevent a direct Si–N interaction. From $\mathbf{R_{prop}}$, the amine group of *N*,*N*-diisopropylethylamine abstracts the H_1

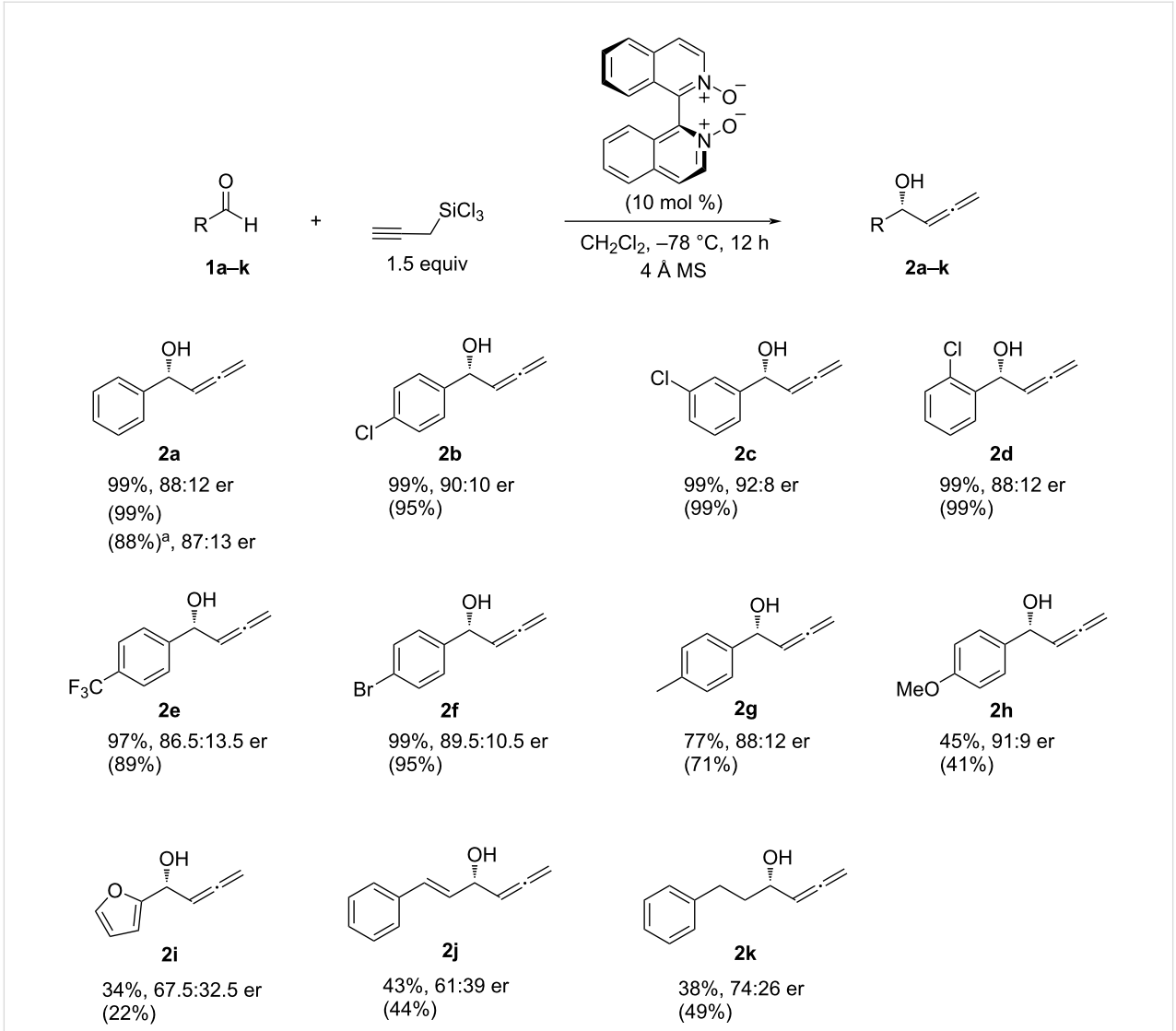

Scheme 5: Evaluation of the extent to which (*S*)-**8** catalyzed the allenylation reaction. Reaction conditions: aldehyde **1a–k** (0.1 mmol), silane (0.15 mmol), (*S*)-**8** (0.01 mmol), CH_2Cl_2 (0.4 mL). Enantiomeric ratios were determined by HPLC on a chiral stationary phase, yields were determined by ^{1}H NMR spectroscopy with 1,1,2,2-tetrachloroethane as an internal standard following workup and isolated yields are given in parentheses. aReaction conditions: **1a** (1.0 mmol), silane (1.5 mmol), (*S*)-**8** (0.1 mmol), CH_2Cl_2 (4.0 mL).

proton with a barrier of 14.2 kcal/mol to form an intermediate (**IN$_1$**). The intermediate **IN$_1$** is unstable (endergonic by 14.0 kcal/mol) and will immediately stabilize to another intermediate (**IN$_2$**) which is 1.2 kcal/mol lower in energy than **IN$_1$**. The **IN$_1$**→**IN$_2$** transformation is driven by the redistribution of the negative charge on C_1 in **IN$_1$**. In particular, the Mulliken charge on C_1 reduces from −0.77*e* to −0.66*e* and the charge on C_3 increases from −0.43*e* to −0.55*e* and facilitate Coulombic interaction between C_3 and H_1. In the next step, from **IN$_2$**, in a barrier-less process the C_3 atom abstracts the H_1 proton that was acquired by the N atom in the previous step to generate allenyltrichlorosilane (**R$_{all}$**). Overall, the **R$_{prop}$**→**R$_{all}$** isomerization is almost thermoneutral, i.e., **R$_{all}$** being 1.7 kcal/mol exergonic from **R$_{prop}$**. These results show that the presence of *N*,*N*-diisopropylethylamine as base makes this process more energetically feasible by substantially stabilizing the transition states and intermediates in the pathway. These results are strongly supported by the experimental data. In a previous study, Hoveyda and co-workers proposed a similar mechanism for the isomerization of alkynes to allenes catalyzed by 1,8-diazabicyclo[5.4.0]undec-7-ene [61].

Conclusion

In this study, we prepared distilled propargyltrichlorosilane with >99% isomeric purity for the first time, developed its asymmetric catalytic regiospecific addition reaction to aldehydes via

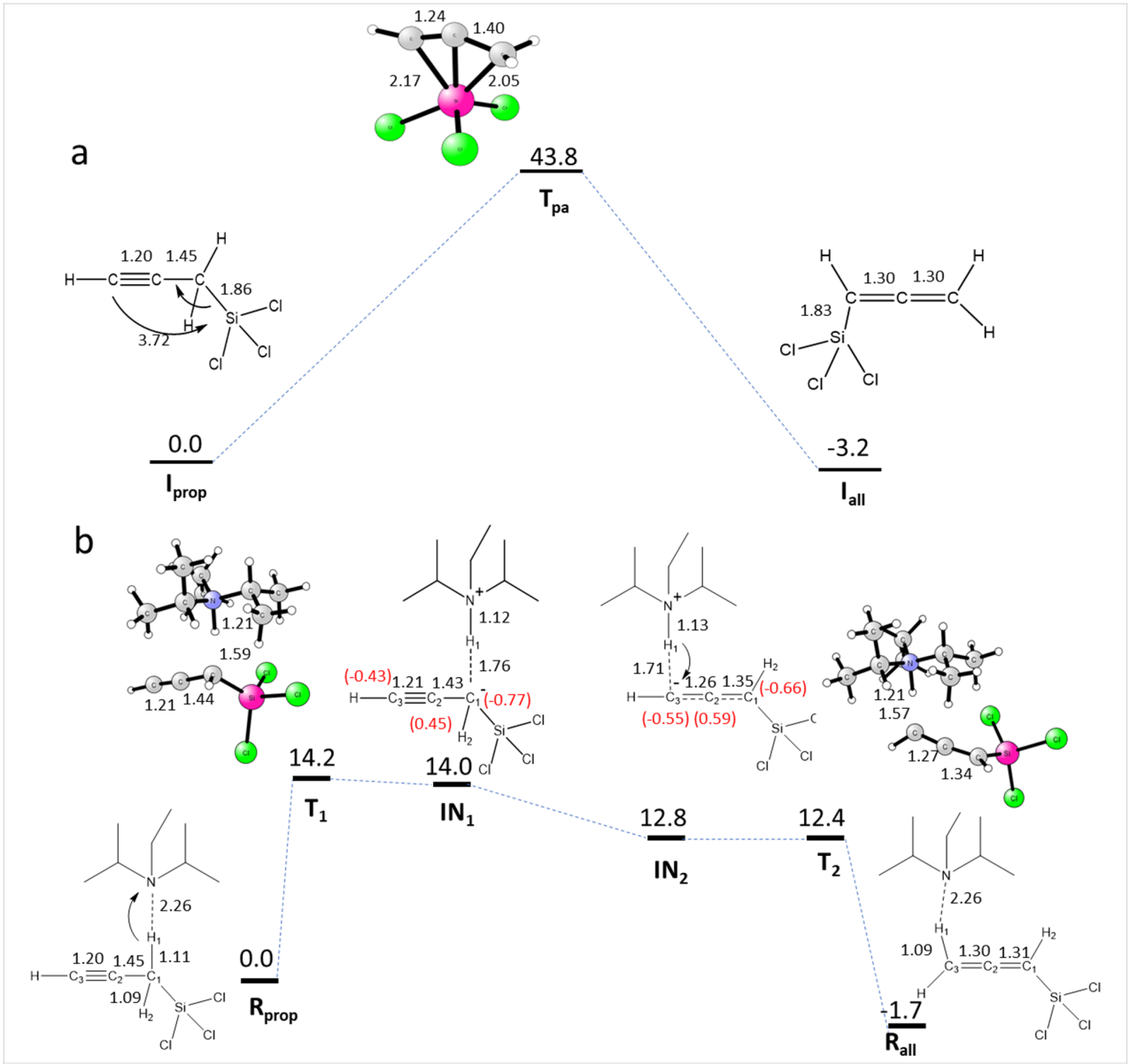

Figure 1: A potential energy surface (PES) for the proposed mechanism for (a) isomerization of propargyltrichlorosilane without *N*,*N*-diisopropylethylamine and (b) with *N*,*N*-diisopropylethylamine. It includes Gibbs free energies (kcal/mol) and Mulliken charges (in parentheses).

a systematic catalyst structure–reactivity and selectivity relationship study, and computationally investigated possible mechanisms of *N*,*N*-diisopropylethylamine-promoted propargyl–allenyl isomerization of propargyltrichlorosilane. The observed catalyst structure–enantioselectivity relationship of the present allenylation reaction was found exactly opposite to that of the extensively investigated analogous allylation reaction, the findings of which raises a possibility that asymmetric induction mechanisms could be fundamentally different between the two transformations. Studies directed toward a better understanding of possible transition-state structures and the design of new catalysts to improve the results are currently underway in our laboratories.

Supporting Information

Supporting Information File 1

Experimental details, characterization data, spectra, and HPLC traces.
[https://www.beilstein-journals.org/bjoc/content/supplementary/1860-5397-20-255-S1.pdf]

Acknowledgements

We thank the Florida Institute of Technology and University of Miami for the generous support of the instrumentation facility.

Funding

This work was financially supported by a grant from the National Institute of Health (1R15 GM139087-01) to N.T. and a grant from the National Science Foundation (Grant Number CHE- 2102563) to R.P.

ORCID® iDs

Noble Brako - https://orcid.org/0009-0008-0406-7399
Sreerag Moorkkannur Narayanan - https://orcid.org/0000-0001-5075-6947
Amber Burns - https://orcid.org/0009-0007-4752-4169
Layla Auter - https://orcid.org/0009-0000-3996-258X
Valentino Cesiliano - https://orcid.org/0009-0005-1076-3313
Rajeev Prabhakar - https://orcid.org/0000-0003-1137-1272
Norito Takenaka - https://orcid.org/0000-0003-3542-1086

Data Availability Statement

All data that supports the findings of this study is available in the published article and/or the supporting information of this article.

References

1. Krause, N.; Belting, V.; Deutsch, C.; Erdsack, J.; Fan, H.-T.; Gockel, B.; Hoffmann-Röder, A.; Morita, N.; Volz, F. *Pure Appl. Chem.* **2008,** *80,* 1063–1069. doi:10.1351/pac200880051063
2. Alonso, J. M.; Almendros, P. *Chem. Rev.* **2021,** *121,* 4193–4252. doi:10.1021/acs.chemrev.0c00986
3. Yoshida, M.; Shoji, Y.; Shishido, K. *Org. Lett.* **2009,** *11,* 1441–1443. doi:10.1021/ol9001637
4. Wang, Y.; Hoen, R.; Hong, R. *Synlett* **2012,** *23,* 2729–2734. doi:10.1055/s-0032-1317566
5. Roy, A.; Bhat, B. A.; Lepore, S. D. *Org. Lett.* **2015,** *17,* 900–903. doi:10.1021/ol503757h
6. Yu, S.; Ma, S. *Angew. Chem., Int. Ed.* **2012,** *51,* 3074–3112. doi:10.1002/anie.201101460
7. Lechel, T.; Pfrengle, F.; Reissig, H.-U.; Zimmer, R. *ChemCatChem* **2013,** *5,* 2100–2130. doi:10.1002/cctc.201200875
8. Adams, C. S.; Weatherly, C. D.; Burke, E. G.; Schomaker, J. M. *Chem. Soc. Rev.* **2014,** *43,* 3136–3163. doi:10.1039/c3cs60416k
9. Muñoz, M. P. *Chem. Soc. Rev.* **2014,** *43,* 3164–3183. doi:10.1039/c3cs60408j
10. Hoffmann-Röder, A.; Krause, N. *Angew. Chem., Int. Ed.* **2004,** *43,* 1196–1216. doi:10.1002/anie.200300628
11. Yamamoto, H.; Usanov, D. L. Propargyl and Allenyl Organometallics. *Comprehensive Organic Synthesis,* 2nd ed.; Elsevier, 2014; Vol. 2, pp 209–242. doi:10.1016/b978-0-08-097742-3.00206-8
12. Thaima, T.; Zamani, F.; Hyland, C. J. T.; Pyne, S. G. *Synthesis* **2017,** *49,* 1461–1480. doi:10.1055/s-0036-1588397
13. Huang, X.; Ma, S. *Acc. Chem. Res.* **2019,** *52,* 1301–1312. doi:10.1021/acs.accounts.9b00023
14. Wisniewska, H. M.; Jarvo, E. R. *J. Org. Chem.* **2013,** *78,* 11629–11636. doi:10.1021/jo4019107
15. Lin, M.-J.; Loh, T.-P. *J. Am. Chem. Soc.* **2003,** *125,* 13042–13043. doi:10.1021/ja037410i
16. Guo, L.-N.; Gao, H.; Mayer, P.; Knochel, P. *Chem. – Eur. J.* **2010,** *16,* 9829–9834. doi:10.1002/chem.201000523
17. Fandrick, K. R.; Ogikubo, J.; Fandrick, D. R.; Patel, N. D.; Saha, J.; Lee, H.; Ma, S.; Grinberg, N.; Busacca, C. A.; Senanayake, C. H. *Org. Lett.* **2013,** *15,* 1214–1217. doi:10.1021/ol400124f
18. Zhang, R.; Xia, Y.; Yan, Y.; Ouyang, L. *BMC Chem.* **2022,** *16,* 14. doi:10.1186/s13065-022-00803-3
19. Dai, X.-L.; Ran, J.; Rajeshkumar, T.; Xu, Z.; Liu, S.; Lv, Z.; Maron, L.; Chen, Y.-H. *Org. Lett.* **2023,** *25,* 3060–3065. doi:10.1021/acs.orglett.3c00824
20. Fu, F.; Hoang, K. L. M.; Loh, T.-P. *Org. Lett.* **2008,** *10,* 3437–3439. doi:10.1021/ol801087s
21. Yu, C.-M.; Yoon, S.-K.; Baek, K.; Lee, J.-Y. *Angew. Chem., Int. Ed.* **1998,** *37,* 2392–2395. doi:10.1002/(sici)1521-3773(19980918)37:17<2392::aid-anie2392>3.0.co;2-d
22. Inoue, M.; Nakada, M. *Angew. Chem., Int. Ed.* **2006,** *45,* 252–255. doi:10.1002/anie.200502871
23. Xia, G.; Yamamoto, H. *J. Am. Chem. Soc.* **2007,** *129,* 496–497. doi:10.1021/ja0679578
24. Reddy, L. R. *Chem. Commun.* **2012,** *48,* 9189–9191. doi:10.1039/c2cc34371a
25. Yu, C.-M.; Yoon, S.-K.; Lee, S.-J.; Lee, J.-Y.; Yoon, S.-K.; Kim, S. S. *Chem. Commun.* **1998,** 2749–2750. doi:10.1039/a807940d
26. Durán-Galván, M.; Connell, B. T. *Eur. J. Org. Chem.* **2010,** 2445–2448. doi:10.1002/ejoc.201000199
27. Durán-Galván, M.; Worlikar, S. A.; Connell, B. T. *Tetrahedron* **2010,** *66,* 7707–7719. doi:10.1016/j.tet.2010.07.065
28. Wang, M.; Khan, S.; Miliordos, E.; Chen, M. *Adv. Synth. Catal.* **2018,** *360,* 4634–4639. doi:10.1002/adsc.201801080
29. Yanagisawa, A.; Bamba, K.; Kawada, A. *ChemistrySelect* **2018,** *3,* 13777–13781. doi:10.1002/slct.201802999
30. Tap, A.; Blond, A.; Wakchaure, V. N.; List, B. *Angew. Chem., Int. Ed.* **2016,** *55,* 8962–8965. doi:10.1002/anie.201603649
31. Zhong, F.; Xue, Q.-Y.; Yin, L. *Angew. Chem., Int. Ed.* **2020,** *59,* 1562–1566. doi:10.1002/anie.201912140
32. Xu, G.; Wang, Z.; Shao, Y.; Sun, J. *Org. Lett.* **2021,** *23,* 5175–5179. doi:10.1021/acs.orglett.1c01712
33. Zhang, F.-H.; Guo, X.; Zeng, X.; Wang, Z. *Nat. Commun.* **2022,** *13,* 5036. doi:10.1038/s41467-022-32614-4
34. Zhang, F.-H.; Guo, X.; Zeng, X.; Wang, Z. *Angew. Chem., Int. Ed.* **2022,** *61,* e202117114. doi:10.1002/anie.202117114
35. Iseki, K.; Kuroki, Y.; Kobayashi, Y. *Tetrahedron: Asymmetry* **1998,** *9,* 2889–2894. doi:10.1016/s0957-4166(98)00290-0
36. Nakajima, M.; Saito, M.; Hashimoto, S. *Tetrahedron: Asymmetry* **2002,** *13,* 2449–2452. doi:10.1016/s0957-4166(02)00640-7
37. Yu, C.-M.; Kim, C.; Kweon, J.-H. *Chem. Commun.* **2004,** 2494–2495. doi:10.1039/b407387h
38. Yang, B.; Zhu, C.; Qiu, Y.; Bäckvall, J.-E. *Angew. Chem., Int. Ed.* **2016,** *55,* 5568–5572. doi:10.1002/anie.201601505
39. Li, W.; Lin, Z.; Chen, L.; Tian, X.; Wang, Y.; Huang, S.-H.; Hong, R. *Tetrahedron Lett.* **2016,** *57,* 603–606. doi:10.1016/j.tetlet.2015.12.098
40. Zhang, T.; Zhu, C. *Synlett* **2024,** *35,* 1170–1174. doi:10.1055/s-0042-1751525
41. Wang, Y.; Zheng, K.; Hong, R. *J. Am. Chem. Soc.* **2012,** *134,* 4096–4099. doi:10.1021/ja300453u
42. Law, C.; Kativhu, E.; Wang, J.; Morken, J. P. *Angew. Chem., Int. Ed.* **2020,** *59,* 10311–10315. doi:10.1002/anie.202001580
43. Kobayashi, S.; Nishio, K. *J. Am. Chem. Soc.* **1995,** *117,* 6392–6393. doi:10.1021/ja00128a043
44. Schneider, U.; Sugiura, M.; Kobayashi, S. *Tetrahedron* **2006,** *62,* 496–502. doi:10.1016/j.tet.2005.08.114

45. Schneider, U.; Sugiura, M.; Kobayashi, S. *Adv. Synth. Catal.* **2006,** *348,* 323–329. doi:10.1002/adsc.200505379
46. Xu, C.; Nader, P.; Xavier, J.; Takenaka, N. *Synlett* **2023,** *34,* 2461–2464. doi:10.1055/s-0042-1751478
47. Nakajima, M.; Saito, M.; Shiro, M.; Hashimoto, S.-i. *J. Am. Chem. Soc.* **1998,** *120,* 6419–6420. doi:10.1021/ja981091r
48. Shimada, T.; Kina, A.; Ikeda, S.; Hayashi, T. *Org. Lett.* **2002,** *4,* 2799–2801. doi:10.1021/ol026376u
49. Malkov, A. V.; Westwater, M.-M.; Gutnov, A.; Ramírez-López, P.; Friscourt, F.; Kadlčíková, A.; Hodačová, J.; Rankovic, Z.; Kotora, M.; Kočovský, P. *Tetrahedron* **2008,** *64,* 11335–11348. doi:10.1016/j.tet.2008.08.084
50. Kadlčíková, A.; Valterová, I.; Ducháčková, L.; Roithová, J.; Kotora, M. *Chem. – Eur. J.* **2010,** *16,* 9442–9445. doi:10.1002/chem.201001523
51. Chen, J.; Captain, B.; Takenaka, N. *Org. Lett.* **2011,** *13,* 1654–1657. doi:10.1021/ol200102c
52. Huang, Y.; Yang, L.; Shao, P.; Zhao, Y. *Chem. Sci.* **2013,** *4,* 3275–3281. doi:10.1039/c3sc50973g
53. Reep, C.; Morgante, P.; Peverati, R.; Takenaka, N. *Org. Lett.* **2018,** *20,* 5757–5761. doi:10.1021/acs.orglett.8b02457
54. Vaganov, V. Y.; Fukazawa, Y.; Kondratyev, N. S.; Shipilovskikh, S. A.; Wheeler, S. E.; Rubtsov, A. E.; Malkov, A. V. *Adv. Synth. Catal.* **2020,** *362,* 5467–5474. doi:10.1002/adsc.202000936
55. Xu, C.; Nader, P.; Xavier, J.; Captain, B.; Takenaka, N. *Tetrahedron* **2023,** *141,* 133496. doi:10.1016/j.tet.2023.133496
56. Sun, S.; Reep, C.; Zhang, C.; Captain, B.; Peverati, R.; Takenaka, N. *Tetrahedron Lett.* **2021,** *81,* 153338. doi:10.1016/j.tetlet.2021.153338
57. Sun, S.; Xu, C.; Jarvis, J.; Nader, P.; Naumann, B.; Soliven, A.; Peverati, R.; Takenaka, N. *Catalysts* **2021,** *11,* 1103. doi:10.3390/catal11091103
58. Fu, J.; Fujimori, S.; Denmark, S. E. Bifunctional Lewis Base Catalysis with Dual Activation of X 3 Si–Nu and C=O (n → σ*). In *Lewis Base Catalysis in Organic Synthesis;* Vedejs, E.; Denmark, S. E., Eds.; Wiley-VCH: Weinheim, Germany, 2016; pp 281–338. doi:10.1002/9783527675142.ch9
59. Malkov, A. V.; Kočovský, P. Lewis Base-Catalyzed Reactions of SiX 3-Based reagents with C=O, C=N (n→σ*). In *Lewis Base Catalysis in Organic Synthesis;* Vedejs, E.; Denmark, S. E., Eds.; Wiley-VCH: Weinheim, Germany, 2016; pp 1011–1038. doi:10.1002/9783527675142.ch20
60. Xing, Y.; Wei, Y.; Zhou, H. *Curr. Org. Chem.* **2012,** *16,* 1594–1608. doi:10.2174/138527212800840973
61. Dabrowski, J. A.; Haeffner, F.; Hoveyda, A. H. *Angew. Chem., Int. Ed.* **2013,** *52,* 7694–7699. doi:10.1002/anie.201303501

License and Terms

BEILSTEIN JOURNAL OF ORGANIC CHEMISTRY

Non-covalent organocatalyzed enantioselective cyclization reactions of α,β-unsaturated imines

Sergio Torres-Oya and Mercedes Zurro*

Review

Open Access

Address:
Departamento de Química Orgánica y Química Inorgánica, Instituto de Investigación Química "Andrés M. del Río" (IQAR), Universidad de Alcalá (IRYCIS), 28805 Madrid, Spain

Email:
Mercedes Zurro* - mercedes.zurro@uah.es

* Corresponding author

Keywords:
α,β-unsaturated imines; asymmetric organocatalysis; cyclization; *N*-heterocycles; inverse electron demand aza-Diels–Alder reaction

Beilstein J. Org. Chem. **2024,** *20,* 3221–3255.
https://doi.org/10.3762/bjoc.20.268

Received: 10 August 2024
Accepted: 22 November 2024
Published: 10 December 2024

This article is part of the thematic issue "New advances in asymmetric organocatalysis II".

Guest Editor: R. Šebesta

Abstract

Asymmetric cycloaddition is a straightforward strategy which enables the synthesis of structurally distinct cyclic derivatives which are difficult to access by other methodologies, using an efficient and atom-economical path from simple precursors. In recent years several asymmetric catalytic cyclization strategies have been accomplished for the construction of *N*-heterocycles using various catalytic systems such as chiral metal catalysts, chiral Lewis acids or chiral organocatalysts. This review presents an overview of the recent advances in enantioselective cyclization reactions of 1-azadienes catalyzed by non-covalent organocatalysts.

Introduction

Nitrogen-containing heterocycles are abundant scaffolds present in natural products, biologically active compounds, pharmaceuticals, synthetic agrochemicals, and functional materials [1,2]. Due to their importance, different synthetic routes involving stoichiometric and catalytic approaches have been developed.

The α,β-unsaturated imines, also known as conjugated imines or 1-azadienes, are useful precursors for the construction of aza-heterocycles. Due to their structure, they can be attacked by a nucleophile and undergo a 1,2-addition or conjugate addition leading to the production of allylic amines or aliphatic imines, respectively. They can also behave as C4 synthons in cycloaddition reactions such as the aza-Diels–Alder reaction, giving access to nitrogen-containing cyclic derivatives. Conjugated imines are usually synthesized from the corresponding carbonyl precursors by reaction with a sulfonamide in the presence of Lewis acids and a dehydrating agent such as molecular sieves [3]. Also, recently a palladium-catalyzed dehydrogenation of aliphatic imines was reported, providing a novel methodology for the construction of α,β-unsaturated imines [4].

There are different types of α,β-unsaturated imines, such as the acyclic imines aldimines, ketimines, or dienimines, depending on whether they are derived from aldehydes, ketones, or doubly unsaturated ketones, respectively. Additionally, the most common cyclic α,β-unsaturated imines involve benzofuran or saccharin-derived azadienes (Figure 1).

Cycloaddition reactions, especially Diels–Alder reactions, have attracted a lot of attention since their discovery as one of the most powerful methodologies for the construction of carbon–carbon bonds [5-10]. The hetero-Diels–Alder reaction is therefore an attractive strategy for the synthesis of heterocyclic compounds. It involves the reaction of dienes or dienophiles which possess a heteroatom in their structure. In this reaction, the HOMO of the diene and the LUMO of the dienophile interact to construct the six-membered heterocyclic derivative and the reaction requires electron-rich dienes and electron-poor dienophiles (Figure 2a). In the inverse electron demand hetero-Diels–Alder reaction (IEDHDA), the LUMO of the diene interacts with the HOMO of the dienophile, and therefore it proceeds through the reaction of electron-poor dienes and electron-rich dienophiles (Figure 2b).

α,β-Unsaturated imines can undergo inverse electron demand aza-Diels–Alder reactions (IEDADA) to produce *N*-heterocyclic compounds. The search for an enantioselective pathway to carry out IEDADA reactions has been a glowing field in recent years [11,12]. In particular, organocatalysis can provide different activation modes to promote enantioselective IEDADA reactions [13,14], based on three strategies (Figure 3): i) LUMO-lowering activation (Brønsted acid catalysis), ii) HOMO-raising activation (amine-based catalysis and *N*-heterocyclic carbenes), and iii) LUMO-lowering and HOMO-raising activation (bifunctional thioureas and squaramides).

Due to the ubiquitous nature of non-covalent interactions in organic systems, they can play a decisive role in asymmetric transformations [15]. Although quite important in all organocatalytic processes, there are specific organocatalysts which activate reactants through non-covalent interactions such as hydrogen bonding. These interactions are crucial to obtain high enantioselectivity in the reaction. The 1-azadienes possess an electronegative nitrogen atom which is prone to interacting with hydrogen-bond donors or Brønsted acids decreasing the LUMO energy of the diene. This review article aims to give an

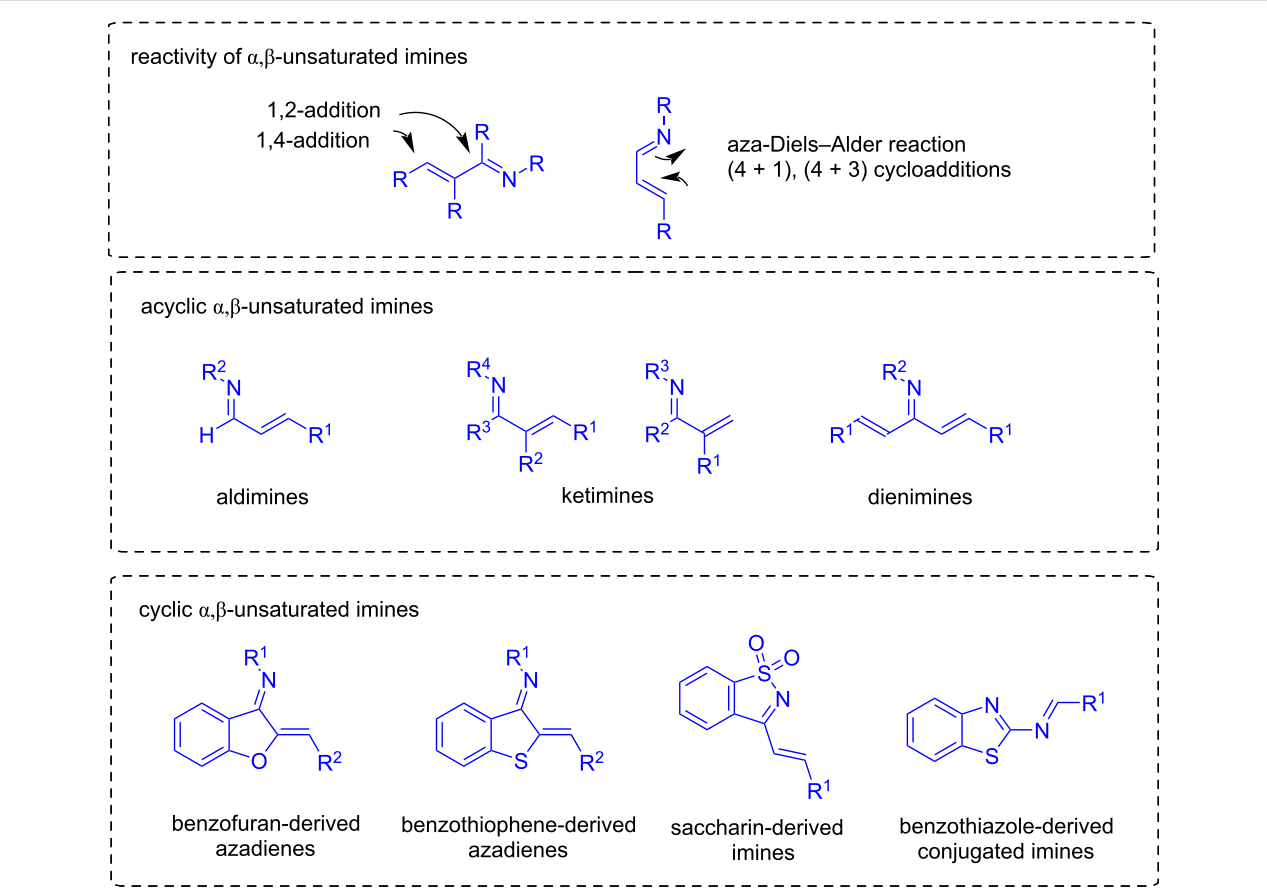

Figure 1: Reactivity of α,β-unsaturated imines and variety of structures.

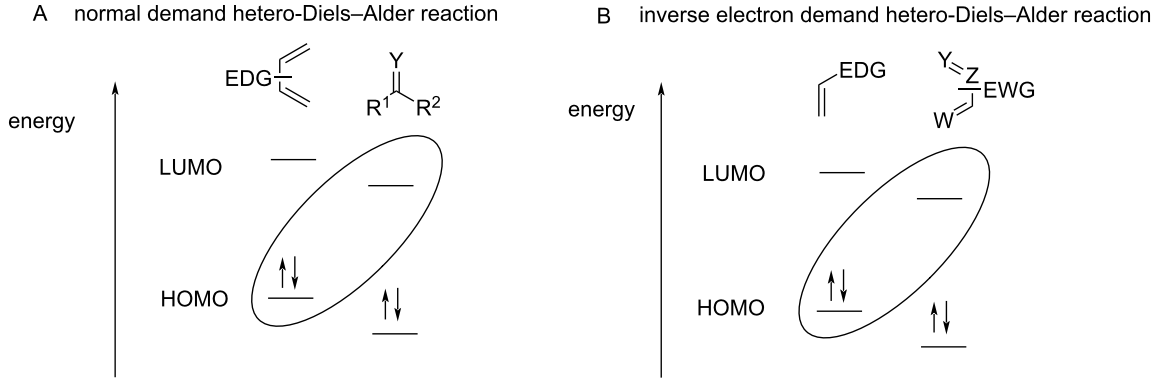

Figure 2: The hetero-Diels–Alder and inverse electron demand hetero-Diels–Alder reactions.

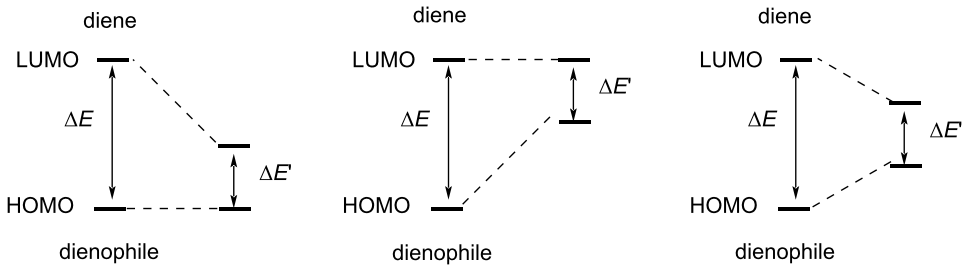

Figure 3: Different strategies to promote the activation of dienes and dienophiles in IEDADA reactions.

overview of the non-covalent organocatalyzed cyclization reactions involving α,β-unsaturated imines. Although most of the cyclization methodologies of 1-azadienes involve a formal [4 + 2] cycloaddition (IEDADA reaction) to construct six-membered nitrogen-containing molecules, α,β-unsaturated imines can also behave as C4 synthons involved in (4 + 1) and (4 + 3) cycloadditions or they act as C2 synthons undergoing (2 + 3) cycloadditions for example. This review discusses different examples involving IEDADA reactions and other cyclizations, with a special focus on the mode of action of the organocatalysts, and aims to show the synthetic applicability of the formed cyclic derivatives. The three non-covalent organocatalysts which will be covered in this review are hydrogen-bond donors such as thioureas and squaramides, Brønsted bases such as tertiary amines, and Brønsted acids such as chiral phosphoric acids. As depicted in Figure 4, a bifunctional squaramide is able to activate both an α,β-unsaturated imine through hydrogen bonding with the squaramide moiety and a nucleophile through deprotonation as Brønsted base. On the other hand, a chiral phosphoric acid provides a confined chiral environment where the reactants are approached, activating both the azadiene by interaction with the acidic hydrogen and a dienophile bearing a carbamate group by interaction with the oxygen atom of the phosphoryl group.

Although recently Rana and co-workers published a review article covering catalytic asymmetric transformations of azadienes [16], there is still room for this review which only focuses on non-covalent organocatalyzed cyclizations, and it will be a useful reference for organic chemists working in the field of asymmetric organocatalysis. The review is divided into sections, each covering a different catalytic system. Additionally, a chronological order is followed in the subchapters. In order to also give a general overview of the field, other dienes bearing two nitrogen atoms in their structure such as 1,3-azadienes or azo-alkenes are also included. On the contrary, asymmetric cyclizations involving aza-*ortho*-quinone intermediates and in situ-formed 1-azadienes were excluded as they have been discussed in other recent reviews [17,18].

Review

Hydrogen bond donors: bifunctional thioureas and squaramides

The use of bifunctional catalysts is commonplace in organocatalyzed transformations [19-23]. These catalysts are able to activate an electrophile and a nucleophile simultaneously and in IEDADA reactions they are employed to promote HOMO-raising and LUMO-lowering of both reactants leading to an en-

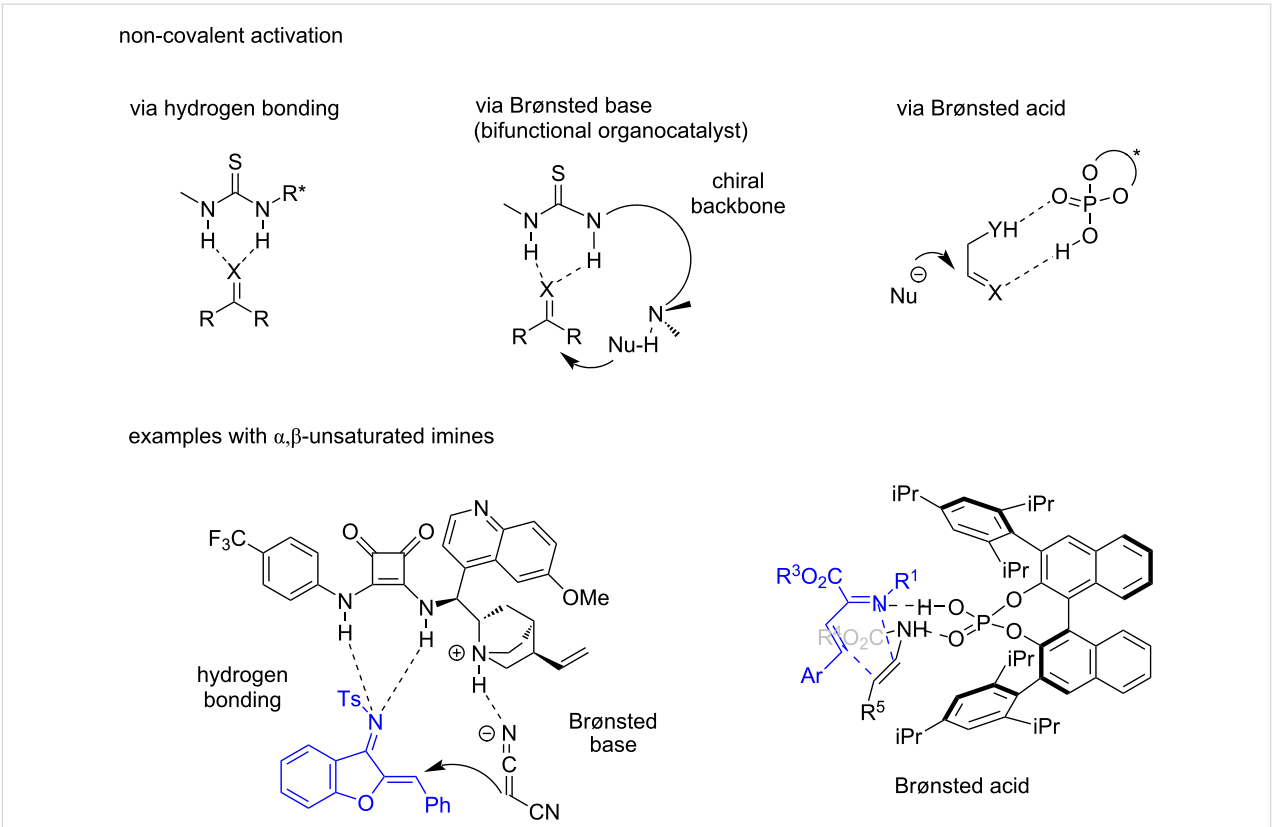

Figure 4: Examples of non-covalent interactions in organocatalysis.

antioselective transformation. In this section, cyclization reactions of α,β-unsaturated imines catalyzed by hydrogen-bond donors, including bifunctional thioureas and squaramides bearing a Brønsted base moiety in their structure will be described.

In 2012, Wang and co-workers reported a bifunctional thiourea-catalyzed aza-Diels–Alder reaction of cyclic keto/enolate salts **1** and *N*-tosyl-2-methylene-but-3-enoates **2** (Scheme 1). After a screening of the reaction conditions they found that organocatalyst **I**, acetic acid as additive and a mixture of toluene and water provided the best results in terms of yield and enantioselectivity. A wide scope was explored, including electron-donating substituents and electron-withdrawing groups, as well as heterocycles, giving densely functionalized chiral azaspirocyclic derivatives **3** in yields up to 99%, up to 20:1 dr, and up to 99% ee [24]. This work represents the first enantioselective bifunctional catalytic inverse electron demand Diels–Alder reaction that occurs with a dual control of the dienophile HOMO and diene LUMO energies of the substrates. The amino group of the organocatalyst acts as a Lewis base forming an enamine which raises the HOMO energy of the dienophile, while the thiourea moiety acts as a Lewis acid, lowering the LUMO level of the diene (Scheme 1). A confined transition state is formed providing a high enantiocontrol of the reaction.

In 2016, Shi and co-workers reported a cinchona alkaloid-derived thiourea-catalyzed regio- and stereoselective cycloaddition of 3-isothiocyanatooxindoles and imines containing two or three electron-deficient unsaturated bonds [25]. Firstly, the (3 + 2) cycloaddition of 3-isothiocyanatooxindoles **4** and aldimines **5** was explored leading to the synthesis of spirooxindole derivatives **6** bearing a thiourea moiety in high yields (91–97%), and with good to excellent diastereoselectivities (10:1–20:1 dr) and enantioselectivities (61–96%) (Scheme 2).

Furthermore, the authors also investigated the reactivity of ketimines and dienimines (Scheme 3). The reaction of 3-isothiocyanatooxindoles **4** and ketimines **7** led to the (3 + 2) cycloaddition through the C=C bond of the α,β-unsaturated imine instead of the C=N bond, affording various spirocyclic derivatives **8** with excellent yields (92–98%), diastereoselectivities (15:1–20:1 dr), and enantioselectivities (90–99% ee). This result could be attributed to the higher steric hindrance at the carbon atom of the imine. On the other hand, the reaction of 3-isothiocyanatooxindoles **4** and dienimines **9** afforded the cascade cycloadducts **10** in high yields (74–94%) and excellent diastereoselectivities (>20:1 dr) and good to excellent enantioselectivities (60–97% ee) when using organocatalyst **III**.

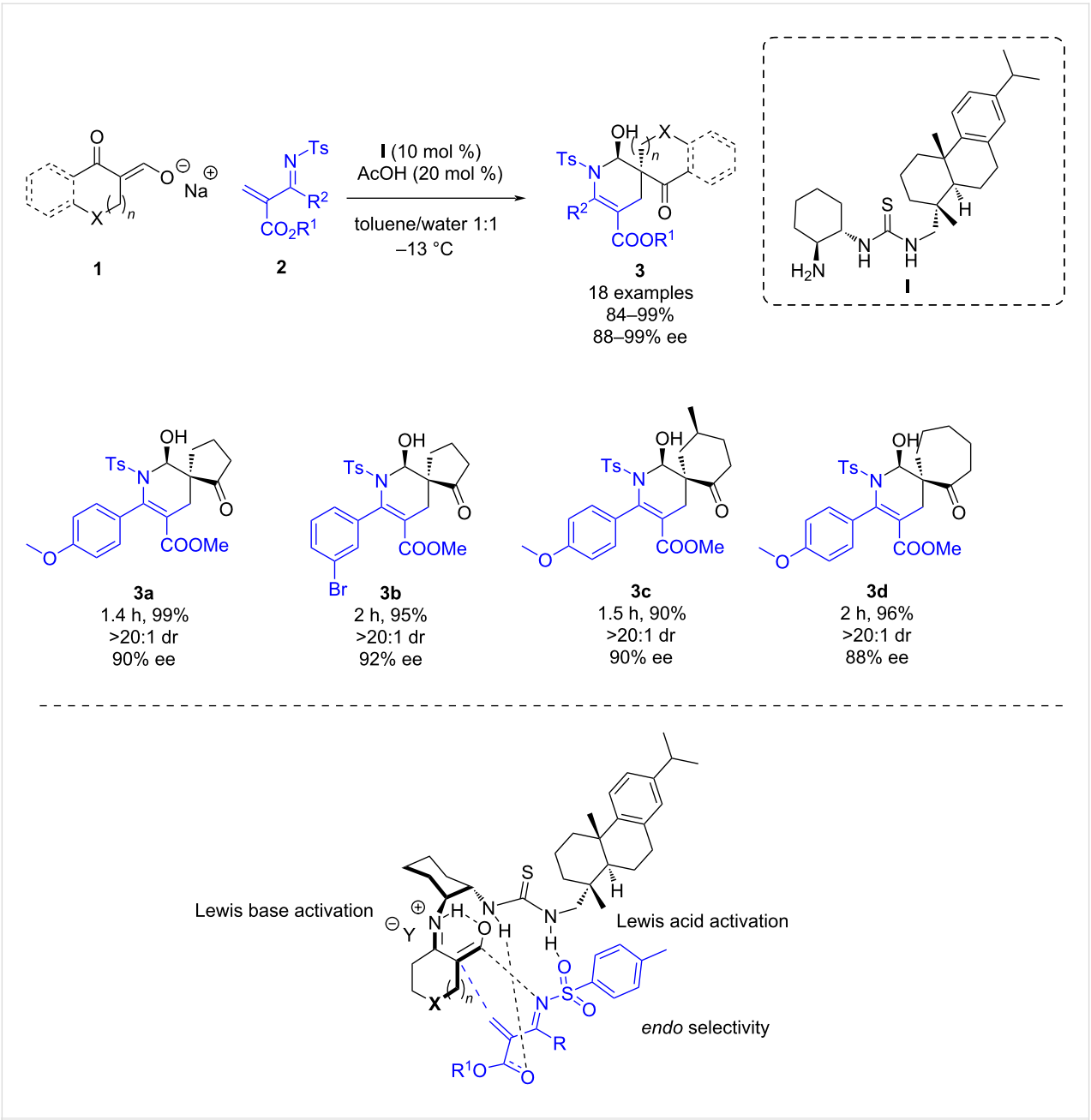

Scheme 1: Enantioselective bifunctional thiourea-catalyzed inverse electron demand Diels–Alder reaction of *N*-tosyl-2-methylene-but-3-enoates and cyclic keto/enolate salts.

Later, in 2018, Zhou and co-workers developed a bifunctional squaramide-catalyzed enantioselective formal [4 + 2] cycloaddition of benzofuran-derived azadienes **11** with malononitrile (**12**) [26]. This work provides an efficient methodology for synthesizing chiral benzofuran-fused 1,4-dihydropyridines **13** in excellent yields (90–99%) and excellent enantioselectivities (92–99% ee) (Scheme 4). The authors also attempted to perform the reaction using 2-tosylacetonitrile instead of malononitrile. However, in this case, the Michael addition product was obtained with low diastereoselectivity.

The mechanism is described in Scheme 4: the bifunctional squaramide activates the azadiene through hydrogen bonding while the malononitrile is deprotonated by the tertiary amine present in the backbone of the catalyst, establishing hydrogen bonding with the protonated tertiary amine. Then, a Michael addition of malononitrile to the azadiene takes place to obtain exclusively the (*S*)-intermediate **A**. Subsequently an intramolecular nucleophilic addition of the nitrile leads to the intermediate **B**, which undergoes tautomerization to furnish the cycloaddition product **13a**.

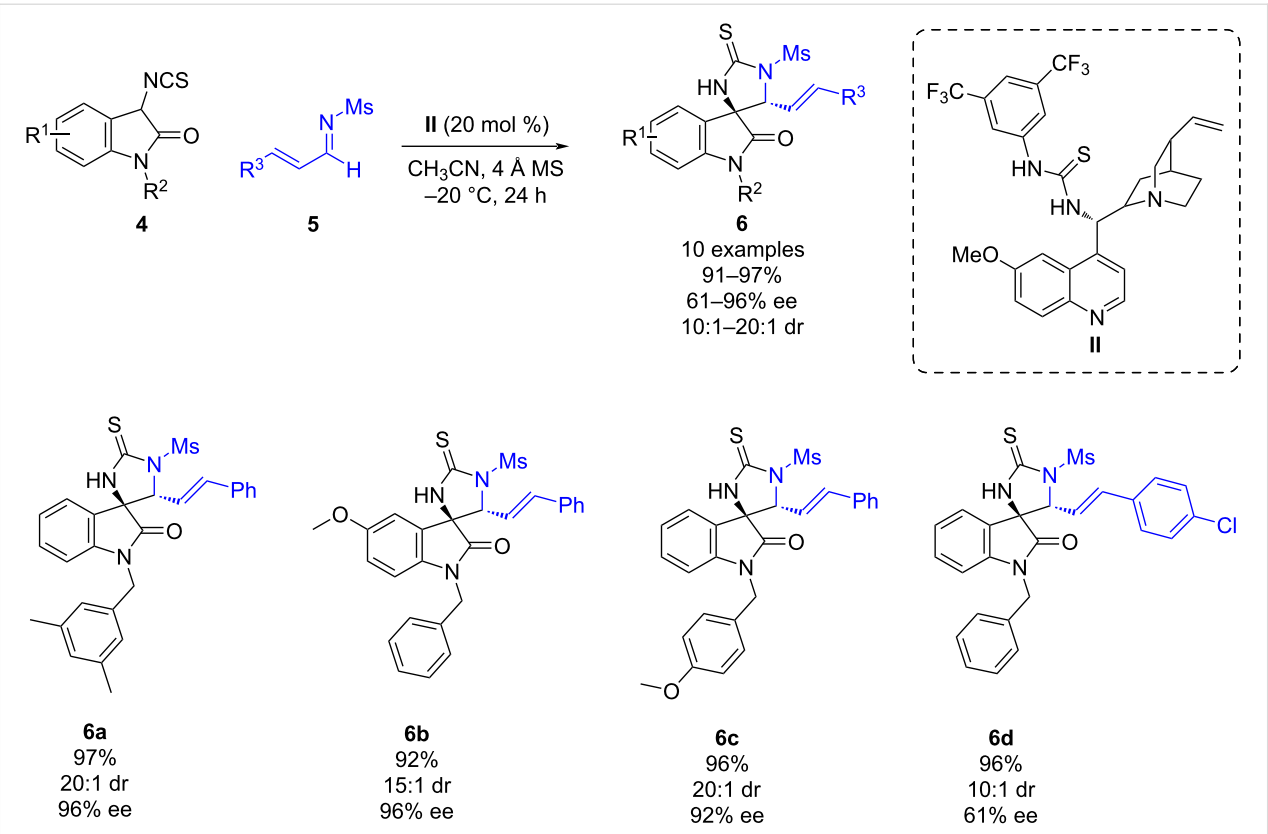

Scheme 2: Cinchona-derived thiourea-catalyzed stereoselective (3 + 2) reaction of α,β-unsaturated imines and 3-isothiocyanatooxindole.

In 2019, Xu's group published a bifunctional squaramide-catalyzed inverse electron demand aza-Diels–Alder reaction of saccharin-derived 1-azadienes **14** and azlactones **15** [27]. This methodology enables chiral tricyclic derivatives **16** bearing a quaternary amino acid moiety in up to 99% yields, up to 93% ee and >20:1 dr (Scheme 5) to be obtained. In general, the steric and electronic properties of the conjugated imines had a slight effect on the enantioselectivities of the reactions. However, the authors pointed out that the azlactones with different substituents at the α-position led to the desired products albeit with unsatisfactory results.

The bifunctional squaramide catalyst **V** has two functions; firstly it deprotonates the enolic form of the azlactone through the Brønsted-base moiety, and secondly it activates the 1-azadiene and enolate form of the azlactones through H-bond interactions with the squaramide moiety. The activated complex undergoes a [4 + 2] cyclization, through the *Si*-face attack of the enolate to the 1-azadiene leading to intermediate **A** which undergoes tautomerization and protonation to yield the chiral tricyclic derivative **16**.

To further investigate the potential utility of this methodology, a gram scale experiment was conducted affording product **16f** in a good yield and a slight decrease of the enantioselectivity. Additionally, a derivatization of product **16f** by hydrogenation was carried out to yield the tricyclic piperidine **17** with high diastereoselectivity (Scheme 5).

In 2019, Shi and co-workers established a guanidine-catalyzed enantioselective (4 + 1) cyclization of benzofuran-derived azadienes **11** with 3-chlorooxindoles **18** [28]. This work provides a useful strategy for the synthesis of chiral spirooxindole derivatives **19** in moderate yields (42–60%), high diastereoselectivities and good enantioselectivities (68–88% ee) (Scheme 6). The authors also attempted the reaction using *N*-benzyl-protected 3-chlorooxindole as a substrate. However, in this case, no reaction was observed, which indicated that the N–H group of the 3-chlorooxindole **18** has an essential role in the reaction.

The proposed reaction pathway for the enantioselective (4 + 1) cyclization is illustrated in Scheme 6. Initially, chiral guanidine **VI**, acts as a Brønsted base deprotonating the enolic form of 3-chlorooxindole whilst simultaneously activating the benzofuran-derived azadiene by H-bonding. This dual activation promotes a stereoselective addition of 3-chlorooxindole to the azadiene leading to intermediate **A**. The latter is also activated

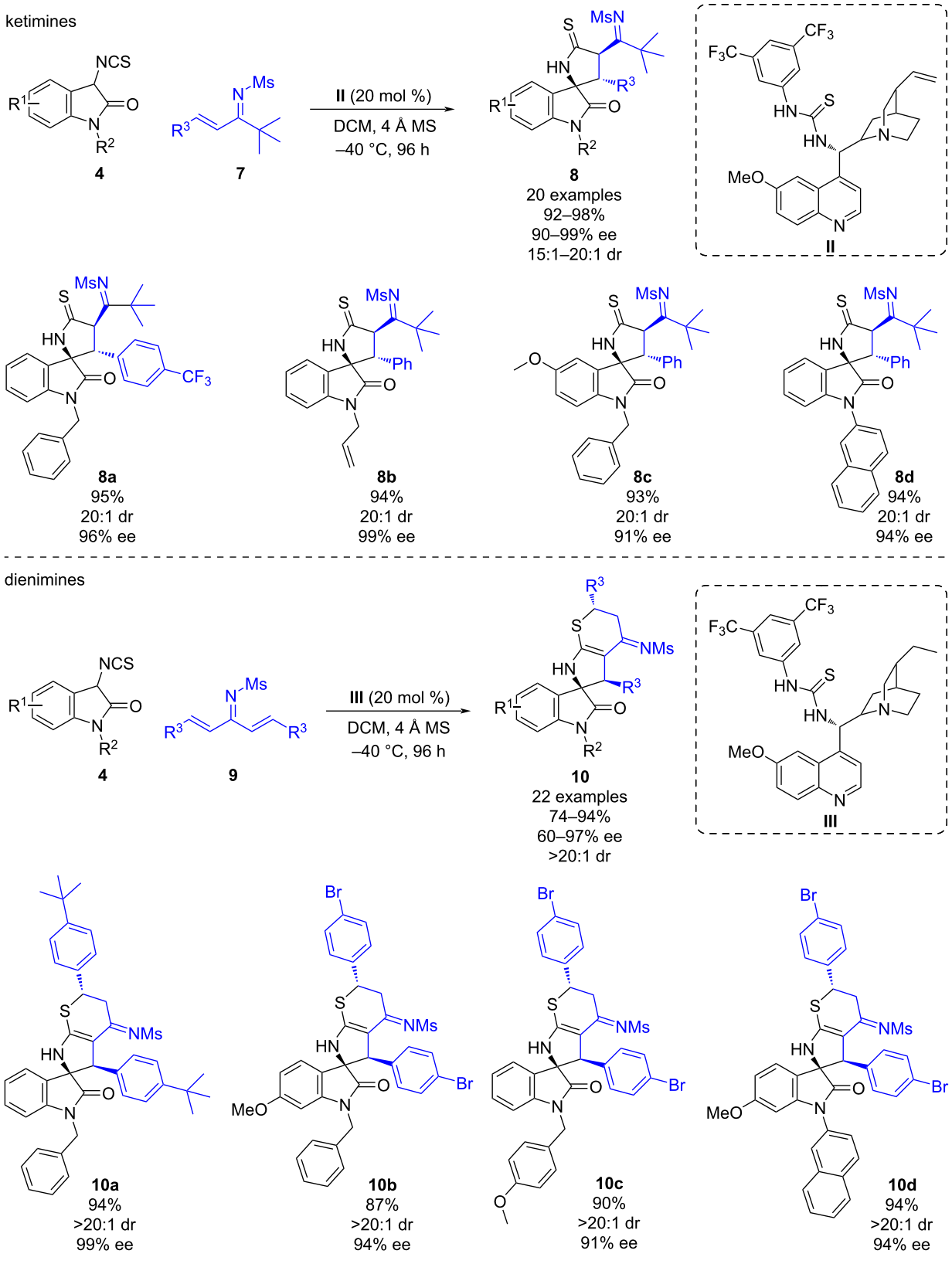

Scheme 3: Cinchona-derived thiourea-catalyzed stereoselective (3 + 2)/(4 + 2) cascade reaction of α,β-unsaturated imines and 3-isothiocyanatooxindole.

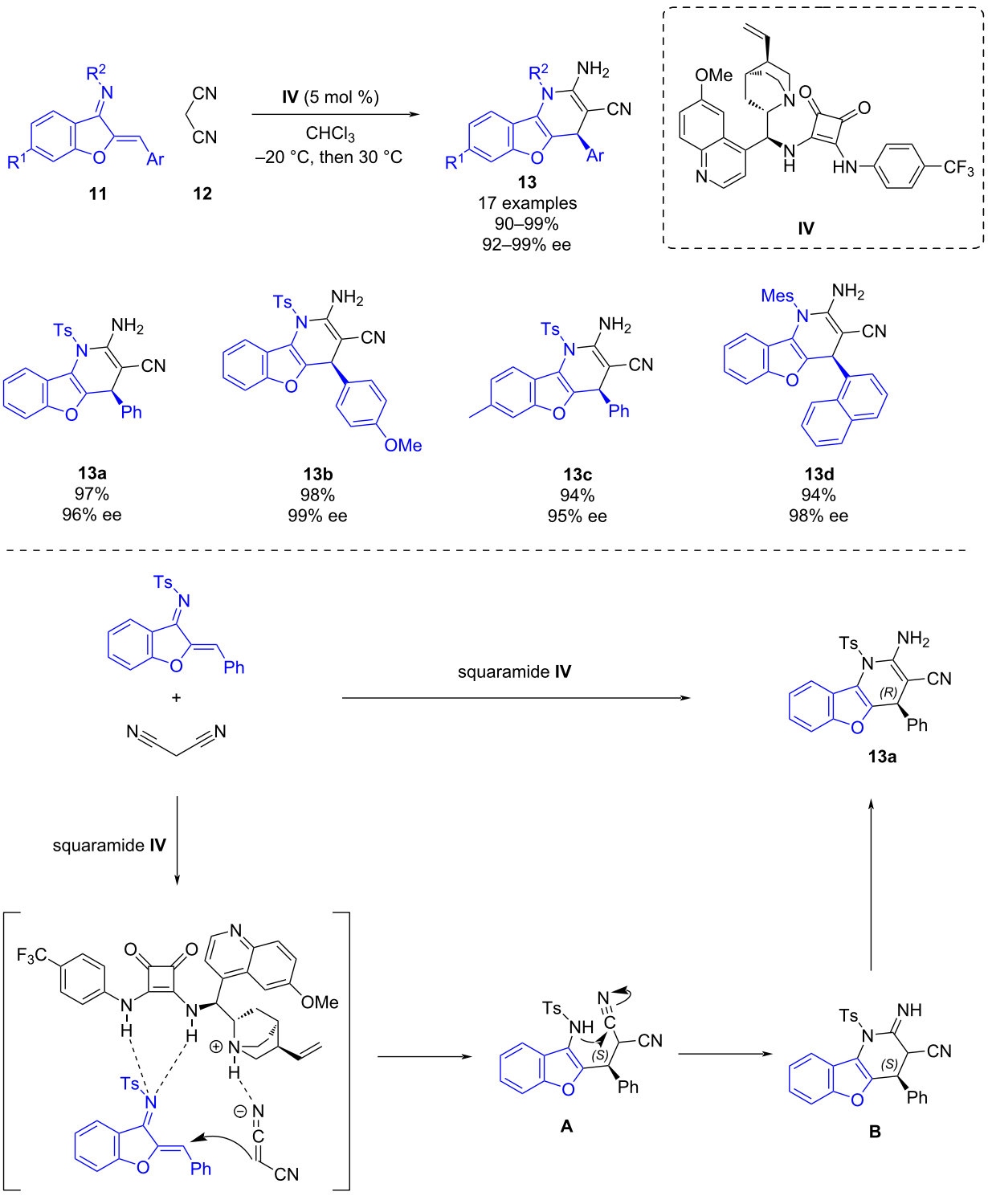

Scheme 4: Enantioselective bifunctional squaramide-catalyzed formal [4 + 2] cycloaddition of malononitrile with benzofuran-derived azadienes.

by the chiral guanidine and undergoes an intramolecular nucleophilic substitution which delivers the product **19b** with the relative configuration depicted in Scheme 6.

Also in 2019, Huang and co-workers reported a bifunctional squaramide-catalyzed [4 + 2] cyclization of benzofuran-derived azadienes **11** and azlactones **15** [29]. This methodology enables

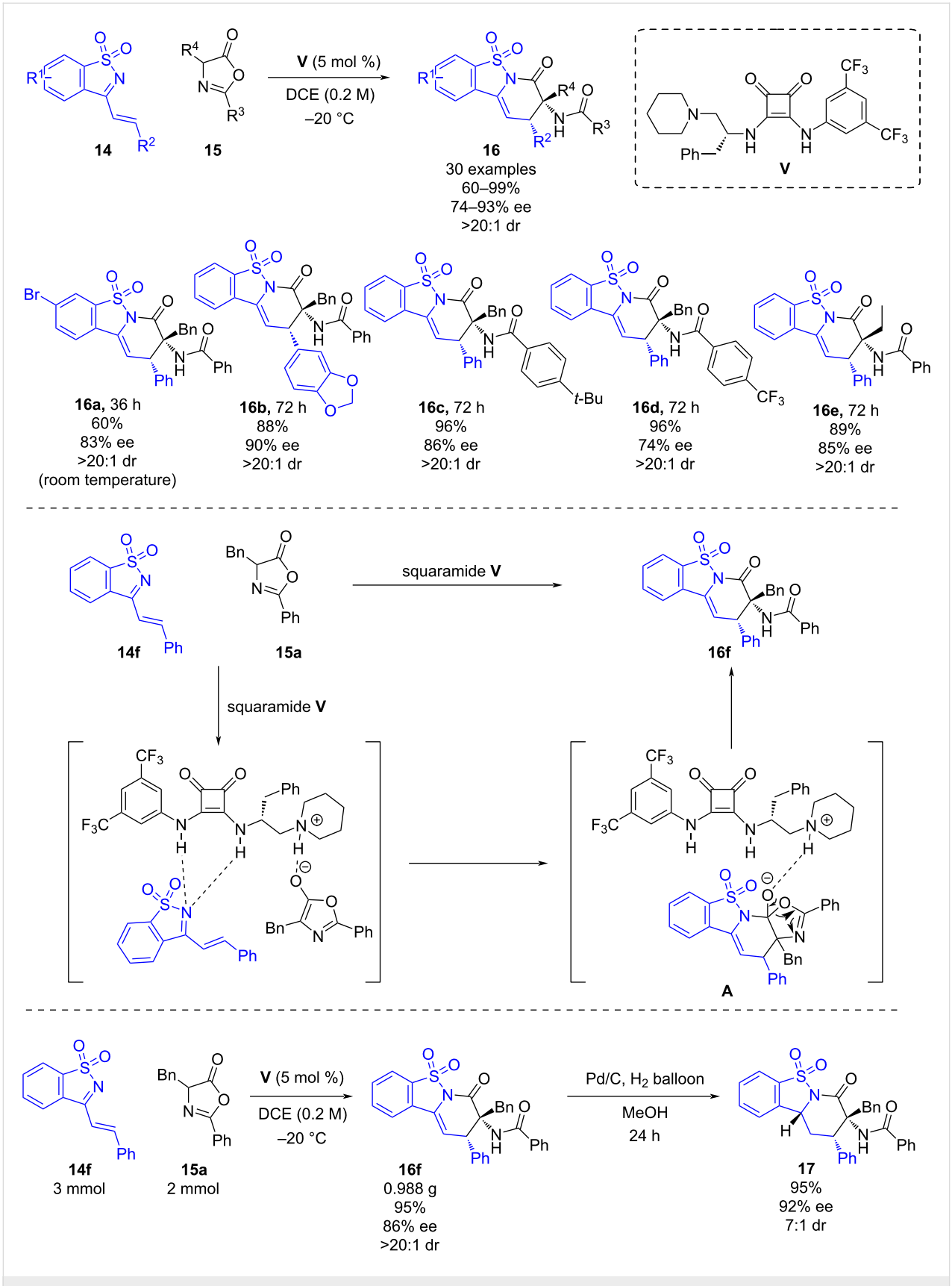

Scheme 5: Bifunctional squaramide-catalyzed IEDADA reaction of saccharin-derived 1-azadienes and azlactones.

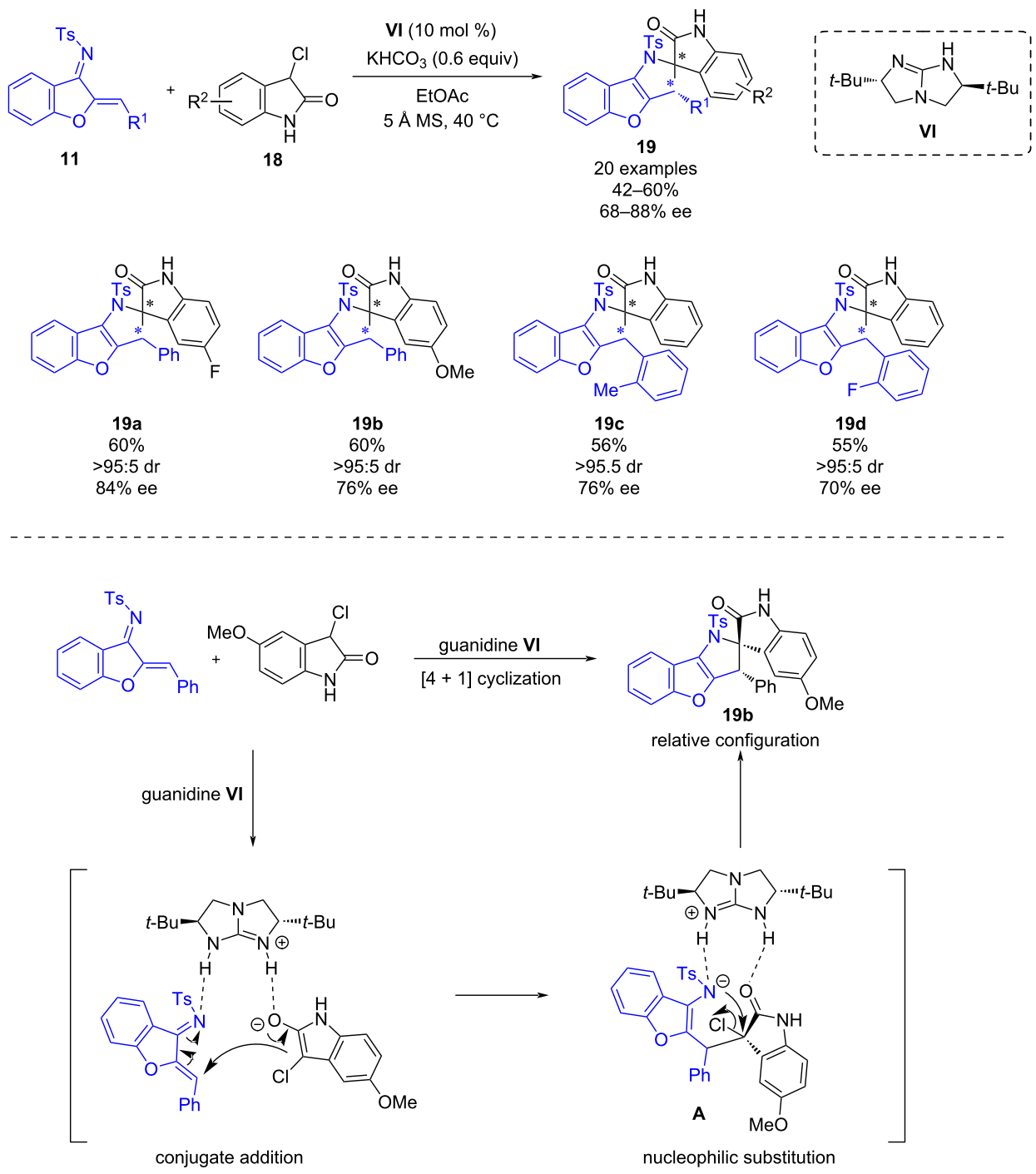

Scheme 6: Chiral guanidine-catalyzed enantioselective (4+1) cyclization of benzofuran-derived azadienes with 3-chlorooxindoles.

the synthesis of benzofuran-fused six-membered heterocycles **20** in yields up to 92%, complete diastereoselectivities and moderate to excellent enantioselectivities (62–99% ee) (Scheme 7). The 1-azadienes bearing electron-rich or electron-poor groups on the *meta* or *para*-position of the phenyl ring led to the derivatives **20** with excellent enantioselectivities. However, when 1-azadienes bearing substituents at the *ortho*-position were tested, the enantioselectivities decreased, probably due to higher steric hindrance.

The mechanism of the reaction is depicted in Scheme 7; firstly, the dual activation of the azadiene and the enol form of the azlactone through hydrogen bonding with the bifunctional squaramide enables a stereoselective Michael addition of the

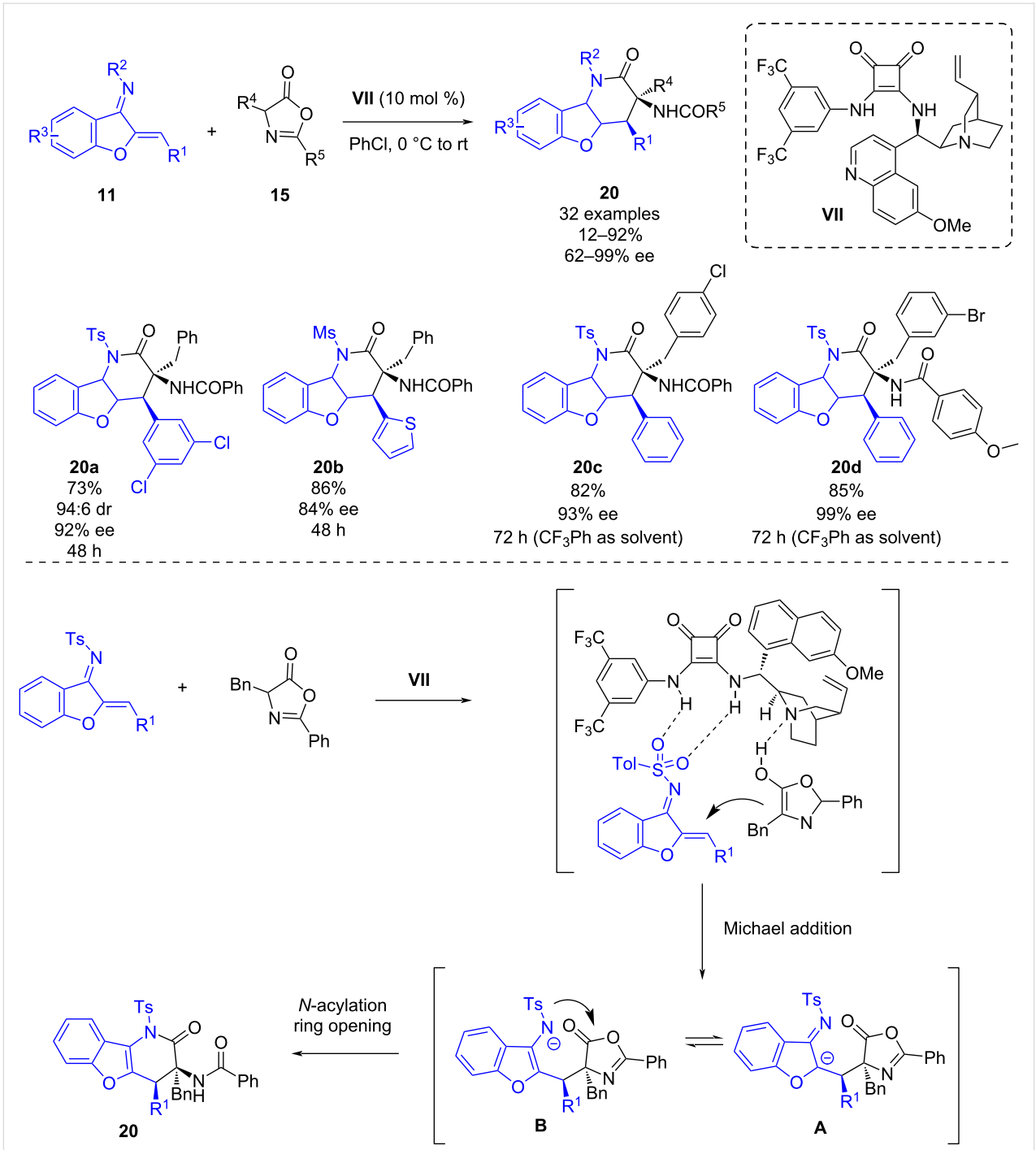

Scheme 7: Bifunctional squaramide-catalyzed [4 + 2] cyclization of benzofuran-derived azadienes and azlactones.

azlactone to the azadiene forming intermediate **A** which transforms into intermediate **B**, which then undergoes an intramolecular cyclization to give the desired product **20**.

In 2020, Ni, Song and co-workers described a bifunctional squaramide-catalyzed asymmetric domino Mannich/formal [4 + 2] cyclization of 2-benzothiazolimines **21** with azlactones **15** [30]. Using cinchona-derived squaramide **VII** it was possible to obtain 25 different chiral benzothiazolopyrimidines **22** bearing adjacent tertiary and quaternary stereocenters in up to 81% yield, up to 20:1 dr, and up to 99% ee (Scheme 8).

The organocatalyst has a bifunctional role; firstly, the tertiary amine deprotonates the azlactone providing its enolate form

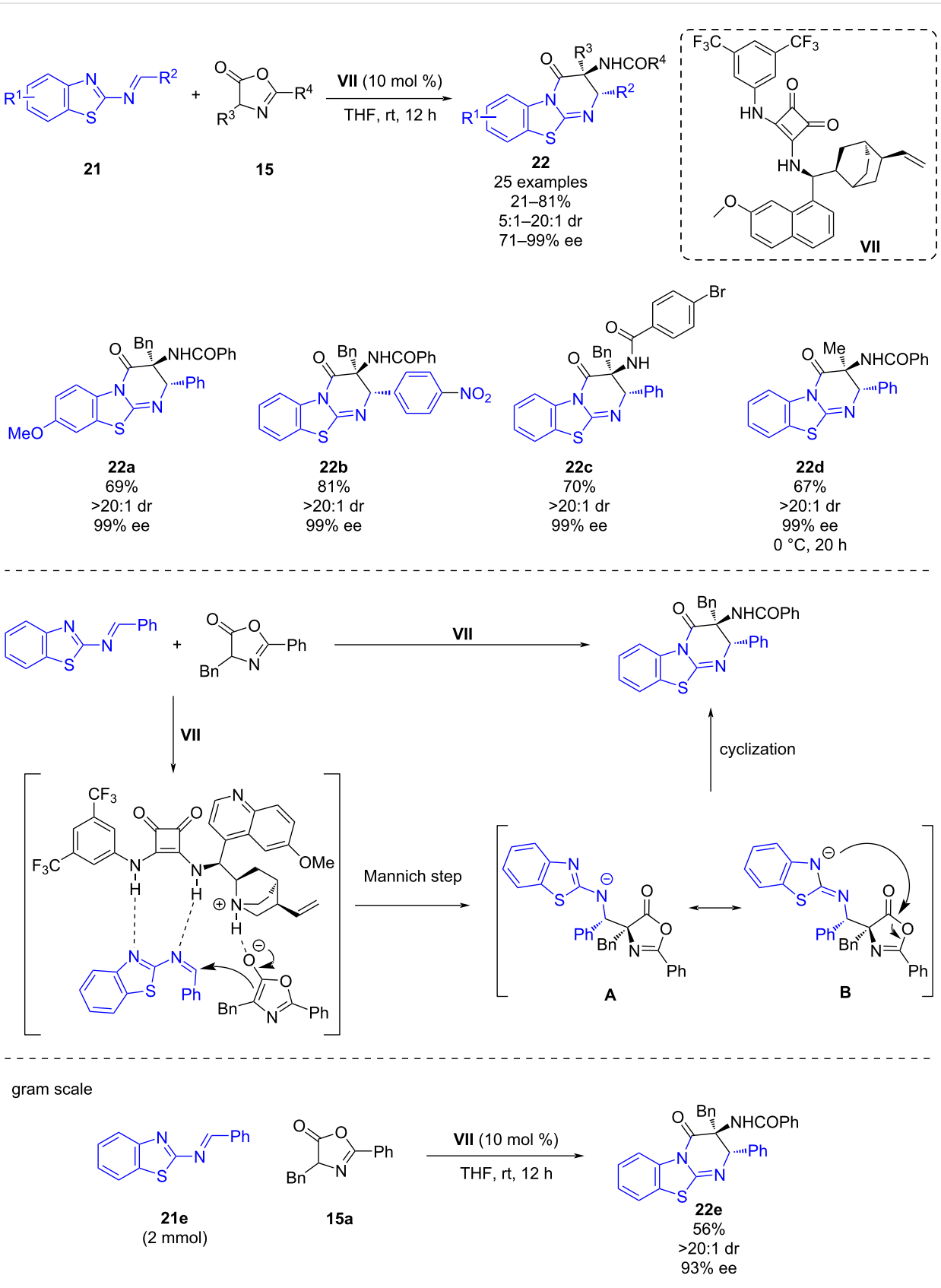

Scheme 8: Chiral bifunctional squaramide-catalyzed domino Mannich/formal [4 + 2] cyclization of 2-benzothiazolimines with azlactones.

while at the same time the squaramide moiety activates the 2-benzothiazolimine by hydrogen-bonding interactions with the nitrogen atoms. Then, the azlactone enolate undergoes a nucleophilic attack on its *Si*-face via Mannich reaction with the 2-benzothiazolimine leading to intermediate **A** which evolves toward its resonance form **B**, responsible of the intramolecular attack of the negatively charged nitrogen to the azlactone moiety leading to the desired chiral benzothiazolopyrimidine. Furthermore, a large-scale experiment was carried out obtaining the product **22e** in 56% yield, >20:1 dr and 93% ee (Scheme 8).

In May 2020, Albrecht and co-workers reported a chiral bifunctional thiourea-catalyzed formal inverse electron demand aza-Diels–Alder reaction (IEDADA) of β,γ-unsaturated ketones **23** and benzofuran-derived azadienes **11** [31]. The procedure enables the straightforward synthesis of benzofuran derivatives **24** bearing an additional tetrahydropyridine ring in good yields (51–94%) and excellent enantioselectivities (90–96% ee) when using thiourea **VIII** with a relatively low catalyst loading (Scheme 9). The authors also attempted to perform the reaction using acyclic azadienes and indene-derived azadiene instead of benzofuran-derived azadienes **11**. However, in these cases, the reactions did not take place.

The authors proposed that the bifunctional thiourea catalyst acts by activating the sulfonyl group of the imine by hydrogen-bonding interactions while at the same time deprotonating the β,γ-unsaturated ketone forming the corresponding dienolate. The latter then participates in the formal IEDADA reaction with the azadiene in a stepwise mechanism: firstly, the vinylogous Michael addition of the dienolate to the double bond of the α,β-unsaturated *N*-sulfonylimine occurs in a stereoselective fashion. Subsequently, cyclization due to an intramolecular aza-Michael reaction and protonation leads to the enantioenriched product **24f**. To show the applicability of this novel methodology, a gram-scale reaction was carried out obtaining comparable results as in a small scale. Besides, an α-bromination of the product **24f** was performed obtaining **25** in 73% yield and complete diastereoselectivity (Scheme 9).

In 2021, Zhao and co-workers reported a dihydroquinine-derived squaramide-catalyzed (3 + 2) cycloaddition reaction of isocyanoacetates **26** and saccharin-derived 1-azadienes **14** [32]. In this work, the azadiene works as a C2 synthon, while the isocyanoacetate, bearing a protected carboxylic acid and a carbene-like divalent isocyanide carbon, behaves a C3 synthon affording benzo[*d*]isothiazole 1,1-dioxide-dihydropyrroles **27** bearing two adjacent stereocenters in high yields (27–98%) and with moderate to excellent stereoselectivities (54–97% ee) when using thiourea **IX** (Scheme 10). The cyclization was observed with all derivatives except for azadienes bearing a bulky *t*-Bu substituent, which led to the Michael product **27e'** albeit with low stereoselectivity. The authors proposed a plausible reaction mechanism to explain the observed stereoselectivity of the reaction. Firstly, the isocyanoacetate is deprotonated by the tertiary amine moiety of the organocatalyst, while the azadiene is activated by hydrogen bonding with the squaramide moiety. Then, the enolate attacks the *Re* face of the azadiene through a Michael addition which leads to intermediate **A**. Next, an intramolecular 5-*endo-dig* cyclization takes place by the attack of the carbanion to the isocyanate group forming intermediate **B** which undergoes protonation yielding the product. The authors attempted to perform different reductions of the products without any success. However, they performed a gram scale version of the transformation obtaining the product in comparable yields and enantioselectivities.

Later in 2021, Fernández-Salas, Alemán and co-workers developed a bifunctional squaramide-catalyzed enantioselective inverse electron demand aza-Diels–Alder reaction (IEDADA) between benzofuran-derived azadienes and silyl (di)enol ethers [33]. This work provides a useful methodology to synthesize interesting benzofuran-fused 2-piperidinol derivatives **29** and **31** bearing three adjacent stereocenters using squaramide **X** as organocatalyst (Scheme 11). Firstly, the reaction between azadiene **11** and trimethylsilyl dienolate **28** was explored obtaining 16 different derivatives in moderate to good yields (53–71%) and excellent enantioselectivities (90–96% ee). Furthermore, with the idea to expand the scope of the reaction, the authors studied the reaction using trimethyl(styryloxy)silane (**30**). This strategy enabled the synthesis of adducts **31** bearing an aromatic ring at the α-position of the activating group with good yields (52–98%), excellent diastereoselectivities and good enantioselectivities (76–94% ee). Additionally, to understand the mechanism of the reaction, the authors performed DFT calculations. Based on the calculations, once the dienolate is hydrolyzed to the free alcohol *E* isomer and it coordinated to the squaramide in an effective orientation, a stepwise mechanism is taking place. Firstly, the dienolate adds to the azadiene which is followed by cyclization with formation of the C–N bond. Finally, protonation leads to the formation of the desired derivative. The calculations also revealed that due to kinetic control the activation of the C2 carbon of the dienolate is preferred vs the C4 atom, therefore only one regioisomer is observed.

Additionally, the asymmetric IEDADA reaction could be performed at a higher scale (1 mmol) leading to the synthesis of the cycloadducts **29e** and **31e** in good yields (Scheme 12). Further derivatizations were also carried out: The treatment of **29e** with

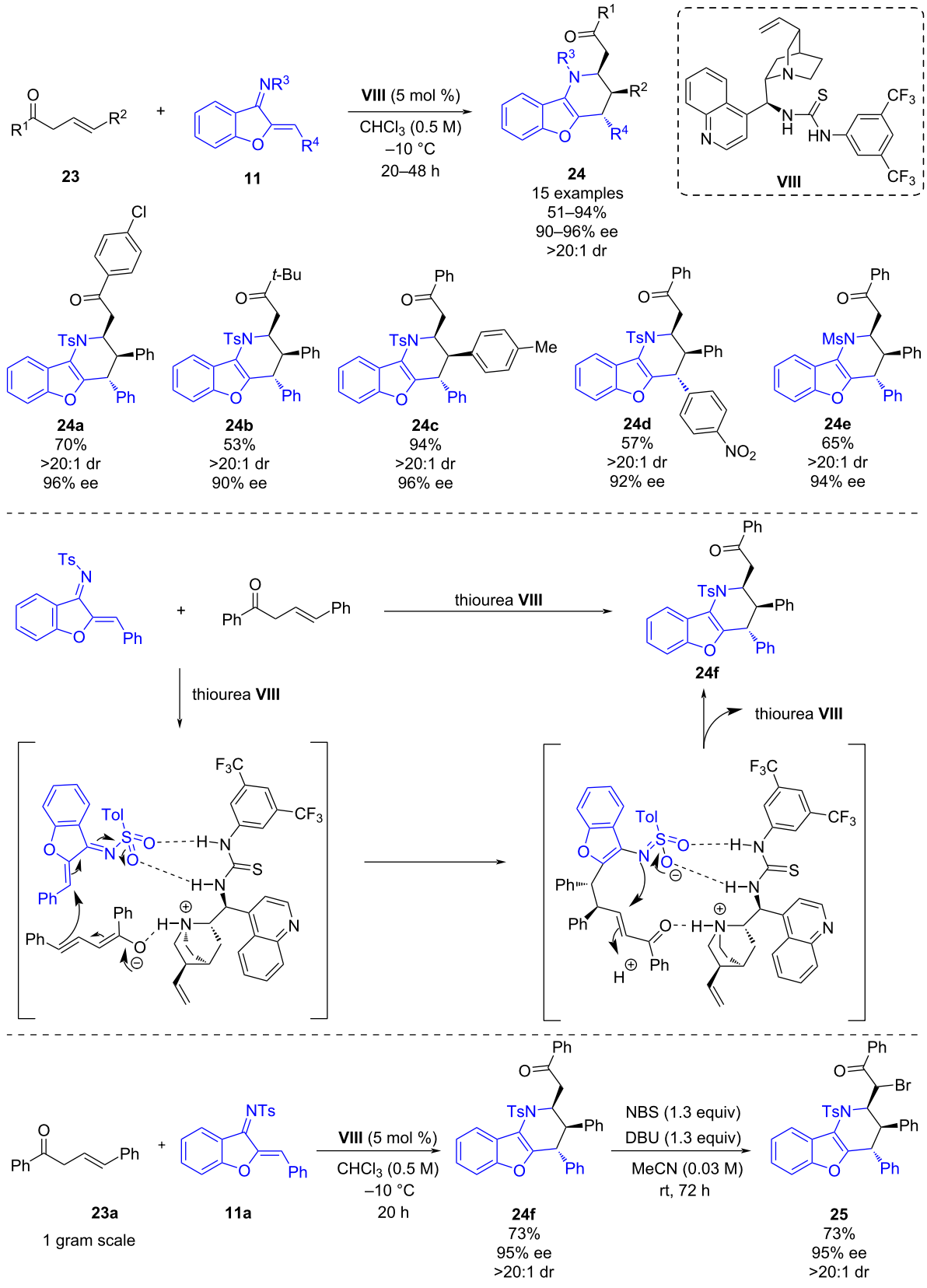

Scheme 9: Chiral bifunctional thiourea-catalyzed formal IEDADA reaction of β,γ-unsaturated ketones and benzofuran-derived azadienes.

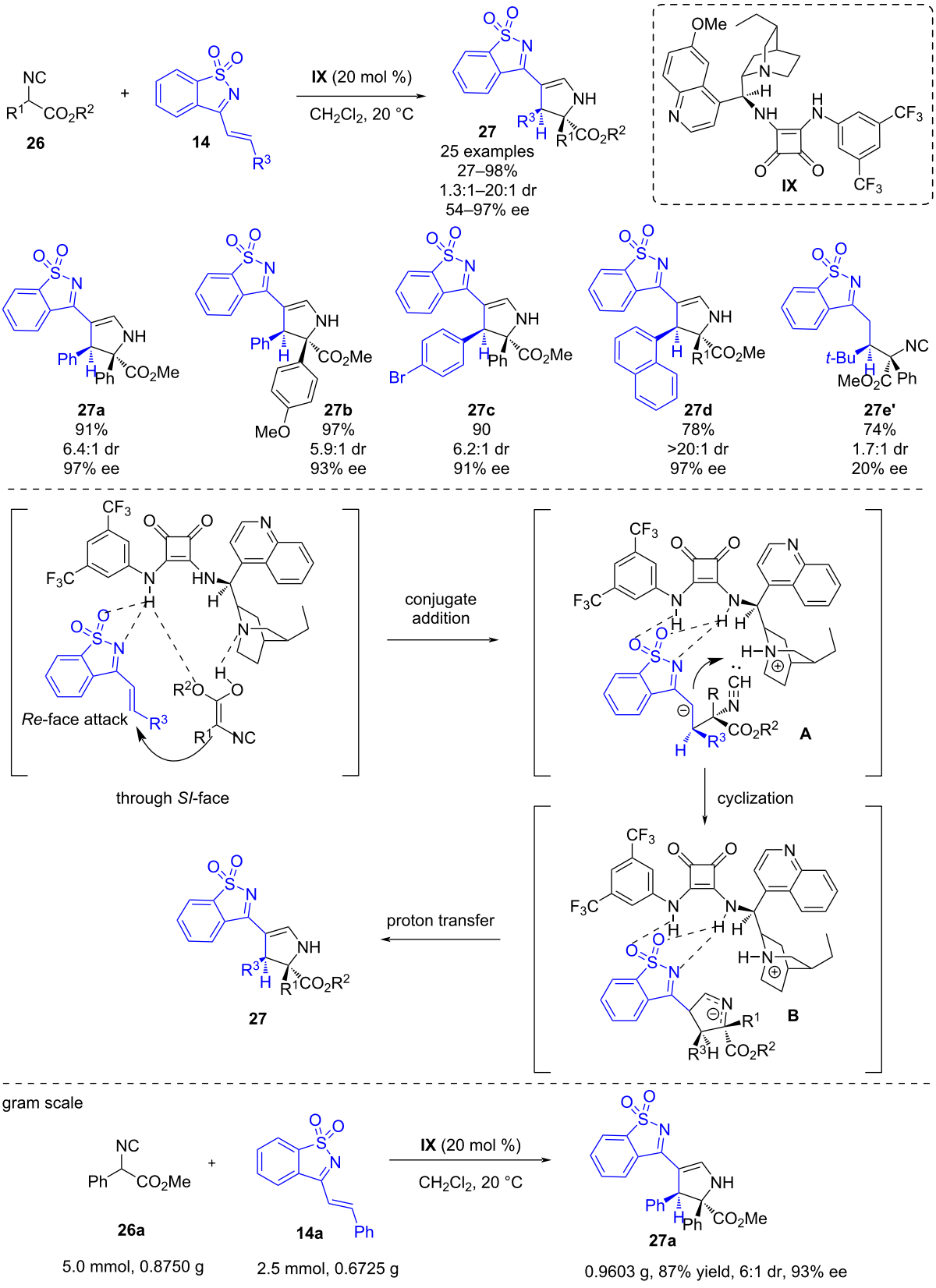

Scheme 10: Dihydroquinine-derived squaramide-catalyzed (3 + 2) cycloaddition reaction of isocyanoacetates and saccharin-derived 1-azadienes.

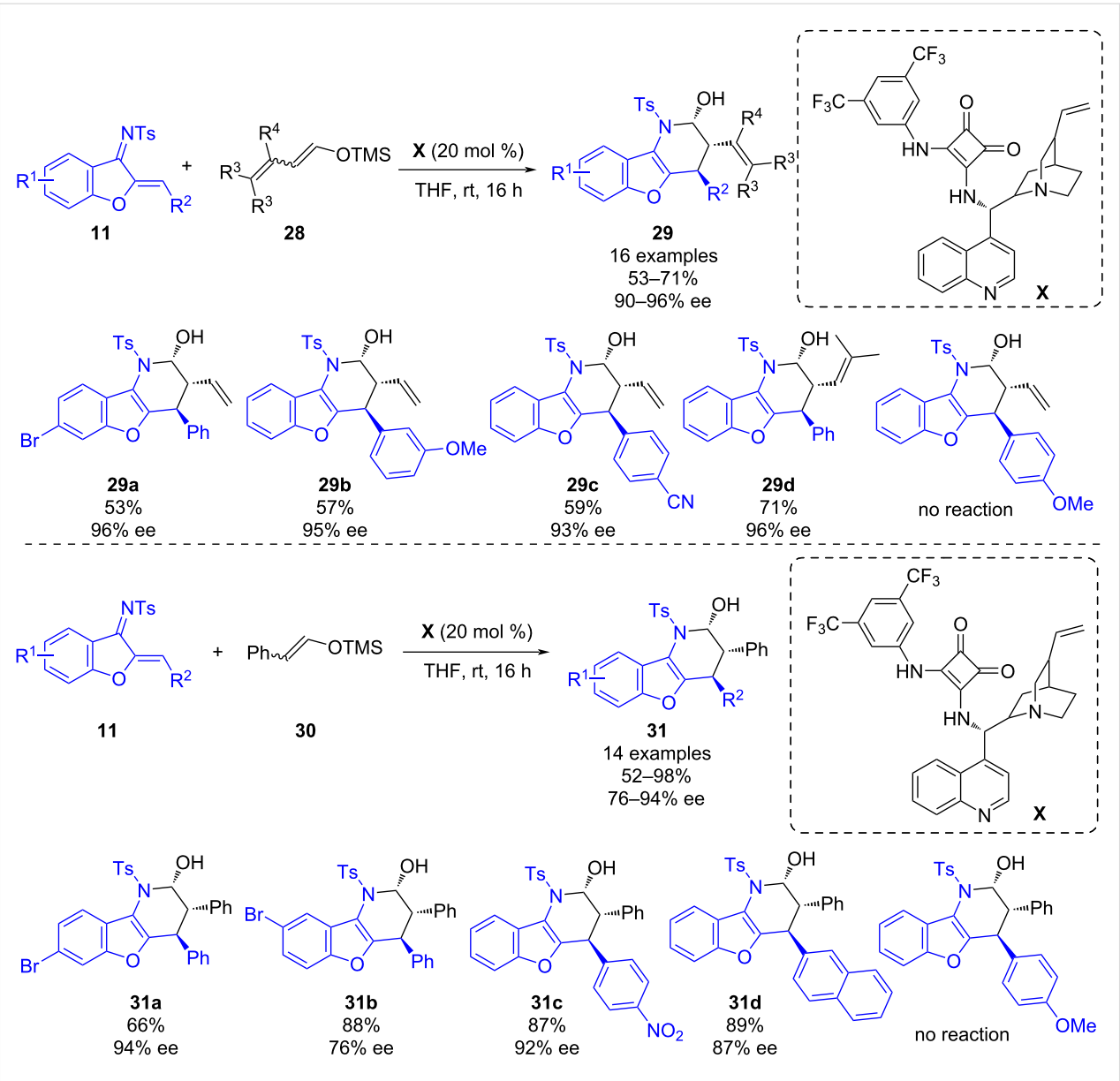

Scheme 11: Enantioselective squaramide-catalyzed asymmetric IEDADA reaction of benzofuran-derived azadienes and silyl (di)enol ethers.

$SOCl_2$ led to interesting unsaturated derivative **32** in a 54% yield. The acetylation of **31e** provided **33** in 76% yield. Next, an alkene metathesis of **33** with styrene led to product **34** in 72% yield. All the derivatizations were carried out without erosion of enantioselectivity.

In 2023, as a follow-up of Zhao's previous work [32], the same group reported a dihydroquinine-derived squaramide-catalyzed Mannich-type reaction of isocyanoacetates with *N*-(2-benzothiazolyl)imines [34]. After a screening of reaction conditions, it was found that the best organocatalyst was also bifunctional squaramide **IX**, but in this case a lower catalyst loading could be used in the reaction (Scheme 13). Under the optimized reaction conditions, 27 different chiral directly linked benzothiazole-dihydroimidazoles **35** bearing two adjacent stereocenters could be obtained in moderate to high yields (47–97%), moderate diastereoselectivities (1:1–3.1:1 dr) and excellent enantioselectivities (94–99% ee). It is worth noting that the steric effect of the isocyanate substituents had an important effect on the reaction, and with bulky substituents, the reaction did not proceed. Further derivatizations of the products were carried out: firstly, the derivative **35e** was reduced using $NaBH_3CN$ to obtain **36** as a single diastereomer in a good yield. Next, a hydrolysis of **36** using concentrated sulfuric acid led to the 1,2-diamino derivative **37** in a good yield and an excellent enantioselectivity.

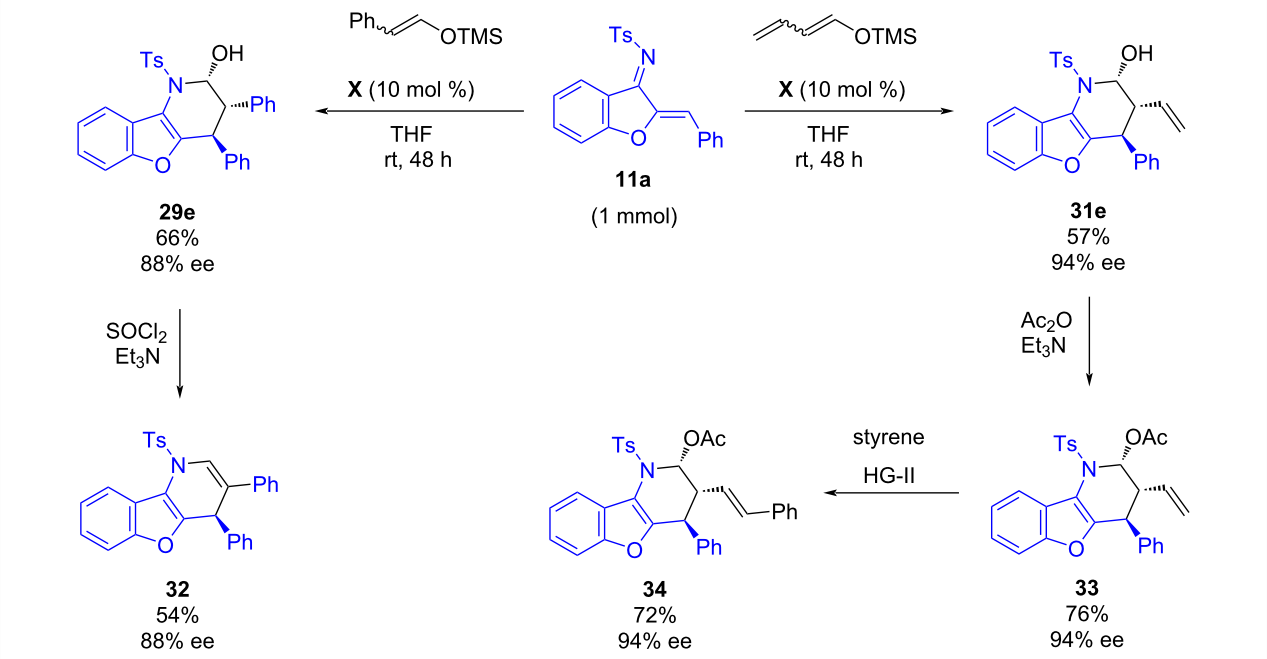

Scheme 12: Scale up and derivatizations of benzofuran-fused 2-piperidinol derivatives.

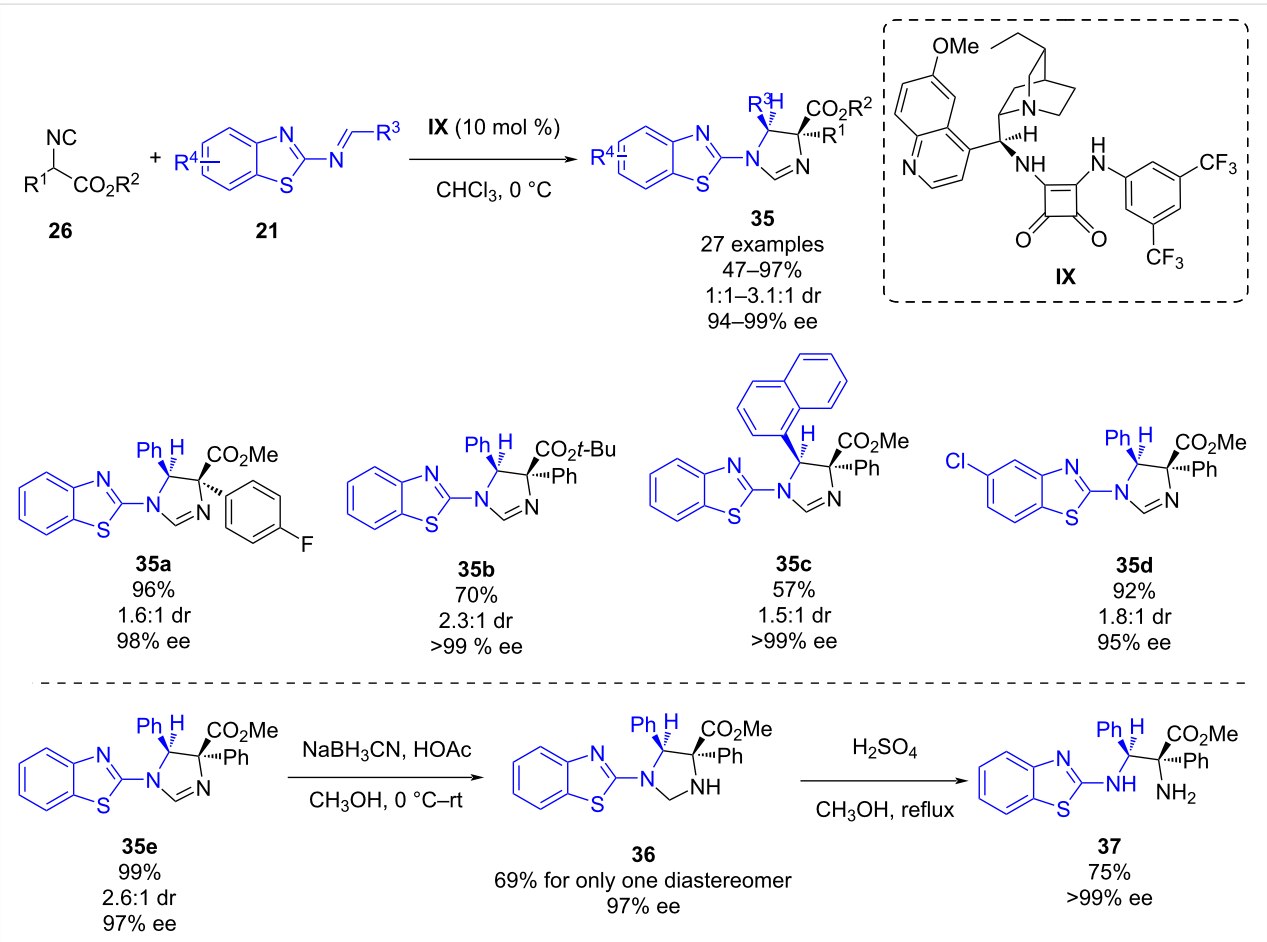

Scheme 13: Dihydroquinine-derived squaramide-catalyzed Mannich-type reaction of isocyanoacetates with *N*-(2-benzo-thiazolyl)imines.

Brønsted bases

Cinchona alkaloids have been established as highly efficient chiral organocatalysts, capable to engage in a wide array of enantioselective processes [35]. They possess a unique structure. Firstly, the bulky quinuclidine moiety can act as a base activating a nucleophile, secondly the secondary hydroxy group can participate in hydrogen bonding or can behave as a Brønsted acid (Figure 5). Additionally, the quinoline moiety can interact through π–π stacking with the reactants.

On the other hand, the $(DHQD)_2$-based catalysts are synthesized by joining together two fragments of cinchona alkaloids. In this manner, it is possible to obtain a symmetric catalyst, which can engage in hydrogen bonding interactions and deprotonation processes. Although they were originally used for Sharpless dihydroxylation, they have been utilized for a wide variety of organocatalytic processes.

In this section, different cyclizations of α,β-unsaturated imines involving Brønsted base organocatalysts such as $(DHQD)_2$-based catalysts will be described.

In 2015, Jiang, Chen and co-worker published a modified cinchona alkaloid-catalyzed [4 + 2] cycloaddition reaction of saccharin-derived 1-azadienes **14** and γ-butenolides **38** [36]. While using $(DHQD)_2$PHAL **XI**, an *endo* cycloadduct **39** could be obtained in good yields (29–57%) and high enantioselectivity (79–99% ee), and the use of the β-isocupreidine-based catalyst **XII** as a catalyst led to the *exo*-type diastereomers **40** with moderate yields (34–61%) and moderate enantioselectivities (55–66% ee). In this case, the addition of tetramethylguanidine (TMG) was necessary to promote the cyclization. This work is one of the first reports in which an enantioselective [4 + 2] cycloaddition of 1-azadienes was performed under Brønsted base conditions. The authors claimed that the reactions to obtain the complex fused polycyclic diastereomeric products is proceeding through a cascade Michael addition–aza-Michael addition, however, they did not propose a plausible reaction pathway for the transformations. In order to evaluate the synthetic utility of this methodology, derivative **39e** was reduced using $BF_3{\cdot}OEt_2$ and Et_3SiH leading to **41** in a good yield and moderate diastereoselectivity (Scheme 14).

In 2017, Li's group developed a chiral $(DHQ)_2$PHAL-catalyzed [2 + 4] annulation reaction of cyclic 1-azadiene **14** with γ-nitro ketones **42** [37]. With this transformation polysubstituted cyclohexanes **43** bearing four consecutive stereocenters are afforded through efficient one-pot cyclization with good yields (43–95%) and with high enantioselectivities (80–97% ee) (Scheme 15). In general, 1-azadienes **14** with different substitution patterns and aryl R^2 substituents led to the desired products. However, the presence of a cyclopropyl or isopropyl R^2 substituent, led to a complex mixture of products (Scheme 15).

In the mechanism proposed by the authors, $(DHQ)_2$PHAL **XIII** provokes the deprotonation of the γ-nitro ketone at the α-position to the nitro group, resulting in the formation of an anionic nucleophilic specie **A**. The latter reacts with the cyclic 1-azadiene via stereoselective Michael addition, forming intermediate **B**, stabilized by π–π stacking interactions between the Ar group and the aromatic cyclic moiety of the 1-azadiene. Then, an intramolecular aldol reaction leads to intermediate **D** which undergoes final protonation to produce the desired chiral product **43f**. The authors proposed that the stereoselectivity of the Michael addition product would direct the stereoselectivity of the intramolecular aldol reaction. To demonstrate the robustness of this novel methodology the model reaction was scaled up to 1.0 mmol, giving the desired product with a slight decrease of the yield and similar results in terms of enantioselectivity, 67% yield, 92% ee and >20:1 dr.

Brønsted acids: chiral phosphoric acids

The employment of Brønsted acid catalysis has been widely studied in asymmetric synthesis [38,39]. While the asymmetric transformations of 2-azadienes have been more intensively investigated, enantioselective derivatizations of 1-azadienes are

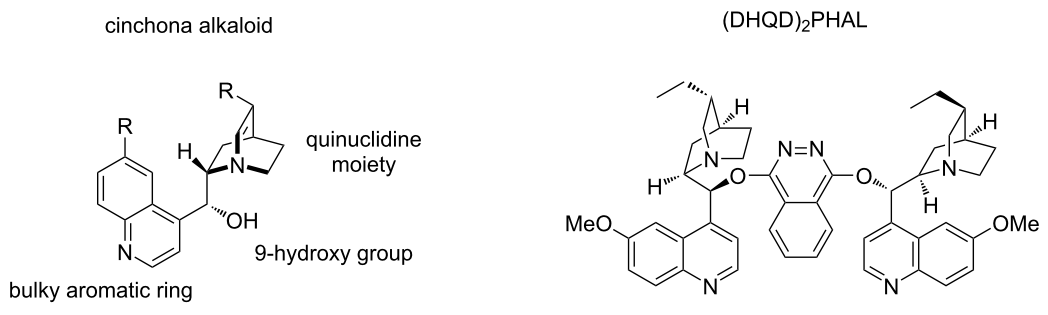

Figure 5: Structure of a cinchona alkaloid and $(DHQD)_2$PHAL.

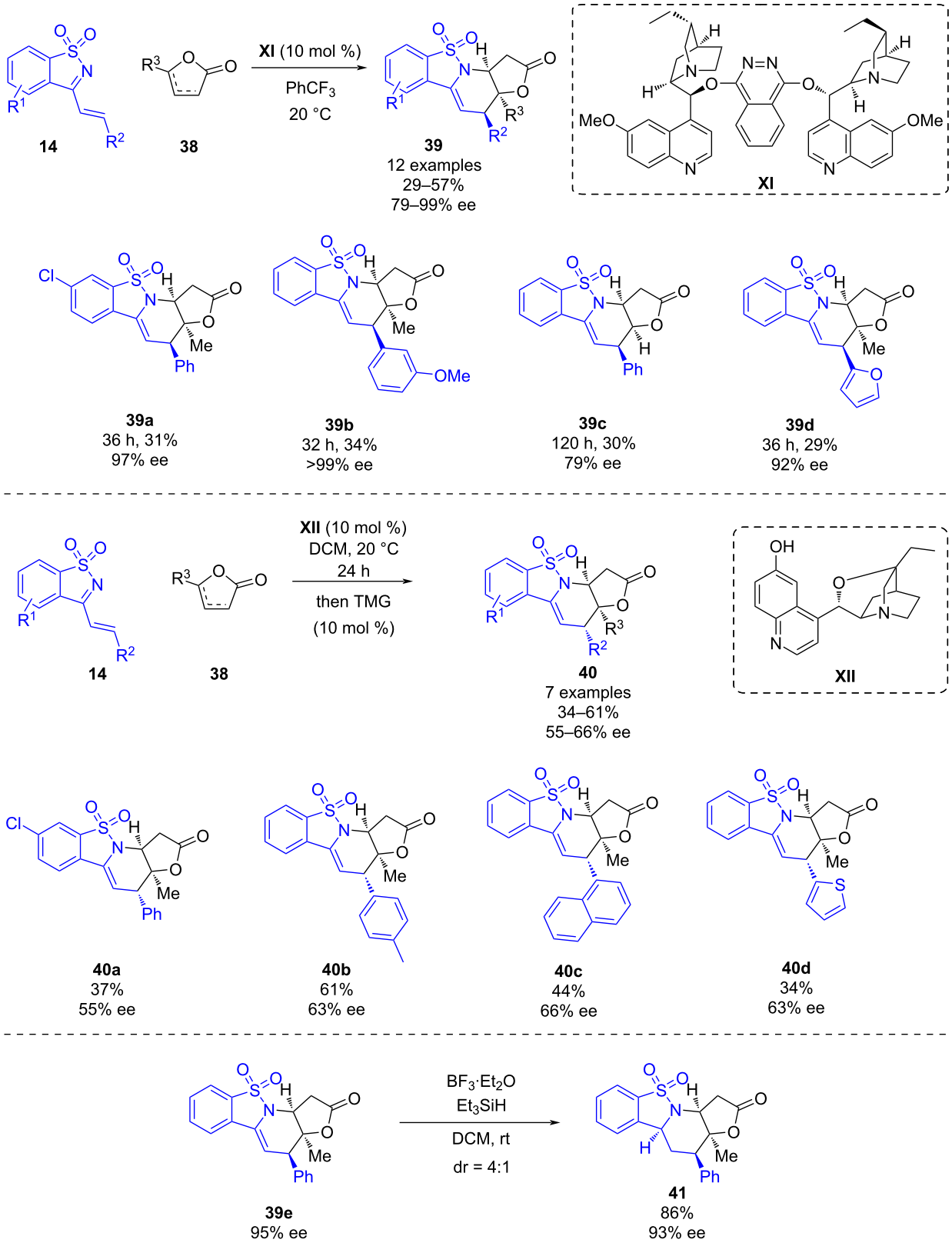

Scheme 14: Enantioselective modified cinchona alkaloid-catalyzed [4 + 2] annulation of γ-butenolides and saccharin-derived 1-azadienes.

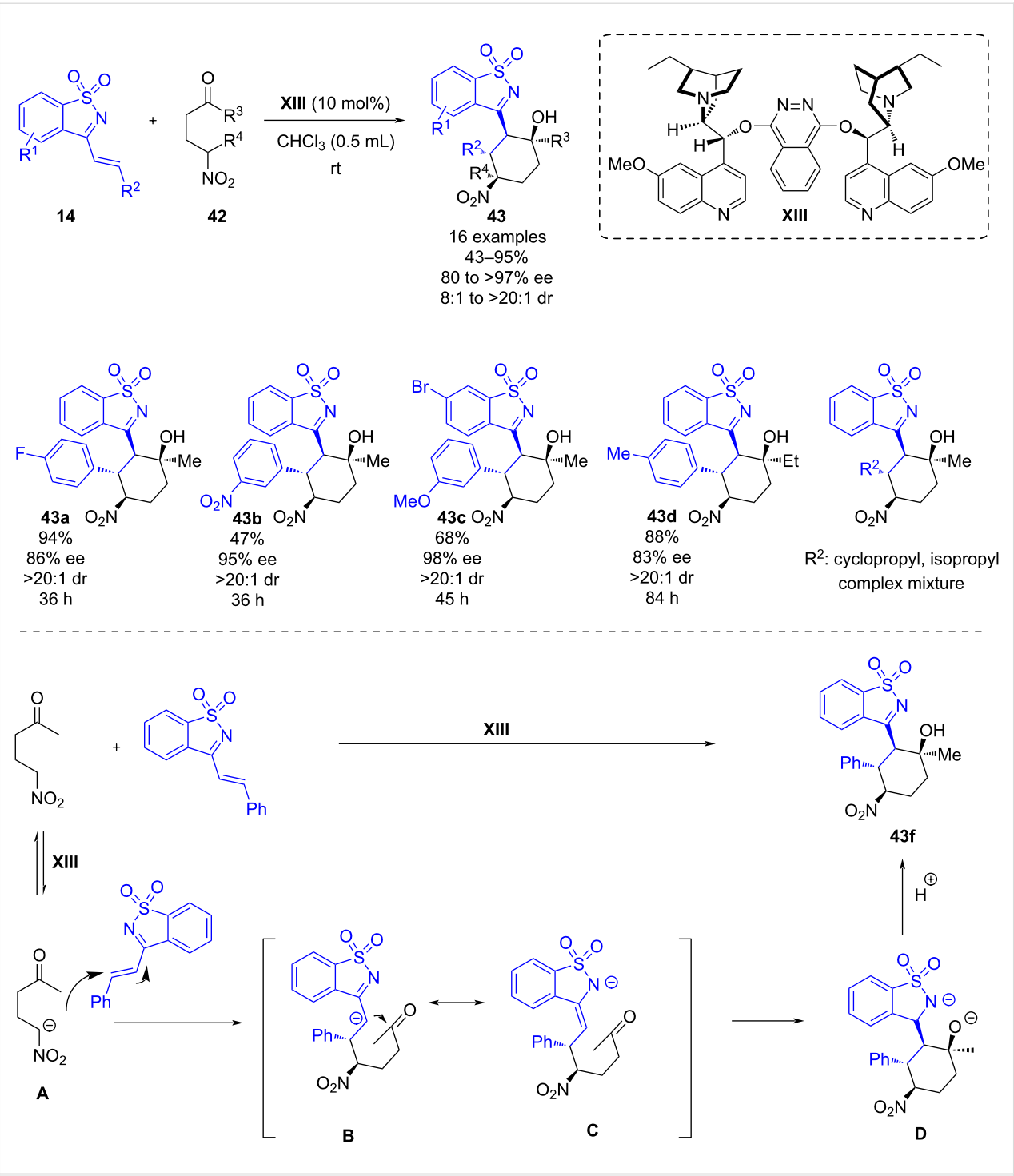

Scheme 15: Chiral tertiary amine-catalyzed [2 + 4] annulation of cyclic 1-azadiene with γ-nitro ketones.

scarce. In this section, the cycloaddition reactions involving α,β-unsaturated imines catalyzed by chiral phosphoric acids will be described.

In 2013, Masson and co-workers reported the enantioselective inverse electron demand aza-Diels–Alder reaction (IEDADA) of 1-azadienes **44** with enecarbamates **45** catalyzed by chiral phosphoric acid **XIV** [40]. Although other works involving a covalent attachment of the catalyst had been previously reported for IEDADA reactions, this work reflects the first Brønsted acid-catalyzed IEDADA reaction of 1-azadienes. This methodology enables the synthesis of a variety of chiral tetrahy-

dropyridine derivatives **46** in good yields (57–84%) and good to excellent enantioselectivities (70–95% ee) when using chiral phosphoric acid **XIV** (Scheme 16).

Mechanistic studies were performed to unveil whether a concerted or stepwise mechanism is taking place, such as trying to trap a possible iminium ion intermediate. The outcome of those experiments pointed towards a concerted mechanism which could be explained by the transition state depicted in Scheme 16: the chiral phosphoric acid could act as a bifunctional catalyst; the OH group acts as a Brønsted acid activating the 1-azadiene, while the phosphoryl oxygen atom activates the enecarbamates as a Lewis base. In order to explain the stereochemistry of the product of the IEDADA reaction, the *Si* face of the azadiene should be attacked by the enecarbamate with *endo* selectivity, thus leading to the (4*S*,5*R*,6*R*)-cycloadduct **46**.

In 2019, as a follow-up work of their previous work, Masson and co-workers published a phosphoric acid-catalyzed enantioselective [4 + 2] cycloaddition of benzothiazolimines **21** and enecarbamates **45** [41]. With this novel methodology benzothiazolopyrimidines **47** bearing three contiguous stereogenic centers were synthesized in good to excellent yields (58–98%), complete diastereoselectivities and excellent enantioselectivities (97–99% ee) using also chiral phosphoric acid **XIV** (Scheme 17). The authors proposed a reaction mechanism in order to explain the observed stereoselectivity of the products in which through hydrogen bonding the chiral phosphoric acid

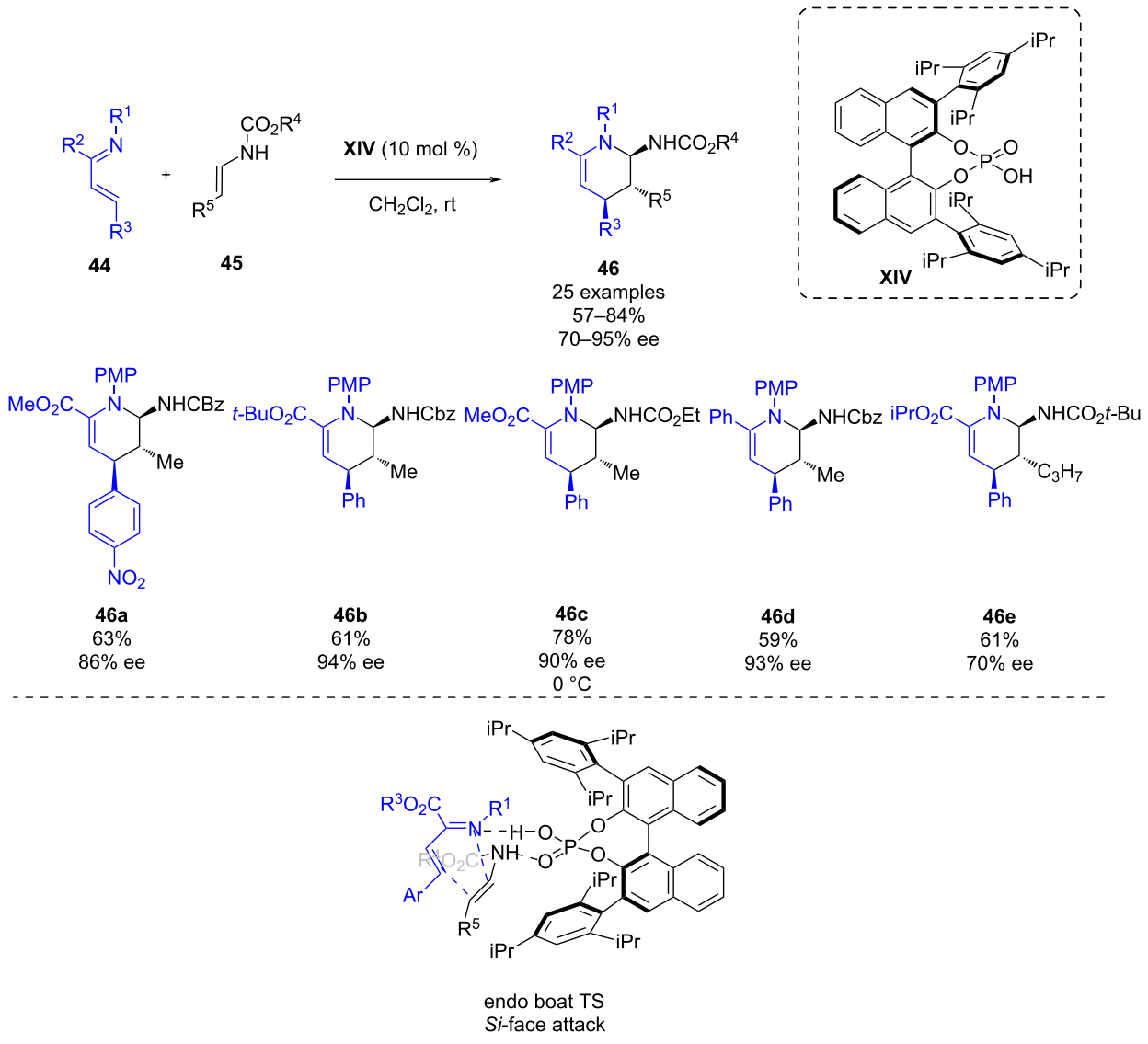

Scheme 16: Inverse electron demand aza-Diels–Alder reaction (IEDADA) of 1-azadienes with enecarbamates catalyzed by chiral phosphoric acid **XIV**.

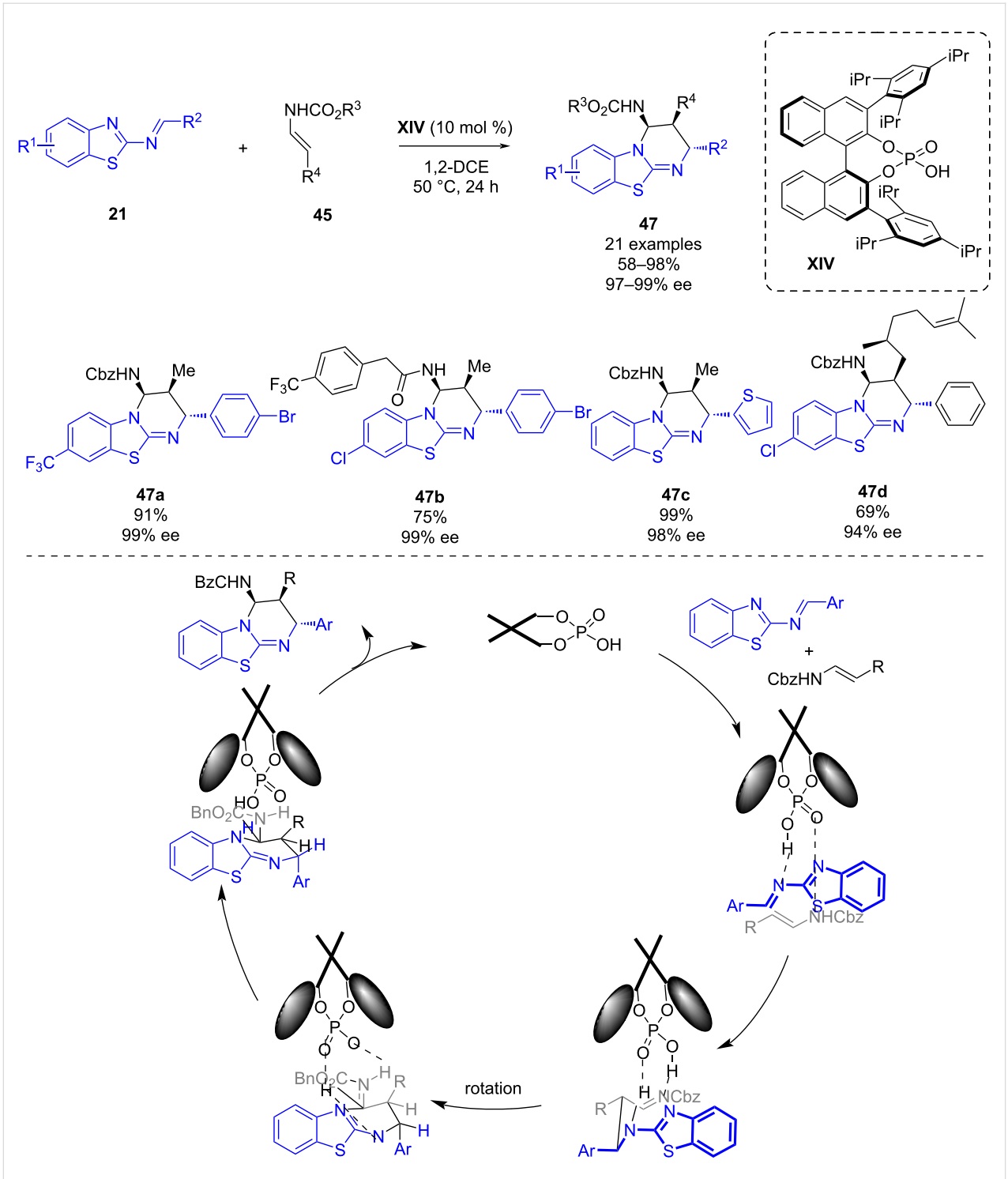

Scheme 17: Phosphoric acid-catalyzed enantioselective [4 + 2] cycloaddition of benzothiazolimines and enecarbamates.

provides a chiral environment where the reaction takes place (Scheme 17).

In 2020, He, Yang and co-workers reported a phosphoric acid-catalyzed enantioselective inverse electron demand aza-Diels–Alder reaction of in situ-generated β,β-disubstituted α,β-unsaturated N–H ketimines and azlactones [42]. This methodology enabled the synthesis of dihydropyridinones **49** and **51** in moderate to good yields (45–76%), excellent diastereoselectivities and high enantioselectivities (85–94% ee) (Scheme 18).

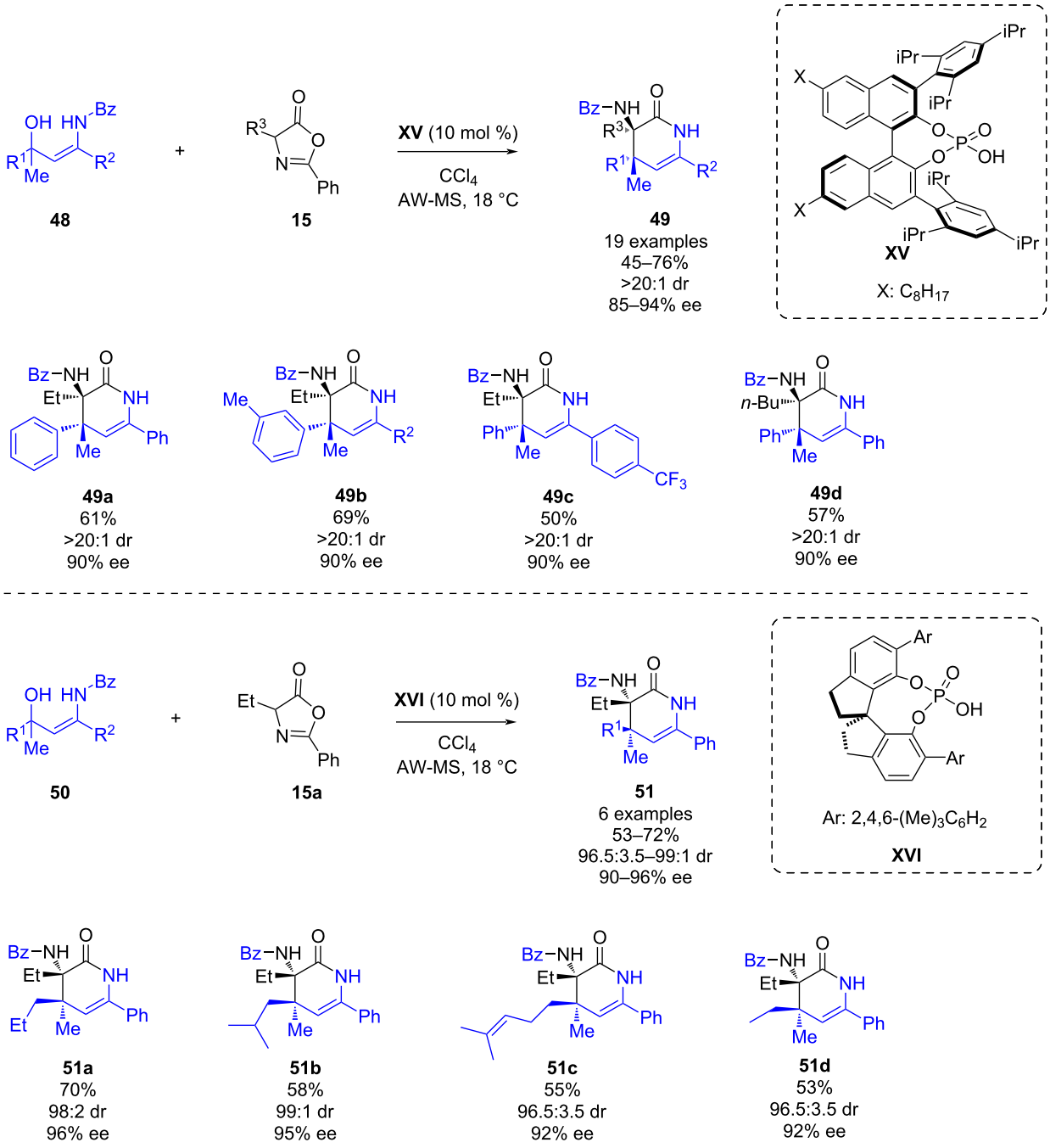

Scheme 18: Phosphoric acid-catalyzed enantioselective inverse electron demand aza-Diels–Alder reaction of in situ-generated β,β-disubstituted α,β-unsaturated N–H ketimines and azlactones.

The reaction was also compatible with 1,1-dialkyl-substituted 3-amidoallylic alcohols **50** as precursors of α,β-unsaturated N–H ketimines; in this case the chiral SPINOL-derived phosphoric acid **XVI** provided the best enantioselectivities (Scheme 18). In both reactions, it was necessary to add acid-washed molecular sieves (AW-MS) in the reaction medium.

The proposed reaction mechanism based on the mechanistic experiments and previous reports is depicted in Scheme 19: the azlactone is activated by the chiral phosphoric acid to generate its active enol form, while at the same time the chiral phosphoric acid mediates the in situ formation of the α,β-unsaturated N–H ketimine, occurring through the formation of an orthoester

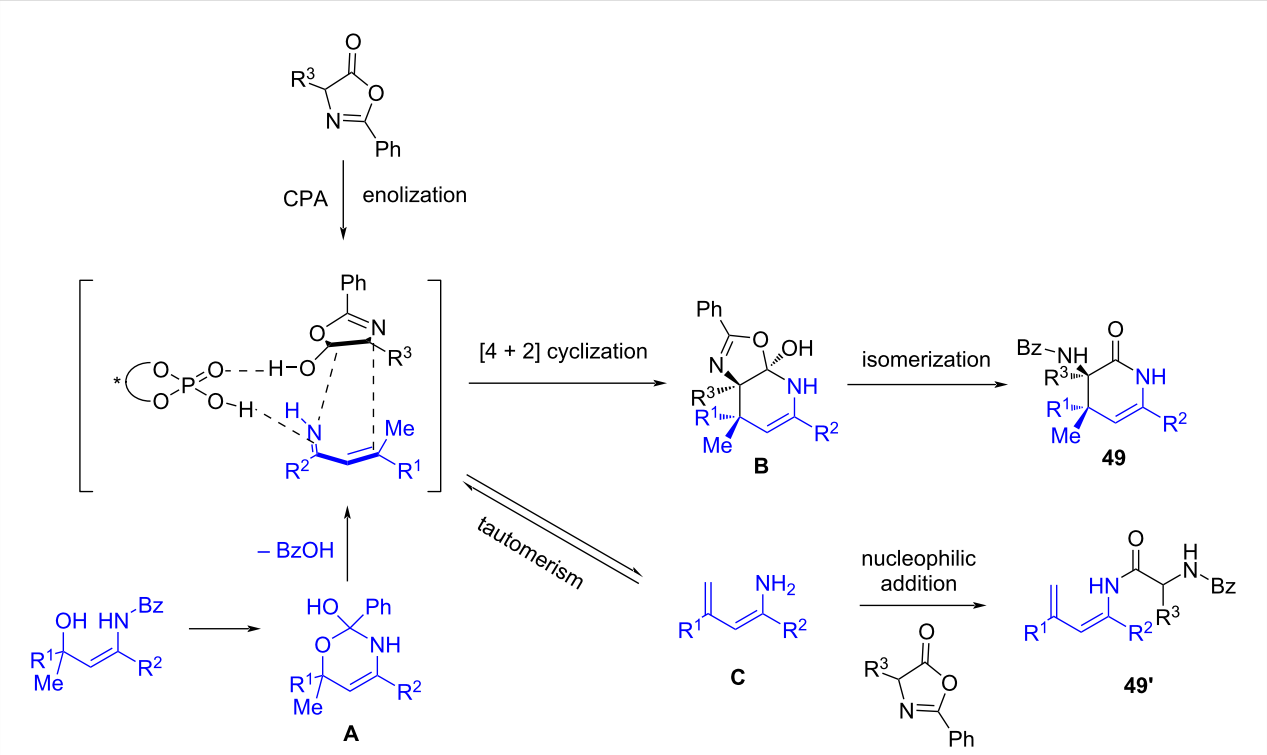

Scheme 19: Proposed reaction mechanism for the phosphoric acid-catalyzed enantioselective inverse electron demand aza-Diels–Alder reaction of in situ generated β,β-disubstituted α,β-unsaturated N–H ketimines and azlactones.

intermediate **A**. Then, the chiral phosphoric acid activates both the enol form of the azlactone and the α,β-unsaturated imine, facilitating the asymmetric [4 + 2] cyclization reaction. The authors proposed the formation of intermediate **B** which subsequently undergoes an isomerization to give the chiral dihydropyridinone derivative **49**. An alternative pathway which occurs is the transformation of the α,β-unsaturated imine into the corresponding enamine **C**, which attacks to the azlactone leading to the addition subproduct **49'**, also observed in the catalytic reactions.

Also in 2020, Lu and co-workers reported an enantioselective dearomatization of indoles **52** via a (3 + 2) cyclization with azoalkenes **53** catalyzed by chiral phosphoric acid **XIV** (Scheme 20). This methodology enables the synthesis of a wide scope of pyrroloindolines **54**, important privileged polycyclic indolines in high yields (72–99%) and high enantioselectivities (90–99%) [43].

The authors proposed a possible mechanism for the reaction which is depicted in Scheme 20. The chiral phosphoric acid activates both the azoalkene acting as a Brønsted acid and the indole acting as a Lewis base promoting a Friedel–Crafts-type 1,4-addition of the indole to the azoalkene. In this manner, a hydrazone intermediate **A** is formed, which tautomerizes to the enamine **B**. Finally, this intermediate undergoes an intramolecular cyclization to yield the desired product.

Besides, to show the synthetic applicability of the pyrroloindoline derivatives, various transformations were performed (Scheme 21). Firstly, hydrogenation with palladium on carbon led to the formation of **55** in a good yield. Secondly, an alkylation of the NH of the indole followed by intramolecular cyclization led to tetracyclic derivative **56** in an 80% yield. Next, a deprotection of the azo nitrogen atom led to derivative **57** in a 92% yield. Finally, the N–N bond could be cleaved forming derivative **58** in 75% yield. All the transformations occurred with the retention of the enantioselectivity.

In July 2021, Tian, Wu, Shi and co-workers published a subsequent article of previous work: a chiral phosphoric acid-catalyzed dearomative (2 + 3) cycloaddition of 3-alkyl-2-vinylindoles **59** and azoalkenes **53** (Scheme 22). This methodology afforded chiral pyrroloindolines **60** bearing two tetrasubstituted stereogenic centers in good yields (61–96%) and excellent stereoselectivities (all >95:5 dr, 86–99% ee) by using chiral phosphoric acid **XVII** [44]. The mechanism of the reaction is taking place in an analogous manner as per the previous article, and the chiral phosphoric acid is activating both the azoalkene and the indole through hydrogen bonding. The newly synthe-

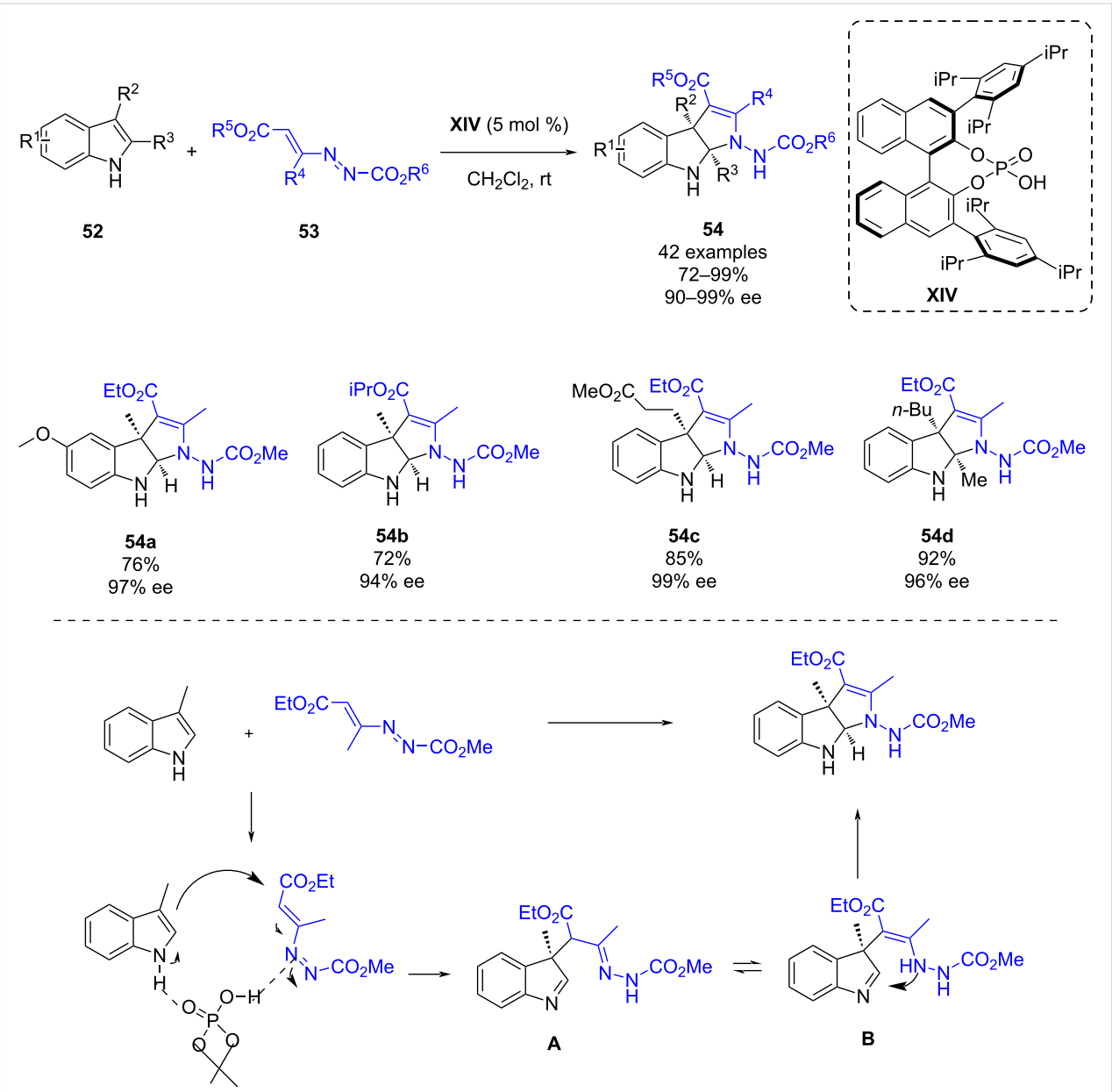

Scheme 20: Enantioselective dearomatization of indoles by a (3 + 2) cyclization with azoalkenes catalyzed by a chiral phosphoric acid.

sized chiral pyrroloindolines were subjected to biological assays confirming that some of the derivatives exhibit strong anticancer activity against Hela and MCF-7 cell lines.

In early 2021, Mei, Lu and co-worker reported a chiral phosphoric acid-catalyzed asymmetric [4 + 2] cycloaddition of aurone-derived 1-azadienes **11** and 3-vinylindoles **61** (Scheme 23). This methodology enables the synthesis of benzofuran-fused tetrahydropyridines **62** bearing three contiguous stereogenic centers in good yields (80–99%), and excellent diastereoselectivities (>20:1 dr) and good to excellent enantioselectivities (63–99% ee) [45]. In general, good enantioselectivities were obtained with all derivatives, only when 2-methyl-3-vinylindole was tested, a lower enantioselectivity was obtained (**62d**, 63% ee). Additionally, the use of 1-azadiene bearing a tosyl substituent led to traces of cycloaddition product **62e**.

The authors proposed a plausible reaction pathway. Firstly, the chiral phosphoric acid is activating both the azadiene and the 3-vinylindole by hydrogen-bonding interactions. However, from this transition state two possible reaction pathways could explain the observed end product. While in path a, a concerted reaction involving an inverse electron demand aza-Diels–Alder reaction could happen, a stepwise mechanism could be also

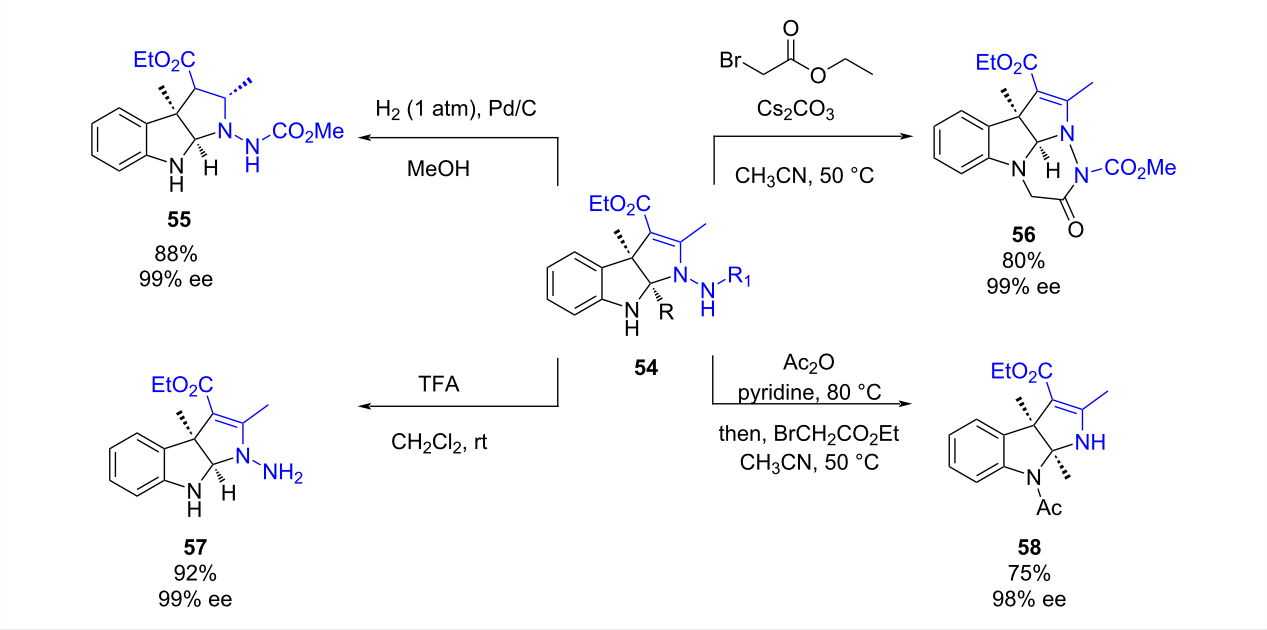

Scheme 21: Synthetic applicability of the pyrroloindoline derivatives.

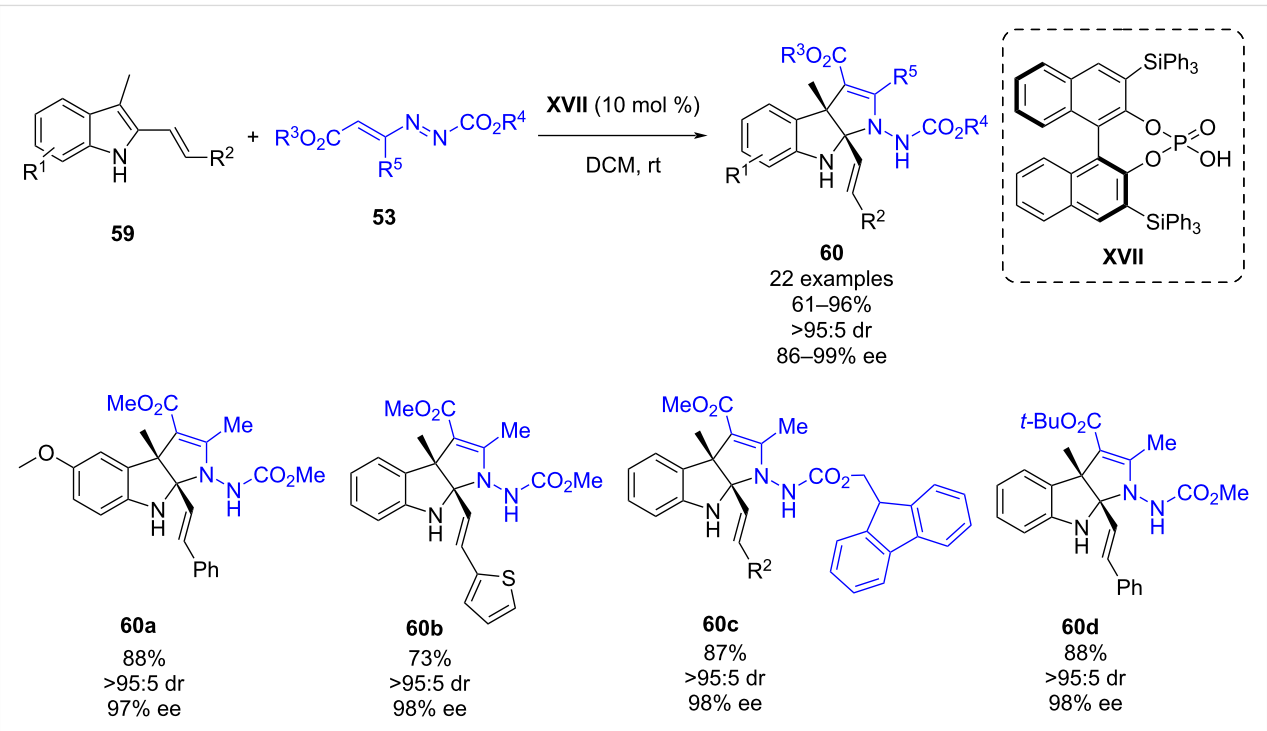

Scheme 22: Chiral phosphoric acid-catalyzed (2 + 3) dearomative cycloaddition of 3-alkyl-2-vinylindoles with azoalkenes.

feasible (path b). In the latter, the addition of the alkene to the azadiene is occurring first and leads to an intermediate which then undergoes an intramolecular cyclization to yield product **62f**. In both pathways, the hydrogen-bonding interaction between the substrate and the product are essential for obtaining the high enantiocontrol in the reaction.

In April 2022, Masson and co-workers published a phosphoric acid-catalyzed enantioselective formal [4 + 2] cycloaddition of 2-benzothioazolimines **21** and dienecarbamates **63** and **65** [46]. Firstly, the reaction between 2-benzothioazolimines **21** and 4-substituted dienes **63** was studied, leading to the synthesis of benzothiazolopyrimidines **64** as major product in moderate to

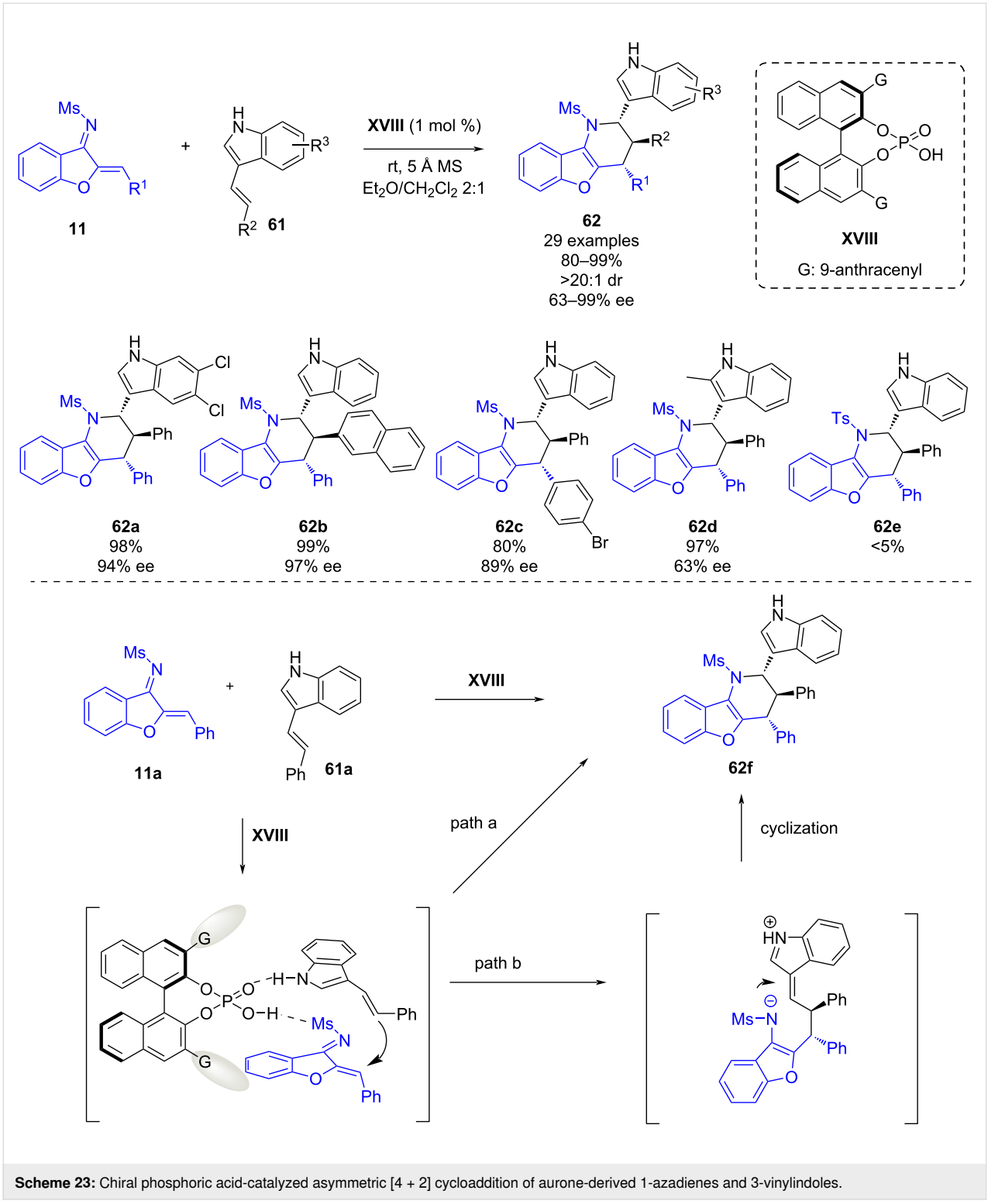

Scheme 23: Chiral phosphoric acid-catalyzed asymmetric [4 + 2] cycloaddition of aurone-derived 1-azadienes and 3-vinylindoles.

good yields (45–67%), complete diastereoselectivities, and in low to high enantioselectivities (10–99% ee) when using organocatalyst **XIV** (Scheme 24). Secondly, the reaction of **21** and 3-substituted dienes **65** led to the production of 1,2,3,4-tetrahydroquinolines diastereomers **66** and **66'** in good to excellent enantioselectivities (68–99% ee) using also chiral phosphoric acid **XIV** (Scheme 24).

In June 2022, Wang, Mei and co-workers reported a chiral phosphoric acid-catalyzed asymmetric inverse electron demand

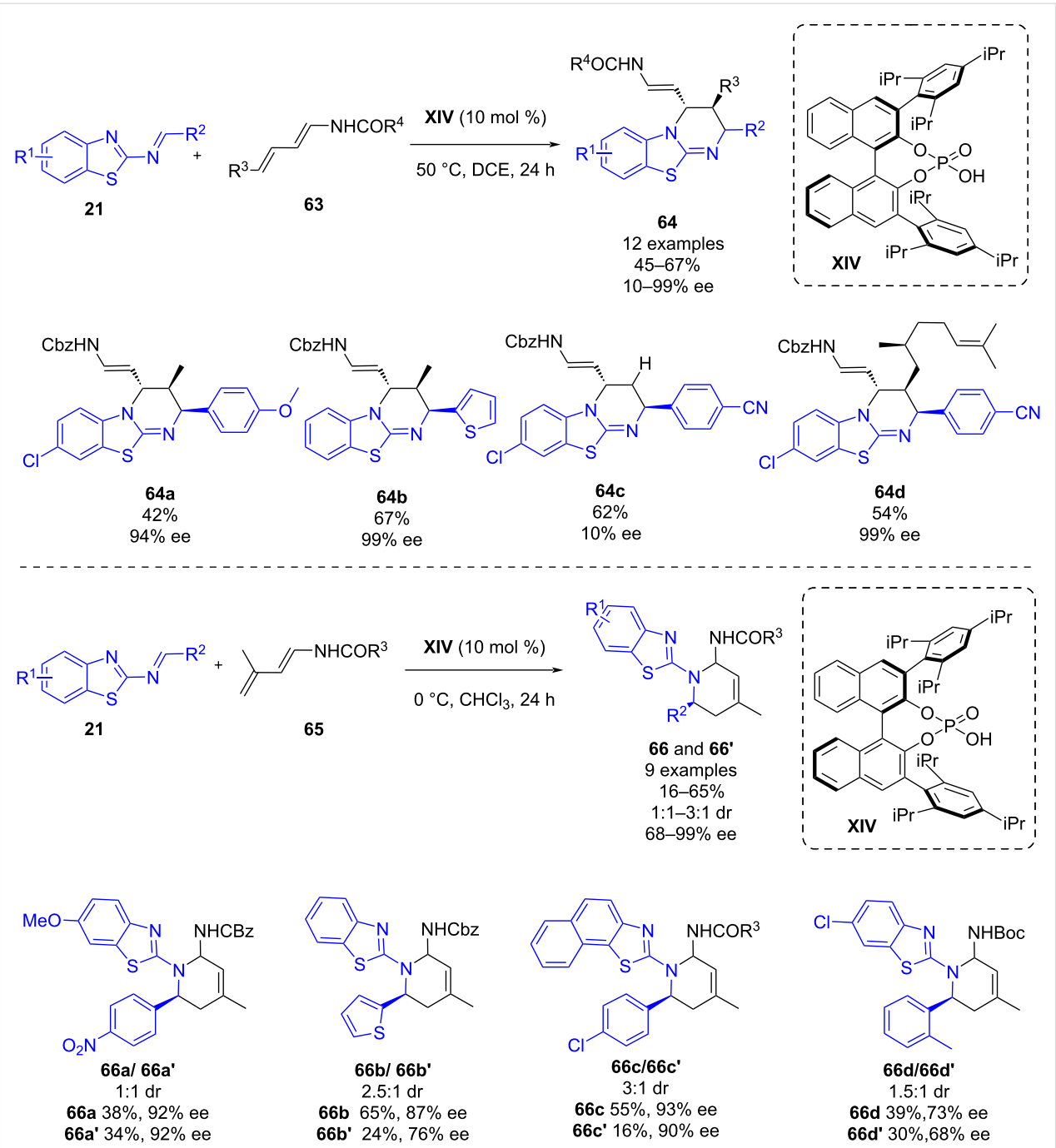

Scheme 24: Phosphoric acid-catalyzed enantioselective formal [4 + 2] cycloaddition of dienecarbamates and 2-benzothioazolimines.

aza-Diels–Alder reaction of 1,3-diazadienes **21** and 3-vinylindoles **61** [47]. After a screening of reaction conditions, chiral phosphoric acid **XIV** was found to be the best organocatalyst, and by using dichloromethane as solvent at room temperature, 43 different benzothiazolopyrimidines **67** were afforded in good yields (52–83%) and good to excellent enantioselectivities (71–99% ee) (Scheme 25). Since the three aromatic residues on the tetrahydropyrimidine ring are placed in a specific *trans–trans* relationship, a concerted reaction pathway seems to be occurring. As depicted in Scheme 25, the chiral phosphoric acid acts as a bifunctional catalyst activating both the 1,3-diazadiene and the indole, procuring a transition state in which both reaction partners are approached.

Also in June 2022, Wang, Xu and Mei reported the chiral phosphoric acid-catalyzed asymmetric Attanasi reaction between

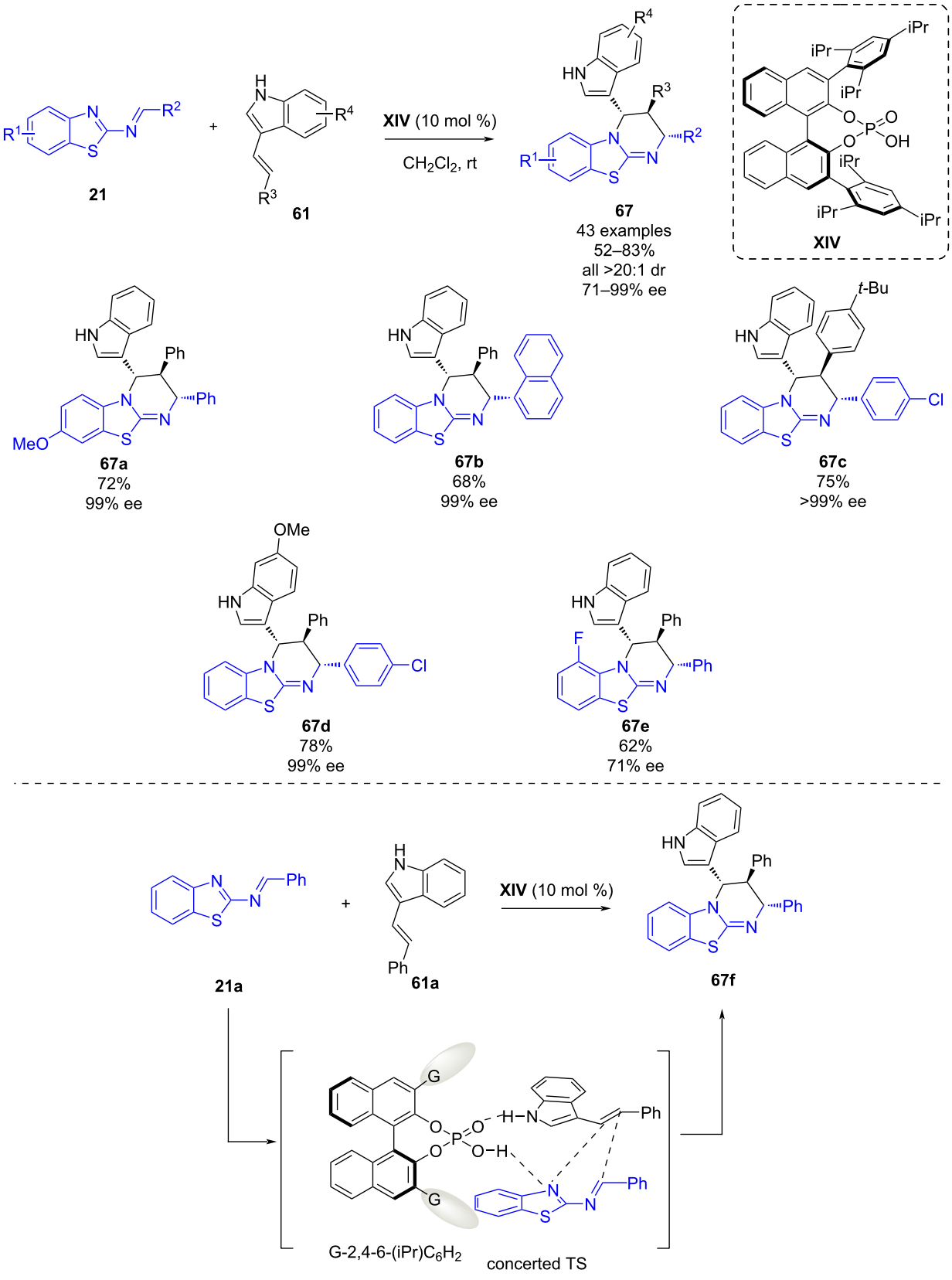

Scheme 25: Chiral phosphoric acid-catalyzed asymmetric inverse electron demand aza-Diels–Alder reaction of 1,3-diazadienes and 3-vinylindoles.

1,3-dicarbonyl compounds **68** and azoalkenes **53** (Scheme 26) [48]. This methodology provides access to C_1-symmetric biarylamino alcohol derivatives (NPNOL) **69** in a wide scope with good yields (45–89%) and good to excellent atroposelectivities (64–99% ee). In order to explain the reaction mechanism and the origin of the enantioselectivity, the authors performed DFT calculations, highlighting the importance of the outer phenyl ring of the chiral phosphoric acid on the enantioinduction.

To demonstrate the synthetic applicability of the chiral axial derivatives a variety of transformations were carried out (Scheme 27). An *N*-alkylation of **69b** was performed leading to **70** bearing two stereogenic axes, the biaryl C–C axis and the N–N axis. The removal of the Boc group led to product **71** in a 98% yield. Then, this derivative was subjected to different transformations. Firstly, the hydrogenation using palladium on carbon led to free alcohol derivative **72** in a 98% yield. Next, a urea **73** and various thioureas **74**–**77** were obtained in good yields and with retention of the enantioselectivity, demonstrating the usefulness of the novel methodology for the synthesis of new organocatalysts.

In April 2023, Huang, Mei and co-workers reported a chiral phosphoric acid-catalyzed asymmetric intermolecular formal (3 + 2) cycloaddition of azoalkenes **53** with azlactones **15** (Scheme 28). This methodology provides fully substituted 4-pyrrolin-2-ones **78** bearing a quaternary carbon atom in high yields (72–95%) and enantioselectivities (87–99% ee) [49]. Furthermore, to demonstrate the synthetic potential of the methodology, further transformations were carried out. Firstly, the *N*-alkylation of **78e** with ethyl bromoacetate led to the synthesis of tetrasubstituted hydrazine **79** in an excellent yield. This derivative has a newly formed N–N axis conducting to the origin of diastereoselectivity in the reaction. The treatment of **79** with base afforded the pyrrolinone **80** in 82% yield. On the other hand, the deprotection of derivative **78f** led to the hydrazine **81** in an excellent yield. All the derivatizations occurred with the enantiomeric ratio retained.

In September 2023, Lan, Huang, Yan and co-workers reported a phosphoric acid-catalyzed enantioselective reaction of acyclic α,β-unsaturated imines and azlactones enabling through an aza-inverse electron demand Diels–Alder reaction, the

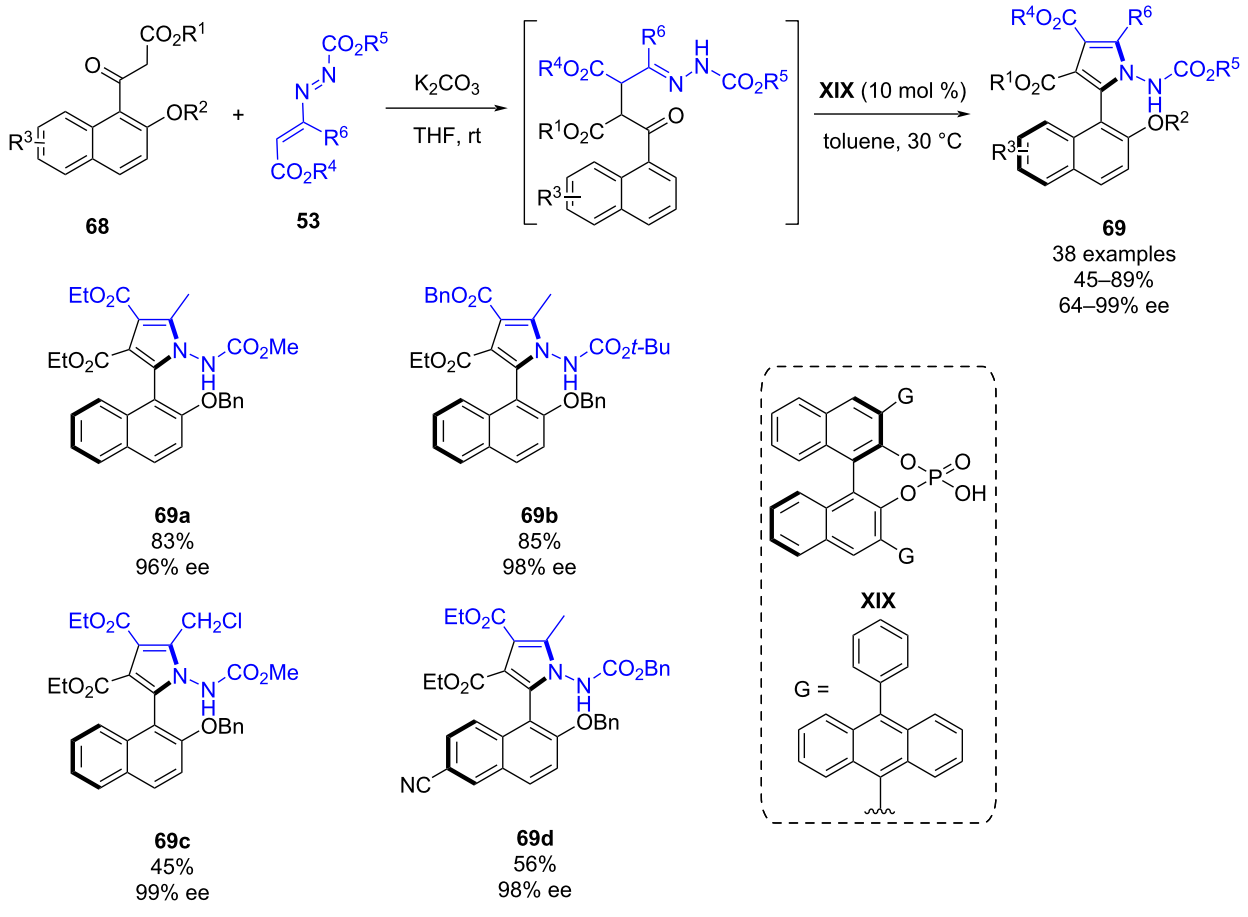

Scheme 26: Chiral phosphoric acid-catalyzed asymmetric Attanasi reaction between 1,3-dicarbonyl compounds and azoalkenes.

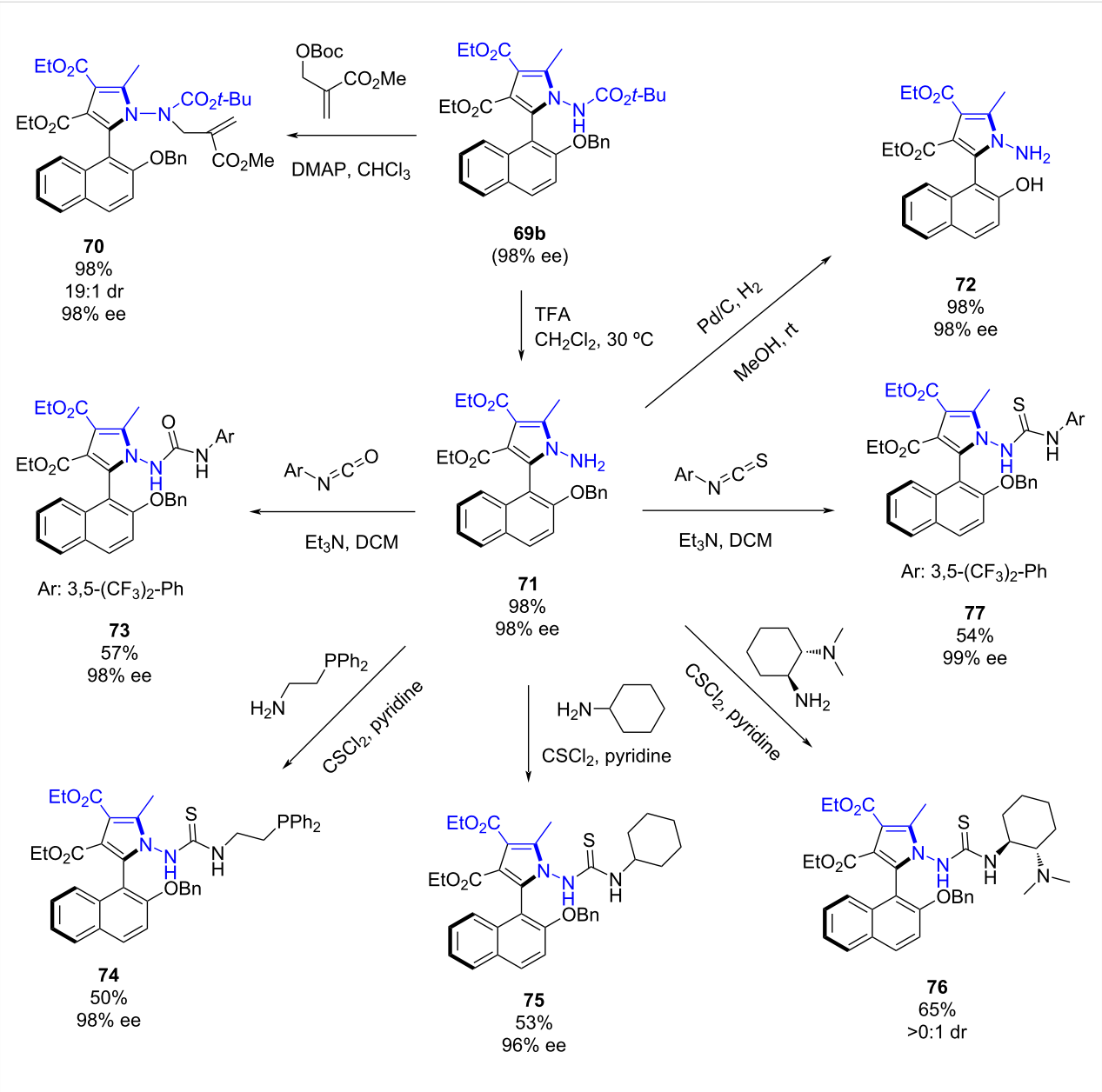

Scheme 27: Synthetic applicability of the NPNOL derivatives.

synthesis of chiral 3-amino-δ-lactams (Scheme 29) [50]. The screening of different Brønsted acids in the reaction between azadiene **82** and azlactone **15** showed that SPINOL-derived catalyst **XX** afforded the best enantioselectivity in the reaction, exploring a scope of 22 derivatives in moderate to excellent yields (46–97%) and enantioselectivities (56–90% ee). Furthermore, under the optimized conditions, the reaction between chalcone-derived azadienes **84** and azlactones **15** was carried out obtaining the chiral 3-amino-δ-lactams **85** in moderate yields (27–57%), good to excellent diastereoselectivities (5:1 to >20:1 dr) and excellent enantioselectivities (92–96% ee).

The proposed reaction pathway is depicted in Scheme 30, the phosphoric acid simultaneously activates the azadiene through hydrogen bonding and the azlactone which is converted to its enol form establishing hydrogen bonding with the phosphoryl group. Next, the 1,4-addition of the azlactone enol through its *Si*-face to the azadiene leads to intermediate **B**, which undergoes an intramolecular lactamization delivering the desired product.

Conclusion

In this review, an overview of the recent advances of cyclization reactions involving α,β-unsaturated imines catalyzed by

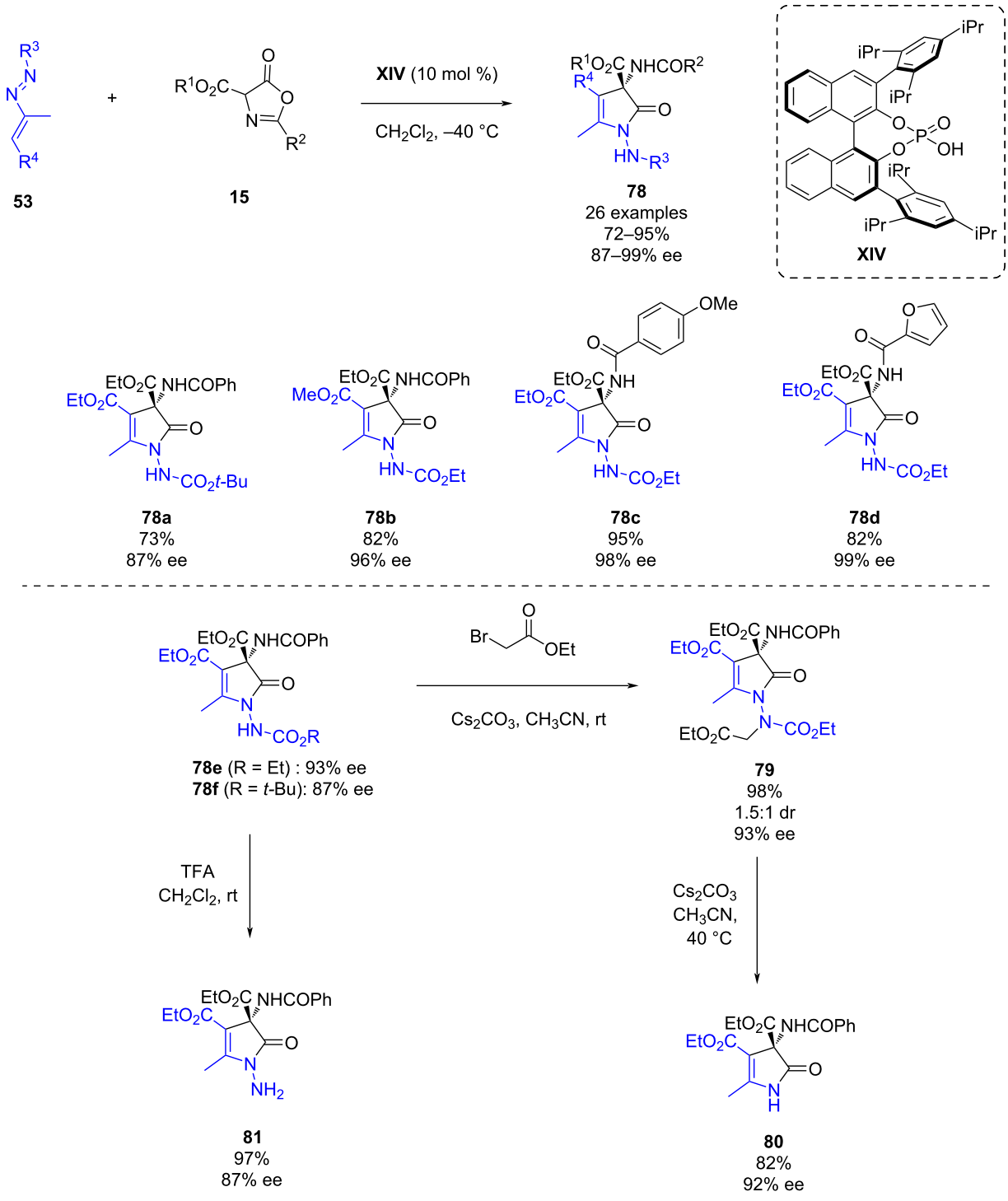

Scheme 28: Chiral phosphoric acid-catalyzed asymmetric intermolecular formal (3 + 2) cycloaddition of azoalkenes with azlactones.

non-covalent organocatalysts has been covered. The chance to use 1-azadienes as electron-poor heterodienes together with available electron-rich dienophiles makes the synthesis of a rich variety of useful *N*-heterocyclic derivatives possible. The right selection of the organocatalyst with different reaction partners enables activation providing stereoselective syntheses to access chiral *N*-heterocyclic scaffolds. While those strategies involving hydrogen-bond donors such as bifunctional thioureas and squaramides or chiral Brønsted acids such as chiral phosphoric acids are more established, reports involving cinchona-derived

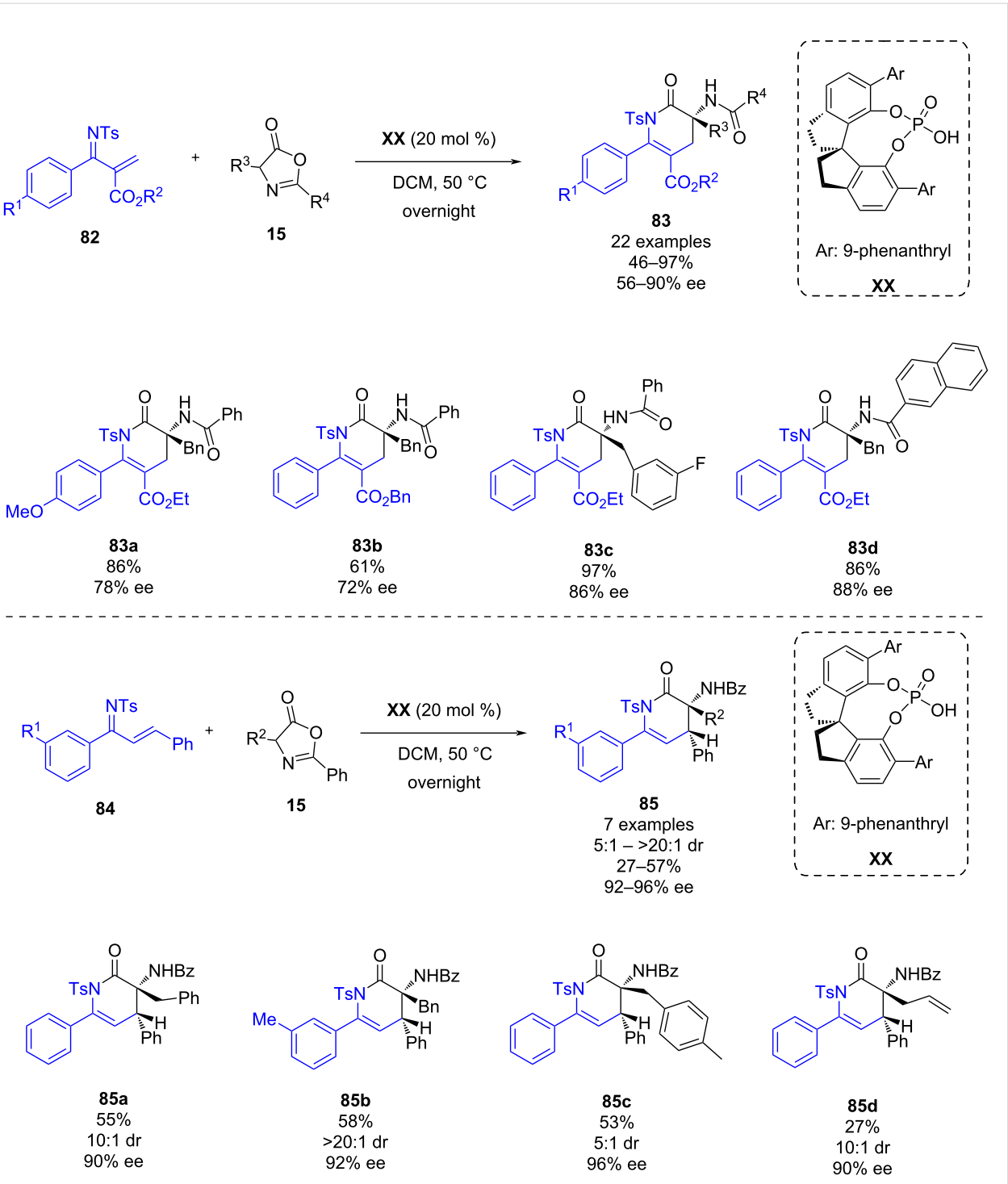

Scheme 29: Enantioselective [4 + 2] cyclization of α,β-unsaturated imines and azlactones.

organocatalysts functioning as Brønsted bases remain rarer. Among the different azadienes employed in the different asymmetric transformations, it is common to identify cyclic α,β-unsaturated imines such as aurone-derived azadienes, saccharin-derived azadienes and benzothiazole-derived imines which in combination with different reaction partners such as azlactones, enecarbamates, vinylindoles, 3-isothiocyanatooxindoles, malononitrile, 3-chlorooxindoles or β,γ-unsaturated ketones lead to the synthesis of a great variety of polycyclic *N*-heterocycles.

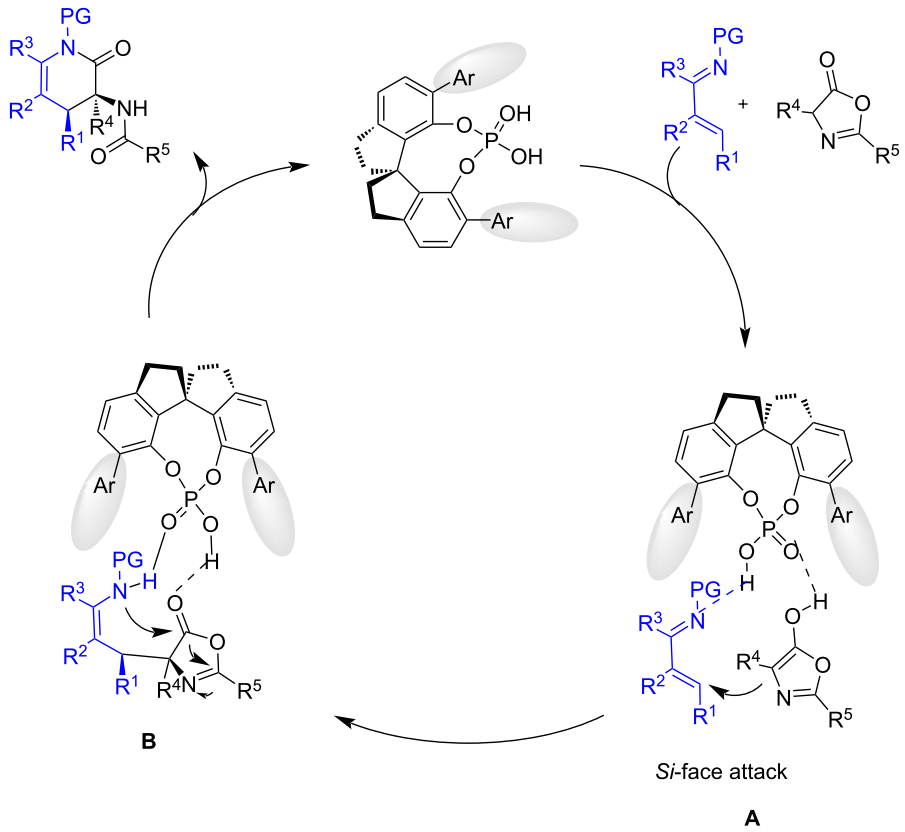

Scheme 30: Catalytic cycle for the chiral phosphoric acid-catalyzed enantioselective [4 + 2] cyclization of α,β-unsaturated imines and azlactones.

To summarize, the asymmetric cycloaddition of 1-azadienes is a straightforward methodology which enables the synthesis of structurally distinct *N*-heterocycles, which are difficult to access by other methodologies. Although in recent years a number of studies have been reported, further novel transformations are likely to be reported in the future.

Funding

S. T.-O. acknowledges a predoctoral contract funded by TED2021-129843B-I00.

Author Contributions

Sergio Torres-Oya: writing – original draft. Mercedes Zurro: conceptualization; supervision; writing – original draft; writing – review & editing.

ORCID® iDs

Sergio Torres-Oya - https://orcid.org/0000-0002-1003-519X
Mercedes Zurro - https://orcid.org/0000-0003-1222-7926

Data Availability Statement

Data sharing is not applicable as no new data was generated or analyzed in this study.

References

1. Alvarez-Builla, J.; Vaquero, J. J.; Barluenga, J., Eds. *Modern Heterocyclic Chemistry;* Wiley-VCH: Weinheim, Germany, 2011. doi:10.1002/9783527637737
2. Joule, J. A.; Mills, K.; Smith, G. F. *Heterocyclic Chemistry;* CRC Press: London, UK, 2020. doi:10.1201/9781003072850
3. Shimizu, M.; Hachiya, I.; Mizota, I. *Chem. Commun.* **2009,** 874–889. doi:10.1039/b814930e
4. Zhao, C.; Gao, R.; Ma, W.; Li, M.; Li, Y.; Zhang, Q.; Guan, W.; Fu, J. *Nat. Commun.* **2024,** *15,* 4329. doi:10.1038/s41467-024-48737-9
5. Gothelf, K. V.; Jørgensen, K. A. *Chem. Rev.* **1998,** *98,* 863–910. doi:10.1021/cr970324e
6. Yet, L. *Chem. Rev.* **2000,** *100,* 2963–3008. doi:10.1021/cr990407q
7. Pandey, G.; Banerjee, P.; Gadre, S. R. *Chem. Rev.* **2006,** *106,* 4484–4517. doi:10.1021/cr050011g
8. Goudedranche, S.; Raimondi, W.; Bugaut, X.; Constantieux, T.; Bonne, D.; Rodriguez Jean, J. *Synthesis* **2013,** *45,* 1909–1930. doi:10.1055/s-0033-1338484
9. Held, F. E.; Tsogoeva, S. B. *Catal. Sci. Technol.* **2016,** *6,* 645–667. doi:10.1039/c5cy01894c
10. Hayashi, Y. Catalytic Asymmetric Diels–Alder Reactions. *Cycloaddition Reactions in Organic Synthesis;* Wiley-VCH: Weinheim, Germany, 2001; pp 5–55. doi:10.1002/3527600256.ch1
11. Kagan, H. B.; Riant, O. *Chem. Rev.* **1992,** *92,* 1007–1019. doi:10.1021/cr00013a013

12. Xie, M.; Lin, L.; Feng, X. *Chem. Rec.* **2017,** *17,* 1184–1202. doi:10.1002/tcr.201700006
13. Laina-Martín, V.; Fernández-Salas, J. A.; Alemán, J. *Chem. – Eur. J.* **2021,** *27,* 12509–12520. doi:10.1002/chem.202101696
14. Skrzyńska, A.; Frankowski, S.; Albrecht, Ł. *Asian J. Org. Chem.* **2020,** *9,* 1688–1700. doi:10.1002/ajoc.202000332
15. Wheeler, S. E.; Seguin, T. J.; Guan, Y.; Doney, A. C. *Acc. Chem. Res.* **2016,** *49,* 1061–1069. doi:10.1021/acs.accounts.6b00096
16. Saha, S. K.; Bera, A.; Singh, S.; Rana, N. K. *Eur. J. Org. Chem.* **2023,** *26,* e202201470. doi:10.1002/ejoc.202201470
17. Zurro, M.; Maestro, A. *ChemCatChem* **2023,** *15,* e202300500. doi:10.1002/cctc.202300500
18. Liao, H.-H.; Miñoza, S.; Lee, S.-C.; Rueping, M. *Chem. – Eur. J.* **2022,** *28,* e202201112. doi:10.1002/chem.202201112
19. Mukherjee, S.; Yang, J. W.; Hoffmann, S.; List, B. *Chem. Rev.* **2007,** *107,* 5471–5569. doi:10.1021/cr0684016
20. MacMillan, D. W. C. *Nature* **2008,** *455,* 304–308. doi:10.1038/nature07367
21. Enders, D.; Niemeier, O.; Henseler, A. *Chem. Rev.* **2007,** *107,* 5606–5655. doi:10.1021/cr068372z
22. Doyle, A. G.; Jacobsen, E. N. *Chem. Rev.* **2007,** *107,* 5713–5743. doi:10.1021/cr068373r
23. Erkkilä, A.; Majander, I.; Pihko, P. M. *Chem. Rev.* **2007,** *107,* 5416–5470. doi:10.1021/cr068388p
24. Jiang, X.; Shi, X.; Wang, S.; Sun, T.; Cao, Y.; Wang, R. *Angew. Chem., Int. Ed.* **2012,** *51,* 2084–2087. doi:10.1002/anie.201107716
25. Du, D.; Xu, Q.; Li, X.-G.; Shi, M. *Chem. – Eur. J.* **2016,** *22,* 4733–4737. doi:10.1002/chem.201600497
26. Gu, Z.; Wu, B.; Jiang, G.-F.; Zhou, Y.-G. *Chin. J. Chem.* **2018,** *36,* 1130–1134. doi:10.1002/cjoc.201800330
27. Ren, X.-R.; Lin, J.-B.; Hu, X.-Q.; Xu, P.-F. *Org. Chem. Front.* **2019,** *6,* 2280–2283. doi:10.1039/c9qo00357f
28. Wang, C.-S.; Li, T.-Z.; Cheng, Y.-C.; Zhou, J.; Mei, G.-J.; Shi, F. *J. Org. Chem.* **2019,** *84,* 3214–3222. doi:10.1021/acs.joc.8b03004
29. Li, X.; Yan, J.; Qin, J.; Lin, S.; Chen, W.; Zhan, R.; Huang, H. *J. Org. Chem.* **2019,** *84,* 8035–8045. doi:10.1021/acs.joc.9b00911
30. Ni, Q.; Wang, X.; Xu, F.; Chen, X.; Song, X. *Chem. Commun.* **2020,** *56,* 3155–3158. doi:10.1039/d0cc00736f
31. Frankowski, S.; Skrzyńska, A.; Sieroń, L.; Albrecht, Ł. *Adv. Synth. Catal.* **2020,** *362,* 2658–2665. doi:10.1002/adsc.202000197
32. Chang, L.; Zhu, G.-Y.; Yang, T.; Zhao, X.-L.; Shi, M.; Zhao, M.-X. *Org. Biomol. Chem.* **2021,** *19,* 3687–3697. doi:10.1039/d1ob00115a
33. Laina-Martín, V.; Humbrías-Martín, J.; Mas-Ballesté, R.; Fernández-Salas, J. A.; Alemán, J. *ACS Catal.* **2021,** *11,* 12133–12145. doi:10.1021/acscatal.1c03390
34. Yang, T.; Yan, S.; Yu, Z.-J.; Zhao, X.-L.; Shi, M.; Zhao, M.-X. *Eur. J. Org. Chem.* **2023,** *26,* e202300275. doi:10.1002/ejoc.202300275
35. Song, C. E., Ed. *Cinchona Alkaloids in Synthesis and Catalysis;* Wiley-VCH: Weinheim, Germany, 2009. doi:10.1002/9783527628179
36. Li, C.; Jiang, K.; Chen, Y.-C. *Molecules* **2015,** *20,* 13642–13658. doi:10.3390/molecules200813642
37. Yu, L.; Cheng, Y.; Qi, F.; Li, R.; Li, P. *Org. Chem. Front.* **2017,** *4,* 1336–1340. doi:10.1039/c6qo00832a
38. Varlet, T.; Masson, G. *Chem. Commun.* **2021,** *57,* 4089–4105. doi:10.1039/d1cc00590a
39. Maji, R.; Mallojjala, S. C.; Wheeler, S. E. *Chem. Soc. Rev.* **2018,** *47,* 1142–1158. doi:10.1039/c6cs00475j
40. He, L.; Laurent, G.; Retailleau, P.; Folléas, B.; Brayer, J.-L.; Masson, G. *Angew. Chem., Int. Ed.* **2013,** *52,* 11088–11091. doi:10.1002/anie.201304969
41. Jarrige, L.; Glavač, D.; Levitre, G.; Retailleau, P.; Bernadat, G.; Neuville, L.; Masson, G. *Chem. Sci.* **2019,** *10,* 3765–3769. doi:10.1039/c8sc05581e
42. He, S.; Gu, H.; He, Y.-P.; Yang, X. *Org. Lett.* **2020,** *22,* 5633–5639. doi:10.1021/acs.orglett.0c01994
43. Mei, G.-J.; Tang, X.; Tasdan, Y.; Lu, Y. *Angew. Chem., Int. Ed.* **2020,** *59,* 648–652. doi:10.1002/anie.201911686
44. Chen, K.-W.; Wang, D.-D.; Liu, S.-J.; Wang, X.; Zhang, Y.-C.; Tian, Y.-M.; Wu, Q.; Shi, F. *J. Org. Chem.* **2021,** *86,* 10427–10439. doi:10.1021/acs.joc.1c01105
45. Koay, W. L.; Mei, G.-J.; Lu, Y. *Org. Chem. Front.* **2021,** *8,* 968–974. doi:10.1039/d0qo01236j
46. Ma, W.-Y.; Montinho-Inacio, E.; Iorga, B. I.; Retailleau, P.; Moreau, X.; Neuville, L.; Masson, G. *Adv. Synth. Catal.* **2022,** *364,* 1708–1715. doi:10.1002/adsc.202200161
47. Miao, Y.-H.; Hua, Y.-Z.; Gao, H.-J.; Mo, N.-N.; Wang, M.-C.; Mei, G.-J. *Chem. Commun.* **2022,** *58,* 7515–7518. doi:10.1039/d2cc02458f
48. Han, T.-J.; Zhang, Z.-X.; Wang, M.-C.; Xu, L.-P.; Mei, G.-J. *Angew. Chem., Int. Ed.* **2022,** *61,* e202207517. doi:10.1002/anie.202207517
49. Mo, N.-N.; Miao, Y.-H.; Xiao, X.; Hua, Y.-Z.; Wang, M.-C.; Huang, L.; Mei, G.-J. *Chem. Commun.* **2023,** *59,* 5902–5905. doi:10.1039/d3cc01194a
50. Zhou, W.-J.; Yu, X.; Chen, C.; Lan, W.; Zhan, G.; Zhou, J.; Liu, Q.; Huang, W.; Yang, Q.-Q. *J. Org. Chem.* **2023,** *88,* 13427–13439. doi:10.1021/acs.joc.3c00663

License and Terms

BEILSTEIN JOURNAL OF ORGANIC CHEMISTRY

Recent advances in organocatalytic atroposelective reactions

Henrich Szabados and Radovan Šebesta*

Review

Open Access

Address:
Department of Organic Chemistry, Faculty of Natural Science, Comenius University Bratislava, Mlynská dolina, Ilkovičova 6, 842 15 Bratislava, Slovakia

Email:
Radovan Šebesta* - radovan.sebesta@uniba.sk

* Corresponding author

Keywords:
asymmetric organocatalysis; atropoisomers; atroposelective synthesis; axial chirality; stereogenic axis

Beilstein J. Org. Chem. **2025,** *21,* 55–121.
https://doi.org/10.3762/bjoc.21.6

Received: 15 August 2024
Accepted: 12 December 2024
Published: 09 January 2025

Associate Editor: M. Rueping

Abstract

Axial chirality is present in a variety of naturally occurring compounds, and is becoming increasingly relevant also in medicine. Many axially chiral compounds are important as catalysts in asymmetric catalysis or have chiroptical properties. This review overviews recent progress in the synthesis of axially chiral compounds via asymmetric organocatalysis. Atroposelective organocatalytic reactions are discussed according to the dominant catalyst activation mode. For covalent organocatalysis, the typical enamine and iminium modes are presented, followed by *N*-heterocyclic carbene-catalyzed reactions. The bulk of the review is devoted to non-covalent activation, where chiral Brønsted acids feature as the most prolific catalytic structure. The last part of the article discusses hydrogen-bond-donating catalysts and other catalyst motifs such as phase-transfer catalysts.

Introduction

Stereoselective catalytic formation of chiral compounds is one of the critical tasks of modern organic synthesis [1]. The catalytic formation of compounds with a center of chirality has been the focus of countless works and can now be considered a matured area. On the other hand, the generation of compounds comprising a stereogenic plane or axis is much less developed. Axially chiral compounds are well known as chiral ligands in asymmetric catalysis, with notable examples of binaphthyl-based derivatives such as BINAP, SEGPHOS, or binaphthyl-based phosphoric acid derivatives, which are among the privileged catalyst frameworks [2]. Axially chiral biaryls have also been found to be useful in materials [3]. Although much less widely occurring than centrochiral compounds, there are also naturally occurring axially chiral compounds. Axially chiral compounds are becoming increasingly relevant also in drug discovery and medicine [4]. However, a lack of reliable synthetic methods for their preparation hindered the broader application of axially chiral compounds. In recent decades, there has been increased interest in the catalytic syntheses of axially chiral compounds by catalytic [5,6], especially organocatalyzed, methods [7-11]. Asymmetric organocatalysis offers efficient and environmentally benign access to numerous chiral compounds [12]. Therefore, an increasing number of researchers are now investigating the organocatalytic formation of compounds

with axial stereogenic axes across various structural motifs [13-17]. Remarkably, these compounds are not limited to the C(sp^2)–C(sp^2) axis, but new developments in the formation of C–N, C–B, or even N–N stereogenic axes have been achieved. To help the research community distill and abstract the relevant new knowledge, this review has been prepared, which aims to provide an update on the last five years of this burgeoning area with some relevant links to key earlier works. The material in this article is divided according to the major activation mode of the organocatalyst, from covalent activation via enamine and iminium activation to NHC-catalyzed reactions. The major part is devoted to chiral Brønsted acid catalysis as it seems so far the most widely used activation principle for the generation of axially chiral compounds. Hydrogen-bond-donating catalysts and various other activation modes complete the discussion of recent advances in organocatalytic atroposelective syntheses.

Review

Atroposelective reactions via enamine and iminium activation

Iminium activation was utilized in the synthesis of axially chiral styrenes. Tan and co-workers developed an atroposelective strategy toward axially chiral alkenylarenes **3** based on an organocatalytic Michael addition to alkynals **2** (Scheme 1) [18]. The authors identified the Jørgensen–Hayashi-type catalyst **C1** as the most efficient organocatalyst. In this way, a range of axially chiral styrenes were obtained in high yields and enan-

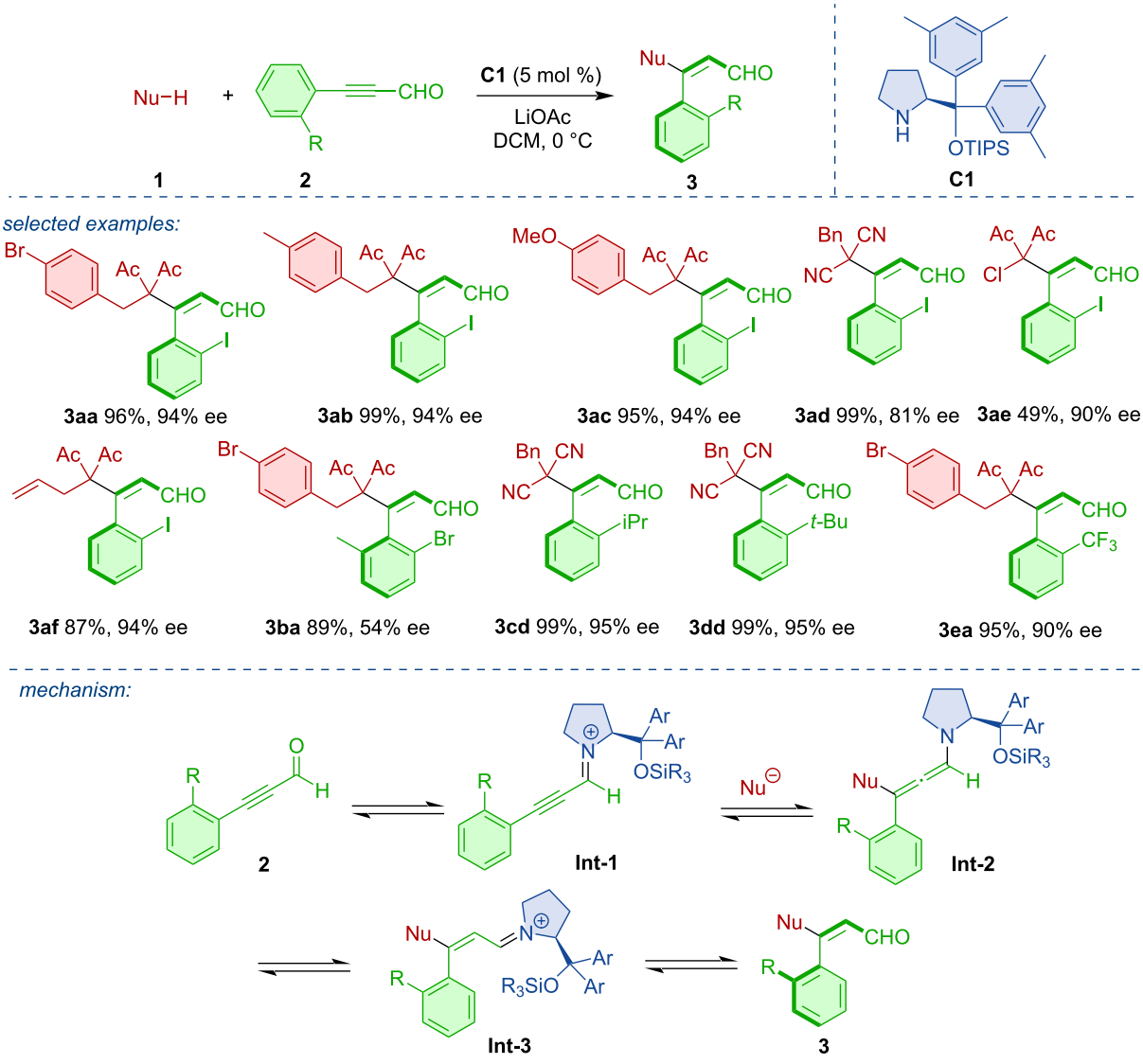

Scheme 1: Formation of axially chiral styrenes **3** via iminium activation.

tiomeric purities. The reaction was based on an iminium activation of propargylic aldehydes with catalyst **Int-1**. Another critical feature was the ability of the organocatalyst to promote the *Z*-selective isomerization of **Int-2** to **Int-3**.

In a related fashion, Wang and co-workers developed an atroposelective heterocycloaddition [19]. The iminium-activated alkynals **4** reacted with aminoarylaldehydes **5** to form axially chiral 2-arylquinoline derivatives **6** (Scheme 2). Using the pyrrolidine derivative **C2** as the most efficient organocatalyst, a range of quinoline derivatives were obtained in high yields and enantiomeric purities. The postulated mechanism consists of iminium activation, atroposelective aza-Michael addition, and intramolecular aldol reaction to form the cationic intermediate **Int-6**. Release of the catalyst **C2**, reduction with $NaBH_4$, and dehydration with acetic acid leads to the desired product **6**.

Recently, an organocatalytic atroposelective intramolecular (4 + 2) annulation of enals with ynamides **8** to afford axially chiral 7-arylindolines **9** was reported [20]. The reaction mechanism, rationalized by DFT calculations, is believed to occur through catalyst **C3** activation of the substrate **8**, dehydration, and deprotonation with tautomerization leading to the enamine intermediate **Int-9**. As the assumed rate-determining step the intramolecular nucleophilic addition takes place, followed by further cyclization and finally, release of the organocatalyst to form the axially chiral product **9**. Various aryl-substituted indolines **9** were obtained in good yields and high enantiomeric purities (Scheme 3).

Sparr and co-workers developed an atroposelective synthesis for tetra-*ortho*-substituted biaryls **11** by non-canonical polyketide cyclizations [21]. This work was based on an earlier report

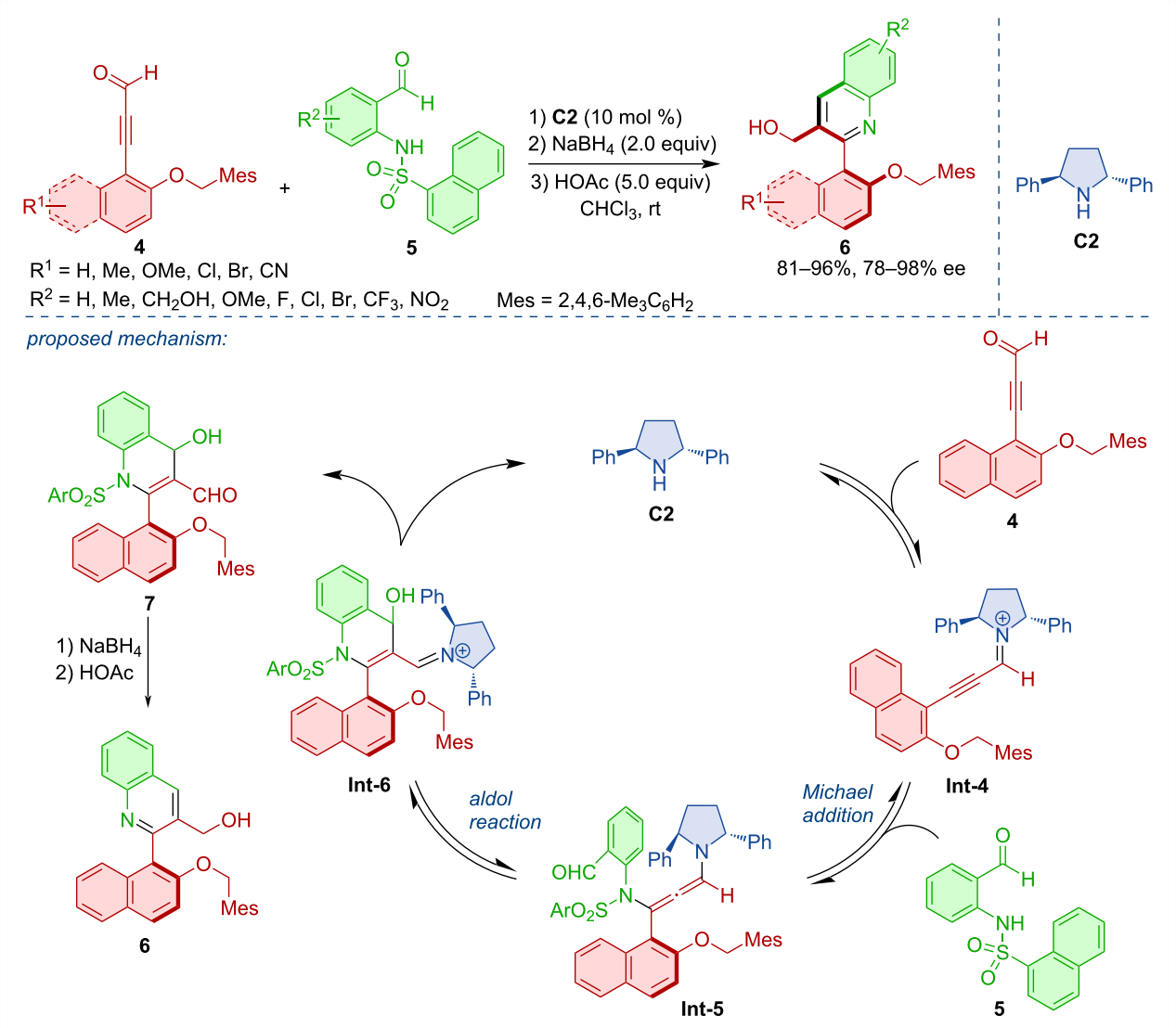

Scheme 2: Synthesis of axially chiral 2-arylquinolines **6**.

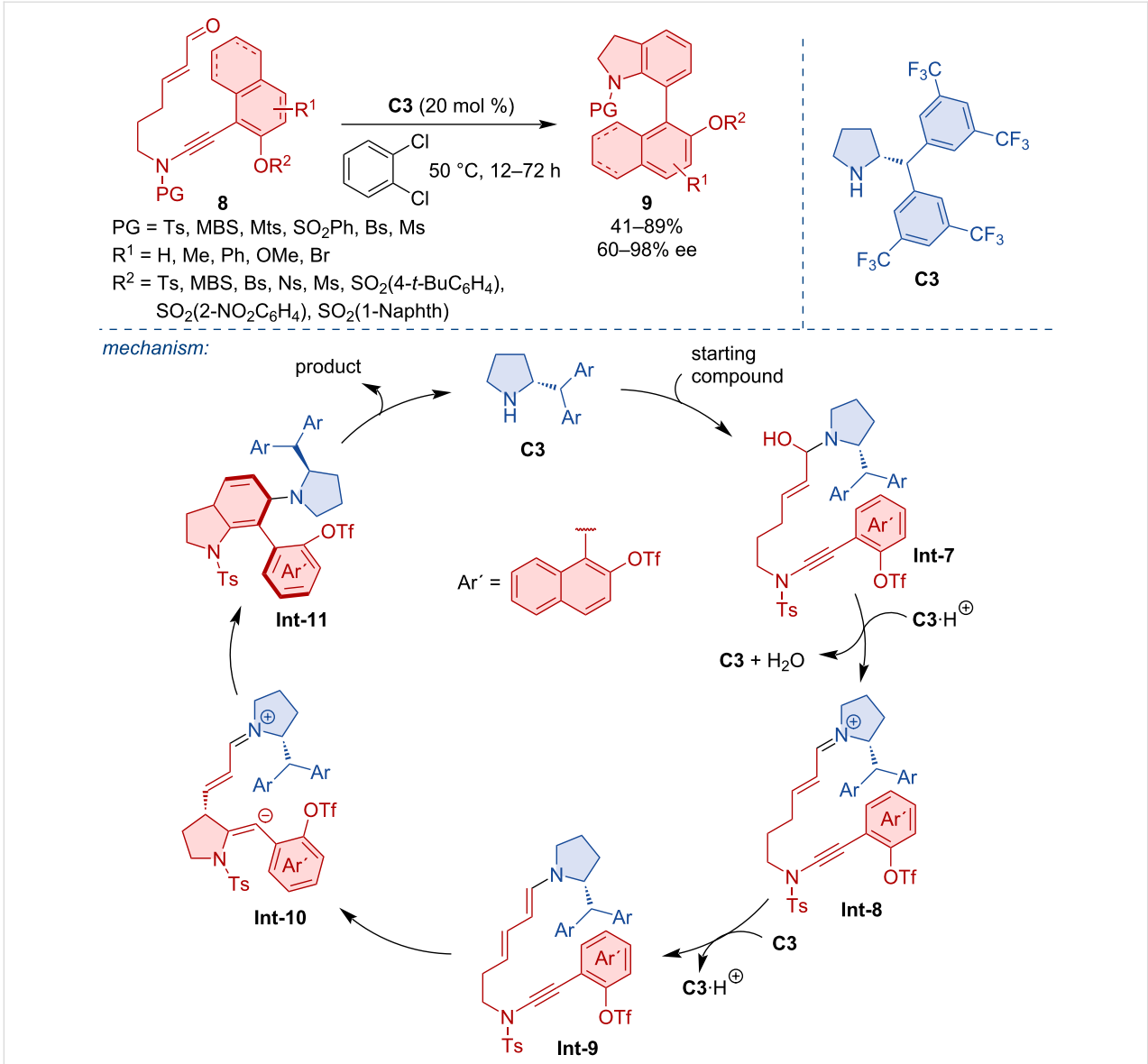

Scheme 3: Atroposelective intramolecular (4 + 2) annulation leading to aryl-substituted indolines.

of the team on the aldol cyclization of naphthyl-substituted unsaturated ketoaldehydes [22]. The process was inspired by the biocatalytic synthesis of aromatic polyketides by polyketide synthase from poly β-carbonyl substrates. Pyrrolidine-based organocatalyst **C4** was able to promote a twofold atroposelective arene-forming 6-*enolendo* aldol condensation (Scheme 4).

Sparr also realized a central-to-axial chirality conversion via catalyst-controlled oxidative aromatization [23]. In this way, the axially chiral starting material **12** comprising an additional stereogenic center was converted into oligonaphthylenes **13** with two, three or even four stereogenic axes. Based on the organocatalyst used, the transformation produced either the (R_a,S_a)-isomer using pyrrolidine tetrazole catalyst **C6** or the (S_a,S_a)-diastereoisomer using quaternary ammonium salt **C5** (Scheme 5). Catalyst-controlled formation of twofold and higher-order stereogenicity in axially chiral arenes was discussed in this account article [15].

Hayashi realized an organocatalytic domino sequence that afforded axially chiral biaryls [24]. The transformation relied on an organocatalytic Michael/Henry cascade. The enamine-type Michael addition was catalyzed by the Hayashi–Jørgensen organocatalyst **C7** (Scheme 6). Then, a series of one-pot reactions was carried out to provide the final biaryl products **17**.

In a related strategy, Hayashi´s team realized an organocatalytic Michael/aldol cascade leading to chiral dihydronaph-

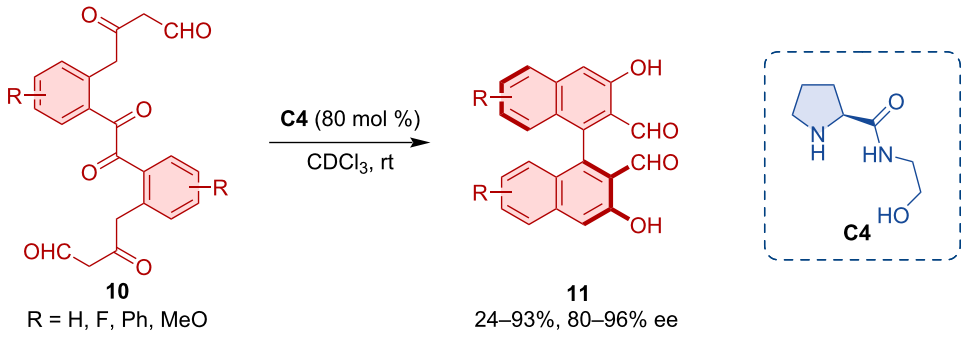

Scheme 4: Atroposelective formation of biaryl via twofold aldol condensation.

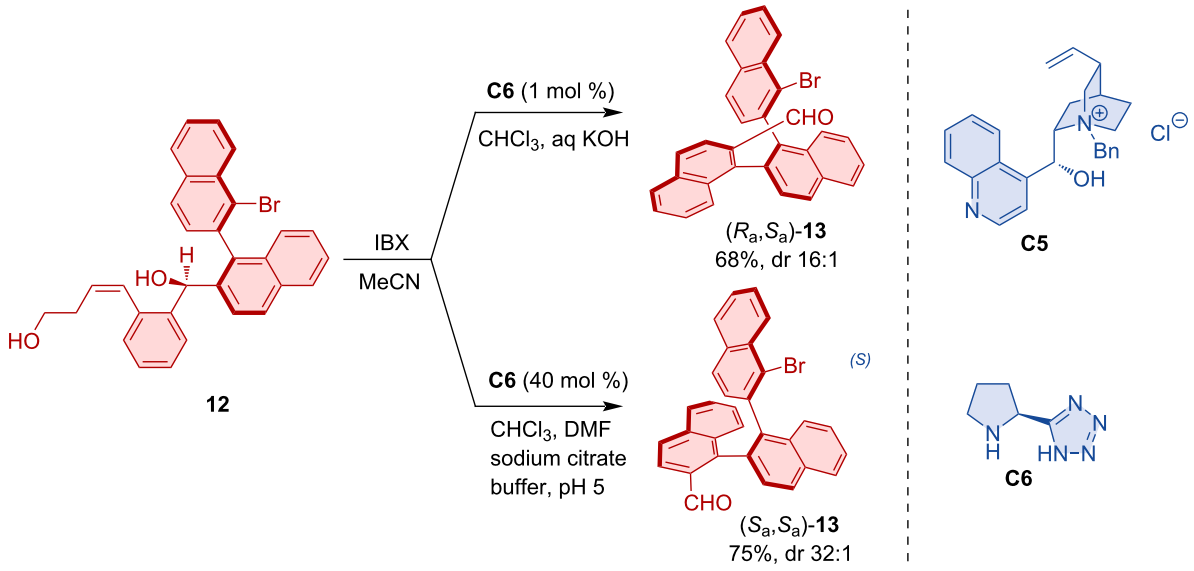

Scheme 5: Strategy towards diastereodivergent formation of axially chiral oligonaphthylenes.

thalene derivatives **20a–e** [25]. Through a series of one-pot reactions, aromatization was achieved with concomitant central-to-axial chirality conversion and formation of axially chiral products **21a–e** (Scheme 7). This critical aromatization was later studied in more detail, and the team was able to achieve enantiodivergent aromatization, which led to different atropoisomers based on the oxidation reagent used [26]. The use of NBS and AgOTf led to the formation of the (S_a)-atropoisomers, whereas NIS afforded the (R_a)-atropoisomers.

Non-biaryl atropoisomers are characterized by at least one non-aryl substituent on the stereogenic axis. Among them, compounds featuring a conformationally stable C(sp^2)–C(sp^3) stereogenic axis are of interest and have been recently investigated by Jørgensen and co-workers. The authors employed an enantioselective aminocatalytic cycloaddition between 5*H*-benzo[*a*]pyrrolizine-3-carbaldehydes **22** and naphthyl-substituted nitroalkenes, α,β-unsaturated ketoesters, or α,β-unsaturated aldehydes **23** [27]. This transformation led to a series of axially chiral cycl[3.2.2]azines **24** in good yields and high enantiomeric purities (Scheme 8). The proposed mechanism comprises enamine activation, condensation with nitroolefin **23**, ring closure, and catalyst elimination to provide the axially chiral product **24**.

NHC-catalyzed atroposelective reactions

Organocatalysis with *N*-heterocyclic carbenes (NHC) became one of the main types of covalent activation strategies, which grew into a very diverse area, allowing the synthesis of a wide array of interesting structures. Also, in atroposelective synthe-

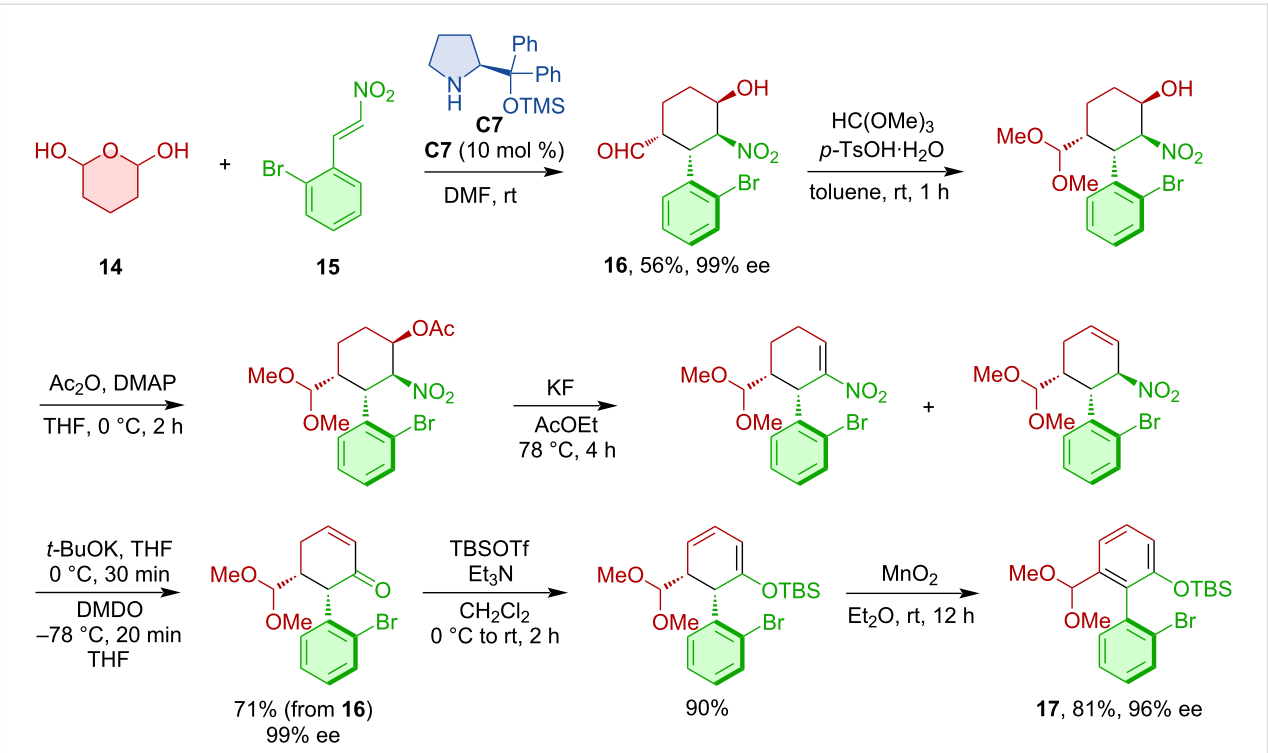

Scheme 6: Atroposelective formation of chiral biaryls based on a Michael/Henry domino reaction.

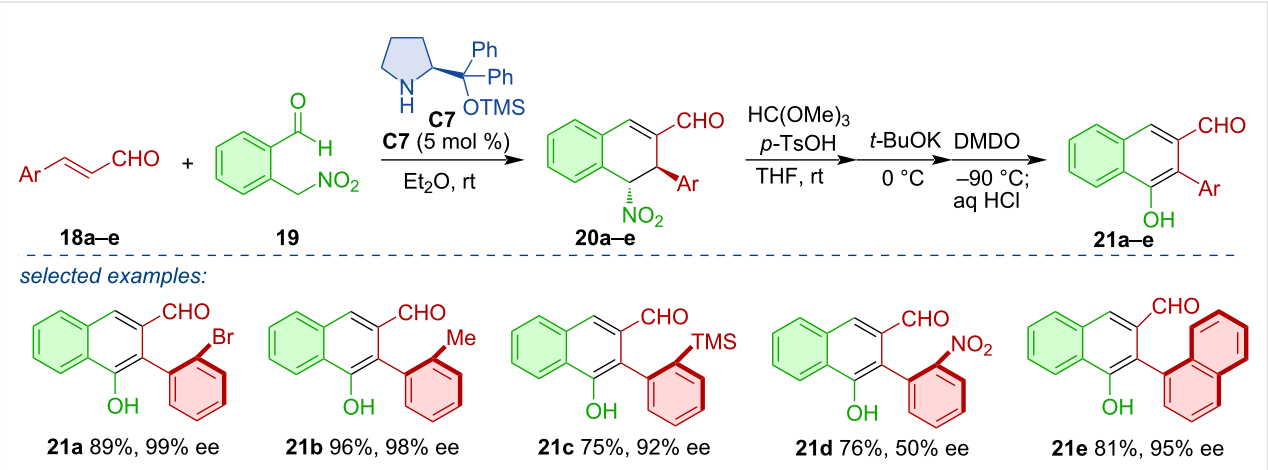

Scheme 7: Organocatalytic Michael/aldol cascade followed by oxidative aromatization.

sis, NHC-catalysis recently led to an array of intriguing transformations.

Axially chiral styrenes **26** were assembled via the NHC-catalyzed reaction of propargylic aldehydes **25**, sulfinic acids, and phenols [28]. The crucial step of this transformation is the 1,4-addition of the sulfinic anion to the triple bond of acylazolium intermediate **Int-16** followed by *E*-selective protonation of **Int-17** (Scheme 9).

NHC-catalysis also proved useful in the atroposelective construction of triaryl derivatives with two stereogenic axes. Wei, Du, and co-workers developed a synthesis of 1,2-diaxially chiral triarylpyranones **29** via an NHC-catalyzed (3 + 3) annulation [29]. A broad scope was demonstrated, comprising more than 50 diversely substituted compounds (Scheme 10).

Wong, Zhao, and co-workers disclosed the intriguing formation of bridged biaryls featuring eight-membered lactone rings **32**

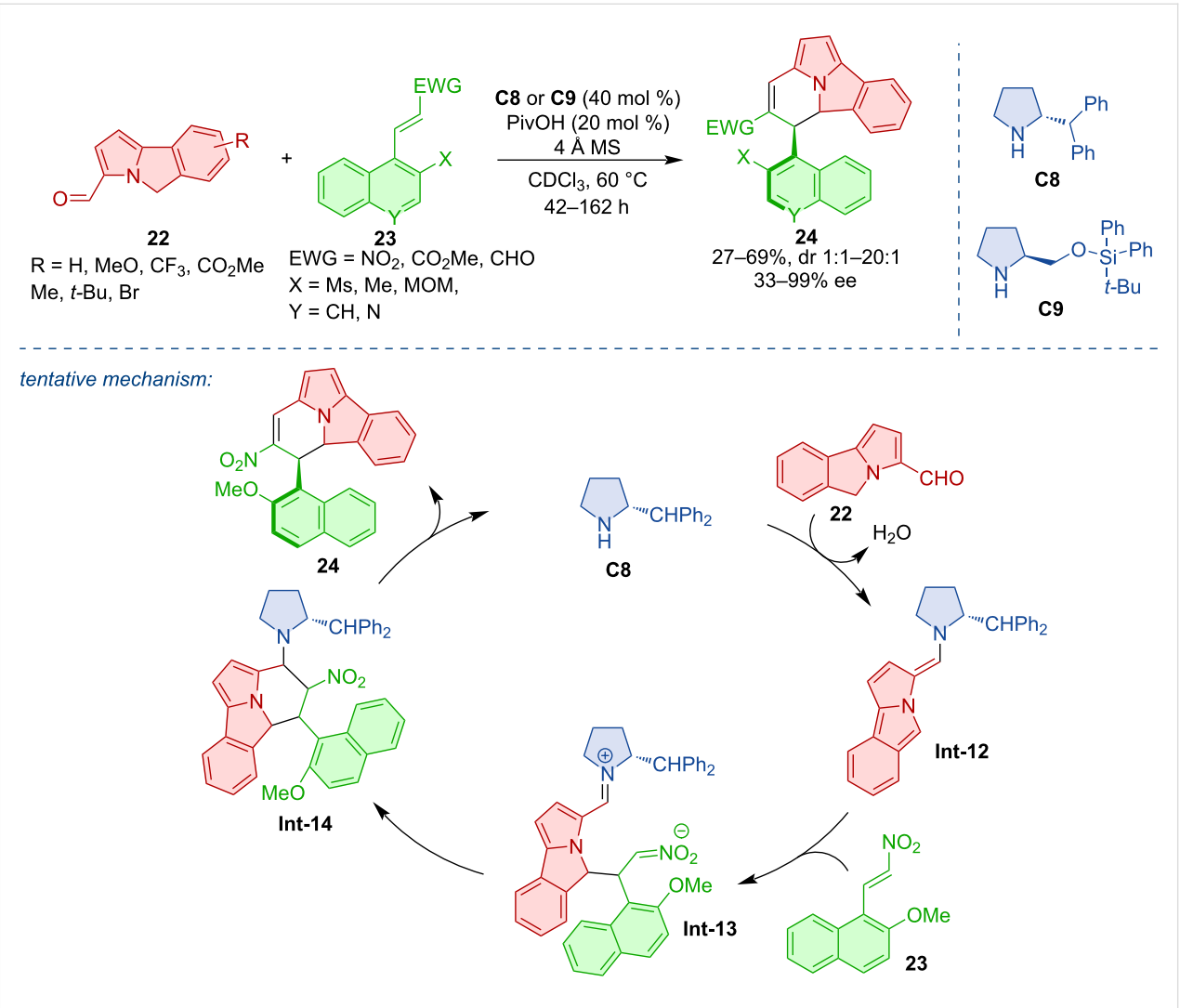

Scheme 8: Atroposelective formation of C(sp^2)–C(sp^3) axially chiral compounds.

[30]. This serendipitously discovered transformation relies on the catalysis with azolium precatalyst **C12** (Scheme 11a). The reaction also allowed the synthesis of indol-derived bridged biaryls **35** (Scheme 11b). The proposed mechanism, supported by DFT calculations, comprises propargylic substitution towards **Int-20** with NHC-derived enolate **Int-19** followed by lactonization to **Int-21** and **Int-22** (Scheme 11c).

Chi and co-workers showed that desymmetrization of urazoles can lead to axially chiral derivatives [31]. The NHC-catalyzed (3 + 2) annulation between α,β-unsaturated aldehydes **36** and urazoles **37** generates atropoisomers **38** with a C–N stereogenic axis (Scheme 12).

Wei, Du, and co-workers developed an atroposelective formal (3 + 3) annulation of 4-nitrophenyl 3-arylpropiolates **39** with 2-sulfonamidoindolines **40** [32]. The NHC catalyst derived from triazolium salt **C14** afforded the best results in terms of chemical yields as well as enantioselectivities (Scheme 13).

Axially chiral compounds with an N–N stereogenic axis can be synthesized by an NHC-catalyzed (3 + 3) annulation [33]. The key feature of this transformation is the cycloaddition of α,β-unsaturated azolium intermediates with thioureas. In this way, a range of diversely substituted N–N axially chiral pyrroles and indoles **44** are obtained (Scheme 14).

Zhu and co-workers developed a method for the atroposelective formation of arenes **48** by an NHC-catalyzed formal (4 + 2) cycloaddition [34]. The triazolium pre-catalyst (*R,S*)-**C11** was the most efficient in providing a range of biaryls in high yields and enantiomeric purities. The reaction was initiated by the formation of acylazolium intermediate **Int-24** that underwent a 1,6-addition with the enol form of the carbonyl substrate to give

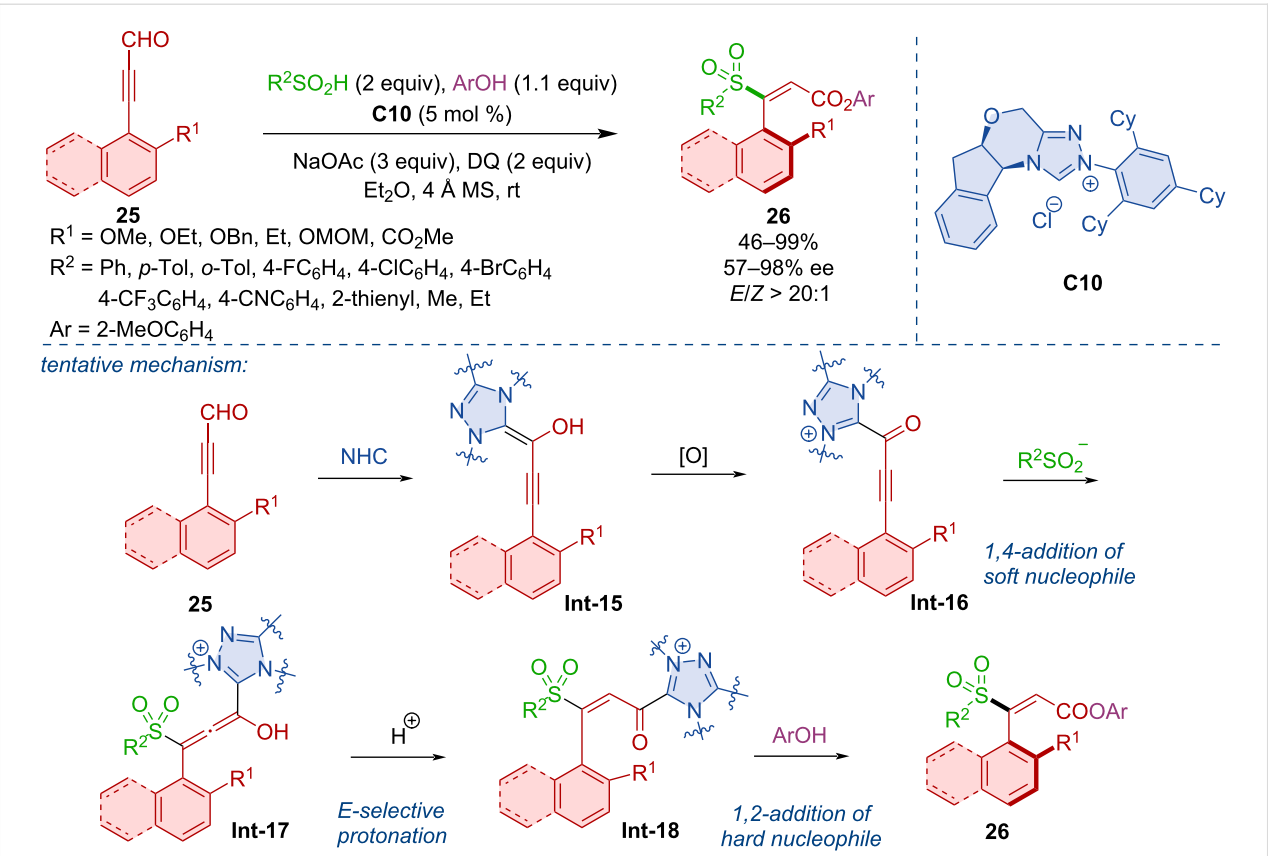

Scheme 9: NHC-catalyzed synthesis of axially chiral styrenes **26**.

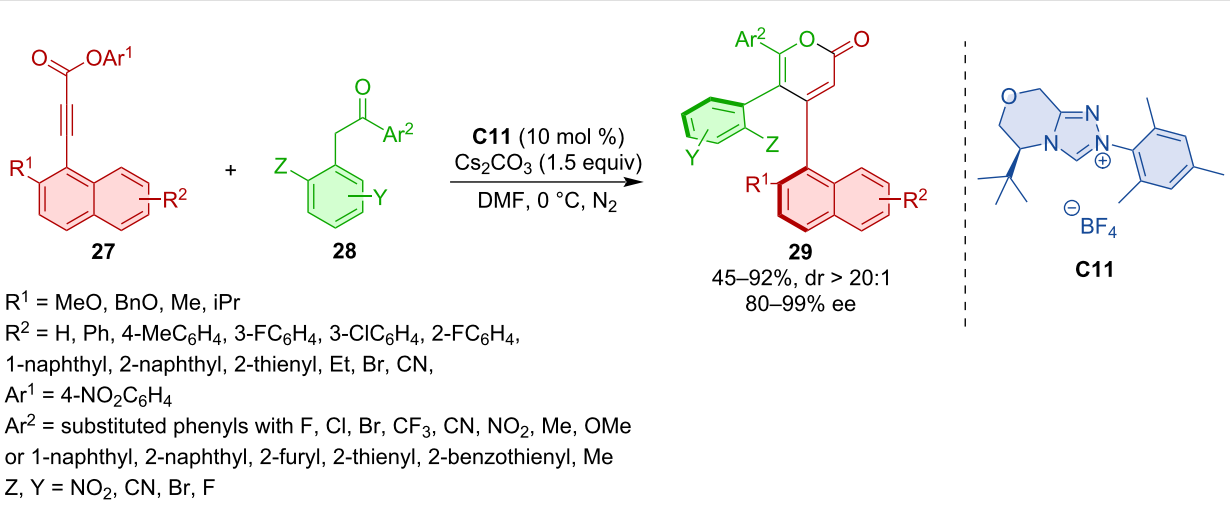

Scheme 10: NHC-catalyzed synthesis of biaxial chiral pyranones.

Int-25. Cyclization was realized via an intramolecular aldol reaction to **Int-26** (Scheme 15).

Ye and co-workers developed atroposelective formation of benzothiophene-fused biaryls via formal (4 + 2) annulation [35]. The NHC catalyst **C12** was the most efficient for realizing the de novo formation of a new aryl ring within the newly formed axially chiral biaryl **51** from enals **49** and 2-benzylbenzothiophene- or benzofuran-3-carbaldehydes **50** (Scheme 16).

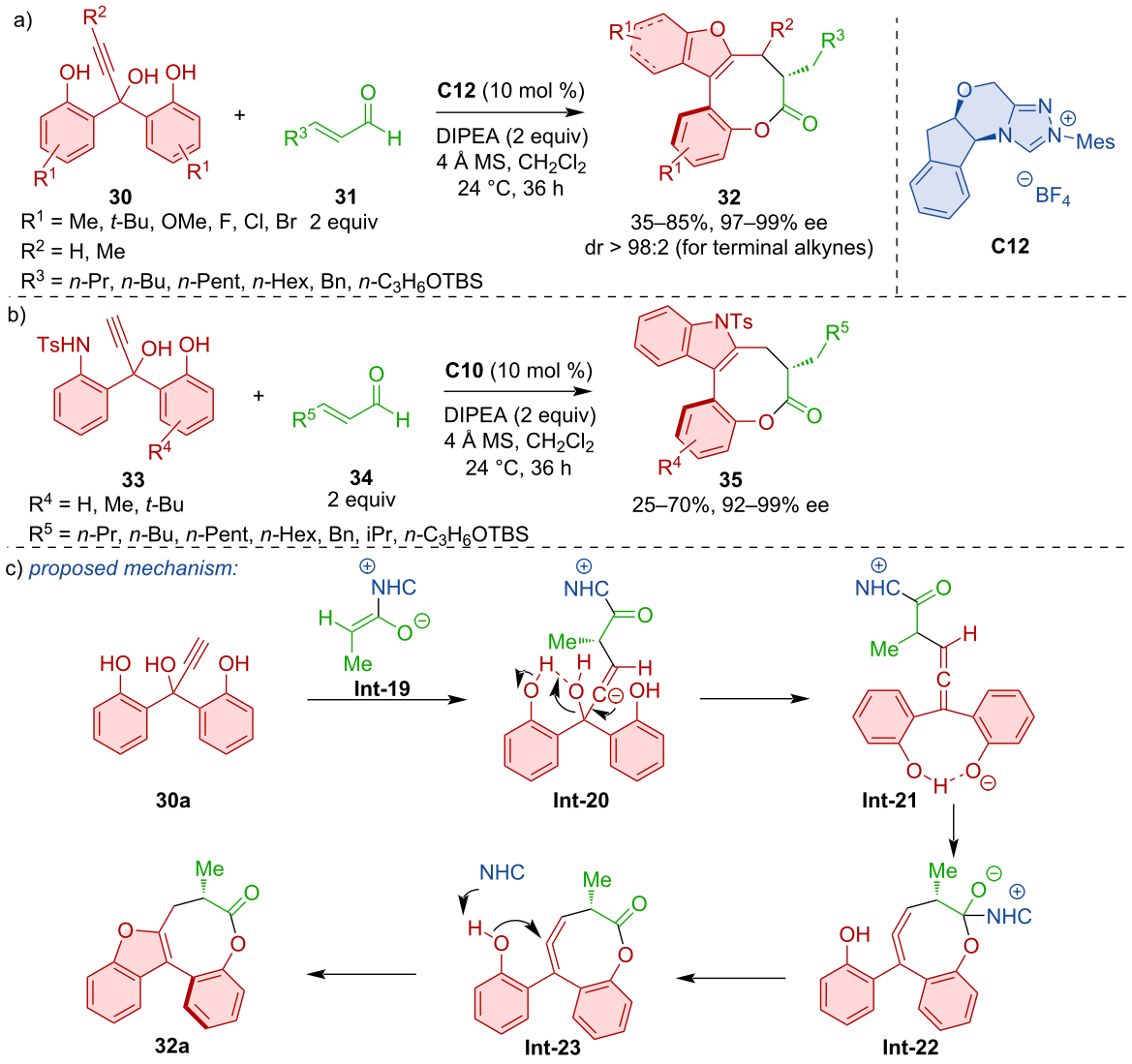

Scheme 11: Formation of bridged biaryls with eight-membered lactones.

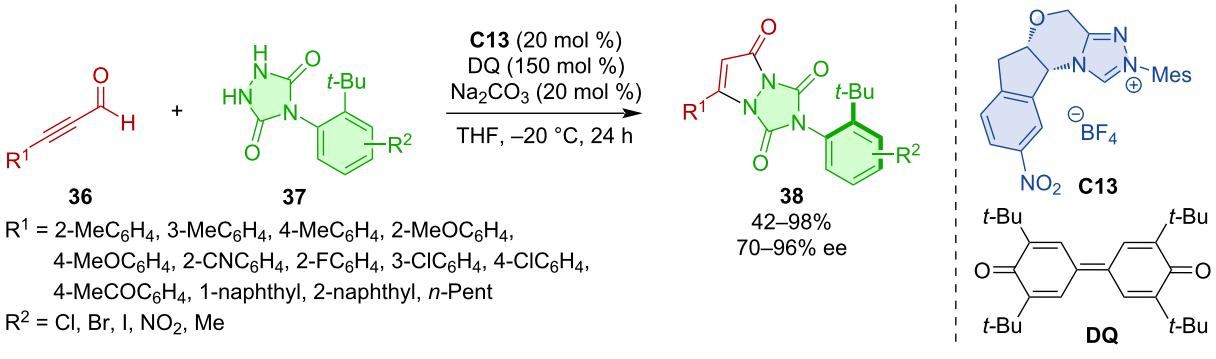

Scheme 12: The NHC-catalyzed (3 + 2) annulation of urazoles **37** and ynals **36**.

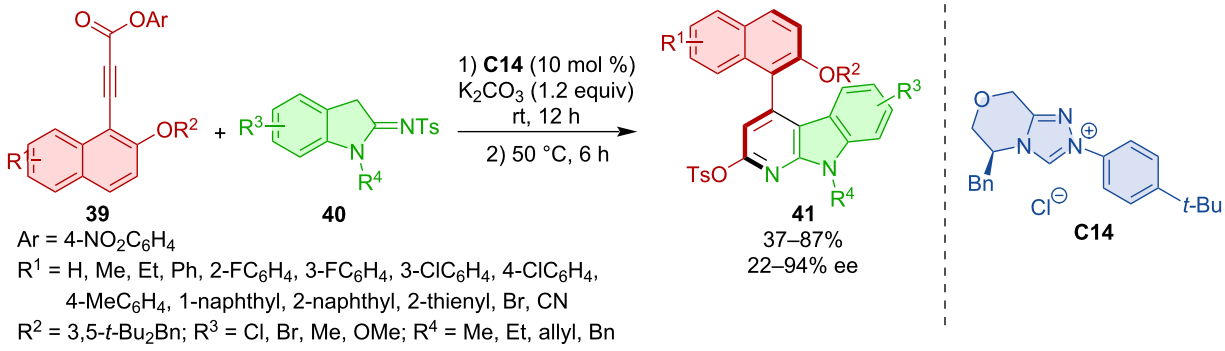

Scheme 13: NHC-catalyzed synthesis of axially chiral 4-aryl α-carbolines **41**.

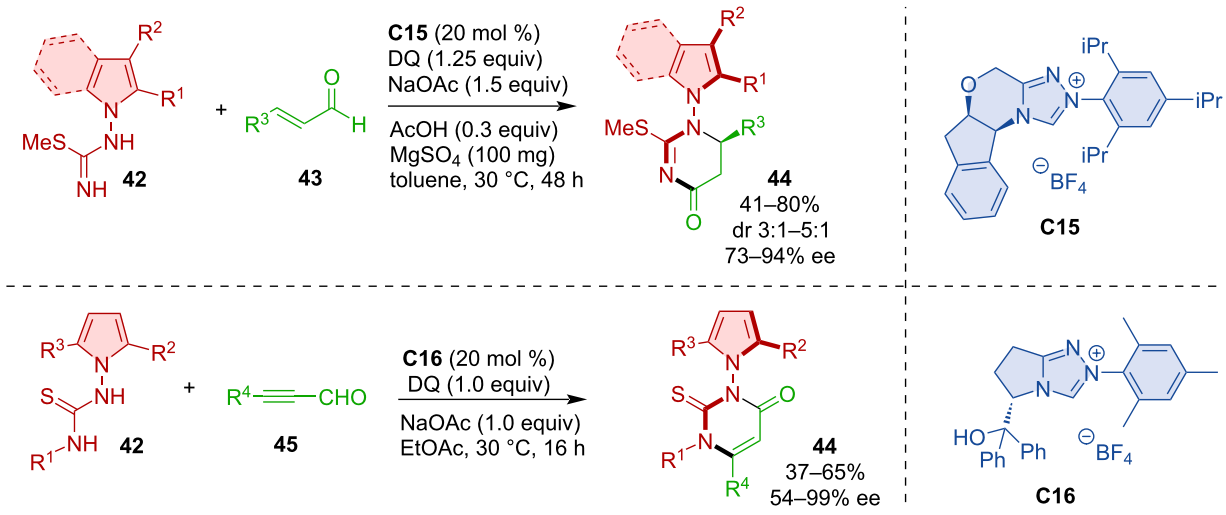

Scheme 14: NHC-catalyzed construction of N–N-axially chiral pyrroles and indoles.

Another demonstration of the atroposelective formation of compounds with a C–N stereogenic axis was developed by Jindal, Mukherjee, Biju, and co-workers [36]. The authors developed an NHC-catalyzed desymmetrization of *N*-aryl maleimides **53**, which afforded a range of axially chiral *N*-aryl succinimides **54**. The tentative mechanism comprises the formation of the Breslow intermediate **Int-31** from the catalyst carbene and aldehyde **52**, which then adds to the electron-deficient double bond of maleimide giving rise to **Int-32** (Scheme 17).

Chi and co-workers developed an atroposelective deracemization of biaryl hydroxy aldehydes **55a–k** [37]. NHC catalyst **C18** afforded a range of axially chiral benzonitriles **56a–k** in high yield and enantiomeric purities (Scheme 18). The reaction likely proceeds via the initial formation of racemic imines, which is followed by the formation of aza-Breslow-type intermediates with the chiral NHC-catalyst and subsequent deprotonation toward the nitrile product.

Zhang, Wang, Ye, and co-workers utilized NHC-catalysis for the atroposelective synthesis of axially chiral diaryl ethers **59** and **61** [38]. This transformation was realized via desymmetrization of prochiral 2-aryloxyisophthalaldehydes **57a**,**b** with a range of aliphatic and aromatic alcohols **58a–g**, as well as heteroaromatic amines **60** (Scheme 19). Chiral diaryl ethers of this type received increased attention lately. Biju, Gao, Zhang, and Zeng groups all reported high degrees of yields and enantioselectivities in similar desymmetrization reactions [39-42].

The dynamic kinetic resolution (DKR) of racemic 2-arylbenzaldehydes **62** with α-bromoenals **63** led to axially chiral prod-

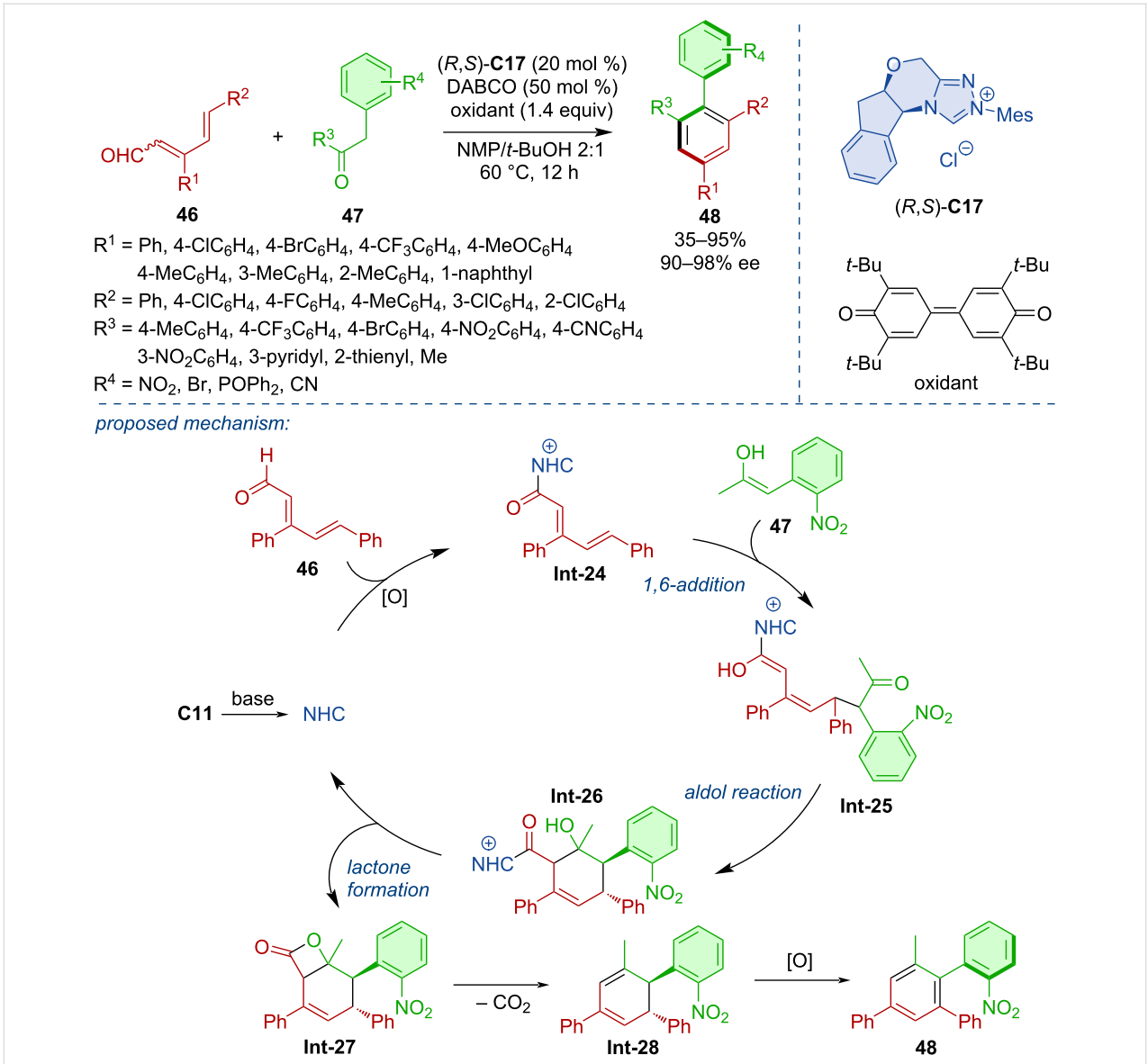

Scheme 15: NHC-catalyzed oxidative Michael–aldol cascade.

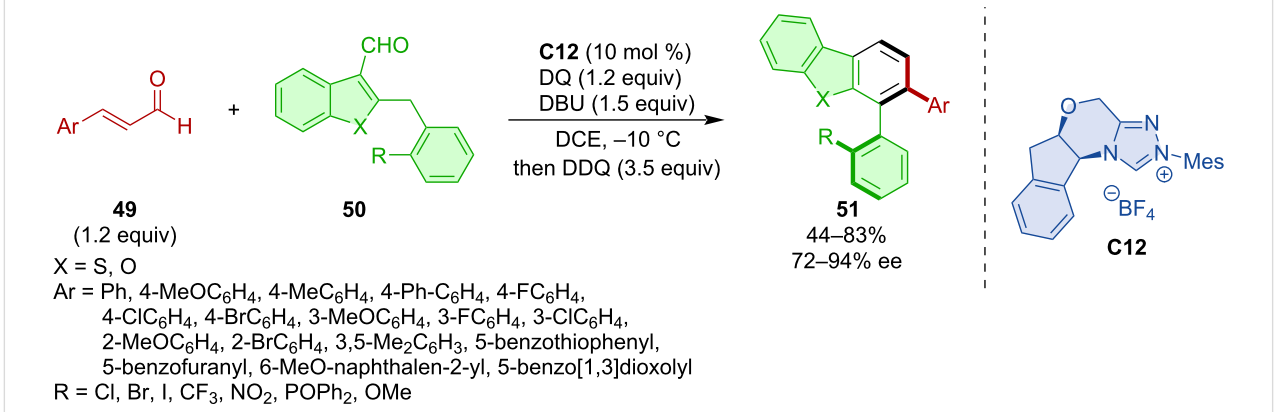

Scheme 16: NHC-catalyzed (4 + 2) annulation for the synthesis of benzothiophene-fused biaryls.

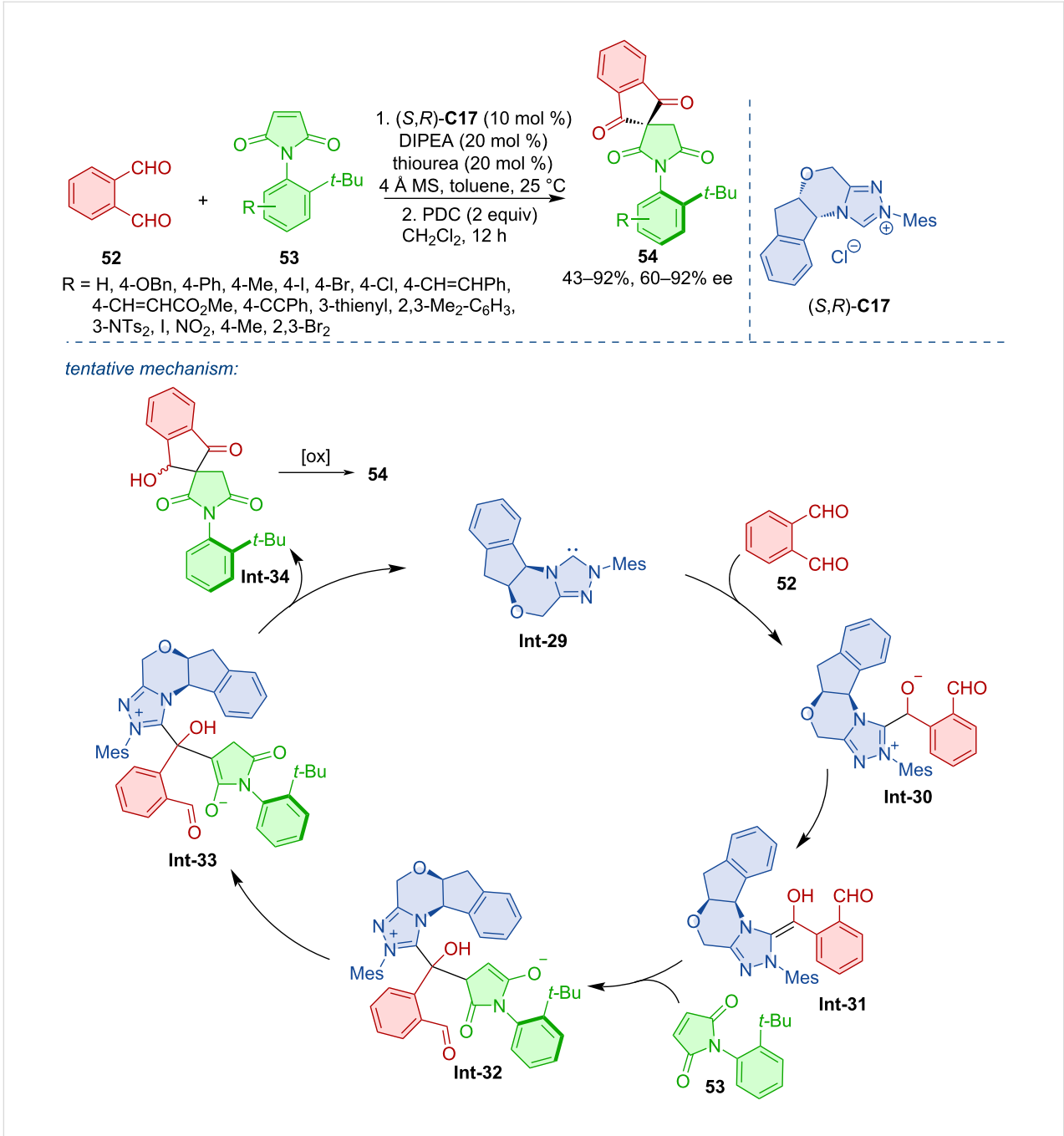

Scheme 17: NHC-catalyzed desymmetrization of *N*-aryl maleimides.

ucts **64** [43]. Triazolium salt **C20** as an NHC pre-catalyst was the most efficient for achieving high yields and enantiomeric purities in this process (Scheme 20).

Chiral Brønsted acid-catalyzed atroposelective reactions

Chiral Brønsted acids became prominent organocatalysts that also promote the syntheses of axially chiral compounds. The amination of aromatic biaryls **65a**–**g** with dibenzylazodicarboxylate catalyzed by organocatalyst **C21** was studied in 2019 (Scheme 21) [44]. A broad range of aniline and phenol substrates was studied. The best results were accomplished with products containing a Boc-protected amino group on the aniline or 2-aminonaphthalene frame (**66a**–**g**), achieving very good yields and excellent enantioselectivities. Compound **66d** was incorporated into a thiourea organocatalyst framework and successfully tested in kinetic resolution with 73% enantioselectivity.

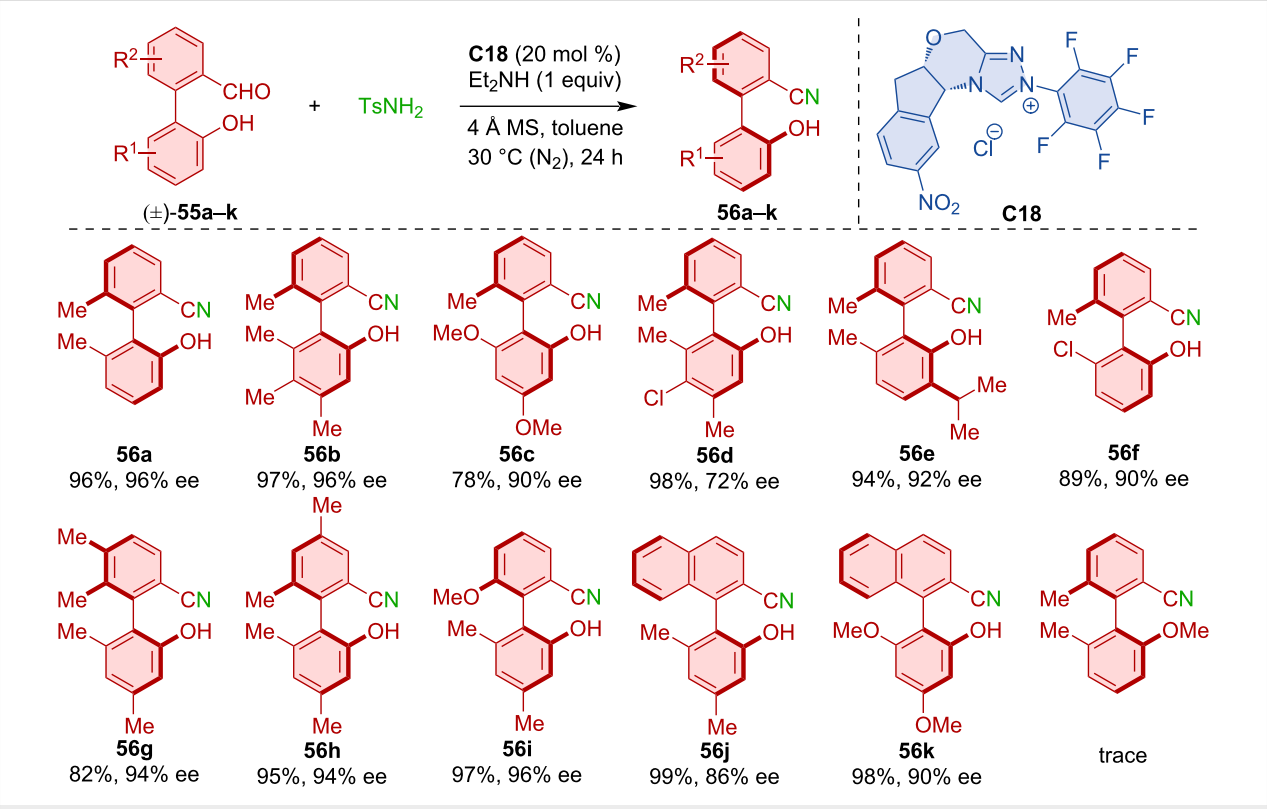

Scheme 18: NHC-catalyzed deracemization of biaryl hydroxy aldehydes **55a–k** into axially chiral benzonitriles **56a–k**.

The chiral phosphoric acid (CPA) (*R*)-**C22** was used to catalyze the formation of a C–N chiral axis in the axially chiral product **68** from biarylamines **67** and di-*tert*-butyl azodicarboxylate (Scheme 22) [45]. An added benefit to these products is that they possess an intramolecular hydrogen bond acting as a stabilizing factor and products **68** were prepared in good to very good yields and excellent enantiomeric purities. Based on the authors' design, previous findings from the literature, and experimental results, a reaction mechanism was proposed [46]. Hydrogen bonding as well as π–π interaction with the catalyst (*R*)-**C22** activates both substrates in the stable intermediate **Int-35**. This stabilized state ensures the concerted control of enantioselectivity during the nucleophilic addition, and the subsequent aromatization completes central-to-axial chirality conversion delivering products **68**.

Dynamic kinetic resolution of naphthylindoles **69** was performed by reaction with bulky electrophiles such as azodicarboxylates **70** or *o*-hydroxybenzyl alcohols **72** (Scheme 23) [47]. These reactions were catalyzed by both BINOL-derived (TRIP) CPA (*S*)-**C23** and SPINOL-derived CPA (*S*)-**C24**, providing axially chiral products **71** and **73**, respectively. Control experiments showed the importance of the N–H group on the indole ring and the presence of both carboxylate groups in the azodicarboxylate as crucial to forming hydrogen bonds with the organocatalyst. Benzylation of this nitrogen or substitution of just one of the carboxylate groups led to no product being observed. A series of naphthylindoles **71** was tested for potential biological activity and showed promising results in one case, providing high cytotoxicity toward the MCF-7 cancer cell line. The stable axial chirality of the products **71** and **73** was confirmed by calculations of the rotational barriers ranging from 30.2 to 46.3 kcal/mol.

Kinetic resolution by amino group protection of biaryls (*R,S*)-**74a–r** with azodicarboxylate catalyzed by CPA (*R*)-**C23** provided axially chiral unprotected biaryls (*S*)-**74a–r** and axially chiral protected biaryls (*R*)-**75a–r** (Scheme 24) [48]. Consistently high enantioselectivities and yields were reported with various binaphthyl and biphenyl substrates. Control experiments revealed the importance of hydrogen on the amino or hydroxy groups, supposedly through the bonding with the catalyst. Substitution of these groups or their hydrogens led to either halted reaction or significantly reduced enantiopurity of the products.

Expanding the scope of available azodicarboxylates **77** and aromatic amines **76** in the C–H amination reaction with CPA **C25**, the authors were able to prepare axially chiral *para*-amination products **78** (Scheme 25) [49]. Such amination products **78**

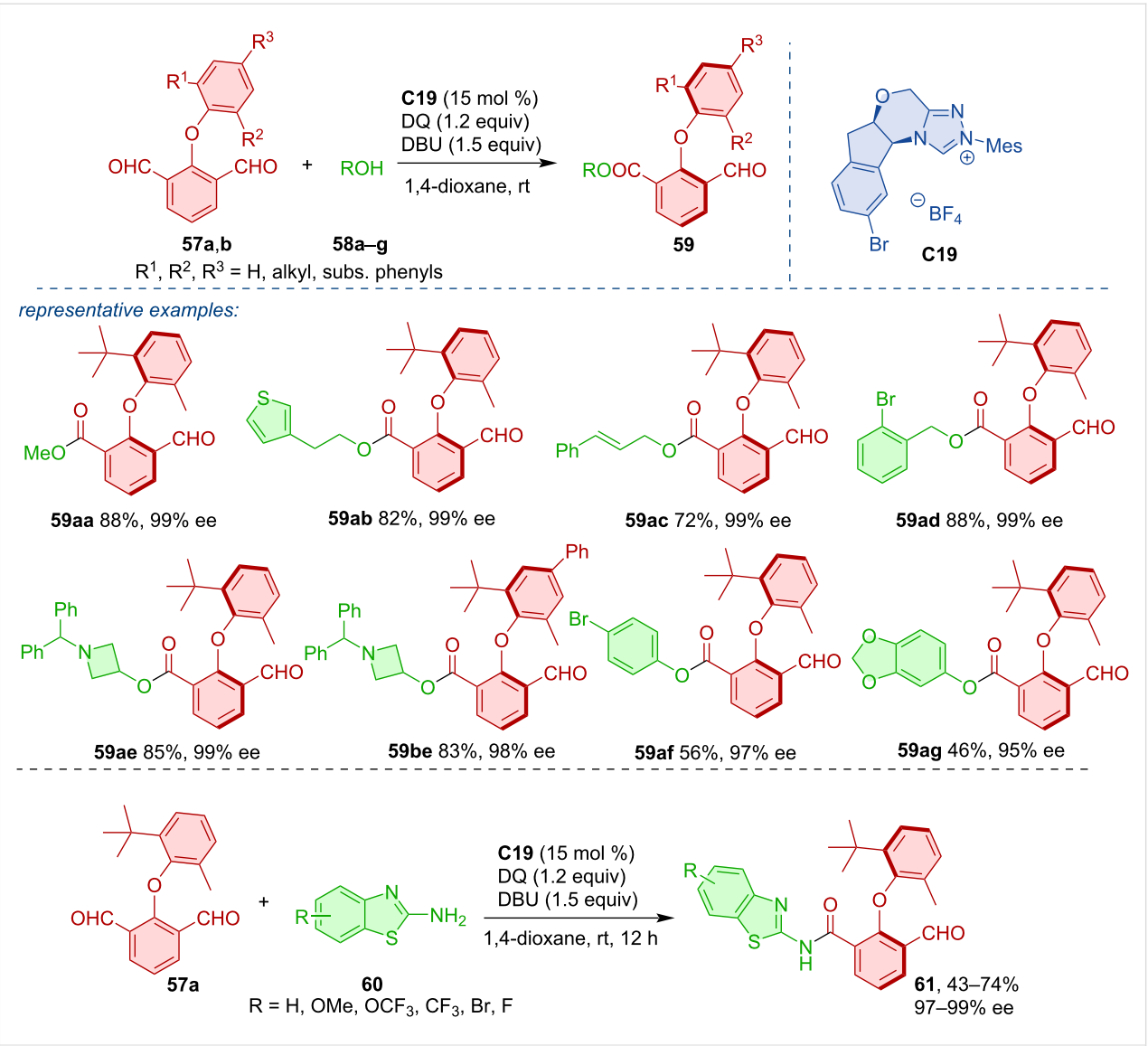

Scheme 19: NHC-catalyzed desymmetrization of 2-aryloxyisophthalaldehydes.

were prepared with high levels of yields and showed remarkable enantiomeric purities. Interestingly, when a phenyl substituent was present on the amino group of the 1,3-benzenediamine, lower yields were reported, and substituting the amino group in position 3 for an *N*-methylamino or *N*,*N*-dimethylamino group led to a reduction in the enantioselectivity.

Shao et al. developed the first organocatalyzed atroposelective Friedländer heteroannulation [50]. The SPINOL-derived chiral phosphoric acid **C26** catalyzed the formation of axially chiral products **81** from diarylketones **79a–f** and ketoesters **80a–c** (Scheme 26). The substrate scope contained a broad range of substituents, including electron-donor groups and whole benzene rings. The authors were able to separate the enamine intermediate formed from diarylketone and ketoester.

Later, the BINOL-derived (TRIP) CPA (*R*)-**C23** was used in a similar Friedländer reaction [51]. Acetylacetone was utilized with diarylketones **82** containing arylethyl chains to form axially chiral products **83** (Scheme 27). The reaction mechanism proposed by the authors was analogous to that of the aforementioned atroposelective Friedländer reaction. Outstanding yields and enantioselectivities were accomplished during the substrate scope screening as well as in a model gram-scale reaction (83%, 91% ee).

Annulation of biaryl ketones **84** with cyclohexanones **85** mediated by the second-generation chiral phosphoric acid **C26** led to the formation of tetrahydroacridines **86** (Scheme 28) [52]. This Friedländer reaction provided products **86** in moderate to good yields with consistently high enantiomeric purities and high dia-

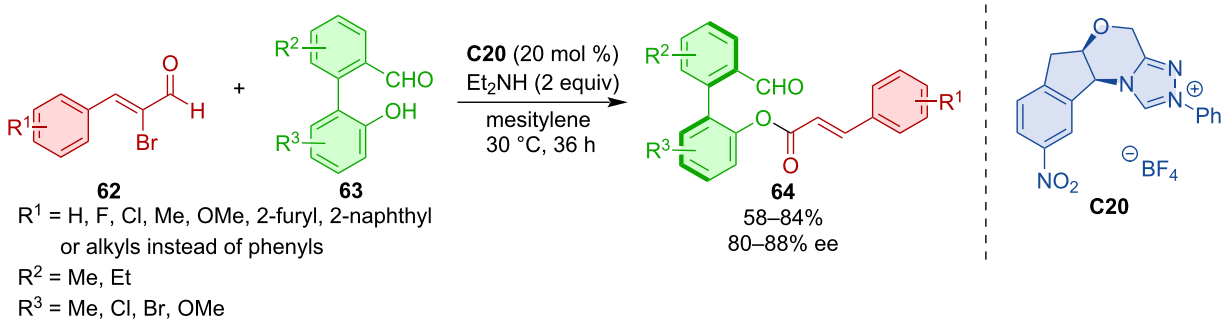

Scheme 20: NHC-catalyzed DKR of 2-arylbenzaldehydes **62**.

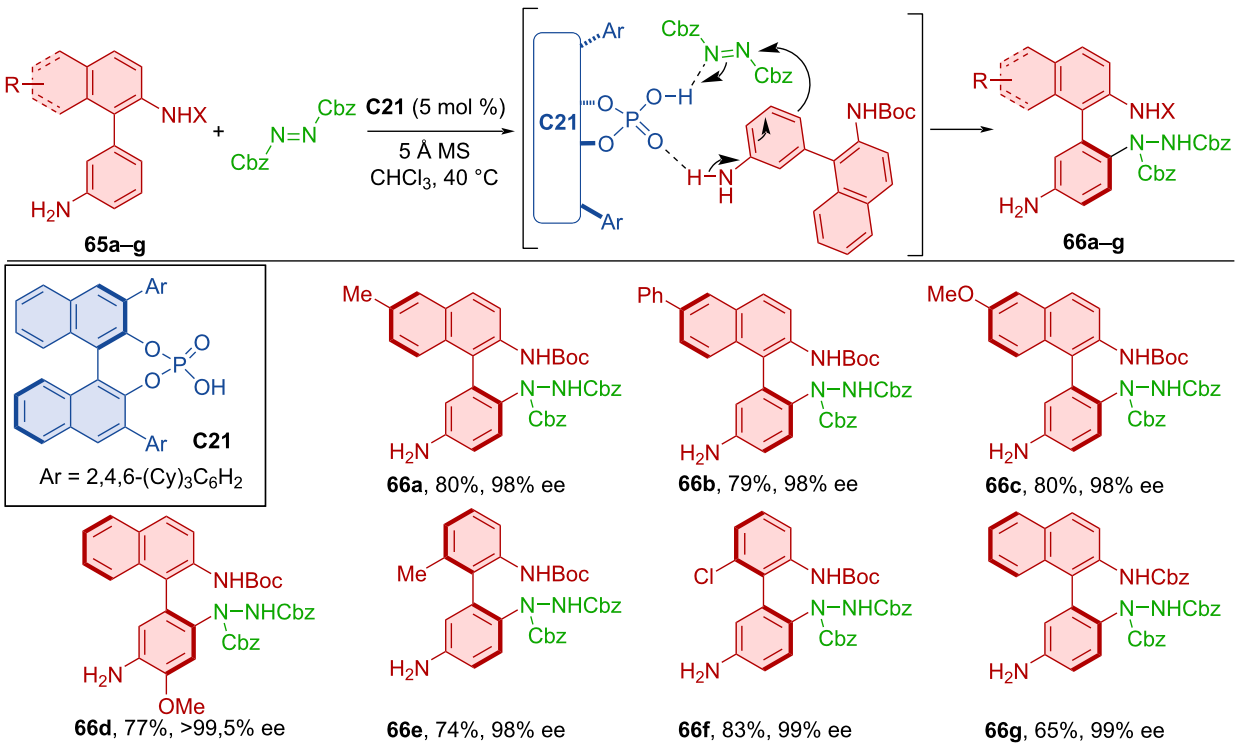

Scheme 21: Atroposelective biaryl amination.

stereomeric ratios in a couple of cases. On a 1 mmol scale with reduced catalyst loading the reaction proceeded in a similar fashion with good yield and enantioselectivity (70%, 89% ee).

The Povarov reaction of imines **87a–h** and alkenylindoles **88a–i** catalyzed by CPA (*R*)-**C23** was utilized to give asymmetric products **89** and their subsequent oxidation with DDQ provided axially chiral quinolines **90** (Scheme 29) [53]. Good retention of the stereoinformation acquired in the first transformation, moderate to excellent yields and consistently high degrees of enantiomeric purity were achieved. The reaction could also be carried out in a one-pot fashion with comparable results and without significant variation from the two-step procedure.

Utilization of the Povarov reaction and subsequent oxidation by DDQ was also done by Wang et al. in 2020 [54]. In situ-formed imines from anilines **91** and benzaldehydes **92** were reacted with alkenyl-2-naphthols **93** in the presence of CPA (*R*)-**C24** to form asymmetric products **94** and eventually axially chiral tetrahydroquinolines **95** through oxidation (Scheme 30). This approach led to the products **95** in high yields and enantiomeric purities. The tosyl group in the product was transformed

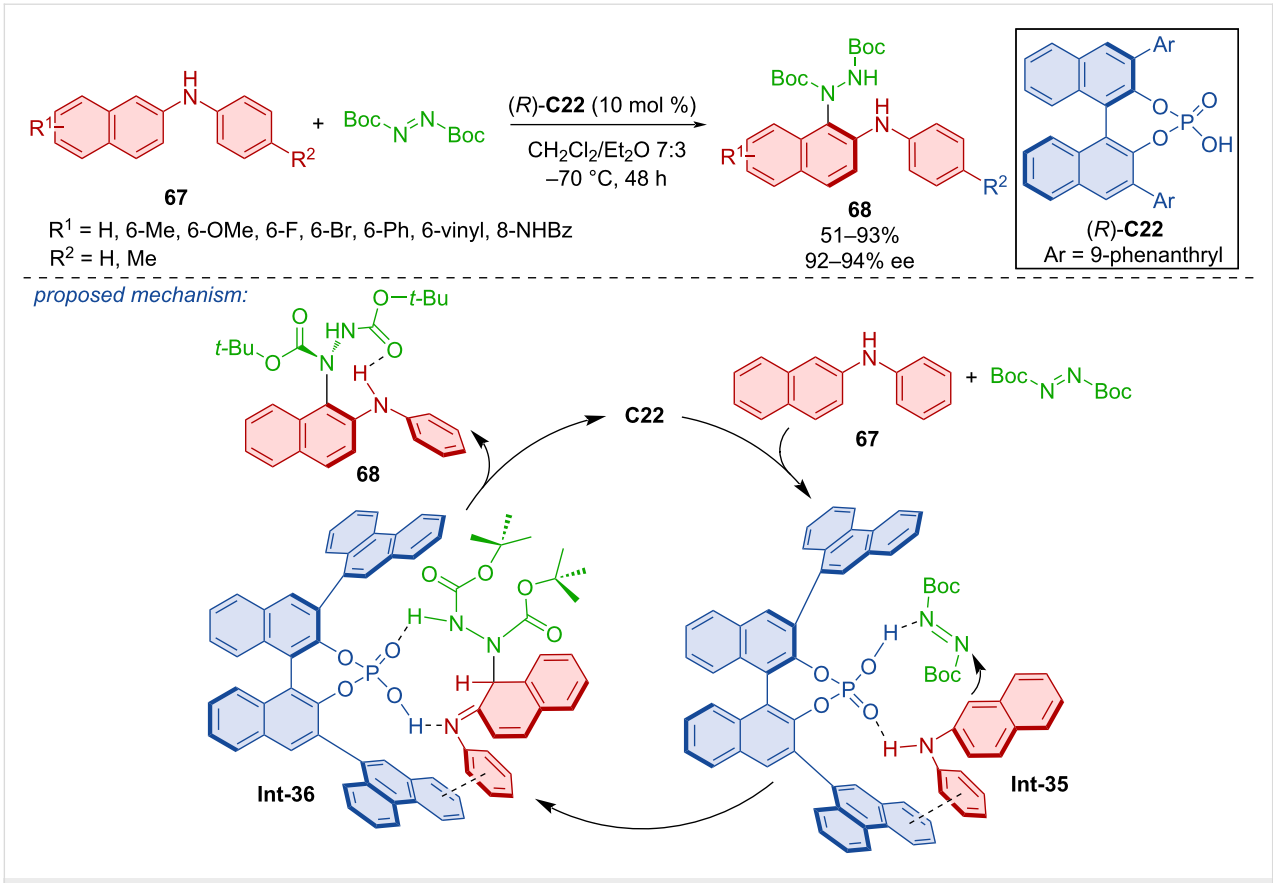

Scheme 22: CPA-catalyzed atroposelective amination of 2-anilinonaphthalenes.

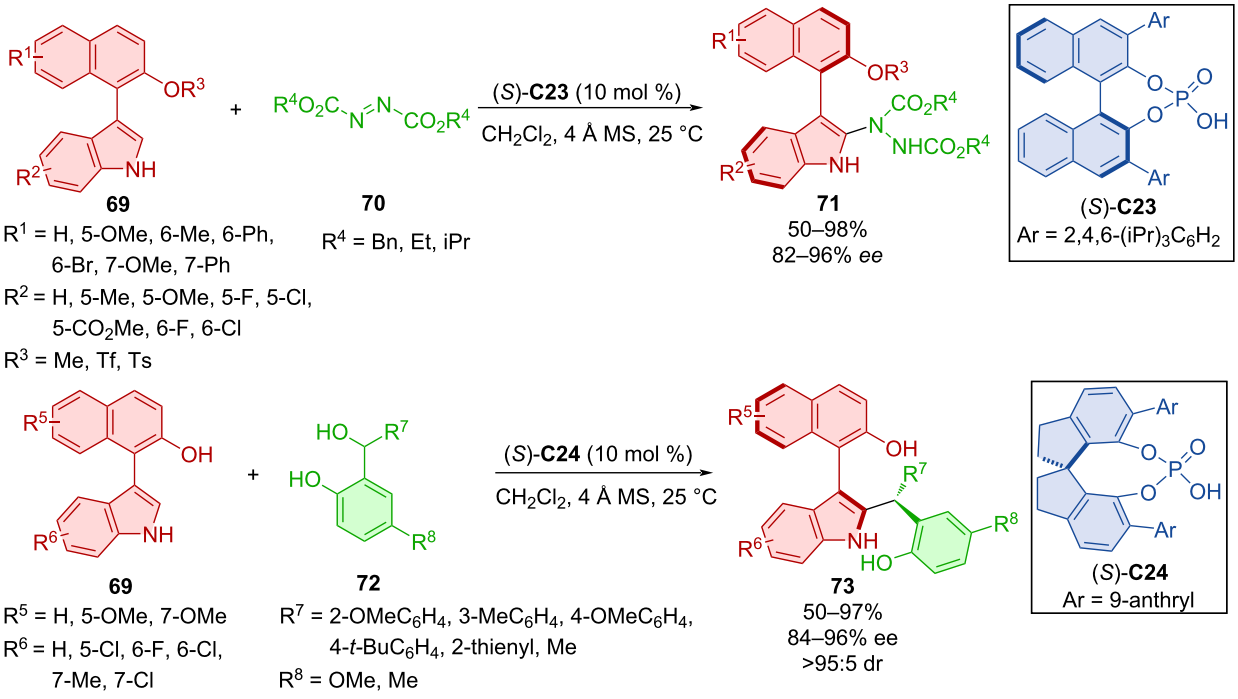

Scheme 23: Atroposelective DKR of naphthylindoles.

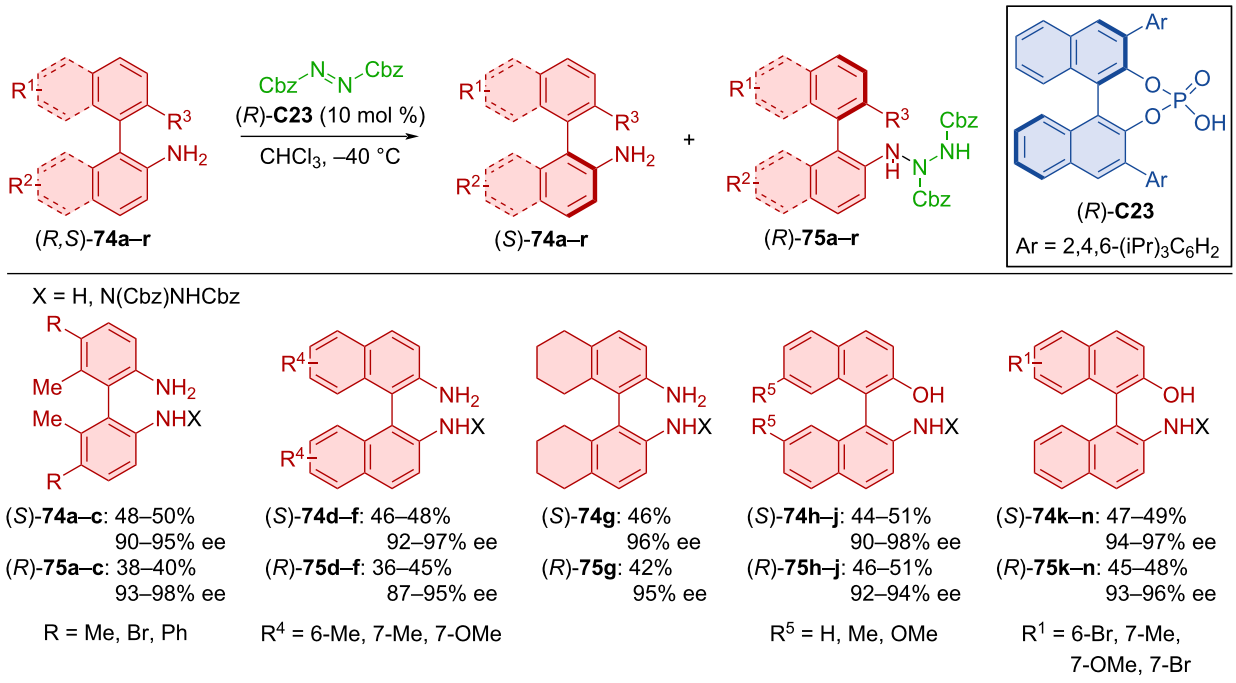

Scheme 24: CPA-catalyzed kinetic resolution of binaphthylamines.

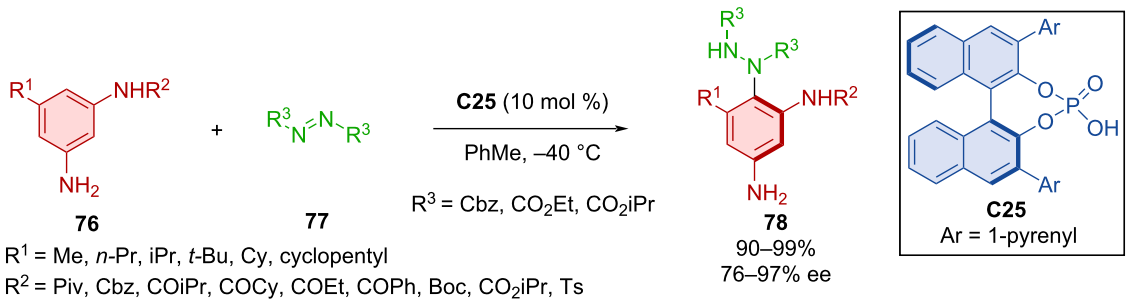

Scheme 25: Atroposelective amination of aromatic amines with diazodicarboxylates.

through a series of reactions to a diphenylphosphine group and used as a ligand for Pd-catalyzed reactions.

De novo ring formation was utilized in the synthesis of N–N axially chiral *N*-pyrrolylindoles **98** and *N*-pyrrolylpyrroles **100** with the help of CPA **C27** (Scheme 31) [55]. Starting from either indoles **96** or pyrroles **99** and 1,4 diketones **97**, respectively, the authors were able to achieve very good to near-perfect yields with consistently high enantioselectivities. Configurational stabilities of the products **98** and **100** were explored in toluene at 110 °C. Rotational barriers were calculated to be 47.7 and 52.2 kcal/mol, respectively, which suggests a high degree of configurational stability. One-mmol-scale reactions provided the corresponding products in comparable yields and enantioselectivities (87–96%, 94–97% ee). Based on a previous report on the CPA-catalyzed Paal–Knorr reaction, a reaction pathway was proposed [56]. The first step is a CPA **C27**-catalyzed condensation giving rise to the imine intermediate followed by isomerization to the enamine stabilized by CPA. An enantioselective intramolecular cyclization followed by dehydration then afford the aromatic ring and desired product **98**.

Concurrently, Gao et al. utilized a similar Paal–Knorr reaction for the synthesis of axially chiral biheteroaryls **103** (Scheme 32) [57]. In the majority of the experiments $Fe(OTf)_3$ was utilized as Lewis acid. The below-mentioned examples are only those, that did not require an additional co-catalyst containing transition metals but are purely of organocatalytic nature. In these ex-

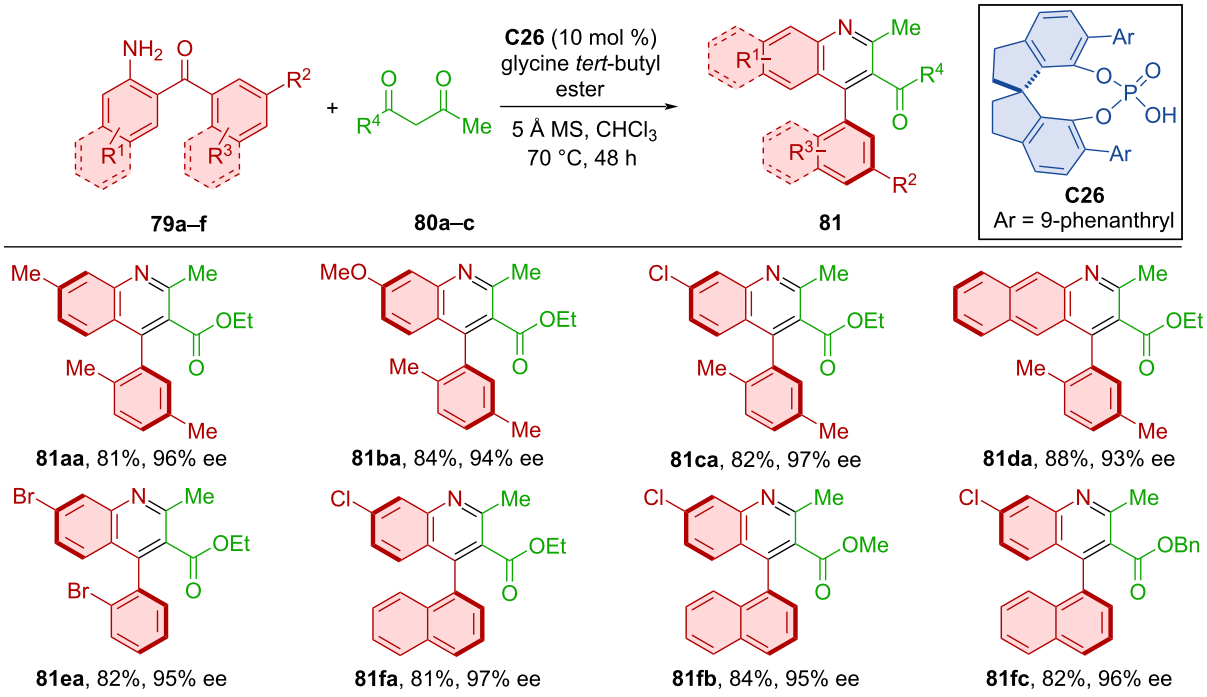

Scheme 26: Atroposelective Friedländer heteroannulation.

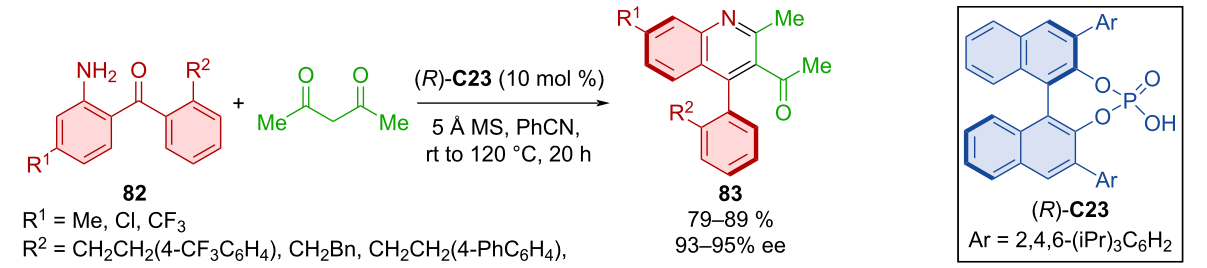

Scheme 27: CPA-catalyzed formation of axially chiral 4-arylquinolines.

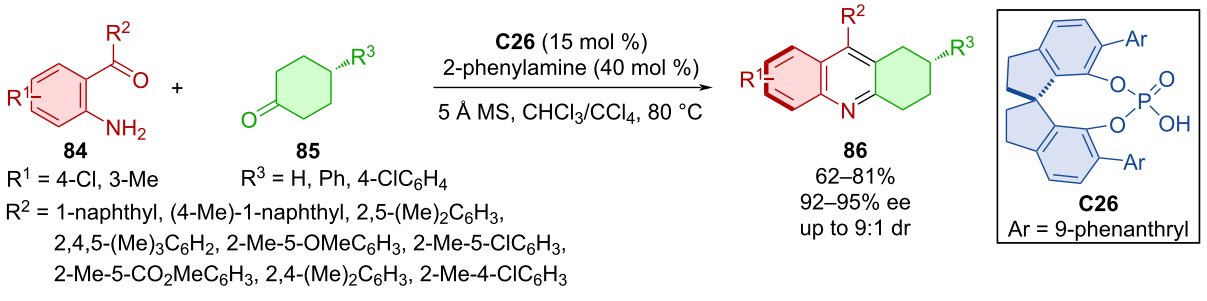

Scheme 28: CPA-catalyzed Friedländer reaction of arylketones with cyclohexanones.

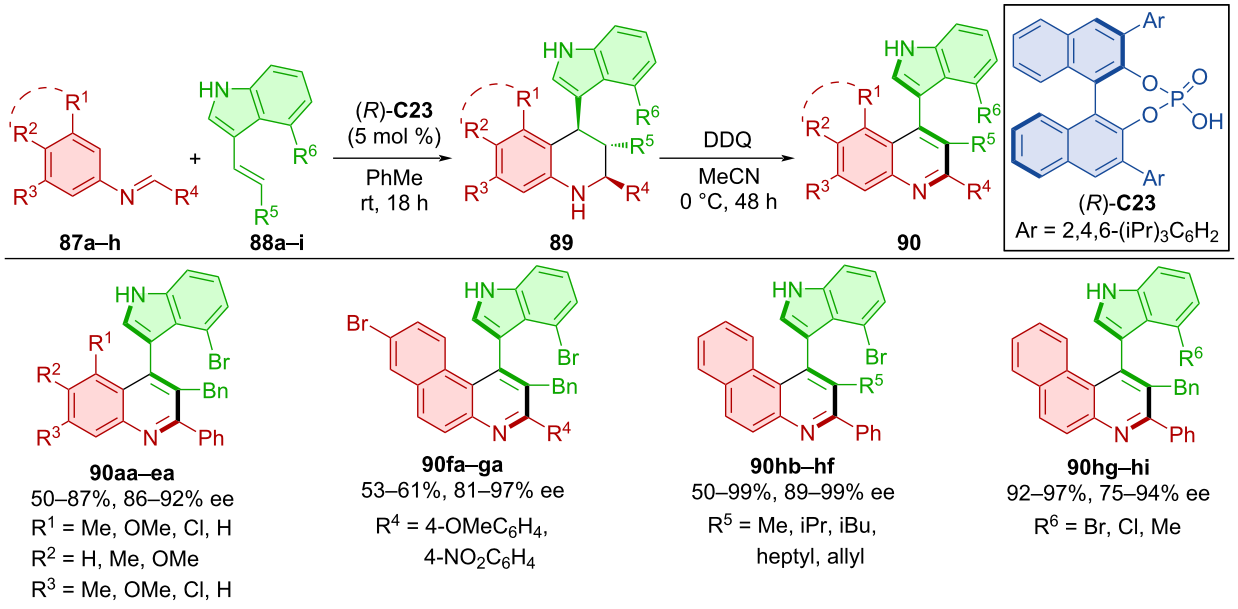

Scheme 29: CPA-catalyzed atroposelective Povarov reaction.

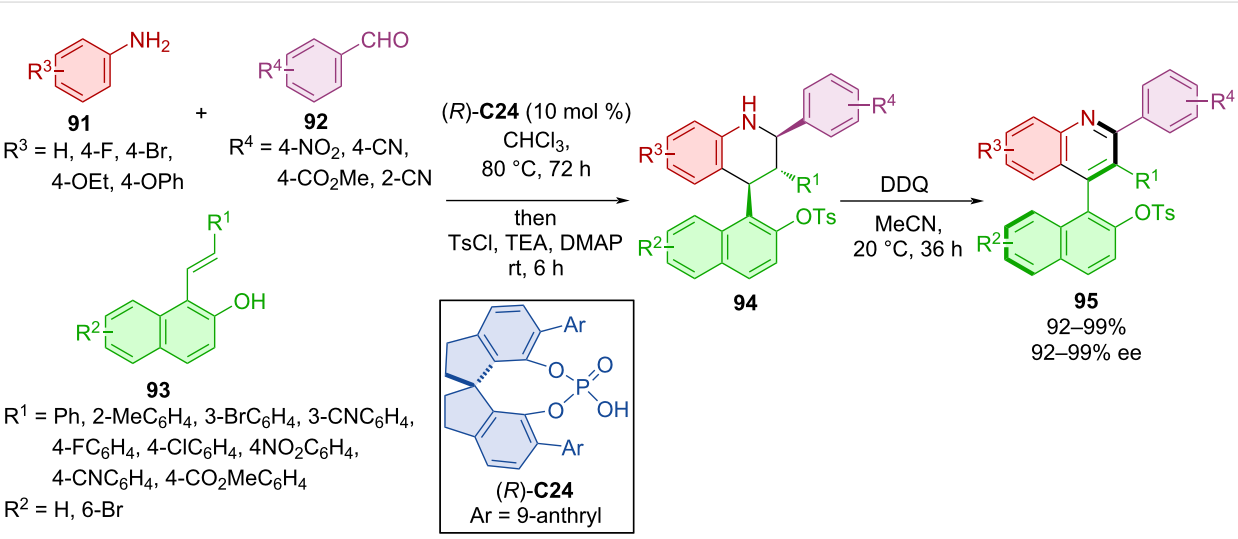

Scheme 30: Atroposelective CPA-catalyzed Povarov reaction.

periments, the chiral phosphoric acid **C28** catalyzed the reaction of aminopyrroles **101** and 1,4-diketones **102**. Under the optimized reaction conditions, the yields were good to excellent, and high levels of enantioselectivities were achieved. The products showed no thermal racemization at 150 °C, what was supported by a calculated high rotational barrier of 49.9 kcal/mol.

The usefulness of chiral phosphoric acids also shows in the atroposelective Pictet–Spengler reaction of *N*-arylindoles **104** with various aldehydes **105** (Scheme 33) [58]. Axially chiral products **106** were prepared in very high yields and exquisite enantiomeric purities. The presence of a methyl group in the aniline ring's *ortho* position proved to have a negative effect on the enantioselectivity, presumably due to the unfavorable steric interaction with the organocatalyst **C21**. A considerable drop in yield and enantioselectivity was also observed in the reaction with dibenzylaniline. Interactions with and steric effects of the CPA **C21** guiding the orientation of the substrates dictate the stereocontrol of the reaction.

The utilization of CPA (*R*)-**C23** in a dynamic kinetic resolution through a Pictet–Spengler reaction, enabled the preparation of

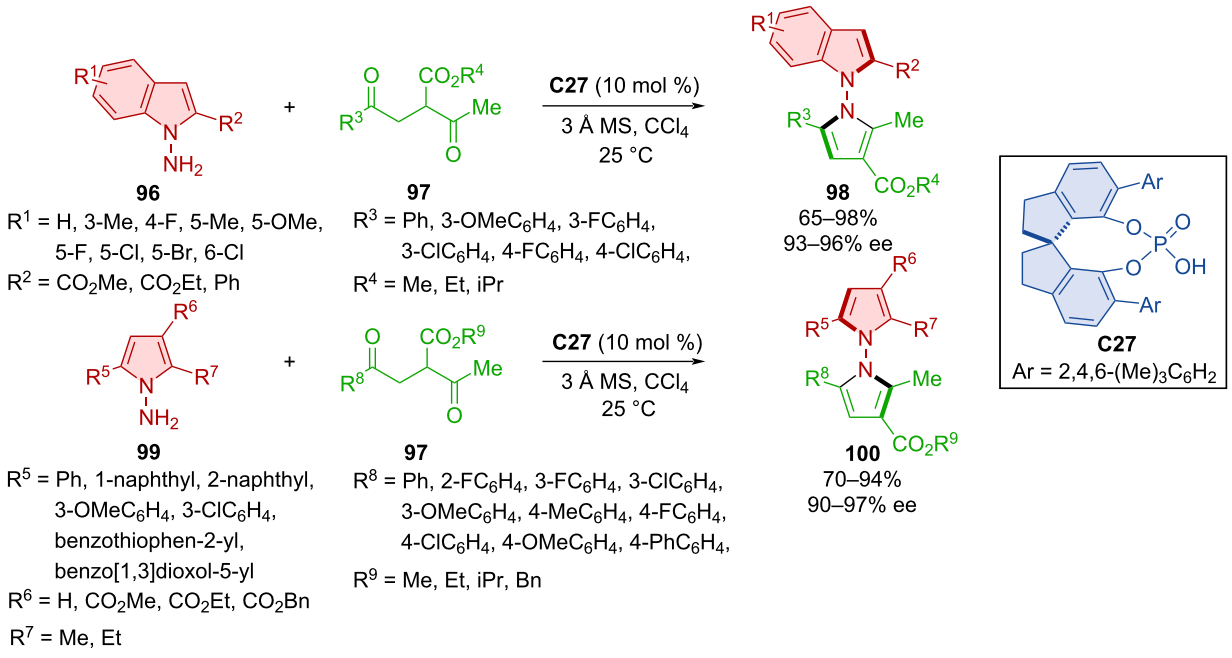

Scheme 31: Paal–Knorr formation of axially chiral *N*-pyrrolylindoles and *N*-pyrrolylpyrroles.

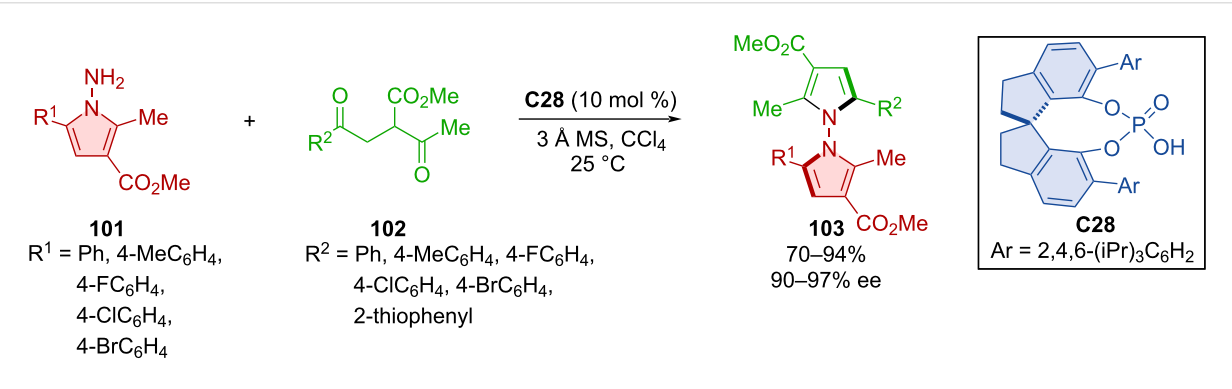

Scheme 32: Atroposelective Paal–Knorr reaction leading to *N*-pyrrolylpyrroles.

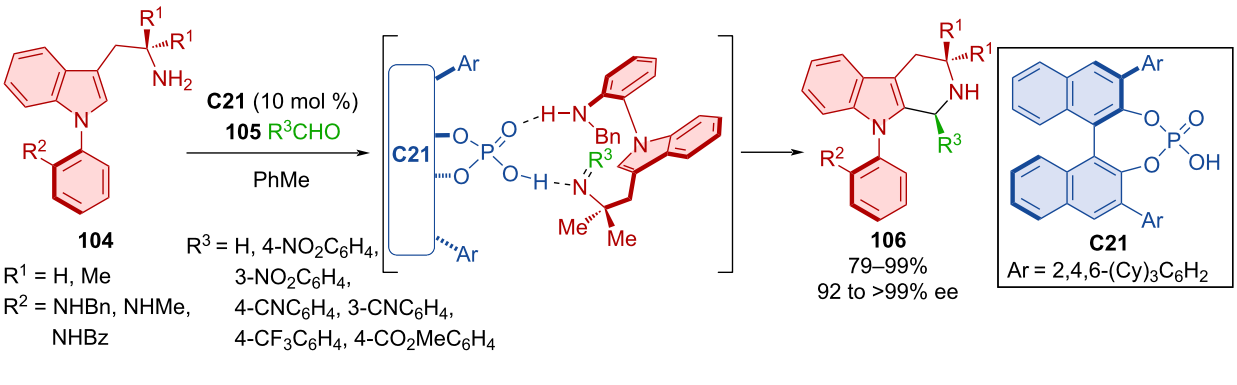

Scheme 33: Atroposelective Pictet–Spengler reaction of *N*-arylindoles with aldehydes.

axially chiral 8-aryltetrahydroisoquinolines **108** starting from aminobiaryl scaffolds **107** and paraformaldehyde (Scheme 34) [59]. For most substrates, excellent enantioselectivities and moderate to excellent yields were reported. However, the reaction did not tolerate a variety of substitutions on the amide group, probably because of its involvement in hydrogen bonding with the organocatalyst (*R*)-**C23**.

Expanding on earlier methodologies of Chen et al. [60,61] and Wang et al. [62] utilizing indole derivatives instead of β-naphthols, new atroposelective reactions of quinones and iminoquinones were developed [63]. The reaction of quinones with an ester group **109** and indoles with alkyl substituents **110** catalyzed by CPA **C29** provided products **112** with regioselectivity on the pyrrole ring of indole (Scheme 35). On the contrary, adding a hydroxy group to the benzene ring of indoles **111** and reacting them with tosyl-protected iminoquinone **109** with the help of CPA **C30** led to the shift in regioselectivity providing different axially chiral products **113**. All products were obtained with high degree of enantiomeric purity as well as significantly high yields. The CPA organocatalyst activates quinones with an acceptor hydrogen bond while indole acts as hydrogen-bond donor. On the other hand, a hydroxy group of hydroxyindole becomes a hydrogen donor and the iminoquinone nitrogen represents an acceptor to the hydrogen from the CPA, resulting in the regioselectivity change.

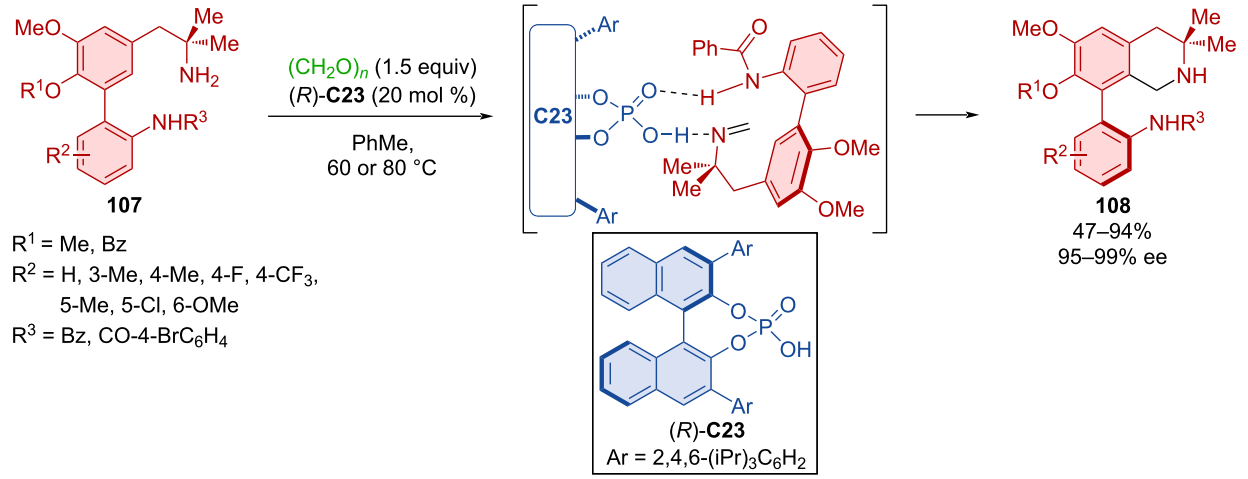

Scheme 34: Atroposelective Pictet–Spengler reaction leading to tetrahydroisoquinolin-8-ylanilines.

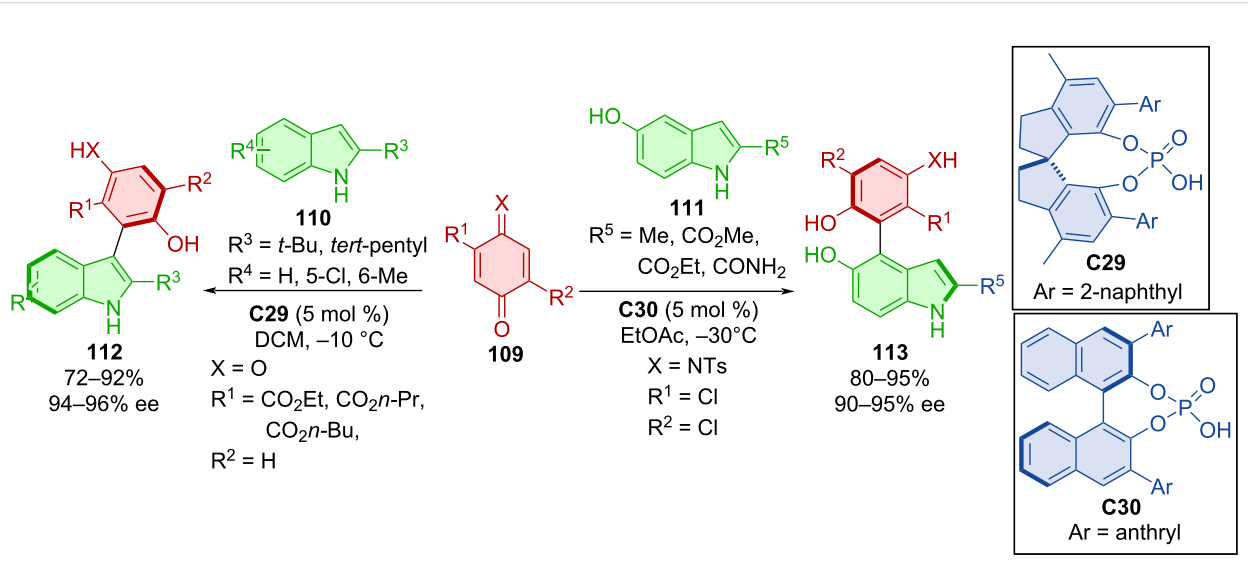

Scheme 35: Atroposelective formation of arylindoles.

Song et al. broadened the scope of usable substrates for the asymmetric arylation of naphthoquinones **115** with indolizines **114** catalyzed by CPA (*R*)-**C23** forming atropoisomers **116** (Scheme 36) [64]. A broad range of indolizine substrates was tested with substituents in positions 6 and 7, but the best results were consistently achieved by exchanging the hydrogen in position 8. Such products along with the ones containing various butyl, methyl, and ethyl esters on the indolizine ring were obtained in moderate to good yields with repeatedly high enantiomeric purity of 97%.

An extensive study on the reactivity of *o*-naphthoquinones **117** and **122** with 2-naphthylamines, 2-naphthols (**118**, **120**), and indoles **123** was done in 2019 (Scheme 37) [65]. Four organo-

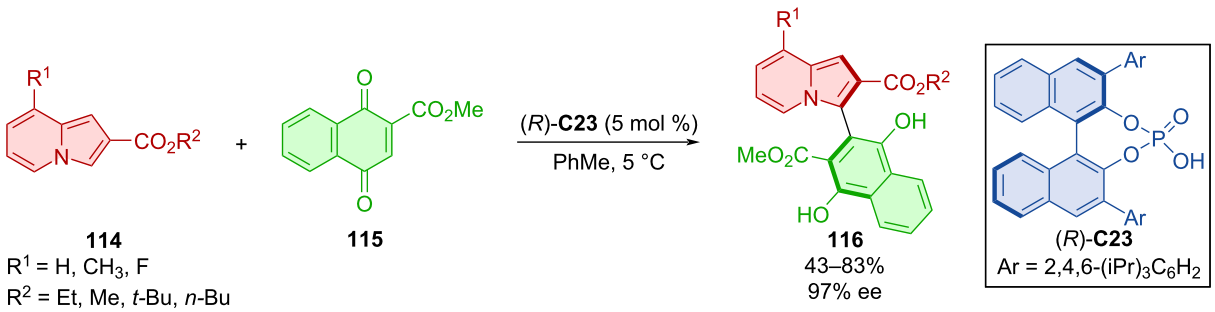

114
R^1 = H, CH_3, F
R^2 = Et, Me, *t*-Bu, *n*-Bu

115

116
43–83%
97% ee

Scheme 36: CPA-catalyzed arylation of naphthoquinones with indolizines.

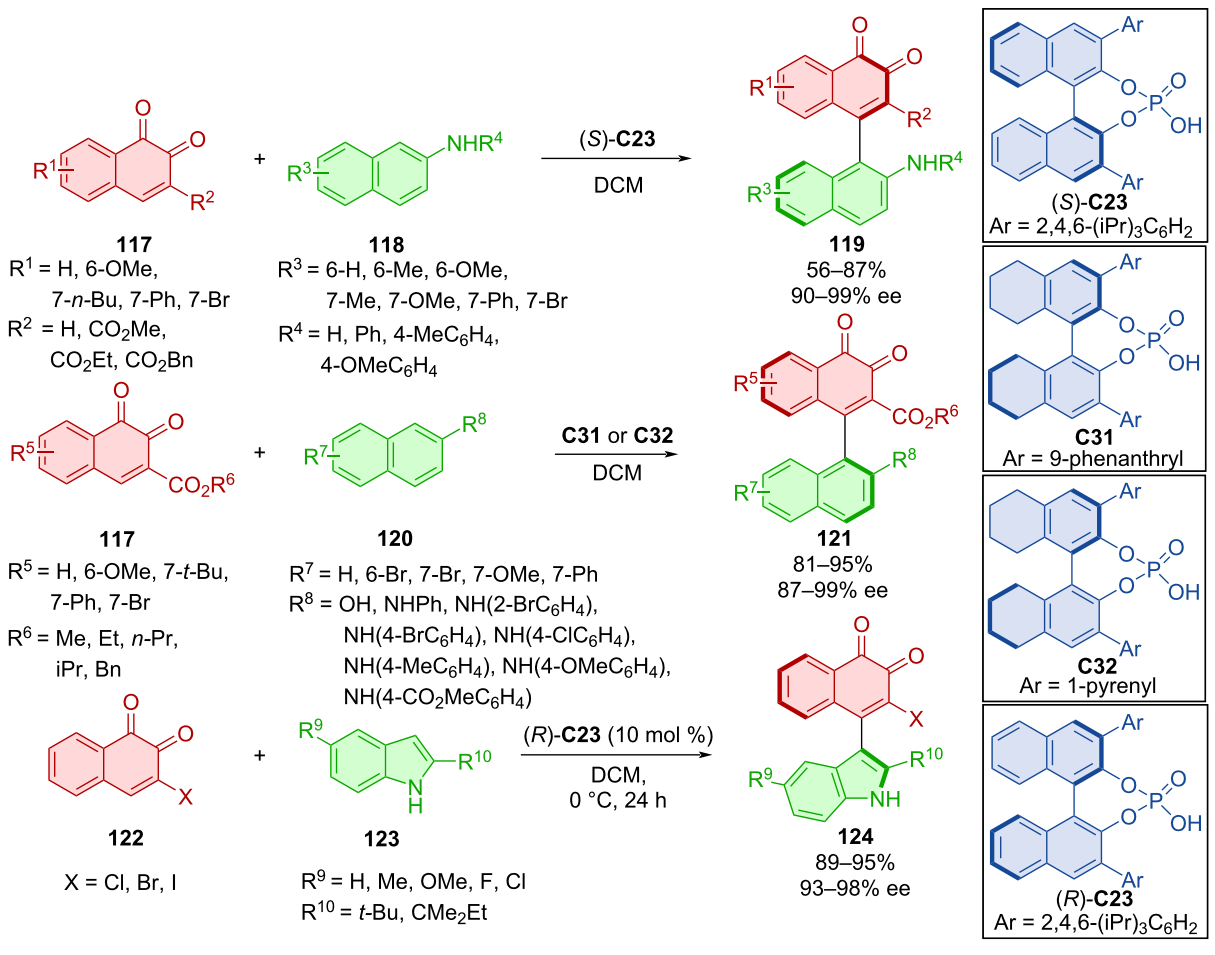

117
R^1 = H, 6-OMe, 7-*n*-Bu, 7-Ph, 7-Br
R^2 = H, CO_2Me, CO_2Et, CO_2Bn

118
R^3 = 6-H, 6-Me, 6-OMe, 7-Me, 7-OMe, 7-Ph, 7-Br
R^4 = H, Ph, 4-MeC_6H_4, 4-$OMeC_6H_4$

119
56–87%
90–99% ee

117
R^5 = H, 6-OMe, 7-*t*-Bu, 7-Ph, 7-Br
R^6 = Me, Et, *n*-Pr, iPr, Bn

120
R^7 = H, 6-Br, 7-Br, 7-OMe, 7-Ph
R^8 = OH, NHPh, NH(2-BrC_6H_4), NH(4-BrC_6H_4), NH(4-ClC_6H_4), NH(4-MeC_6H_4), NH(4-$OMeC_6H_4$), NH(4-$CO_2MeC_6H_4$)

121
81–95%
87–99% ee

122
X = Cl, Br, I

123
R^9 = H, Me, OMe, F, Cl
R^{10} = *t*-Bu, CMe_2Et

124
89–95%
93–98% ee

Scheme 37: Atroposelective reaction of *o*-naphthoquinones.

catalysts ((*S*)-**C23**, **C31**, **C32**, (*R*)-**C23**) proved the most efficient, and stereoinformation was effectively transferred in all cases. High yields and remarkable enantiomeric purities were achieved with all prepared products (**119**, **121**, and **124**).

The proposed reaction pathway indicates the asymmetric conjugated addition from 2-naphthylamine, stabilized by a donor hydrogen bond to the organocatalyst, towards the *o*-naphthoquinone, stabilized with an acceptor hydrogen bond to the chiral phosphoric acid.

Chen et al. developed an organocatalytic atroposelective preparation of arylquinones **127** and **130** utilizing CPA enantiomers (*R*)-**C23** and (*S*)-**C23** (Scheme 38) [66]. In one case quinones **125** were reacted with 2-naphthols **126** and after subsequent oxidation with DDQ provided the respective products **127**. When indoles **129** were utilized with quinone **128**, no further oxidizing reagents were necessary to afford indolylquinones **130**. All products were obtained with high enantiomeric ratios and moderate to good yields. A model reaction performed at a gram scale gave the product with analogous yield and enantioselectivity (73%, 96% ee).

Hydrogen-bond-stabilized axially chiral *N*-arylquinones **133** were prepared by reaction of quinone esters **131** with anilines **132** mediated by CPA (*R*)-**C23** (Scheme 39) [67]. Apart from respectable yields and remarkable enantioselectivities, the authors also calculated the racemization barrier of products **133**. It was determined as a class-3 atropoisomer with 30.1 kcal/mol at 90 °C in toluene. The preparation of **133** on a gram scale yielded 75% of the product with a similar level of enantiomeric purity (90% ee). A key step of this transformation is an asymmetric conjugate addition leading to a central chiral intermediate that tautomerizes to the axially chiral product.

Chiral phosphoric acid **C33** was utilized in the construction of products **136** bearing both axial and central chirality (Scheme 40) [68] through the reaction of bisindoles **134** and isatin-derived 3-indolylmethanols **135**. Over 90% diastereoselectivity, mostly very good yields, and consistently high enantioselectivities were reported. Testing the practicality of the protocol, the gram-scale experiment provided representative product **136** in 93% yield and an excellent stereoselectivity (96% ee, >95:5 dr). No racemization was observed after 36 hours at 150 °C in *o*-xylene.

The asymmetric synthesis of arylindolylindolinones **139** or **141** bearing both central and axial chirality was accomplished by a combination of arylindoles **137** or **140** and indolinones **138** with CPA (*R*)-**C22** acting as the catalyst (Scheme 41) [69]. Following identical reaction conditions two series of different atropoisomers were prepared with very high yields, enantioselectivities, and diastereoselectivities. The corresponding products proved to be stable for up to 12 h in *o*-xylene at 120 °C. Methylation of the indole nitrogen in control experiments led to halted reactivity or loss of enantiocontrol. These results suggest the importance of hydrogen bonding between the NH group and the organocatalyst.

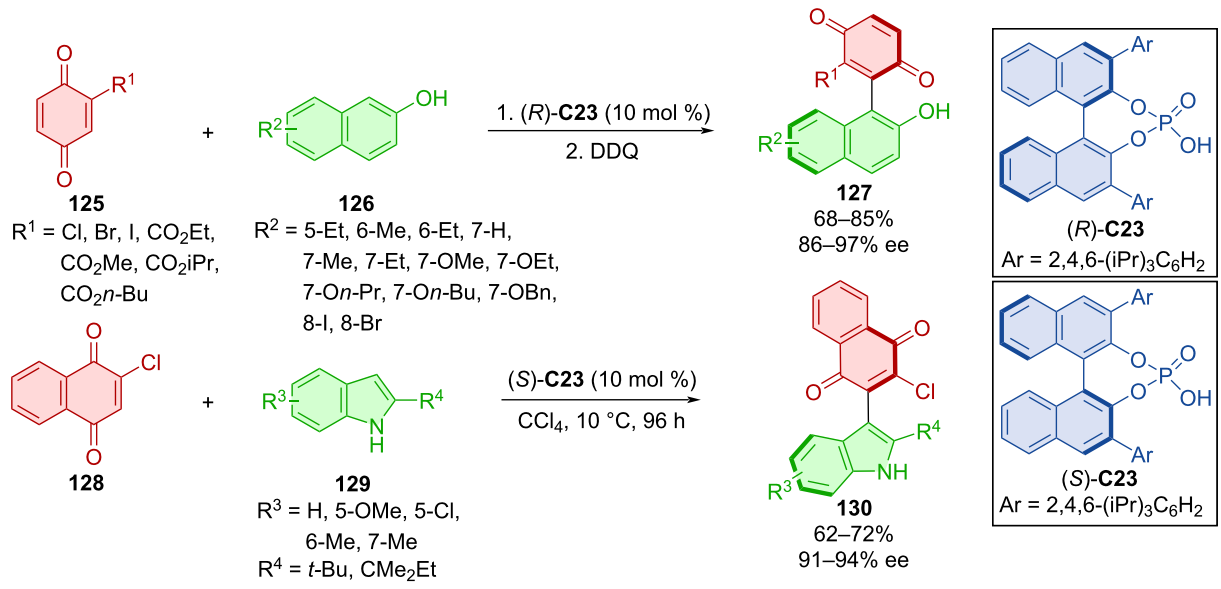

Scheme 38: CPA-catalyzed formation of axially chiral arylquinones.

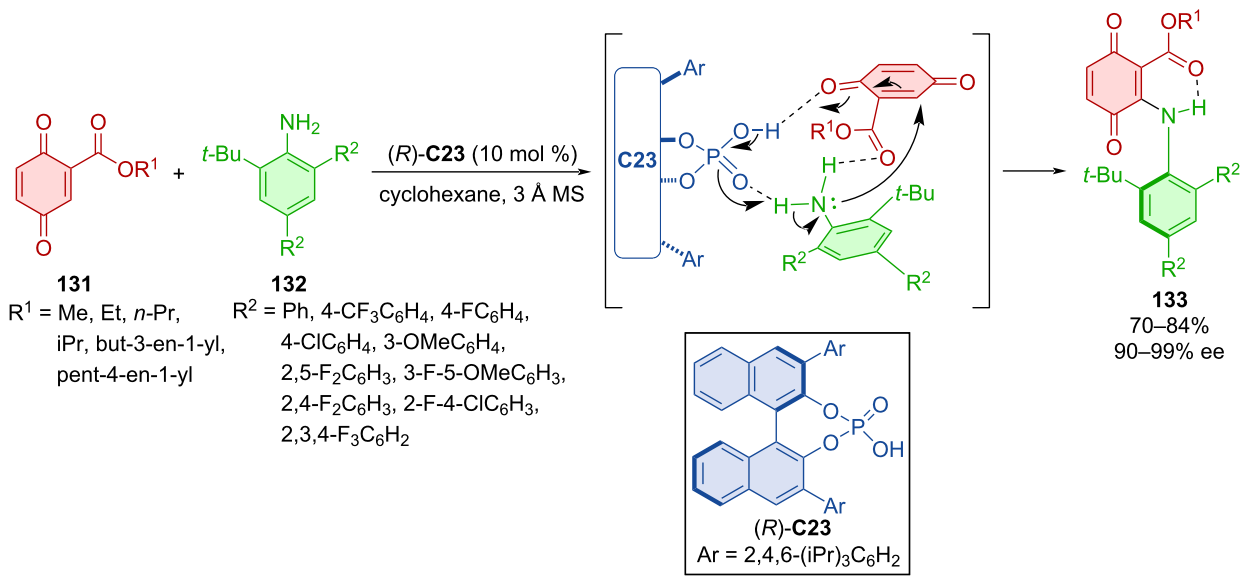

Scheme 39: CPA-catalyzed axially chiral *N*-arylquinones.

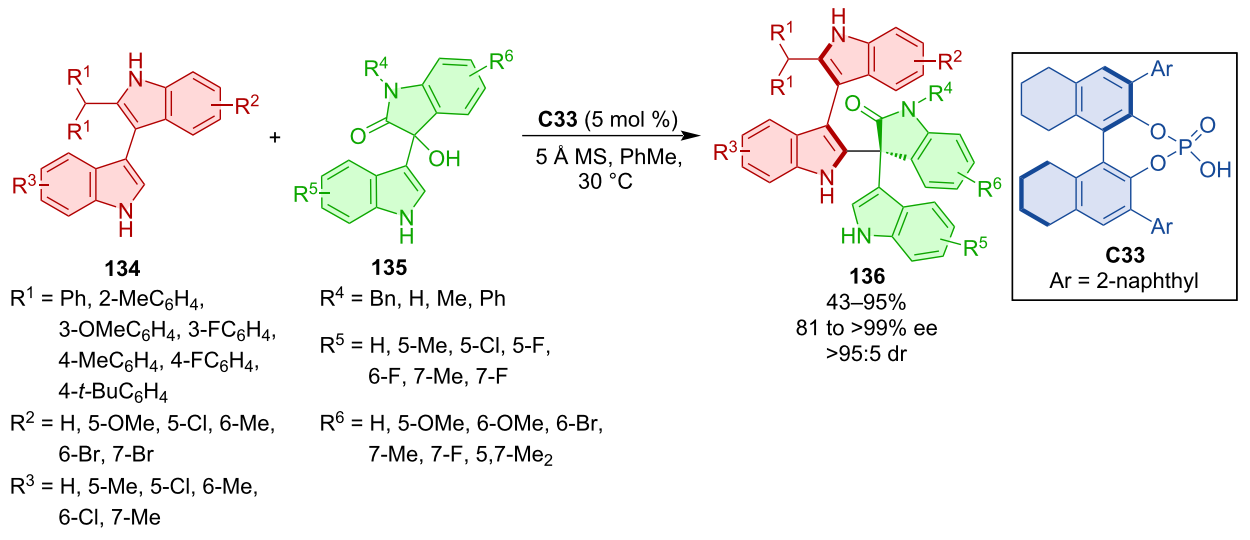

Scheme 40: Atroposelective additions of bisindoles to isatin-based 3-indolylmethanols.

Bisindoles **142** reacted with ninhydrin-derived 3-indoylmethanol **143** in the presence of the CPA (*S*)-**C22** to afford axially chiral products **144** (Scheme 42) [70]. Moderate to decent yields were reported, with enantioselectivities up to 88%. In terms of configurational stability, the representative product **144** could be stirred at 130 °C for 24 h in toluene without loss in yield or enantioselectivity. The calculated rotational barrier of the same compound was found to be 43.8 kcal/mol, which is higher by approximately 30.7 kcal/mol than that of the starting material. This value classifies the corresponding product **144** as class-3 atropoisomer [4]. Experimental results helped with providing possible reaction pathways. The acidic hydrogen of the CPA promotes dehydration and the formation of the vinyliminium intermediate. Chirality control is consistent because of the retarded reaction with the unfavored enantiomer of the bisindole **142** and its low rotational barrier resulting in quick exchange between the two.

Products **147**, bearing both axial and central chirality, were prepared by organocatalytic asymmetric addition of bisindoles **145** and isatin-derived imines **146** catalyzed by CPA **C26** (Scheme 43) [71]. The scope of the reaction showed efficient

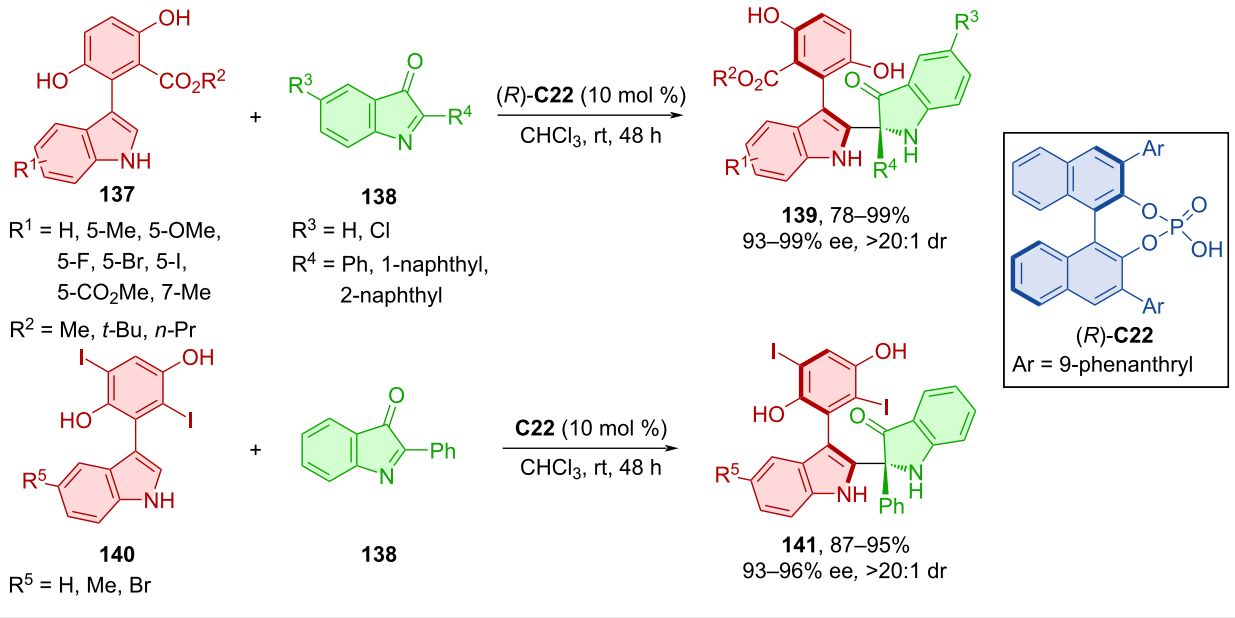

Scheme 41: CPA-catalyzed synthesis of axially chiral arylindolylindolinones.

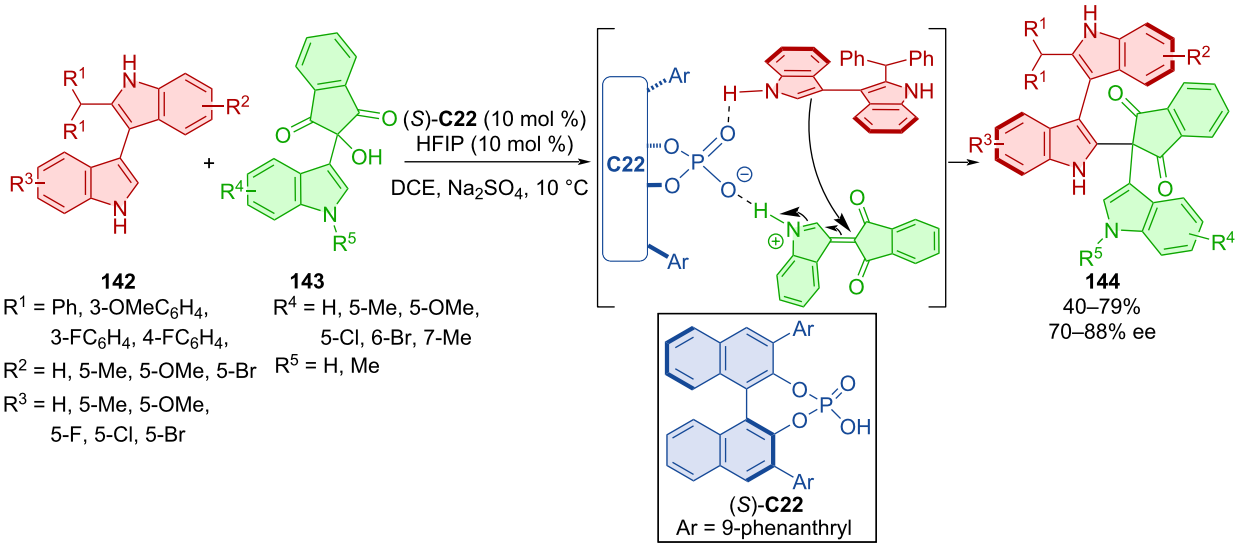

Scheme 42: CPA-catalyzed reaction between bisindoles and ninhydrin-derived 3-indoylmethanols.

stereocontrol by consistently high diastereo- and enantioselectivity with moderate to high yields. A one-mmol-scale reaction of the corresponding product showed a higher yield and similar enantioselectivity. Compared to the low rotational barrier of bisindoles (13.1 kcal/mol), a much higher value (46.3 kcal/mol) was calculated for the final product of the respective reaction. Experiments determining the configurational stability were done in both toluene at 120 °C and *o*-xylene at 150 °C for up to 36 h with retained stereoselectivity but decreasing yields at higher temperatures for prolonged periods of time. The possible activation mode explains the stereocontrol of the reaction with key hydrogen bonds between substrates, organocatalyst, and HFIP.

Sheng et al. utilized the BINOL-derived organocatalyst **C34** in the reaction of benzylindoles **148** and 2-indolylmethanols **149** leading to the bisindoles **150** (Scheme 44) [72]. Very good yields and good to high enantioselectivities were reported. The configurational stability and rotational barrier were also investigated. The enantioselectivity gradually decreased at 70 °C for 12 h in isopropyl alcohol and the calculated value was 28.5 kcal/mol. Control experiments proved the importance of

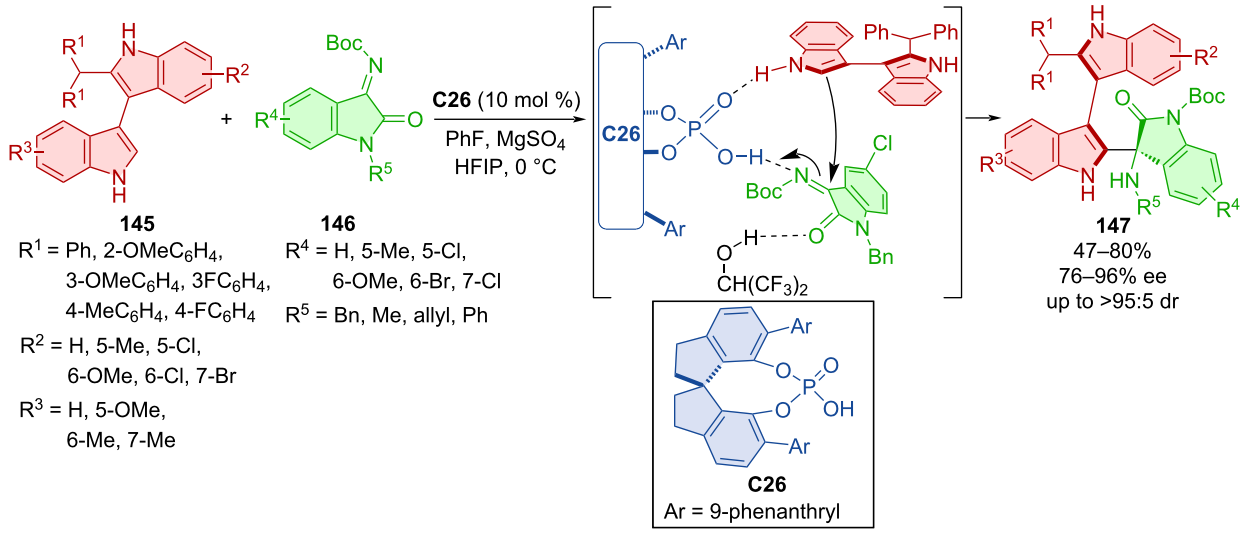

Scheme 43: Atroposelective reaction of bisindoles and isatin-derived imines.

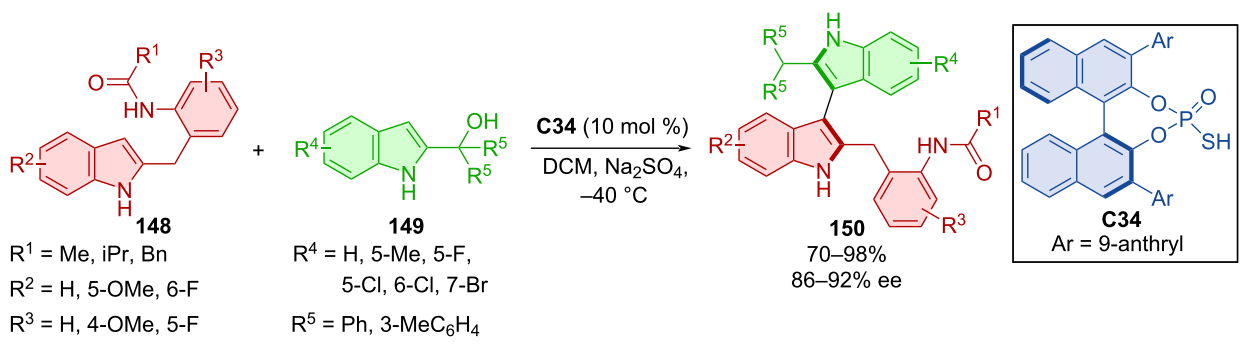

Scheme 44: CPA-catalyzed formation of axially chiral bisindoles.

N–H bonds during the reaction and methylation of just one nitrogen resulted in retarded or halted reactivity.

The combination of 2-naphthols **151** and alkynylhydroxyisoindolinones **152** in the presence of two chiral Brønsted acids **C35** and **C36** provided axially chiral isoindolinones **153** (Scheme 45) [73]. The optimized reaction conditions led to the handful of products in low to satisfactory yields, but having high enantiomeric purities.

An organocatalytic asymmetric (3 + 2) cyclization of 3-arylindoles **154** with either achiral **155** or racemic **157** propargylic alcohols was reported by Wu et al. (Scheme 46) [74]. Utilizing CPA **C37** with 3-arylindoles **154** and achiral propargylic alcohols **155**, the axially chiral arylpyrrolindoles **156** were prepared with excellent enantiomeric purities and high yields. On the other hand, using racemic propargylic alcohols **157** and same 3-arylindoles **155** with CPA **C38** led to the opposite enantiomers **158** with remarkable enantiomeric purities, solid yields and very good diastereomeric ratios. The hydroxy group present in products **156** and **158** could be transformed to provide axially chiral phosphines that could be utilized as chiral ligands in transition-metal-catalyzed reactions. Testing both substrates **156** and **158** for conformational stability in isopropanol at 80 °C for 12 h provided recovered substrates in high yields with maintained diastereo- and enantioselectivities. Based on calculations of rotational barriers, these compounds meet the requirements to be considered class-3 atropoisomers (32.9–37.7 kcal/mol).

Indolylpyrroloindoles **161** were constructed by a (3 + 2) cycloaddition of isoindolinone-substitued propargylic alcohols **160** with bisindoles **159** mediated by CPA **C39** (Scheme 47) [75]. These axially chiral spirocyclic products were prepared with good to very good yields and excellent enantiomeric purities. The slow racemization process of **161** was observed at 70 °C, and the experimentally determined rotational barrier of 30.5 kcal/mol was observed at 100 °C in toluene. Control experiments gave insights into the potential importance of hydrogen

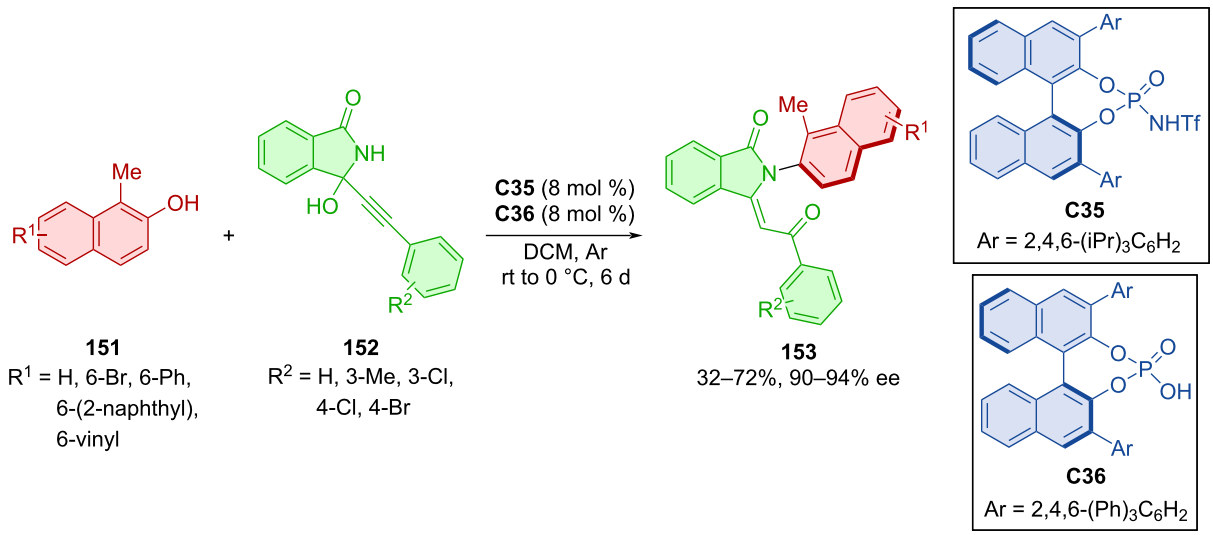

151
R^1 = H, 6-Br, 6-Ph, 6-(2-naphthyl), 6-vinyl

152
R^2 = H, 3-Me, 3-Cl, 4-Cl, 4-Br

153
32–72%, 90–94% ee

Scheme 45: Atroposelective reaction of 2-naphthols with alkynylhydroxyisoindolinones.

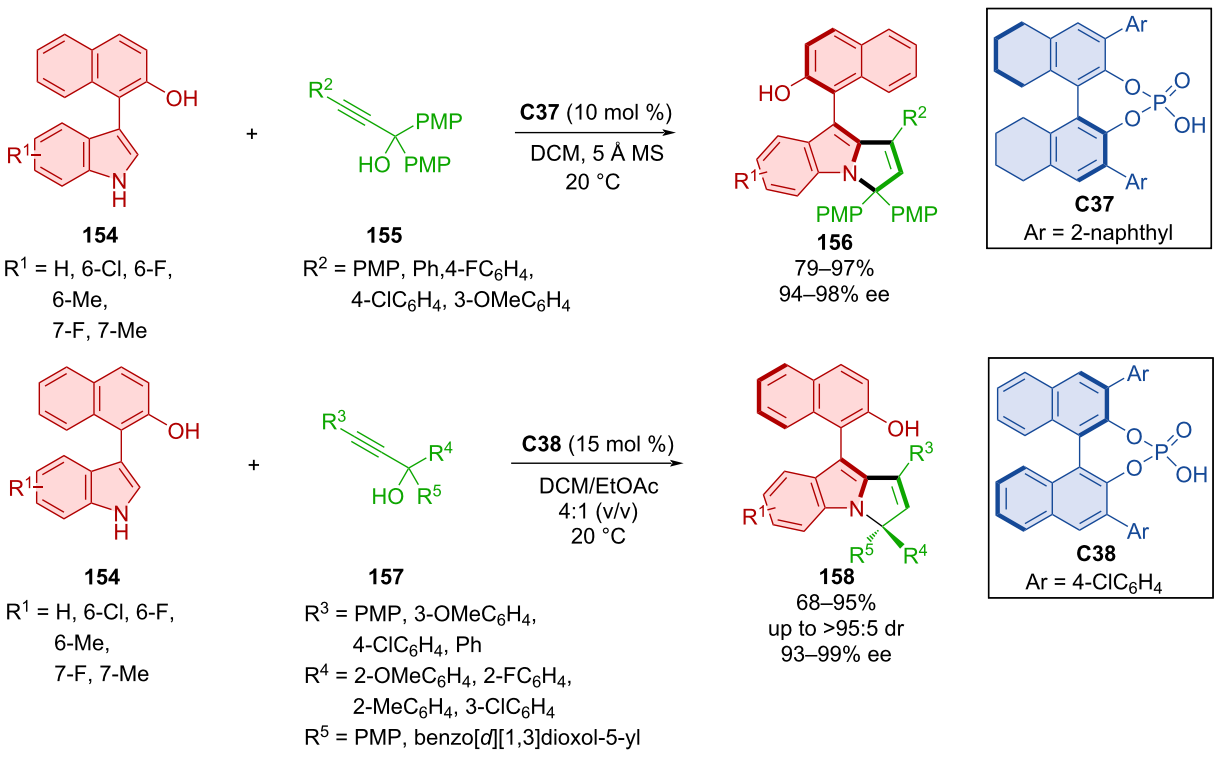

154
R^1 = H, 6-Cl, 6-F, 6-Me, 7-F, 7-Me

155
R^2 = PMP, Ph,4-FC_6H_4, 4-ClC_6H_4, 3-$OMeC_6H_4$

156
79–97%
94–98% ee

154
R^1 = H, 6-Cl, 6-F, 6-Me, 7-F, 7-Me

157
R^3 = PMP, 3-$OMeC_6H_4$, 4-ClC_6H_4, Ph
R^4 = 2-$OMeC_6H_4$, 2-FC_6H_4, 2-MeC_6H_4, 3-ClC_6H_4
R^5 = PMP, benzo[*d*][1,3]dioxol-5-yl

158
68–95%
up to >95:5 dr
93–99% ee

Scheme 46: CPA-catalyzed reaction of indolylnaphthols with propargylic alcohols.

bonds on the nitrogen atoms of the isoindolinone ring in **160** and one indole ring in **159**. Based on these findings, a potential reaction pathway was proposed. It starts with a chiral phosphoric acid-supported dehydration of **160** and reaction with the favored configuration of bisindoles **159** to form an allene intermediate **Int-38**. Proton transfer and subsequent intramolecular cycloaddition occurs to generate indolylpyrroloindole **161**.

Woldegiorgis et al. developed an efficient atroposelective synthesis of axially chiral styrenes connected to axially chiral naph-

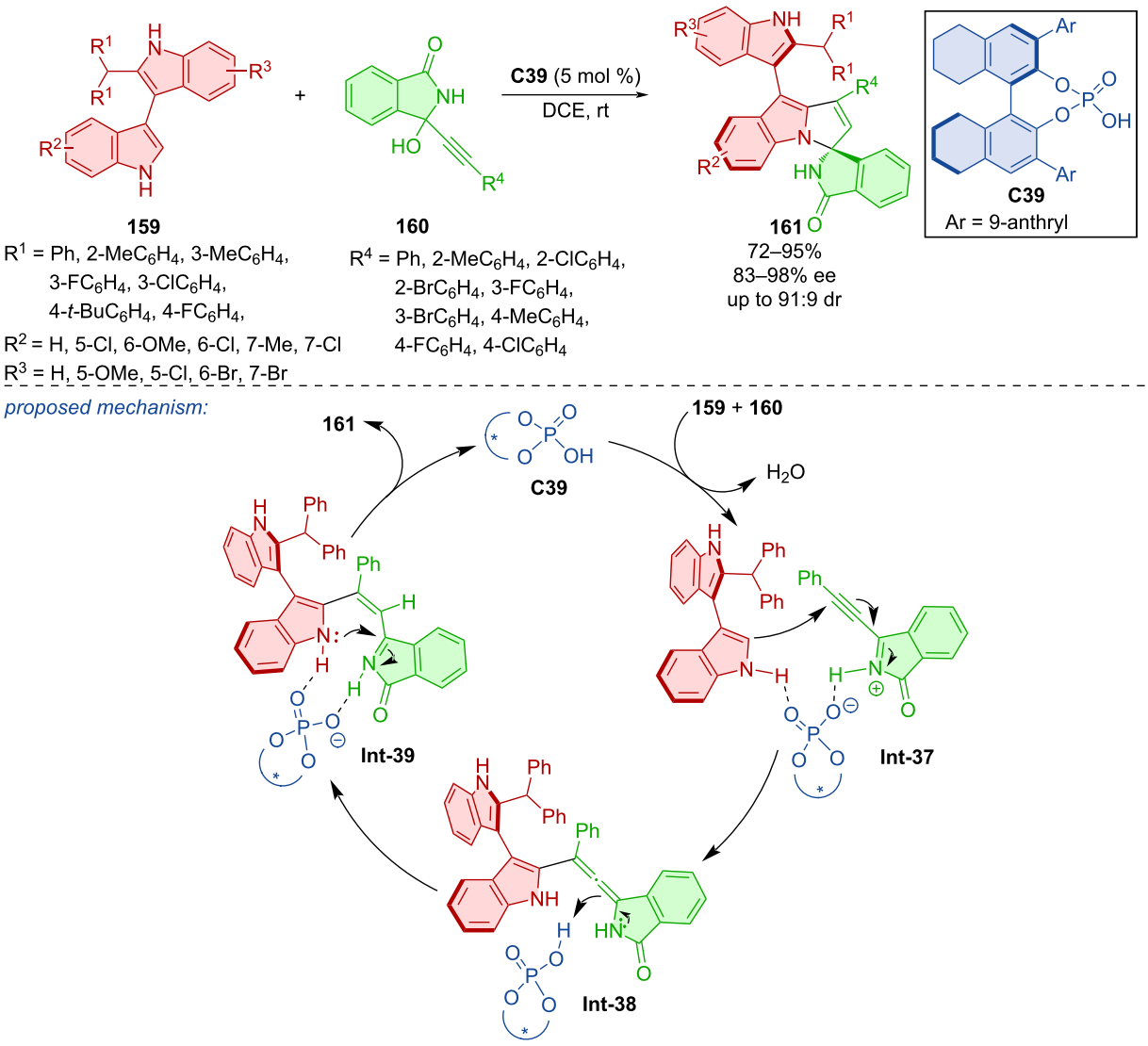

Scheme 47: Atroposelective formation of indolylpyrroloindoles.

thylindoles **164** from naphthylindoles **162** and alkynyl-2-naphthols **163** catalyzed by CPA **C27** (Scheme 48) [76]. The reaction conditions were compatible with many substrates containing methyl, methoxy, halogen, and aryl groups, providing excellent enantioselectivies and moderate to high yields. Control experiments indicated an activation mode through the vinylidene *ortho*-quinone methide (VQM) intermediate as well as the importance of the naphthol's OH group and indole's NH group, presumably through hydrogen bonding with organocatalyst **C27**.

The organocatalytic atroposelective preparation of promising EBINOL scaffolds **167** and **169** was done by Wang et al. with the help of the SPINOL-derived organocatalysts **C40**, **C41**, and **C42** (Scheme 49) [77]. They reacted 2-naphthols **165** either with alkynyl-2-naphthylamines **166** or alkynyl-2-naphthols **168**, respectively. Decent results were achieved with structures containing electron-withdrawing groups such as methyl carboxylate, acetyl, and formyl. The prepared EBINOL **169** was transformed into a CPA to be used as an organocatalyst or to a phosphoramidite to be used as a chiral ligand. Testing these new structures on known stereoselective transformations, the authors achieved high yields and enantioselectivities (up to 98% yield and 97% ee).

Wang et al. performed asymmetric (4 + 3) cyclization of alkynylindolylmethanols **170** and 2-naphthols **171** mediated by chiral phosphoric acid **C37** leading to axially chiral aryl-alkene-indoles **172** (Scheme 50) [78]. Very high enantioselectivities and *E*/*Z* ratios, along with, on average, decent yields, were re-

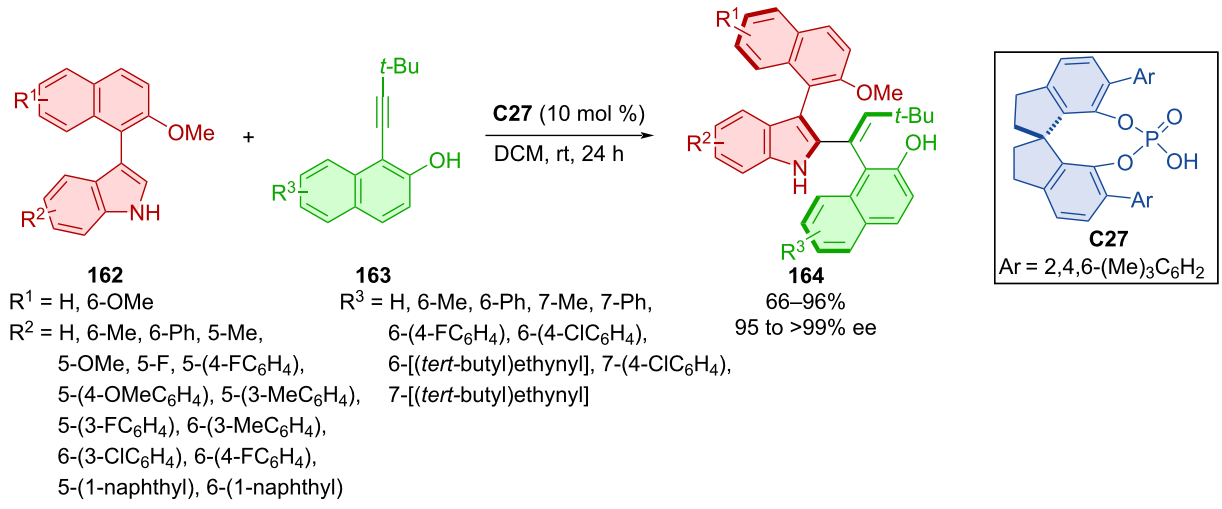

162
R^1 = H, 6-OMe
R^2 = H, 6-Me, 6-Ph, 5-Me, 5-OMe, 5-F, 5-(4-FC_6H_4), 5-(4-$OMeC_6H_4$), 5-(3-MeC_6H_4), 5-(3-FC_6H_4), 6-(3-MeC_6H_4), 6-(3-ClC_6H_4), 6-(4-FC_6H_4), 5-(1-naphthyl), 6-(1-naphthyl)

163
R^3 = H, 6-Me, 6-Ph, 7-Me, 7-Ph, 6-(4-FC_6H_4), 6-(4-ClC_6H_4), 6-[(*tert*-butyl)ethynyl], 7-(4-ClC_6H_4), 7-[(*tert*-butyl)ethynyl]

164
66–96%
95 to >99% ee

Scheme 48: Atroposelective reaction of indolylnaphthalenes with alkynylnaphthols.

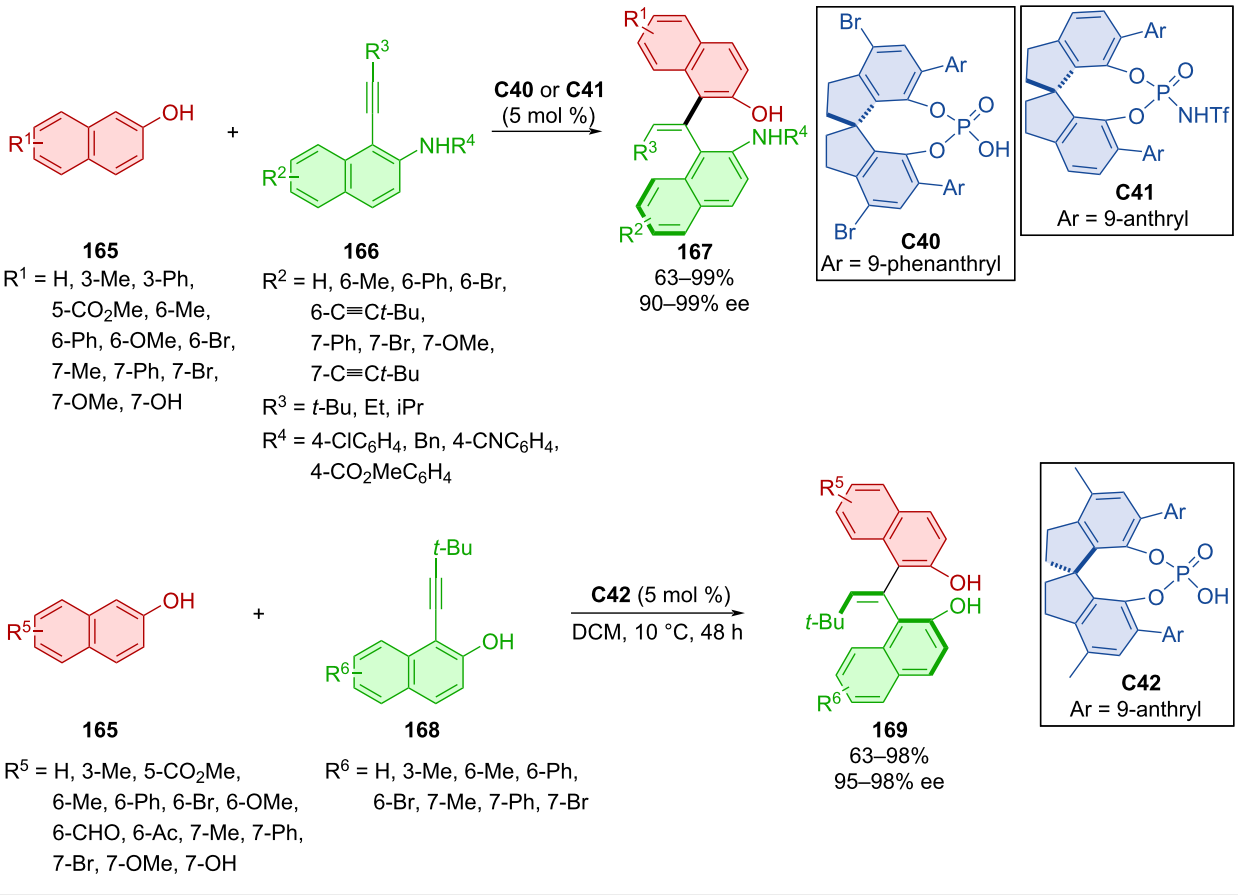

165
R^1 = H, 3-Me, 3-Ph, 5-CO_2Me, 6-Me, 6-Ph, 6-OMe, 6-Br, 7-Me, 7-Ph, 7-Br, 7-OMe, 7-OH

166
R^2 = H, 6-Me, 6-Ph, 6-Br, 6-C≡C*t*-Bu, 7-Ph, 7-Br, 7-OMe, 7-C≡C*t*-Bu
R^3 = *t*-Bu, Et, iPr
R^4 = 4-ClC_6H_4, Bn, 4-CNC_6H_4, 4-$CO_2MeC_6H_4$

167
63–99%
90–99% ee

165
R^5 = H, 3-Me, 5-CO_2Me, 6-Me, 6-Ph, 6-Br, 6-OMe, 6-CHO, 6-Ac, 7-Me, 7-Ph, 7-Br, 7-OMe, 7-OH

168
R^6 = H, 3-Me, 6-Me, 6-Ph, 6-Br, 7-Me, 7-Ph, 7-Br

169
63–98%
95–98% ee

Scheme 49: CPA-catalyzed addition of naphthols to alkynyl-2-naphthols and 2-naphthylamines.

ported. Slow racemization was observed at 40 or 50 °C in isopropanol just after a couple of hours. The racemization barriers of the products were only slightly higher (28 kcal/mol) than the minimal requirement for separation of atropoisomers (24 kcal/mol). Scale-up done on the one-mmol-scale provided the corresponding product in comparable yields and stereoselectivities (85%, 90% ee, >95:5 *E*/*Z*). A biological activity investigation led to promising results in the case of one

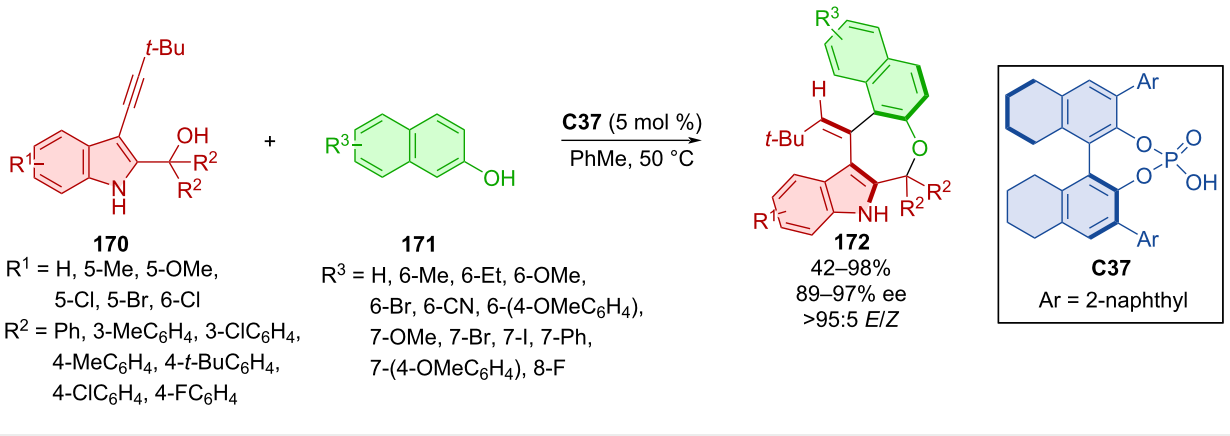

170
R^1 = H, 5-Me, 5-OMe, 5-Cl, 5-Br, 6-Cl
R^2 = Ph, 3-MeC_6H_4, 3-ClC_6H_4, 4-MeC_6H_4, 4-*t*-BuC_6H_4, 4-ClC_6H_4, 4-FC_6H_4

171
R^3 = H, 6-Me, 6-Et, 6-OMe, 6-Br, 6-CN, 6-(4-OMeC_6H_4), 7-OMe, 7-Br, 7-I, 7-Ph, 7-(4-OMeC_6H_4), 8-F

172
42–98%
89–97% ee
>95:5 *E*/*Z*

Scheme 50: CPA-catalyzed formation of axially chiral aryl-alkene-indoles.

substrate displaying cytotoxicity towards several cancer cell lines.

Organocatalytic enantioselective construction of axially chiral styrenes **175** and **177** was done utilizing alkynylnaphthylamines **173** with indoles **174** or coumarins **176** catalyzed with CPA (*R*)-**C23** (Scheme 51) [79]. The extensive scope of alkynylnaphthylamines **173** and indoles **174** led to the products **175** in moderate to high yields with very high enantiomeric purities and decent *E*/*Z* ratio. A gram-scale verson of the reaction provided the product with comparable yield and enantiomeric purity (88%, 93% ee). The more modest scope of coumarins **176** with alkynylnaphthylamines **173** gave rise to axially chiral products **177** in comparable yields to the first reaction with slightly higher enantiomeric purities in general.

Axially chiral alkenylindoles **180** were prepared by the addition of α-amido sulfones **179** to triple bond of alkynylindolyl-

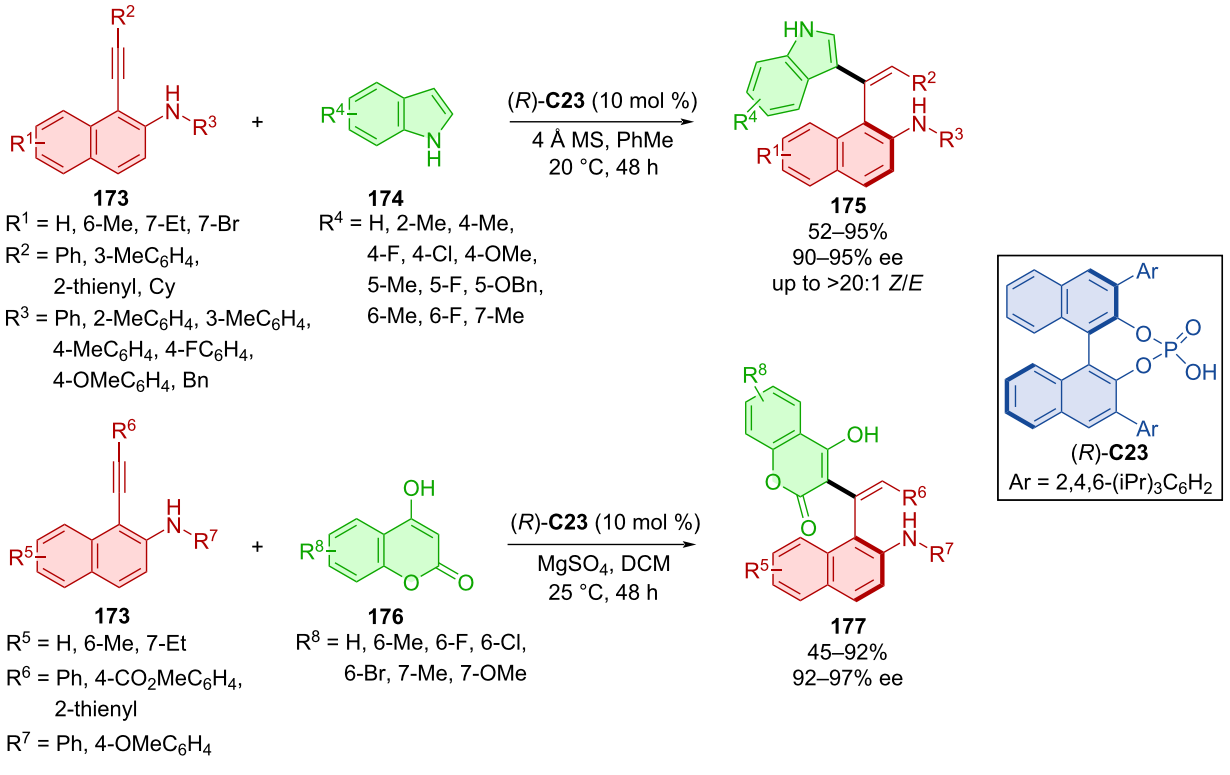

173
R^1 = H, 6-Me, 7-Et, 7-Br
R^2 = Ph, 3-MeC_6H_4, 2-thienyl, Cy
R^3 = Ph, 2-MeC_6H_4, 3-MeC_6H_4, 4-MeC_6H_4, 4-FC_6H_4, 4-OMeC_6H_4, Bn

174
R^4 = H, 2-Me, 4-Me, 4-F, 4-Cl, 4-OMe, 5-Me, 5-F, 5-OBn, 6-Me, 6-F, 7-Me

175
52–95%
90–95% ee
up to >20:1 *Z*/*E*

173
R^5 = H, 6-Me, 7-Et
R^6 = Ph, 4-CO_2MeC_6H_4, 2-thienyl
R^7 = Ph, 4-OMeC_6H_4

176
R^8 = H, 6-Me, 6-F, 6-Cl, 6-Br, 7-Me, 7-OMe

177
45–92%
92–97% ee

Scheme 51: CPA-catalyzed formation of axially chiral styrenes.

methanols **178** catalyzed by CPA **C31** (Scheme 52) [80]. Authors achieved mild to good yields with decent to very good enantioselectivities. Alkenylindole **180** was used for the thermal racemization experiment, which revealed a rotational barrier of 43.2 kcal/mol.

Axially chiral arylquinolines **183** were prepared starting from alkynylnaphthylamines **181** and acetylanilines **182** with the help of CPA **C39** (Scheme 53) [81]. Excellent yields and enantioselectivities were reported for a plenty of different derivatives. The proposed reaction pathway follows hydrogen bonding with alkynylnaphthylamine and later nucleophilic addition of the allene intermediate. The synthesis on the preparative scale provided product **183** with almost no deterioration in yield or enantioselectivity (90%, 91% ee). This product could then be either debenzylated and subsequently transformed into a thiourea organocatalyst or turned into an axially chiral sulfonamide.

In 2022, Yang et al. presented their (3 + 2) formal cycloaddition of alkynylindoles **184** with azonaphthalenes **185** catalyzed by the SPINOL-based CPA **C26** (Scheme 54) [82]. The authors prepared a wide scope of axially chiral products **186** in high yields with excellent enantiomeric purity. The reaction allows lowering of the catalyst loading to 2 mol %. Deprotection of the amino group enabled subsequent transformations, such as a reaction with isocyanate from which a new potential thiourea organocatalyst was prepared.

Hou et al. investigated a way to prepare axially chiral compounds that contain both benzimidazole and quinoline rings **189** (Scheme 55) [83]. One route to access such compounds was

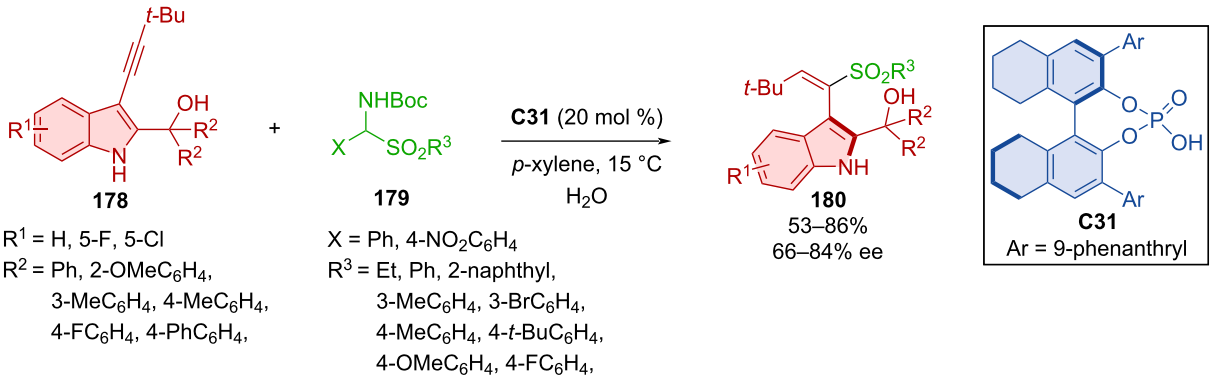

Scheme 52: Atroposelective formation of alkenylindoles.

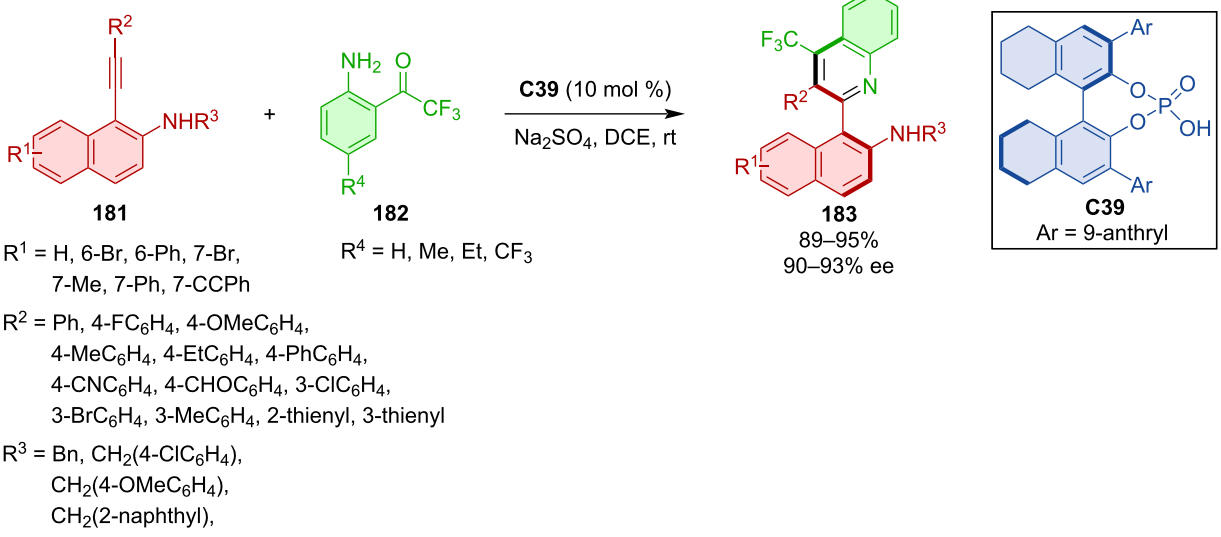

Scheme 53: Atroposelective formation of axially chiral arylquinolines.

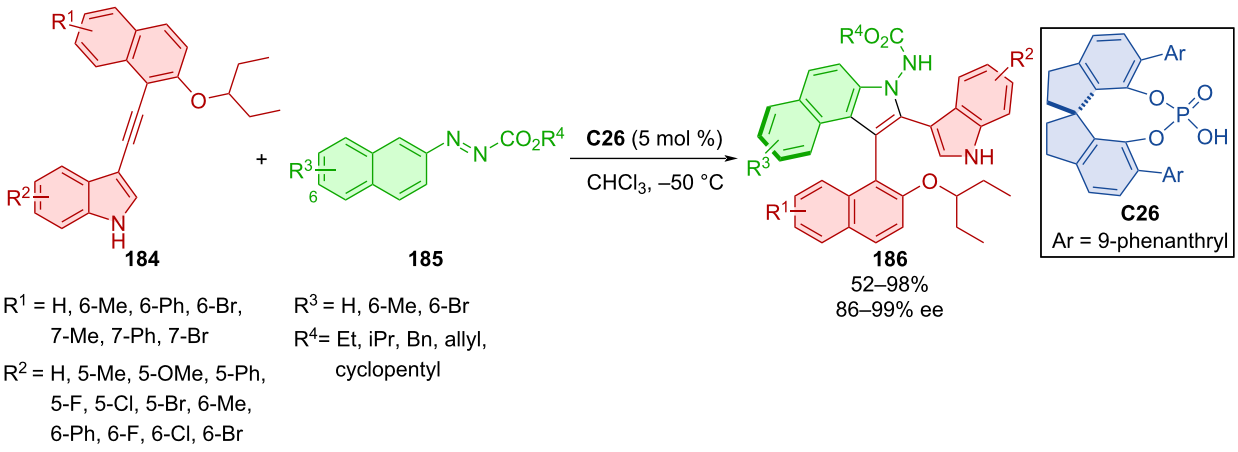

Scheme 54: Atroposelective (3 + 2) cycloaddition of alkynylindoles with azonaphthalenes.

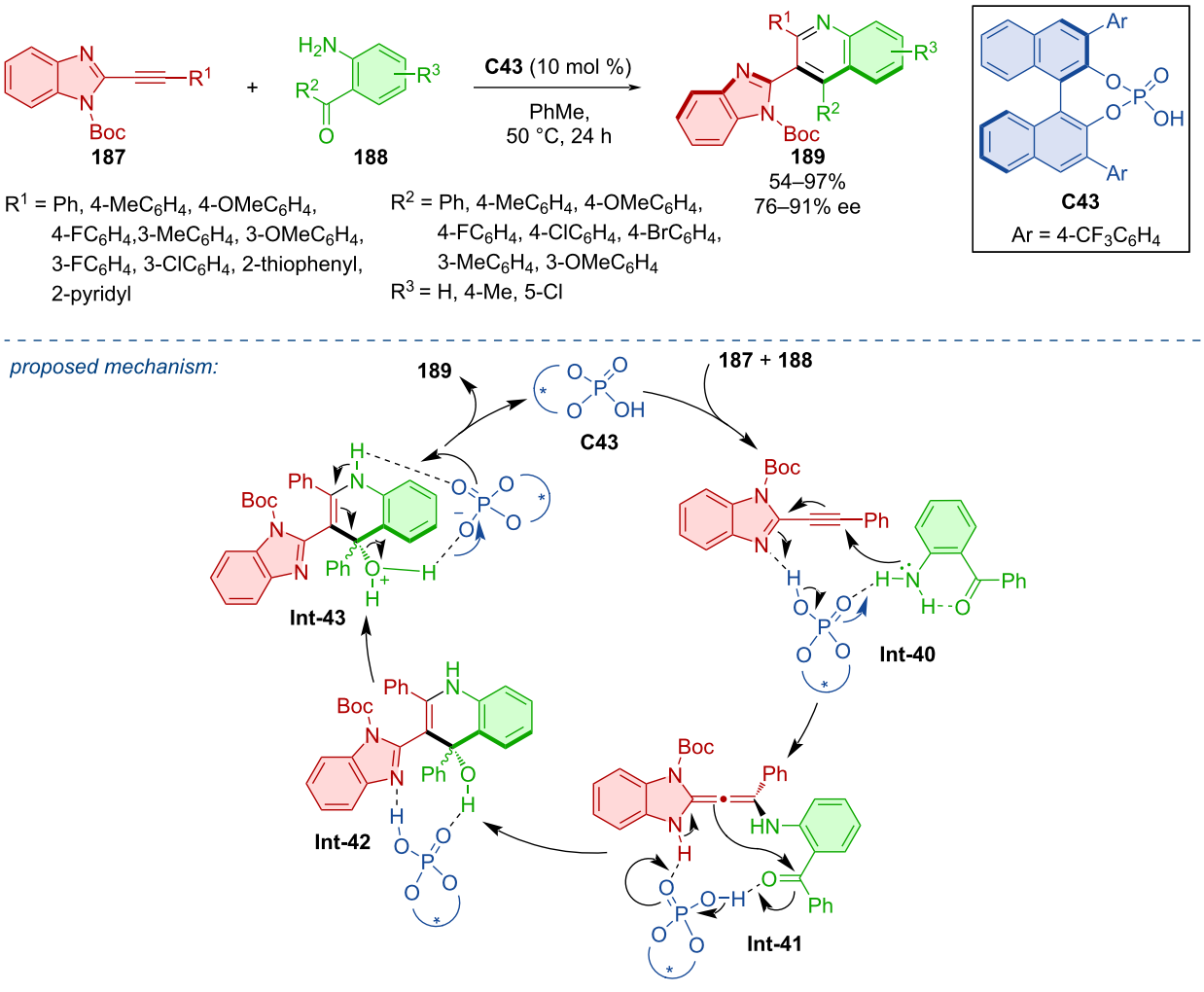

Scheme 55: CPA-catalyzed formation of axially chiral 3-(1*H*-benzo[*d*]imidazol-2-yl)quinolines.

possible through the reaction of 2-alkynylbenzimidazoles **187** with *o*-aminophenylketones **188** mediated by the chiral phosphoric acid **C43**. In general, moderate to excellent yields and very good enantioselectivities were reported. The authors presented a reaction mechanism based on experimental outcomes and previous reports [84,85]. The reaction of the substrates stabilized by hydrogen bonding with catalyst **C43** leads to allene intermediate **Int-41**. The enantiospecific intramolecular enamine–aldol cyclization and further dehydration provide the enantioenriched heterobiaryl product **189**.

The 5-*endo*-*dig*-cyclization reaction of *N*-pyrroloalkynylanilines **190** catalyzed by SPINOL-derived CPA **C44** was utilized in the formation of axially chiral products **191** (Scheme 56) [86]. The authors achieved good results in terms of enantioselectivities and yields with mostly methyl, methoxy, or halogen modifications in various positions. The configurational stability experiments of products **191** confirmed stable enantiopurity at 130 °C for 48 h in toluene. Investigating the biological activity for a number of compounds, good cytotoxicity was reported for five kinds of cancer cells. The mechanistic study suggests that the indole ring of the substrate is having a crucial role in the reaction mechanism because replacing it with another aromatic moiety such as phenyl or 2-thiophenyl led to no product being formed.

An organocatalytic atroposelective three-component cascade heteroannulation was done by Wang et al. [87]. It was a reaction of ketoesters **192**, anilines **193**, and cyclohexadiones **194** catalyzed by SPINOL-derived CPA **C45** (Scheme 57). The authors achieved good to excellent yields and remarkable enantioselectivities and proposed a plausible reaction mechanism. The crucial step of this transformation is believed to be the asymmetric dehydrative cyclization forming biaryl intermediate **Int-48**. Subsequent dehydration, release of the chiral acid, and aromatization through tautomerization of intermediate **Int-50** generate the desired product **195**.

Kwon et al. compared the effectivity of traditional biaryl phosphoric acid **C30** with peptide phosphoric acid **C46** in the cyclodehydration of trifluorophenylaminoacetals **196a**–**k** (Scheme 58) [88]. Both organocatalysts showed comparable effectivity in terms of enantioselectivity across. The difference between these catalysts becomes more visible through DFT calculations. In the case of biaryl phosphoric acid **C30**, stereocontrol is driven by the steric effects of the groups present. On the other hand, peptide phosphoric acid **C46** appears to work through an alternative mode of enantioinduction, where conformational adaptation presumably limits repulsive interactions.

CPA **C40** was utilized in the construction of the imidazole ring of axially chiral products **200** (Scheme 59) [89]. *N*-Naphthylglycine esters **198** reacted with nitrosobenzenes **199** and the authors reported moderate to good yields with remarkable enantioselectivities. Configurational stability of a representative product **200** was observed in toluene at 120 °C for 24 h with no deterioration of the ee. The practicality of the developed protocol was demonstrated on a gram-scale reaction, where the corresponding product **200** was obtained with an acceptable decrease of yield and enantioselectivity (65%, 94% ee). Mechanistically, a chemo- and regioselective nucleophilic addition followed by dehydration leads to diimine intermediate **Int-53**. Control experiments confirmed that this structure could undergo successive reduction and oxidation through intermediate **Int-54** to give benzylimine intermediate **Int-55**. Alternatively, a direct [1,5]-H migration of **Int-53** also leads to **Int-55**. The stereoselectivity of the product is determined in the CPA-catalyzed intramolecular enantioselective addition and oxidative aromatization affords the final products **200**.

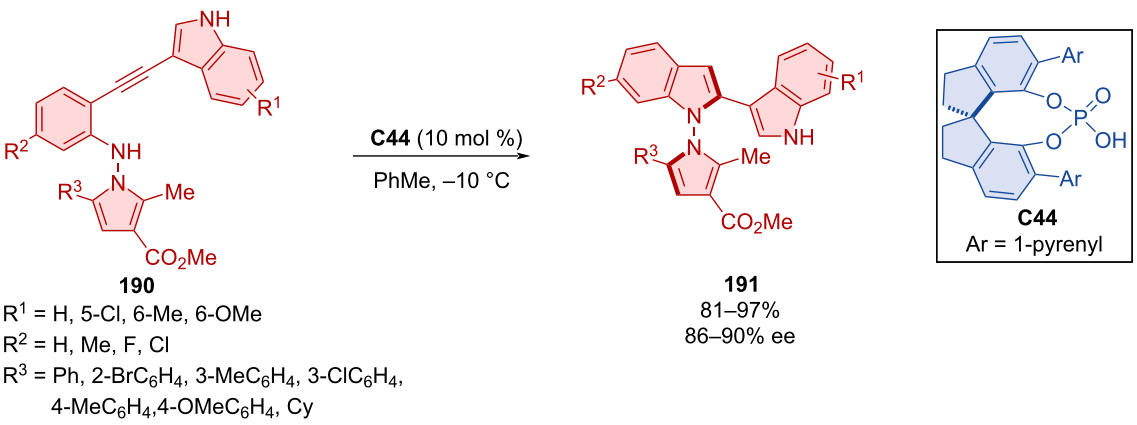

Scheme 56: Atroposelective cyclization of 3-(arylethynyl)-1*H*-indoles.

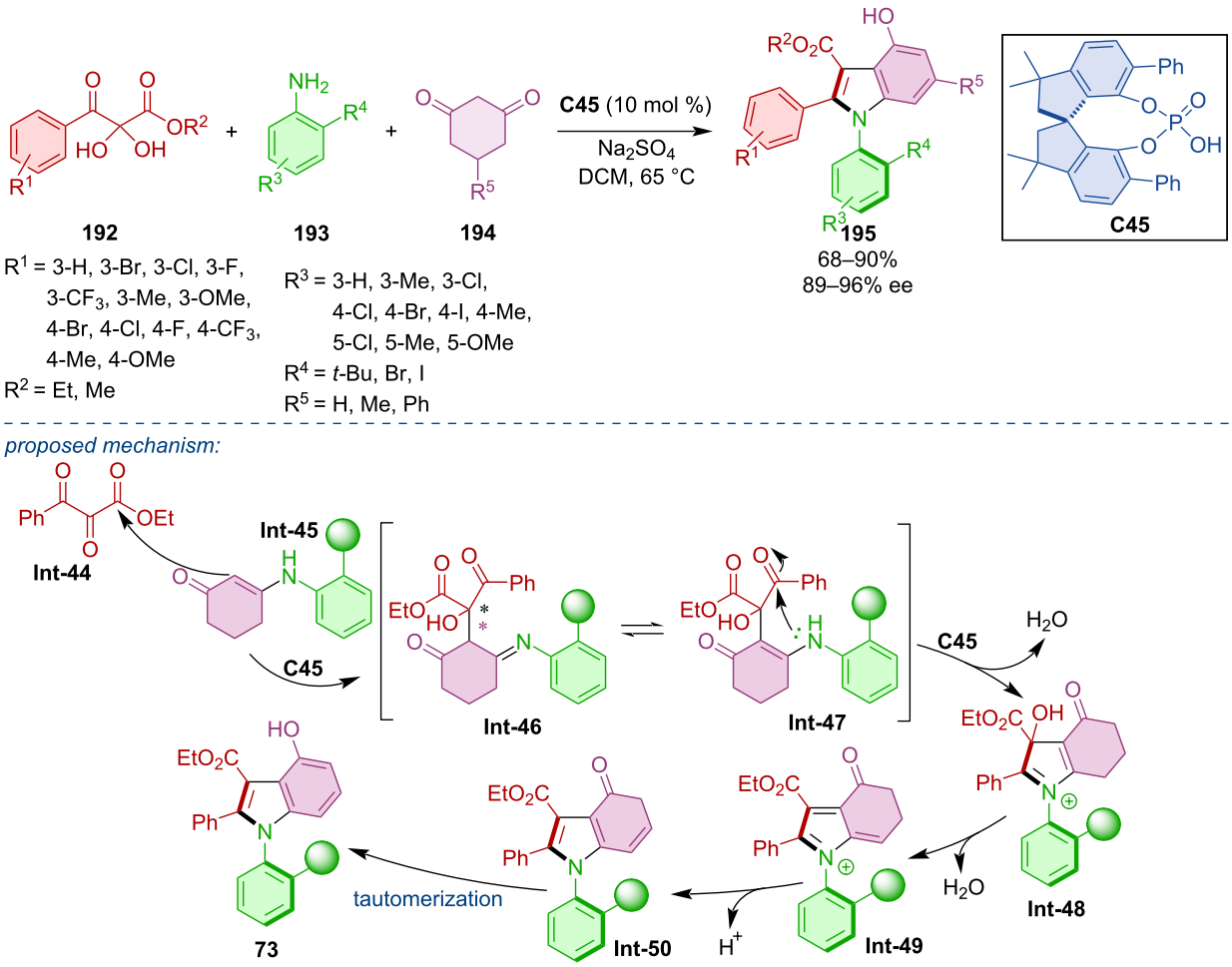

Scheme 57: Atroposelective three-component heteroannulation.

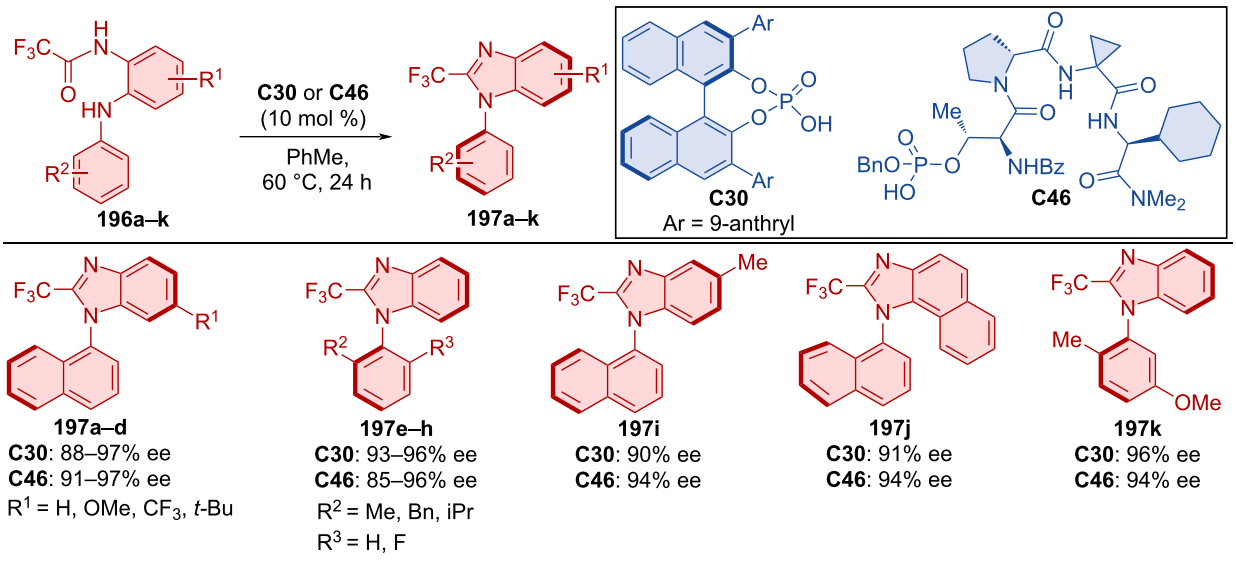

Scheme 58: CPA-catalyzed formation of arylbenzimidazols.

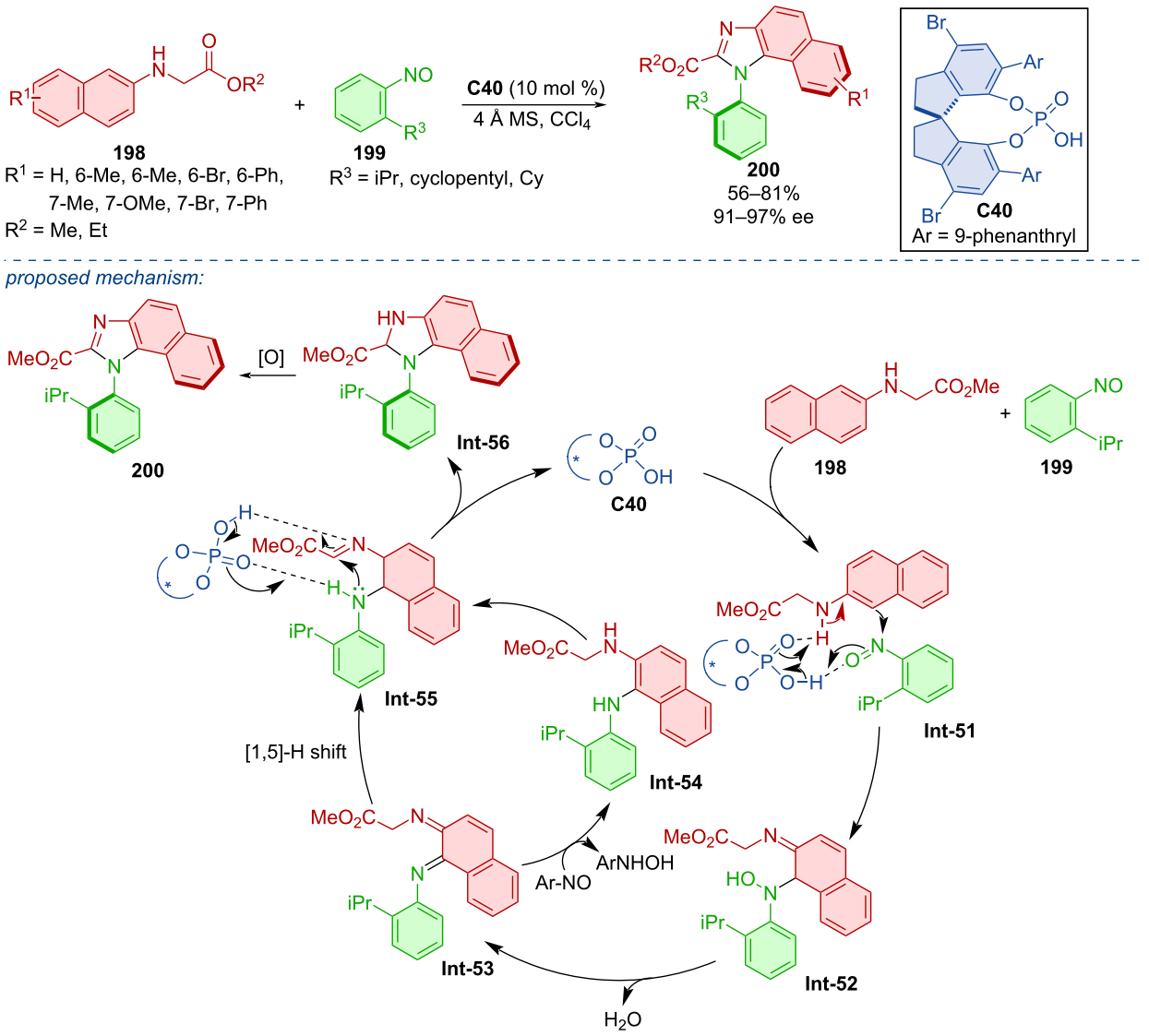

Scheme 59: CPA-catalyzed reaction of *N*-naphthylglycine esters with nitrosobenzenes.

The organocatalytic construction of the imidazole ring to provide axially chiral *N*-arylbenzimidazoles **203** was catalyzed by CPA (*R*)-**C23** (Scheme 60) [90]. It was a reaction of *N*-arylbenzenediamines **201** and β-ketoesters. Testing many different substrates, oxocyclopentane carboxylates **202** consistently provided the highest yields and enantioselectivities. The authors observed no racemization of **203** below 90 °C in toluene, isopropyl alcohol, or DCE. Based on these results, the rotational barrier was calculated to be 32.9 kcal/mol. The proposed reaction pathway starts with CPA activation of the substrates, nucleophilic addition and dehydration leading to imine intermediate **Int-59**. After dehydration to **Int-59**, two possible approaches could be utilized. The first of the two possible approaches consists of isomerization and another catalyst activation promoting an intramolecular Michael addition. The organocatalyst is freed, and cyclization product **Int-62** undergoes racemization to form **Int-64**. The identical intermediate **Int-64** is formed by catalyst activation and direct nucleophilic addition. In the final step of the reaction, ring opening by the C–C bond cleavage yields the desired product **203**.

The first phosphoric acid **C39**-catalyzed asymmetric cycloaddition–elimination cascade reaction of 2-naphthol or phenol enamide derivatives **204** with azonaphthalenes **205** was done by Xu et al. in 2021 (Scheme 61) [91]. After testing a considerable number of substrates, the authors achieved excellent yields and enantioselectivities. The synthetic utility of this approach stems from being able to skip additional reaction steps and thus omit reagents used in those steps, leading to increased efficiency and, by extension, atom economy. Through the thermal racemiza-

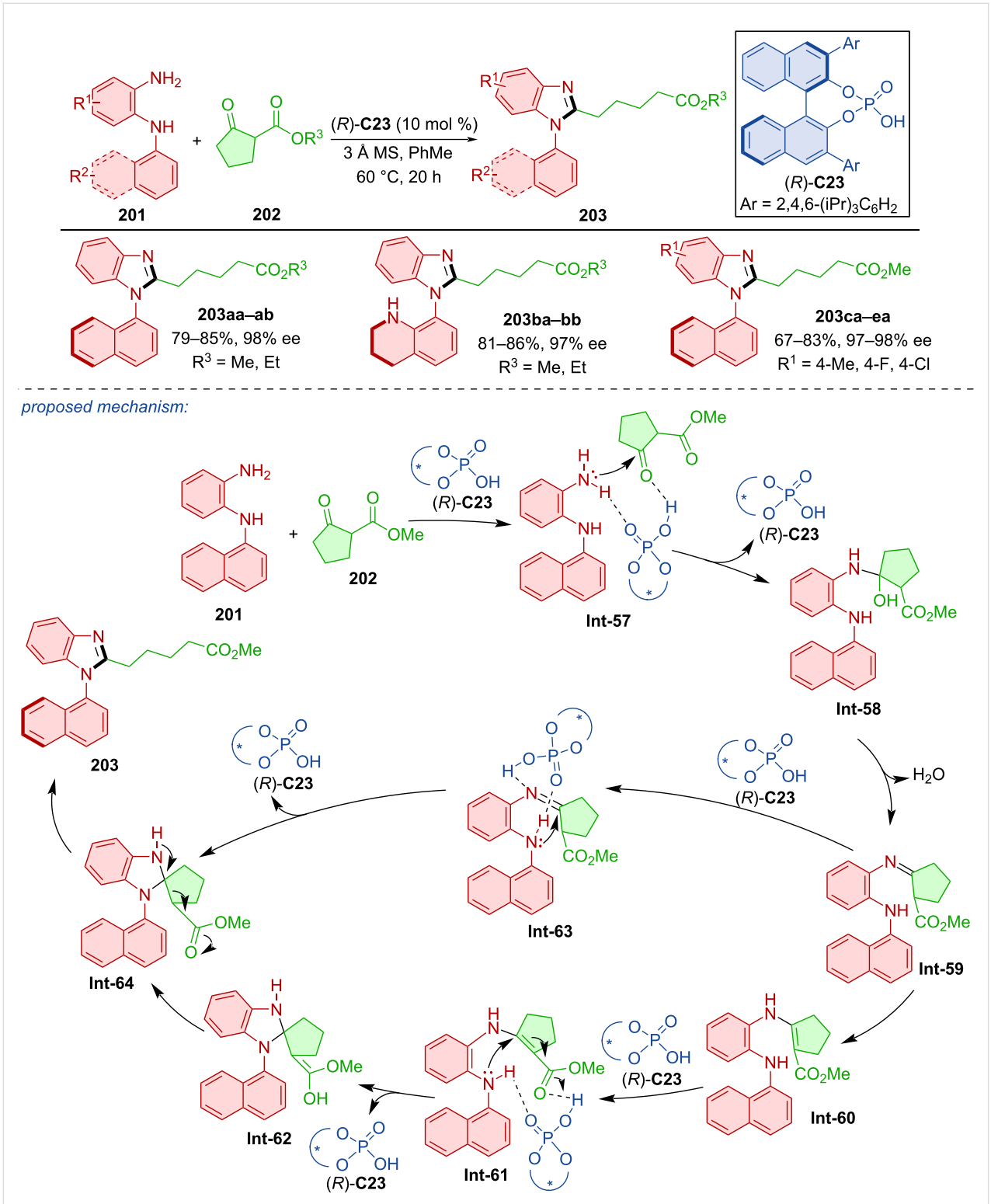

Scheme 60: CPA-catalyzed formation of axially chiral *N*-arylbenzimidazoles.

tion experiment, the rotational barrier of the product **206** was calculated to be 31.1 kcal/mol at 100 °C, corresponding to a half-life of 107 years at 25 °C.

Han et al. developed a protocol to construct pyrrole rings from 1-naphthyl ketoesters **207** and azoalkenes **208** catalyzed by CPA **C47** forming the axially chiral products **209** (Scheme 62)

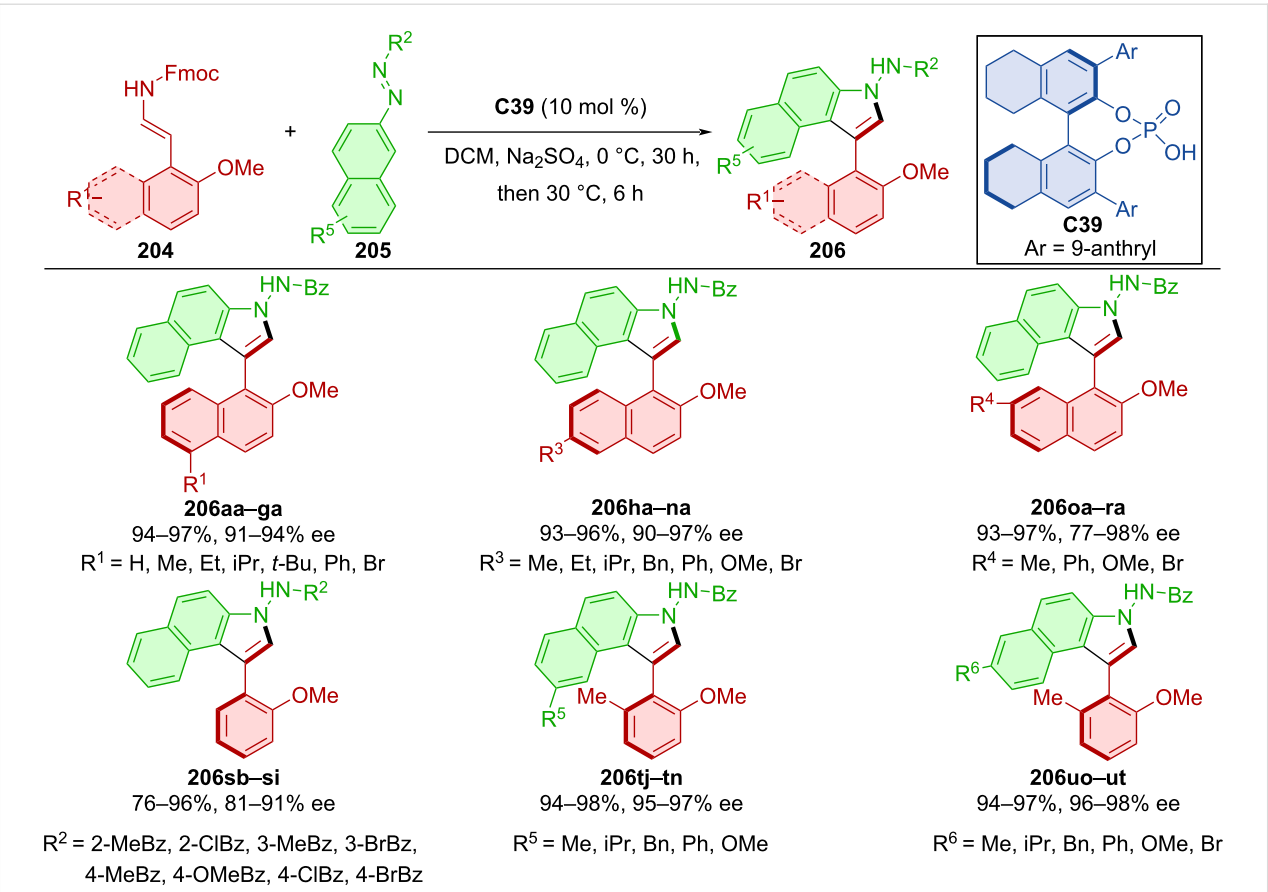

Scheme 61: CPA-catalyzed formation of axially chiral arylbenzoindoles.

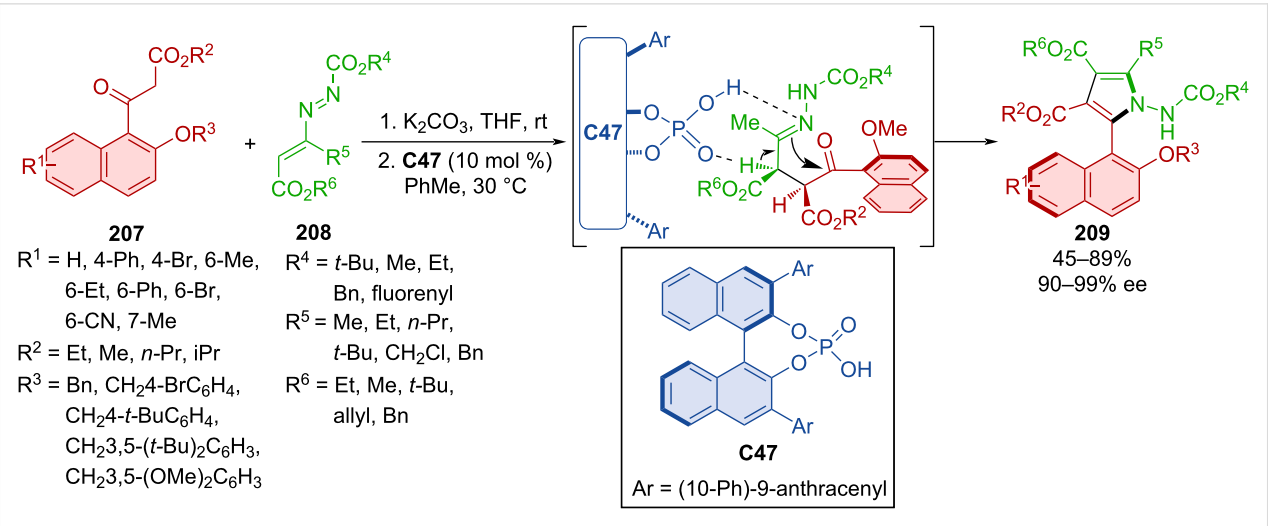

Scheme 62: CPA-catalyzed formation of pyrrolylnaphthalenes.

[92]. The majority of the products were obtained in very good yields and nearly all possessed excellent enantiomeric purities. Racemization experiments were carried out in *m*-xylene and toluene. The rotational barrier of several of products were determined between 30.8 and 32.8 kcal/mol which classifies them as stable class-3 atropoisomers. DFT calculations suggest that the stereoinduction is guided by the hydrogen bonds between catalyst and condensed substrates.

A DFT-guided study of the CPA **C48**-catalyzed reaction of indoles **210** with 2-nitrosonaphthalenes **211** was conducted in 2020 (Scheme 63) [93]. In combination with catalyst hydrogen bonding, the nitroso group was identified as a suitable partner for the nucleophilic substitution by possessing a sufficiently low LUMO energy value. Based on the reaction conditions, two different products were formed. Arylbenzoindoles **212** by standard conditions with 5 mol % catalyst loading and naphthylin-

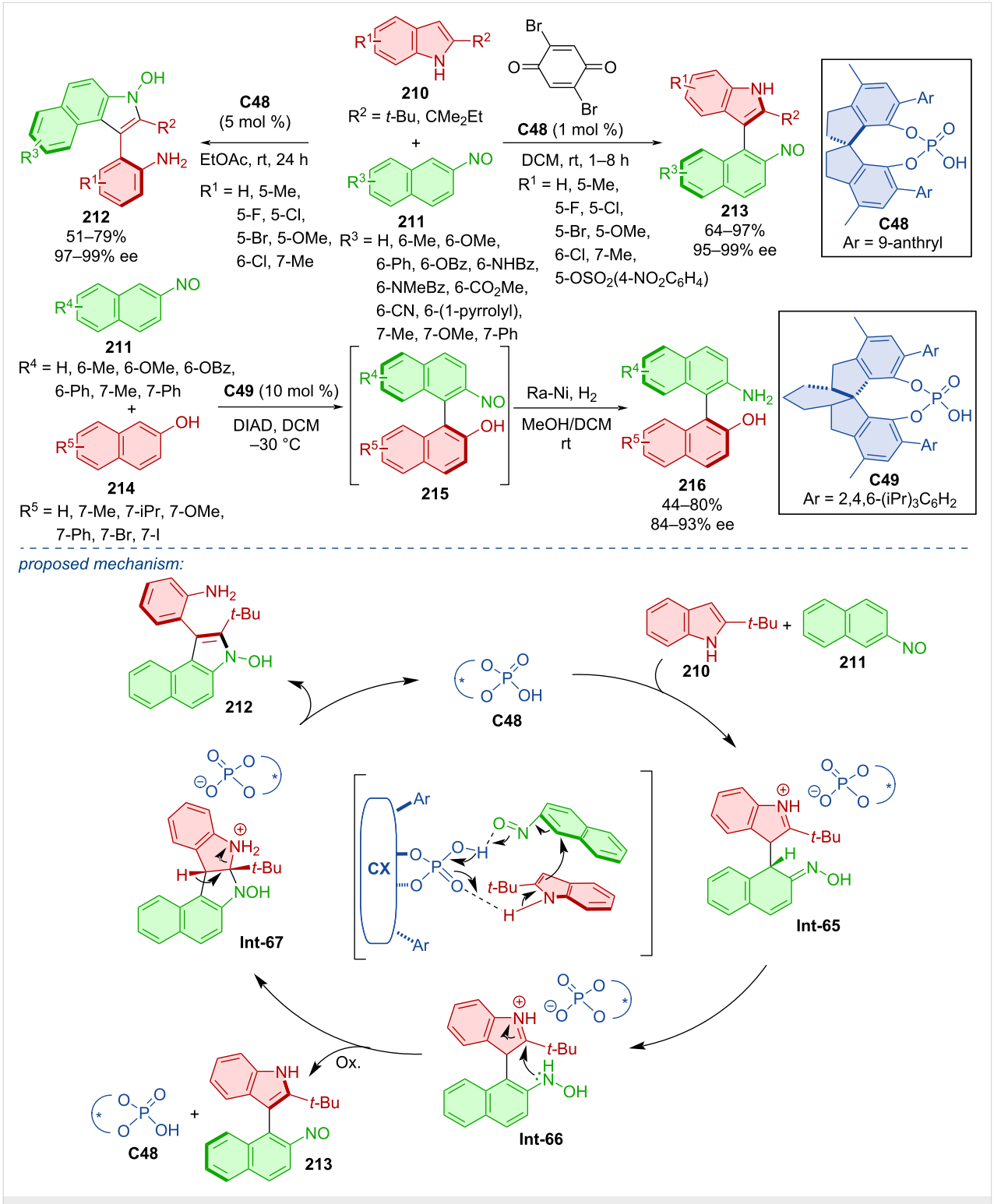

Scheme 63: CPA-catalyzed addition of naphthols and indoles to nitronaphthalenes.

doles **213** by utilization of an oxidant with only 1 mol % catalyst loading. Under these optimized conditions, decent yields and remarkable enantioselectivities were achieved. 2-Nitrosonaphthalenes **211** could also react with 2-naphthols **214** in the presence of CPA **C49** to form axially chiral binaphthyls **215** and finally after hydrogenation atroposelective NOBINs **216**. This reaction yielded products in mostly moderate amounts with good levels of enantiomeric purity. Transition-state calculations gave insight into possible reaction pathways. CPA **C48**-activated substrates react and rearomatization of the benzene ring leads to the intermediate **Int-66**. In the presence of an oxidant, axially chiral product **213** is formed. Otherwise, nitrogen-initiated intramolecular cyclization takes place, subsequent β-H elimination, and C–N-bond cleavage lead to the axially chiral indolylaniline **212**.

Heterobiaryl aldehydes **217a–o** and aminobenzamides **218a–g** reacted in the presence of CPA **C50** leading to axially chiral products **219** (Scheme 64) [94]. Investigating various combinations of naphthyl and phenyl substituents provided satisfactory to good yields in general with high degrees of enantiomeric purity. Scaling up the reaction to a one-mmol scale with reduced catalyst loading of 5 mol % resulted in high yield and slightly decreased enantiomeric purity for the representative product **219oa** (84%, 92% ee).

The unique combination of photochemistry and Brønsted acid-catalysis by CPA (*R*)-**C23** was utilized in the cyclization reaction of cinnamates **220** forming *N*-arylquinolones **221** (Scheme 65) [95]. Optimized reaction conditions led to the formation of products **221** in remarkable yields with astounding enantioselectivities. Both, light and organocatalyst proved crucial for the reaction. The photochemical aspect isomerizes the double bond to (*Z*)-configuration, and CPA stabilizes the structure whilst mediating the cyclization. The wavelength of 405 nm was chosen so that only the starting material, not the organocatalyst nor the product being formed, effectively absorb the light.

An atroposelective C–H amination was done with the help of SPINOL-derived chiral phosphoric acids **C51**, **C40**, and **C42** (Scheme 66) [96]. It was a reaction of naphthalenyldiazene carboxylates **222** with derivatives of carbazole **223** or indole **225**. The reactions provided excellent enantioselectivities and

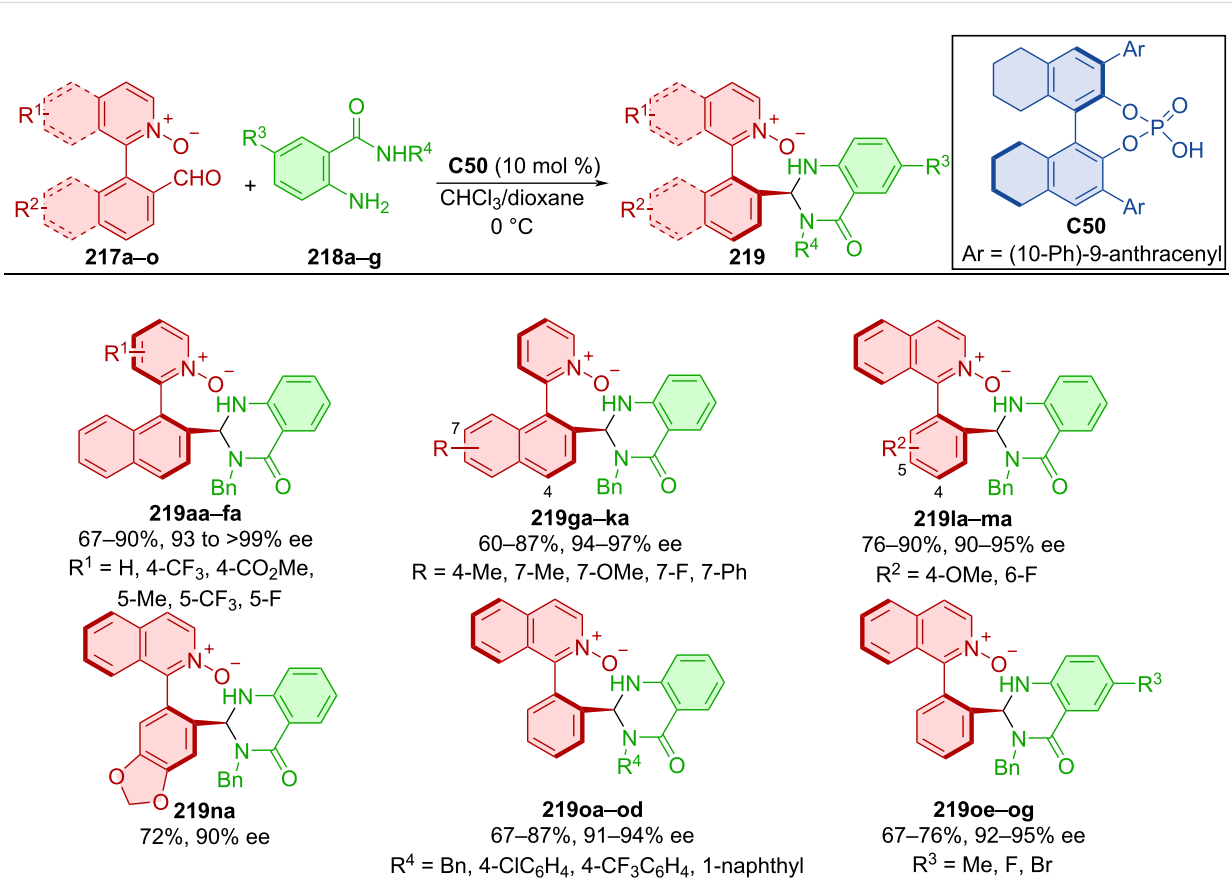

Scheme 64: Atroposelective reaction of heterobiaryl aldehydes and aminobenzamides.

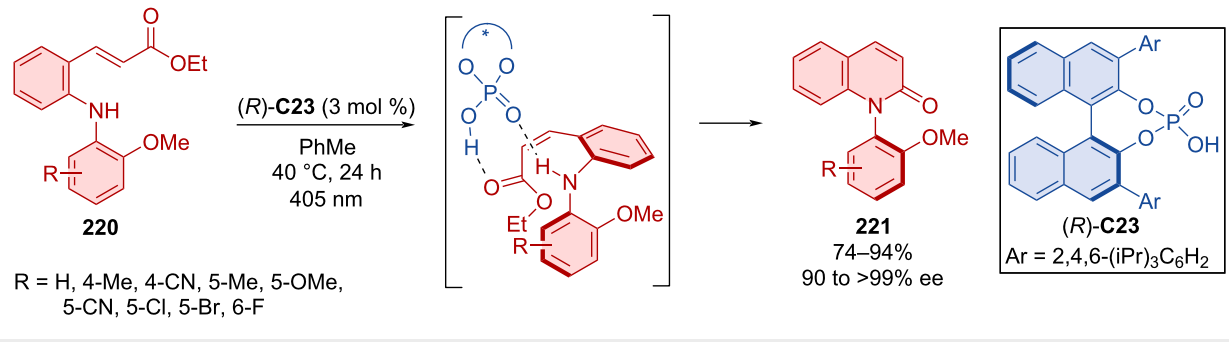

Scheme 65: Atroposelective cyclization forming *N*-arylquinolones.

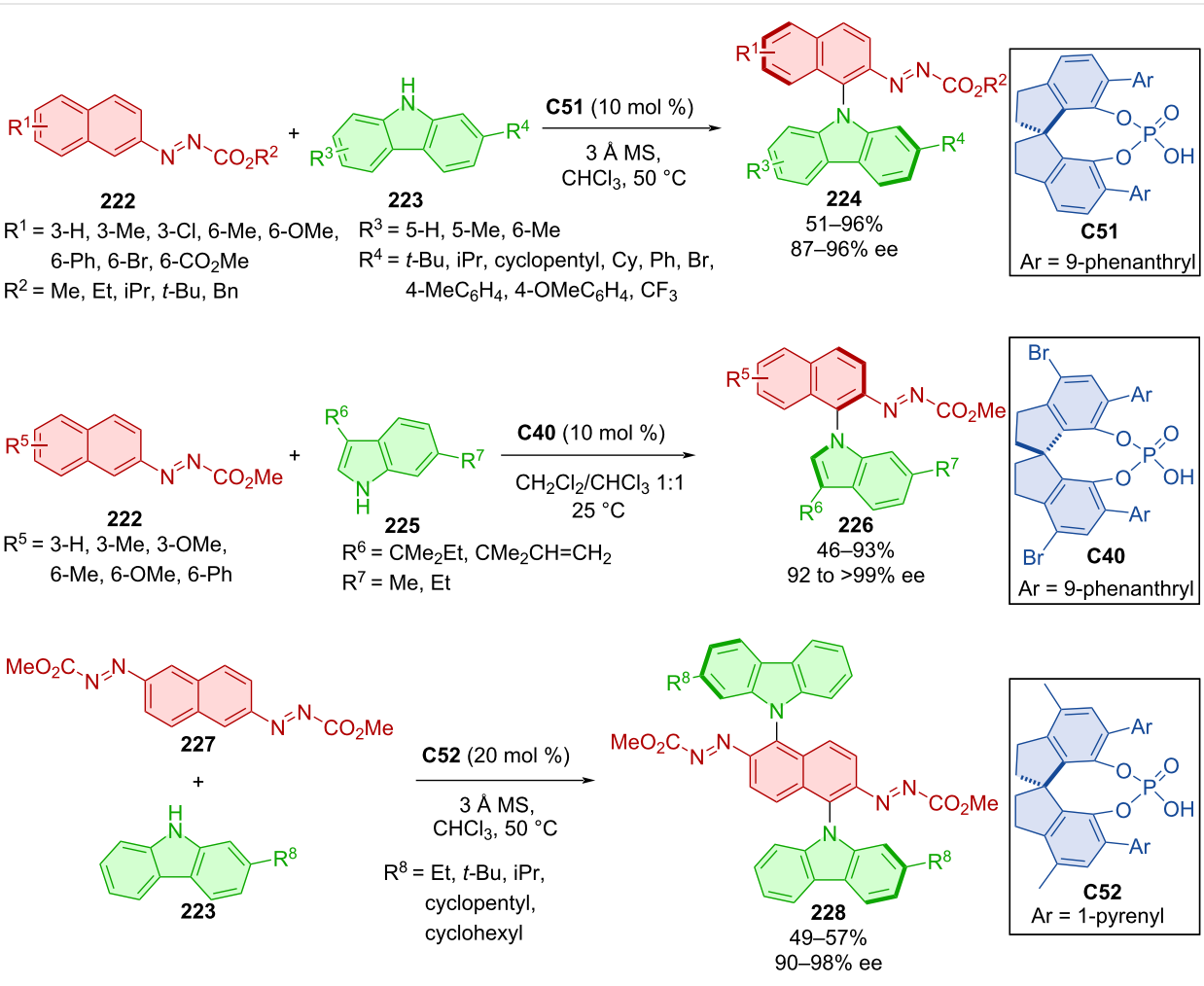

Scheme 66: Atroposelective formation of 9*H*-carbazol-9-ylnaphthalenes and 1*H*-indol-1-ylnaphthalene.

good yields and the best results were achieved with methyl or chlorine substituents in position 3 of the naphthyl ring. Dicarbazoles are generally useful as OLED materials [97]. For this reason, the authors decided to apply the optimized reaction conditions to prepare such compounds. Dicarbazoles **228** were prepared in moderate yields with high enantiomeric purity.

Azonaphthalenes **229** readily reacted with pyrazoles **230** in the presence of CPA **C53** giving access to axially chiral products **231** (Scheme 67) [98]. In the majority of the experiments, great to near-perfect yields and enantioselectivities were reported. The racemization experiment using product **231** in iPrOH at 80 °C resulted in a rotational barrier of 27.3 kcal/mol, which is

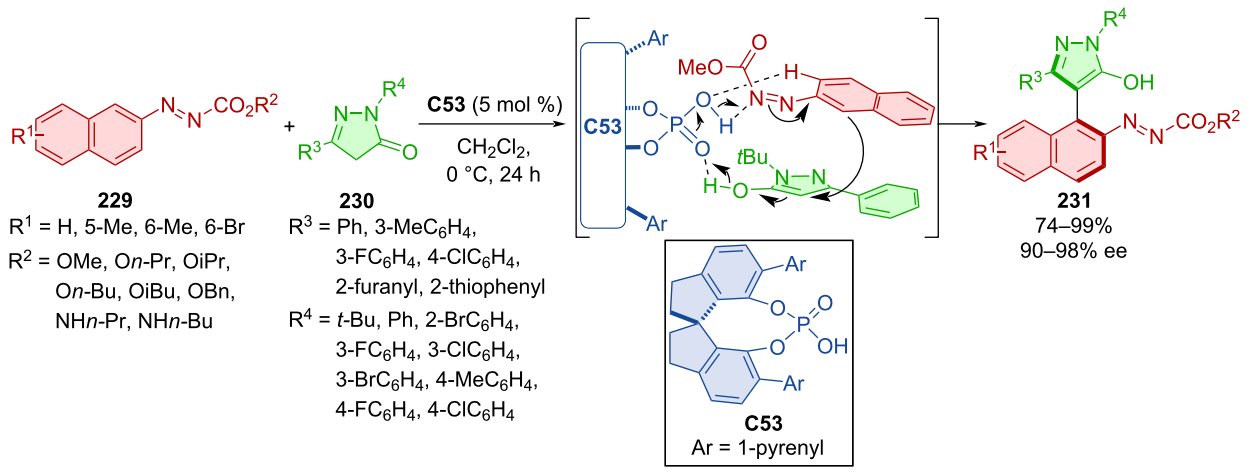

Scheme 67: CPA-catalyzed formation of pyrazolylnaphthalenes.

in good agreement with the calculated value (26.7 kcal/mol). DFT calculations suggest the crucial role of CPA catalyst in the activation of the reaction through corresponding hydrogen bonds.

Gao et al. developed a method of dynamic kinetic resolution providing axially chiral products in good yields, enantio- and diastereoselectivities, but with low rotational barriers (26 kcal/mol) [99].

Yang et al. developed a SPINOL-derived CPA **C54**-catalyzed electrophilic substitution of diazodicarboxamides **233** and azaborinephenols **232** leading to axially chiral products **234** (Scheme 68) [100]. Excellent enantioselectivities and very good yields were reported in almost all cases. More modest yields were reported with different R^3 substituents. The preparative utility of this protocol was demonstrated in the gram-scale reaction providing product **234** in almost identical yield and enantiomeric purity with only 5 mol % catalyst loading (85%, 94% ee). A control experiment without catalyst provided the product (75%), but at a significantly slower rate than the catalyzed one. Methylation of the oxygen in azaborinephenol **232** led to no product being formed. On the other hand, methylation of nitrogen in azaborinephenol **232** still provided the product in decent yield and enantioselectivity (79%, 89% ee) albeit with longer reaction time. A representative axially chiral azaborine exhibited good configurational stability even at 120 °C for 24 h without obvious racemization.

Zhang et al. utilized desymmetrization and kinetic resolution with CPA **C55** in two complementary approaches to prepare atropoisomeric arylpyrrole derivatives (*R*)-**235** and **237** [101]. In the first case, arylpyrroles **235** reacted with either diethyl 2-oxomalonate or dihydroxymalonate ester derivatives **236**

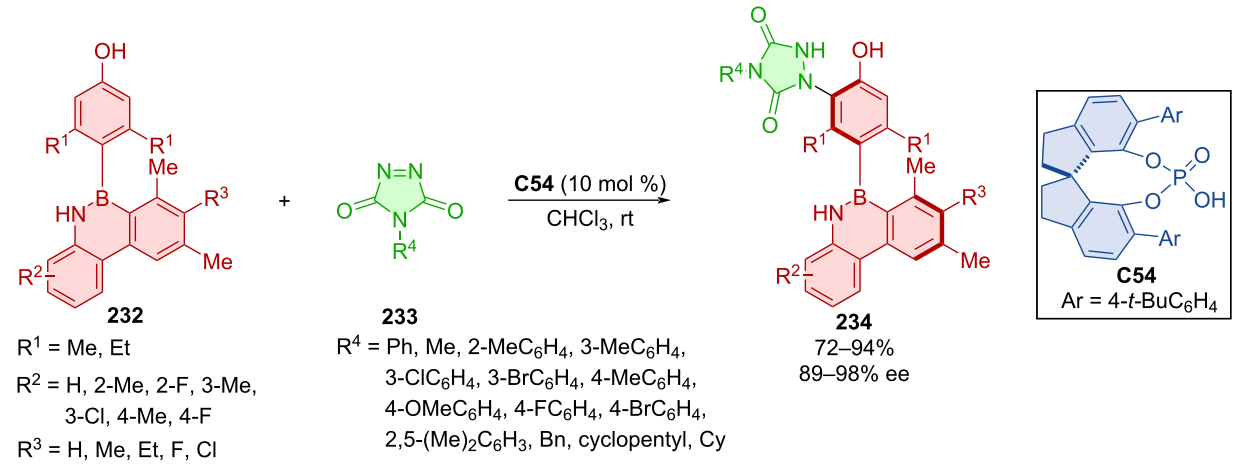

Scheme 68: Atroposelective addition of diazodicarboxamides to azaborinephenols.

(Scheme 69). A kinetic resolution was done with arylpyrroles **235** and diethyl 2-oxomalonate. The possibility of the kinetic resolution was discovered when authors used asymmetrical arylpyrroles **235** instead of symmetrical ones. Both approaches proved effective with high yields and excellent enantioselectivities. Literature research and experimental results gave insight into the potential mechanism of the reaction [102,103]. Hydrogen bonds between the ketomalonate and organocatalyst **Int-68** were shown as the pivotal interaction that formed the chiral pocket for the induction of chirality. Nucleophilic addition followed by rearomatization of the pyrrole ring and protonation of the oxygen forms the axially chiral arylpyrrole **237**.

The organocatalytic cross-coupling reaction of 1-azonaphthalenes **238** with 2-naphthols **239** catalyzed by chiral *N*-triflylphosphoramide **C56** was done in 2023 (Scheme 70) [104]. A remarkable number of axially chiral products **240** were prepared with excellent enantiomeric purities and high yields. Undiminished yields and enantioselectivities (99%, 94% ee) were observed in a gram-scale experiment with only 2 mol % of the organocatalyst **C56**.

The CPA **C57**-catalyzed kinetic resolution was utilized in the formation of axially chiral oxindole-based styrenes (*S*)-**243** and (*R*)-**241** (Scheme 71) [105]. On top of good enantioselectivities and decent yields, very good diastereomeric ratios (up to 94:6)

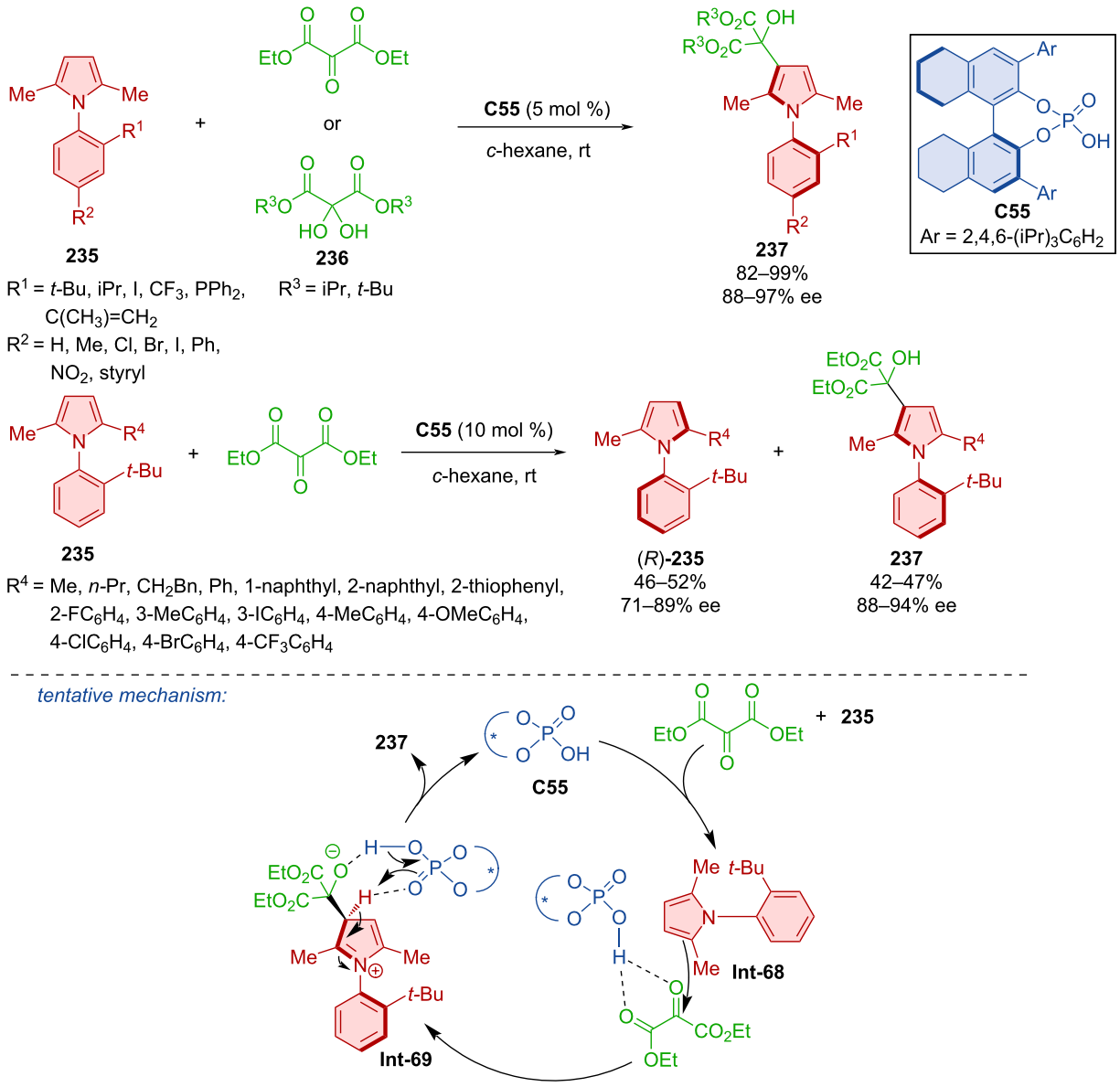

Scheme 69: Catalytic formation of axially chiral arylpyrroles.

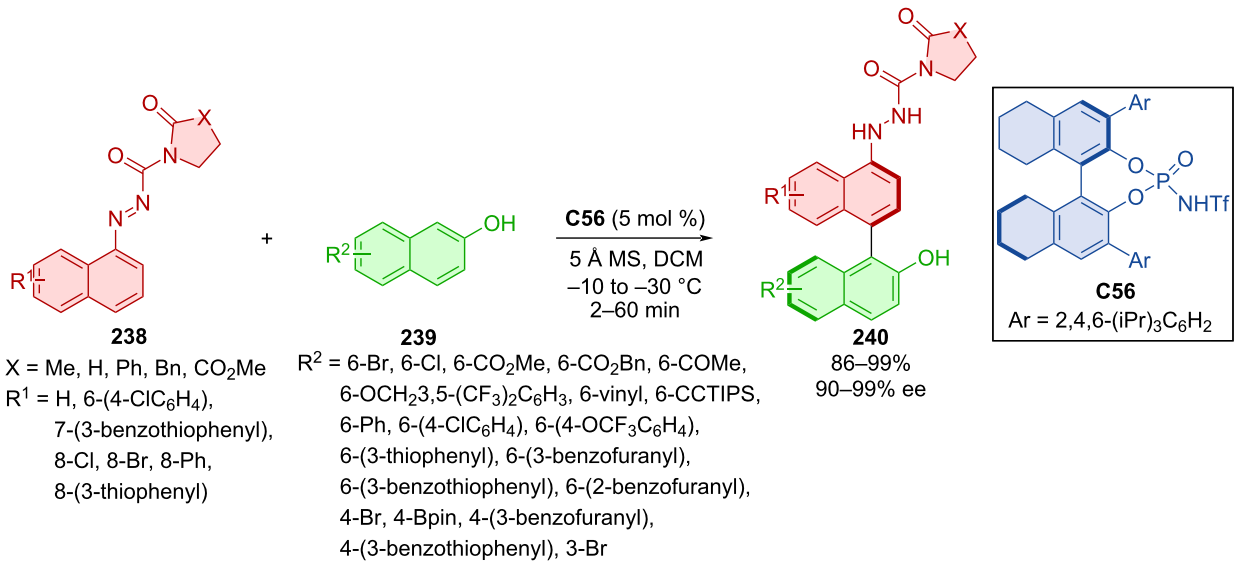

Scheme 70: Atroposelective coupling of 1-azonaphthalenes with 2-naphthols.

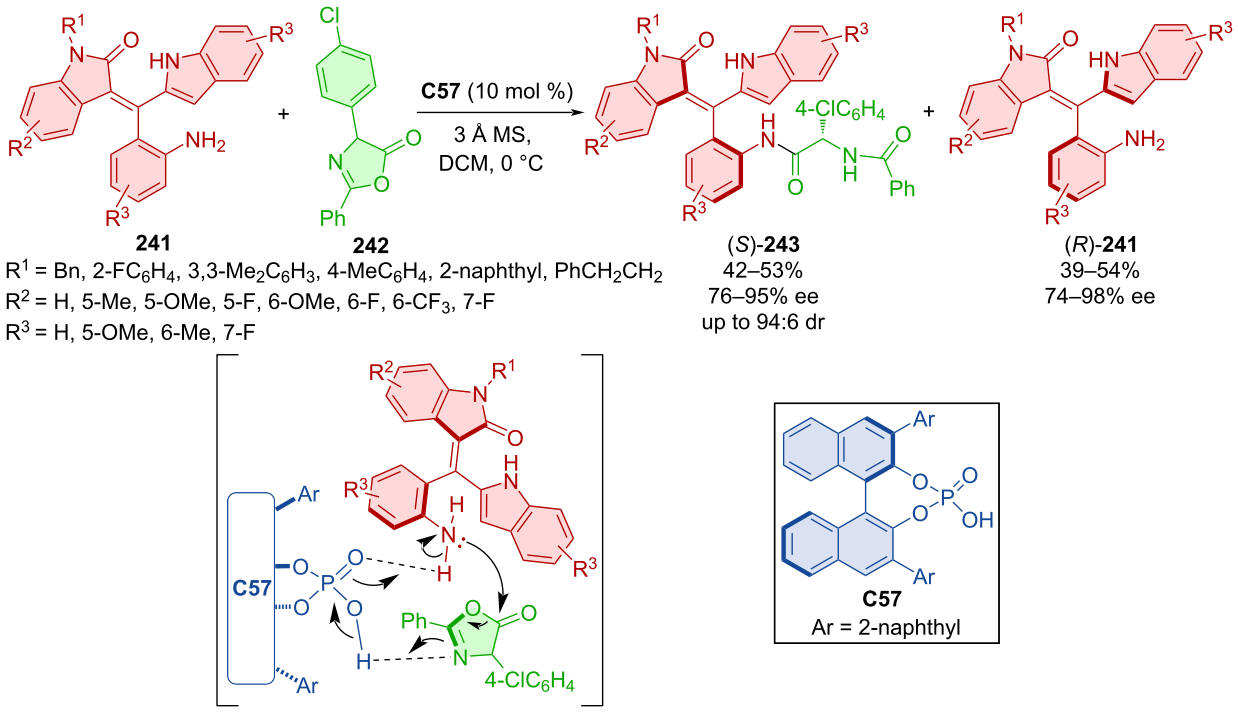

Scheme 71: CPA-catalyzed formation of axially chiral oxindole-based styrenes.

were achieved. The suggested stereoinduction is shown below, with CPA forming hydrogen bonds and activating both substrates. The products incorporated into a thiourea organocatalyst were utilized in (4 + 2) and (3 + 2) annulation reactions providing moderate to high yields, low enantioselectivities, but excellent diastereomeric ratios (57–91%, 32–41% ee, >95:5 dr).

Shao, Cheng, and co-workers developed an atroposelective synthesis of axially chiral styrene-type allylamines [106]. A chiral phosphoric acid organocatalyst catalyzed the key transformation, the reductive amination of 1-enal-substituted 2-naphthols.

Vaidya et al. developed an atroposelective organocatalytic electrophilic halogenation of aminonaphthoquinones **244** with NBS

catalyzed by biaryl catalyst **C33** (Scheme 72) [107]. This seemingly two-axes system is simplified into a single-axis system by a strong intramolecular N–H–O hydrogen bond. Enantiopurities and yields of products **245** were very high. Racemization studies showed that product **245** is a stable class-3 atropoisomer with a barrier of rotation of 30.3 kcal/mol at 100 °C in toluene. Testing in ethanol at 80 °C and in strongly acidic conditions (EtOH/0.5 M HCl 4:1) provided only a slight decrease to 29.1 kcal/mol and 28.9 kcal/mol, respectively, or remained largely unchanged at 30.6 kcal/mol with toluene under buffered aqueous conditions (pH 7.5 in 1 M Tris buffer). These findings suggest this compound would be stereochemically stable in biological environments, showing potential usefulness in medicinal chemistry.

A peculiar class of atropoisomers was prepared in 2024 by bromination catalyzed by CPA (*R*)-**C23** (Scheme 73) [108]. The DABCO-derived cationic bromination agent **247** was used with dienes **246a–o** to form axially chiral dienes **248a–o**. Considerable substrate scope demonstrated via a wide range of products **248a–o** in high yields and remarkable enantiomeric purities. Bromine could subsequently be reacted further, expanding on the synthetic utility of the products. The authors ascertained that the Grignard exchange reaction with PhMgCl could reconvert products **248a–o** into reactive nucleophilic intermediates. The rotational barrier of the product **248a** was determined 36.4 kcal/mol by DFT calculations and 35.5 kcal/mol experimentally.

A dual photoredox and CPA-catalyzed process was developed for the atroposelective construction of axially chiral 5-arylpyrimidines **251** [109]. The strategy relied on a Minisci-type reaction of 5-arylpyrimidines **249** and α-amino acid-derived redox-active esters **250**. This transformation was enabled by 4CzIPN as an organic photoredox catalyst in conjunction with a chiral phosphoric acid catalysts (*R*)-**C23**, **C58**, or **C59** (Scheme 74).

CPA **C60** catalyzed the asymmetric hydrolysis of biaryloxazepines **252a–aa** leading to the formation of axially chiral biarylamides **253a–aa** (Scheme 75) [110]. This method proved to be a reliable strategy providing axially chiral products **253a–aa** in excellent yields and enantiomeric purities. Starting from racemic **253** by subsequent Mitsunobu reaction and CPA-catalyzed asymmetric hydrolysis on a 2.0 mmol scale reaction, a comparably high yield and enantioselectivity was achieved (95%, 96% ee).

The unique preparation of axially chiral biarylsiloxanes **256** from dinaphthosiloles **254** and silylalcohols **255** catalyzed by chiral *N*-triflylphosphoramide **C61** was first done in 2023 (Scheme 76) [111]. Exceptional enantioselectivities and very good yields were achieved with many different dinaphthosiloles containing groups in positions 6 and 7 and a number of silylalcohols as well as in a gram-scale synthesis (90%, 91% ee). The synthetic utility of the reaction stems from efficient atom economy, scalability, operational simplicity, mechanistic novelty, and preparation of axially chiral ligands. The authors presented a proposed reaction mechanism substantiated by DFT calculations. The chiral organocatalyst **C61** forms intermediate **Int-70** stabilized by β-sillicon effect. Subsequent addition, deprotonation, and ring opening leads to the formation of axially chiral biaryl siloxane **256**.

Jiang et al. utilized phenylacrylaldehydes **257** and pinacolborane in combination with CPA **C21**, promoting asymmetric hydrogenation to obtain axially chiral aryl allylalcohols **258** (Scheme 77) [112]. The reaction afforded a wide range of products **258** in synthetically relevant yields with very high enantioselectivities. Heating in isopropanol at 60 °C led to a decrease

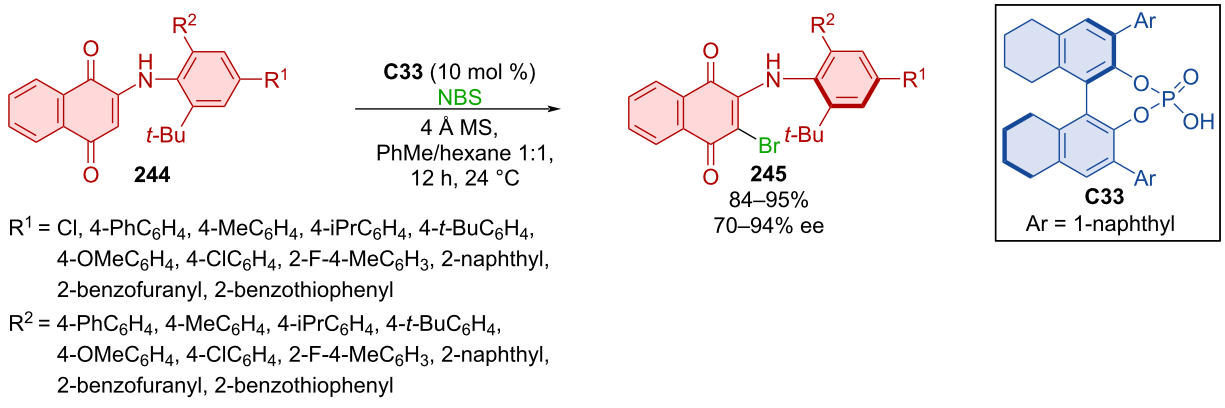

Scheme 72: Atroposelective electrophilic bromination of aminonaphthoquinones.

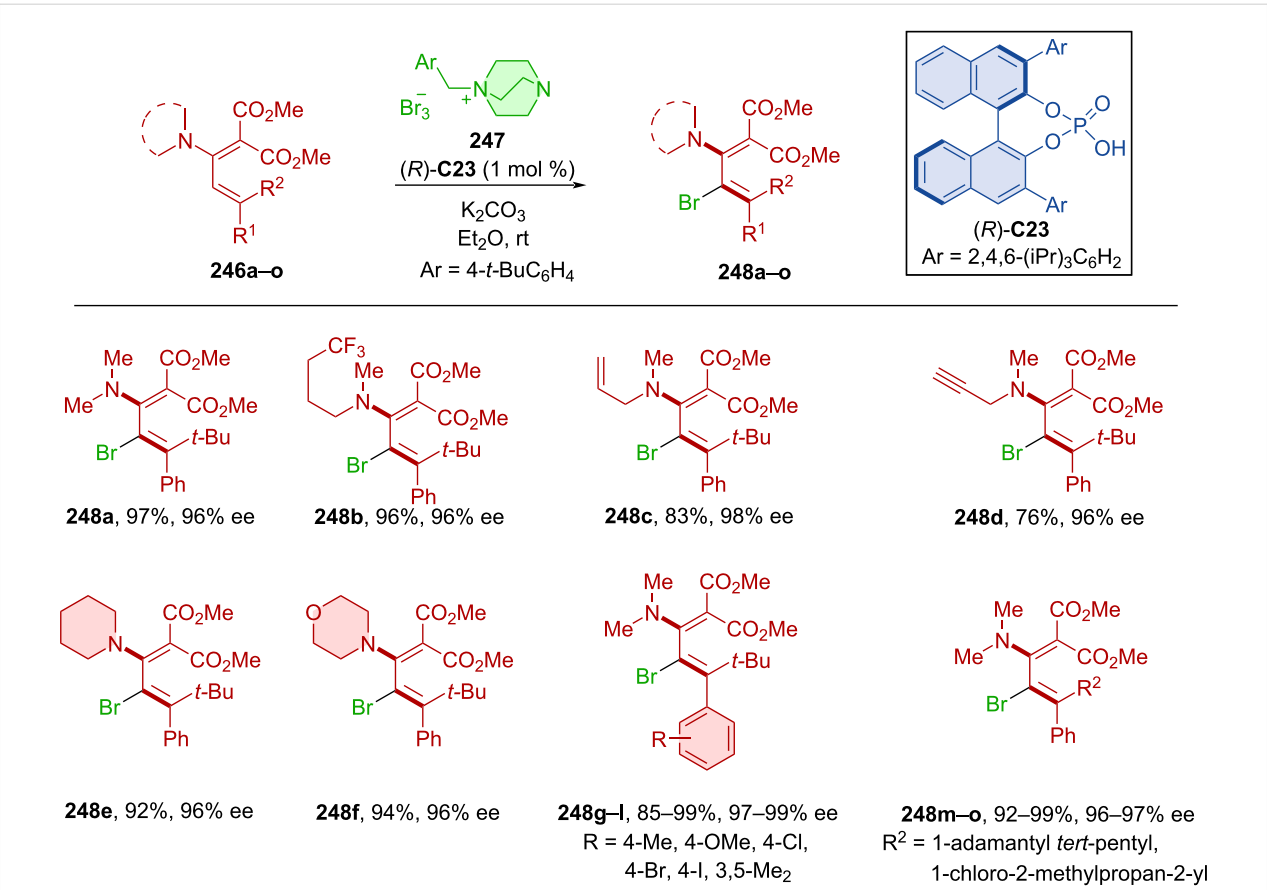

Scheme 73: Atroposelective bromination of dienes.

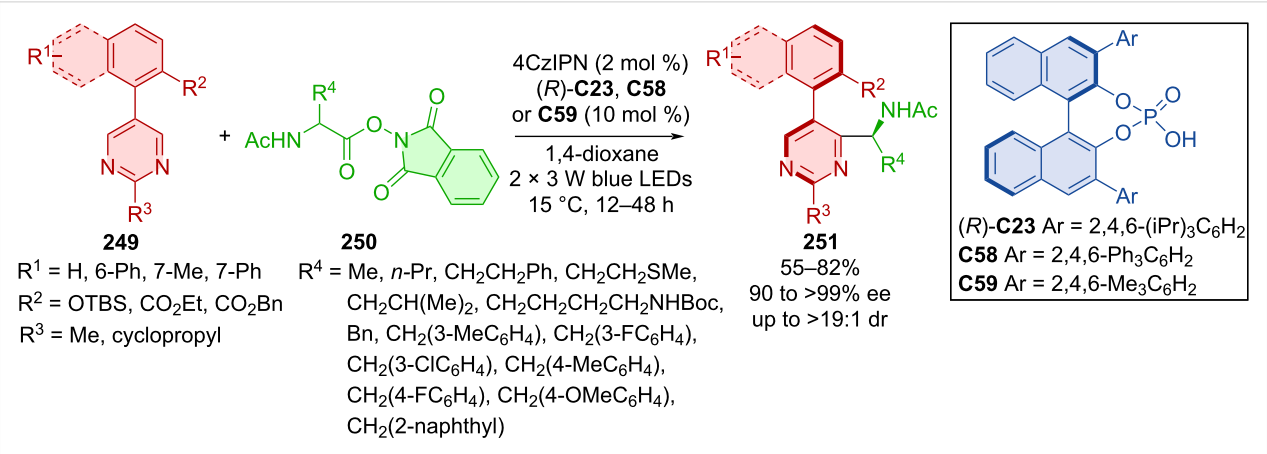

Scheme 74: CPA-catalyzed formation of axially chiral 5-arylpyrimidines.

in ee values and the experimentally calculated racemization barrier was set to 27.9 kcal/mol.

Hydrogen-bond-donating catalysts

Hydroquinine **C62** was utilized in the dynamic kinetic resolution of racemic naphthylamides **259a**,**b** by atroposelective alkylation with carbonates **260a**–**n** forming axially chiral products **261** (Scheme 78) [113]. Good to high yields and excellent enantioselectivities were achieved with a slight decrease of enantioselectivity (66 and 48% ee) on substrates with a methyl or methoxy group in position 4 of 2-naphthol. Comparable results were achieved in the gram-scale preparation of product **261ae**,

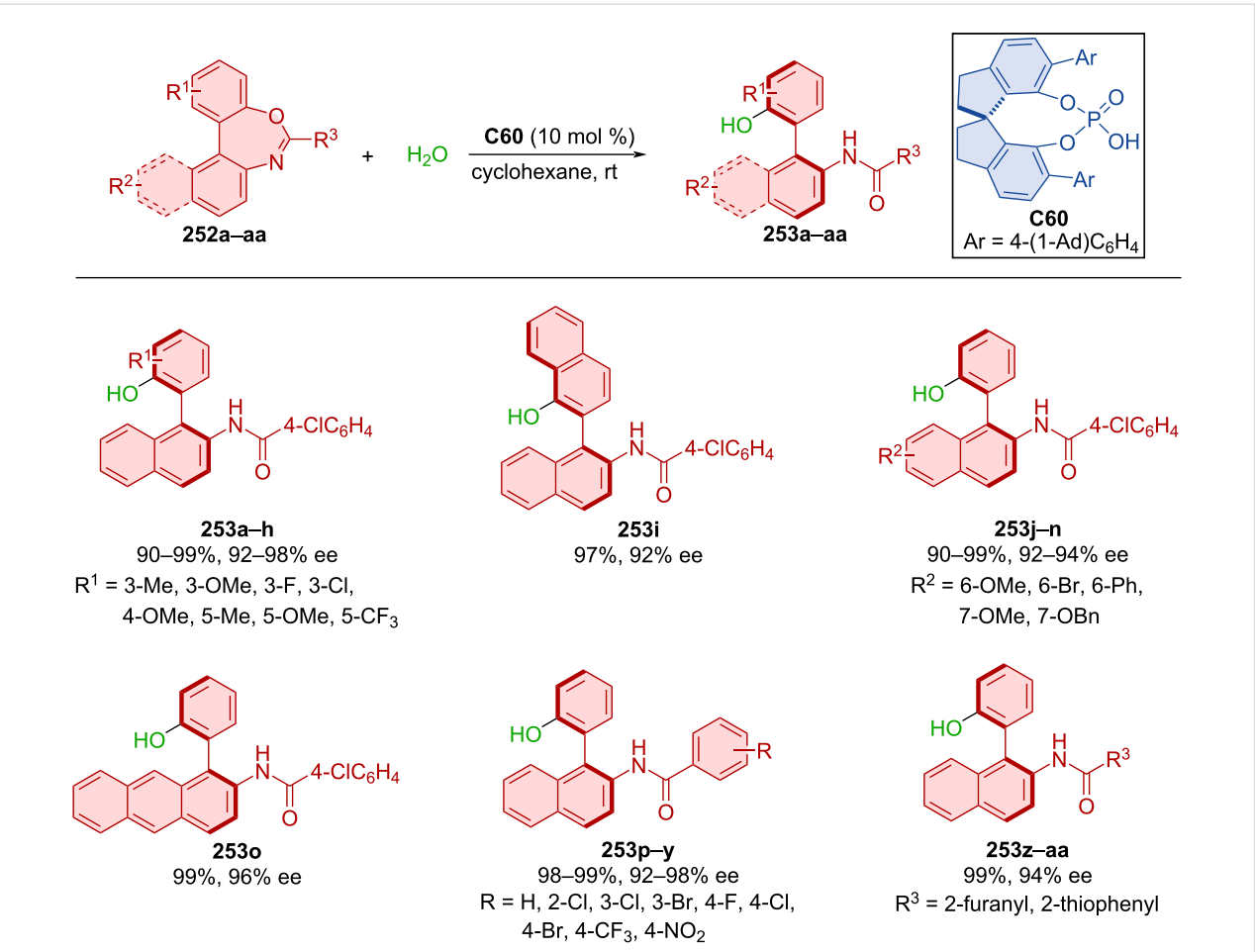

Scheme 75: Atroposelective hydrolysis of biaryloxazepines.

achieving >99% ee after recrystallization. The organocatalyst interacts with the substrates through hydrogen bonds with the oxygen of the naphthylamide and covalent interaction with carbonate.

Yang et al. developed an asymmetric atroposelective *N*-alkylation of phosphinamides **262** with carbonates **263** catalyzed with hydroquinidine **C63** forming axially chiral *N*-alkylated phosphinamides **264** (Scheme 79) [114]. Moderate to high yields and very good enantioselectivities were reported utilizing the optimized reaction conditions. DFT calculations suggest that stereocontrol is derived from a weak hydrogen bond between iodine in the *ortho* position and other hydrogens on sp^2 carbons throughout both substrates. The opposite enantiomer would require the methyl group to vacate this chiral pocket, which would cause steric repulsion. This unfavorable transition state was calculated to have a 2.0 kcal/mol higher energy than the favorable one. Hypervalent iodine(III) present in the products could be used to catalyze the asymmetric oxidative dearomatization of phenols.

Atroposelective *N*-alkylations catalyzed by quinidine **C64** were also done by Mei et al. in 2021 (Scheme 80) [115]. In one reaction, carbonates **266a–d** were used as alkylation reagents, along with aminopyrroles **265a–g**. The second was the reaction of aminoquinazolinones **268** with similar carbonates **266**. Axially chiral products **267** and **269**, respectively, were prepared with very high levels of enantiopurity and high yields. Racemization experiments carried out on product **269** led to decreased ee values over time. Through these experiments and DFT calculations, rotational barriers were calculated between 29.6 and 32.3 kcal/mol.

Carbonates **271** proved suitable reaction partners for arylsulfinamides **270** in the presence of hydroquinine **C62** affording alkylated axially chiral sulfinamides **272** (Scheme 81) [116]. A wide range of moderate to high yields were achieved with consistently high enantioselectivities and mostly high diastereoselectivities. The investigation of the rotational barrier provided a good result (31.1 kcal/mol) for the chosen product **272**, indicating a half-life of up to 11.1 hours at 105 °C.

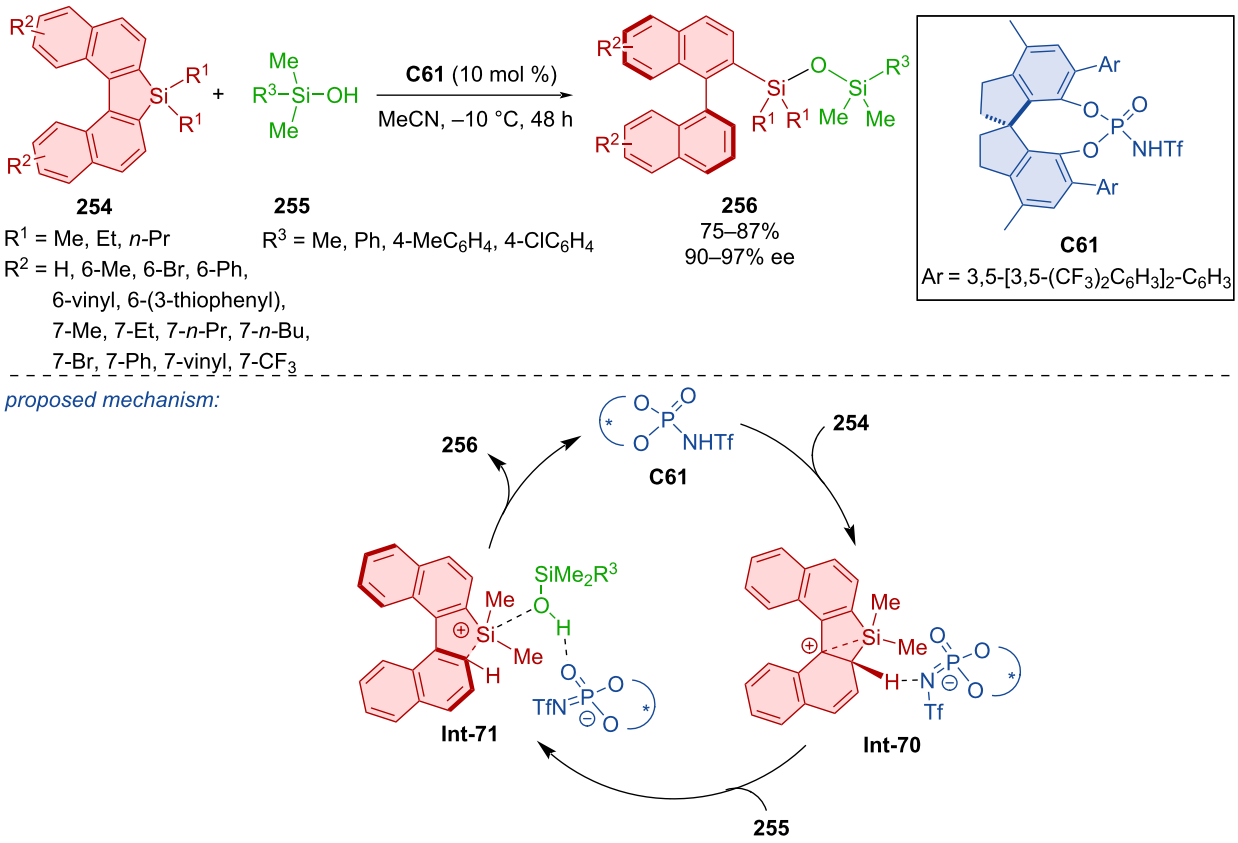

Scheme 76: Atroposelective opening of dinaphthosiloles.

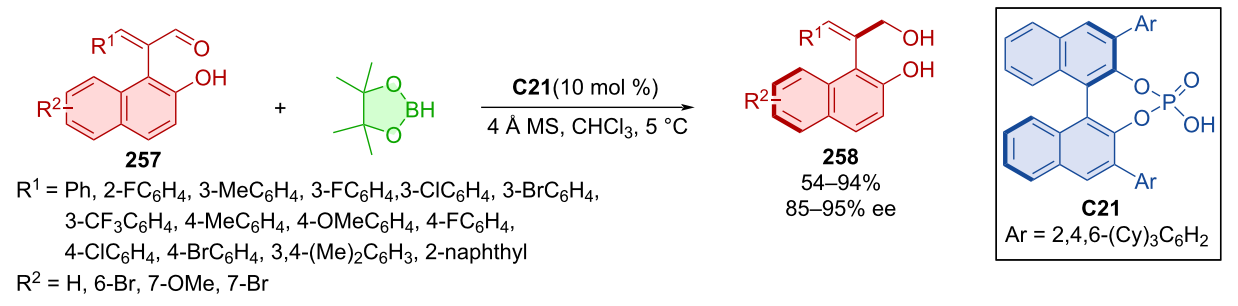

Scheme 77: Atroposelective reduction of naphthylenals.

Huang et al. demonstrated one case of asymmetrically prepared selenovinylsulfones in the presence of quinine-derived squaramide in moderate yield and good enantioselectivity (43%, 84% ee) [117].

Aminosulfones **274** acted as nucleophiles in the reaction with arylynones **273** mediated by cinchona alkaloid squaramide **C65** resulting in axially chiral products **275** (Scheme 82) [118]. In all cases, the *E*-isomer was predominant and good to excellent yields with very high enantioselectivities were reported. The model product **275** was successfully tested in reactions with a Grignard reagent and sodium tetrahydroborane resulting in the expected products.

Alkynyl-2-naphthols **276** with 5*H*-oxazolones **277** in the presence of chiral squaramide bearing quinine units **C66** were being utilized in the formation of axially chiral products **278** (Scheme 83) [119]. These unique structures containing a double bond, central and axial asymmetry were prepared in amazing yields, great enantiomeric purities, and high diastereomeric

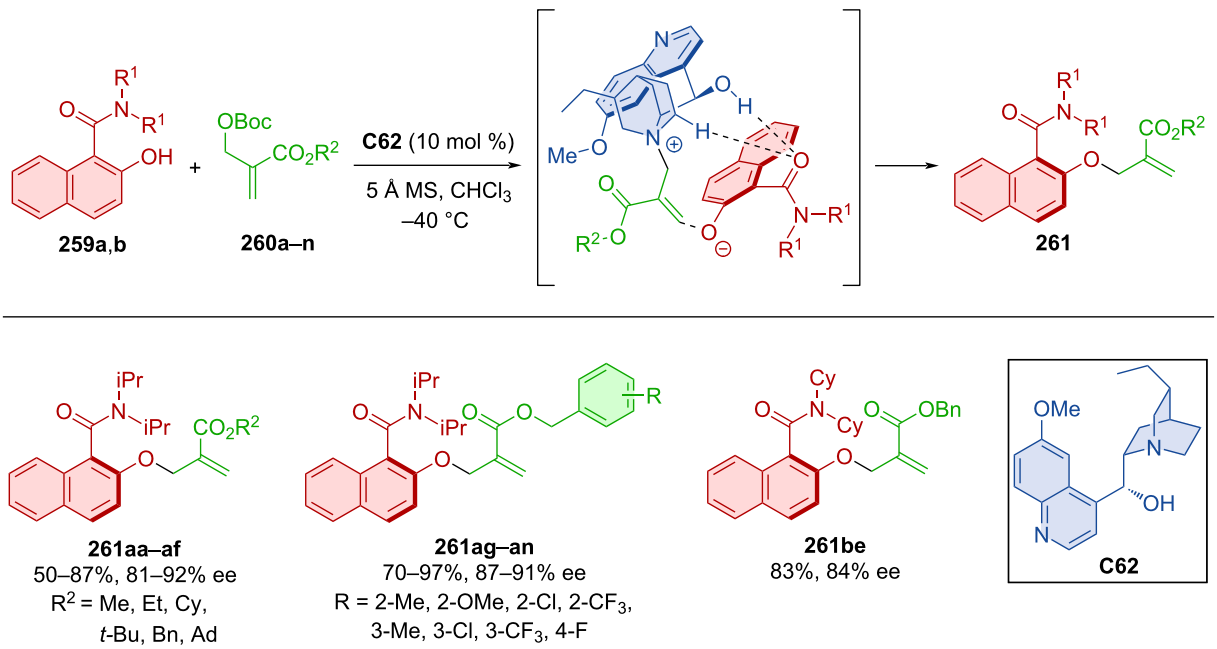

Scheme 78: Atroposelective allylic substitution with 2-naphthols.

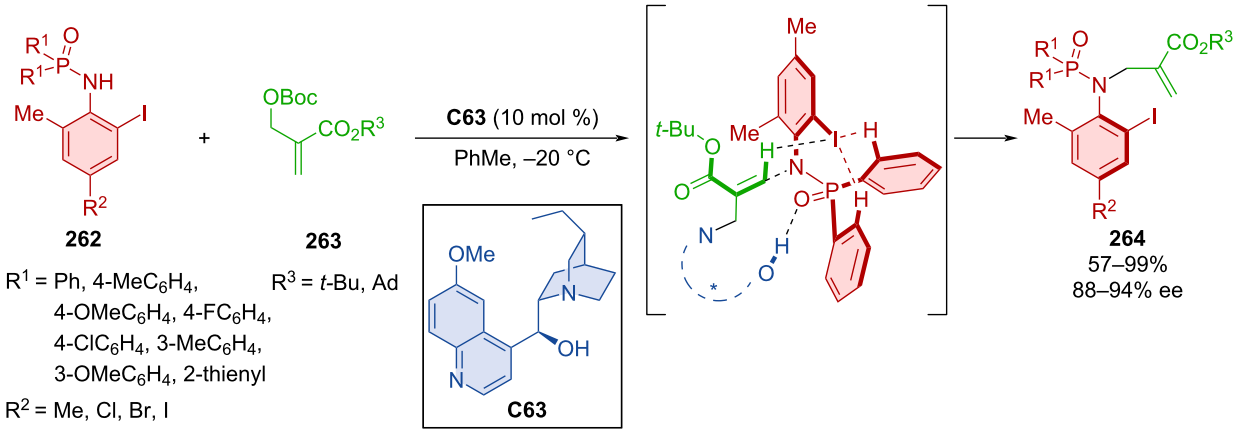

Scheme 79: Atroposelective allylic alkylation with phosphinamides.

ratios as one *E*/*Z* isomer. A possible mode of activation is shown below with amino squaramide hydrogens participating in hydrogen bonds with in situ-formed VQM intermediate from alkynyl-2-naphthol. The activated oxazolone in enol form on the other hand is stabilized by the quinine nitrogen. The favorability of this approach is based upon the phenyl group of the alkynyl-2-naphthol being oriented in a way that provides decreased sterical hinderance.

Zhang et al. developed a methodology involving cyclopropane-ring opening of **280** and alkynyl-2-naphthols **279** with the help of hydroquinine-derived squaramide **C67** leading to axially chiral products **281** (Scheme 84) [120]. Optimized reaction conditions afforded products **281** in moderate to decent yields with consistently high enantiomeric purities.

Zhang et al. leveraged photochemical conditions, mesityl acridinium as photocatalyst and chiral squaramide **C67** to prepare axially chiral products **284** starting from alkynyl-2-naphthols **282a–g**, alkyl fluoroborates **283a–e** and a source of sulfur dioxide (Scheme 85) [121]. A wide variety of products **284** were separated as single enantiomers with great diastereoselec-

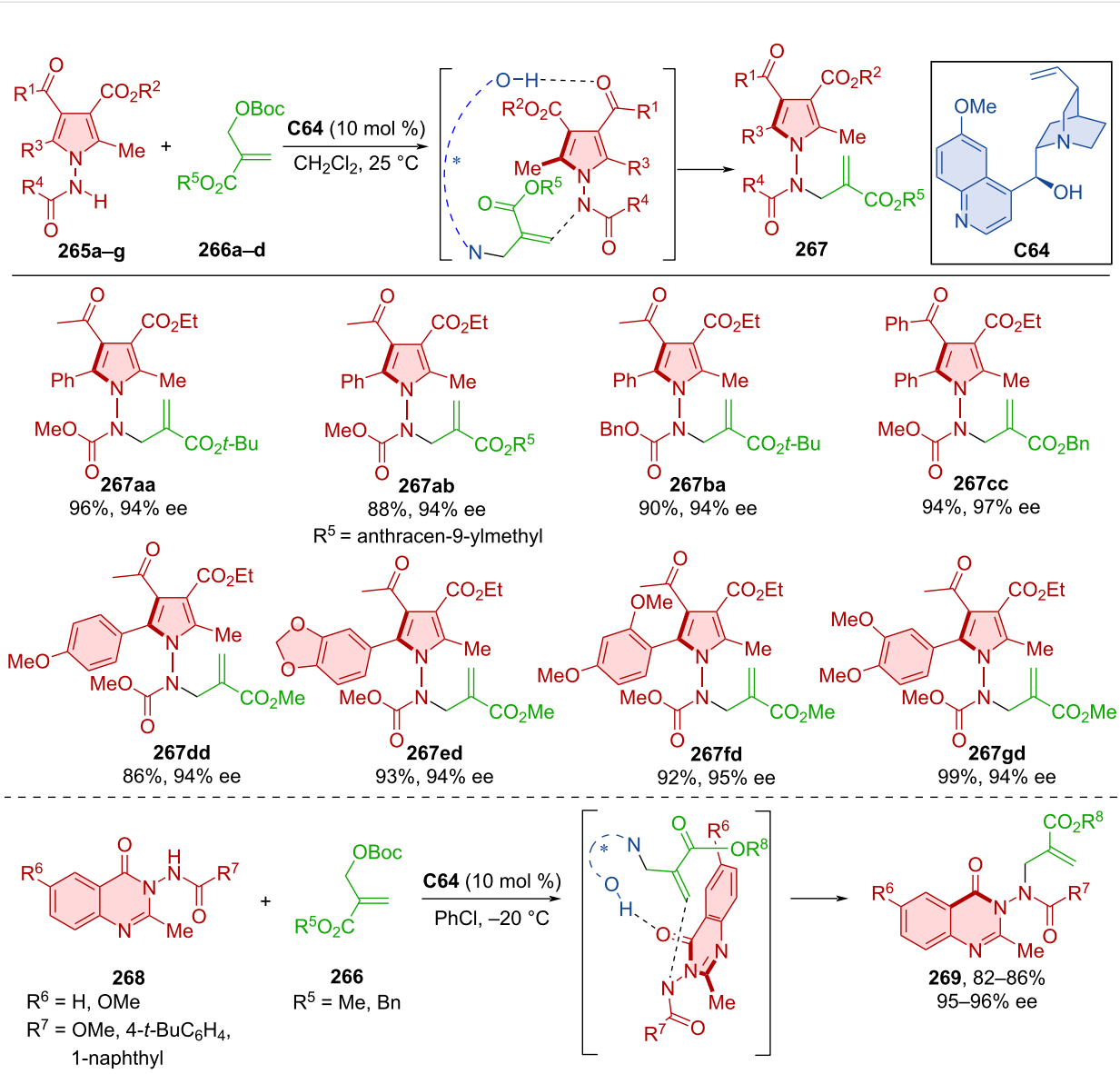

Scheme 80: Atroposelective allylic substitution with aminopyrroles.

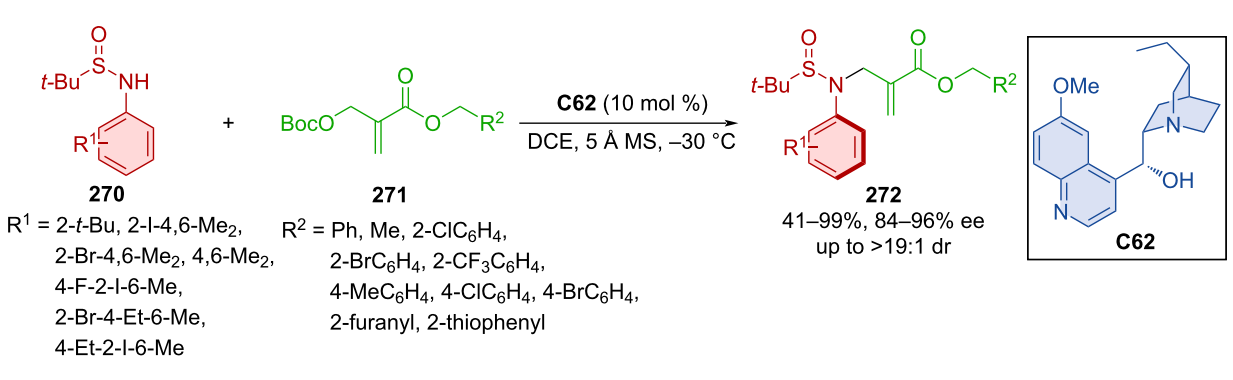

Scheme 81: Atroposelective allylic substitution with aromatic sulfinamides.

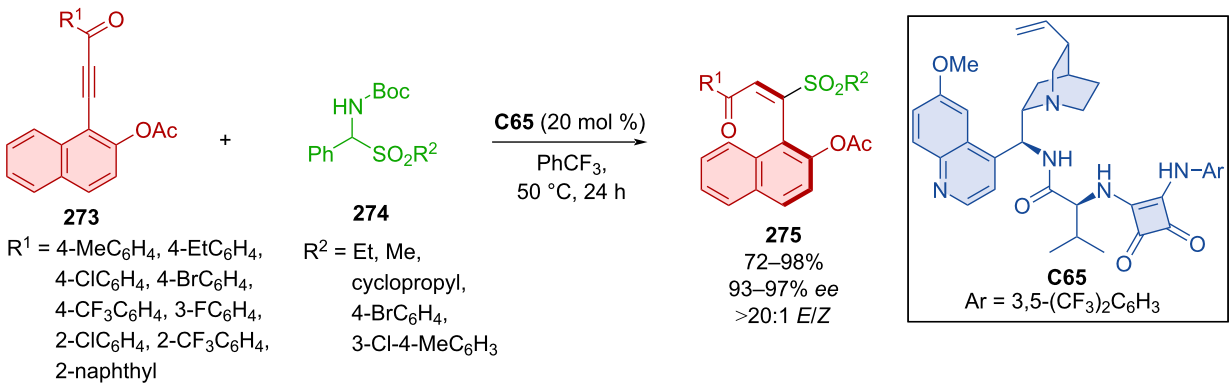

273
R^1 = 4-MeC_6H_4, 4-EtC_6H_4, 4-ClC_6H_4, 4-BrC_6H_4, 4-$CF_3C_6H_4$, 3-FC_6H_4, 2-ClC_6H_4, 2-$CF_3C_6H_4$, 2-naphthyl

274
R^2 = Et, Me, cyclopropyl, 4-BrC_6H_4, 3-Cl-4-MeC_6H_3

275
72–98%
93–97% *ee*
>20:1 *E*/*Z*

C65
Ar = 3,5-$(CF_3)_2C_6H_3$

Scheme 82: Atroposelective sulfonylation of naphthylynones.

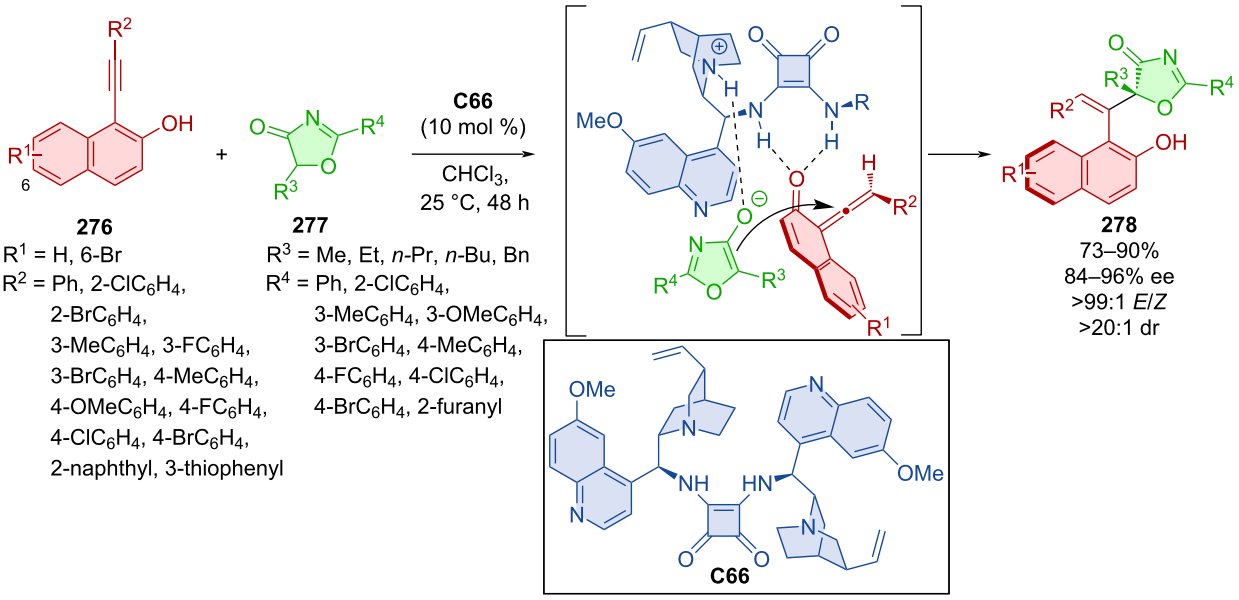

276
R^1 = H, 6-Br
R^2 = Ph, 2-ClC_6H_4, 2-BrC_6H_4, 3-MeC_6H_4, 3-FC_6H_4, 3-BrC_6H_4, 4-MeC_6H_4, 4-$OMeC_6H_4$, 4-FC_6H_4, 4-ClC_6H_4, 4-BrC_6H_4, 2-naphthyl, 3-thiophenyl

277
R^3 = Me, Et, *n*-Pr, *n*-Bu, Bn
R^4 = Ph, 2-ClC_6H_4, 3-MeC_6H_4, 3-$OMeC_6H_4$, 3-BrC_6H_4, 4-MeC_6H_4, 4-FC_6H_4, 4-ClC_6H_4, 4-BrC_6H_4, 2-furanyl

278
73–90%
84–96% ee
>99:1 *E*/*Z*
>20:1 dr

Scheme 83: Squaramide-catalyzed reaction of alkynyl-2-naphthols with 5*H*-oxazolones.

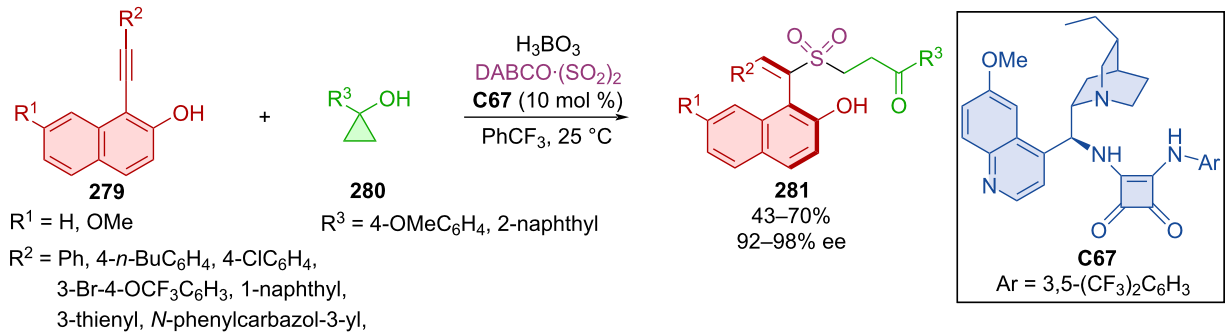

279
R^1 = H, OMe
R^2 = Ph, 4-*n*-BuC_6H_4, 4-ClC_6H_4, 3-Br-4-$OCF_3C_6H_3$, 1-naphthyl, 3-thienyl, *N*-phenylcarbazol-3-yl, $CH_2CH(CO_2Me)_2$

280
R^3 = 4-$OMeC_6H_4$, 2-naphthyl

281
43–70%
92–98% ee

Scheme 84: Formation of axially chiral styrenes via sulfonylative opening of cyclopropanols.

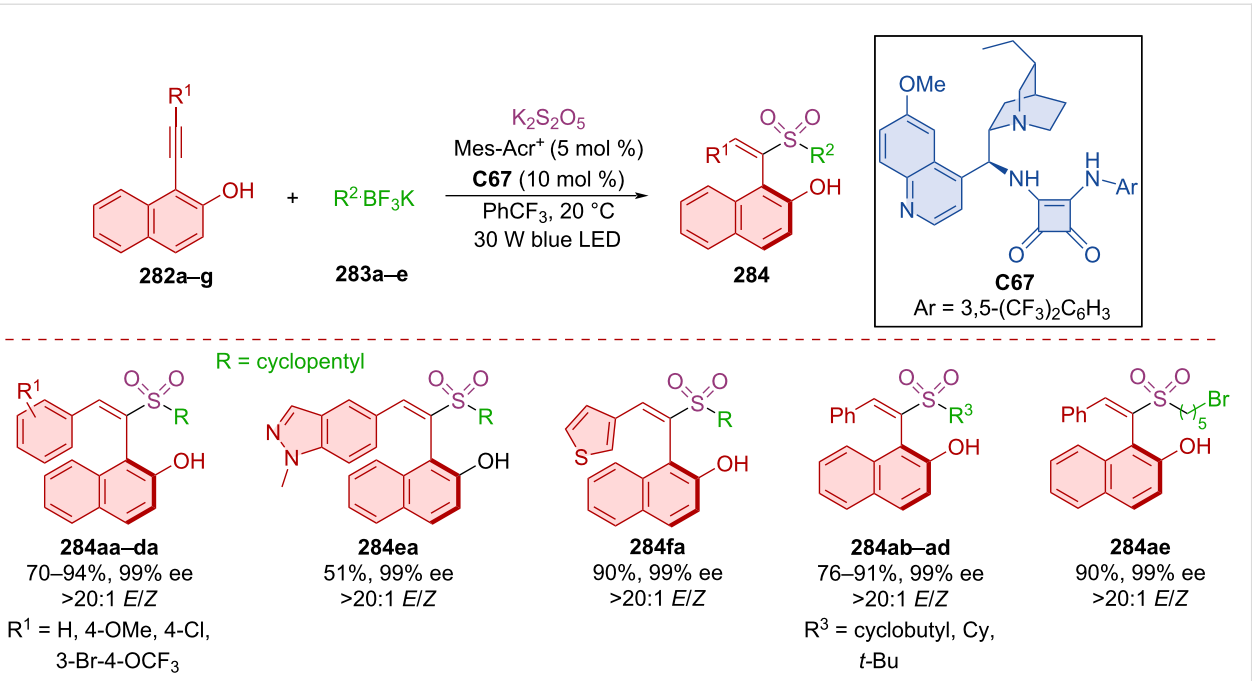

Scheme 85: Atroposelective organo-photocatalyzed sulfonylation of alkynyl-2-naphthols.

tivity in moderate to very good yields. Demonstrating the practicality of the method, the gram-scale synthesis of a corresponding product **284** resulted in almost no deterioration in chemical yield and enantioselectivity (84%, 99% ee). A plausible radical process has been proposed based on observations and computational results.

Wada et al. contributed with their quinine-derivative-catalyzed enantioselective bromination of axially chiral cyanoarenes, achieving mild enantioselectivities in general [122]. These precedents gave solid stepping stone for further development in this field.

Asymmetric annulation of *o*-alkynylanilines **285** catalyzed by quinidine-derived thiourea organocatalyst **C68** led to the formation of axially chiral aryl-C2-indoles **286** (Scheme 86) [123]. High to excellent yields and enantioselectivities were achieved through optimized reaction conditions with many substrates. The transformation is presumed to occur through a VQM intermediate. After the reaction, organocatalyst **C68** could be regenerated and used again without significant loss of catalytic activity or achieved enantioselectivity. The decagram-scale reaction has led to the representative product **286** in near quantitative yield and enantiopure form (90%, >99% ee) through recrystallization without the use of column chromatography.

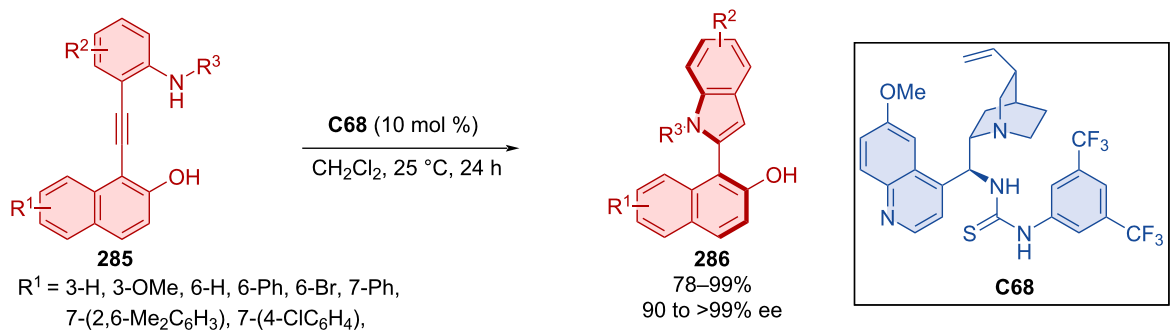

R1 = 3-H, 3-OMe, 6-H, 6-Ph, 6-Br, 7-Ph, 7-(2,6-Me2C6H3), 7-(4-ClC6H4), 7-(2-OMeC6H4)
R2 = 5-H, 5-Cl, 6-H, 6-Me, 6-F, 6-Cl, 6-Br
R3 = *t*-Bu, Ts

Scheme 86: Thiourea-catalyzed atroposelective cyclization of alkynylnaphthols.

A chiral thiourea organocatalyst was used in asymmetric transformations leading to products in poor to moderate yields and decent enantioselectivities (17–66%, 39–80% ee) [124].

Chang et al. focused their attention on the atroposelective construction of arylisothiazoles and arylpyrazoles [125]. Unique modified VQM precursor structures were designed as substrates to accomplish this task. Kinetic resolution by brominative cyclization using quinidine-derived squaramide **C65** as organocatalyst, were utilized to prepare axially chiral naphthylisothiazoles **288** starting from sulfinamides **287** (Scheme 87). The preparation of naphthylpyrazoles **290** and **291** was realized with quinidine-derived squaramide organocatalyst **C66** or **C69** and hydrazones **289**. Utilization of substrates bearing sulfonylbenzene groups with organocatalyst **C69** led to the formation of one enantiomer, and ones bearing a diphenylphosphine oxide group reacted with NBS and organocatalyst **C66** to provide another. Excellent enantioselectivities were achieved with all products and moderate to high yields. Some products **290** and **291** showed mild biological activity and even good antiproliferation effects during biological assays.

Cinchona alkaloid squaramide also catalyzed a double cyclization reaction through VQM leading to unique products with both helical and axial chirality [126].

The fascinating work of Xu et al. demonstrated synthetic utility of alkynyl substrates in annulation reactions with the help of NIS catalyzed by quinine-based squaramides [127]. In the first case, alkynylsilanol **292** reacted to form axially chiral product **293** where organocatalyst **C65** served for chirality transfer (Scheme 88). Second was the reaction catalyzed by organocatalyst **C69** where alkynylanilines **294** formed products **295** with two stereogenic axes. High yields and high to near-perfect enantioselectivities were reported. Catalyst **C69** could be successfully utilized for up to six continuous feedings of substrate **294** and NIS to provide product **295** with good degree of enantiomeric purity. Both products **293** and **295** were also prepared in a

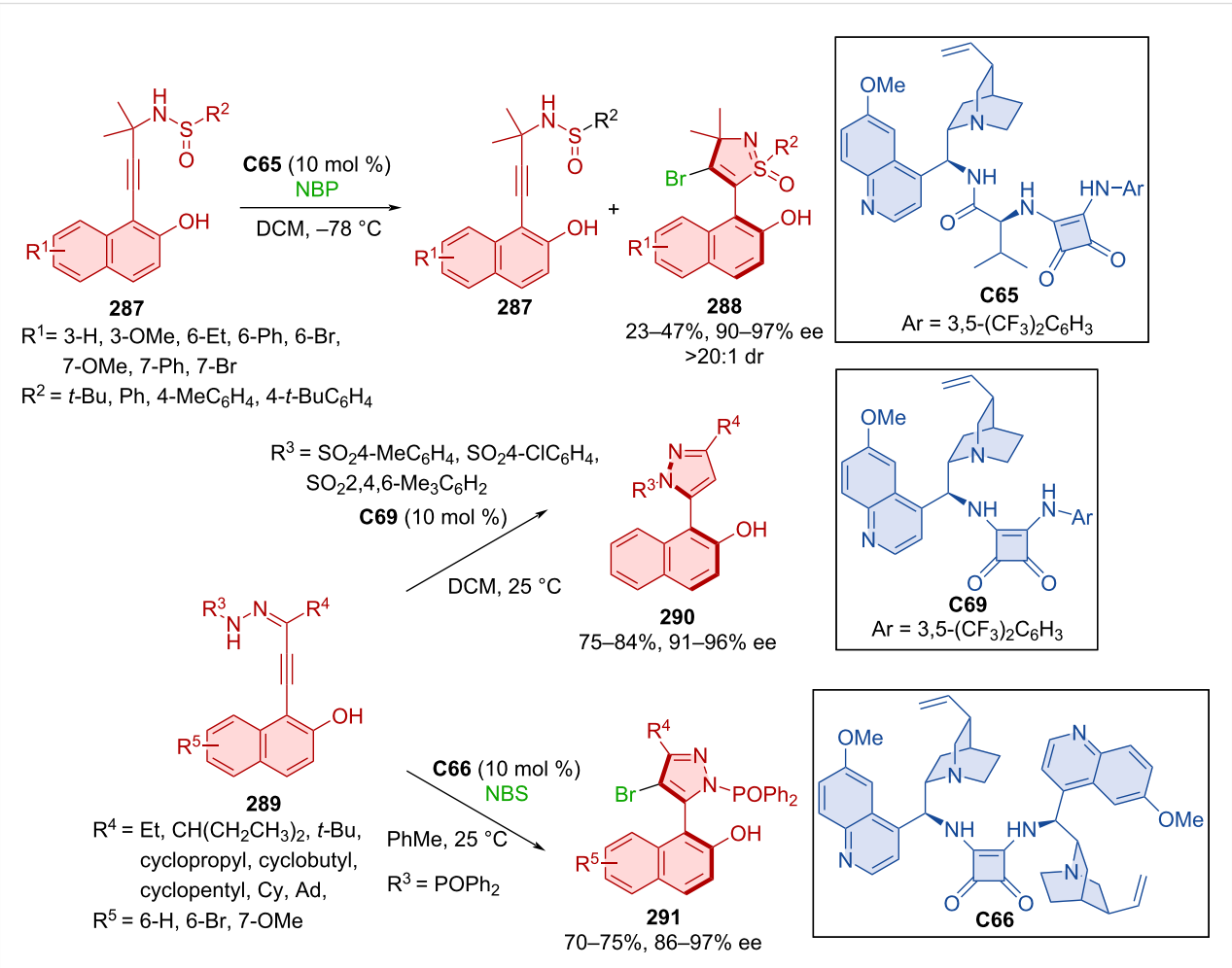

Scheme 87: Squaramide-catalyzed formation of axially chiral naphthylisothiazoles.

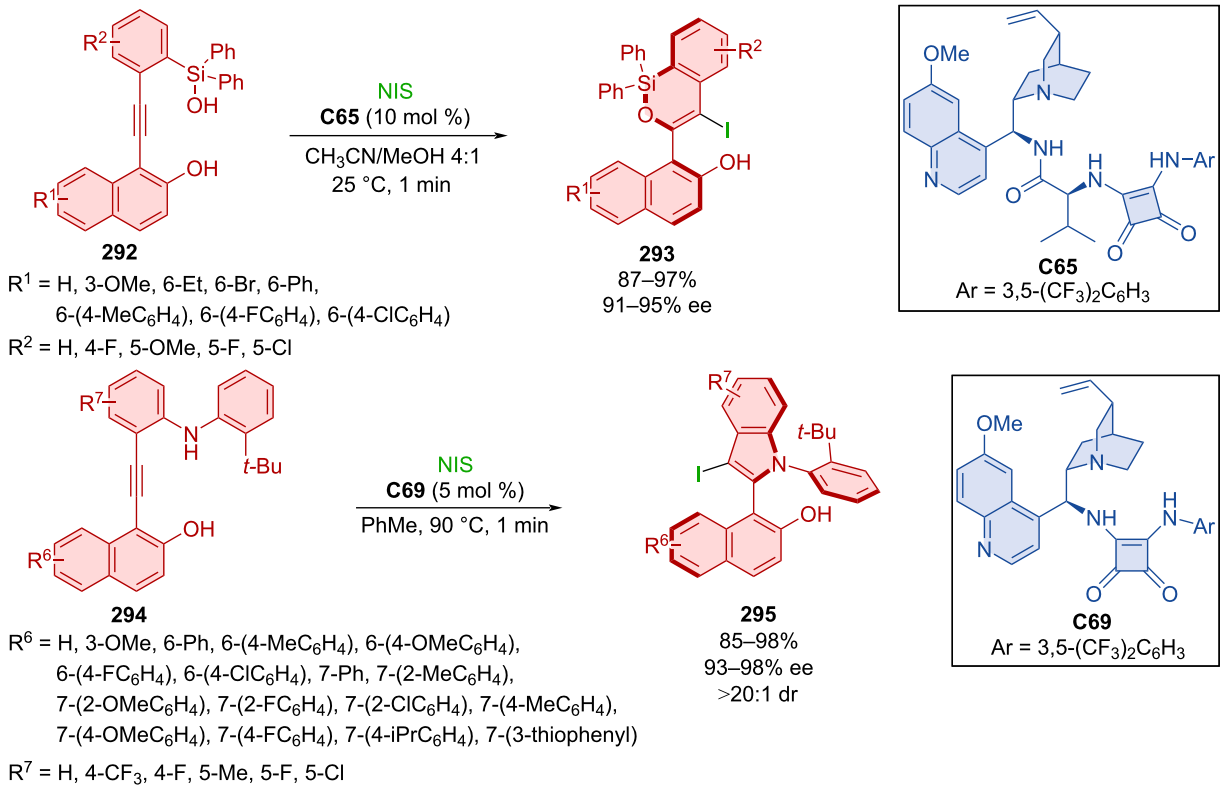

Scheme 88: Atroposelective iodo-cyclization catalyzed by squaramide **C69**.

gram-scale experiment with excellent yields and enantiomeric purities (>90%, >91% ee).

A quinine-derived thiourea organocatalyst was efficient in realizing an intramolecular reaction using VQM intermediates [128]. This atroposelective cyclization allows access to axially chiral nonsymmetric biaryltriols with up to 98% yield and 99% ee.

Diastereomeric oligoarenes were prepared with the help of a bifunctional squaramide organocatalyst in 2020 [129]. Afterwards, MnO_2 was successfully utilized in central-to-axial chirality conversion (Scheme 89).

Activation of the C–N bond of cyclic *N*-sulfonylamides **300a**,**b** with alcohols **301a**–**e** and quinidine-derived squaramide organocatalyst **C69** provided biaryl amino acid esters **302** with high levels of enantiomeric purities in near-perfect yields (Scheme 90) [130]. Stereocontrol through donor hydrogen bonds of amino squaramide groups with the oxygen on the *N*-sulfonylamide and acceptor hydrogen bond of nitrogen from quinidine to the alcohol hydrogen was proven by DFT calculations. Conformational stability was concluded by a racemization experiment, where product **302aa** could be stirred at 140 °C in *o*-xylene for 4 hours without any loss of enantiomeric purity. The rotational barrier, calculated by DFT, was 37.4 kcal/mol. Transformation of the ester group in **302aa** could lead to the formation of axially chiral amino alcohols, tripeptides, or bifunctional amines.

Using Cinchona alkaloids as catalysts, the atroposelective decarboxylative transamination of biarylaldehydes was also developed [131]. The transformation operated as a dynamic kinetic resolution and afforded the corresponding products in up to 92% yield and 66% ee.

Zheng et al. prepared Barton–Zard intermediate (*S*,*R*)-**303** as a single diastereomer in a racemic mixture. Thiourea quinine-derived organocatalyst **C68** was then employed to promote kinetic resolution, forming axially chiral naphthylpyrroles **304** (Scheme 91) [132]. Central-to-axial chirality conversion is proposed to take place through *syn*-elimination of the nitrous acid with the help of organocatalyst **C68** and subsequent aromatization. This enantioselective aromatization applies to a broad range of substrates, leading to high enantiomeric purities and sufficient conversions. The racemization barrier of the model

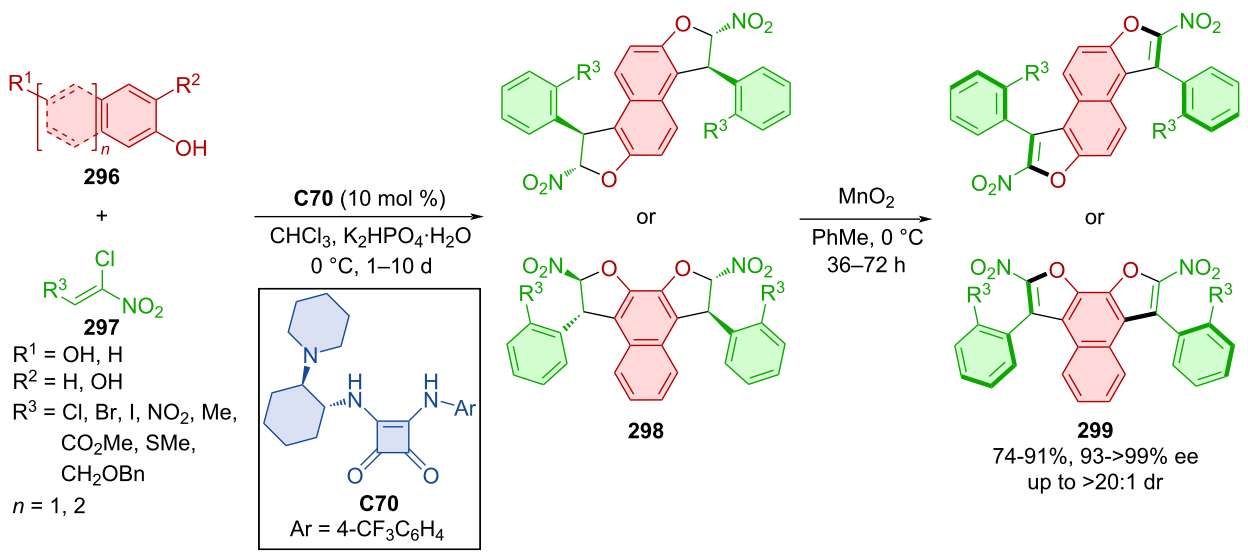

Scheme 89: Squaramide-catalyzed formation of axially chiral oligoarenes.

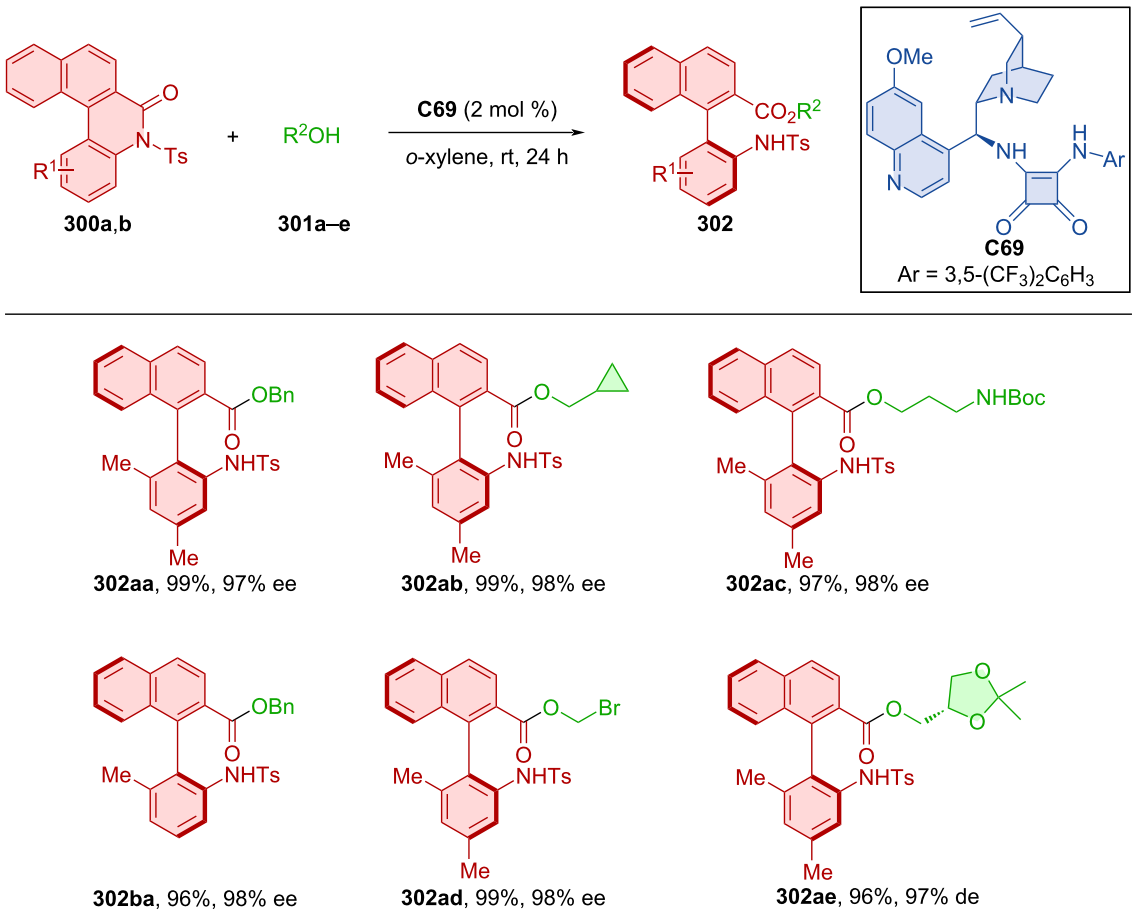

Scheme 90: Atroposelective ring-opening of cyclic *N*-sulfonylamides.

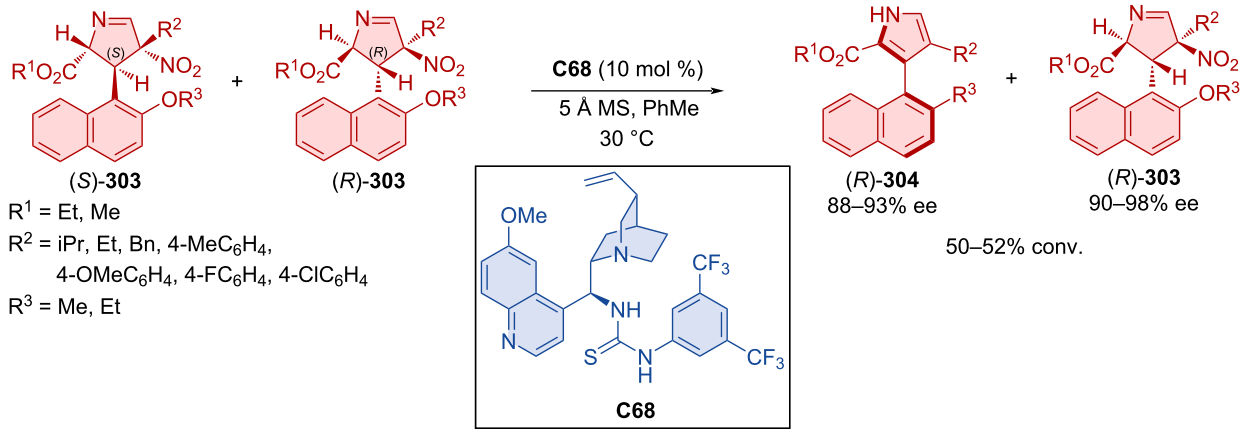

Scheme 91: Thiourea-catalyzed kinetic resolution of naphthylpyrroles.

product (*R*)-**304** was calculated to be 34.6 kcal/mol at 140 °C, which corresponds with a half-life of one day at this temperature.

A chiral squaramide organocatalyst was also employed in a dynamic kinetic resolution of hemi-stable arylnaphthoquinones [133]. The transformation comprised atroposelective 1,4-addition of thiosugars followed by stereoretentive oxidation.

Alkenyl-substituted pyrazolone derivatives featuring an axially chiral styrene unit were obtained in high yields and with excellent diastereoselectivity and enantioselectivity [134]. The key transformation was an atroposelective addition of enolizable pyrazolones to alkynylnaphthols.

Hong et al. utilized dynamic kinetic resolution by alcohols **306a–u** with *N*-Boc-*N*-arylindole lactams **305a–t** in the presence of bifunctional squaramide catalyst **C69** (Scheme 92) [135]. Extensive substrate scope provided an overwhelming majority of the axially chiral *N*-arylindoles **307** in near quantitative yields with next to perfect enantiomeric purity. A chosen product **307** was then tested for configurational stability in *o*-xylene at 140 °C for 12 h without any observed loss in ee. As shown below, a possible transition state consists of chiral organocatalyst **C69** providing hydrogen bonds to both substrates, dictating stereocontrol of the reaction. Demonstrating practicality of the method, gram-scale experiments provided products in comparable yields and enantioselectivities.

Fang et al. successfully carried out the Atherton–Todd reaction of 1-naphthyl-2-tetralones **308** and diarylphosphine oxides **309** catalyzed by thiourea phosphonium salt phase-transfer catalyst **C71** forming axially chiral phosphates **310** (Scheme 93) [136]. The atropoisomeric product **310** stirred in anisole at 160 °C proved to have a half-life of the enantiopurity around 24 h. The rotational barrier of this process was around 36.4 kcal/mol. Investigation of the synthetic utility of the reaction on the gram-scale led to the product **310** with comparable yield and enantiomeric purity (82%, 92% ee). Performed DFT calculations led to the proposition of a potential intermediate responsible for enantiocontrol. Thiourea amino groups provide donor hydrogen bonds to the phosphine oxide oxygen atom. Another stabilizing interaction potentially occurs between tetralone oxygen and phosphonium adjacent hydrogen on the organocatalyst.

Iminoquinones **312** as widely applicable reaction partners in arylation reactions, where they also play a role of oxidants, were utilized in the reaction with 5-hydroxyindoles **311** (Scheme 94) [137]. The authors present the first case of axially chiral arylindoles **313** being prepared with thiourea organocatalyst **C72**, omitting usage of CPAs, which were utilized much more in the past. This approach led to near-perfect yields and enantioselectivities in best cases, with great results being achieved on the lower end as well. Chosen product **313** was tested as chiral ligand in a model reaction, providing the corresponding product in good results with a high degree of enantiomeric purity (87%, 87% ee). NMR experiments suggested the importance of hydrogen bonding in the reaction mechanism. Furthermore, in large-scale experiments (90%, >99% ee), organocatalyst **C72** was repeatedly (up to 5-times) recovered after the reaction with excellent yields (98–99%).

Other types of organocatalysts

Phase-transfer catalyst **C73** was utilized in the kinetic resolution of BINOLs (*R,S*)-**314** through benzylation by benzyl tosylate affording resolved axially chiral (*R*)-**314** and benzylated axially chiral (*S*)-**315** (Scheme 95) [138]. Slightly better enantioselectivities were achieved with unprotected BINOLs

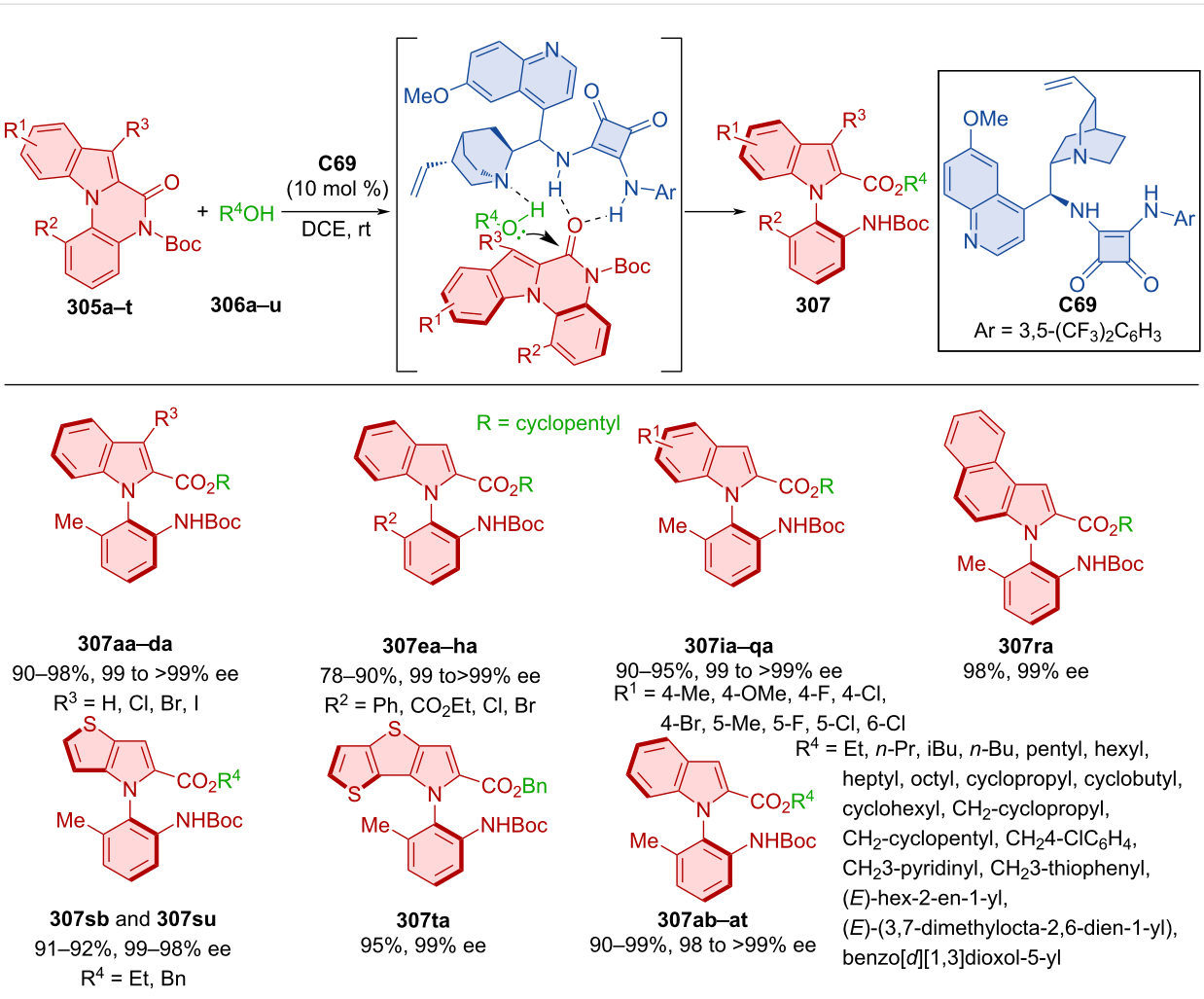

Scheme 92: Atroposelective ring-opening of arylindole lactams.

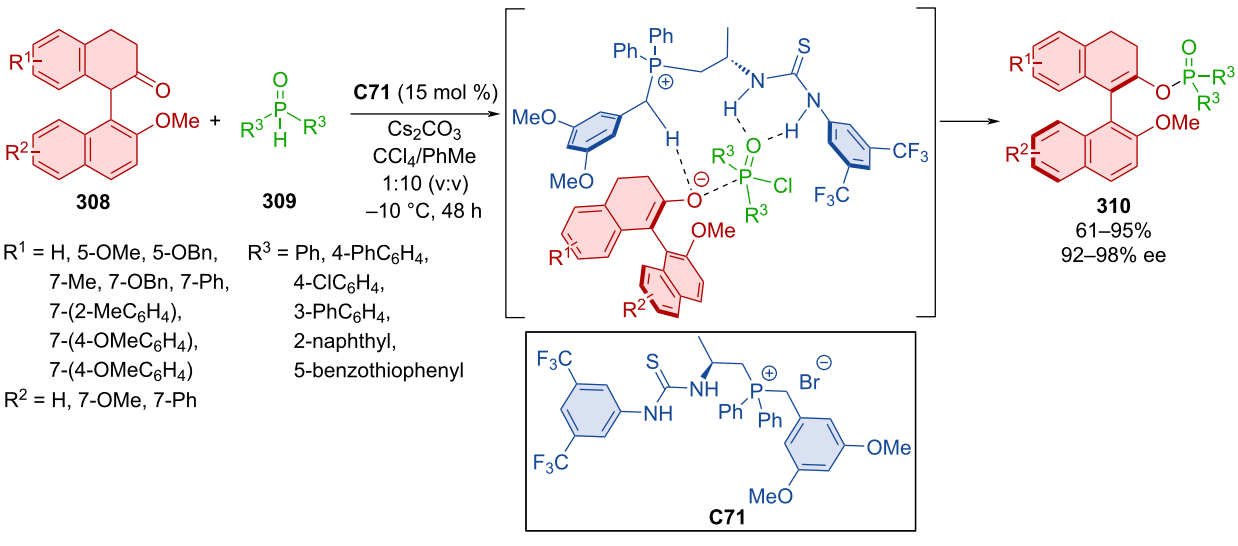

Scheme 93: Atroposelective reaction of 1-naphthyl-2-tetralones and diarylphosphine oxides.

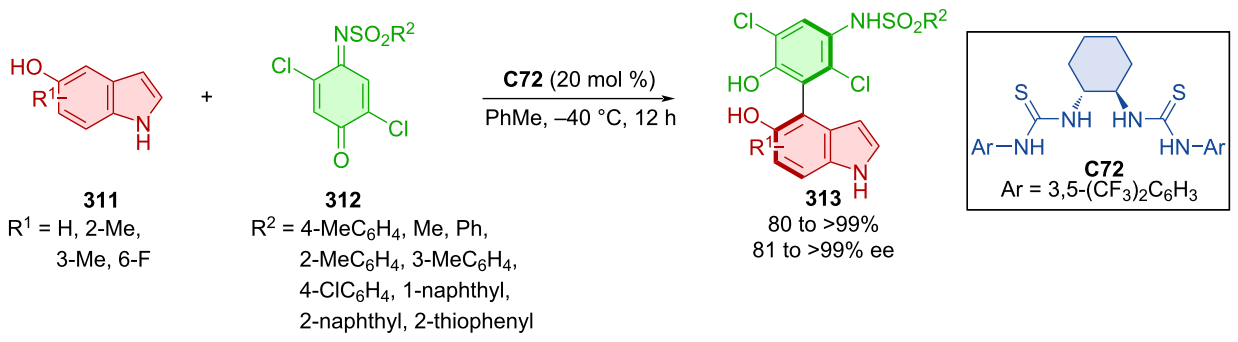

Scheme 94: Atroposelective reaction of iminoquinones with indoles.

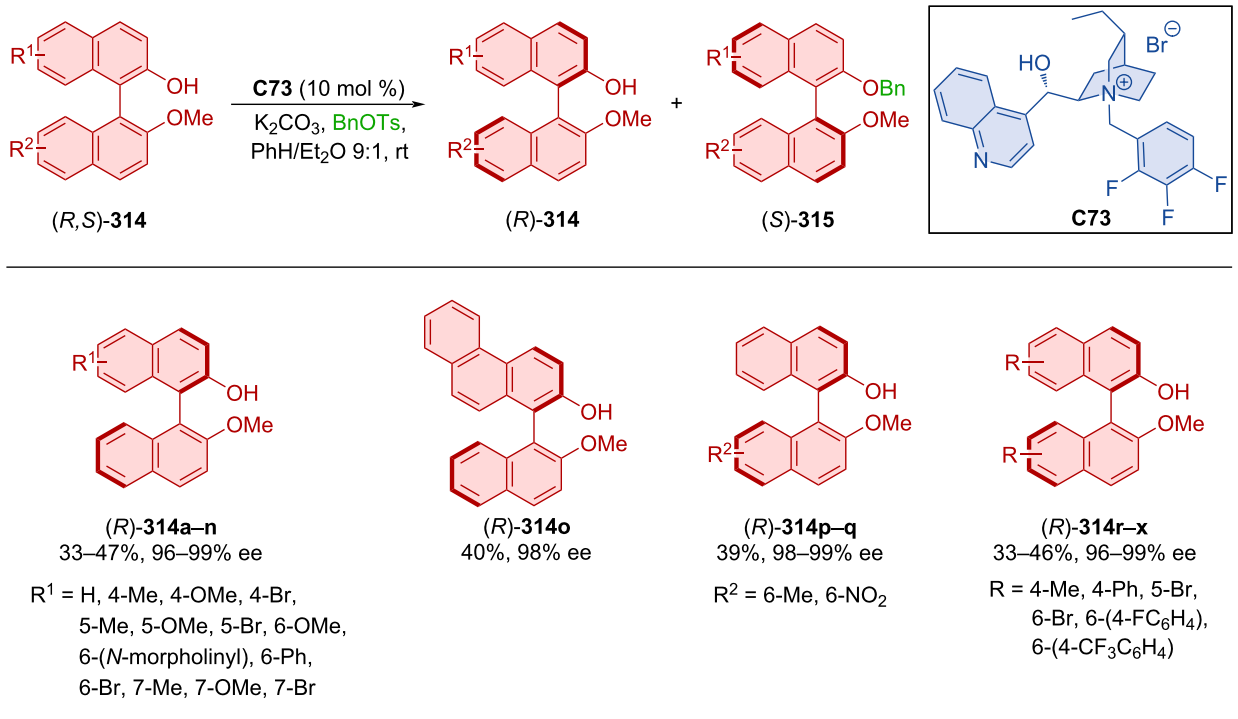

Scheme 95: Kinetic resolution of binaphthylalcohols.

(*R*)-**314** than with benzylated ones. The practicality of the process was demonstrated on a 22 mmol scale reaction with comparable results for both products (**314** – 98% ee and **315** – 80% ee). In accordance with literature, the authors proposed that the mechanism takes place through rapid and reversible deprotonation followed by slow conversion for the disfavored and fast conversion for the favored enantiomer.

Fugard et al. developed a highly enantioselective route to axially chiral naphthamides **317a–l** (Scheme 96) [139]. Through dynamic kinetic resolution by benzylation of racemic naphthamides **316a–l** catalyzed with phase-transfer organocatalyst **C74**, moderate to high yields with excellent enantioselectivities were achieved. The utilization of aromatic rings in position 8 of the naphthamide led to a slight decrease in yields (**317g–k**). The rotational barrier of starting material **316l** containing a hydroxy group was calculated to be 22.8 kcal/mol. On the other hand, the benzylated product **317l** had a rotational barrier of 31.4 kcal/mol. The authors suggest that the high rotational barrier of the starting material is due to the intramolecular hydrogen bond between the hydroxy group and amide nitrogen. This interaction was then used to promote dynamic kinetic resolution providing products with even higher rotational barrier.

Phase-transfer quinine-based organocatalyst **C75** was utilized in the transformation of arylenamines **318** with aliphatic and aro-

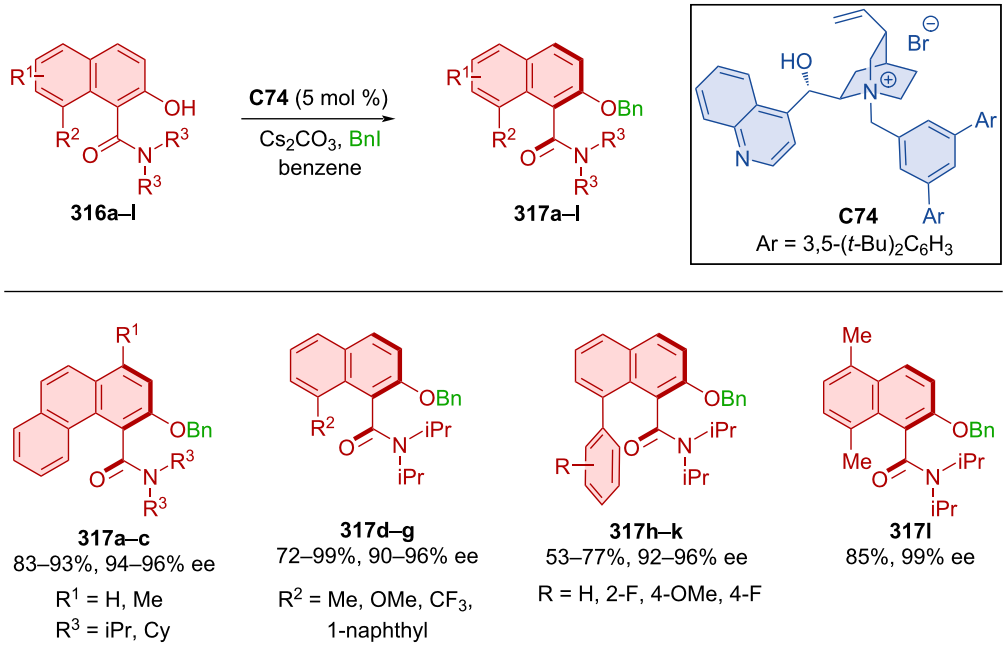

Scheme 96: DKR of hydroxynaphthylamides.

matic bromo derivatives **319** that led to axially chiral amino esters **320** (Scheme 97) [140]. The addition of LAH subsequently led to the cyclization and formation of a pyrrole ring providing axially chiral 2-arylpyrroles **321** in good to high yields and very good enantioselectivities retaining stereoinformation from the previous step. The possibility for a one-pot two-step reaction protocol was explored with satisfying yield and enantioselectivity of the corresponding product (83%, 93% ee).

A phase-transfer catalyst was also utilized in dynamic kinetic resolution by benzylation resulting in products with good yields, but moderate enantiomeric purities (53–86%, 40–80% ee) [141].

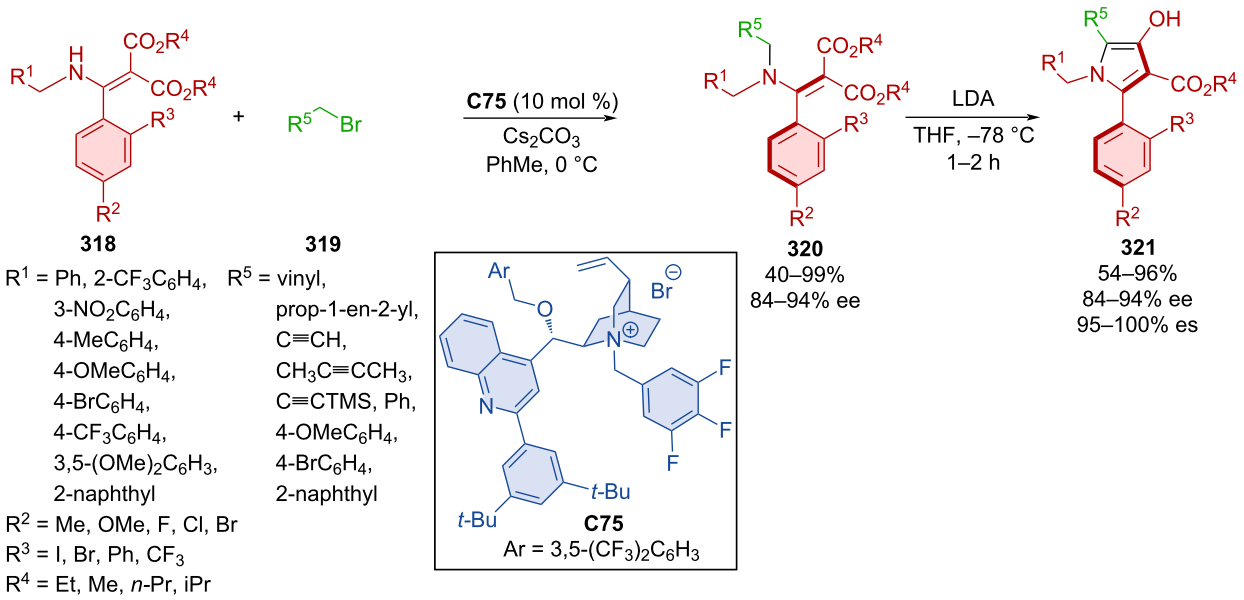

Scheme 97: Atroposelective *N*-alkylation with phase-transfer catalyst **C75**.

Lu et al. developed kinetic resolution by *N*-alkylation reaction of racemic biaryls **322a**–**h** with carbonate **323** catalyzed by dimeric hydroquinone organocatalyst **C76** (Scheme 98) [142]. *N*-Alkylated axially chiral products (*S*)-**324a**–**h** were prepared with moderate to good enantiomeric purities, and enantio-enriched products (*R*)-**322a**–**h** were prepared in almost enan-

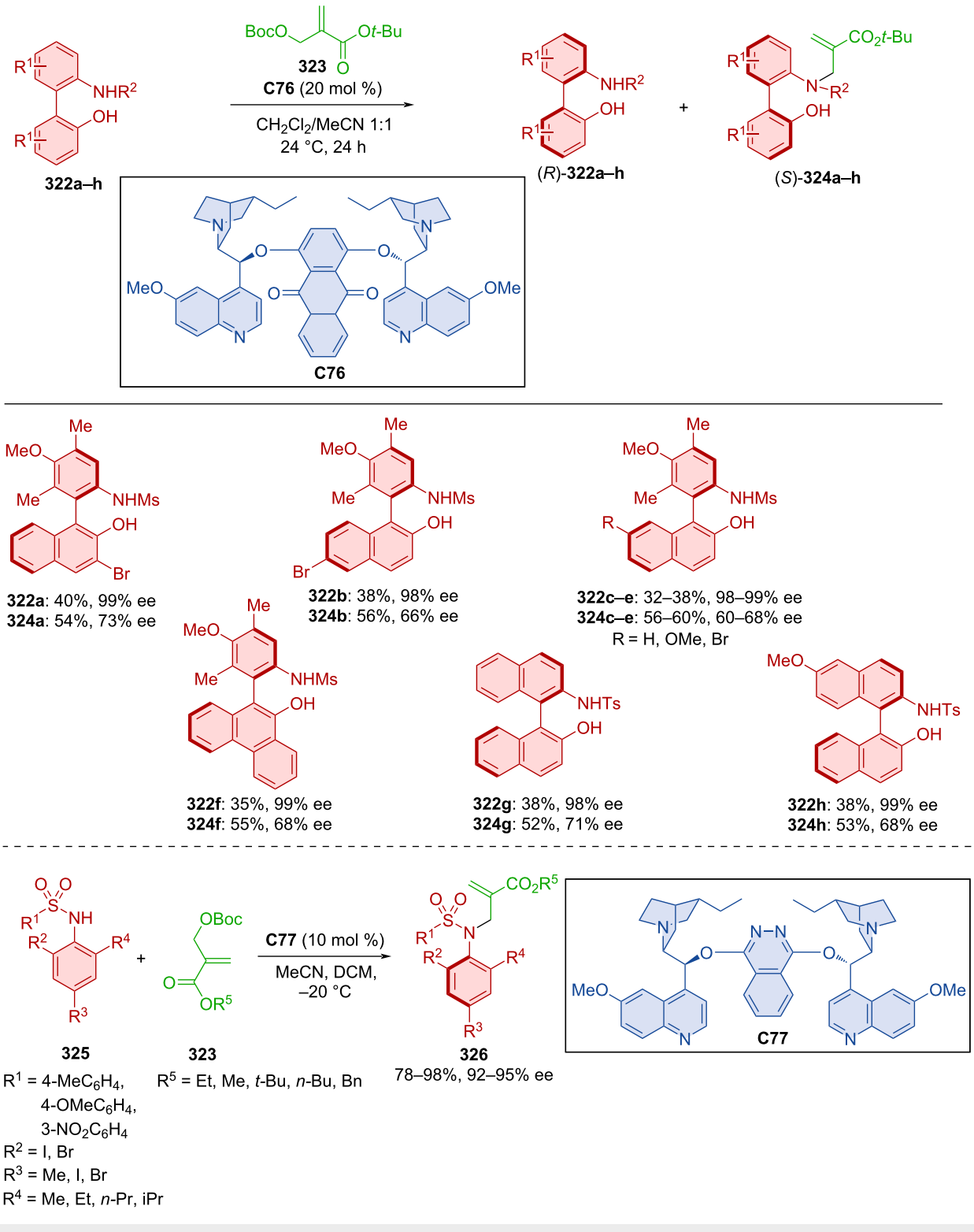

Scheme 98: Atroposelective allylic substitution via kinetic resolution of biarylsulfonamides.

tiopure form. The organocatalyst **C76** was successfully regenerated after the reaction and could be readily used again with comparable efficiency. During the study of the reaction conditions, in some cases, the authors observed the formation of tertiary sulfonamides as two different isomers, with their ratios changing over time. These isomers were defined as atropoisomers of alkylated arylsulfonamides. Expanding on this methodology, axially chiral products **326** were prepared starting from arylsulfonamides **325** and carbonates **323** mediated by dimeric hydrochinone **C77**. Di-*ortho*-substituted substrates were utilized, providing a significantly higher rotational barrier than mono-*ortho*-substituted ones. The optimized reaction conditions led to the formation of a considerable number of *N*-alkylarylated sulfonamides **326** with excellent yields and enantiomeric purities.

Wu et al. primarily focused on diastereoselective halogenations of double bonds [143]. In the process of substrate scoping they also developed a protocol, where halogenation happens on the triple bond of a suitable substrate **327** with the help of hydroquinine-based organocatalyst **C78** leading to axially chiral products **328** (Scheme 99). By this approach decent to near perfect yields and very good enantioselectivities were achieved.

Liang et al. constructed axially chiral amino sulfide vinyl arenes **331** by cyclization of alkynylanilines **329a–m** and electrophilic sulfur reagents **330a–h** in the presence of TMSOTf and organocatalyst **C79** (Scheme 100) [144]. This approach led to a wide range of axially chiral products in high yields and high degrees of enantiomeric purity. The thio and amino groups were subject to further transformations. For example, sulfur oxidation to sulfonyl, followed by substitution and reduction or deprotection of the amine, and diazotization can be done with subsequent bromination. The plausible reaction mechanism starts by the activation of the electrophilic sulfur reagent **330a** by organocatalyst **C83** and the Lewis acid. Thiirenium ion intermediate **Int-74** is formed with **329a** and by further conversion through aza-vinylidene-quinone-methide (aza-VQM) intermediate **Int-75**. Cyclization and rearomatization then afford the axially chiral product **331aa**.

An interesting report of catalysis by ketoreductase (KRED) for the preparation of atropoisomers was published in 2023 [145]. DKR of *N*-arylindolecarbaldehydes provided axially chiral products with consistently good yields and high levels of enantiomeric purities. The model product was successfully incorporated into a bifunctional thiourea organocatalyst.

The cinchona alkaloid-derived phase-transfer chiral organocatalyst **C80** was utilized in dynamic kinetic resolution by sulfonylation of isochromenone-indoles **332** with sulfonyl chlorides **333** (Scheme 101) [146]. Axially chiral isochromenone-indoles **334** were prepared in moderate to excellent yields with a high degree of enantiomeric purity. Reaction mechanism studies suggest that the key reaction step responsible for the stereocontrol happens when the axially chiral enolate ion forms an ionic pair with the quaternary ammonium salt. This activated complex then forms the corresponding enantiomeric product faster, than the opposite one. Configurational stability was determined after stirring one of the products **334** in isopropanol at 110 °C for 9 h with no erosion of the enantioselectivity. The rotational barrier was theoretically calculated to be 39.7 kcal/mol, which defines it as class-3 atropoisomer.

Compounds with a C–N stereogenic axis are an interesting type of axially chiral derivatives. Dong and co-workers developed an atroposelective *N*-acylation of aniline-derived sulfonamides **335** (Scheme 102) [147]. The reaction afforded a range of sulfonyl-

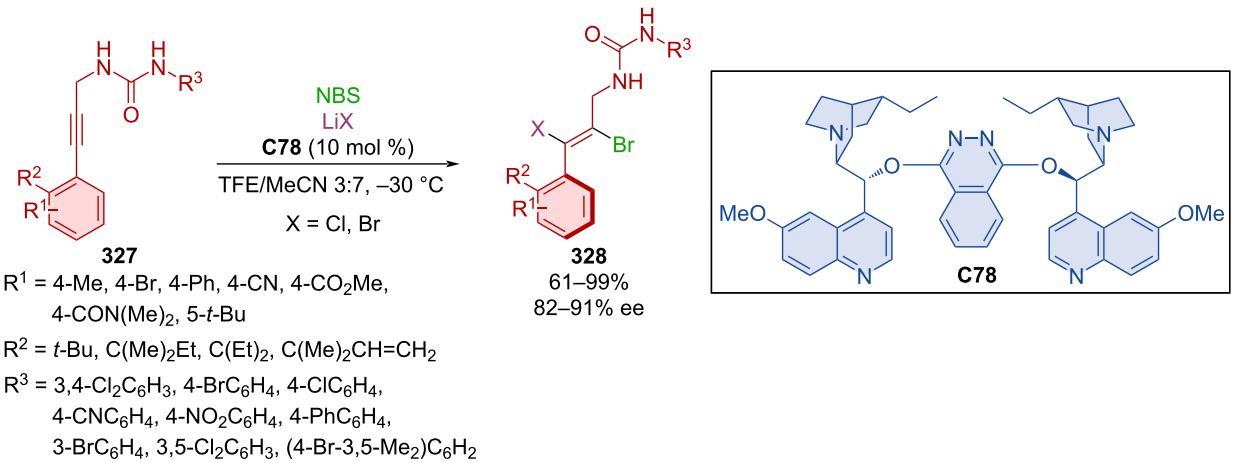

R^1 = 4-Me, 4-Br, 4-Ph, 4-CN, 4-CO_2Me, 4-CON$(Me)_2$, 5-*t*-Bu

R^2 = *t*-Bu, C$(Me)_2$Et, C$(Et)_2$, C$(Me)_2$CH=CH_2

R^3 = 3,4-$Cl_2C_6H_3$, 4-BrC_6H_4, 4-ClC_6H_4, 4-CNC_6H_4, 4-$NO_2C_6H_4$, 4-PhC_6H_4, 3-BrC_6H_4, 3,5-$Cl_2C_6H_3$, (4-Br-3,5-Me_2)C_6H_2

Scheme 99: Atroposelective bromo-functionalization of alkynylarenes.

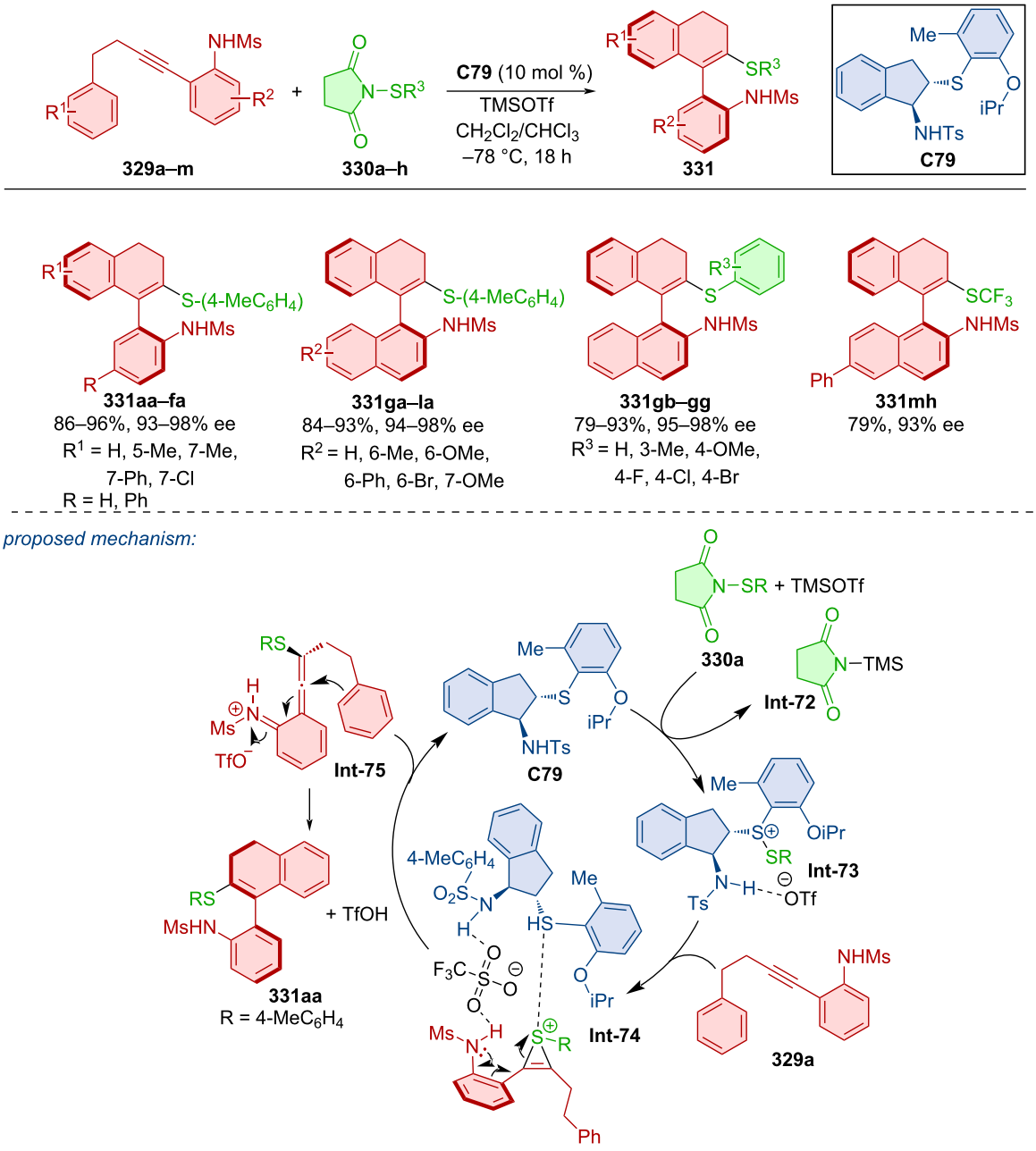

Scheme 100: Sulfenylation-induced atroposelective cyclization.

substituted anilide products **337** in good yields and high enantiomeric purities.

Beleh et al. presented a tandem dynamic kinetic resolution catalyzed by two different peptide organocatalysts **C82** and **C83** in 2020 (Scheme 103) [148]. Products of these subsequent transformations were axially chiral structures **339a–f** bearing two axially chiral axes. The first of the two reactions was the atroposelective lactone-ring opening of racemic polycyclic substrate **338a–f**, after which atroposelective chlorination of the central benzene ring took place. Despite the stereochemical complexity of the reaction, excellent enantioselectivities and moderately good yields were reported. A number of different approaches were tested, such as utilizing **C82** as a catalyst in both reactions and adding the chlorination reagent after the first twenty hours of reaction time. Decreased enantio- and diastereoselectivities were achieved by this method as opposed to standardized methodology (76% ee, 3.5:1 dr). Combining both organocatalysts and chlorination reagents from the get-go did not provide any product after 20 h. Lastly, by adding both

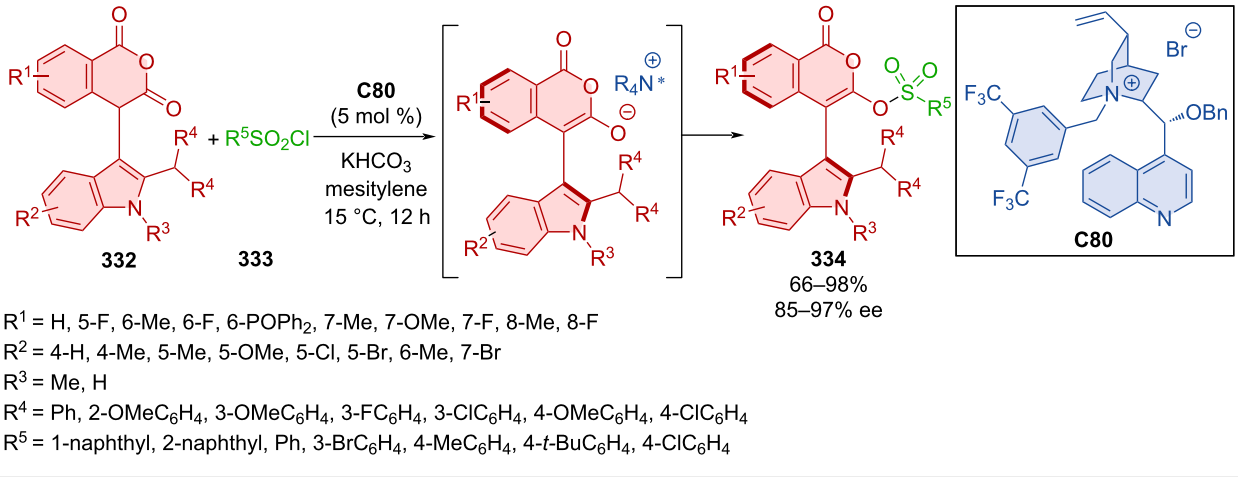

Scheme 101: Atroposelective *O*-sulfonylation of isochromenone-indoles.

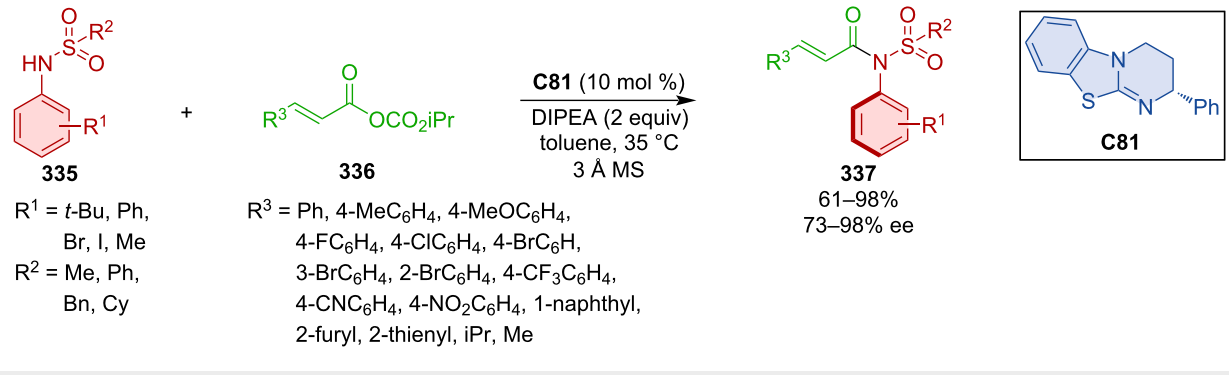

Scheme 102: NHC-catalyzed atroposelective *N*-acylation of anilines.

organocatalysts initially and the chlorination reagent after 24 h, the product was formed with decent enantiomeric purity (84% ee, 5.5:1 dr), proving the superior efficiency of the tandem approach.

Peptide **C84** was successfully utilized in the coupling reaction of 2-naphthols **340** with quinones **341** giving rise to the axially chiral naphthylhydroquinones **342** in moderate to excellent yields and good enantioselectivities (Scheme 104) [149]. A substrate containing a nitrile group in position 6 of the 2-naphthol deviates from otherwise decent yields, providing the product in only 48% yield. In a preparative scale reaction, the authors were able to achieve nearly enantiopure products after recrystallization, where significant product enantioenrichment happened after just one recrystallization cycle.

Similar peptide-catalyzed asymmetric cyclizations led to the formation of pharmaceutically relevant atropoisomeric *N*-arylquinazolinediones in mostly great yields, but with limited enantiomeric purity (70–97%, 32–84% ee) [150].

In 2023, a unique chiral phosphonium salt **C85**-catalyzed reaction of alkenyl-2-naphthols **343** with fluorobenzenes **344** forming axially chiral products **345** was carried out (Scheme 105) [151]. With the optimized reaction conditions near perfect yields and enantioselectivities were reported.

Conclusion

Axially chiral compounds rose from stereochemical peculiarities to diverse groups of compounds with many interesting properties and applications that range from catalysis, through materials to medicine. Atroposelective organocatalysis became one of the main methods for efficient synthesis of compounds chirality axes. Analysis of recent progress in this area has shown that all major organocatalytic activation modes are employed for realizing atroposelective transformations. From among covalent activation, classical enamine/iminium activation as well as NHC-catalyzed reactions were utilized to engage predominantly carbonyl-based transformations. The majority of recent organocatalytic reactions were catalyzed by non-covalent catalysts. Here the greatest share and the broadest diversity

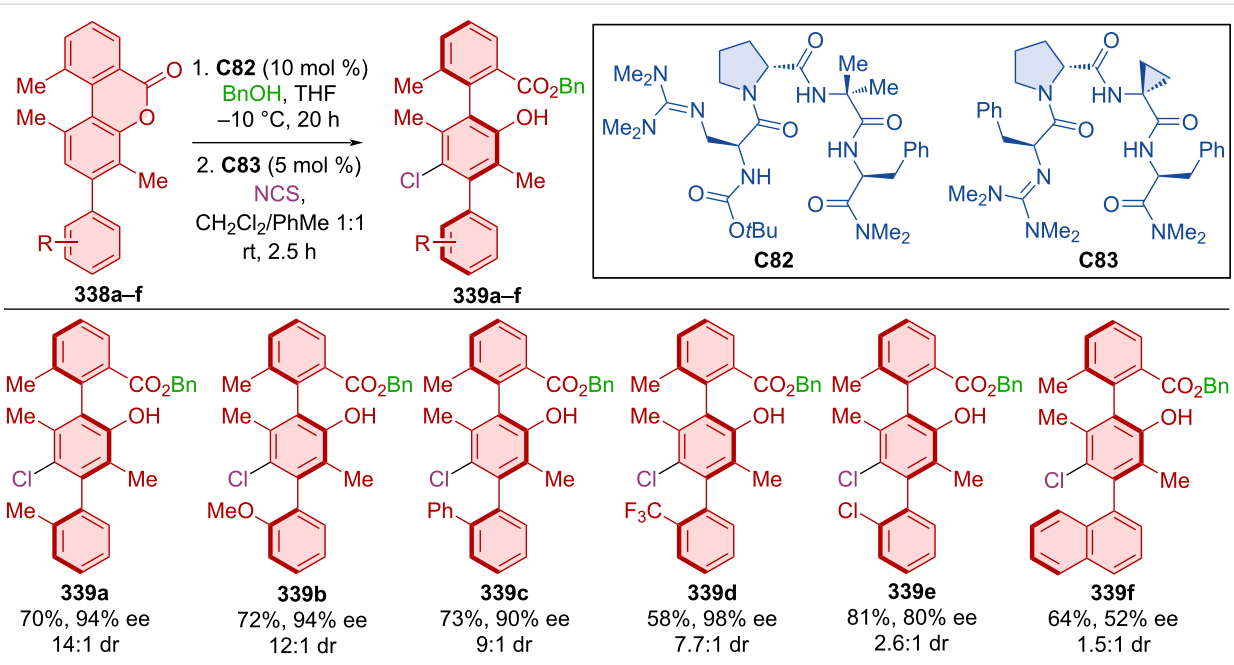

Scheme 103: Peptide-catalyzed atroposelective ring-opening of lactones.

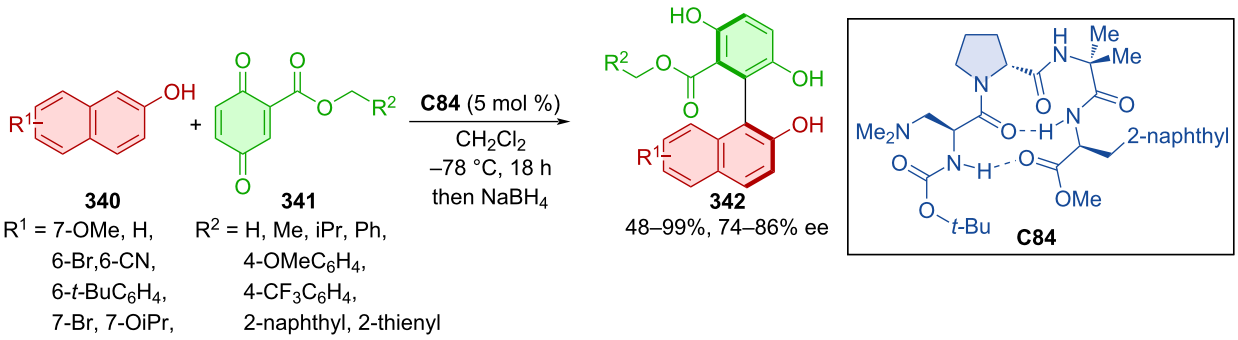

Scheme 104: Peptide-catalyzed coupling of 2-naphthols with quinones.

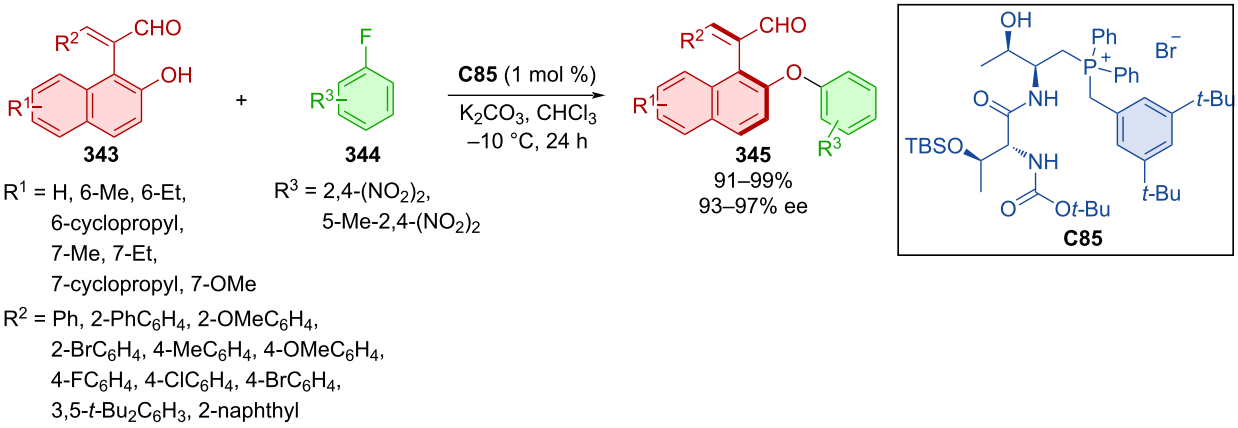

Scheme 105: Atroposelective nucleophilic aromatic substitution of fluoroarenes.

can be found in the chiral Brønsted acid catalysts. Interesting to note is also the fact that the most efficient structural motif for catalyst construction is actually an axially chiral binaphthylphosphoric acid and its congeners. From among other non-covalent organocatalysts, hydrogen-bond-donating thioureas and squaramides as well as other types of donors such alcohols or peptides were successfully employed in the stereoselective formation of axially chiral compounds. Several examples of phase-transfer-catalyzed reactions conclude the discussion. This review documents continuing development of this burgeoning area of research and documents tremendous creativity of our research community in assembling complex compounds with axial chirality. One can also note that some synthetic potential of all organocatalytic approaches was not yet utilized. For instance, methodologies utilizing peptide or carbonyl catalysis were not yet developed. Similarly, other non-covalent strategies such as those utilizing ion-paring catalysis, halogen bonds will hopefully also find use in the atroposelective organocatalysis. With this overview of recent progress of atroposelective organocatalytic reactions we hope to provide readers in various areas with an update of how this field develops and were new directions may lay.

Funding

This work was supported by the Slovak Grant Agency VEGA, grant no. VEGA 1/0445/24.

ORCID® iDs

Henrich Szabados - https://orcid.org/0009-0000-6067-4267
Radovan Šebesta - https://orcid.org/0000-0002-7975-3608

Data Availability Statement

Data sharing is not applicable as no new data was generated or analyzed in this study.

References

1. Cossy, J., Ed. *Comprehensive Chirality,* 2nd ed.; Academic Press, 2024.
2. Zhou, Q.-L., Ed. *Privileged Chiral Ligands and Catalysts;* Wiley-VCH: Weinheim, Germany, 2011. doi:10.1002/9783527635207
3. Wang, Y.; Li, Q. *Adv. Mater. (Weinheim, Ger.)* **2012,** *24,* 1926–1945. doi:10.1002/adma.201200241
4. LaPlante, S. R.; Edwards, P. J.; Fader, L. D.; Jakalian, A.; Hucke, O. *ChemMedChem* **2011,** *6,* 505–513. doi:10.1002/cmdc.201000485
5. Cheng, J. K.; Xiang, S.-H.; Li, S.; Ye, L.; Tan, B. *Chem. Rev.* **2021,** *121,* 4805–4902. doi:10.1021/acs.chemrev.0c01306
6. Kitagawa, O. *Acc. Chem. Res.* **2021,** *54,* 719–730. doi:10.1021/acs.accounts.0c00767
7. Cheng, J. K.; Xiang, S.-H.; Tan, B. *Acc. Chem. Res.* **2022,** *55,* 2920–2937. doi:10.1021/acs.accounts.2c00509
8. Song, R.; Xie, Y.; Jin, Z.; Chi, Y. R. *Angew. Chem., Int. Ed.* **2021,** *60,* 26026–26037. doi:10.1002/anie.202108630
9. Woldegiorgis, A. G.; Lin, X. *Beilstein J. Org. Chem.* **2021,** *17,* 2729–2764. doi:10.3762/bjoc.17.185
10. Feng, J.; Du, D. *Tetrahedron* **2021,** *100,* 132456. doi:10.1016/j.tet.2021.132456
11. Wang, Y.-B.; Tan, B. *Acc. Chem. Res.* **2018,** *51,* 534–547. doi:10.1021/acs.accounts.7b00602
12. Krištofíková, D.; Modrocká, V.; Mečiarová, M.; Šebesta, R. *ChemSusChem* **2020,** *13,* 2828–2858. doi:10.1002/cssc.202000137
13. Luc, A.; Wencel-Delord, J. *Chem. Commun.* **2023,** *59,* 8159–8167. doi:10.1039/d3cc01328f
14. Wang, X.; Chen, X.; Lin, W.; Li, P.; Li, W. *Adv. Synth. Catal.* **2022,** *364,* 1212–1222. doi:10.1002/adsc.202200085
15. Schmidt, T. A.; Sparr, C. *Acc. Chem. Res.* **2021,** *54,* 2764–2774. doi:10.1021/acs.accounts.1c00178
16. Li, T.-Z.; Liu, S.-J.; Tan, W.; Shi, F. *Chem. – Eur. J.* **2020,** *26,* 15779–15792. doi:10.1002/chem.202001397
17. Zhang, Z.-X.; Hu, T.-Q.; Ye, L.-W.; Zhou, B. *Synthesis* **2024,** *56,* 2316–2328. doi:10.1055/a-2241-3571
18. Zheng, S.-C.; Wu, S.; Zhou, Q.; Chung, L. W.; Ye, L.; Tan, B. *Nat. Commun.* **2017,** *8,* 15238. doi:10.1038/ncomms15238
19. Yang, G.; Sun, S.; Li, Z.; Liu, Y.; Wang, J. *Commun. Chem.* **2021,** *4,* 144. doi:10.1038/s42004-021-00580-5
20. Zhang, Z.-X.; Liu, L.-G.; Liu, Y.-X.; Lin, J.; Lu, X.; Ye, L.-W.; Zhou, B. *Chem. Sci.* **2023,** *14,* 5918–5924. doi:10.1039/d3sc01880f
21. Witzig, R. M.; Fäseke, V. C.; Häussinger, D.; Sparr, C. *Nat. Catal.* **2019,** *2,* 925–930. doi:10.1038/s41929-019-0345-0
22. Link, A.; Sparr, C. *Angew. Chem., Int. Ed.* **2014,** *53,* 5458–5461. doi:10.1002/anie.201402441
23. Lotter, D.; Castrogiovanni, A.; Neuburger, M.; Sparr, C. *ACS Cent. Sci.* **2018,** *4,* 656–660. doi:10.1021/acscentsci.8b00204
24. Hayashi, Y.; Takikawa, A.; Koshino, S.; Ishida, K. *Chem. – Eur. J.* **2019,** *25,* 10319–10322. doi:10.1002/chem.201902767
25. Koshino, S.; Takikawa, A.; Ishida, K.; Taniguchi, T.; Monde, K.; Kwon, E.; Umemiya, S.; Hayashi, Y. *Chem. – Eur. J.* **2020,** *26,* 4524–4530. doi:10.1002/chem.201905814
26. Koshino, S.; Taniguchi, T.; Monde, K.; Kwon, E.; Hayashi, Y. *Chem. – Eur. J.* **2021,** *27,* 15786–15794. doi:10.1002/chem.202102797
27. Bertuzzi, G.; Corti, V.; Izzo, J. A.; Ričko, S.; Jessen, N. I.; Jørgensen, K. A. *J. Am. Chem. Soc.* **2022,** *144,* 1056–1065. doi:10.1021/jacs.1c12619
28. Yan, J.-L.; Maiti, R.; Ren, S.-C.; Tian, W.; Li, T.; Xu, J.; Mondal, B.; Jin, Z.; Chi, Y. R. *Nat. Commun.* **2022,** *13,* 84. doi:10.1038/s41467-021-27771-x
29. Zhang, S.; Wang, X.; Han, L.-L.; Li, J.; Liang, Z.; Wei, D.; Du, D. *Angew. Chem., Int. Ed.* **2022,** *61,* e202212005. doi:10.1002/anie.202212005
30. Lu, S.; Ong, J.-Y.; Yang, H.; Poh, S. B.; Liew, X.; Seow, C. S. D.; Wong, M. W.; Zhao, Y. *J. Am. Chem. Soc.* **2019,** *141,* 17062–17067. doi:10.1021/jacs.9b08510
31. Jin, J.; Huang, X.; Xu, J.; Li, T.; Peng, X.; Zhu, X.; Zhang, J.; Jin, Z.; Chi, Y. R. *Org. Lett.* **2021,** *23,* 3991–3996. doi:10.1021/acs.orglett.1c01191
32. Ma, R.; Wang, X.; Zhang, Q.; Chen, L.; Gao, J.; Feng, J.; Wei, D.; Du, D. *Org. Lett.* **2021,** *23,* 4267–4272. doi:10.1021/acs.orglett.1c01221
33. Wang, S.-J.; Wang, X.; Xin, X.; Zhang, S.; Yang, H.; Wong, M. W.; Lu, S. *Nat. Commun.* **2024,** *15,* 518. doi:10.1038/s41467-024-44743-z
34. Xu, K.; Li, W.; Zhu, S.; Zhu, T. *Angew. Chem., Int. Ed.* **2019,** *58,* 17625–17630. doi:10.1002/anie.201910049

35. Zhang, C.-L.; Gao, Y.-Y.; Wang, H.-Y.; Zhou, B.-A.; Ye, S. *Angew. Chem., Int. Ed.* **2021,** *60,* 13918–13922. doi:10.1002/anie.202103415
36. Barik, S.; Shee, S.; Das, S.; Gonnade, R. G.; Jindal, G.; Mukherjee, S.; Biju, A. T. *Angew. Chem., Int. Ed.* **2021,** *60,* 12264–12268. doi:10.1002/anie.202016938
37. Lv, Y.; Luo, G.; Liu, Q.; Jin, Z.; Zhang, X.; Chi, Y. R. *Nat. Commun.* **2022,** *13,* 36. doi:10.1038/s41467-021-27813-4
38. Zhou, B.-A.; Li, X.-N.; Zhang, C.-L.; Wang, Z.-X.; Ye, S. *Angew. Chem., Int. Ed.* **2024,** *63,* e202314228. doi:10.1002/anie.202314228
39. Shee, S.; Shree Ranganathappa, S.; Gadhave, M. S.; Gogoi, R.; Biju, A. T. *Angew. Chem., Int. Ed.* **2023,** *62,* e202311709. doi:10.1002/anie.202311709
40. Li, L.; Ti, W.; Miao, T.; Ma, J.; Lin, A.; Chu, Q.; Gao, S. *J. Org. Chem.* **2024,** *89,* 4067–4073. doi:10.1021/acs.joc.3c02912
41. Wu, Y.; Guan, X.; Zhao, H.; Li, M.; Liang, T.; Sun, J.; Zheng, G.; Zhang, Q. *Chem. Sci.* **2024,** *15,* 4564–4570. doi:10.1039/d3sc06444a
42. Liu, Y.; Yuan, L.; Dai, L.; Zhu, Q.; Zhong, G.; Zeng, X. *J. Org. Chem.* **2024,** *89,* 7630–7643. doi:10.1021/acs.joc.4c00330
43. Zheng, Z.; Liu, Q.; Peng, X.; Jin, Z.; Wu, J. *Org. Lett.* **2024,** *26,* 917–921. doi:10.1021/acs.orglett.3c04189
44. Wang, D.; Liu, W.; Tang, M.; Yu, N.; Yang, X. *iScience* **2019,** *22,* 195–205. doi:10.1016/j.isci.2019.11.024
45. Bai, H.-Y.; Tan, F.-X.; Liu, T.-Q.; Zhu, G.-D.; Tian, J.-M.; Ding, T.-M.; Chen, Z.-M.; Zhang, S.-Y. *Nat. Commun.* **2019,** *10,* 3063. doi:10.1038/s41467-019-10858-x
46. Li, S.; Zhang, J.-W.; Li, X.-L.; Cheng, D.-J.; Tan, B. *J. Am. Chem. Soc.* **2016,** *138,* 16561–16566. doi:10.1021/jacs.6b11435
47. Jiang, F.; Chen, K.-W.; Wu, P.; Zhang, Y.-C.; Jiao, Y.; Shi, F. *Angew. Chem., Int. Ed.* **2019,** *58,* 15104–15110. doi:10.1002/anie.201908279
48. Liu, W.; Jiang, Q.; Yang, X. *Angew. Chem., Int. Ed.* **2020,** *59,* 23598–23602. doi:10.1002/anie.202009395
49. Wang, D.; Jiang, Q.; Yang, X. *Chem. Commun.* **2020,** *56,* 6201–6204. doi:10.1039/d0cc02368j
50. Shao, Y.-D.; Dong, M.-M.; Wang, Y.-A.; Cheng, P.-M.; Wang, T.; Cheng, D.-J. *Org. Lett.* **2019,** *21,* 4831–4836. doi:10.1021/acs.orglett.9b01731
51. Wan, J.; Liu, H.; Lan, Y.; Li, X.; Hu, X.; Li, J.; Xiao, H.-P.; Jiang, J. *Synlett* **2019,** *30,* 2198–2202. doi:10.1055/s-0039-1690228
52. Shao, Y.-D.; Han, D.-D.; Ma, W.-Y.; Cheng, D.-J. *Org. Chem. Front.* **2020,** *7,* 2255–2262. doi:10.1039/d0qo00534g
53. Bisag, G. D.; Pecorari, D.; Mazzanti, A.; Bernardi, L.; Fochi, M.; Bencivenni, G.; Bertuzzi, G.; Corti, V. *Chem. – Eur. J.* **2019,** *25,* 15694–15701. doi:10.1002/chem.201904213
54. Wang, S.-J.; Wang, Z.; Tang, Y.; Chen, J.; Zhou, L. *Org. Lett.* **2020,** *22,* 8894–8898. doi:10.1021/acs.orglett.0c03285
55. Chen, K.-W.; Chen, Z.-H.; Yang, S.; Wu, S.-F.; Zhang, Y.-C.; Shi, F. *Angew. Chem., Int. Ed.* **2022,** *61,* e202116829. doi:10.1002/anie.202116829
56. Zhang, L.; Zhang, J.; Ma, J.; Cheng, D.-J.; Tan, B. *J. Am. Chem. Soc.* **2017,** *139,* 1714–1717. doi:10.1021/jacs.6b09634
57. Gao, Y.; Wang, L.-Y.; Zhang, T.; Yang, B.-M.; Zhao, Y. *Angew. Chem., Int. Ed.* **2022,** *61,* e202200371. doi:10.1002/anie.202200371
58. Kim, A.; Kim, A.; Park, S.; Kim, S.; Jo, H.; Ok, K. M.; Lee, S. K.; Song, J.; Kwon, Y. *Angew. Chem., Int. Ed.* **2021,** *60,* 12279–12283. doi:10.1002/anie.202100363
59. Kim, A.; Moon, J.; Lee, C.; Song, J.; Kim, J.; Kwon, Y. *Org. Lett.* **2022,** *24,* 1077–1082. doi:10.1021/acs.orglett.1c04330
60. Chen, Y.-H.; Cheng, D.-J.; Zhang, J.; Wang, Y.; Liu, X.-Y.; Tan, B. *J. Am. Chem. Soc.* **2015,** *137,* 15062–15065. doi:10.1021/jacs.5b10152
61. Chen, Y.-H.; Qi, L.-W.; Fang, F.; Tan, B. *Angew. Chem., Int. Ed.* **2017,** *56,* 16308–16312. doi:10.1002/anie.201710537
62. Wang, J.-Z.; Zhou, J.; Xu, C.; Sun, H.; Kürti, L.; Xu, Q.-L. *J. Am. Chem. Soc.* **2016,** *138,* 5202–5205. doi:10.1021/jacs.6b01458
63. Lu, D.-L.; Chen, Y.-H.; Xiang, S.-H.; Yu, P.; Tan, B.; Li, S. *Org. Lett.* **2019,** *21,* 6000–6004. doi:10.1021/acs.orglett.9b02143
64. Song, X.; Fan, Y.; Zhu, Z.; Ni, Q. *Org. Lett.* **2022,** *24,* 2315–2320. doi:10.1021/acs.orglett.2c00461
65. Zhu, S.; Chen, Y.-H.; Wang, Y.-B.; Yu, P.; Li, S.-Y.; Xiang, S.-H.; Wang, J.-Q.; Xiao, J.; Tan, B. *Nat. Commun.* **2019,** *10,* 4268. doi:10.1038/s41467-019-12269-4
66. Chen, Y.-H.; Li, H.-H.; Zhang, X.; Xiang, S.-H.; Li, S.; Tan, B. *Angew. Chem., Int. Ed.* **2020,** *59,* 11374–11378. doi:10.1002/anie.202004671
67. Guo, C.-Q.; Lu, C.-J.; Zhan, L.-W.; Zhang, P.; Xu, Q.; Feng, J.; Liu, R.-R. *Angew. Chem., Int. Ed.* **2022,** *61,* e202212846. doi:10.1002/anie.202212846
68. Ma, C.; Jiang, F.; Sheng, F.-T.; Jiao, Y.; Mei, G.-J.; Shi, F. *Angew. Chem., Int. Ed.* **2019,** *58,* 3014–3020. doi:10.1002/anie.201811177
69. Yuan, X.; Wu, X.; Peng, F.; Yang, H.; Zhu, C.; Fu, H. *Chem. Commun.* **2020,** *56,* 12648–12651. doi:10.1039/d0cc05432a
70. Chen, K.-W.; Wang, Z.-S.; Wu, P.; Yan, X.-Y.; Zhang, S.; Zhang, Y.-C.; Shi, F. *J. Org. Chem.* **2020,** *85,* 10152–10166. doi:10.1021/acs.joc.0c01528
71. Sheng, F.-T.; Li, Z.-M.; Zhang, Y.-Z.; Sun, L.-X.; Zhang, Y.-C.; Tan, W.; Shi, F. *Chin. J. Chem.* **2020,** *38,* 583–589. doi:10.1002/cjoc.202000022
72. Sheng, F.-T.; Yang, S.; Wu, S.-F.; Zhang, Y.-C.; Shi, F. *Chin. J. Chem.* **2022,** *40,* 2151–2160. doi:10.1002/cjoc.202200327
73. Qian, C.; Huang, J.; Huang, T.; Song, L.; Sun, J.; Li, P. *Chem. Sci.* **2024,** *15,* 3893–3900. doi:10.1039/d3sc06707f
74. Wu, P.; Yu, L.; Gao, C.-H.; Cheng, Q.; Deng, S.; Jiao, Y.; Tan, W.; Shi, F. *Fundam. Res.* **2023,** *3,* 237–248. doi:10.1016/j.fmre.2022.01.002
75. Wang, H.-Q.; Wu, S.-F.; Yang, J.-R.; Zhang, Y.-C.; Shi, F. *J. Org. Chem.* **2023,** *88,* 7684–7702. doi:10.1021/acs.joc.2c02303
76. Woldegiorgis, A. G.; Gu, H.; Lin, X. *Org. Lett.* **2023,** *25,* 2068–2072. doi:10.1021/acs.orglett.3c00425
77. Wang, Y.-B.; Yu, P.; Zhou, Z.-P.; Zhang, J.; Wang, J.; Luo, S.-H.; Gu, Q.-S.; Houk, K. N.; Tan, B. *Nat. Catal.* **2019,** *2,* 504–513. doi:10.1038/s41929-019-0278-7
78. Wang, C.-S.; Li, T.-Z.; Liu, S.-J.; Zhang, Y.-C.; Deng, S.; Jiao, Y.; Shi, F. *Chin. J. Chem.* **2020,** *38,* 543–552. doi:10.1002/cjoc.202000131
79. Zhang, D.; Chen, Y.; Cai, H.; Yin, L.; Zhong, J.; Man, J.; Zhang, Q.-F.; Bethi, V.; Tanaka, F. *Org. Lett.* **2020,** *22,* 6–10. doi:10.1021/acs.orglett.9b03527
80. Wang, J.-Y.; Sun, M.; Yu, X.-Y.; Zhang, Y.-C.; Tan, W.; Shi, F. *Chin. J. Chem.* **2021,** *39,* 2163–2171. doi:10.1002/cjoc.202100214
81. Zhang, L.; Shen, J.; Wu, S.; Zhong, G.; Wang, Y.-B.; Tan, B. *Angew. Chem., Int. Ed.* **2020,** *59,* 23077–23082. doi:10.1002/anie.202010598

82. Yang, H.; Sun, H.-R.; He, R.-Q.; Yu, L.; Hu, W.; Chen, J.; Yang, S.; Zhang, G.-G.; Zhou, L. *Nat. Commun.* **2022,** *13,* 632. doi:10.1038/s41467-022-28211-0
83. Hou, L.; Zhang, S.; Ma, J.; Wang, H.; Jin, T.; Terada, M.; Bao, M. *Org. Lett.* **2023,** *25,* 5481–5485. doi:10.1021/acs.orglett.3c01905
84. Wang, Y.-Y.; Kanomata, K.; Korenaga, T.; Terada, M. *Angew. Chem., Int. Ed.* **2016,** *55,* 927–931. doi:10.1002/anie.201508231
85. Hou, L.; Kikuchi, J.; Ye, H.; Bao, M.; Terada, M. *J. Org. Chem.* **2020,** *85,* 14802–14809. doi:10.1021/acs.joc.0c01840
86. Wang, C.-S.; Xiong, Q.; Xu, H.; Yang, H.-R.; Dang, Y.; Dong, X.-Q.; Wang, C.-J. *Chem. Sci.* **2023,** *14,* 12091–12097. doi:10.1039/d3sc03686c
87. Wang, L.; Zhong, J.; Lin, X. *Angew. Chem., Int. Ed.* **2019,** *58,* 15824–15828. doi:10.1002/anie.201909855
88. Kwon, Y.; Li, J.; Reid, J. P.; Crawford, J. M.; Jacob, R.; Sigman, M. S.; Toste, F. D.; Miller, S. J. *J. Am. Chem. Soc.* **2019,** *141,* 6698–6705. doi:10.1021/jacs.9b01911
89. An, Q.-J.; Xia, W.; Ding, W.-Y.; Liu, H.-H.; Xiang, S.-H.; Wang, Y.-B.; Zhong, G.; Tan, B. *Angew. Chem., Int. Ed.* **2021,** *60,* 24888–24893. doi:10.1002/anie.202111251
90. Man, N.; Lou, Z.; Li, Y.; Yang, H.; Zhao, Y.; Fu, H. *Org. Lett.* **2020,** *22,* 6382–6387. doi:10.1021/acs.orglett.0c02214
91. Xu, W.-L.; Zhao, W.-M.; Zhang, R.-X.; Chen, J.; Zhou, L. *Chem. Sci.* **2021,** *12,* 14920–14926. doi:10.1039/d1sc05161j
92. Han, T.-J.; Zhang, Z.-X.; Wang, M.-C.; Xu, L.-P.; Mei, G.-J. *Angew. Chem., Int. Ed.* **2022,** *61,* e202207517. doi:10.1002/anie.202207517
93. Ding, W.-Y.; Yu, P.; An, Q.-J.; Bay, K. L.; Xiang, S.-H.; Li, S.; Chen, Y.; Houk, K. N.; Tan, B. *Chem* **2020,** *6,* 2046–2059. doi:10.1016/j.chempr.2020.06.001
94. Yuan, X.; Wang, J. *Sci. China: Chem.* **2022,** *65,* 2512–2516. doi:10.1007/s11426-022-1402-9
95. Arunachalampillai, A.; Chandrappa, P.; Cherney, A.; Crockett, R.; Doerfler, J.; Johnson, G.; Kommuri, V. C.; Kyad, A.; McManus, J.; Murray, J.; Myren, T.; Fine Nathel, N.; Ndukwe, I.; Ortiz, A.; Reed, M.; Rui, H.; Silva Elipe, M. V.; Tedrow, J.; Wells, S.; Yacoob, S.; Yamamoto, K. *Org. Lett.* **2023,** *25,* 5856–5861. doi:10.1021/acs.orglett.3c02117
96. Xia, W.; An, Q.-J.; Xiang, S.-H.; Li, S.; Wang, Y.-B.; Tan, B. *Angew. Chem., Int. Ed.* **2020,** *59,* 6775–6779. doi:10.1002/anie.202000585
97. Wex, B.; Kaafarani, B. R. *J. Mater. Chem. C* **2017,** *5,* 8622–8653. doi:10.1039/c7tc02156a
98. Yuan, H.; Li, Y.; Zhao, H.; Yang, Z.; Li, X.; Li, W. *Chem. Commun.* **2019,** *55,* 12715–12718. doi:10.1039/c9cc06360a
99. Gao, Z.; Qian, J.; Yang, H.; Hang, X.-C.; Zhang, J.; Jiang, G. *Chem. Commun.* **2020,** *56,* 7265–7268. doi:10.1039/d0cc02380a
100. Yang, J.; Zhang, J.-W.; Bao, W.; Qiu, S.-Q.; Li, S.; Xiang, S.-H.; Song, J.; Zhang, J.; Tan, B. *J. Am. Chem. Soc.* **2021,** *143,* 12924–12929. doi:10.1021/jacs.1c05079
101. Zhang, L.; Xiang, S.-H.; Wang, J.; Xiao, J.; Wang, J.-Q.; Tan, B. *Nat. Commun.* **2019,** *10,* 566. doi:10.1038/s41467-019-08447-z
102. Gridnev, I. D.; Kouchi, M.; Sorimachi, K.; Terada, M. *Tetrahedron Lett.* **2007,** *48,* 497–500. doi:10.1016/j.tetlet.2006.11.017
103. Rueping, M.; Nachtsheim, B. J.; Ieawsuwan, W.; Atodiresei, I. *Angew. Chem., Int. Ed.* **2011,** *50,* 6706–6720. doi:10.1002/anie.201100169
104. Da, B.-C.; Wang, Y.-B.; Cheng, J. K.; Xiang, S.-H.; Tan, B. *Angew. Chem., Int. Ed.* **2023,** *62,* e202303128. doi:10.1002/anie.202303128
105. Ma, C.; Sheng, F.-T.; Wang, H.-Q.; Deng, S.; Zhang, Y.-C.; Jiao, Y.; Tan, W.; Shi, F. *J. Am. Chem. Soc.* **2020,** *142,* 15686–15696. doi:10.1021/jacs.0c00208
106. Shao, Y.-D.; Feng, J.-S.; Han, D.-D.; Pan, K.-H.; Zhang, L.; Wang, Y.-F.; Ma, Z.-H.; Wang, P.-R.; Yin, M.; Cheng, D.-J. *Org. Chem. Front.* **2022,** *9,* 764–770. doi:10.1039/d1qo01672e
107. Vaidya, S. D.; Toenjes, S. T.; Yamamoto, N.; Maddox, S. M.; Gustafson, J. L. *J. Am. Chem. Soc.* **2020,** *142,* 2198–2203. doi:10.1021/jacs.9b12994
108. Wu, Q.-H.; Duan, M.; Chen, Y.; Yu, P.; Wang, Y.-B.; Cheng, J. K.; Xiang, S.-H.; Houk, K. N.; Tan, B. *Nat. Catal.* **2024,** *7,* 185–194. doi:10.1038/s41929-023-01097-x
109. Liang, D.; Chen, J.-R.; Tan, L.-P.; He, Z.-W.; Xiao, W.-J. *J. Am. Chem. Soc.* **2022,** *144,* 6040–6049. doi:10.1021/jacs.2c01116
110. Wei, L.; Li, J.; Zhao, Y.; Zhou, Q.; Wei, Z.; Chen, Y.; Zhang, X.; Yang, X. *Angew. Chem., Int. Ed.* **2023,** *62,* e202306864. doi:10.1002/anie.202306864
111. Wu, M.; Chen, Y.-W.; Lu, Q.; Wang, Y.-B.; Cheng, J. K.; Yu, P.; Tan, B. *J. Am. Chem. Soc.* **2023,** *145,* 20646–20654. doi:10.1021/jacs.3c07839
112. Jiang, H.-X.; Han, D.-D.; Song, R.-P.; Shi, Q.; He, X.-F.; Kou, W.-Q.; Zhao, Q.; Shao, Y.-D.; Cheng, D.-J. *Adv. Synth. Catal.* **2023,** *365,* 1398–1404. doi:10.1002/adsc.202300042
113. Li, S.-L.; Wu, Q.; Yang, C.; Li, X.; Cheng, J.-P. *Org. Lett.* **2019,** *21,* 5495–5499. doi:10.1021/acs.orglett.9b01796
114. Yang, G.-H.; Zheng, H.; Li, X.; Cheng, J.-P. *ACS Catal.* **2020,** *10,* 2324–2333. doi:10.1021/acscatal.9b05443
115. Mei, G.-J.; Wong, J. J.; Zheng, W.; Nangia, A. A.; Houk, K. N.; Lu, Y. *Chem* **2021,** *7,* 2743–2757. doi:10.1016/j.chempr.2021.07.013
116. Zheng, G.; Li, X.; Cheng, J.-P. *Org. Lett.* **2021,** *23,* 3997–4001. doi:10.1021/acs.orglett.1c01201
117. Huang, S.; Chen, Z.; Mao, H.; Hu, F.; Li, D.; Tan, Y.; Yang, F.; Qin, W. *Org. Biomol. Chem.* **2019,** *17,* 1121–1129. doi:10.1039/c8ob02967a
118. Zhang, N.; He, T.; Liu, Y.; Li, S.; Tan, Y.; Peng, L.; Li, D.; Shan, C.; Yan, H. *Org. Chem. Front.* **2019,** *6,* 451–455. doi:10.1039/c8qo01241e
119. Huang, A.; Zhang, L.; Li, D.; Liu, Y.; Yan, H.; Li, W. *Org. Lett.* **2019,** *21,* 95–99. doi:10.1021/acs.orglett.8b03492
120. Zhang, C.; Ye, S.; Wu, J. *Org. Lett.* **2024,** *26,* 3321–3325. doi:10.1021/acs.orglett.4c01011
121. Zhang, C.; Tang, Z.; Qiu, Y.; Tang, J.; Ye, S.; Li, Z.; Wu, J. *Chem Catal.* **2022,** *2,* 164–177. doi:10.1016/j.checat.2021.12.008
122. Wada, Y.; Matsumoto, A.; Asano, K.; Matsubara, S. *RSC Adv.* **2019,** *9,* 31654–31658. doi:10.1039/c9ra05532k
123. Peng, L.; Li, K.; Xie, C.; Li, S.; Xu, D.; Qin, W.; Yan, H. *Angew. Chem., Int. Ed.* **2019,** *58,* 17199–17204. doi:10.1002/anie.201908961
124. Deng, Y.-H.; Qin, L.; Li, R.; Wang, Y.-B.; Zhu, J.-Y.; Fu, J.-Y.; Zhang, C.-B.; Zhao, L. *Org. Lett.* **2022,** *24,* 8277–8282. doi:10.1021/acs.orglett.2c03179
125. Chang, Y.; Xie, C.; Liu, H.; Huang, S.; Wang, P.; Qin, W.; Yan, H. *Nat. Commun.* **2022,** *13,* 1933. doi:10.1038/s41467-022-29557-1
126. Jia, S.; Li, S.; Liu, Y.; Qin, W.; Yan, H. *Angew. Chem., Int. Ed.* **2019,** *58,* 18496–18501. doi:10.1002/anie.201909214
127. Xu, D.; Huang, S.; Hu, F.; Peng, L.; Jia, S.; Mao, H.; Gong, X.; Li, F.; Qin, W.; Yan, H. *CCS Chem.* **2022,** *4,* 2686–2697. doi:10.31635/ccschem.021.202101154

128. Jia, S.; Qin, W.; Wang, P.; Yan, H. *Org. Chem. Front.* **2022,** *9,* 923–928. doi:10.1039/d1qo01821c
129. Bao, X.; Rodriguez, J.; Bonne, D. *Chem. Sci.* **2020,** *11,* 403–408. doi:10.1039/c9sc04378k
130. Wang, G.; Shi, Q.; Hu, W.; Chen, T.; Guo, Y.; Hu, Z.; Gong, M.; Guo, J.; Wei, D.; Fu, Z.; Huang, W. *Nat. Commun.* **2020,** *11,* 946. doi:10.1038/s41467-020-14799-8
131. Guo, D.; Wang, J. *Synthesis* **2022,** *54,* 3193–3200. doi:10.1055/a-1767-6153
132. Zheng, S.-C.; Wang, Q.; Zhu, J. *Angew. Chem., Int. Ed.* **2019,** *58,* 9215–9219. doi:10.1002/anie.201903589
133. Wu, Y.; Zhou, W.-J.; Yao, L.; Niu, Y.; Zhao, H.; Peng, C.; Han, B.; Huang, W.; Zhan, G. *Chem. Commun.* **2023,** *59,* 7279–7282. doi:10.1039/d3cc01705b
134. Zhang, W.; Wei, S.; Wang, W.; Qu, J.; Wang, B. *Chem. Commun.* **2021,** *57,* 6550–6553. doi:10.1039/d1cc01123e
135. Hong, X.; Guo, J.; Liu, J.; Cao, W.; Wei, C.; Zhang, Y.; Zhang, X.; Fu, Z. *Sci. China: Chem.* **2022,** *65,* 905–911. doi:10.1007/s11426-021-1209-2
136. Fang, S.; He, J.; Liu, Z.; Su, Z.; Guo, F.; Wang, T. *ACS Catal.* **2023,** *13,* 13077–13088. doi:10.1021/acscatal.3c03304
137. Liu, J.-Y.; Yang, X.-C.; Liu, Z.; Luo, Y.-C.; Lu, H.; Gu, Y.-C.; Fang, R.; Xu, P.-F. *Org. Lett.* **2019,** *21,* 5219–5224. doi:10.1021/acs.orglett.9b01828
138. Jones, B. A.; Balan, T.; Jolliffe, J. D.; Campbell, C. D.; Smith, M. D. *Angew. Chem., Int. Ed.* **2019,** *58,* 4596–4600. doi:10.1002/anie.201814381
139. Fugard, A. J.; Lahdenperä, A. S. K.; Tan, J. S. J.; Mekareeya, A.; Paton, R. S.; Smith, M. D. *Angew. Chem., Int. Ed.* **2019,** *58,* 2795–2798. doi:10.1002/anie.201814362
140. Wang, Y.-B.; Wu, Q.-H.; Zhou, Z.-P.; Xiang, S.-H.; Cui, Y.; Yu, P.; Tan, B. *Angew. Chem., Int. Ed.* **2019,** *58,* 13443–13447. doi:10.1002/anie.201907470
141. Sweet, J. S.; Wang, R.; Manesiotis, P.; Dingwall, P.; Knipe, P. C. *Org. Biomol. Chem.* **2022,** *20,* 2392–2396. doi:10.1039/d2ob00177b
142. Lu, S.; Ng, S. V. H.; Lovato, K.; Ong, J.-Y.; Poh, S. B.; Ng, X. Q.; Kürti, L.; Zhao, Y. *Nat. Commun.* **2019,** *10,* 3061. doi:10.1038/s41467-019-10940-4
143. Wu, S.; Xiang, S.-H.; Li, S.; Ding, W.-Y.; Zhang, L.; Jiang, P.-Y.; Zhou, Z.-A.; Tan, B. *Nat. Catal.* **2021,** *4,* 692–702. doi:10.1038/s41929-021-00660-8
144. Liang, Y.; Ji, J.; Zhang, X.; Jiang, Q.; Luo, J.; Zhao, X. *Angew. Chem., Int. Ed.* **2020,** *59,* 4959–4964. doi:10.1002/anie.201915470
145. Rodríguez-Salamanca, P.; de Gonzalo, G.; Carmona, J. A.; López-Serrano, J.; Iglesias-Sigüenza, J.; Fernández, R.; Lassaletta, J. M.; Hornillos, V. *ACS Catal.* **2023,** *13,* 659–664. doi:10.1021/acscatal.2c06175
146. Hang, Q.-Q.; Wu, S.-F.; Yang, S.; Wang, X.; Zhong, Z.; Zhang, Y.-C.; Shi, F. *Sci. China: Chem.* **2022,** *65,* 1929–1937. doi:10.1007/s11426-022-1363-y
147. Li, D.; Wang, S.; Ge, S.; Dong, S.; Feng, X. *Org. Lett.* **2020,** *22,* 5331–5336. doi:10.1021/acs.orglett.0c01581
148. Beleh, O. M.; Miller, E.; Toste, F. D.; Miller, S. J. *J. Am. Chem. Soc.* **2020,** *142,* 16461–16470. doi:10.1021/jacs.0c08057
149. Coombs, G.; Sak, M. H.; Miller, S. J. *Angew. Chem., Int. Ed.* **2020,** *59,* 2875–2880. doi:10.1002/anie.201913563
150. Tampellini, N.; Mercado, B. Q.; Miller, S. J. *Chem. – Eur. J.* **2024,** *30,* e202401109. doi:10.1002/chem.202401109
151. Guo, F.; Fang, S.; He, J.; Su, Z.; Wang, T. *Nat. Commun.* **2023,** *14,* 5050. doi:10.1038/s41467-023-40840-7

License and Terms

BEILSTEIN JOURNAL OF ORGANIC CHEMISTRY

Development and mechanistic studies of calcium–BINOL phosphate-catalyzed hydrocyanation of hydrazones

Carola Tortora[‡1], Christian A. Fischer[‡2], Sascha Kohlbauer[1], Alexandru Zamfir[1], Gerd M. Ballmann[2], Jürgen Pahl[2], Sjoerd Harder[*2] and Svetlana B. Tsogoeva[*1]

Full Research Paper

Open Access

Address:
[1]Department of Chemistry and Pharmacy, Organic Chemistry Chair I and Interdisciplinary Center for Molecular Materials (ICMM), Friedrich-Alexander-Universität Erlangen-Nürnberg, Nikolaus-Fiebiger Strasse 10, 91058 Erlangen, Germany and [2]Department of Chemistry and Pharmacy, Chair of Inorganic and Organometallic Chemistry, Friedrich-Alexander-Universität Erlangen-Nürnberg, Egerlandstrasse 1, 91058 Erlangen, Germany

Email:
Sjoerd Harder[*] - sjoerd.harder@fau.de; Svetlana B. Tsogoeva[*] - svetlana.tsogoeva@fau.de

* Corresponding author ‡ Equal contributors

Keywords:
asymmetric synthesis; calcium–BINOL phosphate catalysis; hydrocyanation; hydrazones; isocyanides

Beilstein J. Org. Chem. **2025,** *21,* 755–765.
https://doi.org/10.3762/bjoc.21.59

Received: 30 October 2024
Accepted: 11 February 2025
Published: 14 April 2025

This article is part of the thematic issue "New advances in asymmetric organocatalysis II".and is dedicated to Professor Rudi van Eldik on the occasion of his 80th birthday.

Guest Editor: R. Šebesta

Abstract

Asymmetric hydrocyanation of hydrazones, catalyzed by a calcium–BINOL phosphate complex, has been studied for the first time both experimentally and computationally with DFT methods. A full catalytic cycle for the enantioselective synthesis of α-hydrazinonitriles is proposed based on insights gained from DFT calculations. Trimethylsilyl cyanide (TMSCN) has been used as a sacrificial cyanide source. We found that isocyanide (rather than cyanide) is a preferred coordination to calcium during the catalytic cycle, while the active catalyst prefers a side-on coordination of cyanide. The configuration-determining step is a hydrocyanation via a calcium isocyanide complex, whereas the rate-limiting step is that which recovers the calcium catalyst and replaces the TMS-bound product from the catalyst. While our experimental data demonstrate enantioselectivity values as high as 89% under certain conditions, the overall enantioselectivity achieved with the calcium catalyst remains modest, mainly due to competing pathways for the *Z*- and *E*-hydrazone isomers leading to opposite enantiomers. The experimental results confirm these computational proposals.

Introduction

Catalytic applications of non-toxic earth abundant metals like calcium are currently on the rise [1-4]. Prominent recent examples that witness the versatility of calcium catalysis include calcium-catalyzed amination of π-activated alcohols [5], the Beckmann rearrangement under mild conditions [6], and the Nazarov-type electrocyclization of alkenyl aryl carbinols [7]. Exploiting the ease with which calcium forms hydrides, hydrogenation of aldimines, transfer hydrogenation of alkenes, and

even deuteration of benzene by an S_NAr mechanism, have been recently achieved through calcium catalysis [8-10]. Asymmetric synthesis has also been achieved via, e.g., 1,4-addition and [3 + 2] cycloaddition of 3-tetrasubstituted oxindoles with a calcium Pybox catalyst [11,12], or through enantioselective Friedel–Crafts and carbonyl–ene reactions [13]. Since the pioneering studies by the groups of Akiyama and Terada in 2004 [14,15], many excellent results have been achieved by applying BINOL-derived phosphoric acids, which can act as proton donor and acceptor [16-19], possessing both Brønsted acid and Lewis base character [20]. Substantial effort has been invested in elucidating the mechanism by which these bifunctional compounds act as powerful catalysts [21-29]. Since Ishihara disclosed the crucial role of calcium in many purportedly purely organocatalytic BINOL phosphate-catalyzed reactions [30,31], several asymmetric synthesis applications of calcium complexes with axially chiral BINOL phosphate ligands have been reported in recent years [28,32-38], as well as complexes with other chiral phosphoric acid ligands [39]. Since then, other main group metal complexes with BINOL phosphate ligands have been discovered [40-44]. However, this catalytic system has not yet been employed explicitly in the hydrocyanation of hydrazones. In 2010, our group reported the first organocatalytic enantioselective hydrocyanation of hydrazones catalyzed by BINOL phosphate [45], giving valuable and potentially bioactive α-hydrazino acids [46-48]. This reaction has also been achieved by a lanthanide–PYBOX complex [49] and through asymmetric transfer hydrocyanation of aldimines with a boron compound [50]. Hence, we reasoned that the enantioselective hydrocyanation of hydrazones might be possible with a calcium–BINOL phosphate complex as catalyst.

Herein, we report the development of the first Ca–BINOL phosphate-catalyzed asymmetric hydrocyanation of hydrazones and the results from DFT calculations to elucidate the mechanism of this transformation.

Results and Discussion

We first set out to study the hydrocyanation of hydrazone **1** towards product **2** (Table 1) using an achiral model calcium-based catalyst (**4**, Figure 1) with monodentate biphenyl phosphate ligands. This model catalyst **4**, derived from the literature-known phosphoric acid $BIPO_4$-H **3** [51], was synthesized by reacting **3** with $Ca(OiPr)_2$ under inert conditions. The product was isolated as colorless crystals in good yield of 81% (Scheme 1). Complex **4** crystallizes as a C_2-symmetric chiral mononuclear complex in which Ca is bound to two monodentate phosphate ligands (Figure 1). Four MeOH ligands complete the slightly distorted octahedral coordination sphere. The phosphate ligands are in *cis*-position with respect to each other. The structure of **4** shows similarities to that of a BINOL-derived calcium phosphate complex that also crystallizes with four methanol ligands, creating an octahedral coordination sphere

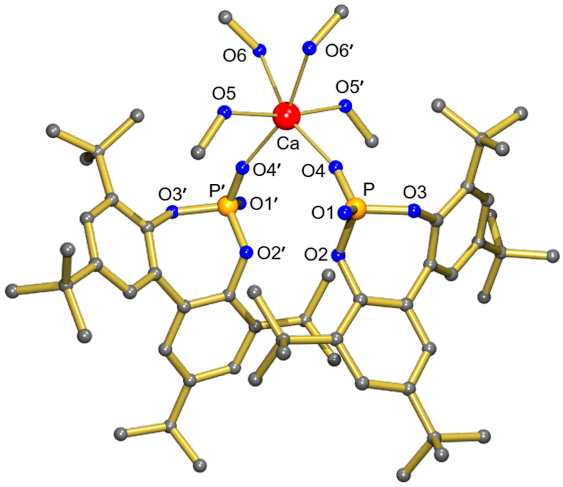

Figure 1: Crystal structure of the calcium diphenyl phosphate complex **4**. Hydrogen atoms are omitted for clarity. Selected bond lengths (in Å) and angle: Ca1–O4 2.2510(13), Ca1–O6 2.4004(14), Ca1–O5 2.3438(13), P–O4 1.4793(13), P–O1 1.4914(13), O4–Ca-O4′ 99.09(7)°.

Table 1: Hydrocyanation of **1** catalyzed with calcium phosphate model complex **4**.

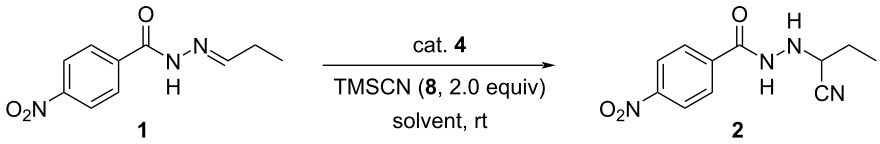

Entry	Cat. loading [mol %]	Solvent[a]	Time [h]	Conversion [%]
1	10	DCM	2	>99
2	5	DCM	6	>99
3	2.5	DCM	12	>99
4	10	THF	12	>99

[a]DCM = dichloromethane, THF = tetrahydrofuran.

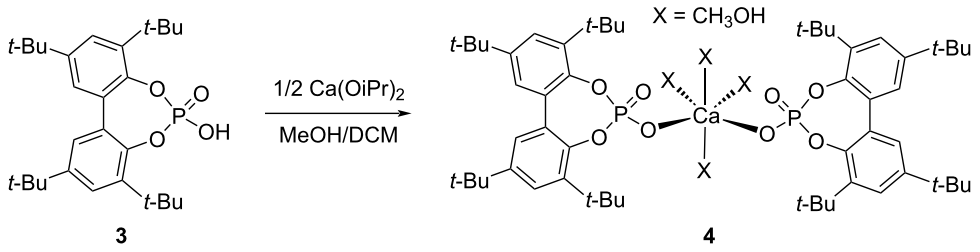

Scheme 1: Synthesis of the calcium diphenyl phosphate model complex **4** from phosphoric acid **3** and $Ca(OiPr)_2$.

with phosphate ligands in *cis*-position [52]. As observed earlier [53], *cis*/*trans* preferences in octahedral calcium complexes are influenced by small changes in sterics. Further details on the structure of **4** can be found in Supporting Information File 1.

Complex **4** appeared to be a well-defined achiral model system for the catalyst combination BINOL phosphate/$Ca(OiPr)_2$. In the presence of two equivalents of TMSCN, complex **4** gave a quantitative conversion to the product **2**, whereby the phosphoric acid $BIPO_4$-H ligand **3** did not catalyze this hydrocyanation. At room temperature, a nearly full conversion can already be achieved within 2–12 hours, depending on the catalyst loading. This result underscores the importance of calcium in complex **4** for this particular transformation. We assume that the conversion of complex **4** to the active catalytic species might rely on the in situ formation of the cyanide species from the reaction between Ca complex **4** and TMSCN (**8**).

Model complex **4** initially reacts with TMSCN to give MeOTMS and HCN. Even under methanol-free conditions, an excess of TMSCN is therefore needed to achieve complete conversion (Table 1), which hints at a mechanism of catalyst activation through reaction of the metal complex with the cyanide source. This observation complies with the results from the computational study (Figure 2). In addition, some TMSCN is consumed together with an amount of BINOL phosphate through the probably parasitic formation of catalytically inactive trimethylsilyl phosphate **3a**, which we were able to characterize (see Supporting Information File 1). Unfortunately, the computationally proposed catalytically active calcium cyanide complex **7** itself could not be isolated.

Substrate conversion is retarded when the non-coordinating solvent DCM is replaced by THF (Table 1, entry 4 vs 1), which might be due to competition between Ca-hydrazone and Ca–THF binding. Considering smoothness of catalytic hydrazone hydrocyanation, similar hydrofluorination or hydroiodination seemed feasible. However, replacement of TMSCN by TMSF or TMSI did not give any product.

After establishing the activity of the model achiral catalyst **4** for non-enantioselective hydrocyanation of hydrazone **1**, we sought to demonstrate the enantioselective hydrocyanation by employing enantiopure BINOL phosphate **5** as ligand for calcium (Table 2).

In order to compare the activity of this complex with that of BINOL phosphate **5** itself, as reported in our previous work [45], we carried out the enantioselective hydrocyanation of hydrazones using Ca–BINOL phosphate complex **6** at −10 °C in DCM for 72 h. In addition to those reaction conditions, we initially used *t*-BuOH as an additive [45]. The Ca–BINOL phosphate complex **6** was prepared in situ by reaction of the chiral ligand **5** with $Ca(OiPr)_2$, varying the ratio from 2:1 to 6.6:1, respectively (Table 2, entries 1–3).

The amount of calcium salt added influences the reaction yield, which decreases when the fraction of $Ca(OiPr)_2$ is lowered (Table 2, entry 3), while the good enantioselectivity remains unaffected (87–89% ee (*R*-enantiomer), entries 1–3). Because we assumed complex **6** (with two bidentate phosphate ligands) to be a precursor to the actual catalytically active species, we pre-formed it, following the procedure employed to prepare achiral complex **4** (with two monodentate phosphates, Scheme 1) and used it after isolation and characterization. In these cases, BINOL phosphate **5** was purchased, and used either without any further purification (Table 2, entries 5–7), or it was washed first with 2 N HCl solution, then rinsed with water, to remove possible traces of Ca^{2+}, which could stem from industrial production (Table 2, entries 4, 8, and 9). All these experiments gave only low ee values (4–19% ee, Table 2, entries 4–9), with a preference for the *S*-enantiomer. Use of aromatic alcohol or (*R*)-1-phenylethanol as additives did not improve either yields or enantioselectivities (Table 2, entries 5 and 6 vs entry 4). Accordingly, experiments without additive performed better in terms of yield and enantioselectivity than those with additives but the ee values remain low (Table 2, entries 7–9 vs entries 4–6).

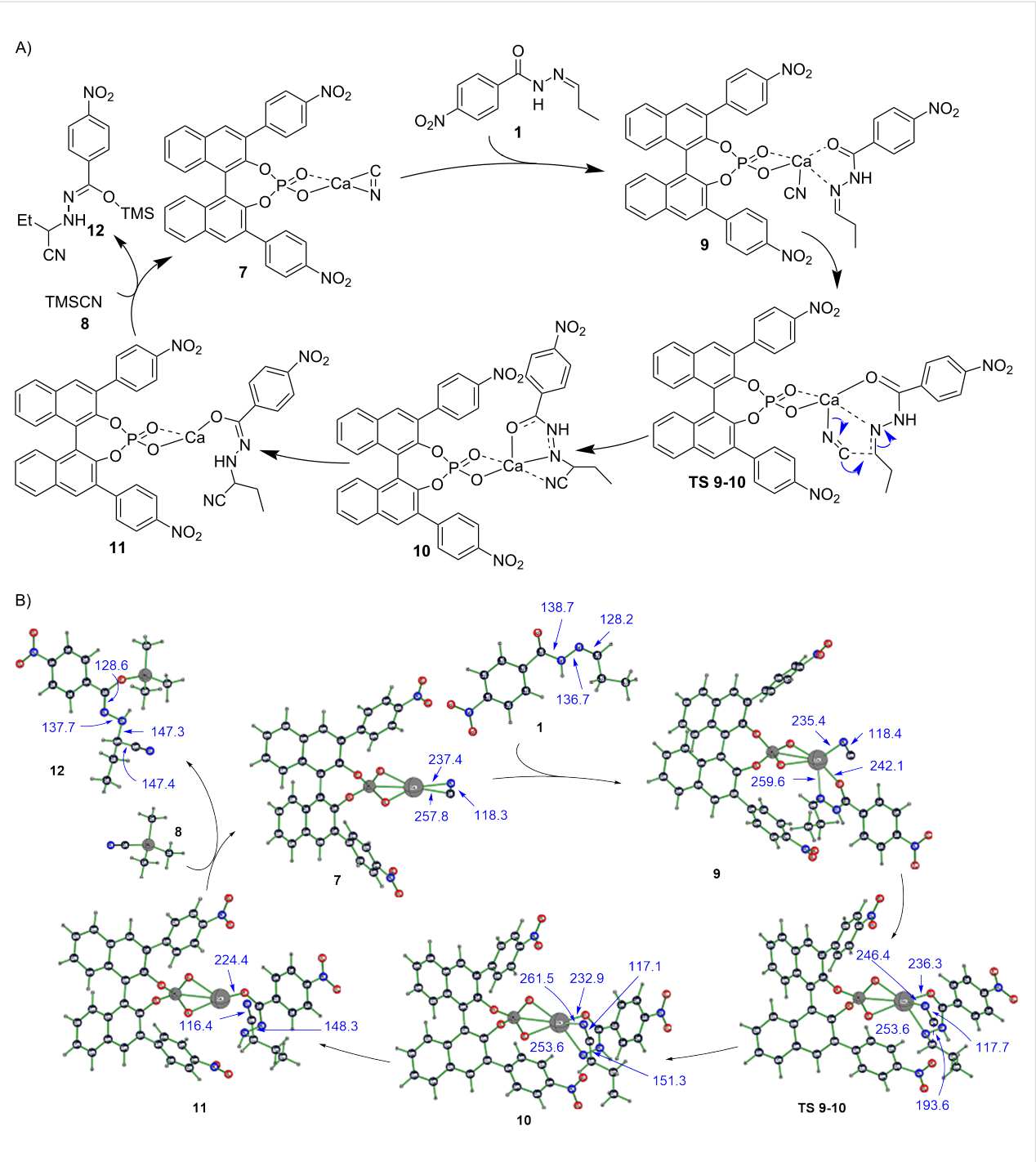

Figure 2: (A) Proposed catalytic cycle for the hydrocyanation of hydrazones with the Ca–BINOL phosphate catalyst. (B) Catalytic cycle for asymmetric hydrocyanation of a *Z*-hydrazone, giving the "*S*" product, catalyzed by a Ca–BINOL phosphate complex as computed at B3LYP/6-31G* level of theory. Axial chirality configuration of the BINOL phosphate is as used in experiment (i.e., "*R*"). Bond lengths and distances are given in pm. For discussion see text. Species numbers represent all respective stereoisomeric forms.

Surprisingly, in all experiments with the pre-formed catalyst **6** (Table 2, entries 4–9), a hydrocyanation product with opposite chirality was obtained, in comparison to experiments with the in situ formed Ca complex (Table 2, entries 1–3). It appears that the way in which catalyst **6** is generated (pre-formed or in situ), has a major influence on enantioselectivity, while the addition of *t*-BuOH has little to no effect (Table 2, entry 4 vs entries 1–3). This made us wonder whether the same active catalytic species is involved, when **6** is either pre-formed or presumably generated in situ.

Table 2: Asymmetric hydrocyanation of hydrazones catalyzed by calcium–BINOL phosphate complex.

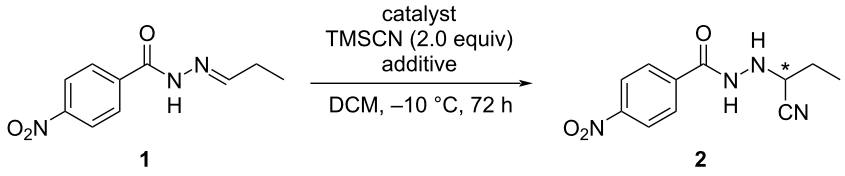

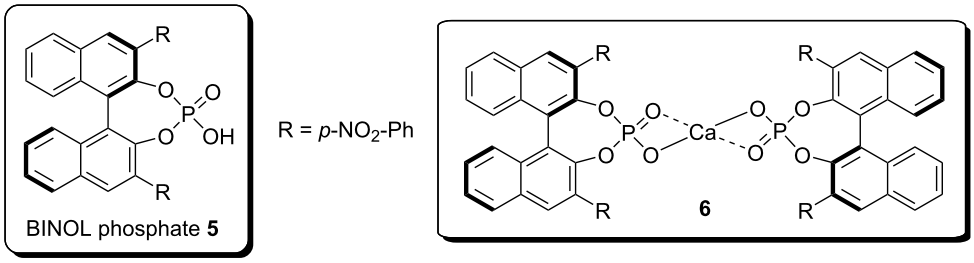

Entry	Ca complex [mol %]	BINOL phosphate **5** [mol %]	Additive [equiv]	Yield [%]	ee [%][a]
1[b,c]	$Ca(OiPr)_2$ [2.50]	5.0	*t*-BuOH [0.20]	95[d]	89 (*R*)
2[b,c]	$Ca(OiPr)_2$ [1.25]	5.0	*t*-BuOH [0.20]	89[d]	87 (*R*)
3[b,c]	$Ca(OiPr)_2$ [0.75]	5.0	*t*-BuOH [0.20]	71[d]	87 (*R*)
4	Cat **6** [5.0][e,f]	–	*t*-BuOH [0.20]	88[d]	4 (*S*)
5	Cat **6** [5.0][e,g]	–	phenol [2.0]	82[h]	6 (*S*)
6	Cat **6** [5.0][e,g]	–	(*R*)-1-phenylethanol [2.0]	50[h]	*rac*
7	Cat **6** [5.0][e,g]	–	–	92[d]	19 (*S*)
8	Cat **6** [5.0][e,i]	–	–	>99[d]	19 (*S*)
9	Cat **6** [5.0][e,f]	–	–	>99[d]	9 (*S*)

[a]Determined by chiral HPLC. [b]BINOL phosphate **5** was prepared according to the procedure reported in literature [15]. After purification by column chromatography, the catalyst was washed with 2 N HCl then water, crystallized and subsequently used for the reaction. [c]Ca complex **6** was generated in situ. [d]Yield of isolated product. [e]Ca–BINOL complex **6** was preformed according to the procedure employed to prepare the complex **4**. [f]Second batch of BINOL phosphate **5** purchased by abcr GmbH and washed with 2 N HCl then water before use. [g]BINOL phosphate **5** was purchased by abcr GmbH and directly used. [h]Determined after calibration curve measured using compound **2** on chiral HPLC. [i]First batch of BINOL phosphate **5** purchased by abcr GmbH and washed with 2 N HCl then water before use.

As the mechanism of action of the calcium-BINOL phosphate catalyst remains still computationally unexplored, we set out to elucidate it by using DFT computations (Figure 2). As we have chosen as substrate in our experiments a self-prepared mixture of *E*- and *Z*-isomers (9:1) of *N*-acyl hydrazone **1**, which allows for additional binding to oxophilic calcium via the carbonyl oxygen, we did not know a priori which of the two isomers undergoes the hydrocyanation reaction more facile and therefore we studied both reaction pathways for the *Z*- and for the *E*-hydrazone. The assumed resting state of the catalyst is complex **7** (Figure 2), in which BINOL phosphate serves as a bidentate ligand to calcium in a pseudo-tetrahedral coordination environment with cyanide, stemming from a common reagent (vide infra) and binding to the metal in a preferred side-on (π-complex) mode [54].

When the hydrazone substrate enters the catalytic cycle, it coordinates also as a bidentate ligand to calcium via oxygen and nitrogen atoms, resulting in detachment of the cyanide carbon from the calcium atom to yield an isocyanide complex **9** [55], in which the preferred side of attack on the imine carbon of the hydrazone is already predetermined (i.e., from either *Re* or *Si* face). Notably, in both complexes formed from *E*- and *Z*-hydrazone, an attack from the *Si* side is favored. Formation of hydrazone complex **9** is strongly exothermic (Figure 3), rendering this reaction step effectively irreversible. Relative stabilities of diastereomers for *Z*- and *E*-hydrazones play therefore a minor role, as relative amounts of the four possible stereoisomers of **9** (for *Z*- and *E*-configuration, and for *Re* or *Si* side attack) should be more or less equal and the actual stereoselectivity must hence be determined in later stages of the reaction.

Ligand sites in the pre-complex **9** form a pseudo-tetragonal pyramid, with isocyanide at the apex. Atoms in the Ca–NC moiety are non-linear with a Ca–N–C angle of 100°. Due to the stereospecificity of the reaction, racemization would have to

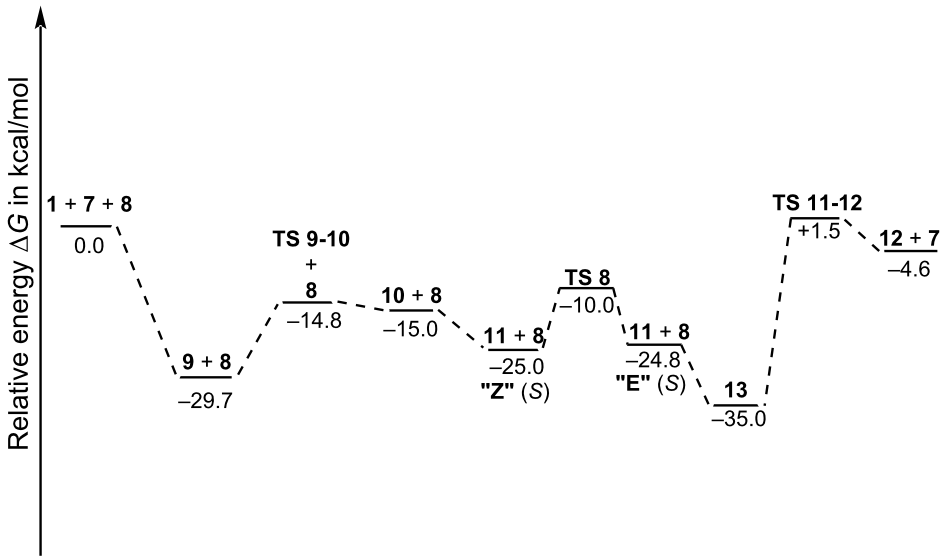

Figure 3: Reaction energy profile for the hydrocyanation of *Z*-hydrazone **1**, (depicted is the pathway that gives the "*S*" product), catalyzed by in situ-formed calcium BINOL phosphate complex **7**, as computed at the B3LYP/6-31G* level of theory, including zero-point energy, thermodynamic, and dispersion energy corrections (with Grimme's semiempirical D3 correction and Becke–Johnson damping, cutting off terms with higher than r^{-6} asymptotic dependence).

occur already in **9** through a topomerization (e.g., similar to a Berry pseudorotation) of the metal complex, considering that species with a quaternary carbon, as they appear in later stages of the catalytic cycle, are less likely to racemize without bond breaking. The barrier to pyramidal inversion has been found to be 15.1 kcal·mol^{-1}. Berry rotation itself proceeds via a tetragonal pyramid as transition-state structure and does therefore not occur here. A second isocyanide isomer, with a more acute Ca–N–C angle of 92°, has greater resemblance to a (here absent) side-on form (found to dominate computationally for $Ca(CN)_2$ in the gas phase) [54]. Fortunately, that isomer in which the isonitrile carbon is closer to the imine carbon (i.e., the hydrocyanation reaction center), is 0.5 kcal·mol^{-1} lower in energy. Substrate **1** may conceivably undergo a tautomerization towards an iminol form, 14.2 kcal·mol^{-1} higher in energy. Hence, amounts of this isomer are negligible in equilibrium and do not play a role also in the formation of the pre-complex **3**.

The competing cyanide form of **9** (with a collinear arrangement of Ca–C–N) was found to be a sizable 3.3 kcal·mol^{-1} higher in energy than the preferred isonitrile, conforming to earlier anticipations based on computations of alkaline earth metal dicyanides [54]. Similarly, it also has been recently observed that boron-catalyzed transfer hydrocyanation of alkenes proceeds via (boron) isocyanides [50].

If calcium cyanide would be preferred over isocyanide, hydrocyanation would hardly be possible. A principally conceivable "hydroisocyanation" of hydrazone is therefore precluded. The relative stability of alkaline earth metal cyanides versus isocyanides had been subject of high-level quantum chemical computations [54], and has gained interest lately [56-58].

Thanks to preferred isocyanide (rather than cyanide) coordination to calcium, the carbon atom in **9** has increased nucleophilicity, compared to that in **7** – an important provisioning for the following reaction step. Hydrocyanation hence proceeds facially with a barrier of only 10.2 kcal·mol^{-1} via the configuration-determining **TS 9-10** by attack of isocyanide at the imine carbon of hydrazone. If the configuration-determining step would be also rate limiting, experimental observation of enantioselectivity must be explained by relative energies of stereoisomeric forms of **TS 9-10**. Reversible formation of product **10** from nucleophilic addition step via **TS 9-10** is slightly endothermic (Figure 3). In **10**, cyanide is still attached via nitrogen to calcium, forming a formal Ca–N–C–C–N–(Ca) five-ring. This initial product is consumed in a tautomerization step to give slightly more stable **11**, in which the cyanide group is no longer bound to the calcium atom. Tautomerization **10** → **11** (with N_β hydrogen shifting to N_α, the former imine nitrogen) is most likely intermolecular, as direct [1,2]H shift is orbital symmetry forbidden and has, hence, a high barrier of 39.8 kcal·mol^{-1}, and also because a – conceivable – intermittently at carbonyl oxygen protonated species (i.e., on an iminol-type pathway) is considerably higher in energy than **10** or **11**.

The TMS-bound product **12**, proposed in the computational investigation, could not be isolated either – probably due to its

high sensitivity to hydrolysis. However, a 2D ^{1}H-^{15}N NMR correlation spectrum showed no interactions of hydrogen nuclei in silicon-bound methyl groups and any of the nitrogens in the product. This led us to conclude that silicon is bound via the carbonyl oxygen in **12**, as also shown by DFT computations. This is further corroborated by observation of a ^{13}C NMR signal at 146 ppm for an sp^2 carbon in the backbone of the product, which fits better for a C=N than a C=O bond.

Recovery of the catalyst resting state **7** is achieved by reacting **11** with stoichiometric reagent TMSCN (**8**). This "reloads" calcium with cyanide and replaces TMS-bound isolated product **12** from the metal complex and in which silicon, rather than calcium, is bound to the carbonyl oxygen. The addition reaction itself is rather exothermic (Figure 3) and provides (together with the similarly exothermic complexation of calcium complex **7** with hydrazone) driving force for the catalytic cycle, but, on the other hand, may impede enantioselectivity, because of a "backwater" effect equaling out outcomes from different reaction pathways before intermediates are allowed to overcome the rate-limiting barrier. The actual replacement step itself (Figure 5), which recovers the catalyst and releases product **12**, is endothermic and slow (Figure 3). The overall reaction energy of the catalytic cycle is, hence, a mere 4.6 kcal·mol^{-1}, taking into account zero-point energy and thermodynamic corrections. Getting acceptable yields experimentally at all is only possible because of swiftness and practical irreversibility of formation of new **9** from released **7**. Furthermore, it could be helpful to constantly remove the product from the reaction zone.

Moreover, the replacement step will occur only from a conformation in which the ethyl group at the former imine carbon stands opposite to the TMS moiety. While the CN double bond of imine **1** became a single bond in complexes **10** and **11** through the hydrocyanation step, internal rotation around this bond is still massively hindered with a sizable barrier of 15.0 kcal·mol^{-1} via **TS 8** (Figure 4), interchanging two almost equienergetic conformations of **11** (**11Z**, with an N–N–C–C_{Et} torsion angle of 32°, and **11E**, with an torsion angle of 111°), which have a strong reminiscence of their predecessors' former geometric isomerism, an effect that might similarly occur also in related addition reactions of alkenes, for example.

After **11E** had reacted with TMSCN, adduct **13** forms, 3.8 kcal·mol^{-1} more stable than the competing unreactive adduct obtained from "*Z*" conformation.

Outside from the catalytic cycle, **12** could be further hydrolyzed in a subsequent step to yield hydrazino nitrile **2** (Table 2) from which α-hydrazino acids could be obtained by harsher hydrolysis conditions. It is important to note that compound **12** also exhibits geometric isomerism (Figure 2 depicts the lower-energy configuration), which arises from the newly formed CN double bond.

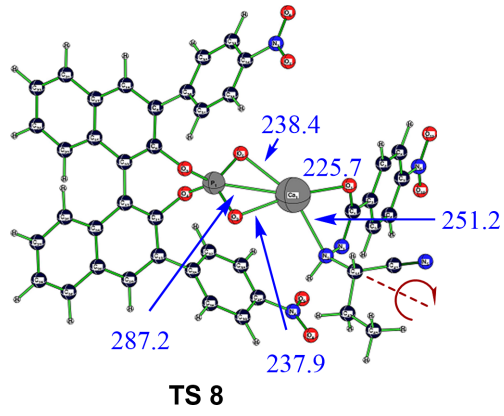

Figure 4: Transition-state structure **TS 8** for internal rotation, mixing conformational (*Z*/*E*)-pathways with opposite enantioselectivity. Bond lengths and distances are given in pm.

One of the most important quantities which allows comparison with experimental data is enantioselectivity. The most favorable **TS 9-10** is that which leads to the "*S*"-configured product, when the substrate is *Z*-hydrazone. Product of opposite handedness is reached via a transition state, 1.0 kcal·mol^{-1} higher in energy, resulting in a theoretical ee value of 74% (at 263 K), if pure *Z*-hydrazone would be used and under the assumption of kinetic reaction control. In contrast, the *E*-hydrazone gives preferably the "*R*" product (with a theoretical ee value of 64%). The transition state which gives the *R*-product from *E*-hydrazone is slightly lower in energy (Table 3).

Table 3: Relative energies (in kcal·mol^{-1}) at B3LYP/6-31G* for different pathways involving the configuration-determining hydrocyanation step. Absolute configuration (*R* or *S*) refers to that in hydrocyanation product **10**.

Pathway	E_{rel} of **9**	E_{rel} of **TS 9-10**	E_{rel} of **10**
Z (*S*)	1.6	11.8	6.0
Z (*R*)	2.6	12.8	6.9
E (*S*)	0.0	11.7	5.1
E (*R*)	0.3	10.9	4.2

However, the activation barrier for the rate-limiting step is 0.4 kcal·mol^{-1} lower for the pathway shown in Figure 2 and that yields the *S*-product from the *Z*-hydrazone. As the activation barrier to thermal *E*/*Z*-isomerization is more than twice as high as the barrier to hydrocyanation [59], the initial *E*/*Z* ratio is mostly conserved and affects strongly the experimentally

achievable ee value, which must necessarily be much lower than the theoretical values because of the opposite handedness of products preferred for *E*- and *Z*-hydrazones, respectively.

A thermodynamic control of the reaction outcome (i.e., especially enantioselectivity) would require the possibility to approach an equilibrium between **9** and **10** (seeing the reversibility of step **9** → **10**), in which case the relative energies of stereoisomeric forms of **10** determine the experimentally achievable ee values. Maximal theoretical ee values are 70% "*S*" for *Z*-hydrazone and 70% "*R*" for *E*-hydrazone. The relatively high racemization barriers in **9** preclude a Curtin–Hammett scenario (with fast pre-equilibrium), which would otherwise render the enantiomeric outcome (ee value) independent of the relative stabilities of different forms of this complex. Consequently, under kinetic reaction control, enantioselectivity would decrease over time as the reaction progresses. This occurs because slower-reacting complexes would accumulate, leading to a gradual equilibration of reaction rates for the *S*- and *R*-forming stereoisomers of **9**. The final step in the catalytic cycle (Figure 5), i.e., replacement step **13** → **7**, is rate limiting in calcium–BINOL phosphate-catalyzed asymmetric hydrocyanation of hydrazones and proceeds via a transition-state structure **TS 11-12**, 1.5 kcal·mol^{-1} higher in energy than that of the entry channel (**1** + **7** + **8**, Figure 3). Because the rate-determining and configuration-determining steps are different, reaction control of the whole multistep transformation in terms of enantioselectivity is therefore neither predominantly thermodynamic nor predominantly kinetic. However, trends in (and even extent of) enantioselectivity are very similar for both kinetic and thermodynamic control for the configuration-determining hydrocyanation step and for both *Z*- and *E*-hydrazones, respectively.

The replacement step is initiated by forming an adduct **13** from reaction of **11E** with TMSCN (**8**), giving a rather low energy complex as an energetic "sink" in the mechanism and with an almost linear Si–CN–Ca chain with a bridging cyanide ligand (Figure 5).

Catalyst **7** is released in the subsequent endothermic step via **TS 11-12**, which also yields the TMS-bound product **12**. In this

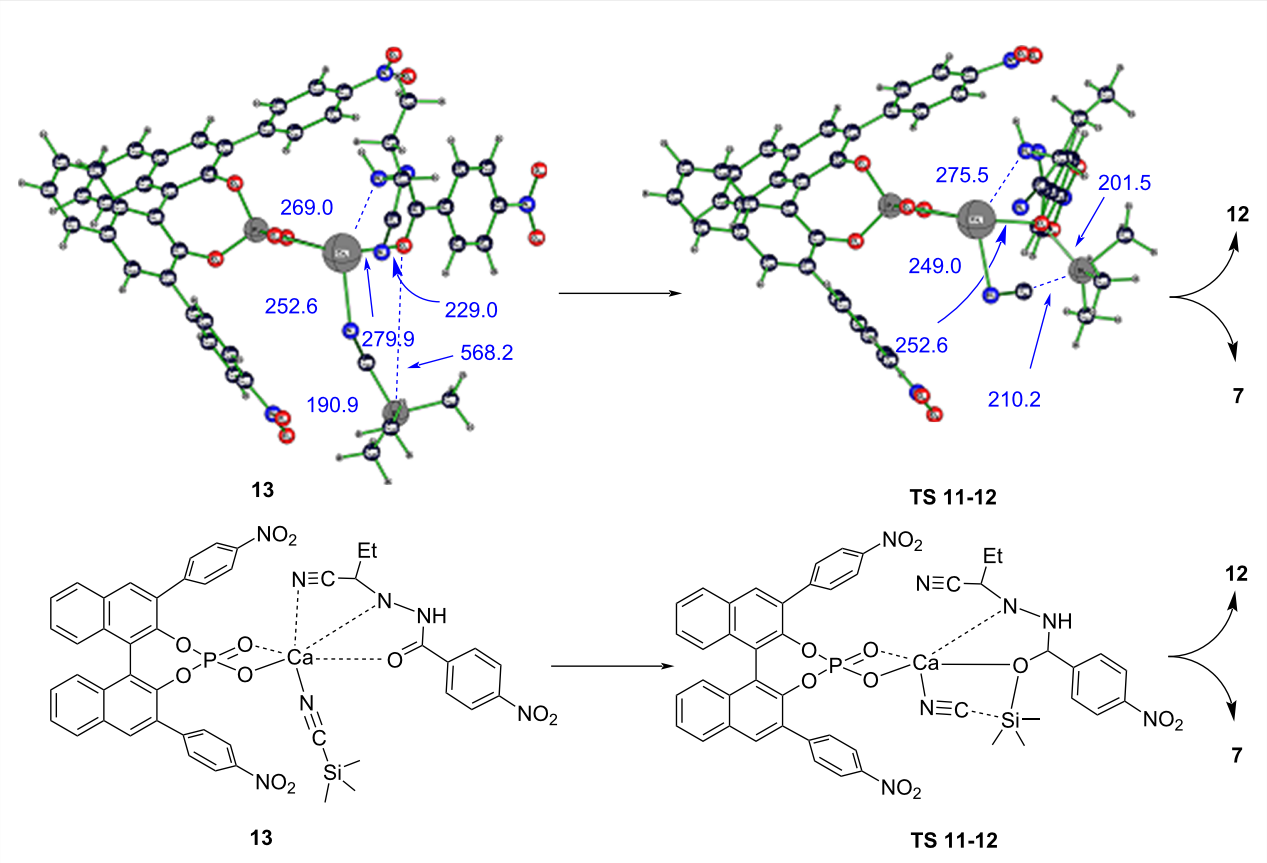

Figure 5: Replacement step after internal rotation in **11** via **TS8** and reaction with TMSCN to give adduct **13** (see Figure 3). Distances and bond lengths are given in pm. Catalyst **7** is replaced in **TS 11-12** by concerted electrophilic intramolecular substitution with formal trimethylsilyl cation as electrophile. Please note the surprisingly short Ca···N distance to the product nitrile nitrogen atom in **13**.

transition-state structure, two bonds (Ca–O and Si–C) are broken, while a Si–O bond is simultaneously formed, in a concerted step implying a cyclic flow of six electrons in a five-membered ring. The isocyanide Ca–N–C bond angle in **TS 11-12** lies between that of **7** and **9**. While the replacement step is slow, and hence, the bottleneck of the hydrocyanation, it is practically irreversible because the released free catalyst **7** is rapidly engaged again by reaction with further hydrazone in a distinctly exothermic reaction step.

Conclusion

In summary, we demonstrated that calcium-BINOL phosphates are able to catalyze the hydrocyanation reaction of hydrazones, towards precursors of α-hydrazino acids. Model achiral catalyst **4**, pre-formed by reaction of $Ca(OiPr)_2$ and biphenyl phosphate **3**, led to racemic product **2** in nearly full conversion in different reaction times, depending on the amount of catalyst used. Biphenyl phosphate **3** alone did not catalyze the reaction, showing that the catalytically active species is formed in situ by reaction between the Ca complex **4** and TMSCN. We also performed the reaction using chiral Ca complex **6**, either formed in situ or pre-formed as mentioned above for **4**, using enantiopure BINOL phosphate **5** as ligand. By generating the pre-catalyst **6** directly in the reaction vessel, we proved the involvement of Ca^{2+} in the catalysis, since the yield decreases by reducing the amount of $Ca(OiPr)_2$ with respect to the BINOL phosphate **5**. When Ca complex **6** is prepared and isolated prior to the reaction, use of alcohols as additives has a negative effect on both yield and enantioselectivity. The enantioselectivity was generally low (Table 2, entries 4–9) and with preference for the *S*-configured hydrocyanide employing the pre-formed Ca complex **6**. In addition, product **2** was obtained with absolute configuration opposite to the results with in situ-formed Ca complex **6**, for which BINOL phosphate was newly synthesized, instead of purchased, and with which we achieved much higher ee values (87–89% ee (*R*), Table 2, entries 1–3). These distinctly different outcomes, when methods to generate Ca complex **6**, or source and purification of ligand **5**, are varied, showed that these parameters strongly influence the hydrocyanation enantioselectivity.

In order to elucidate the mechanism of action of the pre-catalyst complex **6** and to explain the observed low enantioselectivity, we have carried out DFT computations with both *E*- and *Z*-hydrazone **1**, which revealed that Ca–BINOL phosphate complex **7** with side-on-coordinated cyanide is likely to be the active catalytic species and catalyst resting state. This complex reacts with hydrazone to give an encounter complex **9** with end-on-bound isocyanide, that attacks the imine carbon in the hydrazone to give species **10** in which cyanide is bound to both calcium and the imine carbon and which readily rearranges to cyanide **11**. This process is only slightly faster for the *Z*-hydrazone than for the *E*-hydrazone. Moreover, according to computations, the *Z*-hydrazone gives preferentially the *S*-, whereas the more stable *E*-hydrazone gives preferentially the *R*-configured product. However, in order to replace TMS-bound product **12** from the calcium complex and retrieve catalyst **7**, prior internal rotation in **11** from *Z*-hydrazone pathway to *E*-hydrazone pathway is required, i.e., both hydrazone isomers give the same hydrocyanation product and with low ee, because pathways with opposite preference for either product enantiomer mix via internal rotation **TS8**, which explains also the low enantioselectivity observed in our experiments and with preformed pre-catalyst **6**. Which absolute configuration prevails eventually in the product (i.e., *R* or *S*), is difficult to predict theoretically due to the fact that the configuration and rate-determining steps are not the same.

The good enantioselectivities observed when the catalytic species was presumed to be in situ-generated pre-catalyst **6**, indicate that catalysis must have followed therein a route different from the one with preformed pre-catalyst **6**, and involves a different active species. Seeing that calcium is prone to form complexes with mono- and bidentate phosphate ligands, bridged multicentered particles may form in solution during in situ generation of the calcium complex, as known from, e.g., Posner's well-defined colloidal calcium phosphates [60].

Supporting Information

CCDC 1824279 (**4**), CCDC 1824280 (**3**), and CCDC 1824281 (product O=C(C1=CC=C(Br)C=C1)NNC(C#N)CC2=CC=CC=C2, **2''**) contain the supplementary crystallographic data for this paper. These data are provided free of charge by The Cambridge Crystallographic Data Centre via http://www.ccdc.ac.uk/data request/cif.

Supporting Information File 1

Synthetic procedures, ^{1}H, ^{13}C, and ^{31}P NMR as well as mass-spectrometric data of all synthesized compounds and selected crystal structures.
[https://www.beilstein-journals.org/bjoc/content/supplementary/1860-5397-21-59-S1.pdf]

Acknowledgements

Portions of this work are included in the doctoral thesis of Christian Andreas Fischer, "Insights in Group 2 Metal Catalysis: New Ways and New Obstacles", Friedrich-Alexander-Universität Erlangen-Nürnberg, 2020.

Funding

The authors gratefully acknowledge the financial support from the Deutsche Forschungsgemeinschaft (DFG) by grants TS 87/28-1 and HA-3218/8-1.

ORCID® iDs

Christian A. Fischer - https://orcid.org/0000-0002-5691-5248
Sascha Kohlbauer - https://orcid.org/0009-0008-7840-9902
Alexandru Zamfir - https://orcid.org/0009-0005-7029-7617
Sjoerd Harder - https://orcid.org/0000-0002-3997-1440
Svetlana B. Tsogoeva - https://orcid.org/0000-0003-4845-0951

Data Availability Statement

Data generated and analyzed during this study is available from the corresponding author upon reasonable request.

References

1. Harder, S. *Chem. Rev.* **2010,** *110,* 3852–3876. doi:10.1021/cr9003659
2. Albrecht, M.; Bedford, R.; Plietker, B. *Organometallics* **2014,** *33,* 5619–5621. doi:10.1021/om5010379
3. Schafer, L. L.; Mountford, P.; Piers, W. E. *Dalton Trans.* **2015,** *44,* 12027–12028. doi:10.1039/c5dt90105g
4. Hill, M. S.; Liptrot, D. J.; Weetman, C. *Chem. Soc. Rev.* **2016,** *45,* 972–988. doi:10.1039/c5cs00880h
5. Haubenreisser, S.; Niggemann, M. *Adv. Synth. Catal.* **2011,** *353,* 469–474. doi:10.1002/adsc.201000768
6. Kiely-Collins, H. J.; Sechi, I.; Brennan, P. E.; McLaughlin, M. G. *Chem. Commun.* **2018,** *54,* 654–657. doi:10.1039/c7cc09491d
7. Martin, M. C.; Sandridge, M. J.; Williams, C. W.; Francis, Z. A.; France, S. *Tetrahedron* **2017,** *73,* 4093–4108. doi:10.1016/j.tet.2017.03.041
8. Bauer, H.; Alonso, M.; Färber, C.; Elsen, H.; Pahl, J.; Causero, A.; Ballmann, G.; De Proft, F.; Harder, S. *Nat. Catal.* **2018,** *1,* 40–47. doi:10.1038/s41929-017-0006-0
9. Bauer, H.; Thum, K.; Alonso, M.; Fischer, C.; Harder, S. *Angew. Chem., Int. Ed.* **2019,** *58,* 4248–4253. doi:10.1002/anie.201813910
10. Rösch, B.; Gentner, T. X.; Elsen, H.; Fischer, C. A.; Langer, J.; Wiesinger, M.; Harder, S. *Angew. Chem., Int. Ed.* **2019,** *58,* 5396–5401. doi:10.1002/anie.201901548
11. Tsubogo, T.; Saito, S.; Seki, K.; Yamashita, Y.; Kobayashi, S. *J. Am. Chem. Soc.* **2008,** *130,* 13321–13332. doi:10.1021/ja8032058
12. Shimizu, S.; Tsubogo, T.; Xu, P.; Kobayashi, S. *Org. Lett.* **2015,** *17,* 2006–2009. doi:10.1021/acs.orglett.5b00749
13. Rueping, M.; Bootwicha, T.; Kambutong, S.; Sugiono, E. *Chem. – Asian J.* **2012,** *7,* 1195–1198. doi:10.1002/asia.201200063
14. Uraguchi, D.; Terada, M. *J. Am. Chem. Soc.* **2004,** *126,* 5356–5357. doi:10.1021/ja0491533
15. Akiyama, T.; Itoh, J.; Yokota, K.; Fuchibe, K. *Angew. Chem., Int. Ed.* **2004,** *43,* 1566–1568. doi:10.1002/anie.200353240
16. Yamanaka, M.; Itoh, J.; Fuchibe, K.; Akiyama, T. *J. Am. Chem. Soc.* **2007,** *129,* 6756–6764. doi:10.1021/ja0684803
17. Simón, L.; Goodman, J. M. *J. Org. Chem.* **2011,** *76,* 1775–1788. doi:10.1021/jo102410r
18. Kshatriya, R. *ACS Omega* **2023,** *8,* 17381–17406. doi:10.1021/acsomega.2c05535
19. del Corte, X.; Martínez de Marigorta, E.; Palacios, F.; Vicario, J.; Maestro, A. *Org. Chem. Front.* **2022,** *9,* 6331–6399. doi:10.1039/d2qo01209j
20. Tsogoeva, S. B. *Nat. Catal.* **2024,** *7,* 7–9. doi:10.1038/s41929-023-01099-9
21. Akiyama, T. *Chem. Rev.* **2007,** *107,* 5744–5758. doi:10.1021/cr068374j
22. Terada, M. *Chem. Commun.* **2008,** 4097–4112. doi:10.1039/b807577h
23. Kampen, D.; Reisinger, C. M.; List, B. *Top. Curr. Chem.* **2010,** *291,* 395–456.
24. Zamfir, A.; Schenker, S.; Freund, M.; Tsogoeva, S. B. *Org. Biomol. Chem.* **2010,** *8,* 5262–5276. doi:10.1039/c0ob00209g
25. Freund, M.; Schenker, S.; Zamfir, A.; Tsogoeva, S. B. *Curr. Org. Chem.* **2011,** *15,* 2282–2310. doi:10.2174/138527211796150750
26. Rueping, M.; Kuenkel, A.; Atodiresei, I. *Chem. Soc. Rev.* **2011,** *40,* 4539–4549. doi:10.1039/c1cs15087a
27. Schenker, S.; Zamfir, A.; Freund, M.; Tsogoeva, S. B. *Eur. J. Org. Chem.* **2011,** 2209–2222. doi:10.1002/ejoc.201001538
28. Parmar, D.; Sugiono, E.; Raja, S.; Rueping, M. *Chem. Rev.* **2014,** *114,* 9047–9153. doi:10.1021/cr5001496
29. Held, F. E.; Grau, D.; Tsogoeva, S. B. *Molecules* **2015,** *20,* 16103–16126. doi:10.3390/molecules200916103
30. Hatano, M.; Moriyama, K.; Maki, T.; Ishihara, K. *Angew. Chem., Int. Ed.* **2010,** *49,* 3823–3826. doi:10.1002/anie.201000824
31. Simón, L.; Paton, R. S. *J. Am. Chem. Soc.* **2018,** *140,* 5412–5420. doi:10.1021/jacs.7b13678
32. Drouet, F.; Lalli, C.; Liu, H.; Masson, G.; Zhu, J. *Org. Lett.* **2011,** *13,* 94–97. doi:10.1021/ol102625s
33. Lalli, C.; Dumoulin, A.; Lebée, C.; Drouet, F.; Guérineau, V.; Touboul, D.; Gandon, V.; Zhu, J.; Masson, G. *Chem. – Eur. J.* **2015,** *21,* 1704–1712. doi:10.1002/chem.201405286
34. Nimmagadda, S. K.; Mallojjala, S. C.; Woztas, L.; Wheeler, S. E.; Antilla, J. C. *Angew. Chem., Int. Ed.* **2017,** *56,* 2454–2458. doi:10.1002/anie.201611602
35. Li, X.-Y.; Yuan, W.-Q.; Tang, S.; Huang, Y.-W.; Xue, J.-H.; Fu, L.-N.; Guo, Q.-X. *Org. Lett.* **2017,** *19,* 1120–1123. doi:10.1021/acs.orglett.7b00143
36. Ibáñez, I.; Kaneko, M.; Kamei, Y.; Tsutsumi, R.; Yamanaka, M.; Akiyama, T. *ACS Catal.* **2019,** *9,* 6903–6909. doi:10.1021/acscatal.9b01811
37. Liu, R.; Krishnamurthy, S.; Wu, Z.; Tummalapalli, K. S. S.; Antilla, J. C. *Org. Lett.* **2020,** *22,* 8101–8105. doi:10.1021/acs.orglett.0c03059
38. Wu, Z.; Krishnamurthy, S.; Satyanarayana Tummalapalli, K. S.; Xu, J.; Yue, C.; Antilla, J. C. *Chem. – Eur. J.* **2022,** *28,* e202200907. doi:10.1002/chem.202200907
39. Cao, R.; Antilla, J. C. *Org. Lett.* **2020,** *22,* 5958–5962. doi:10.1021/acs.orglett.0c02048
40. Ingle, G. K.; Liang, Y.; Mormino, M. G.; Li, G.; Fronczek, F. R.; Antilla, J. C. *Org. Lett.* **2011,** *13,* 2054–2057. doi:10.1021/ol200456y
41. Ingle, G.; Mormino, M. G.; Antilla, J. C. *Org. Lett.* **2014,** *16,* 5548–5551. doi:10.1021/ol502527q
42. Wang, Y.; Wang, S.; Shan, W.; Shao, Z. *Nat. Commun.* **2020,** *11,* 226. doi:10.1038/s41467-019-13886-9
43. Capel, E.; Rodríguez-Rodríguez, M.; Uria, U.; Pedron, M.; Tejero, T.; Vicario, J. L.; Merino, P. *J. Org. Chem.* **2022,** *87,* 693–707. doi:10.1021/acs.joc.1c02699
44. Wen, H.-C.; Chen, W.; Li, M.; Ma, C.; Wang, J.-F.; Fu, A.; Xu, S.-Q.; Zhou, Y.-F.; Ni, S.-F.; Mao, B. *Nat. Commun.* **2024,** *15,* 5277. doi:10.1038/s41467-024-49435-2
45. Zamfir, A.; Tsogoeva, S. B. *Org. Lett.* **2010,** *12,* 188–191. doi:10.1021/ol9025974

46. Morley, J. S.; Payne, J. W.; Hennessey, T. D. *J. Gen. Microbiol.* **1983,** *129,* 3701–3708. doi:10.1099/00221287-129-12-3701
47. Lam, L. K.; Arnold, L. D.; Kalantar, T. H.; Kelland, J. G.; Lane-Bell, P. M.; Palcic, M. M.; Pickard, M. A.; Vederas, J. C. *J. Biol. Chem.* **1988,** *263,* 11814–11819. doi:10.1016/s0021-9258(18)37858-x
48. Chen, S.; Chrusciel, R. A.; Nakanishi, H.; Raktabutr, A.; Johnson, M. E.; Sato, A.; Weiner, D.; Hoxie, J.; Saragovi, H. U.; Greene, M. I. *Proc. Natl. Acad. Sci. U. S. A.* **1992,** *89,* 5872–5876. doi:10.1073/pnas.89.13.5872
49. Keith, J. M.; Jacobsen, E. N. *Org. Lett.* **2004,** *6,* 153–155. doi:10.1021/ol035844c
50. Orecchia, P.; Yuan, W.; Oestreich, M. *Angew. Chem., Int. Ed.* **2019,** *58,* 3579–3583. doi:10.1002/anie.201813853
51. Yao, L.-H.; Shao, S.-X.; Jiang, L.; Tang, N.; Wu, J.-C. *Chem. Pap.* **2014,** *68,* 1381–1389. doi:10.2478/s11696-014-0585-z
52. Liang, T.; Li, G.; Wojtas, L.; Antilla, J. C. *Chem. Commun.* **2014,** *50,* 14187–14190. doi:10.1039/c4cc06520d
53. Harder, S.; Müller, S.; Hübner, E. *Organometallics* **2004,** *23,* 178–183. doi:10.1021/om0341350
54. Kapp, J.; Schleyer, P. v. R. *Inorg. Chem.* **1996,** *35,* 2247–2252. doi:10.1021/ic9511837
55. Katz, A. K.; Glusker, J. P.; Beebe, S. A.; Bock, C. W. *J. Am. Chem. Soc.* **1996,** *118,* 5752–5763. doi:10.1021/ja953943i
56. Lanzisera, D. V.; Andrews, L. *J. Phys. Chem. A* **1997,** *101,* 9666–9672. doi:10.1021/jp972098i
57. Andrews, L.; Cho, H.-G.; Yu, W.; Wang, X. *J. Phys. Chem. A* **2019,** *123,* 3743–3760. doi:10.1021/acs.jpca.9b01286
58. Ballmann, G.; Elsen, H.; Harder, S. *Angew. Chem., Int. Ed.* **2019,** *58,* 15736–15741. doi:10.1002/anie.201909511
59. Landge, S. M.; Tkatchouk, E.; Benítez, D.; Lanfranchi, D. A.; Elhabiri, M.; Goddard, W. A., III; Aprahamian, I. *J. Am. Chem. Soc.* **2011,** *133,* 9812–9823. doi:10.1021/ja200699v
60. Mancardi, G.; Hernandez Tamargo, C. E.; Di Tommaso, D.; de Leeuw, N. H. *J. Mater. Chem. B* **2017,** *5,* 7274–7284. doi:10.1039/c7tb01199g

License and Terms